Mechanically Interlocked Architectures *via* Active-metal Template Strategies

by

Kevin D. Hänni

Degree of Doctor of Philosophy
School of Chemistry
The University of Edinburgh
August 2009

A ceux qui ont cru en moi.

Table of Content

Abstract *vii*

Declaration *viii*

Meeting and Lectures Attended and Presentations Given *ix*

Acknowledgements *x*

List of Abbreviations *xiii*

General Remarks on Experimental Data *xv*

Layout of the Thesis *xvi*

Chapter I, Introducing Mechanically Interlocked Architectures **1**

1.1 Nomenclature and Definitions **2**

1.2 Early Synthetic Methodologies **2**

1.2.1 Statistical Approaches 2

1.2.2 Covalent Bond Directed Synthesis 3

1.3 Template Directed Synthesis of Interlocked Architectures **4**

1.4 Non Transition Metal Template-based Methodologies to MIAs **5**

1.4.1 Hydrophobic Interactions 5

1.4.2 Aromatic Interactions 6

1.4.3 Hydrogen-bonding Interactions 8

1.4.3.1 Amide Hydrogen-bonding Interactions *8*

1.4.3.2 Ammonium-crown Ether Template *11*

1.5 Transition-Metal Template for the Preparation of MIAs **12**

1.5.1 Passive Templates 12

1.5.1.1 Linear (1+1) Template *14*

1.5.1.2 Tetrahedral (2+2) TM Geometry *14*

1.5.1.3 Square-Planar (3+1) Pd Geometry *17*

1.5.1.4 Trigonal-bipyramidal (3+2) Geometry *19*

1.5.1.5 Octahedral (3+3) TM Geometry *20*

1.5.1.6 Octahedral (3+2+1) Template Strategy *22*

1.5.1.7 Octahedral (4+2) Template Strategy *24*

1.5.1.8 Octahedral (2+2+2) TM Strategy *25*

1.5.2 Interlocked Architecture Containing Metal Ions in Their Framework 26
1.5.2.1 Pd-containing Catenanes 27
1.5.2.2 Mixed Cu^{II}/Cu^{III} Dithiocarbamate Catenane 28
1.5.2.3 Palladium First- and Second-sphere Coordination Template 28
1.5.2.4 Macrocycle Shrinking by Palladium Template 29
1.5.2.5 Gold-acetylide-based Catenane 30
1.6 The Active-metal Template Approach **30**
1.6.1 Presentation of the Concept 30
1.6.2 CuAAC Active-metal Template 32
1.6.3 Glaser and Ulmann Active-metal Template 32
1.6.4 Rotaxanes *via* Cadiot-Chowkiewicz Active-metal Template 33
1.6.5 Pd(II) Michael Addition towards the Synthesis of Rotaxanes 35
1.6.6 Scope of the Thesis 37
1.7 References **37**
Chapter II, Catalytic CuAAC-AMT Synthesis of [2]Rotaxanes, [3]Rotaxanes and Molecular Shuttles **41**
2.1 Synopsis **42**
2.2 Introduction **43**
2.3 Results and Discussion **45**
2.3.1 Initial Results 45
2.3.2 Effect of the Macrocyclic Structure on [2]Rotaxane Formation 48
2.3.2.1 Mono- and Tridentate Macrocycles 50
2.3.2.2 Bidentate Macrocycles 51
2.3.3 ^{1}H NMR of Metal-free [2]Rotaxanes 53
2.3.4 Effect of the Nature of the Cu(I) Source 55
2.3.5 Template CuAAC Reaction at High Macrocycle:Cu(I) Ratios: Unexpected Formation of [3]Rotaxanes 55
2.3.6 Stoichiometric and Catalytic Active-metal Template Synthesis of *Bis*triazole [2]Rotaxanes 60

2.3.7 Transition Metal-mediated Control of the Shuttling Rate in Degenerate *Bis*Triazole-Station Molecular Shuttles 61

2.4 Conclusion ***64***

2.5 Experimental Section ***65***

2.5.1 General Procedure for the Formation of AMT-CuAAC Rotaxanes 65

2.5.2 Preparation of Half-threads 66

2.5.3 Preparation of Macrocycles 68

2.5.4 Preparation of CuAAC-AMT Rotaxanes 76

2.6 References ***88***

Chapter III: A Catalytic Palladium Active-metal Template Pathway to [2]Rotaxanes **91**

3.1 Synopsis ***92***

3.2 Introduction ***93***

3.3 Results and Discussion ***93***

3.3.1 Effect of the Macrocycle Structure on [2]Rotaxane Formation 98

3.3.2 ^{1}H NMR of the Interlocked Compound 100

3.4 Conclusion ***100***

3.5 Experimental Section ***101***

3.5.1 Preparation of Half-thread **3** 101

3.5.2 Preparation of Pd-complexes 102

3.5.3 Preparation of AMT Alkynes Homocoupling Rotaxanes 113

3.6 References ***116***

Chapter IV: [2]Rotaxanes through Palladium Active-Template Oxidative Heck Cross-Couplings **117**

4.1 Synopsis ***118***

4.2 Introduction ***119***

4.3 Results and Discussion ***120***

4.3.1 Initial Attempts using Pd^{0}-mediated Heck Cross-coupling 120

4.3.2 Pd(II) Oxidative Heck: Initial Screening Conditions 121

4.3.3 ^{1}H NMR of the Interlocked Structure 125

4.3.4 Substrate Scope 125

4.4 Conclusion ***127***

4.5 Experimental Section ***127***

4.5.1 Preparation of Half-threads 127

4.5.2 General Experimental Procedure for the Oxidative Heck Active-Metal Template Reaction 136
4.5.3 Spectroscopic Data of Corresponding Non-interlocked Threads 140
4.6 References **142**
Chapter V: [2]Rotaxanes through Diels-Alder Active-Metal Template Strategy Mediated by Lewis Acids **144**
5.1 Synopsis **145**
5.2 Introduction **146**
5.3 Results and Discussion **147**
5.3.1 ^{1}H NMR of the Interlocked Product 151
5.3.2 Influence of the Macrocyclic Ligand on the DA-AMT Rotaxane Formation Reaction 152
5.3.3 Transition Metal-mediated Control of the Shuttling in Two-Station Molecular Shuttle 153
5.4 Conclusion **155**
5.5 Experimental Section **156**
5.5.1 General Procedure for Preparation of Metal-complexes 156
5.5.2 Preparation of Half-threads 163
5.5.3 General Procedure for DA-rotaxane Formation Reaction 170
5.5.4 Spectroscopic Data of Corresponding Non-interlocked Threads 176
5.6 References **177**
Outlook **179**
Appendix: Published Papers **180**

Abstract

In contrast to the classic 'passive template' approach,[1] an 'active-metal' template strategy involves a metal centre which acts as both a template and the catalyst for covalent bond formation in the construction of mechanically interlocked architectures. The crucial formation of a covalent bond between two 'half-threads' is promoted by the catalyst and directed through the cavity of the macrocycle by the catalyst's coordination requirements.

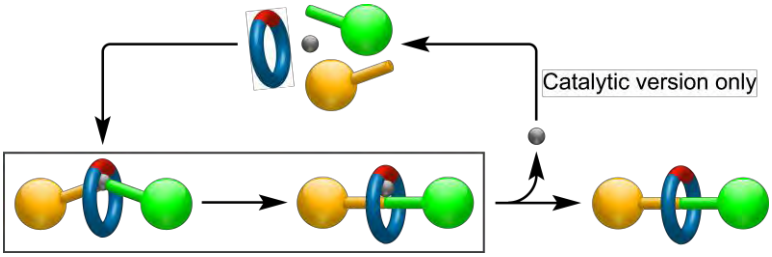

Scheme 1. Schematic representation of the active-metal template strategy to interlocked architectures.

The main attractive features of such a synthetic approach are the efficiency (as one step is required instead of two), the rapid assembly of inaccessible structures, the possibility of 'traceless' assemblies, the versatility, the possibility to use catalytic amount of the metal template and to provide mechanistic insight.

This novel concept was successfully introduced by our group and applied to a wide range of well-known transition metal-catalysed reactions. The thesis will present several examples of active-metal template reactions for the synthesis of interlocked architectures, including Cu(I)-catalysed alkyne-azide cycloaddition (CuAAC popularised as the click reaction),[2] Pd(II)-catalysed alkyne homocouplings[3] Pd(II)-catalysed oxidative Heck cross-couplings[4] and Lewis acids mediated Diels-Alder reactions.

(1) M. C. Thompson, D. H. Busch, *J. Am. Chem. Soc*. **1964**, *86*, 3651-3656.

(2) a) V. Aucagne, K. D. Hänni, D. A. Leigh, P. J. Lusby, D. B. Walker, *J. Am. Chem. Soc*. **2006**, *128*, 2186-2197. b) V. Aucagne, J. Berná J. D. Crowley, S. M. Goldup, K. D. Hänni, D. A. Leigh, P. J. Lusby, V. E. Ronaldson, A. M. Z. Slawin, A. Viterisi, D. B. Walker, *J. Am. Chem. Soc*. **2007**, *129*, 11950-11963.

(3) J. Berná J. D. Crowley, S. M. Goldup, K. D. Hänni, A.-L. Lee, D. A. Leigh, *Angew. Chem. Int. Ed*. **2007**, *46*, 5709-5713.

(4) J. D. Crowley, K. D. Hänni, A.-L. Lee, D. A. Leigh, **2007**, *J. Am. Chem. Soc*. *129*, 12092-12093.

Declaration

The scientific work described in the present thesis was carried out in the School of Chemistry at the University of Edinburgh between August and December 2005 and between September 2006 and May 2009. Unless otherwise stated, it is the work of the author. Part of the work presented in sections 2.3.1, 2.3.2 and 2.3.6 (Chapter II) has been submitted for a MSc degree in Molecular and Biological Chemistry at the Ecole Polytechnique Fédérale de Lausanne (Switzerland) in December 2005.

Signed: 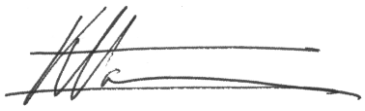

Date: 19th November 2009

Meeting and Lectures Attended and Presentations Given

1. **Organic Research Seminars**, School of Chemistry, University of Edinburgh, UK, 2006-2009.
    a) *Rotaxanes from Active-metal Template Strategies*, March 2007.
    b) *Rotaxanes from Active-metal Template Strategies*, February 2008.
    c) *Rotaxanes via Active-metal Template Methodologies*, April 2009.
2. **School of Chemistry Visiting Speaker Colloquia**, School of Chemistry, University of Edinburgh, UK, 2006-2009.
3. **The Young(ish!) Giants of Chemistry: A Symposium Marking the Sixty-Fifth Birthday of Sir J. Fraser Stoddart**, University of Edinburgh, UK, June 2007.
4. **RSC Perkin Division 35th Scottish Regional Meeting**, University of Glasgow, UK, December 2007.
5. **Molecular Nanoscience Symposium**, University of Reading, UK, June 2008.
    Poster presentation: *Diels-Alder Active Template for the Synthesis of [2]Rotaxanes.*
6. **3rd Internationnal Symposium on Macrocyclic and Supramolecular Chemistry**, Las Vegas NV, USA, July 2008.
    Poster presentation: *Diels-Alder Active Template for the Synthesis of [2]Rotaxanes.*
7. **Swiss Chemical Society Fall Meeting 2008**, University of Zürich, Switzerland, Sept. 2008.
    Oral presentation: *Rotaxane via Palladium Active-metal Template Strategies.*
8. **20th SCI Postgraduate Symposium**, University of St. Andrew, UK, April 2009.
    Oral presentation: *Rotaxanes via Active-metal Template Strategies.*
9. **Exploiting the Chemistry of Metals for Catalysis Synthesis and Spectroscopy**, University of York, UK, May 2009.
    Oral presentation: *Rotaxanes via Active-metal Template Strategies.*
10. **42nd IUPAC Meeting 2009**, SECC, Glasgow, UK, August 2009.
    Oral presentation: *Molecular Interlocked Architecture via Active-metal Template Methodologies.*

Acknowledgments

For starters, I would especially like to thank my supervisor Professor David A. Leigh, who not only gave me the opportunity to work in his marvellous international research group, but also gave me the chance to work in a field of chemistry that I particularly like, with all the independence, advice and resources I needed to conduct a successful PhD. *Encore merci Dave!*

The adventure would have probably never started without the support of Professor Paul J. Dyson at the EPFL (Switzerland) and without the enthusiastic classes of Joyce Rupp, a chemistry teacher at the Morges High School (Switzerland), who turned my first excitement into a deep true love for the science that is chemistry.

For the main course, I would like to acknowledge all the talented chemists and precious friends who shared my everyday life in Edinburgh.

I would like to thank two persons in particular; as they helped me enormously during my PhD. Firstly, Dr. Vincent Aucagne, presently, a *chargé de recherche* at the CNRS in Orléans. He introduced me to the wonderful world of the active-metal template when I was still a young and innocent Erasmus student. He guided me during my first stay in Edinburgh and it is probably due to his enthusiasm that I had the urge to return. The second person is Dr. James Crowley, now back home in *Middle Earth* (New Zealand) at the University of Otago. I thank him for his valuable advices, guidance and friendship all along the one-and-half year I worked with him. *Merci les gars!*

Aside from these characters, I thank those with whom it has been my pleasure to work over the last three years (in roughly chronological order): Dr. Aurélien Viterisi, Dr. Ai-Lan Lee, Dr. José Berná, Dr. Steve Goldup and Max von Delius, who not only shares my love of green alcoholic beverages but also the love of brewing and enjoying good ales.

As far as collaborators at other universities are concerned, I would like to thank the Professor Alexandra M. Z. Slawin for solving various X-ray crystal structures shown in this thesis.

Then there are those guys that I did not work with, but that have helped to make the group such a great place to work. My PhD fellows: Anthony, Mike and Roy. My Bay Comrades: Bryan, Marius, Nick and Takeshi. And all the others: Adam, Amaya, Barry, Bea, Christoph, Diego, Daniel (I and II), David, Dominik, Jhenyi (Jhen-Jhen), Katherine,

Louise, Luca, Luciana, Martin (Party Meister), Monica, Nathalie, Paul L., Paul M., Romen, Satoshi, Stewart, Tao, Teresa, Thomas and of course all that I have surely forgotten…

I should address special thanks to those who shared the common office computer with me (i.e. who coped with me not sharing the computer): Christiane, Vicki and Armando, and of course, thank you Edzard, for your contribution!

Thanks also to all the support staff here at the University of Edinburgh: Amanda and Annette upstairs, Derek, Kenny, Raymond and Tim in stores, the NMR team and the EPSRC (i.e. the British taxpayer) for funding.

For the cheese (for a French-speaking Swiss citizen it is the very important part) we have the people that really matter! The people, without whom, nothing would have been possible.

I would like to thank Dr. (medical, this time) Semanur Cengelli for her encouragements and love during the eight years that she shared my life.

I would like to thank my parents: Rénald, my father, who left us far too early and Nicole, my mother for their unconditional love and support (morally, emotionally and financially) over the past 28 years. I would also like to thank my brother Alfonso, my grandmother Liliane and my dearest friends Alexandre, Luc and *Les Zigotos*: Caroline, Hugo and Thomas. *Merci, merci et encore merci!*

I also would also like to thank the members of *La Fine Equipe*, a group of chemistry alumni from the EPFL, with whom I shared many laughs and good times in non French-speaking European capitals: Adrien (small blond guy to be wary of), Laélia (to be wary of at any time), Sébastien and Antoine (*dit* Berth), whose (flawed) theories proved each time to be accurate (damn!).

For the des(s)ert, I acknowledge Dr. Mark Symes for answering patiently my administration/English language/British customs questions during the three (and a bit more) years we spent together. I also want to thank him for playing the role of Louise in the remake of the famous movie *Thelma and Louise*, during our trip to Las Vegas to attend the ISMSC 2008 conference. We drove across the desert from Las Vegas to San Francisco (where we met nice people with flowers in their hair) *via* Flagstaff (AZ) passing through important places for chemists such as Antimony (UT), Boron (CA) and Chloride City (AZ). That's the spirit which built America!

And finally, as digestive, I would like to thank the Easyjet™ logistic team, which had the very good idea to establish a direct connection between Edinburgh and Geneva, which made my travelling much easier. I thank Les Paul for his invention of the electric guitar and made the sound of rock and roll possible; musical groups such as Deep Purple, The Rolling Stones, Led Zepplin, Muse, etc. probably appreciate this fact more than me. I am grateful to the Swiss people who has been responsible enough to vote positively to the Swiss-European treaties in 2000 and 2005 (that does not forgive them for having voted *no* in 1992…) which allowed me to live, work and pass the borders more easily in Europe and in the United Kingdom. I thank all the artists from whom I stole pictures on the internet to compose the images shown in the beginning of each Chapter, and finally I would have thanked Rick Hartung at the University of Nebraska if only I knew him...

List of Abbreviations

AMT	Active-metal Template
Amt.	amount
bipy	2,2′-bipyridine
calcd.	calculated
CuAAC	Copper(I)-Catalysed Azide Alkyne Cycloaddition
BQ	benzoquinone
BR	Borromean Rings
CD	cyclodextrin
Conv.	convertion
Da	Dalton
DA	Diels-Alder
DB24C8	Dibenzo-24-crown-8
DBU	1,8-Diazabiciclo[5,4,0]undec-7-ene
DCM	dichloromethane
dec.	decomposition
δ	chemical shift
EDCI	1-(3-dimethylaminopropyl)-3-ethylcarbodiimide
EDTA	ethanediaminetetraacetate
ESI	electrospray ionisation
Et_2O	diethylether
equiv.	equivalent
EtOAc	ethyl acetate
EtOH	ethanol
DIAD	diisopropylazodicarboxylate
DIPA	diisopropylamine
DIPEA	diisopropylethylamine
DMA	*N,N*'-dimethylacetamide
DMAP	4-dimethylaminopyridine
DMF	*N,N*'-dimethylformamide

DMSO	dimethylsulfoxide
FAB	Fast Atom Bombardment
FC	flash column
HRMS	High Resolution Mass Spectrometry
Hz, MHz	Hertz, megahertz
IPA	isopropyl alcohol
LA	Lewis acid
LRMS	Low Resolution Mass Spectrometry
Me_2CO	acetone
MeOH	methanol
MIA	Molecular Interlocked Architecture
min	minutes
m.p.	melting point
NMR	Nuclear Magnetic Resonance
3-NOBA	3-nitrobenzyl alcohol
Paraquat	*N,N′*-dimethyl-4,4′-bipyridinium dichloride
phen	1,10-phenanthroline
ppm	part per million
SP	Square planar
rot.	rotaxane
RT	room temperature
Terpy	2,2′:6′,2″-terpyridine
TFA	trifluoroacetic acid
THF	tetrahydrofuran
THIOG	thioglycerol
TLC	Thin Layer Chromatography
TM	Transition Metal

Note: conventional abbreviations for units and physical quantities are not included.

General Comments on Experimental Data

Unless otherwise stated, all reagents and solvents were purchased from Aldrich Chemicals and used without further purification. Tetrahydrofuran, dichloromethane, chloroform, acetonitrile and *N*,*N*-dimethylformamide were dried using a solvent purification system manufactured by Innovative Technology, Newburyport, MA, USA. Unless otherwise stated, all reactions were carried out under an atmosphere of nitrogen at room temperature. Column chromatography was carried out using Silica 60A (particle size 35-70 μm, Fisher, UK) as the stationary phase, and TLC was performed on precoated silica gel plates (0.25 mm thick, 60 F_{254}, Merck, Germany) and observed under UV light. By petrol is meant the fraction of petroleum ether boiling between 40 °C - 60 °C. ^{1}H spectra were recorded on Bruker AV 400, Bruker DMX 500 and Bruker AVA 600 instruments whilst all ^{13}C NMR spectra were recorded on a Bruker AV 400 instrument. Chemical shifts are reported in parts per million (ppm) from low to high frequency and referenced to the residual solvent resonance. Coupling constants (*J*) are reported in hertz (Hz). Standard abbreviations indicating multiplicity were used as follows: s = singlet, d = doublet, t = triplet, dd = double doublet, q = quartet, m = multiplet, b = broad, ddd = doublet of double doublets. Melting points (m.p.) were determined using a Sanyo Gallenkamp apparatus and are reported uncorrected. Mass spectrometry was carried out by the services at the University of Edinburgh and the EPSRC National Mass Spectrometry Service Centre, Swansea, UK.

Layout of the Thesis

Chapter I outlines some of the more pertinent strategies towards the synthesis of molecular interlocked architectures using various templating methodologies. Chapters II, III and IV describe different active-metal template strategies. They are each presented in the form of articles that have recently been published in peer-reviewed journals. No attempt has been made to re-write this work out of context, other than to insert cross-reference to other Chapters (where appropriate) and to ensure consistency of presentation throughout this thesis. These chapters are also reproduced in the Appendix, in their published formats. Chapter V details the extension of the concept of the active-metal template to the well-known Diels-Alder cycloaddition. The outlook contains closing remarks about the work that has been presented and prospective ideas for its application to more complicated systems.

Chapter I

Introducing Mechanically Interlocked Architectures

Acknowledgments

Dr. Barry A. Blight, Paul McGonigal and especially Adam Wilson are gratefully thanked for their proof-reading of this thesis.

1.1 Nomenclature and Definitions

Mechanically interlocked architectures (MIAs) are the result of an assembly of two or more separate molecules connected to each other not through traditional chemical (i.e. covalent) bonds but through what chemists more recently define as mechanical bonds.[1] Although their components are not covalently connected, the assemblies are true molecules and not supramolecular species, as the cleavage of one covalent bond is necessary to separate the constituent parts. Schematic representations of the most representatives MIAs are shown in Figure 1.1.[2]

Figure 1.1 Representation of the common MIAs, [2]rotaxane, [2]catenane and Borromean rings.

Interest in such molecules grew with the ability of scientists to produce them in efficient and facile ways. From early inefficient statistical methods (where a linear molecule is randomly threaded through a macrocycle),[3] until the emergence of supramolecular chemistry and template-directed synthesis, chemists have deployed their ingenuity to develop efficient protocols towards the preparation of MIAs. Because of their different properties compared to their non-interlocked analogues, MIAs have a huge number of potential applications, such as in Molecular Electronic Devices (MEDs), drug delivery systems,[4] surface transportation devices, molecular rotors and molecular machinery.[5]

1.2 Early Synthetic Methodologies

1.2.1 Statistical Approaches

It is claimed that in early 1900s, Willstatter first discussed the possibility of synthesising mechanically interlocked macrocyclic rings.[2] Early synthetic paths explored were based on statistical approaches: the random threading of a linear molecule through a macrocyclic followed by its cyclisation. The first preparation of interlocked rings was reported in 1960 by Wassermann; he achieved the synthesis of [2]catenane **3** from the penta-deutarated macrocycle **1** and the linear thread **2** in less than 1% yield (Scheme 1.1).[3a]

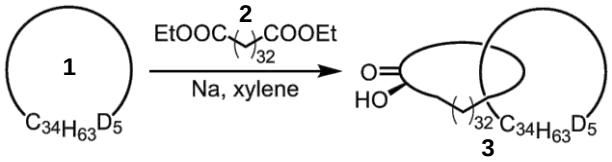

*Scheme 1.1 The first synthesis of a [2]catenane **2** by Wasserman exploiting the statistical threading of a linear chain through a macrocycle.*

The first synthesis of a [2]rotaxane was published by Harrison and Harrison seven years later using the same methodology as seen above.[3b] Pseudo-rotaxane **6** is obtained by the random threading of the linear diol **4** through a 30-membered ring attached on a Merrifield resin. Stoppering reaction followed by cleavage from the solid support yielded [2]rotaxane **7** in a very moderate 6% yield after seventy iterations (Scheme 1.2).

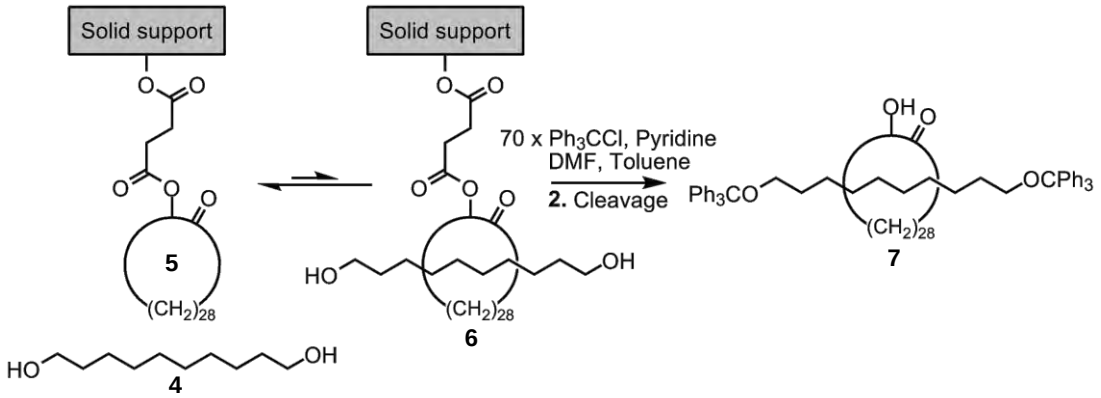

*Scheme 1.2 Synthesis of the first rotaxane **7** in 6% yield by statistical methodology (70 iterations).*

The extremely low yields in the above examples highlight the problem of using statistical methods: there is no thermodynamic driving force to facilitate the formation of interlocked species.

1.2.2 Covalent Bond Directed Synthesis

In 1964, Schill and Lüttringhaus described the use of covalent bonds as templates in the first directed synthesis of an MIAs.[6] In this multistep synthesis, **8** is the key intermediate: the geometry design - bond angles, lengths, tetrahedral structure of the ketal carbon atom, size of the macrocycle, lengths of the alkyl chloride chains - imposes intramolecular macrocyclisation in a unique and predetermined way. Alkylation of the amino group occurs only with the two alkyl chloride chains located one above and one below the plane of the central benzene ring to give **9**. Selective cleavage of the aryl-nitrogen bond and hydrolysis of the ketal group leads to the [2]catenane **10** in 30% yield.

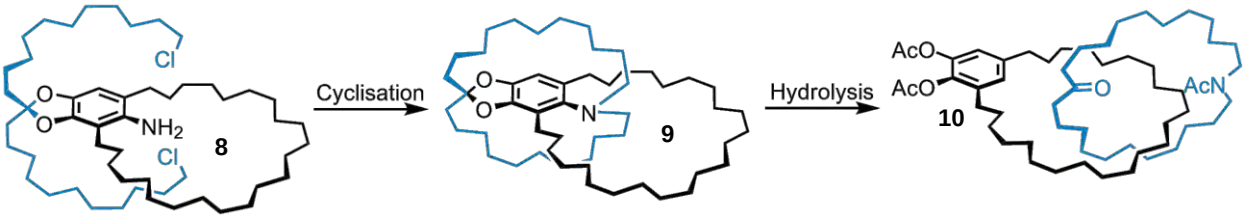

*Scheme 1.3 Synthesis of the first catenane **10** by covalently directed synthesis*

In spite of Schill's ingenious synthetic routes using a covalent bond template, this methodology did not resolve the major and limiting problem of poor yields in the synthesis of such interlocked molecules. Research aimed at improving the yields of interlocked species focused on the use of template interactions.

1.3 Template Directed Synthesis of Interlocked Architectures

The advent of both supramolecular chemistry and template synthesis marked a new era for MIAs: the use of non-covalent and weak intermolecular interactions allowed the formation of stable interlocked systems in high yields. It is undeniable that the work of Sauvage in the early 1980's turned MIAs from chemical curiosities into readily accessible molecules.[7] Over the past two decades, diverse recognition motifs such as donor-acceptor π-stacking systems,[8] hydrogen bonds[9] and metal coordination[10] have been utilized as a toolbox for the synthesis of complex interlocked structures.

To date, four distinct template approaches have been adopted for the synthesis of [2]rotaxanes (Scheme 1.4). The **capping** method[11,12] employs the conversion of a dynamic *pseudo*-rotaxane, wherein the thread and the macrocycle are held together *via* non-covalent interactions (i.e. the template), into the corresponding rotaxane by covalent attachment of two bulky stoppered units at both ends of the linear thread. The macrocycle is therefore trapped on the thread and its disassociation (or dethreading) is prevented by the presence of the two bulky stoppers. The **clipping** methodology[13] is quite similar to the capping reaction except that the thread is already capped. The rotaxane is obtained by the closure of an acyclic ligand (U-shape) templated around the stoppered thread. The **slipping** strategy[14,15] involves the macrocyclic unit passing over the stoppers of a thread at elevated temperatures followed by cooling to render the complex kinetically trapped. Note that the size of the stoppers must fit perfectly with the macrocycle cavity. **The active-metal template** strategy, which Leigh and Saito research groups have recently began to explore, is a methodology in which the template plays an active role in promoting the crucial covalent bond in order to capture

the interlocked structure.[16] The metal centre has a dual function: it acts both as a template *and* a catalyst for the formation the covalent bond between two "half-threads" through the cavity of a macrocycle. The present thesis discusses in detail the discovery, developments and application of this new technique.

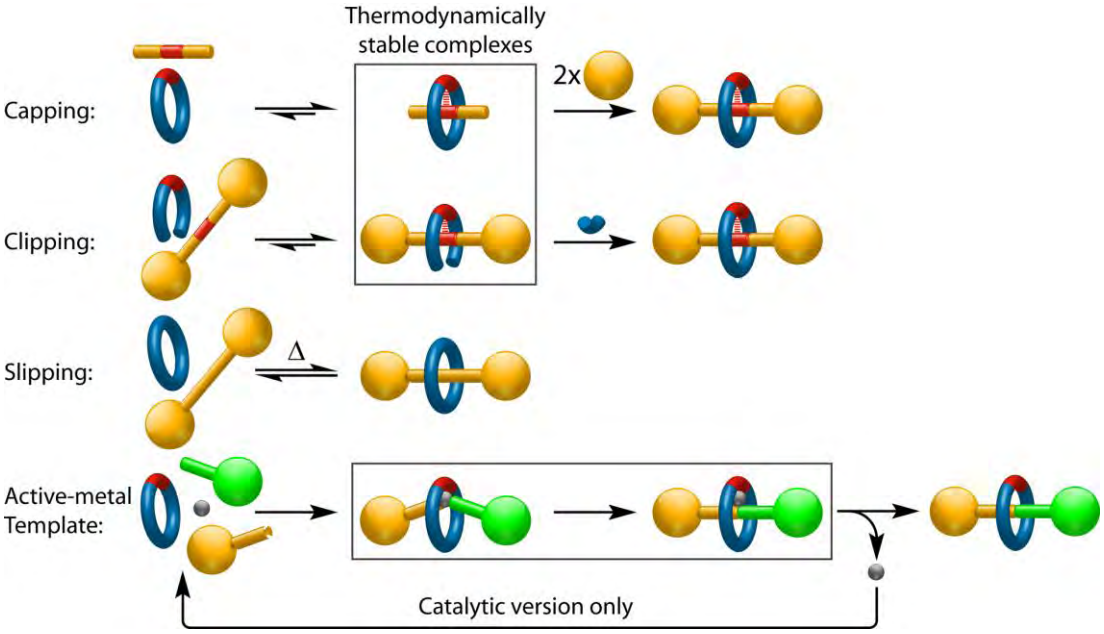

Scheme 1.4 Strategies towards the synthesis of [2]rotaxanes.

1.4 Non Transition Metal Template-based Methodologies to MIAs

1.4.1 Hydrophobic Interactions

The most extensively studied type of rotaxanes formed by the use of hydrophobic interactions is those with a cyclodextrin-based structure. Cyclodextrins (CDs) are cyclic oligosaccharides consisting of six or more α-1,4-linked D-glucopyranose units that yield a truncated cone shape. The exterior of their cavity is hydrophilic, due to the hydroxyl groups on the outer surface while their core is hydrophobic due to the hydrocarbon units of the interior. Such physicochemical properties make them both water-soluble and convenient hosts for complexing lipophilic molecular guests in aqueous media. Examples of CD-based [2]rotaxanes, reflecting the diversity of possible structures, are shown in Figure 1.2.

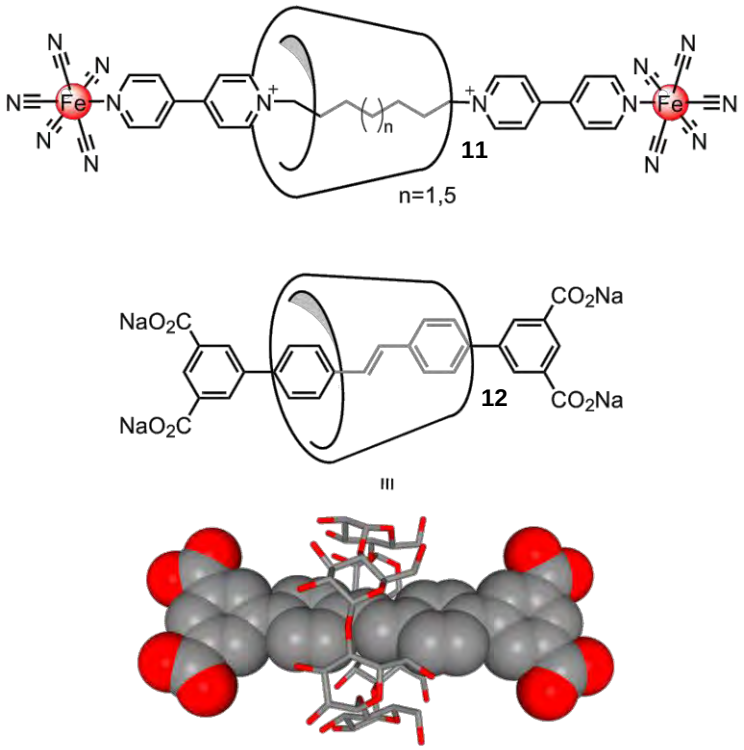

*Figure 1.2 Examples of cyclodextrin-based [2]rotaxane **11**[17] and **12**[18].*

1.4.2 Aromatic Interations

The discussion of synthetic molecular architectures assembled using aromatic interactions must be centred on the extensive research of Stoddart. In the late 1980s, they reported the discovery of a route to catenanes that worked using π-π stacking interactions.[19] Stoddart's research group studied the inclusion complexes of the π-electron deficient derivative **14** with π-electron-rich guests such as the crown ethers **13** to form host-guest complex **15** (Figure 1.2). Treatment of an acetonitrile solution of the *pseudo*-rotaxane with 1,4-dibenzyl bromide resulted in the formation of paraquat-containing catenane **16** in an impressive 70% yield.

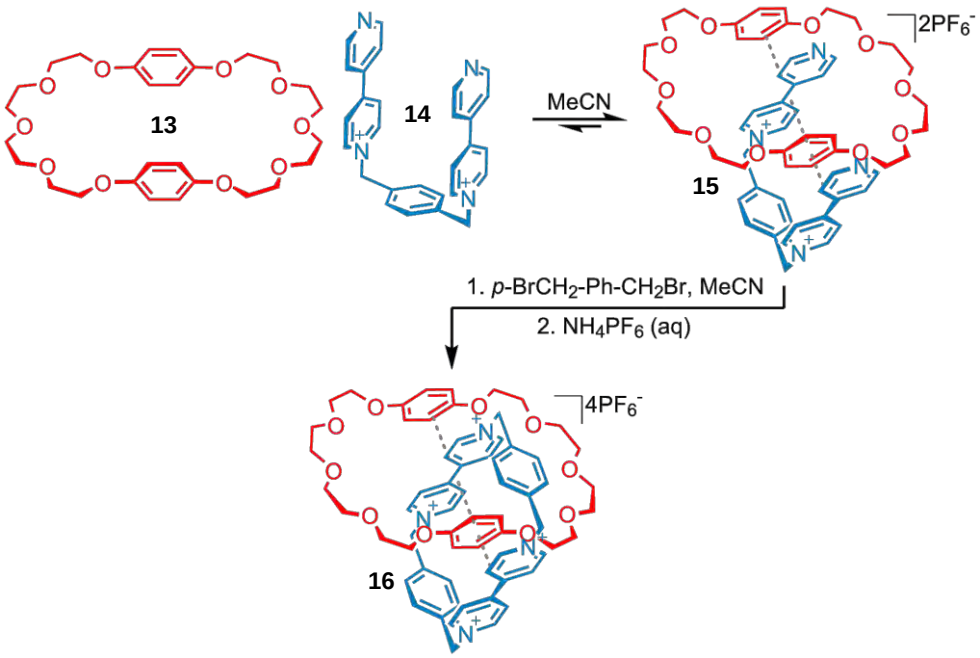

Scheme 1.5 Inclusion complexes using aromatic π-π stacking interactions.

Stoddart used this methodology for the synthesis of a multitude of MIAs such as rotaxanes,[20] catenanes,[21] lariats,[20b] molecular shuttles[20b,22] and other devices.[23,24] The general synthetic protocol involves the creation of thermodynamically stable *pseudo*-rotaxanes between a *bis*-functionalized π-donating unit threaded through a π-accepting macrocycle (or *vice-versa*). The latest strategy to date used by Stoddart and co-workers is the combination of the copper catalysed alkyne-azide cycloaddition (CuAAC or "click" chemistry) together with the donor-acceptor π-stacking strategy. One example is shown in Scheme 1.6, wherein rotaxanes **21a** (X = H) and **21b** (X =F) are obtained by trapping *pseudo*-rotaxanes **19a** and **19b** with a CuAAC stoppering reaction (82% and 11% respectively).

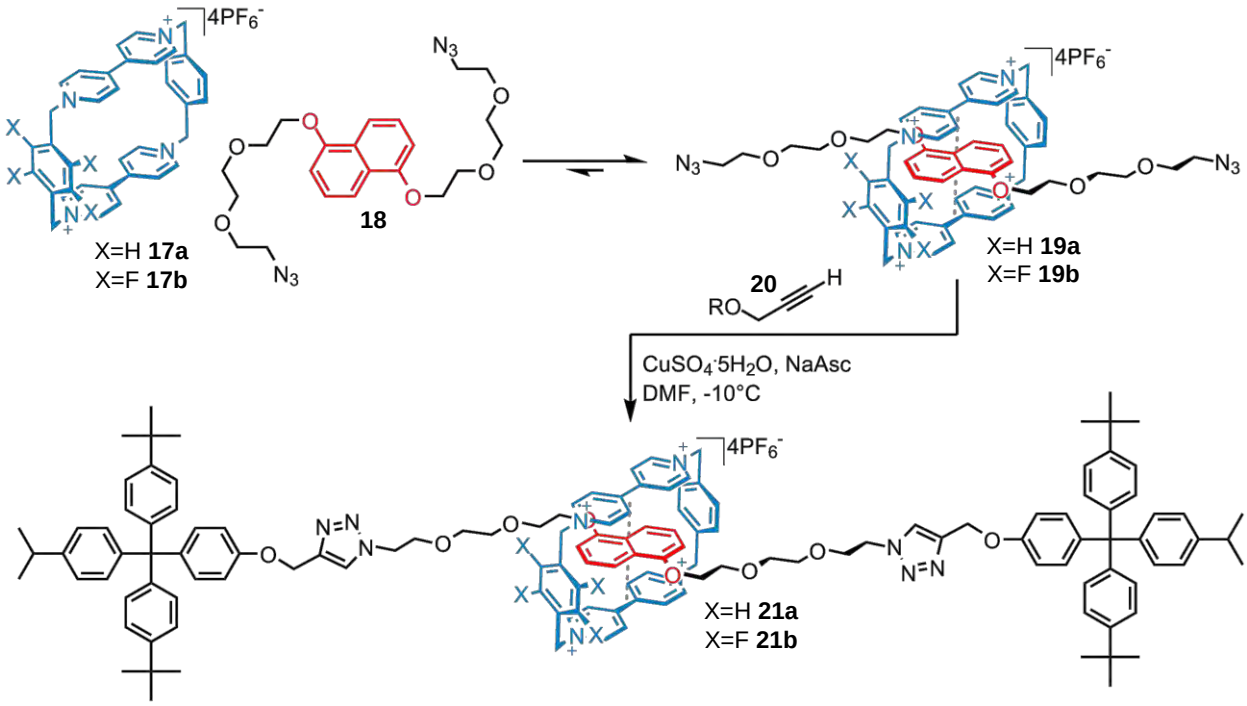

*Scheme 1.6 Synthesis of [2]rotaxanes **21a** and **21b** by the "threading-followed-by-stoppering" method via the CuAAC reaction.*

1.4.3 Hydrogen-bonding Interactions

Hydrogen bonds are much weaker than covalent bonds or those involved between a metal centre and ligands. As a consequence, effective H-bonding templates are generally made up of multi-point recognition sites. The most effective H-bonding templates are those with a high level of pre-organisation.

1.4.3.1 Amide Hydrogen-bonding Interactions

a) Anion-Based Catenanes and Rotaxanes

Vögtle and co-workers reported the first example of a [2]rotaxane assembled around an anionic phenolate template in 1999.[25] They utilised the binding of an anionic species to amides present in a macrocycle to template the formation of a [2]rotaxane in an excellent yield of 95%. The phenoxide-macrocycle complex **22** reacts with the mono-stoppered thread **23** to form the [2]rotaxane **24** as shown in Scheme 1.7.

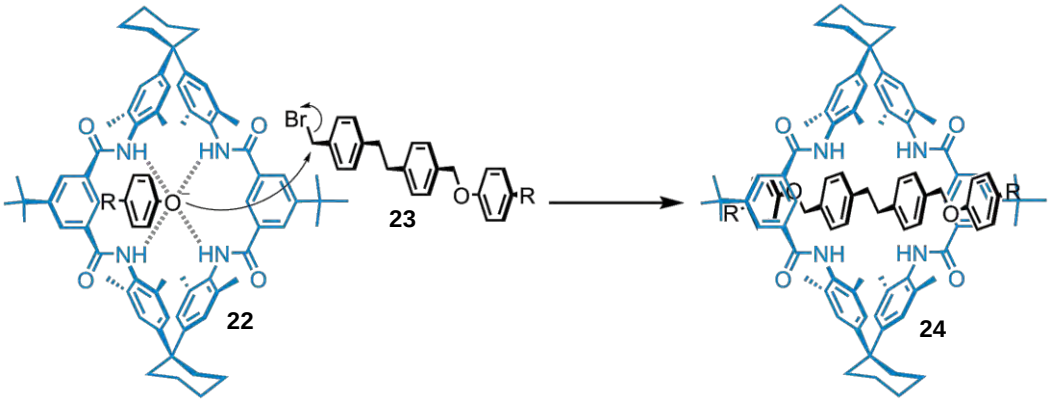

*Scheme 1.7 Synthesis of Vögtle's [2]rotaxane **24** assembled using a phenoxide template.*

More recently, Beer and co-workers have elegantly shown how chloride ion recognition motifs can be utilised to assemble rotaxanes[26] and catenanes[27] (Figure 1.3).

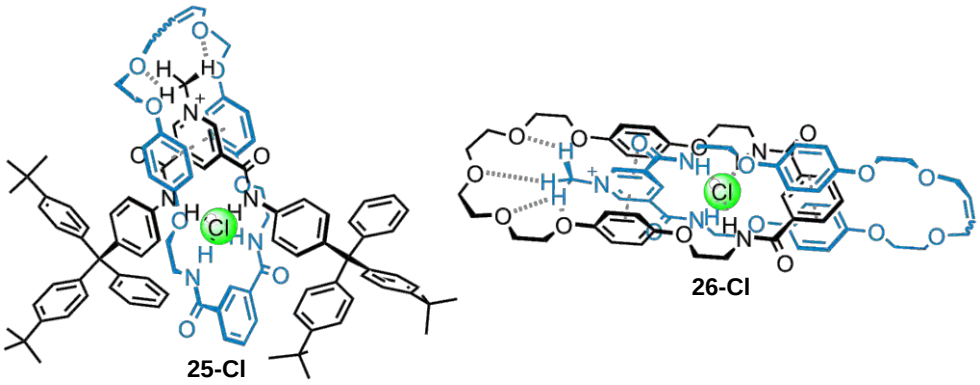

*Figure 1.3 Beer's anion templated MIAs, rotaxane **25-Cl** and catenane **26-Cl**.*

b) Amide-Based Catenanes and Rotaxanes

In an attempt to increase the yield of a macrocyclisation, Hunter discovered a one step synthesis of the first amide-based catenane **27a** in 1992.[28] This supramolecular self-assembly process, wherein multiple H-bonds direct the formation of two interlocking rings, resulted in a 34% yield of [2]catenane. The remainder of the product is a tetrameric species and the free macrocycle. This was closely followed by the publication of a very similar molecule by Vögtle **27b** (Figure 1.4).[29]

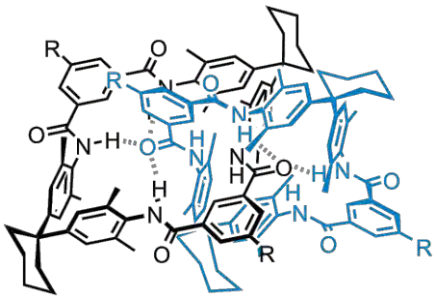

27a R=H: Hunter
27b R=OMe: Vögtle

Figure 1.4 First amide-based [2]catenane reported by Hunter (R = H) and Vögtle (R =OMe).

David Leigh published in 1995 his now-famous hydrogen bonding system to produce MIAs. He reported the synthesis of benzylic amide [2]catenane **30** in 20% yield from the reaction of isophthaloyl dichloride **28** and para-xylylenediamine **29** in dichloromethane with the presence of triethylamine at high dilution (Scheme 1.8, top).[9c] The catenane was the only product left in solution at the end of the reaction, all other products precipitated. Subsequently, it was observed that if the condensation reaction was carried out in the presence of a suitably stoppered benzylic 1,3-diamide thread, [2]rotaxanes could be easily obtained. The more rigid fumaric rotaxane **31a** was synthesized in 97% yield (Scheme 1.8, bottom). This excellent yield is due to the near-ideal spatial arrangement of the two amide carbonyl groups to template the formation of the benzylic amide macrocycle. The presence of a double bond also prevents the thread from forming intramolecular hydrogen bonds, which can disfavour the rotaxane formation. Leigh has since utilised this methodology to explore the fascinating world of molecular machinery.[30]

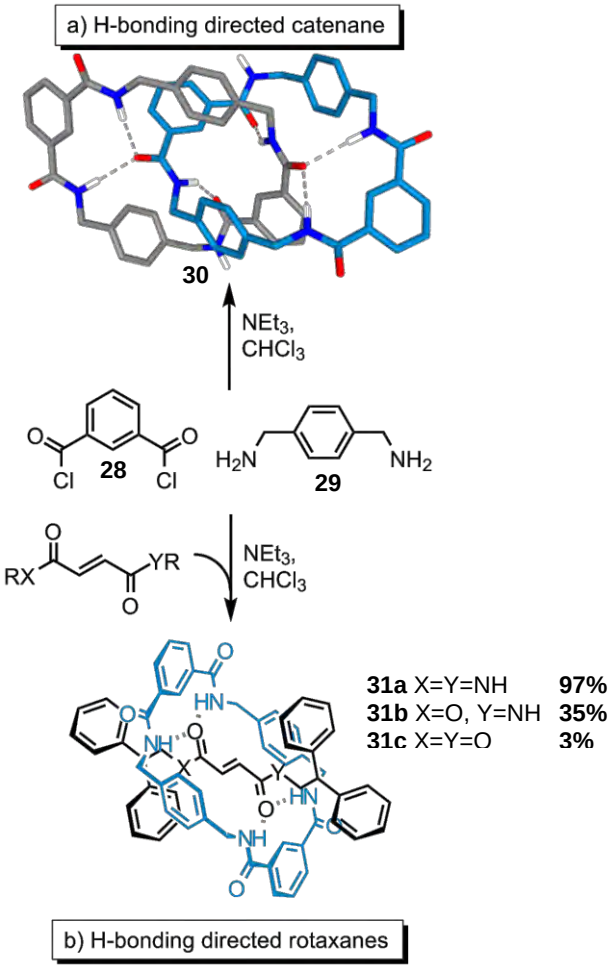

Scheme 1.8 a) Synthesis and crystal structure of the leigh-type benzylic amide [2]catenane ***30****, b) Synthesis of fumaramide-containing rotaxanes* ***31a-c****.*

1.4.3.2 *Ammonium-Crown Ether Template*

Crown ethers have also been extensively used to achieve the synthesis of rotaxanes. Hydrogen bonding between the oxygen donor atoms of the crown ether and the secondary dialkylammonium unit of the thread offer a suitable host-guest complex ready for subjection to the capping methodology.[31,32] Stoddart converted crown ether-containing *pseudo*-rotaxane **33** (Scheme 1.9), into the corresponding [2]rotaxane **34** (31% yield) by reacting it with an excess of di-*tert*-butylacetylenedicarboxylate at reflux in dichloromethane for several days.[33]

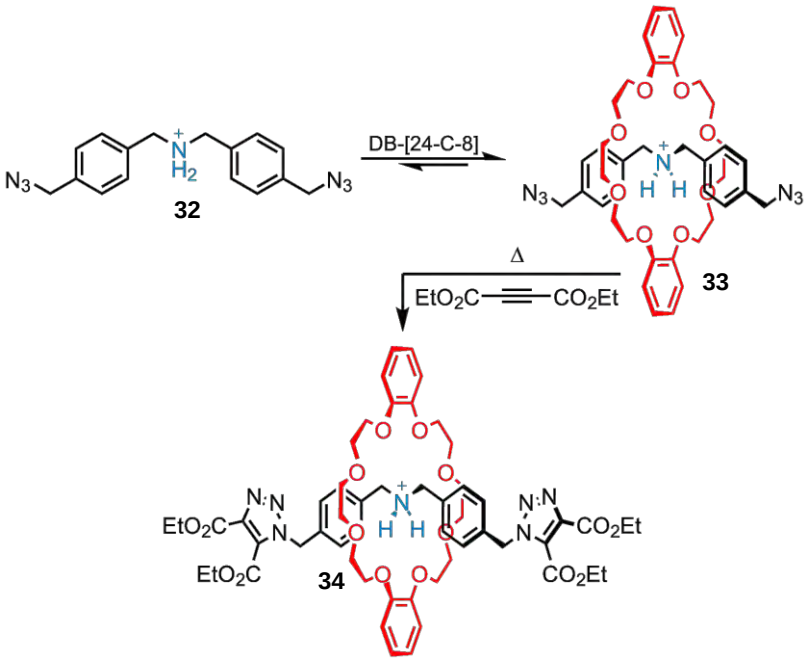

*Scheme 1.9 Stoddart's synthesis of a [2]rotaxane **34** exploiting the binding of secondary dialkyl ammonium salts by crown ethers.*

1.5 Transition Metal Template for the Preparation of MIAs

As suggested above, the work published by Sauvage in 1983 marked a new area in the preparation of MIAs. Sauvage took advantage of the transition metal's ability to predispose ligands in a predictable spatial orientation, creating a cross-over point that directs subsequent macrocyclisation or capping reactions towards the threaded architectures. To date, most of these routes depend on the use of neutral or cationic species to achieve the desired template effect.

1.5.1 Passive Template

Since the synthesis of the first metal template catenanes and rotaxanes, a wide range of metals with preferences for different coordination geometries have been used with numerous ligands to template the formation of interlocked architectures. Examples shown in Figure 1.5 employing a) linear,[34] b) tetrahedral,[7] c) square planar,[35] d) octahedral[36,37,38] and e) trigonal bipyramidal or square pyramidal[39] geometries will be detailed further in this chapter.

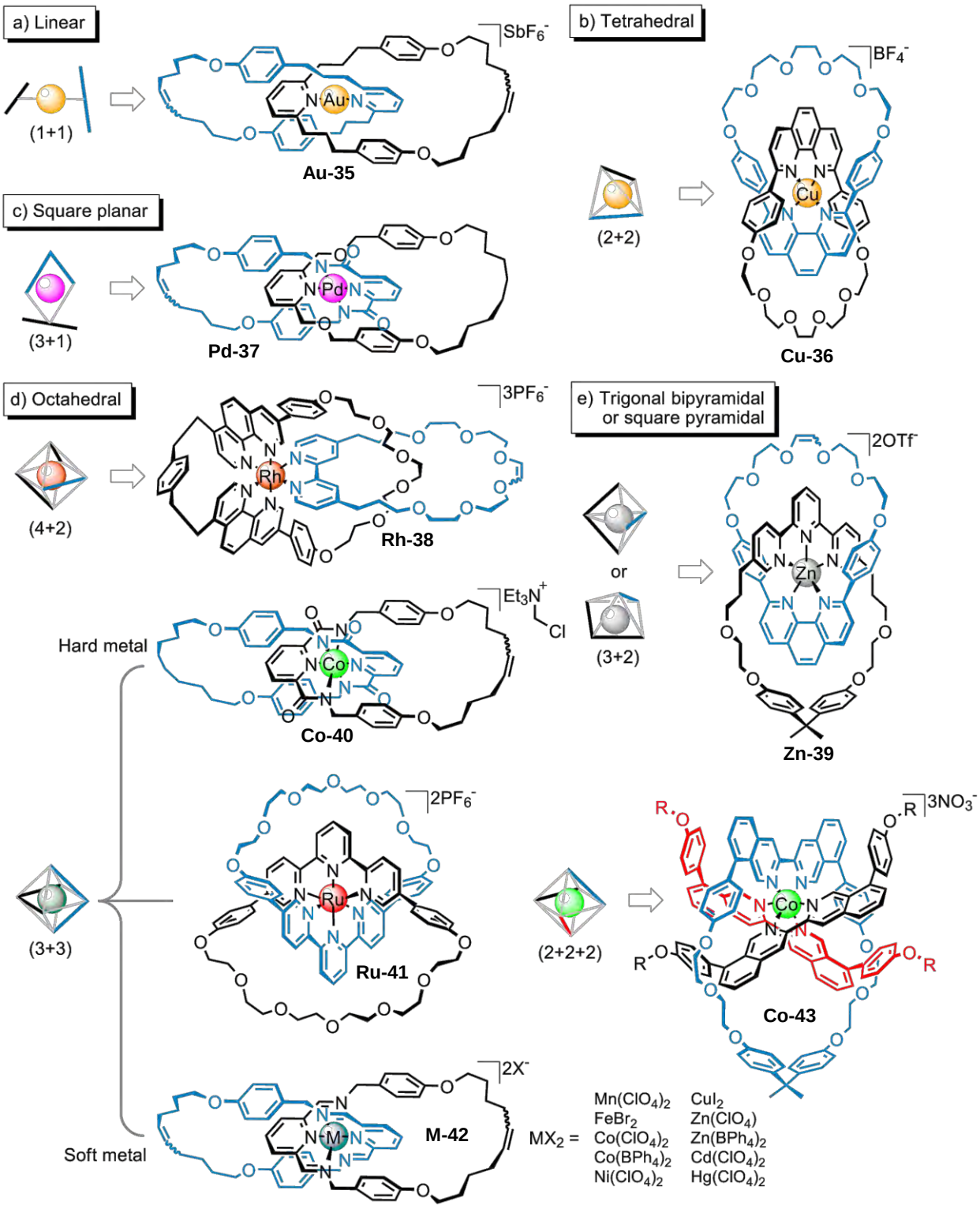

Figure 1.5 Examples of metal geometries used in a classic passive-metal template strategy towards the synthesis of MIAs. Interlocked architectures are shown before hydrogenation.

1.5.1.1 *Linear (1+1) Template*

The achievement of a linear (1+1) template was reported by Leigh and co-worker in 2008.[34] The authors exploited the linear geometry of a gold(I) metal centre to achieve the preparation of the [2]catenane **45** in 26% yield. Coordination of two pyridine acyclic moieties around the Au(I) ion gave the pre-arranged complex **44**. Conversion to the corresponding catenane was achieved by subjecting **44** to ring closing metathesis conditions followed by hydrogenation of the newly formed double bond.

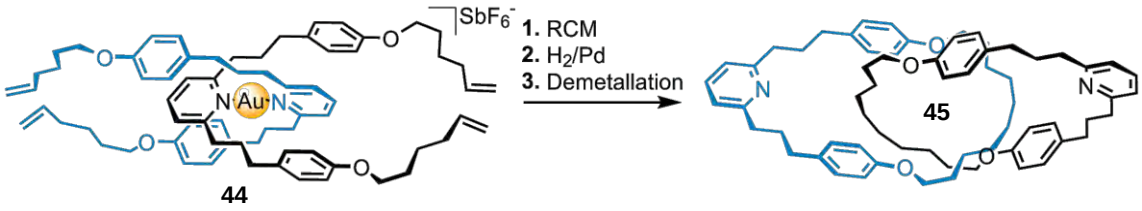

*Scheme 1.10 Gold(I) templated synthesis of catenane **45**.*

1.5.1.2 *Tetrahedral (2+2) TM Geometry*

Jean-Pierre Sauvage employed the preferred tetrahedral geometry of Cu(I) to organise two bidentate phenanthroline (phen)-containing ligands in a mutually orthogonal manner (Scheme 1.11, Route A).[7a] The copper-containing *pseudo*-rotaxane **47** is obtained by subjecting pre-made macrocycle **46** with Cu(I) and acyclic phen ligand **48**. Alkylation of **47** with *bis*alkyl-iodide gives metal-catenane (or catenate) **Cu-50** in 40% yield. The complementary Route B (Scheme 1.11) was achieved one year later.[7b] The alkylation of Cu(I)-complex **49** with a *bis*alkyl-iodide led to catenate **Cu-50** in 27% yield. Free catenand **50** (indicating a catenane which has been assembled using a metal template) can be obtained by removing the copper template by treatment with KCN.

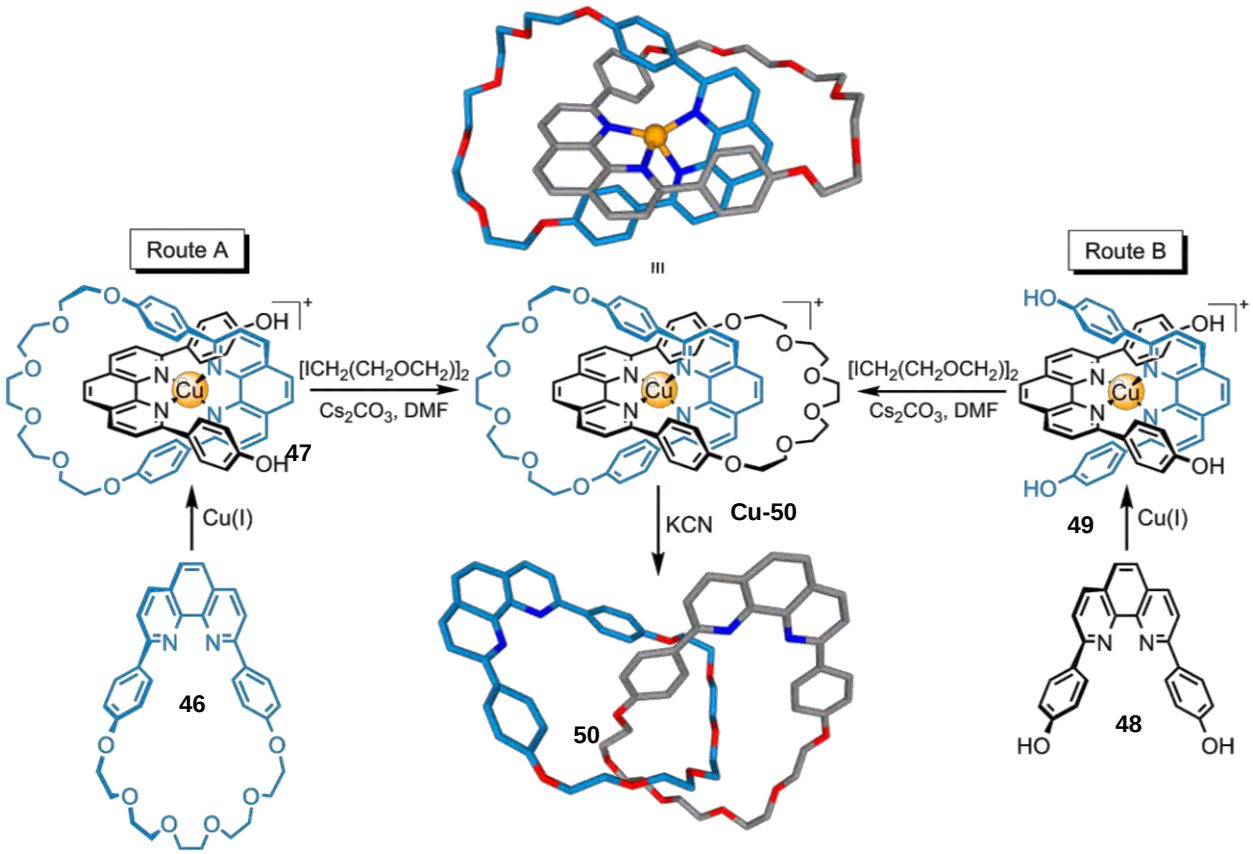

*Scheme 1.11 Sauvage's phen-Cu(I) directed strategies for the synthesis of [2]catenane **50**.*

Surprisingly, it was not until 1991 - eight years after Sauvage's original paper on the Cu(I)-phenanthroline motif - that the first preparation of a [2]rotaxane using that methodology was achieved by Gibson and co-workers. They demonstrated that Sauvage's *pseudo*-rotaxane **49** could be alkylated with two bulky stoppered units to generate (after decomplexation with a cyanide-derivatised resin) metal-free rotaxane **51** in 42% yield.

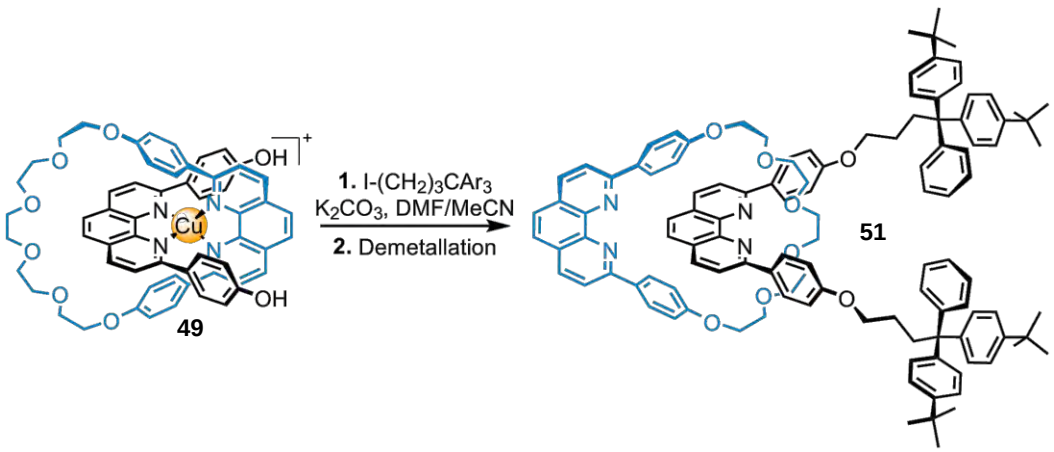

*Scheme 1.12 Synthesis of rotaxane **51** via transition metal coordination.*

By incorporating a terpyridine (terpy) unit in one of their phenanthroline-containing catenane, Sauvage and co-workers were able to realise a molecular switch based on the redox chemistry of copper.[40] In the lower oxidation state of the copper (Scheme 1.13, left, **Cu^{I}-52**), the two phenanthroline (phen) moieties are coordinatied to the metal centre in a tetrahedral geometry. Positional isomerisation was achieved by oxidation of the Cu(I) into Cu(II) allowing the terpy and the phenanthroline ligands to be hold in a trigonal bipyramidal manner (Scheme 1.13, right, **Cu^{II}-52**). The reverse process is achieved under reducing conditions.

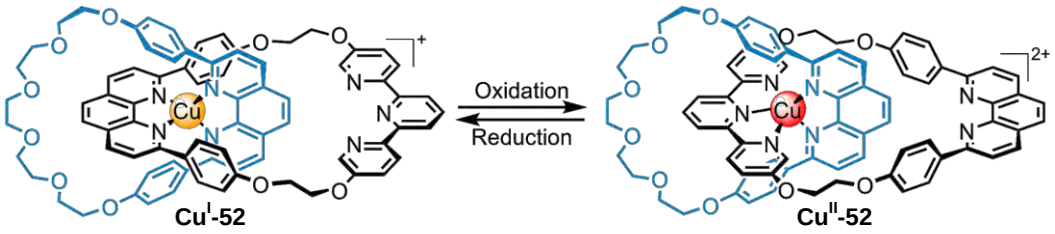

Scheme 1.13 Positional control between the tetradentate (phen-phen) and the pentadentate (terpy-phen) coordination modes.

A few years later, Sauvage accomplished the synthesis of a switchable molecular shuttle using the same Cu(I)/Cu(II) chemistry in which the Cu-phen-macrocycle complex is displaced between a terpy and a phenanthroline station.[41]

Combining the Cu(I)-phenanthroline motif with the CuAAC reaction, Sauvage and co-workers published recently the preparation of a "clicked" Cu(I)-rotaxane complex.[42] Subjecting diazide functionalised *pseudo*-rotaxane **54** to standard Cu-catalysed alkyne azide cycloaddition (CuAAC) provided Cu(I)-rotaxane complex **Cu-56** in 62% yield.

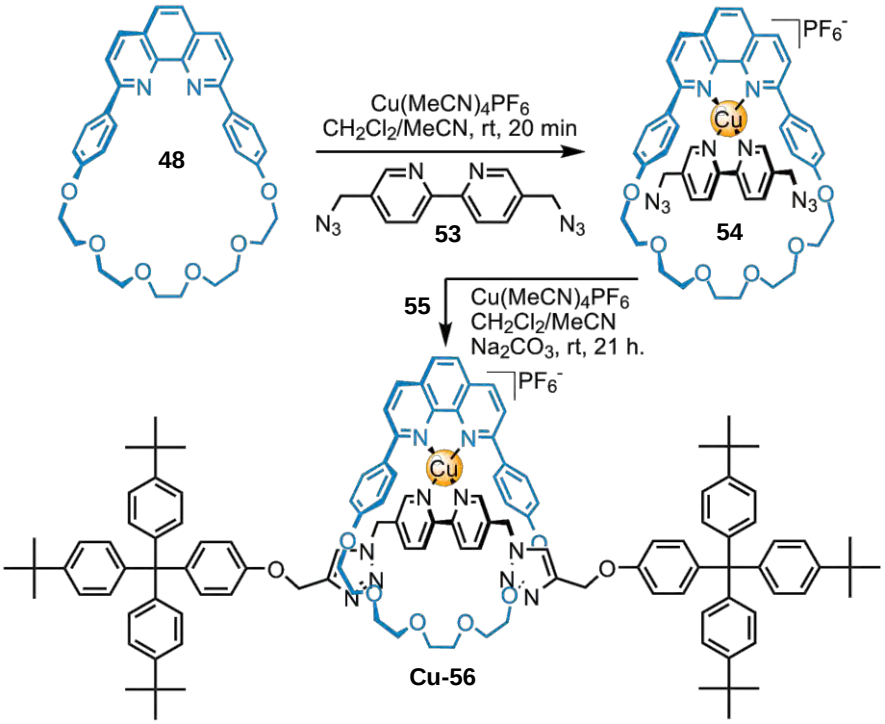

Scheme 1.14 Passive-metal template synthesis of the Cu(I)-[2]rotaxane 22.

Replacing the diazido-bipyridyl thread **53** by a more hindered phenanthroline-based thread showed more stability under the CuAAC stoppering conditions and yielded the corresponding Cu(I)-rotaxane complex in 67%.[43]

1.5.1.3 Square planar (3+1) Pd Geometry

One year after Sauvage's first example utilizing a palladium square planar (3+1) strategy towards the synthesis of a Pd-*pseudo*-rotaxane complex,[44] Leigh and co-workers published in 2004 the preparation of a [2]rotaxane using a palladium square planar (SP) template.[35] The clipping strategy involved the exchange of the labile acetonitrile molecule in 2,6-dicarboxamide-pyridine-Pd complex **Pd-58** by the monodentate 2,6-disubstitued pyridine thread **57**. The pre-rotaxane obtained was stable enough to be isolated in 63% yield. RCM followed by hydrogenation gave **Pd-61** (77%) which could then be demetallated by KCN to afford the metal-free rotaxane in 97% yield (Scheme 1.15, bottom). The Leigh group extended the methodology to the preparation of [2]catenanes.[45] Catenate **Pd-60** is obtained in 78% yield from the assembly of **Pd-58** and pyridine macrocyclic ligands **59** around a Pd template followed by RCM and hydrogenation (Scheme 1.15, top).

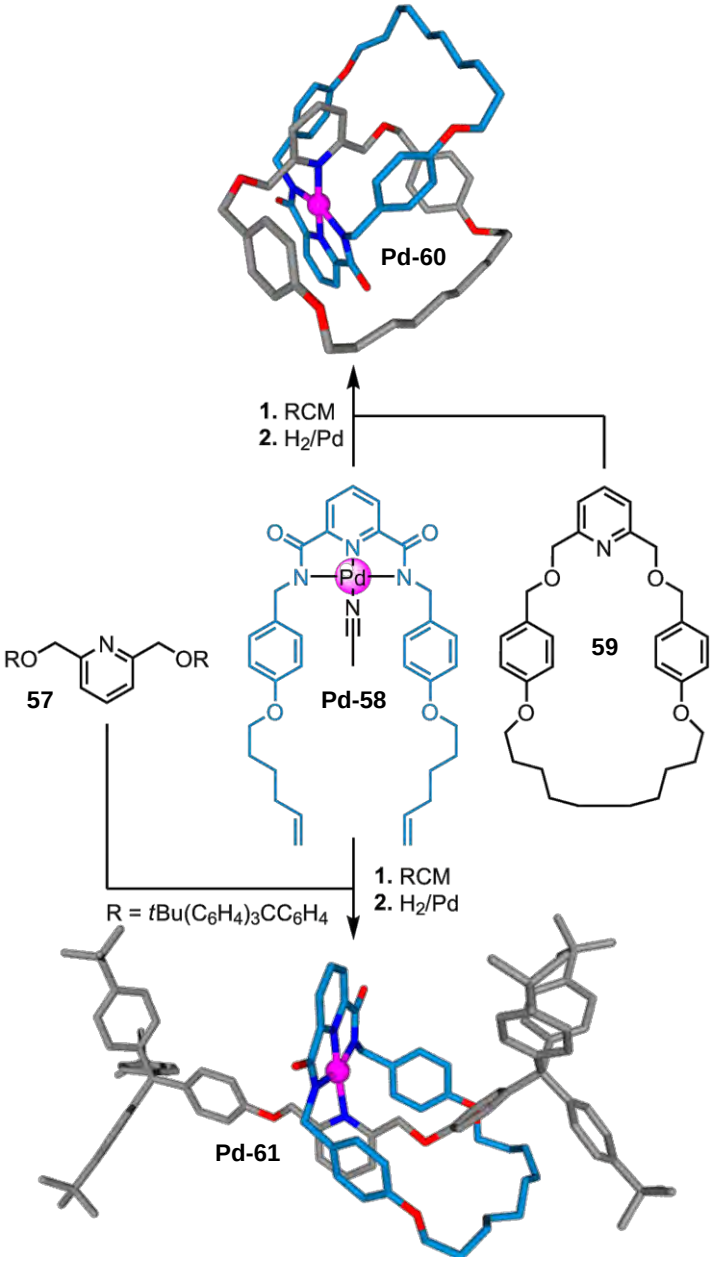

Scheme 1.15 Synthesis of a square-planar metal coordinated [2]rotaxane.

This successful Pd (3+1) methodology was extensively used to achieve the synthesis of various MIAs. Takata and Hirano reported the synthesis of rotaxanes using similar ligands but in a capping method.[46] David Leigh published an easy and efficient protocol towards the iterative synthesis of [n]rotaxanes: A pyridine unit (not centred on the thread) is used as handle to introduce sequentially Pd-U-shape complexes on the thread. The authors used the following cycle to proceed: complexation of **Pd-58** on the thread *via* the pyridine unit; RCM; hydrogenation and demetallation. After the first cycle a [2]rotaxane was obtained and subsequently the second cycle gave [3]rotaxane

62, the third cycle yielded [4]rotaxane **63** (see Scheme 1.16 for the last step). The only limiting factor in the synthesis of higher order rotaxane is the length of the thread used.

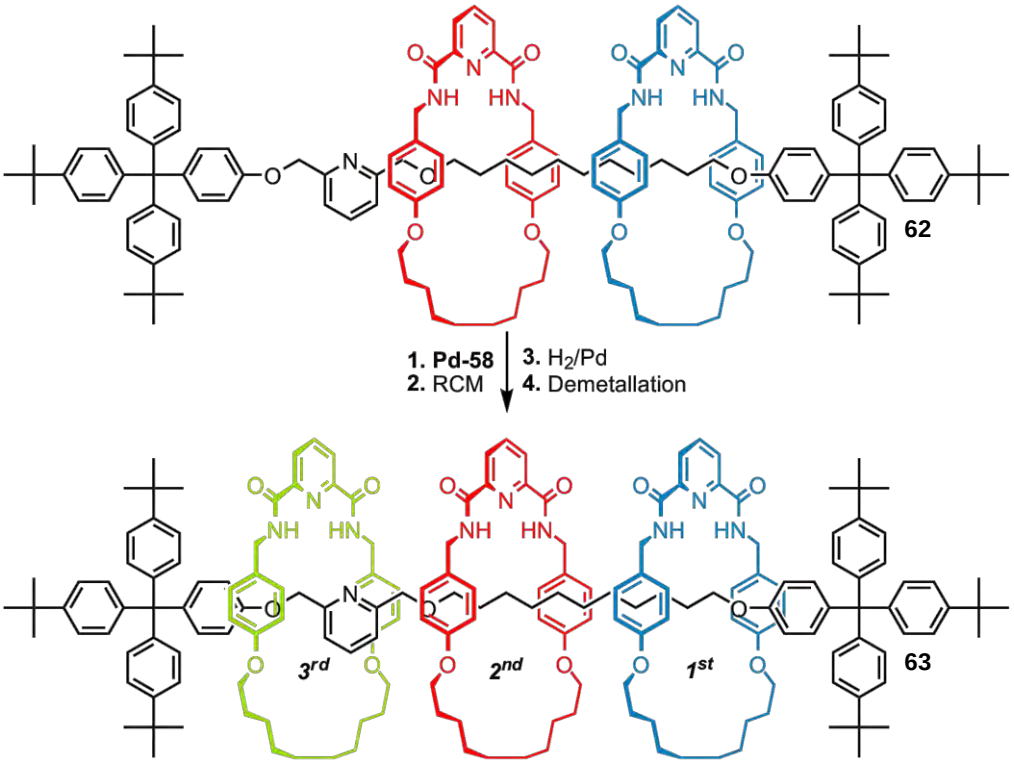

*Scheme 1.16 Iterative synthesis of [4]rotaxane **63** using a Pd-SP template.*

1.5.1.4 *Trigonal-bipyramidal (3+2) Geometry*

The first example of an interlocked architecture obtained by a (3+2) passive template strategy was reported by Sauvage and collaborators in 2003.[39] The Alsatian group combined divalent zinc ion with bidentate and tridentate ligands. The coordination of zinc trifluoromethanesulfonate into a terpy-based macrocycle followed by the replacement of the triflates ligands by a phen U-shaped ligand formed penta-coordinated Zn-*pseudo*-rotaxane complex **66**. Subjecting this complex to RCM conditions followed by hydrogenation led to corresponding [2]catenand **Zn-67**. Decomplexation by stirring a solution of this catenand in a CH_2Cl_2 with an aqueous base afforded the metal-free catenane in 40% yield over the 3 last steps.

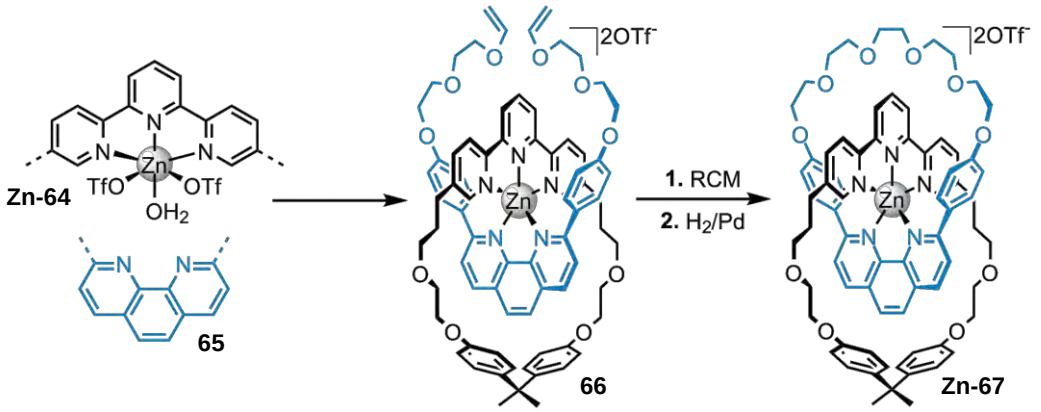

*Scheme 1.17 Synthesis of five coordinate Zn(II) catenate **Zn-67**.*

1.5.1.5 Octahedral (3+3) TM Geometry

The first example of a MIA assembled via an octahedral metal centre was reported by Sauvage in 1991.[47] He used a (3+3) strategy wherein a Ru(II) ion holds two terpy ligands in an orthogonal manner. Cyclisation by Williamson alkylation provided the Ru-catenane **Ru-70** in a moderate yield of 11%. Unfortunatelly, due to the stability of the complex, demetallation has proven to be impossible. Later, Siegel and co-workers developped strategies using Fe(II) and Ru(II) towards the prepartation of (3+3) catenanes.[48]

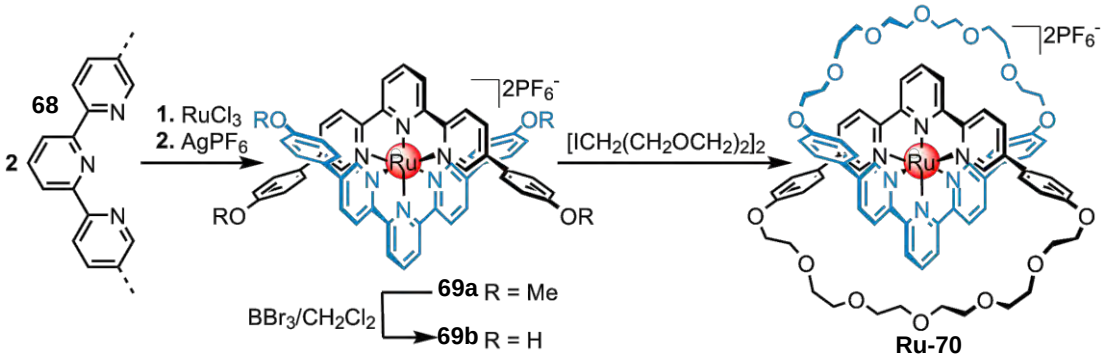

*Scheme 1.18 Octahedral (3+3) template synthesis of catenate **Ru^{II}-70** using Williamson macrocyclization.*

In 2001, Leigh and co-workers reported a simple, general and efficient protocol for the preparation of catenanes around a wide range of divalent octahedral TM ions (Figure 1.5).[36] The ligating moieties are based on tridentate benzylic 2,6-di-iminopyridine and two distinct strategies can be applied towards the preparation of catenanes. The first approach consists of treating the metal-di-iminopyridine complexes of type **74** with Grubb's catalyst to afford catenates in good yield (Scheme 1.19, Route A). As example, Zinc perchlorate complex **Zn-74** was readily prepared in 83% yield from simple

addition of a solution of ligand **71** in dichloromethane to a methanolic solution of $Zn(ClO_4)_2(H_2O)_6$. Free imines are not normally compatible with RCM conditions but, in this case, coordination to the TM ion effectively protects the sensitive functionality allowing Grubbs' catalyst to mediate the clean conversion of the tetra-olefin complex to the zinc catenate in 73% yield. The tolerance of this approach was investigated using a wide range of divalent TM ions with a octahedral geometric preference (i.e Mn(II)-Zn(II) across the 1st row and Zn(II)-Hg(II) down to group 12) and catenanes were isolated in each case. The highly preorganised *bis*-tridentate ligand system introduces high kinetic stability to the interlocked complexes. Demetallation was achieved by reduction of the imine functionalities with $NaBH_4$ followed by treatment with Na_2H_2EDTA to give the metal-free catenand **76**. Since this publication, the Leigh group has extended this (3+3) strategy: they took advantage of the thermodynamical stability of metal-complexes **M-75** to achieve a five component self-assembly process around a divalent octahedral TM template (Scheme 1.19, Route B) and they used tridentate pyridine-diamide ligands around a hard trivalent metal ion such as Co(III) (Figure 1.5, **Co-40**) to achieve the synthesis of a [2]catenane.[49]

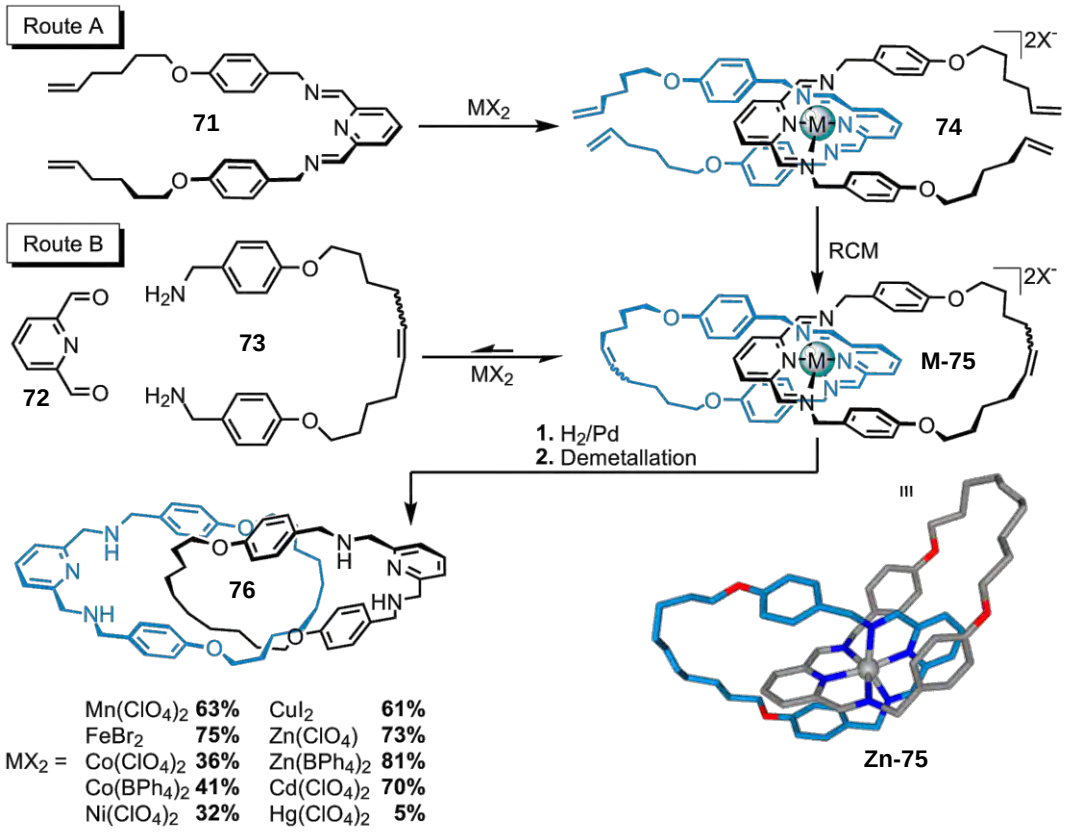

*Scheme 1.19 Synthesis of octahedral catenates (**M-75**) by ring closing metathesis, using a large range of divalent TM (Mn-Zn, Cd-Hg).*

1.5.1.6 Octahedral (3+2+1) Template Strategy

Although Seeman and co-workers achieved the synthesis of Borromean rings (BRs) using DNA strands,[50] the chemical assembly of molecular BRs was first realised in 2004 by Stoddart and co-workers. Using computer-aided design to optimise the π-π stacking interactions and coordination geometries, the Californian group achieved the self-assembly of BRs from 18 building blocks, arguably one of the most impressive thermodynamically controlled multi-component reactions described to date.[51] This spectacular synthesis was performed utilising the reversible nature of imine bonds. The [2+2] macrocyclisation reaction between the 2,6-diformylpyridine unit **72** and the bipyridyl-containing diamine **77**, produced the *endo*-tridentate diiminopyridyl binding site. Addition of $Zn(OAc)_2$ directed the formation of BRs by binding the exo-bidentate and endo-tridentate ligands in a slightly distorted octahedral geometry. By following the reaction by ^1H NMR, it was observed that after two days the major (>90%) product was the desired Borromean rings complex **Zn_6-78**. This was confirmed by X-ray crystal structure determination shown in Scheme 1.20, top (sixth coordination site have been removed for clarity). The authors proved later that zinc could be replaced by copper (II) to yield the corresponding BR's (**Cu_6-78**). Interestingly, when they used a mixed Zn/Cu 1:1 template, the formation of a Solomon knot (a doubly entwined catenane) was observed (Scheme 1.20, bottom, **Zn_2Cu_2-79**). Although various molecular species compete with each other in solution, the Solomon's knot is formed over the other species (notably BRs) owing to a favourable crystal packing effect (dynamic kinetic resolution).[52]

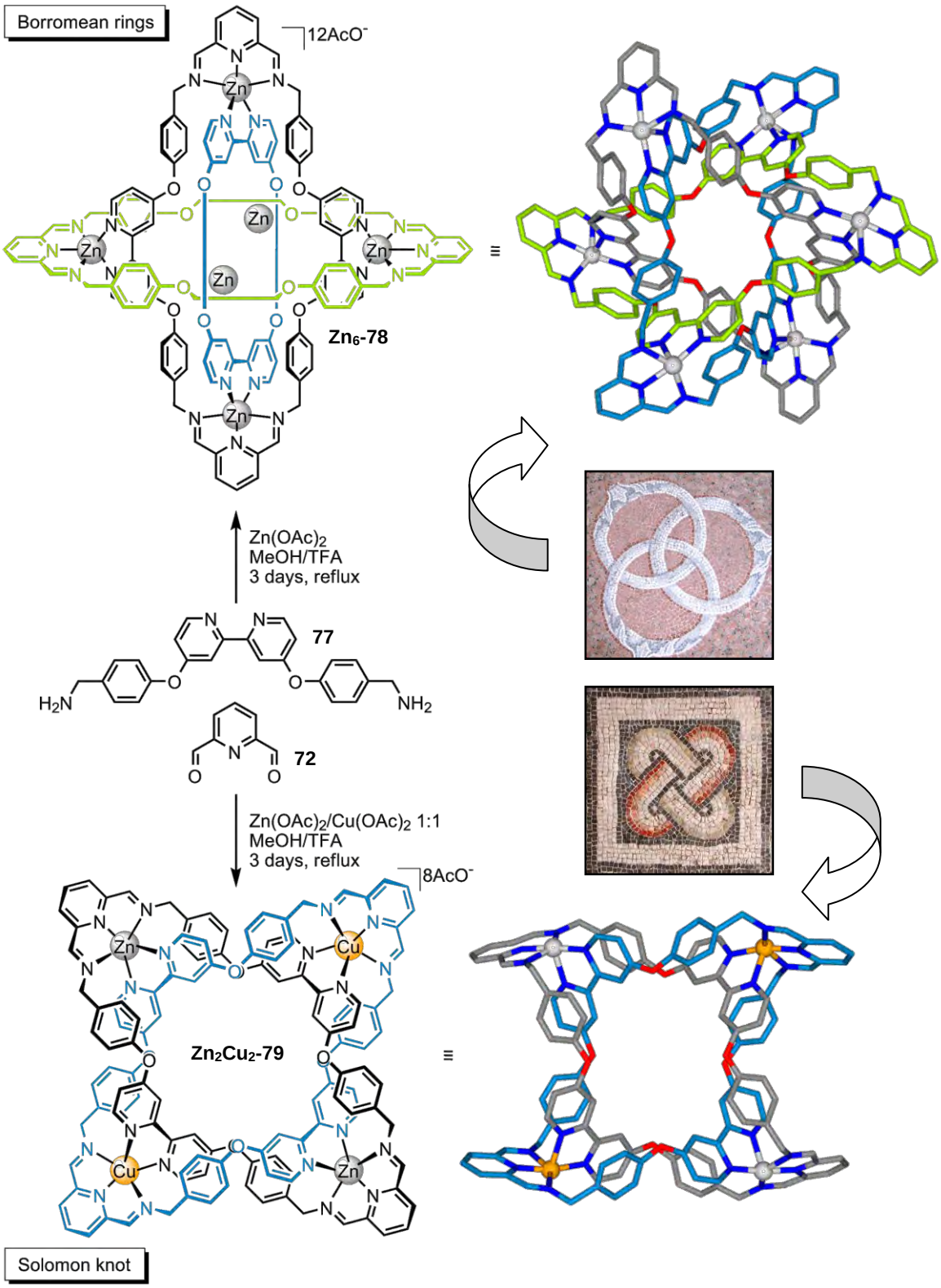

Scheme 1.20 Impressive achievements of complex interlocked structures via Zn(II) and Cu(II) template using imine reversible bond. Top: molecular borromean rings and bottom: Solomon knot.

1.5.1.7 *Octahedral (4+2) Template Strategy*

Jean-Pierre Sauvage, once again, proved his expertise in the introduction of novel strategies towards the preparation of MIAs utilising transition metals and noteworthy ligands. Sauvage's research group introduced a (4+2) octahedral template,[53] complex **Ru-80**, which is obtained by coordination of the tetradentate (two phen units) macrocycle around a divalent ruthenium centre. Replacement of the two acetonitriles by a bipy U-shaped ligand afforded the Ru-pre-catenane complex **82** which can be converted into the corresponding Ru-catenate **Ru-83** (68% yield) by subsequent RCM followed by hydrogenation (Scheme 1.21).

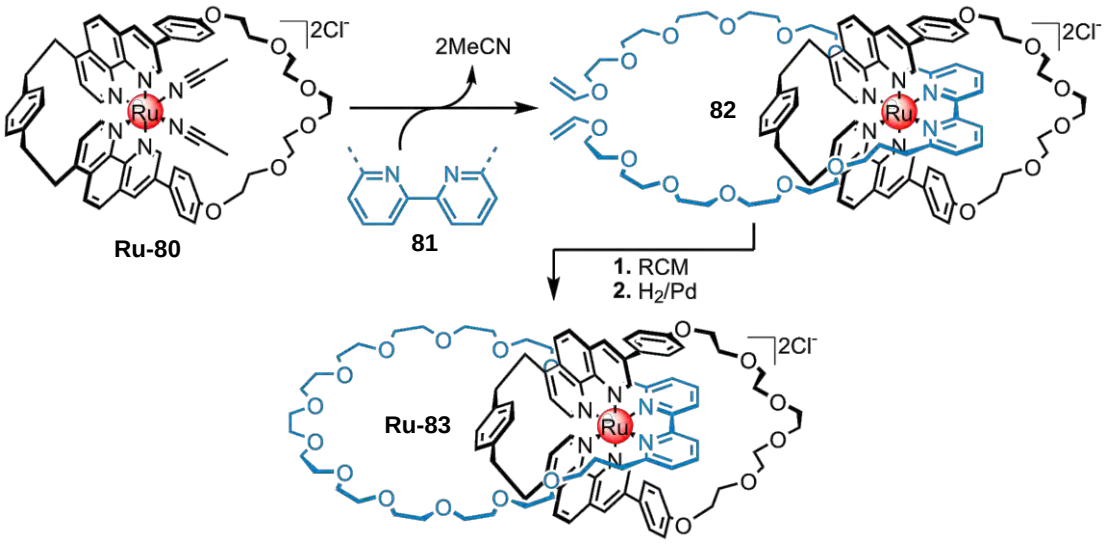

*Scheme 1.21 Synthesis of complex **Ru-83** with the (4+2) strategy.*

Sauvage's research group investigated the possibility of using of a double macrocyclisation technique to prepare **Ru-83** (46%).[54] Structural modifications of both macrocyclic and the acyclic ligands were proved to be possible: modifications of the macrocycle poly-ether backbone increased the yield (76%)[55] and the use of a 4,4'-disubstitued bipy ligand afforded a catenane in which the RCM occurred around the poly-ether thread and not around the metal coordination core, this example used a Rh(III) metal centre as shown in Figure 1.5 (34% yield, **Rh-38**).[56] In contrast with the previous Ru-(3+3)-octahedral methodology applied (Paragraph 1.5.1.5), where demetallation is impossible due to the high stability of the ruthenium complex, the lability of the Ru-bipy can be achieved by irradiating (UV) the complex in presence of chloride ions. Unfortunately, the methodology showed a lack of success when second-row TM such as Zn(II) or Fe(II) were used as template. This methodology was also extended for the preparation of [2]rotaxanes.[57]

1.5.1.8 Octahedral (2+2+2) TM Strategy

After the success of his (4+2) octahedral strategy, Sauvage explored a novel octahedral (2+2+2) methodology in which the assembly of three distinct bidentate ligands is achieved around a same transition metal centre. *Bis*-isoquinoline ligands were preferred, as phen or bipy are less encumbered and allow for a less sterically congested metal coordination site. Triply entwined complexes, such as **86** were generated *via* an octahedral (2+2+2) strategy with three bidentate ligands such as **84a** (R = Me) around a divalent ruthenium ion.[58] The solid structure of **86** revealed an intriguing entwinement around the metal ion which was later exploited by Sauvage's group to create interlocked architectures such as the impressive [3]rotaxane shown in Scheme 1.22.[59] Two *bis*-isoquinoline rods decorated at each end with azide functionalities (**84b**) were threaded into the cavity of macrocycle **85** to generate metal-complexes **M-87** (M = Fe(II) or Co(III)). Stoppering with bulky alkyne-stoppered unit **55** was realised *via* CuAAC reaction to afford **Fe^{II}-88** and **Co^{III}-88** in very high yields (82% and 89% yield respectively). The iron(II) complex showed an extreme stability over standard demetallation conditions (H_2O/MeOH 1:1, Na_3HEDTA, rt), while attempts to use harsher conditions (Cs_2CO_3, DMF, 80 °C) resulted in the concerted dethreading of the two stoppered threads through the cavity. The metal-free [3]rotaxane was achieved by replacing iron(II) with cobalt(III).[60] Owing to the kinetic stability of **Co^{III}-88** - and because it is paramagnetic – the study and characterisation of this complex is possible by ^{1}H NMR. Oxidation of Co(III) into labile Co(II) complex made the decomplexation quick and efficient (DMSO, Na_3HEDTA) affording the metal-free [3]rotaxane **88** in a quantitative yield. The dethreading process of **88** was followed by ^{1}H NMR and its half-life was determined to be one week in CH_2Cl_2 at room temperature.

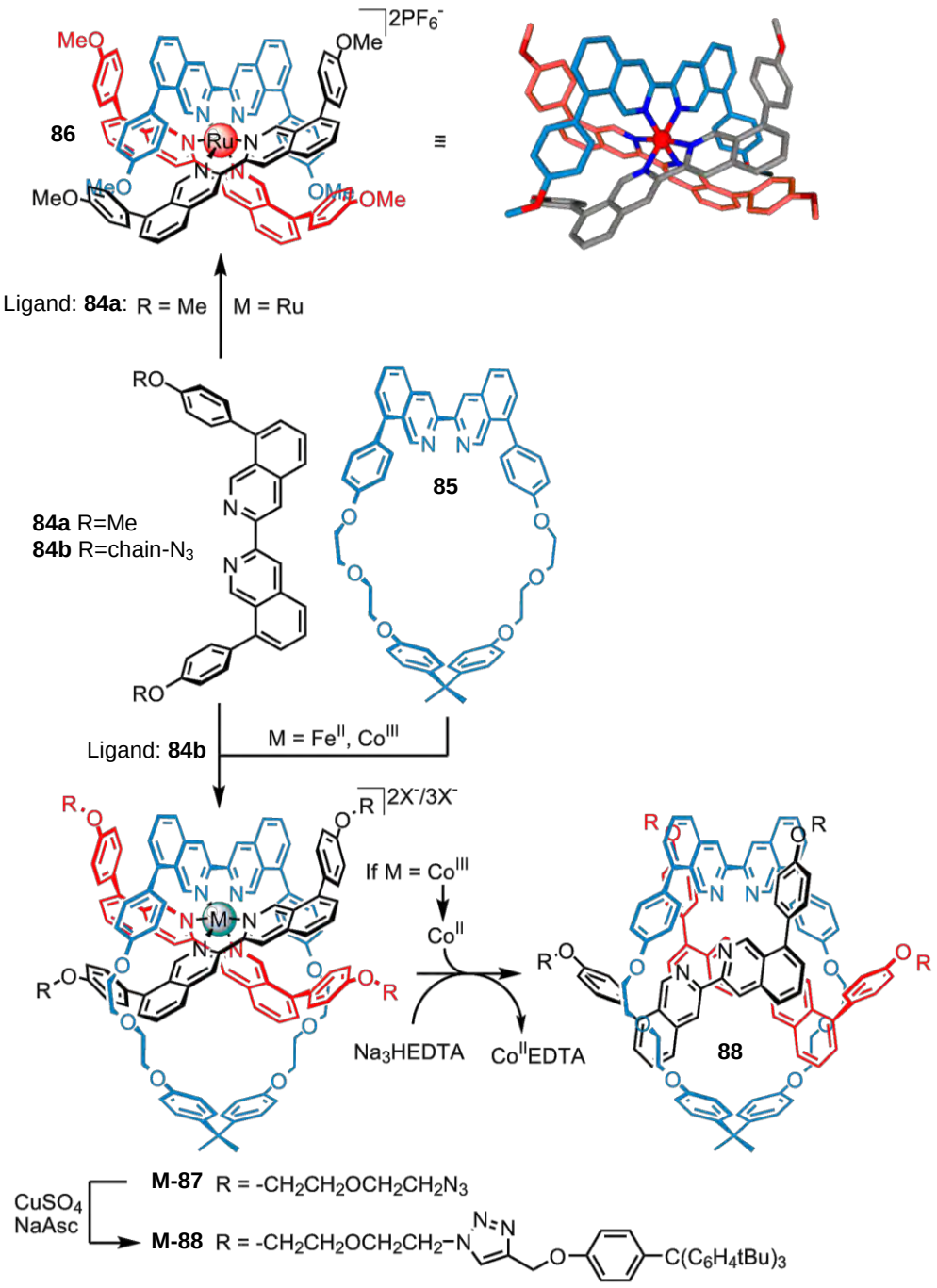

*Scheme 1.22 (2+2+2) Octahedral strategy to the preparation of complex **86**, pre-rotaxanes **Fe^{II}-87** and **Co^{III}-87**, and [3]rotaxane **88**.*

1.5.2 Interlocked Architectures Containing Metal Ions in Their Framework

The rich variation in properties of TMs and alkali metals has led to an exotic selection of [2]catenanes containing metal ions in their structure being reported in the literature. The relationship between the complexes, other than their obvious topological congruity, is their thermodynamically controlled assembly. It has been demonstrated

that a cyclic structure containing reversible coordination bonds can reorganise to form a stable interpenetrated TM complex. The energetic gain in stability through intercomponent recognition outweighs the entropic cost of unifying the two species.

1.5.2.1 Pd-containing Catenanes

This field of research is dominated by the work of Fujita[61,62,63] who, in 1994, reported a Pd(II) containing [2]catenane accessed *via* the quantitative self-assembly of simple component molecules.[64] By mixing $Pd(NO_3)_2(en)$ with 1,4-*bis*[(4-pyridyl)-methyl]benzene **90a** in aqueous solution, macrocycle **92a** and corresponding [2]catenane **93a** were shown to be in rapid equilibrium with one another (Scheme 1.23). Consequently, by Le Chatelier's Principle, at concentrations of greater than 50 mM, the reaction conditions favour the single component [2]catenane species **93a**. It has been suggested that the [2]catenane spontaneously forms as a result of double molecular recognition, i.e. the molecules bind each other in their respective hydrophobic cavities. By increasing the polarity of the reaction medium through addition of $NaNO_3$, the yield of [2]catenane **93a** was increased to greater than 99% even at high dilution, which supports this hypothesis.

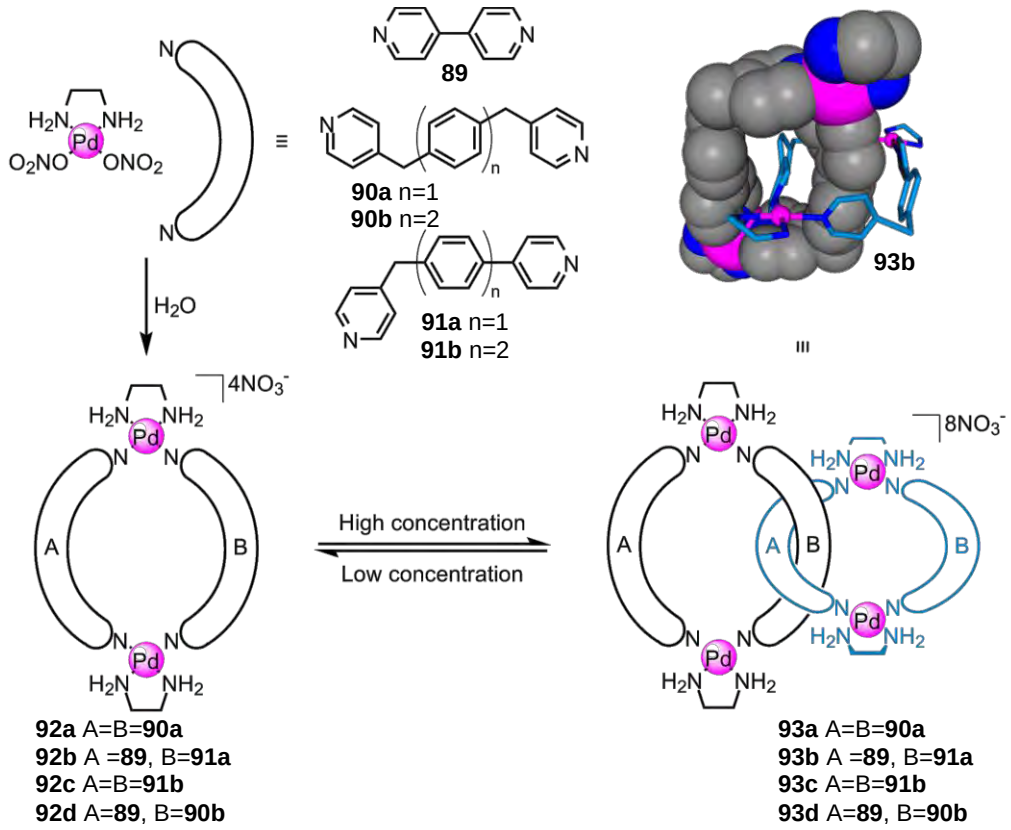

Scheme 1.23 Fujita's original Pd(II) catenane synthesis.

1.5.2.2 *Mixed Cu(II)/Cu(III) Dithiocarbamate Catenane*

Beer described the synthesis of serendipitous mixed Cu(II)/Cu(III) interlocked systems.[65] The preformed dinuclear copper(II) dithiocarbamate macrocycle **94** was submitted to oxidation to afford tetra metal-containing catenane **95** in quantitative yield. Characterisation techniques (i.e. structural, magnetic susceptibility, ESI-MS and electrochemical studies) all support the mixed cationic nature of **95** (i.e. $Cu^{II}Cu^{III}Cu^{II}Cu^{III}$). The authors later published a protocol in which copper(III) is replaced by gold(III).[66]

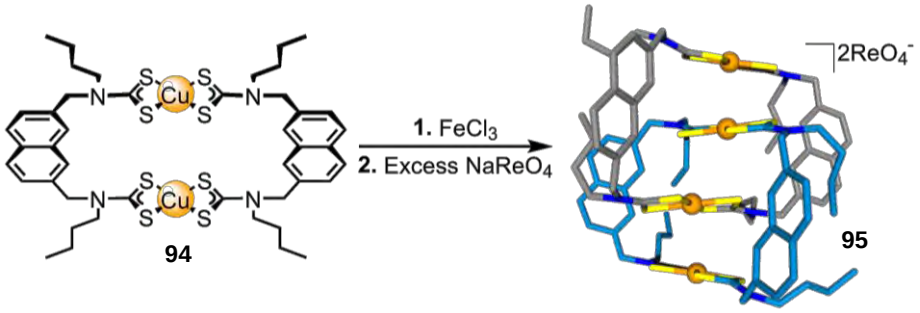

*Scheme 1.24 Dicationic Cu(II)/Cu(III)-containing catenane **95**.*

1.5.2.3 *Assemblies via First- and Second-sphere Coordination Palladium*

Following the work of Chang and Jeong, wherein they clipped a hydrogen-bond based macrocycle around a thread using a Re(I) metal centre,[67] the Wisner research group recently investigated the preparation of self-assembly though first- and second- sphere coordination. Here, the palladium metal centre acts as both as a template and as a "covalent" link between the components of the interlocked architecture. In 2006, they published a very facile protocol towards the preparation of [2]rotaxanes.[68] Coordination of *trans-bis*benzonitrile palladium(II) dichloride inside the cavity of the tetra-amide macrocycle is driven *via* hydrogen-bonding; further replacement of the two labile nitrile ligands by stronger-coordinating pyridine moieties gave the Pd-containing rotaxane **96** in 89% yield (Figure 1.6, top). The authors later extended this methodology replacing halides by thiocyanate ligands.[69] The unexpected unsymmetrical geometry of the obtained rotaxane (coordination of the thiocyanate ligands to the Pd centre *via* the nitrogen atoms) suggests that the SCN moieties act as a ratchet between two degenerated stations; this hypothesis was supported by variable temperature ^{1}H-NMR experiments. A similar double-clipping strategy was utilised to achieve the preparation of [2]catenane **97** (Figure 1.6, bottom).[70]

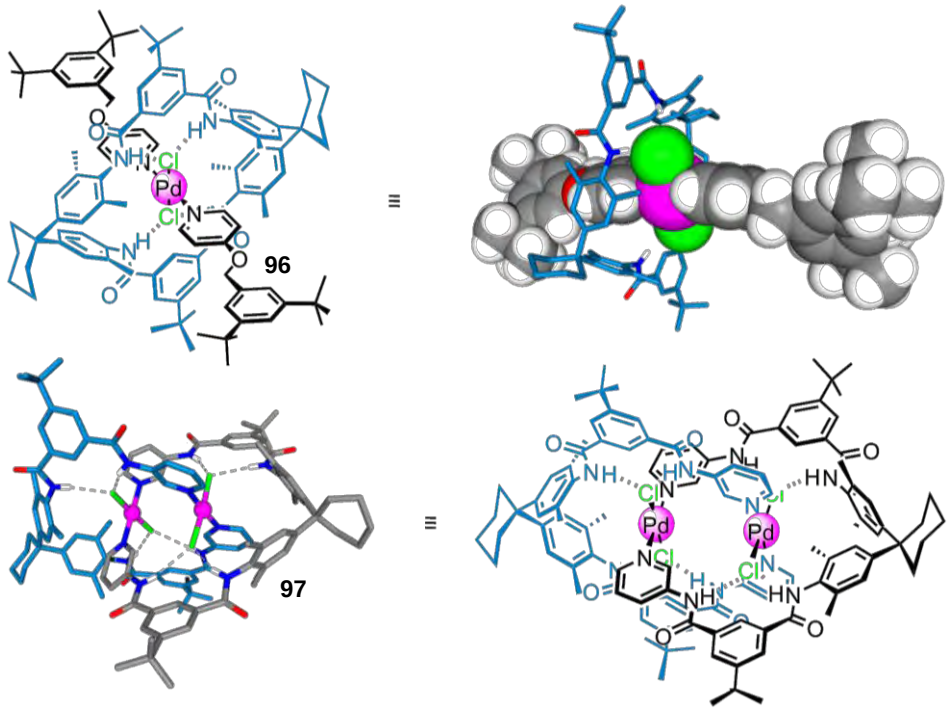

*Figure 1.6 $PdCl_2$-containing rotaxane **96** and catenane **97** achieved by Blight et al.*

1.5.2.4 *Macrocycle Shrinking by Palladium Template*

In 2004, Asakawa and collaborators introduced the novel threading-followed-by-shrinking methodology.[71] The presence of a binding site (two imine and two hydroxyl functionalities) designed to accommodate a square planar metal centre permits the modulation of the cavity size of **98**. The reversible threading of dialkylammonium salt **99** though **98** forms the unlocked *pseudo*-rotaxane **100**. Addition of $Pd(OAc)_2$ afforded the corresponding locked Pd-rotaxane **Pd-100** (30%) by shrinking the macrocycle around the thread.

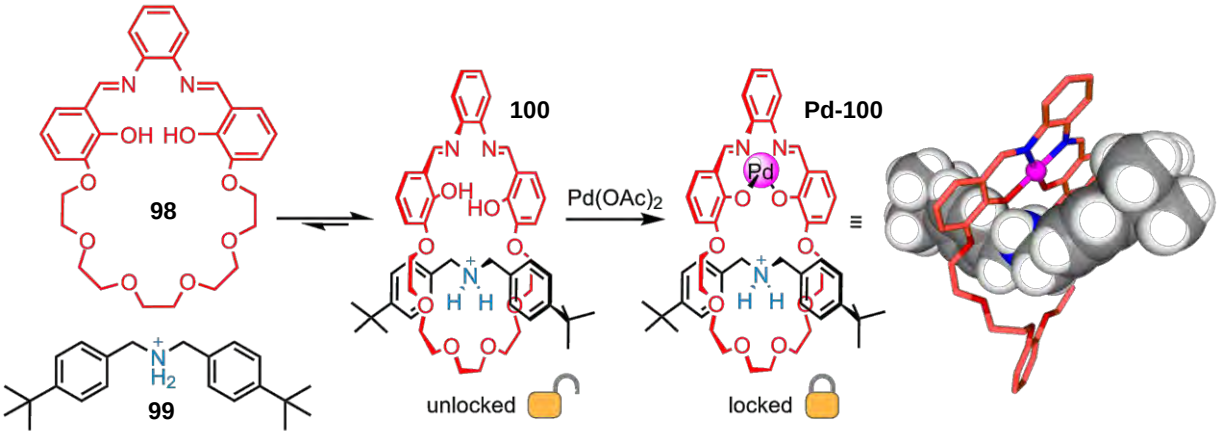

*Scheme 1.25 Synthesis of [2]rotaxane **Pd-100** by shrinking methodology.*

1.5.2.5 *Gold-acetylide Based Catenanes*

Gold-containing catenanes were first reported by Puddelphatt[72] following his description of Au-diacetylide aggregates.[73] The authors subjected gold-acetylide polymers with neutral bidentate phosphine ligands and obtained macrocycles and [2]catenanes in good yields. Using a diphosphine ligand with a short spacer (n = 1 or 2, Scheme 1.26, left) yielded macrocycles **103a** and **103b** respectively in 70% and 81% yield. Catenanes **104a-c** were easily obtained through self-assembly using a longer spacer (n = 3, 4 or 5, Scheme 1.26, right). Interestingly, the crystal structures of the interlocked structures show an intramolecular gold-gold distance of 2.968 Å suggesting a significant aurophilic interaction which might be responsible for enhancing the formation of interlocked products over the formation of macrocycles.

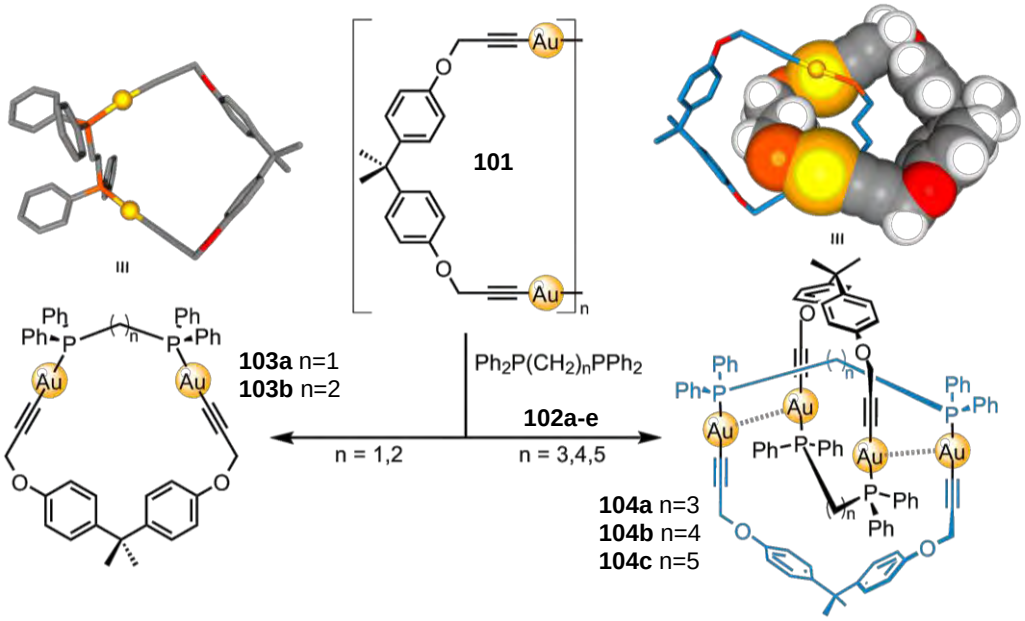

*Scheme 1.26 Preparation of gold-containing macrocycle **103a-b** and catenanes **104a-c**, Phenyl groups attached to the phosphorus atoms are not shown for clarity.*

1.6 *The Active-Metal Template Approach*

1.6.1 Presentation of the Concept

As seen above, a wide variety of metal template methodologies towards the preparation of interlocked architectures are available. However, in these approaches metal centres act only in a passive way (like a glue to hold fragment together while the mechanical bond is formed), require a stoichiometric quantity of template, and generally[74] require strongly binding recognition motifs to preorganise the components for a facile interlocking step. Building on well-documented principles of transition

metal catalysis in a wide range of organic bond forming reactions, the Leigh group envisages a new kind of approach wherein the metal template also plays an **active** role in the bond formation: the metal ion acts simultaneously as *both* a template *and* a catalyst for the formation of an interlocked structure. This active-metal template (AMT) approach would only require a permanent coordination site on the macrocycle. The rest of the compound would be assembled through functional groups that react together under catalysis by the metal-macrocycle complex. The fragments are held in position such that their metal catalyzed reaction leads to an interlocked product. The process is shown schematically in Figure 1.7 under a) stoichometric conditions and b) catalytic ones.

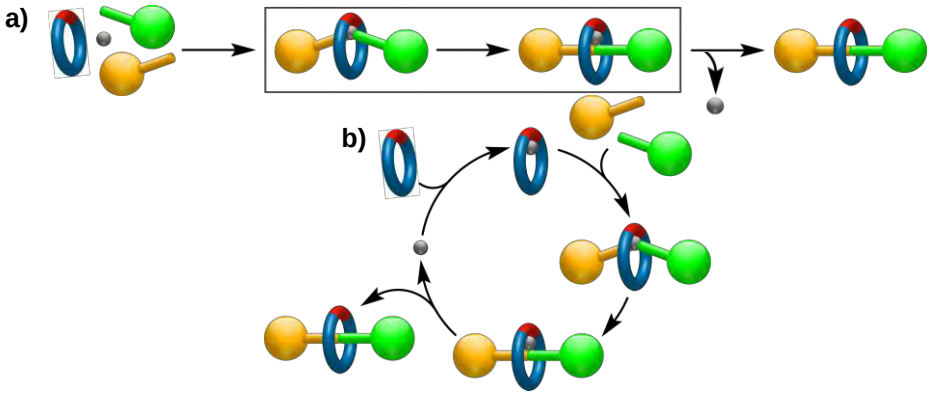

Figure 1.7 Schematic representation of the active template approach to interlocked architectures. a) Stoichiometric active-metal template synthesis of a [2]rotaxane with de-metallation; b) Catalytic active-metal template synthesis of a [2]rotaxane.

There are several potentially attractive features of such a synthetic approach to mechanically interlocked architectures, the inherent efficiency of a reaction in which the macrocycle-metal complex performs multiple functions; the lack of requirement for permanent recognition elements in each component of the interlocked product which increases the structural diversity possible in catenanes and rotaxanes and enables their formation to be "traceless"; in some cases only substoichiometric quantities of the active template may be required (i.e. the catalytic active-metal template variant, Figure 1.7b); the strategy should prove applicable to many different types of well-known transition metal catalysed (and even organocatalytic) reactions; reactions that only proceed through a threaded intermediate would allow access to several currently inaccessible mechanically linked macromolecular architectures; and finally, the coordination requirements during key stages of the catalytic cycle of active-template reactions could provide insight into the mechanisms of metal-catalysed reactions.[75]

1.6.2 CuAAC Active-metal Template

The use of the CuAAC reaction in the synthesis of rotaxanes starts with the publication by Leigh and co-workers of a novel and elegant active-metal template protocol.[16] They took advantage of both geometrical requirements and catalytic proprieties of the copper(I) to form a disubstitued triazole ring from half-threads **55** (alkyne) and **105** (azide) through the cavity of the pyridine-containing macrocycle **59** (Scheme 1.27). The second chapter of the present thesis describes in detail the discovery, extension and applications of this particular AMT methodology.[76]

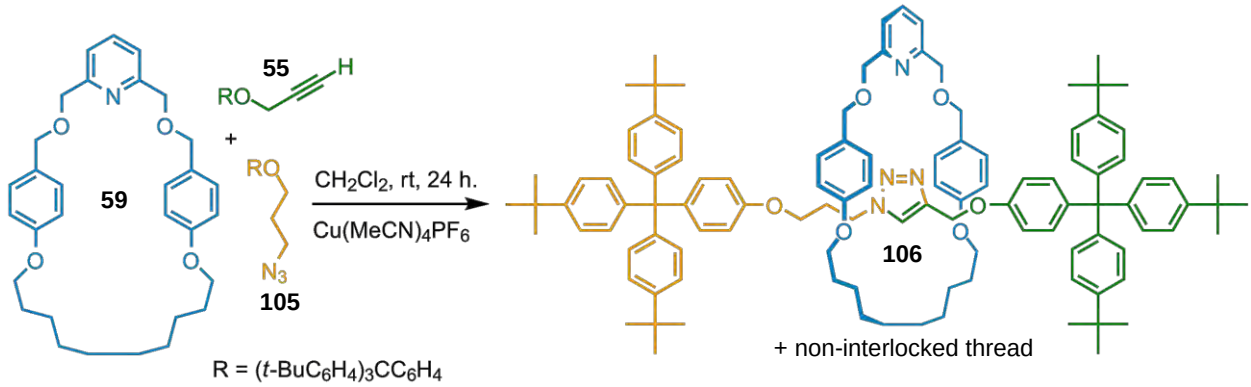

*Scheme 1.27 Active-metal template synthesis of the [2]rotaxane **106** via CuAAC reaction.*

1.6.3 Glaser and Ullman Active-metal Template

Saito and co-workers were the next to report an example of an AMT strategy. The authors investigated Glaser diyne coupling and Ullman C-S bond formation – both reactions are catalysed by Cu(I) – for the preparation of MIAs.[77] The Glaser homo-coupling of two aryl-alkyne half-threads occurs through the cavity of pre-formed complex **Cu-107** to produce rotaxane **108** in 72% yield (Scheme 1.28, top). In the same publication they also reported the Ullman coupling between a thiol and a aryl-iodide half-threads inside the cavity of the same macrocycle-Cu(I) complex, although in this case more than 10 equivalents of both half-threads were necessary to generate only a small amount of rotaxane **109** (27% yield, Scheme 1.28, centre left). Two years later, they reported the first preparation of catenanes by Glaser alkyne homo-coupling using the same CuI-macrocycle complex and a wide range of double-functionalised U-shapes (8-64%).[78] The most relevant example of the synthesis of a Glaser AMT catenane is shown in Scheme 1.28, bottom. Later the Leigh group reported an alkyne homo-coupling AMT towards rotaxanes using palladium as catalyst (see Chapter III).[79]

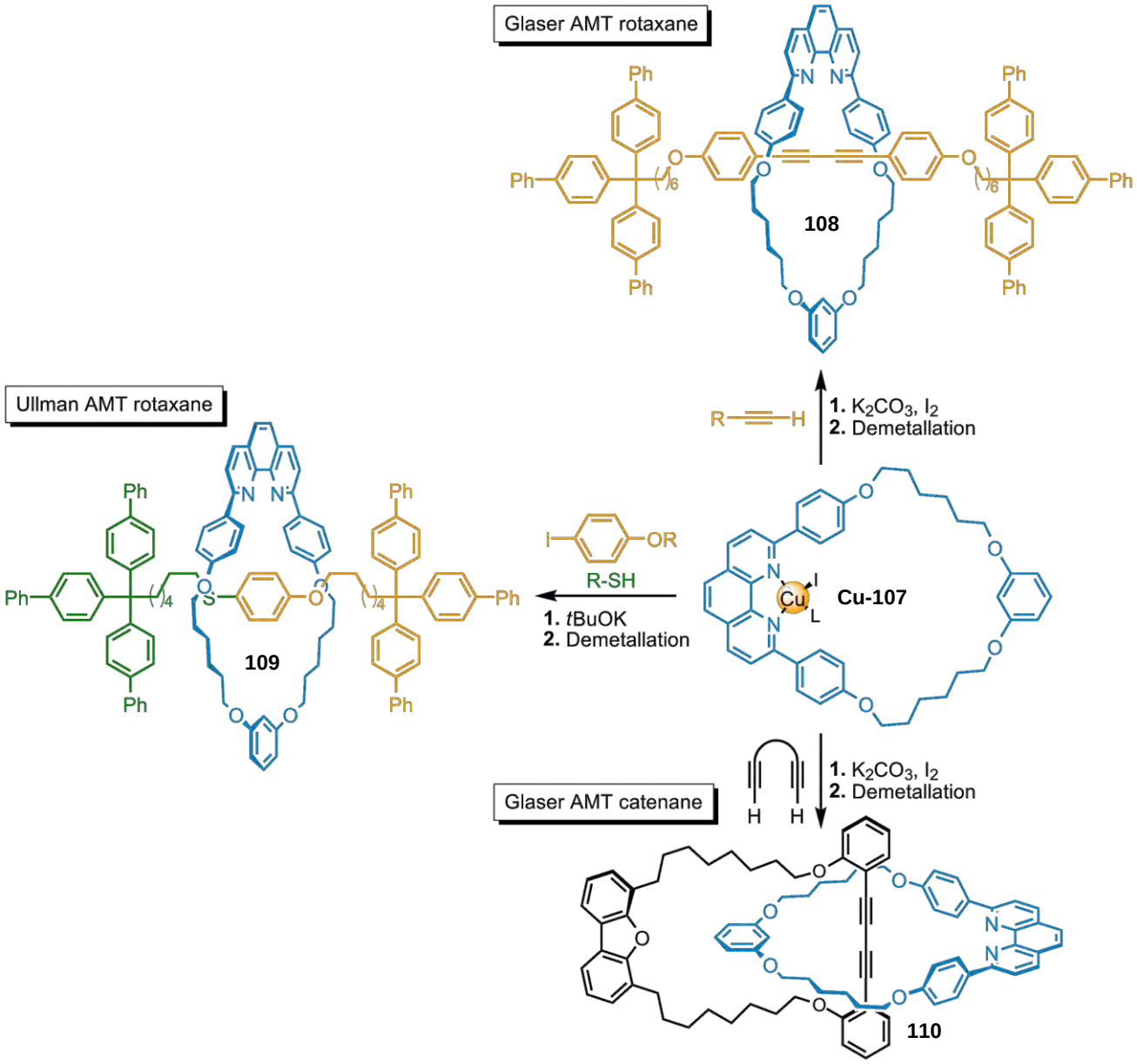

Scheme 1.28 Saito's Glaser and Ullman AMT strategies for the preparation of MIAs.

1.6.4 Rotaxanes via Cadiot-Chodkiewicz Active-metal Template

The Leigh research group published a protocol in which rotaxanes were assembled *via* an alkyne cross-coupling Cadiot-Chodkiewicz AMT protocol. Coordination of the preformed copper acetylide half-thread **Cu-112** to the bidentate bipy binding side of macrocycle **111** leads to the complex of type **I** (Scheme 1.29). Oxidative addition of the bromo-alkyne half-thread **113** occurs to the opposite side of the macrocycle to afford a Cu(III) intermediate of type **II** (Scheme 1.29). Reductive elimination of this complex yielded [2]rotaxane **114** in 85% yield.

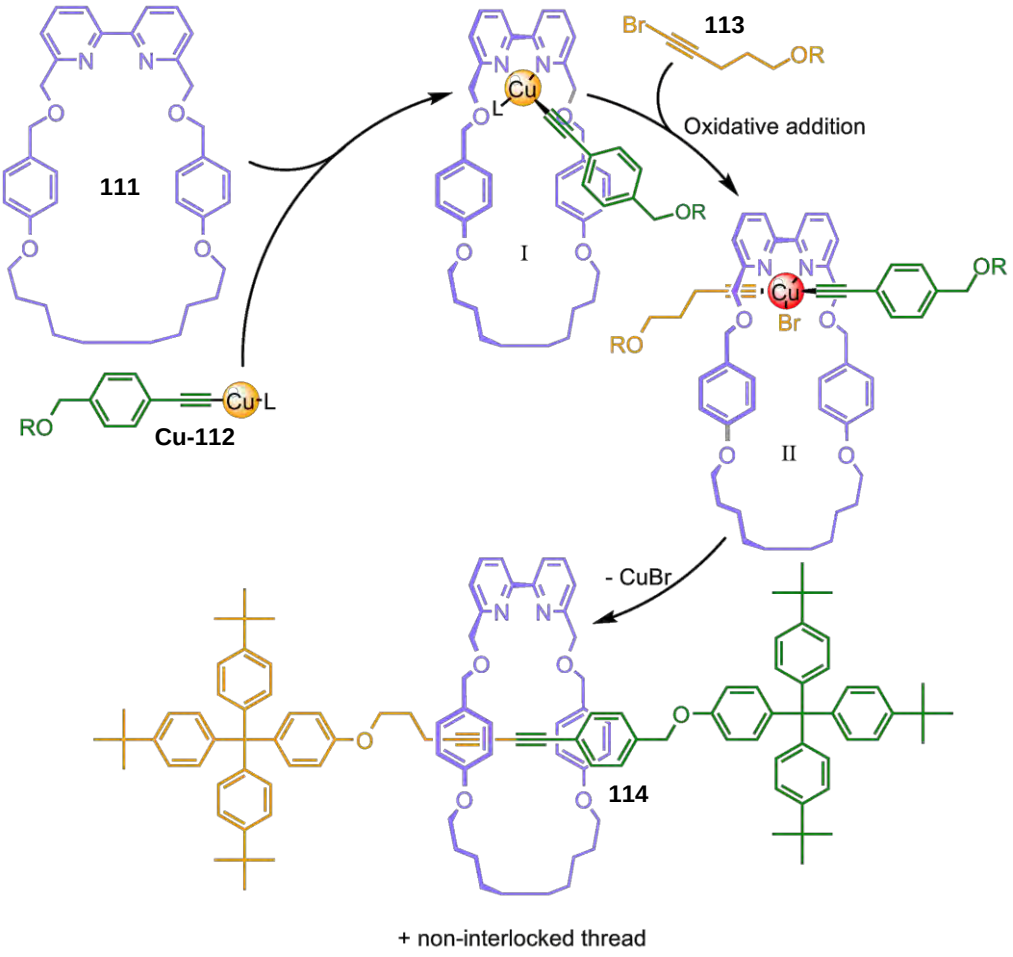

Scheme 1.29 Cadiot-Chodkiewicz active-metal template synthesis of rotaxanes.

To demonstrate the utility of this novel AMT strategy, Leigh and co-workers published the synthesis and the study of a molecular shuttle obtained by this method. They created a [2]rotaxane containing two distinct stations which can be switched utilising weak interactions. In the neutral form of **115** the bipy macrocycle resides predominantly on the aniline station due to the hydrogen bonding interactions between the aniline proton and one (or both) N-donor atoms of the bipy unit (Figure 1.8, top). Addition of either *p*-toluene sulfonic acid or lithium iodide leads to the displacement of the macrocycle from the aniline to the DMAP station as the positively-charged centre acts as bridging agent between the DMAP and the bipy units. Return to the neutral form is achieved either by washing **M$^+$-115** with $NaHCO_3$ (in the case of TsOH treatment) or with H_2O (LiI).

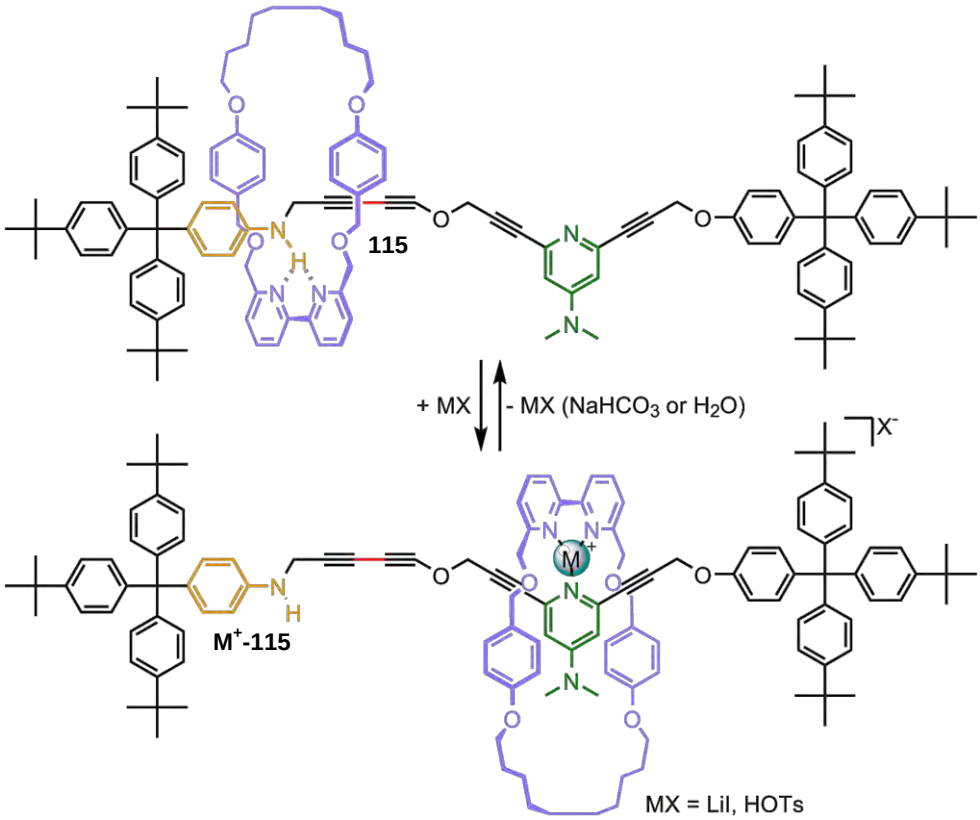

Figure 1.8 Shuttling process in the Cadiot-shuttle. The newly formed bond is shown in red.

1.6.5 Pd(II) Michael Addition towards the Synthesis of Rotaxanes

Combining their previous Pd square-planar strategy (Paragraph 1.5.1.3) with the newly introduced AMT methodology, Leigh and collaborators investigated the possibility to construct rotaxanes and molecular shuttles *via* a double Michael addition strategy promoted by a Pd(II)-pyridine-2,6-*bis*-carboxamido complex.[80] Reaction of complex **Pd-116** with ethyl cyanoacetate **118** in CH_2Cl_2 leads to – after evaporation of the combined solvent and acetonitrile - palladium complex **119**. Solid state structures of complexes **Pd-116** and **119** show that the nitrile ligands are occupying the fourth coordination site of the palladium and are located centrally within the cavity of the macrocycle allowing therefore two successive Michael additions of the vinyl ketone half-thread **117** to both sides of the macrocycle generate rotaxane **Pd-120** in 99% yield (Scheme 1.30).

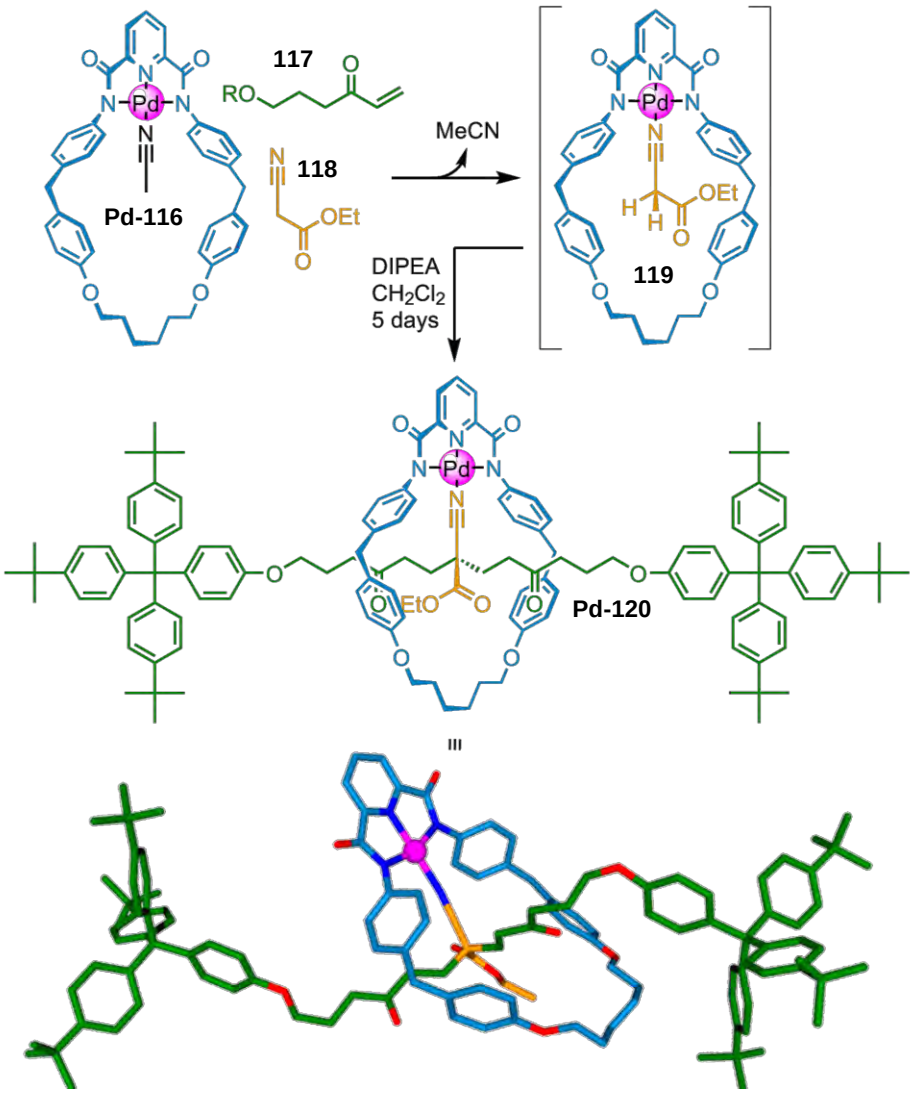

*Scheme 1.30 Pd(II) promoted Michael addition for the preparation of Rotaxane **Pd-45**.*

Demetallation with KCN gave metal-free rotaxane **120** in which the macrocycle preferentially resides near one of - or quickly shuttle between – the two carbonyl groups present in the thread due to its ability to establish hydrogen – bonding interactions between the carbonyls and the amide groups. As the nitrile ligand is retained in the final interlocked product, the authors also synthesised a degenerate shuttle containing two nitrile stations and studied the dynamics of the Pd-macrocycle complex between those two stations. At room temperature, NMR studies (293 K, d_7-DMF) showed that the Pd-macrocycle complex is unable to shuttle between the nitrile stations at the NMR time scale. In contrast, increasing the temperature to 300 K promoted a fast shuttling of the macrocycle. Exchange rates were determined by 2D-EXSY NMR experiments showing that solvent molecules are involved in the shuttling process (i.e. the rate in d_7-DMF is 600 times faster than in $CDCl_3$).

1.6.6 Scope of the Thesis

The present thesis exemplifies the active-metal template methodology for the facile preparation of MIAs *via* several well-known metal-catalysed reactions. As seen in Paragraph 1.6.2, Chapter II focuses on the use of the CuAAC reaction to achieve an AMT synthesis of [2]rotaxanes, [3]rotaxanes and molecular shuttles. Chapters III and IV describe the use of palladium(II) as a catalyst to achieve AMT syntheses of MIAs *via* alkyne homocoupling[79] and oxidative Heck cross-coupling[81] reactions, respectively. Finally, Chapter V illustrates the use of the Diels-Alder reaction mediated by Lewis acids such as copper and zinc triflate to achieve [2]rotaxanes and a molecular shuttle.

1.7 References

(1) W. R. Dichtel, O. Š. Miljanić, W. Zhang, J. M. Spruell, K. Patel, I. Aprahmian, J. R. Heath, J. F. Stoddart, *Acc. Chem. Res.* **2008**, *41*, 1750-1761.

(2) G. Shill, *Catenanes, Rotaxanes and Knots*, **1971**, Academic Press, New York.

(3) a) E. Wasserman, *J. Am. Chem. Soc*. **1960**, *82*, 4433-4434. b) I. T Harrison, S. J. Harrison, *J. Am. Chem. Soc*. **1967**, *89*, 5723-5724.

(4) A. Fernandes, A. Viterisi, F. Coutrot, S. Potok, D. A. Leigh, V. Aucagne, S. Papot, *Angew. Chem. Int. Ed.* **2009**, *48*, 6443-6447.

(5) E. R. Kay, D. A. Leigh, F. Zerbetto, *Angew. Chem. Int. Ed*. **2006**, *46*, 72-191.

(6) G. Schill, H. Zollenkopf, *Liebig. Ann. Chem*. **1979**, *721*, 53-74.

(7) a) C. O. Dietrich-Buchecker, J.-P. Sauvage, J. P. Kintzinger, *Tetrahedron Lett*. **1983**, *24*, 5095-5098. b) C. O. Dietrich-Buchecker, J.-P. Sauvage, J.-M. Kern, *J. Am. Chem Soc*. **1984**, *106*, 3043-3045.

(8) a) P. R. Ashton, B. Odell, M. V. Reddington, A. M. Z. Slawin, J. F. Stoddart, D. J. Williams, *Angew. Chem. Int. Ed*. **1988**, *27*, 1550-1553. b) P. R. Ashton, R. Ballardini, V. Balzani, M. Bělohradský, M. T. Gandolfi, D. Philp, L. Prodi, F. M. Raymo, M. V. Reddington, N. Spencer, J. F. Stoddart, M. Venturi, D. J. Williams, *J. Am. Chem. Soc*. **1996**, *118*, 4931-4951.

(9) a) C. A. Hunter, *J. Am. Chem. Soc*. **1992**, *114*, 5303-5311. F. Vögtle, S. Meier, R. Hoss, *Angew. Chem. Int. Ed*. **1992**, *31*, 1619-1622. c) A. G. Johnston, D. A Leigh, L. Nezhat, J. P. Smart, M. D Deegan, *Angew. Chem. Int. Ed*. **1995**, *34*, 1212-1216.

(10) Bipyramidal and square pyramidal: L. Raehm, J. M. Kern, J.-P. Sauvage, *Chem. Eur. J*. **1999**, *5*, 3310-3317. Octahedral: D. A Leigh, P. J. Lusby, S. J. Teat, A. J. Wilson, J. K. Y. Wong, *Angew. Chem. Int. Ed*. **2001**, *40*, 1538-1543. Trigonal pyramid: L. Hogg, D. A. Leigh, P. J. Lusby, A. Morelli, S. Parsons, J. K. Y. Wong, *Angew. Chem. Int. Ed*. **2004**, *43*, 1218-1221. Square planar: A.-M. Fuller, D. A. Leigh, P. J. Lusby, I. D. H. Oswald, S. Parsons, D. B. Walker, *Angew. Chem. Int. Ed*. **2004**, *43*, 3914-3918.

(11) C. Wu, P. R. Lecavalier, Y. X. Shen, H. W.Gibson, *Chem. Mat.* **1991**, *3*, 569-572.

(12) a) P. L. Anelli, P. R. Ashton, R. Ballardini, V. Balzani, M. Delgado, M. T. Gandolfi, T. T. Goodnow, A. E. Kaifer, D. Philp, M. Pietraszkiewicz, L. Prodi, M. V. Reddington, A. M. Z. Slawin, N. Spencer, J. F. Stoddart, C. Vincent, D. J. Williams, *J. Am. Chem. Soc.* **1992**, *114*, 193-218.

b) A. G. Kolchinski, D. H. Bush, N. W. Alcook, *J. Chem. Soc. Chem. Commun.* **1995**, 1289-1290. c) P. L. Anelli, N. Spencer, J. F. Stoddart, *J. Am. Chem. Soc*. **1991**, *113*, 5131-5133.

(13) D. Philp, J. F. Stoddart, *Synlett* **1991**, 445-458.

(14) P. R. Ashton, M. Bělohradský, D. Philp, J. F. Stoddart, *J. Chem. Soc. Chem. Commun.* **1993**, *16*, 1269-1274.

(15) M. Händel, M. Plevoets, S. Gestermann, F. Vögtle, *Angew. Chem. Int. Ed. Engl.* **1997**, *368*, 1199-1200.

(16) V. Aucagne, K. D. Hänni, D. A. Leigh, P. J. Lusby, D. B. Walker, *J. Am. Chem. Soc*. **2006**, *128*, 2186-2187.

(17) J. F. Stoddart, *Angew. Chem. Int. Ed. Engl.* **1992**, *31*, 846-848.

(18) H. Murakami, A. Kawabuchi, K. Kotoo, M. Kunitake, N. Nakashima, *J. Am. Chem. Soc.* **1997**, *119*, 7605-7606.

(19) P. R. Ashton, B. Odell, M. V. Reddington, A. M. Z. Slawin, J. F. Stoddart, D. J. Williams, *Angew. Chem., Int. Ed.* **1988**, *27*, 1550-1553.

(20) a) W. R. Dichtel, O. Š. Miljanić, J. M. Spruell, J. R. Heath, J. F. Stoddart, J. Am. Chem. Soc. 2006, 128, 10388-10390. b) A. B. Braunschweig, W. R. Dichtel, O. Š. Miljanić, M. A. Olson, J. M. Spruell, S. I. Khan, J. R. Heath, J. F. Stoddart, *Chem. Asian J*. **2007**, *2*, 634-647. c) For polyrotaxane: W. Zhang, W. R. Dichtel, A. Z. Stieg, D. Benítez, J. K. Gimzewski, J. R. Heath, J. F. Stoddart, *Proc. Natl. Acad. Sci*. **2008**, *105*, 6514-6519.

(21) a) O. Š. Miljanić, W. R. Dichtel, S. Mortezaei, J. F. Stoddart, *Org. Lett*. **2006**, *8*, 4835-4838. b) O. Š. Miljanić, W. R. Dichtel, S. I. Khan, S. Mortezaei, J. R. Heath, J. F. Stoddart, *J. Am. Chem. Soc*. **2007**, *129*, 8236-8246.

(22) a) I. Aprahamian, W. R. Dichtel, T. Ikeda, J. R. Heath, J. F. Stoddart, Org. Lett. 2007, 9, 1287-1290. b) I. Aprahamian, T. Yasuda, T. Ikeda, S. Saha, W. R> Dichtel, K Isoda, T. Kato, J. F. Stoddart. *Angew. Chem. Int. Ed*. **2007**, *46*, 4675.

(23) I. Aprahamian, J.-C. Olsen, A. Trabolsi, J. F. Stoddart, *Chem. Eur. J*. **2008**, *14*, 3889-3895.

(24) P. R. Ashton, R. Ballardini, V. Balzani, M. Belohradský, M T. Gandolfi, D. Philp, L. Prodi, F. M. Raymo, M. V. Reddington, N. Spencer, J. F. Stoddart, M. Venturi, D. J. Williams, *J. Am. Chem. Soc.* **1996**, *118*, 4931-4951.

(25) G. M. Hubner, J. Glaser, C. Seel, F. Vogtle, *Angew. Chem. Int. Ed. Engl.*, **1999,** *38*, 383-386.

(26) J. A. Wisner, P. D. Beer, M. G. B. Drew, M. R. Sambrook, *J. Am. Chem. Soc.*, **2002,** *124*, 12469-12476.

(27) M. R. Sambrook, P. D. Beer, P. D, J. A. Wisner, R. L. Paul, A. R. Cowley, *J. Am. Chem. Soc*, **2004,** *126*, 15364-15365.

(28) C. A. Hunter, *J. Am. Chem. Soc.*, **1992,** *114*, 5303-5311.

(29) F. Vögtle, S. Meier, R. Hoss, *Angew. Chem. Int. Ed.* **1992,** *31*, 1619-1622.

(30) For a reversible molecular motor, see: a) J. V. Hernández, E. R. Kay, D. A. Leigh, *Science*, **2004**, *306*, 1532-1537. b) D. A. Leigh, J. K. Y. Wong, F. Dehez, Francesco Zerbetto, *Nature*, **2003**, *424*, 174-179. For a transportation device using molecular machines, see: J. Berná, D. A. Leigh, M. Lubomska, S. M. Mendoza, E. M. Pérez, P. Rudolf, G. Teobaldi, F. Zerbetto, *Nature Mater*, **2005**, *4*, 704-710.

(31) P. R. Ashton, P. T. Glink, J. F. Stoddart, P.A. Tasker, A. J. P. White, D. J. Williams, *Chem. Eur. J.* **1996**, *2*, 729-736.

(32) (a) J-Y. Ortholand, A. M. Z. Slawin, N. Spencer, J. F. Stoddart, D. J. Williams, *Anew. Chem. Int. Ed.*, **1988**, *28*, 1394-1395. (b) P. R. Ashton, A. M. Z. Slawin, N. Spencer, J. F. Stoddart, D. J. Williams, *J. Chem. Soc., Chem. Commun.* **1987**, 1066-1069. (c) B. L. Allwood, H. Shahriari-Zavareh, J. F. Stoddart, D. J. Williams, *J. Chem. Soc., Chem.* Commun. **1987**, 1064-1066. (d) B. L. Allwood, H. Shahriari-Zavareh, J. F. Stoddart, D. J. Williams, *J. Chem. Soc., Chem. Commun.*, **1987**, 1058-1061.

(33) P. R. Ashton, E. J. T. Chrystal, P. T. Glink, S. Menzer, C. Schiavo, N. Spencer, J. F. Stoddart, P.A. Tasker, A. J. P. White, D. J. Williams, *Chem. Eur. J.* **1996**, *2*, 709-728.

(34) S. M. Goldup, D. A. Leigh, P. J. Lusby, R. T. McBurney A. M. Z. Slawin, *Angew. Chem. Int. Ed.* **2008**, *47*, 6999-7003.

(35) A-M. Fuller, D. A. Leigh, P. J. Lusby, I. D. H. Oswald, S. Parsons, D. B. Walker, Angew. Chem. Int. Ed. **2004**, 43, 3194-9198.

(36) D. A. Leigh, P. J. Lusby, S. J. Teat, A. J. Wilson, J. K. Y. Wong, *Angew. Chem. Int. Ed.* **2001**, *40*, 1538-1543.

(37) D. Pomeranc, D. Jouvenot, J-C. Chambron, J-P. Collin, V. Heitz, J-P. Sauvage, *Chem. Eur. J.* **2003**, *9*, 4247-4254.

(38) L. Hogg, D. A. Leigh, P. J. Lusby, A. Morelli, S. Parsons, J. K. Y. Wong, *Angew. Chem.* **2004**, *116*, 1238-1241. *Angew. Chem. Int. Ed.* **2004**, *43*, 1218-1221.

(39) C. Hamann, J.-M. Kern, J.-P. Sauvage, *Inorg. Chem.* **2003**, *42*, 1877-1883.

(40) A. Livoreil, C. O. Dietrich-Buchecker, J.-P. Sauvage, *J. Am. Chem. Soc.* **1994**, *116*, 9399-9400.

(41) a) J.-P. Collin, P. Gaviña, J.-P. Sauvage, *Chem. Commun.* **1996**, 2005-2006; b) P. Gaviña, J.-P. Sauvage, *Tetrahedron Lett.* **1997**, *38*, 3521-3524; c) N. Armaroli, V. Balzani, J.-P. Collin, P. Gaviña, J.-P. Sauvage, B. Ventura, *J. Am. Chem. Soc.* **1999**, *121*, 4397-4408.

(42) P. Mobian, J.-P. Collin, J.-P. Sauvage, Tetrahedron Lett. **2006**, 47, 4907-4909.

(43) S. Durot, P. Mobian, J.-P. Collin, J.-P. Sauvage, Tetrahedron Lett. **2008**, 64, 8496-8503.

(44) C. Hamann, J.-M. Kern, J.-P. Sauvage, *Dalton Trans.* **2003**, 3770-3775.

(45) A.-M. L. Fuller, D. A. Leigh, P. J. Lusby, A. M. Z. Slawin, D. B. Walker, *J. Am. Chem. Soc.* **2005**, *127*, 12612-12619.

(46) Y. Furusho, T. Matsuyama, T. Takata, T. Moriuchi, T. Hirao, *Tetrahedron Lett.* **2004**, *45*, 9593-9597.

(47) J.-P. Sauvage, M. Ward, *Inorg. Chem.* **1991**, *30*, 3869-3874.

(48) J. C. Loren, P. Gantzel, A. Linden, J. S. Siegel, Org. Biomol. Chem. **2005**, 3, 3105-3116.

(49) D. A. Leigh, P. J. Lusby, R. T. McBurney, A. Morelli, A. M. Z. Slawin, A. R. Thomson, D. B. Walker, *J. Am. Chem. Soc*, **2009**, *131*, 3762-3771.

(50) C.D. Mao, W. Q. Sun, N. C. Seeman, *Nature*, **1997,** *386*, 137-138.

(51) K. S. Chichak, S. J. Cantrill, A. R. Pease, S. H. Chiu, G. W. V. Cave, J. L. Atwood, J. F. Stoddart, *Science*, **2004,** *304*, 1308-1312.

(52) a) C. D. Pentecost, K. S. Chichak, A. J. Peters, G. W. V. Cave, S. J. Cantrill, J. F. Stoddart, *Angew. Chem. Int. Ed.* **2007**, *46*, 218-222.

(53) For a review see: a) J.-C. Chambron, J.-P. Collin, V. Heitz, D. Jouvenot, J.-M. Kern, P. Mobian, D. Pomeranc, J.-P. Sauvage, *Eur. J. Org. Chem.* **2004**, 1627-1638; b) P. Mobian, J.-M. Kern, J.-P. Sauvage, *J. Am. Chem. Soc.* **2003**, *125*, 2016-2017.

(54) F. Arico, P. Mobian, J.-M. Kern, J.-P. Sauvage, *Org. Lett.* **2003**, *5*, 1887-1890.
(55) P. Mobian, J.-M. Kern, J.-P. Sauvage, *Helv. Chim. Acta* **2003**, *86*, 4195-4213.
(56) P. Mobian, J.-M. Kern, J.-P. Sauvage, *Inorg. Chem.* **2003**, *42*, 8633-8637.
(57) a) D. Pomeranc, D. Jouvenot, J.-C. Chambron, J.-P. Collin, V. Heitz, J.-P. Sauvage, *Chem. Eur. J.* **2003**, *9*, 4247-4254; b) J.-P. Collin, D. Jouvenot, M. Koizumi, J.-P. Sauvage, *Eur. J. Inorg. Chem.* **2005**, 1850-1855.
(58) F. Durola, L. Russo, J.-P. Sauvage, K. Rissanen, O. S. Wenger, *Chem. Eur. J.* **2007**, *13*, 8749-8753.
(59) A. I. Prikhod'ko, F. Durola, J.-P. Sauvage, *J. Am. Chem. Soc.* **2008**, *130*, 448-449.
(60) A. I. Prikhod'ko, J.-P. Sauvage, *J. Am. Chem. Soc*. **2009**, *131*, 6794-6807.
(61) M. Fujita, *Chem. Soc. Rev.* **1998,** *27*, 417-425.
(62) M. Fujita, *Acc. Chem. Res.* **1999,** *32*, 53-61
(63) M. Fujita, K. Ogura, *Coord. Chem. Rev*. **1996,** *148*, 249-264.
(64) M. Fujita, F. Ibukuro, H. Hagihara, Ogura, K., *Nature*, **1994,** *367*, 720-3
(65) M. E. Padilla-Tosta, O. D. Fox, M. G. B. Drew, P. D. Beer. *Angew. Chem. Int. Ed*. **2001**, *40*, 4235-4239.
(66) W. W. H. Wong, J. Cookson, E. A. L. Evans, E. J. L. McInnes, J. Wolowska, J. P. Maher, P. Bishop, P. D. Beer, *Chem. Commun*. **2005**, *17*, 2214-2216.
(67) S.-Y. Chang, K.-S. Jeong, *J. Org. Chem*. **2003**, *68*, 4014-4019.
(68) B. A. Blight, J. A. Wisner, M. C. Jennings, *Chem. Commun*, **2006**, 4593-4595.
(69) B. A. Blight, X. Wei, J. A. Wisner, M. C. Jennings, *Inorg. Chem*. **2007**, *46*, 8445-8447.
(70) B. A. Blight, J. A. Wisner, M.C. Jennings, *Angew. Chem. Int. Ed*. **2007**, *119*, 2893-2896.
(71) I. Yoon, M. Narita, T. Shimizu, M. Asakawa, *J. Am. Chem. Soc.* **2004**, *126*, 16740-16741.
(72) a) C.P. McArdle, J.J. Vittal, R.J. Puddephatt, *Angew. Chem. Int. Ed.* **2000**, *39*, 3819; b) C.P. McArdle, M.C. Jennings, J.J. Vittal, R.J. Puddephatt, Chem.Eur. J. 2001, 7, 3572.
(73) G. Jia, R. J. Puddephatt, J. D. Scott, J. J. Vittal, *Organometallics* **1993**, *12*, 3565 -3574.
(74) J. S. Hannam, S. M. Lacy, D. A. Leigh, C. G. Saiz, A. M. Z. Slawin, S. G. Stitchell, Angew. Chem. Int. Ed. 2004, 43, 3260-3264.
(75) J. D. Crowley, S. M. Goldup, A.-L. Lee, D. A. Leigh, R. T. McBurney, *Chem. Soc. Rev.* **2009**, *38*, 1530-1541.
(76) V. Aucagne, J. Berná, J. D. Crowley, S. M. Goldup, K. D. Hänni, D. A. Leigh, P. J. Lusby, V. E. Ronaldson, A. M. Z. Slawin, A. Viterisi, D. B. Walker, *J. Am. Chem. Soc.* **2007**, *129*, 11950-11963.
(77) S. Saito, E. Takahashi, K. Nakazono, *Org. Lett.* **2006**, *8*, 5133-5136.
(78) Y. Sato, R. Yamasaki, S. Saito, *Angew. Chem. Int. Ed*. **2009**, *48*, 504 –507.
(79) a) J. Berná, J. D. Crowley, S. M. Goldup, K. D. Hänni, A.-L. Lee, D. A. Leigh, *Angew. Chem.* **2007**, *119*, 5811-5815; *Angew. Chem. Int. Ed.* **2007**, *46*, 5709-5713; b) T. M. Swager, R. M. Moslin, *Synfacts* **2007**, 1158.
(80) S. M. Goldup, D. A. Leigh, P. J. Lusby, R. T. McBurney, A. M. Z. Slawin, *Angew. Chem. Int. Ed.* **2008**, *43*, 3381-3384.
(81) J. D. Crowley, K. D. Hänni, A.-L. Lee, D. A. Leigh, *J. Am. Chem. Soc.* **2007**, *129*, 12092-12093.

Chapter II

Catalytic CuAAC-AMT Synthesis of [2]rotaxanes, [3]rotaxanes, and Molecular Shuttles

Published as *Catalytic "Click" Rotaxanes: A Substoichiometric Metal-Template Pathway to Mechanically Interlocked Architectures*, V. Aucagne, K. D. Hänni, D. A. Leigh, P. J. Lusby, D. B. Walker, *J. Am. Chem. Soc.* **2006**, *128*, 2168-2187, and as *Catalytic "Active-Metal" Template Synthesis of [2]Rotaxanes, [3]Rotaxanes, and Molecular Shuttles, and Some Observations on the Mechanism of the Cu(I)-Catalyzed Azide-Alkyne 1,3-Cycloaddition*, V. Aucagne, J. Berná, J. D. Crowley, S. M. Goldup, K. D. Hänni, D. A. Leigh, P. J. Lusby, V. E. Ronaldson, A. M. Z. Slawin, A. Viterisi, D. B. Walker, *J. Am. Chem. Soc.* **2007**, *129*, 11950-11963.

Acknowledgments

The following people are gratefully acknowledged for their contribution to this Chapter: Dr. Vincent Aucagne synthesised rotaxane **4a** for the first time and prepared suitable amounts of macrocycles **1b-1i** and **1k-1m**. Aurélien Viterisi isolated and characterised rotaxanes **4b-4m**, created the stacked plots presented in Paragraphs 2.3.3 and 2.3.5, and finally obtained an X-ray quality crystal of **6l** (Scheme 2.5). Dr. D. Barney Walker investigated the introduction of transition metals into rotaxane **9a** and provided the corresponding stacked plot (Figure 2.5). Dr. James Crowley and Dr. Paul Lusby provided useful advice and crucial involvement in the project design and writing process. Dr. Stephen Goldup and Dr. Vicki Ronaldson developed synthetic routes to macrocycles **1j** and **1n** and finally, Dr. José Berná investigated alternative synthetic strategies that are not described here.

2.1 Synopsis

This chapter reports the synthetic approach to rotaxane architectures in which metal atoms catalyse covalent bond formation while simultaneously acting as the template for the assembly of the MIA. This active-metal template strategy is exemplified using the Huisgen-Meldal-Fokin Cu(I)-catalyzed 1,3-cycloaddition of azides with terminal alkynes (the CuAAC or "click" reaction). Coordination of Cu(I) to an endotopic pyridine-containing macrocycle allows the alkyne and azide to bind to metal atoms in such a way that the metal-mediated bond-forming reaction takes place through the cavity of the macrocycle forming a rotaxane.

A variety of mono- and bidentate macrocyclic ligands are shown to form [2]rotaxanes in this way, and addition of pyridine enables the metal to turn over during the reaction, giving a catalytic AMT assembly process. Both the stoichiometric and catalytic versions of the reaction were also used to synthesise more complex two-station molecular shuttles. The dynamics of the translocation of the macrocycle by ligand exchange in these two-station shuttles could be controlled by coordination to different metal ions (rapid shuttling is observed with Cu(I), slow shuttling with Pd(II)).

Under AMT reaction conditions that feature a high macrocycle:copper ratio, [3]rotaxanes are also produced during the reaction. The latter observation shows that under these conditions the mechanism of the CuAAC involves a reactive intermediate that features at least two metal ions.

2.2 *Introduction*

Since the introduction in 2001 of the Cu(I)-catalysed variant of the Huisgen[1] 1,3-dipolar alkyne-azide cycloaddition (CuAAC) by Meldal[2] and the discovery of both rate and regio selectivity enhancement independently by Meldal[3] and Fokin[4] research groups, there has been a tremendous surge of interest in so-called "click" methodologies for functional molecule synthesis.[5] In contrast with the uncatalysed thermal conditions (Scheme 2.1, b)[1] which lead to a mixture of 1,4- and 1,5- disubstitued triazole isomers and require elevated temperature to proceed, the presence of a Cu(I) catalyst accelerates the rate of the cycloaddition and affords exclusively the 1,4- isomer (Scheme 2.1, a). The most common catalyst systems for this reaction are aqueous or alcoholic media and use a Cu(II) salt in the presence of a reducing agent (often sodium ascorbate – NaAsc – or ascorbic acid) to generate the required Cu(I) catalyst *in situ*.[4,6] Metallic copper[4,6] or copper clusters[7] have also been employed as pre-catalysts, and in some cases Cu(I) salts can be used directly. However, in apolar solvents Cu(I) salts usually require the presence of ligands (nitrogen[4,6,8] or phosphorus[9]), or acetonitrile as a co-solvent, to stabilise the Cu(I) oxidation state. Under these conditions, undesired diyne homocoupling products are often observed. Sharpless and co-workers have also reported the use of a ruthenium based catalyst to achieve the complementary formation of 1,5-triazole isomers (Scheme 2.1, c).[10]

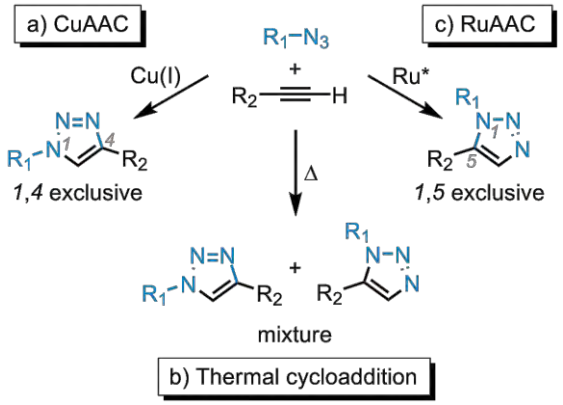

Scheme 2.1 Cycloaddition of terminal alkynes with organic azides over a) Cu(I) catalysis, b) thermal (uncatalysed) conditions, c) Ru-based catalysis.

The basic mechanism of the CuAAC reaction is believed to proceed *via* a formal Cu(III) metallacycle which DFT calculations have determined to be more favourable than the thermal pathway by 11.7 kcal·mol^{-1}.[11] However, the exact nature of this reactive intermediate is unclear (Scheme 2.1, types I-III).

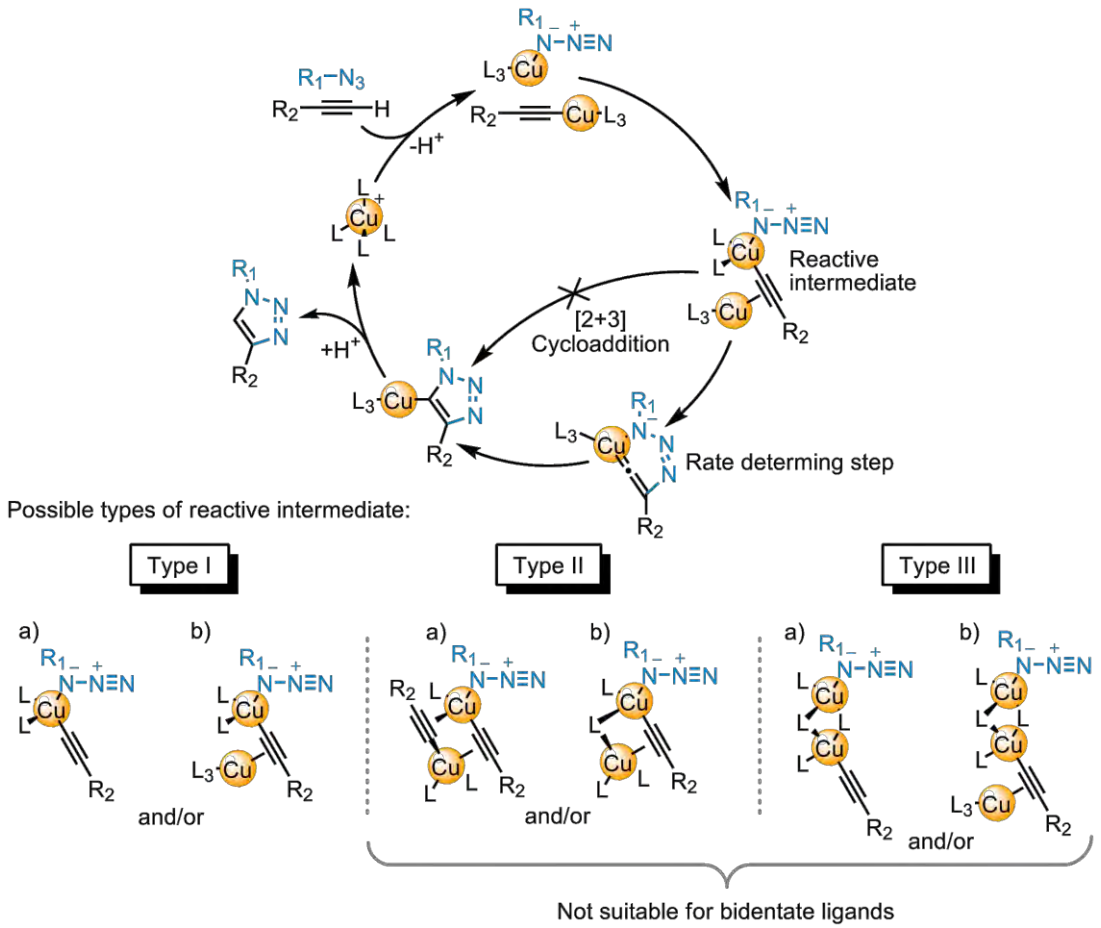

Scheme 2.2 Proposed mechanism of the CuAAC reaction.

In absence of competing ligands (referred to as ligandless or ligand-free in the present thesis), Cu(I) acetylides exist as complex multi metal atom aggregates,[12] and kinetic studies by Fokin and Finn on the generic ligand-free CuAAC reaction show that in DMSO-water mixtures the reaction mechanism is second-order with respect to copper.[8a,13] The same studies found first-order kinetics with respect to the azide and alkyne (actually slightly higher than first-order with respect to the alkyne). However, relatively little is known about the ligand-promoted Cu(I)-catalysed cycloaddition in organic solvents. Recent experiments by Straub,[14] in which mononuclear copper(I) acetylides ligated to a sterically demanding *N*-heterocyclic carbene react efficiently with bulky azides at room temperature, support the notion that a single copper atom mechanism (Scheme 2.2, Ia) is viable for the reaction, at least when the copper is bound to bulky ligands. Recent DFT calculations[11b,15] suggest that π-activation of the copper acetylide unit by coordination of a second copper atom (i.e. Type Ib or, more likely under ligand-free conditions or with small monodentate ligands, bridged[16] intermediates such as IIa or IIb, Scheme 2.2) greatly enhances the reactivity of the

copper π-acetylide, accelerating formation of the metallacycle. Alternatively, a pathway in which the reacting azide and alkyne are coordinated to different copper atoms (intermediate IIIa or IIIb, Scheme 2.2) would also be consistent with the second-order kinetics observed in DMSO-water. It may well be that several of these types of intermediates can provide viable pathways for the CuAAC reaction, with the different characteristics of the intermediates being relatively favored or inhibited by factors such as the solvent, bulk and coordination number of an added ligand, the strength of ligand-copper binding, and the amount of ligand-free Cu(I) present in solution. Given the tendency of copper(I) acetylides to aggregate, we can postulate that doubly bridged intermediates such as **II** or **III** should be abundant species under most conditions. Accordingly, if coordination of the azide to the same copper atom significantly increases the reactivity of the σ-acetylide, type IIb intermediates are probably involved in the dominant pathways in most reported CuAAC reactions.

2.3 Results and Discussions

2.3.1 Initial Results

In organic solvents, tertiary amines or, better, pyridines, considerably enhance the reaction kinetics,[4,8b] suggesting that a macrocycle bearing an endotopic ligating nitrogen atom could direct such a catalysed reaction through its cavity. The 2,6-*bis*[(alkyloxy)methyl]pyridine macrocycle (**1a**), previously used[17] as both a mono- and bidentate ligand for various transition metals in classical passive template syntheses, seemed a suitable candidate for our initial investigations. $Cu(MeCN)_4PF_6$ was chosen as the copper source, avoiding ligands that might compete too strongly for the metal with the macrocycle and other reactants.

Pleasingly, stirring an equimolar mixture of the pyridine-containing macrocycle **1a**, alkyne **2**, azide **3**, and $Cu(MeCN)_4PF_6$ in CH_2Cl_2 for 24 h afforded - after demetalation with KCN - a mixture of [2]rotaxane **4a** (57%), the non-interlocked triazole thread **5** (41%) and some of the unconsumed starting macrocycle (Scheme 2.3 and Table 2.1, entry 1).[18] By varying the reaction conditions and reactant stoichiometry (Table 2.1), yields of up to 94% of [2]rotaxane (with respect to **1a**) were achieved using conditions shown in Table 2.1, entry 4. The use of substoichiometric amounts of copper was investigated to determine whether the metal would turn over as both a template and a cycloaddition catalyst. When using 0.2 equivalent (with respect to **1a**) of $Cu(MeCN)_4PF_6$ at room temperature, the reaction appeared to stop after an amount of [2]rotaxane

equivalent to the amount of copper present had been formed, suggesting that the multidentate rotaxane sequesters the transition metal during the reaction, inhibiting further catalytic activity. Addition of pyridine as a competing ligand enabled the catalyst to turn over, producing a substoichiometric reaction. However the reaction was extremely slow at 25 °C (Table 2.1, entry 5). Elevating the temperature (70 °C, dichloroethane) and using a five-fold excess of both half-threads gave an improved yield (82%) of rotaxane **4a** in a reasonable time period (36 h in total) using only 4 mol % Cu(I) with respect to both **2** and **3** (Table 2.1, entry 9).

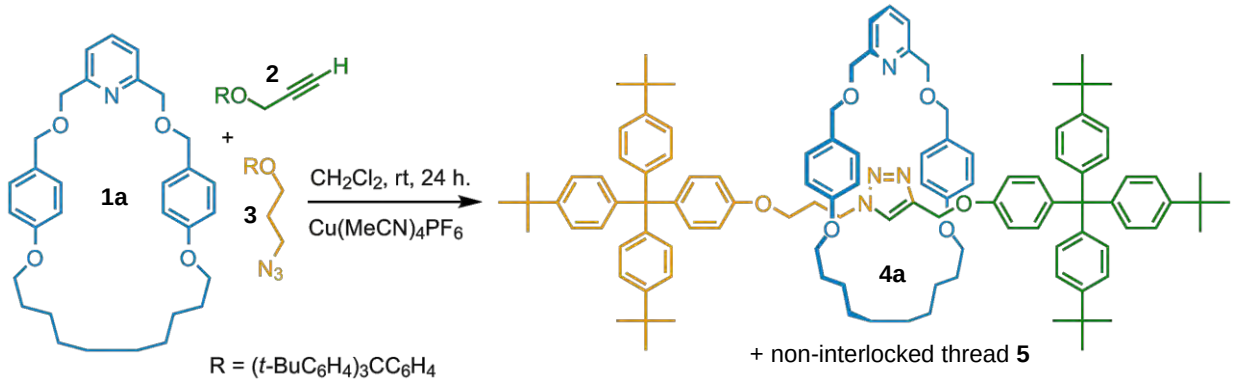

*Scheme 2.3 Active-metal template synthesis of the [2]rotaxane **4a** via CuAAC reaction.*

*Table 2.1 Variations in the Experimental Conditions and Reactant Stoichiometry for the Synthesis of [2]Rotaxane **4a**.*[a]

Entry	Amt. of **2** and **3** [equiv]	Amt. of CuL_4PF_6 [equiv]	Solvent	T [°C]	Time	Conv. to triazoles **2+3→4a+5** [%]	Yield of rot. **1a→4a** [%]
1	1	1	CH_2Cl_2	25	12 h	>95	57
2	1	1	H_2O/*t*BuOH	25	10 d	>95	22
3	3	1	CH_2Cl_2	25	24 h	>95	83
4	**5**	**1**	**CH_2Cl_2**	**25**	**72 h**	**92**	**94**
5	1	0.2	CH_2Cl_2	25	10 d	30	20
6[b]	1	0.2	CH_2Cl_2	25	10 d	>95	38
7[b]	5	0.2	CH_2Cl_2	25	20 d	44	59
8[b]	1	0	$(CH_2Cl)_2$	25 → 70	12 h → 72 h	<5	0
9[b]	**5**	**0.2**	**$(CH_2Cl)_2$**	**25 → 70**	**12 h → 24 h**	**94**	**82**

[a]*All reactions were carried out at 0.1 mM concentration with respect to **2** and **3**, with 1 equiv of macrocycle **1a**, and without the need for an inert atmosphere nor distilled or dried solvents. A general experimental procedure is provided in the experimental section.* [b]*With 3 equiv of pyridine* [c]*To assess the efficacy of the rotaxane and thread as ligands for a catalytic copper species, the*

reaction conditions from entry 4 were repeated with no macrocycle present but starting with 1 equiv of ***4*** *or* ***5*** *instead. The resulting conversions of* ***2+3→5*** *were 2% and 9%, respectively.*

Although halogenated solvents give the highest yields of rotaxane, the reaction proved to be tolerant to a range of media, including semi-aqueous conditions as shown in Table 2.1, entry 2. Later our group investigated various substrate scopes for the CuAAC active-template rotaxane formation reaction.[19]

The ^{1}H NMR spectrum of **4a** in $CDCl_3$ (Figure 2.1, b) shows upfield shifts of several signals with respect to its non-interlocked components **1a** and **5** (Figure 2.1, a and c, respectively). The shielding, typical of interlocked architectures in which the aromatic rings of one component are positioned face-on to another component, is observed for all the non-stoppered resonances of the axle ($H_{f\text{-}j}$) in **4a**, indicating that the macrocycle is able to access the full length of the thread. In contrast, the equivalent spectrum of the re-metalated rotaxane Cu**4a**PF_6 (Me_2CO, RT, 1 h, quantitative, Figure 2.1, d) shows pronounced shielding of H_j and H_k with respect to **5** (Figure 2.1, c) but *not* H_h, H_g, or H_f. This suggests that the Cu(I) binds to the macrocycle and thread in the rotaxane via two sets of bidentate N,O donor interactions, fixing the interlocked components in a position consistent with the observed shielding effects.

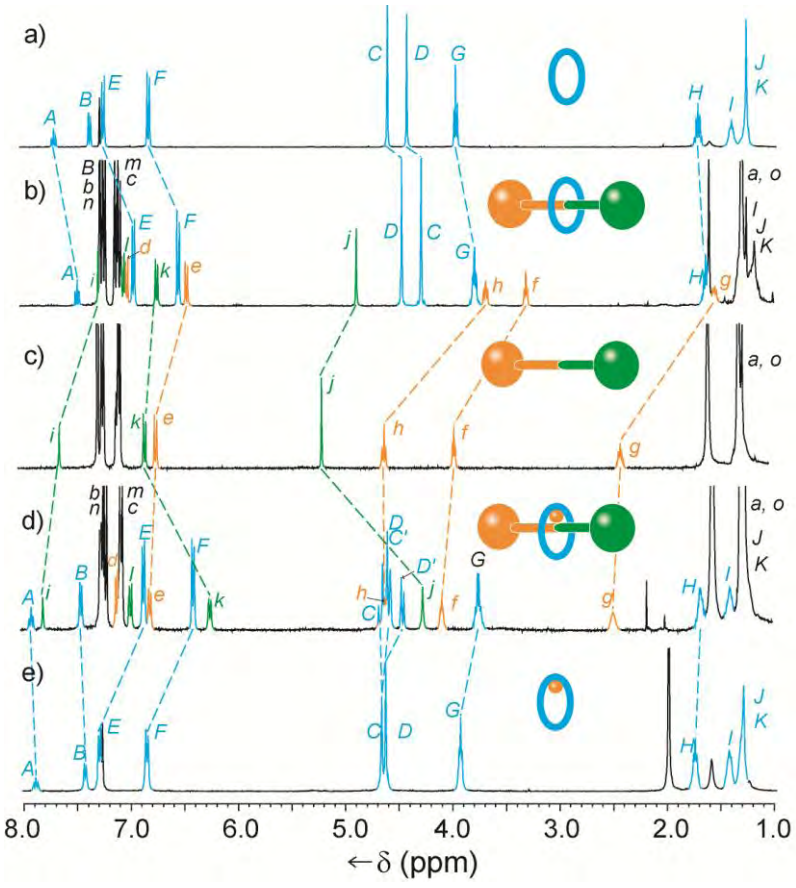

*Figure 2.1 ^{1}H NMR spectra (400 MHz, $CDCl_3$, 298 K) of a) macrocycle **1a**, b) [2]rotaxane **4a**, c) non-interlocked thread **5**, d) complex Cu**4a**PF6 and e) complex Cu**1a**PF6.*

2.3.2 Effect of the Macrocycle Structure on [2]Rotaxane Formation

To further investigate both the scope and the mechanism of the active-template rotaxane-forming reaction shown in Scheme 2.3, we varied the structure of the pyridine-based macrocycle. The macrocyclic ligands used in the study are shown in Figure 2.2 (their syntheses are detailed in the Experimental section). To compare the relative yields of rotaxane and thread within the ligand series, the macrocyclic ligands were screened using the standard stoichiometric conditions (1 equiv of macrocycles **1a-o**, alkyne **2**, azide **3**, and $Cu(MeCN)_4PF_6$, 0.01 M in CH_2Cl_2, RT, 24 h). In most cases the starting alkyne **2** and azide **3** were completely consumed during the course of the reaction. After 24 h (72 h for **1n** and **1o**) each reaction was treated with KCN to remove the Cu(I) template, analysed by ^{1}H NMR to determine the yield and then purified to give authentic samples of each [2]rotaxane. The yield (the percentage shown in red in Figure 2.2) of each rotaxane is the conversion of the macrocycles **1a-o** to the corresponding [2]rotaxanes **4a-o**. The conversion to triazole (the percentage in parentheses in Figure 2.2) is the overall conversion of the alkyne **2** and azide **3** into both thread **5** and rotaxanes **4a-o**.

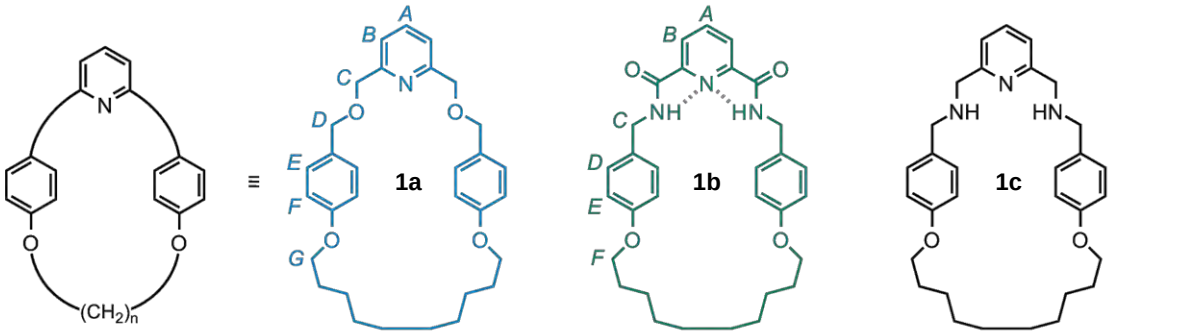

[2]rotaxane **4a** 57% (>95%) [2]rotaxane **4b** 6% (>95%) [2]rotaxane **4c** 0% (>95%)

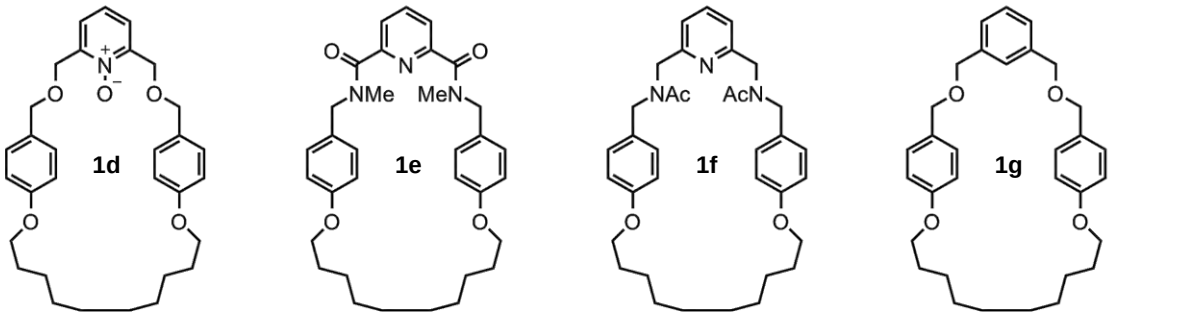

[2]rotaxane **4d** trace (>95%) [2]rotaxane **4e** trace (>95%) [2]rotaxane **4f** trace (>95%) [2]rotaxane **4g** 0% (>95%)

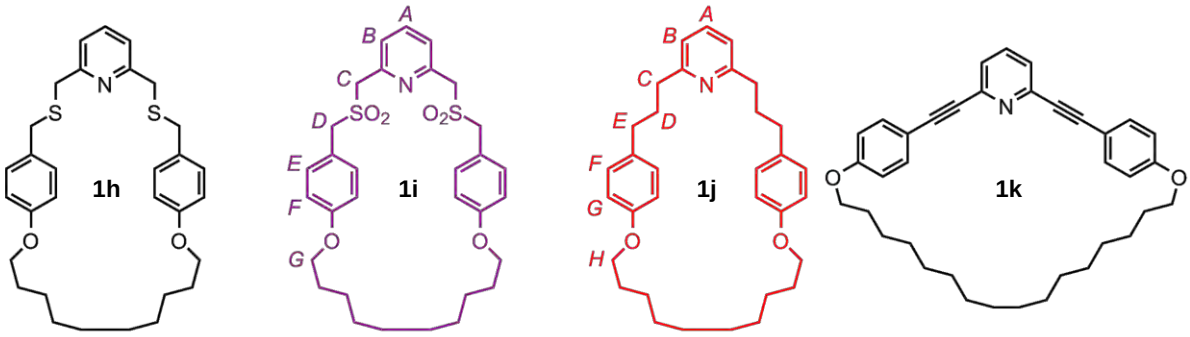

[2]rotaxane **4h** 0% (30%) [2]rotaxane **4i** 13% (>95%) [2]rotaxane **4j** 60% (>95%) [2]rotaxane **4k** 0% (25%)

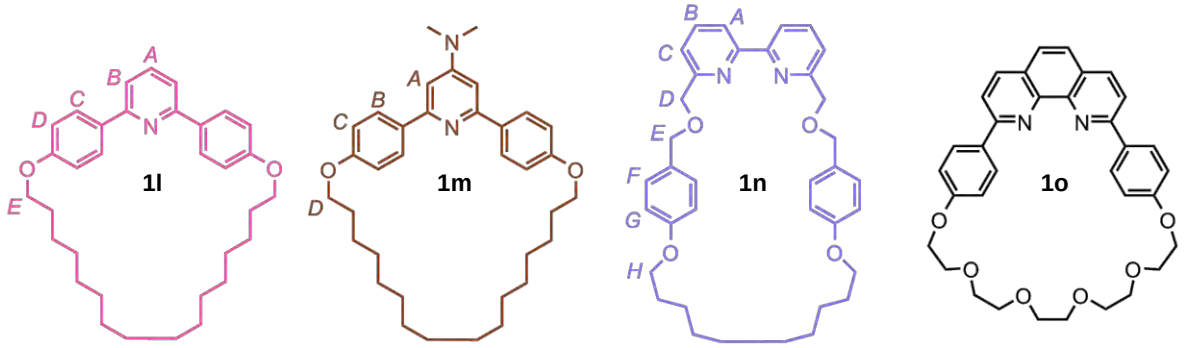

[2]rotaxane **4l** 25% (>95%) [2]rotaxane **4m** 20% (>95%) [2]rotaxane **4n** 45% (>95%) [2]rotaxane **4o** 0% (<1%)

*Figure 2.2 Influence of the macrocyclic ligand on the AMT CuAAC rotaxane-forming reaction under standard conditions. Conversion of macrocycle into rotaxane (**1**→**4**) is given in red, overall conversion (**2+3**→**4+5**) is given in brackets. Traces mean that rotaxane was detected by ESI-MS but not by ^{1}H NMR. The colour and lettering correspond to the signal assignment of ^{1}H NMR spectra shown in Figure 2.3.*

2.3.2.1 *Mono- and Tridentate Macrocycles*

In addition to the strongly coordinating pyridine nitrogen, macrocycle **1a** has two ether oxygen atoms that could potentially be involved in (albeit weak) coordination to the metal atom during the AMT reaction, making **1a** a monodentate, a weak bidentate or a very weak tridentate ligand. Not only is macrocycle **1b** missing the ether oxygen atoms, but the pyridine nitrogen atom lone pair is tied up in strong intramolecular hydrogen bonds to the adjacent amide groups, therefore it was surprising to isolate [2]rotaxane **4b** in 6% yield. Coordination of **1b** to the copper occurs at the expense of the intramolecular hydrogen bonds.[20] In contrast, the use of **1c** - a tridentate macrocyclic ligand with three hard donor atoms - gave a similar overall conversion to triazole products but the corresponding rotaxane was not formed. Upon addition of **1c** to the copper catalyst, the solution turned from colourless to blue-green suggesting that most of the Cu(I) is rapidly oxidised to Cu(II) upon coordination to **1c**. The resulting Cu^{II}-**1c** complex is then not able to catalyse the CuAAC reaction. In addition, any tridentate complexes such as Cu^{I}-**1c** lack the free coordination sites necessary to bind azide and alkyne in the same aggregate. However, enough copper(I) remains in solution (i.e. not tied up by **1c**) for the ligandless thread-forming triazole reaction to proceed to completion within 24 h. Macrocycle **1d** has a similar structure compared to **1a** except that the pyridine nitrogen atom is oxidised. The resulting CuAAC reaction leads to >98% conversion to triazole-containg products but only traces of rotaxane were detected by ESI-MS. This shows, as expected, that the *N*-oxygen atom greatly affects the ligand's ability to coordinate copper(I) inside the cavity of **1d**. Macrocycle **1e** also has a constitution similar to **1b**: the difference is that the secondary amides are methylated, eliminating their ability to form hydrogen bonds. Computer assisted calculations (Spartan™) show that the methyl groups distort and partially fill the cavity, with the result that (as with **1d**) little of the CuAAC reaction is directed through the macrocycle cavity to form the corresponding rotaxane. The same effect is seen for macrocycle **1f**, the *bis*-*N*-acetylated analogue of **1c**. Removing the pyridine nitrogen atom as in macrocycle **1g**, completely switches off rotaxane formation, confirming the importance of the presence of a ligating donor atom. Replacing the benzylic oxygens of **1a** with more strongly coordinating sulfur atoms produces another tridentate macrocycle (**1h**). As with **1c**, no rotaxane is formed - consistent with the premise that Cu(I)-tridentate ligand complexes lack the vacant coordination sites necessary to bind both azide and alkyne. The yield of triazole products is also only 30%, indicating that **1h** is particularly

effective in sequestering the catalyst. Oxidation of the sulfide groups into sulfones led to macrocycle **1i**, wherein its binding ability towards Cu(I) is restored and despite the increased bulk around the coordinated metal ion, a significant amount (13%) of [2]rotaxane **4i** is formed. In contrast with **4h**, substitution of the benzylic ether oxygen atoms for methylene groups confirms that only a monodentate macrocycle with a single strongly coordinating donor atom is required for an efficient AMT rotaxane-forming reaction: macrocycle **1j** generates just as much [2]rotaxane as the parent macrocycle **1a**. To test whether other macrocycle geometries would be tolerated by the active-template reaction, macrocycles **1k** and **1l** were prepared**,** in which the substituted benzylic units were replaced by arylalkynyl and aryl groups, respectively. The 2,6-*bis*alkynylpyridine unit proved to be unstable under the reaction conditions, suppressing the overall yield of the CuAAC reaction and suppressing all production of rotaxane. The AMT CuAAC reaction proceeded smoothly with **1l**, albeit generating rather less rotaxane (25%) than the most effective examples of other macrocycle geometries (**1a** and **1j**). The phenyl groups flanking the pyridine sterically encumber the nitrogen donor atom, and a combination of sterics and electronic factors probably reduces the binding affinity of this ligand for Cu(I) metal centres. The weaker binding leads to the presence of more ligandless Cu(I) in solution, resulting in higher conversion of the substrates into the non-interlocked thread **5** and the relatively modest yield of [2]rotaxane **4l** (25%). Increasing the steric bulk at the *4*-position of the pyridine group by adding a DMAP unit which simultaneously increases the electron-donating ability of the heterocyclic nitrogen atom, macrocycle **1m**, had little effect on the rotaxane yield (20%).

2.3.2.2 *Bidentate Macrocycles*

Having established that monodentate macrocyclic ligands geometries and donor atom orientations (**1a**, **1j**, **1l**, **1m**) efficiently promote the active-template rotaxane formation, whereas strongly tridentate macrocycles (**1c** and **1h**) do not, we investigated the efficacy of bidentate macrocycles **1n** and **1o**. The bipyridyl macrocycle **1n** directs the CuAAC reaction through its cavity to form rotaxane almost as efficiently as the best monodentate macrocycles (45% for **1n→4n** compared to 57% for **1a→4a** and 60% for **1j→4j**). However, it severely inhibits the rate of the CuAAC and it took 3 days for the AMT reaction **1n→4n** to go to completion, compared to 24 h for **1a→4a** and 6 h for the ligand-free Cu(I)-catalysed control reaction (kinetic studies in reference 19, not shown here). The inhibition of the Cu(I)-catalysed cycloaddition is even more

dramatic with another bidentate ligand investigated. The 2,9-diphenylphenanthroline macrocycle **1o** used extensively to assemble MIAs by the Sauvage research group (See Chapter I) completely inhibits the CuAAC reaction. Even after 3 days under the standard stoichiometric conditions, no triazole products were obtained. This latter result is particularly interesting given that phenanthroline ligands have previously been reported[8] to promote the reaction. The lack of reactivity is presumably a result of the steric bulk around the Cu(I) centre in the complex preventing it from undergoing the various structural variations required for reaction to take place (i.e. tolerating the change in geometry from Cu(I) to the formal Cu(III) species, Scheme 2.1), together with the ability of the macrocycle to sequester effectively the Cu(I) in its unreactive form. As seen in Chapter I, Section 1.5.2.2, a similar Cu(I)-macrocycle complex has been reported to promote the formation of MIAs *via* a Glaser diyne coupling and Ullman C-S bond formation.[21] In that case, however, intermediates of type II (Scheme 2.2) are possible with a bidentate ligand for copper because no azides need be coordinated to the metal atom.

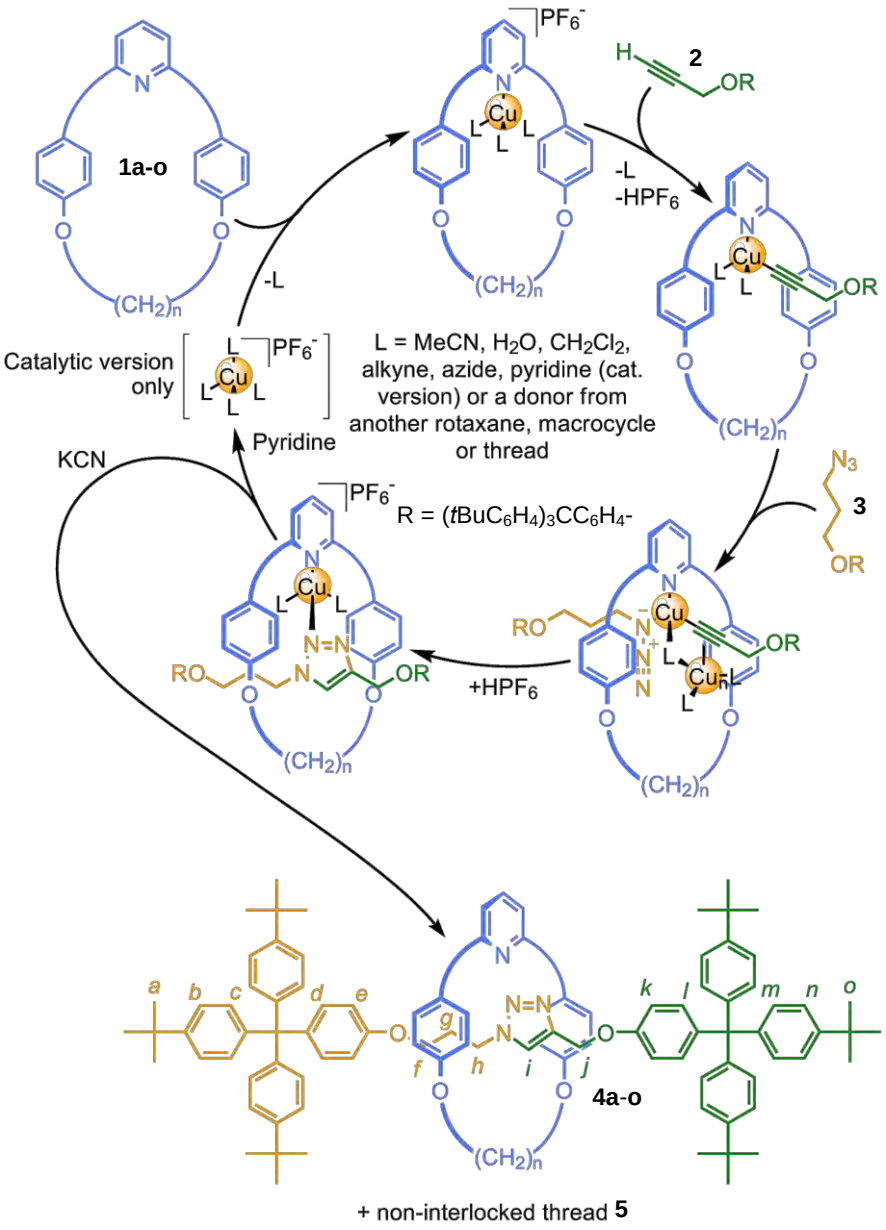

*Scheme 2.4 Proposed catalytic cycle for the active-metal Template CuAAC Sythesis of [2]rotaxanes **4a-o** from alkyne **2**, azide **3** and macrocycles **1a-o**.*

2.3.3 ^{1}H NMR Spectra of Metal-Free [2]Rotaxanes

The ^{1}H NMR spectra (400 MHz, 298 K, $CDCl_3$) of each rotaxane formed in more than 5% yield are shown in Figure 2.3. The ^{1}H NMR spectra of the rotaxanes (Figure 2.3b-g) all show upfield shifts of several signals with respect to the signals of the non-interlocked components (thread **5**, Figure 2.3a, and the macrocycles **1a**, **1b**, **1i**, **1j**, **1m**, and **1n**; see reference 19). Such shielding is typical of interlocked structures in which the aromatic rings of one component are positioned face on to another component and is observed for all the non-stopper resonances of the axle ($H_{f\text{-}j}$), indicating that the macrocycle

accesses the full length of the thread, as there are no strong intercomponent non-covalent interactions between the thread and the macrocycle in the metal-free rotaxanes. The one exception is the amide-containing rotaxane **4b** (Figure 2.3c), which exhibits a significant downfield shift of the amide resonance with respect to the free macrocycle. This can be attributed to hydrogen bonding between the amides of the macrocycle and the triazole ring of the thread in an interaction similar to that previously observed between interlocked amide and pyridine components in rotaxanes and catenanes.[17,22]

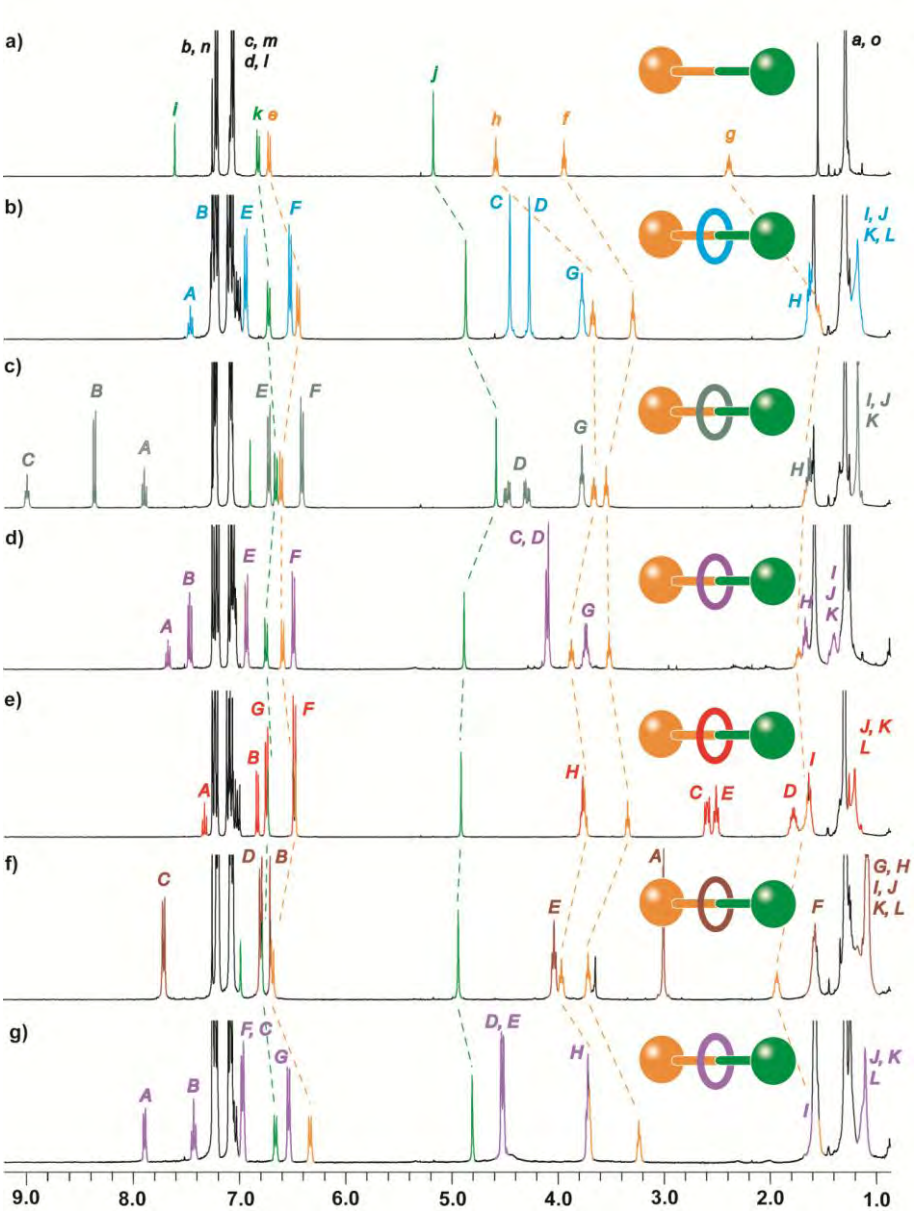

*Figure 2.3 ^{1}H NMR spectra (400 MHz, $CDCl_3$, 298 K) of a) triazole thread **5**, b) [2]rotaxane **4a**, c) [2]rotaxane **4b**, d) [2]rotaxane **4i**, e) [2]rotaxane **4j**, f) [2]rotaxane **4m** and g) [2]rotaxane **4a**. The assignments correspond to the lettering in Figure 2.2 and in Scheme 2.4.*

2.3.4 Effect of the Nature of the Cu(I) Source

A number of different Cu(I) salts were screened for the reaction shown in Scheme 2.3 using the conditions shown in Table 2.1, entry 1, but replacing the $Cu(MeCN)_4PF_6$ salt with other Cu(I) sources. The use of CuOTf·benzene gave a 78% conversion of **2** and **3** into triazole products after 24 h but only a 46% yield of [2]rotaxane **4a**. By letting the reaction continue for a further 2 days (72 h in total), complete conversion of the starting azide and alkyne to triazole products was achieved (48% rotaxane). Substituting $Cu(MeCN)_4PF_6$ with CuI (copper iodide) led to very little reaction during the first 24 h (8% conversion to triazole products), presumably owing to the low solubility of CuI in CH_2Cl_2, but interestingly, what little alkyne and azide had reacted formed rotaxane with high selectivity (88:12 rotaxane:thread). The reaction proceeded slowly to completion (>98% conversion) over three weeks. However, at the end the product ratio (56:44 rotaxane:thread) was similar to that of the analogous $CuMeCN_4PF_6$-mediated experiment. We also synthesised and isolated various discrete Cu^I-**1a** complexes and tested their efficiency in the AMT reaction. Submitting macrocycle **1a** with several different Cu(I) salts in acetonitrile yielded the corresponding Cu^I-**1a** complexes which were obtained through precipitation with diethyl ether. The preformed Cu^I-**1a** complexes were submitted to the standard rotaxane-forming reaction conditions (Table 2.1, entry 1). Complex Cu**1a**PF_6 gave 76% conversion to triazole products and 53% yield of [2]rotaxane **4a**; the preformed Cu**1a**OTf complex gave 53% conversion to triazoles but only a little 5% yield of [2]rotaxane while the Cu**1a**I complex gave results identical to those of the Cu**1a**I complex formed *in situ* (i.e. >98% triazole conversion over 3 weeks, 56% rotaxane). Although there is some variation in the efficiency of the various Cu(I) salts on the rotaxane-forming reaction and some unexplained variation in the rotaxane:thread ratio. Our initial attempt using $Cu(MeCN)_4PF_6$ as a copper(I) source is the most convenient and efficient way of maximising the CuAAC rotaxane-formation reaction.

2.3.5 Template CuAAC Reaction at High Macrocycle:Cu(I) Ratios: Unexpected Formation of [3]Rotaxanes

The picture of the AMT CuAAC reaction that we can build up is consistent with the experimental observations: the ligand-free $Cu(MeCN)_4PF_6$ salt and macrocycles **1a-o** are in equilibrium with the corresponding copper(I)-macrocycle complexes in which, in most cases, the metal atom directs the cycloaddition of the azide and alkyne through the macrocycle cavity. Although the ligand-free reaction is inherently faster than the

AMT one (see kinetic studies in reference 19), the coordinating ability of the macrocycle means that the rotaxane-forming reaction competes with the thread-forming reaction. In general, a stronger binding macrocyclic ligand (i.e. **1a** compared to **1b**) should move this equilibrium in favor the rotaxane formation. However, some changes in coordination geometry about the metal are required for the CuAAC mechanism to operate (Scheme 2.2). For example, the most strongly binding macrocycle **1o** does not tolerate such changes and actually inhibits the rotaxane-forming reaction. In view of this, we decided to investigate other conditions in which the rotaxane formation might be increased at the expense of the thread. In an attempt to minimise the amount of ligandless Cu(I) present in solution, we carried out the AMT CuAAC protocol under the standard set of conditions (1 equiv of **2**, **3**, and $CuMeCN_4PF_6$, CH_2Cl_2, rt) used previously but in the presence of 10 equivalents of macrocycle (Scheme 2.5). Our initial experiments were carried out with monodentate macrocycle **1l**, and the reaction was shown to be much slower with 10 equivalents of the macrocyclic ligand than it had been with 1 equivalent (more than one week was necessary for the reaction to go to completion). Upon reaching the end point, the mixture of triazole products was found to consist of non-interlocked thread **5**, [2]rotaxane **4l**, and [3]rotaxane **6l** (30%, 37% and 33% respectively), yields are quoted with respect to the alkyne and azide half-threads) as shown in Scheme 2.6. The reaction using macrocycle **1a** under the same conditions was also slower (3 days to reach completion compared to 24 h), generating a product mixture of thread **5** (5%), [2]rotaxane **4a** (90%), and [3]rotaxane **6a** (5%). A similar but less dramatic trend was seen with bidentate macrocycle **1n**: with 10 equivalents of **1n** the reaction took 10 days to complete (cf. 3 days with 1 equivalent), producing 3% thread **5** and 97% [2]rotaxane **4n** but no [3]rotaxane **6n** was detected by ^{1}H NMR spectroscopy or by ESI-MS.

Single crystals of **6l** suitable for X-ray crystallography were grown by slow cooling of a hot saturated solution of **6l** in acetonitrile. The solid-state structure (Scheme 2.5, bottom) confirmed the constitution of **6l** as a [3]rotaxane. Although it may superficially appear that face-to-face π-stacking interactions might aid the relative orientation of the two macrocycles on the thread, in the solid state the aromatic rings of adjacent macrocycles are not coplanar and their separation (>3.8 Å) is greater than that typically associated with aromatic stacking interactions.

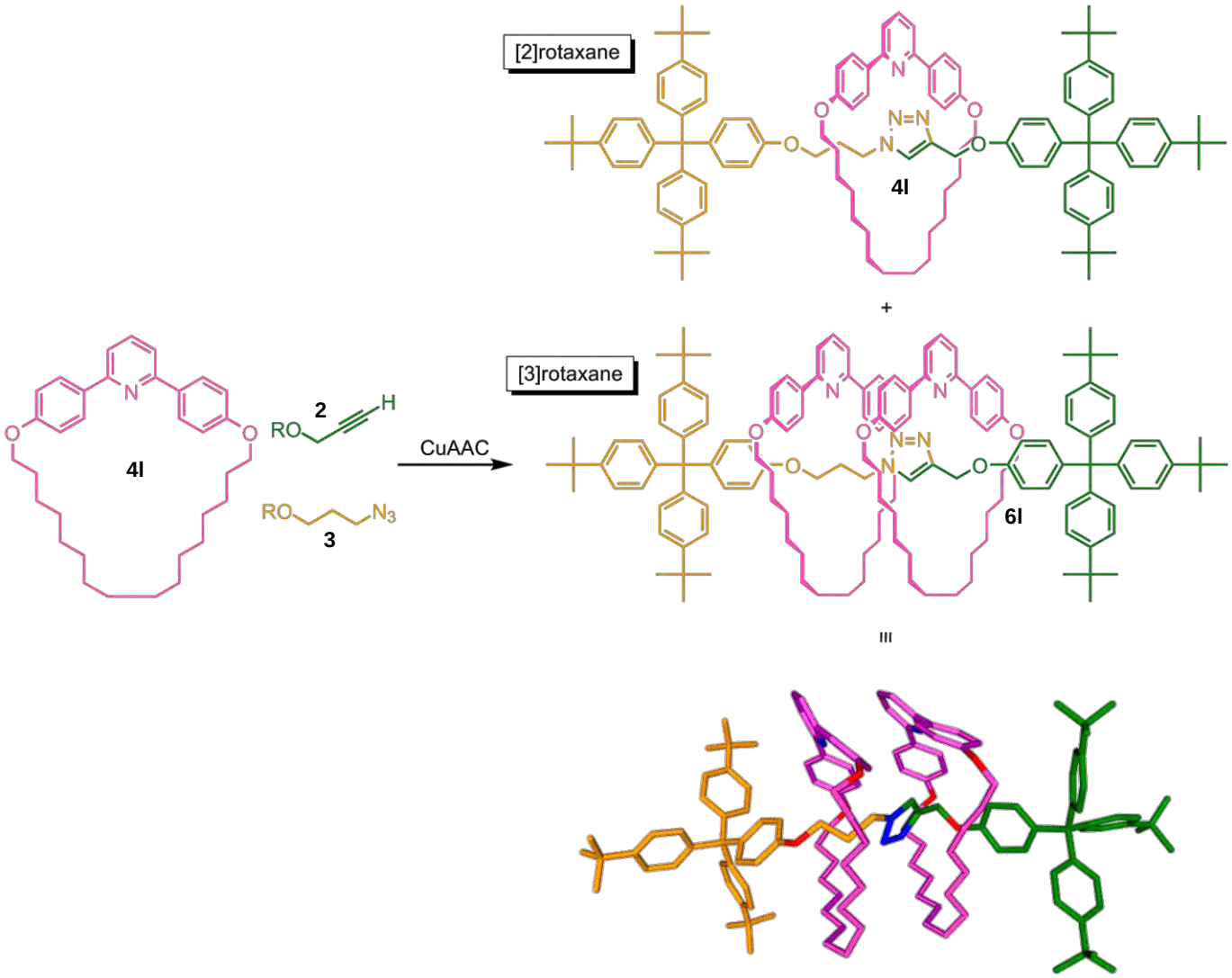

*Scheme 2.5 Serendipitous synthesis of [3]rotaxane **6l** by using 10 equivalents of macrocycle **1n**.*

The remarkable features of these high macrocycle:Cu(I) ratio active-metal template reactions are:

(i) Exceptional combined rotaxane yields: 95% (**4a** + **6a**) compared to 57% for **4a** with 1 equivalent of **1a**; 70% (**4l** + **6l**) compared to 25% for **4l** with 1 equivalent of **1l**; 97% (**4n**) compared to 45% for **4n** with 1 equivalent of **1n**.

(ii) Significant decrease of the reaction rates compared to the low macrocycle:Cu(I) ratio reactions. The largest effect on the rate is seen with the weakly copper-binding macrocycle **1l**; the smallest effect on the rate occurs for the strongly copper-binding macrocycle **1n**. This is strongly suggestive experimental evidence that the dominant mechanism of the CuAAC reaction under these conditions involves activation of the

copper σ-acetylide unit by a second, preferably ligandless for steric reasons, copper atom (i.e. **I** or **II**, Scheme 2.6).

(iii) Formation of [3]rotaxane (in 33% yield using macrocycle **1l**) - i.e. *two* macrocycles being threaded during the formation of *one* triazole ring. Molecular models (Spartan™) show that it is possible for this to occur through the bridged two copper atom intermediate **III** shown in Scheme 2.6. Since such a doubly bridged intermediate cannot occur with bidentate ligands (no [3]rotaxane is observed with **1n**), it seems likely that monodentate pyridine ligand promoted CuAAC reactions proceed via doubly bridged intermediates such as **I** (Scheme 2.6 ≡ intermediate IIb in Scheme 2.2), whereas bidentate bipyridyl ligand promoted CuAAC reactions proceed via simple π-coordinated complexes such as **II** (Scheme 2.6 ≡ intermediate Ia in Scheme 2.2).

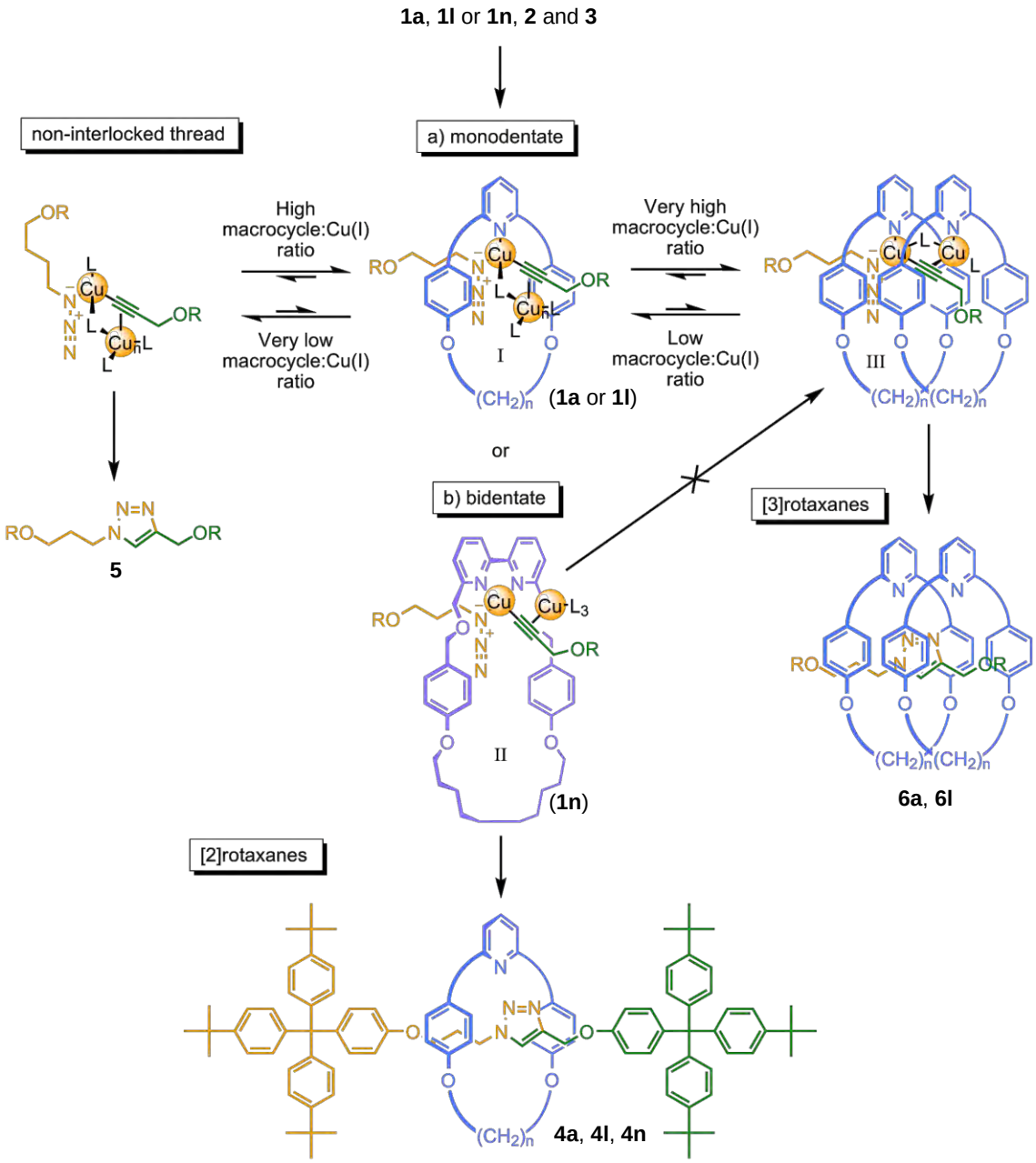

Scheme 2.6 Effect of the macrocycle:Cu(I) ratio on the active-metal template CuAAC reaction.

The ^{1}H NMR spectra of [2]rotaxane **4l** and [3]rotaxane **6l** are shown in parts b and c, respectively, Figure 2.4. The resonances for the axle ($H_{f\text{-}j}$) of the rotaxanes are shifted upfield compared to the signal for the non-interlocked thread **5** (Figure 2.4, a). The effect is more pronounced in the [3]rotaxane (Figure 2.4, c) than in the [2]rotaxane (Figure 2.4, b). Owing to the asymmetry of the thread, the ^{1}H NMR spectrum of [3]rotaxane **6l** displays inequivalent but overlapping peaks for the two macrocycle components, which are twice as intense as those of the corresponding macrocycle signals in the [2]rotaxane.

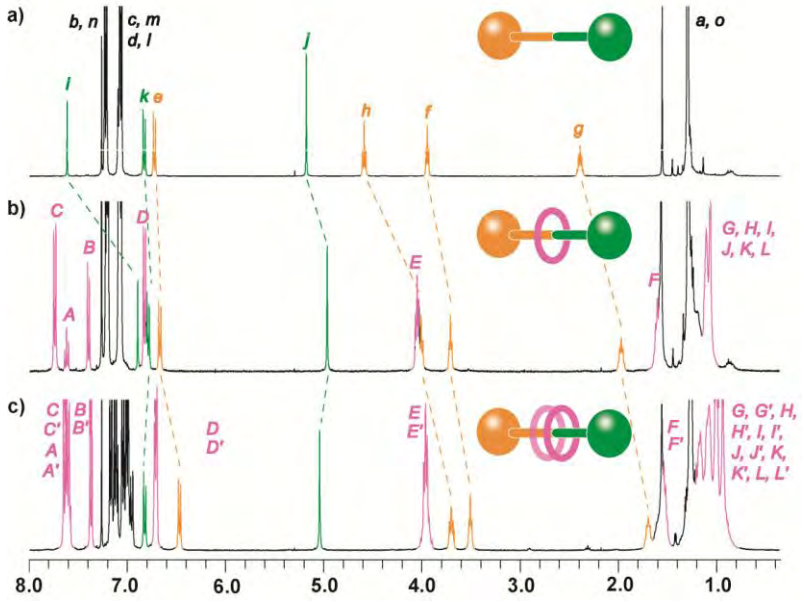

*Figure 2.4 ^{1}H NMR spectra (400 MHz, $CDCl_3$, 298 K) of a) triazole thread **5**, b) [2]rotaxane **4l** and c) [3]rotaxane **6l**. The assignments correspond to the lettering shown in Figure 2.2 and Scheme 2.1.*

2.3.6 Stoichiometric and Catalytic Active-metal Template Synthesis of *Bis*triazole [2]Rotaxanes

To see whether the copper(I) would turn over catalytically during the formation of a single molecule, we investigated systems which require *two* cycloaddition reactions to be catalysed in the formation of one molecule: [2]Rotaxanes **9a** and **11a** were each obtained in good yields (81% and 74%, respectively) using the conditions shown in Scheme 2.1 (0.5 equiv of Cu(I) for each triazole ring formed in a rotaxane) with either **1a**, **2**, and the diazide **7** or **1a**, **3**, and the dialkyne **8**. Since the rotaxane-Cu(I) complex in **4a** is strong enough to sequester the metal in the absence of pyridine, the lack of formation of more than trace amounts of [3]rotaxane in the reaction mixtures suggests that only *one* macrocycle-Cu(I) complex acts processively to catalyse the formation of *two* triazole rings in an individual rotaxane thread. Such observation is consistent with the publication of Rodionov *et al*. in which they reported a strong kinetic enhancement in the second cycloaddition reaction when using diazide reactants (albeit this is in a ligand-free Cu(I) system).[13] Reducing the amount of the copper salt to 0.2 equivalent with respect to **1a** (10 mol % with respect to each triazole ring formed) and utilising 3 equivalents of pyridine in the reaction of **1a**, **2**, and **7** allowed the catalyst to turn over intermolecularly and still generated [2]rotaxane **9a** in 63% yield.

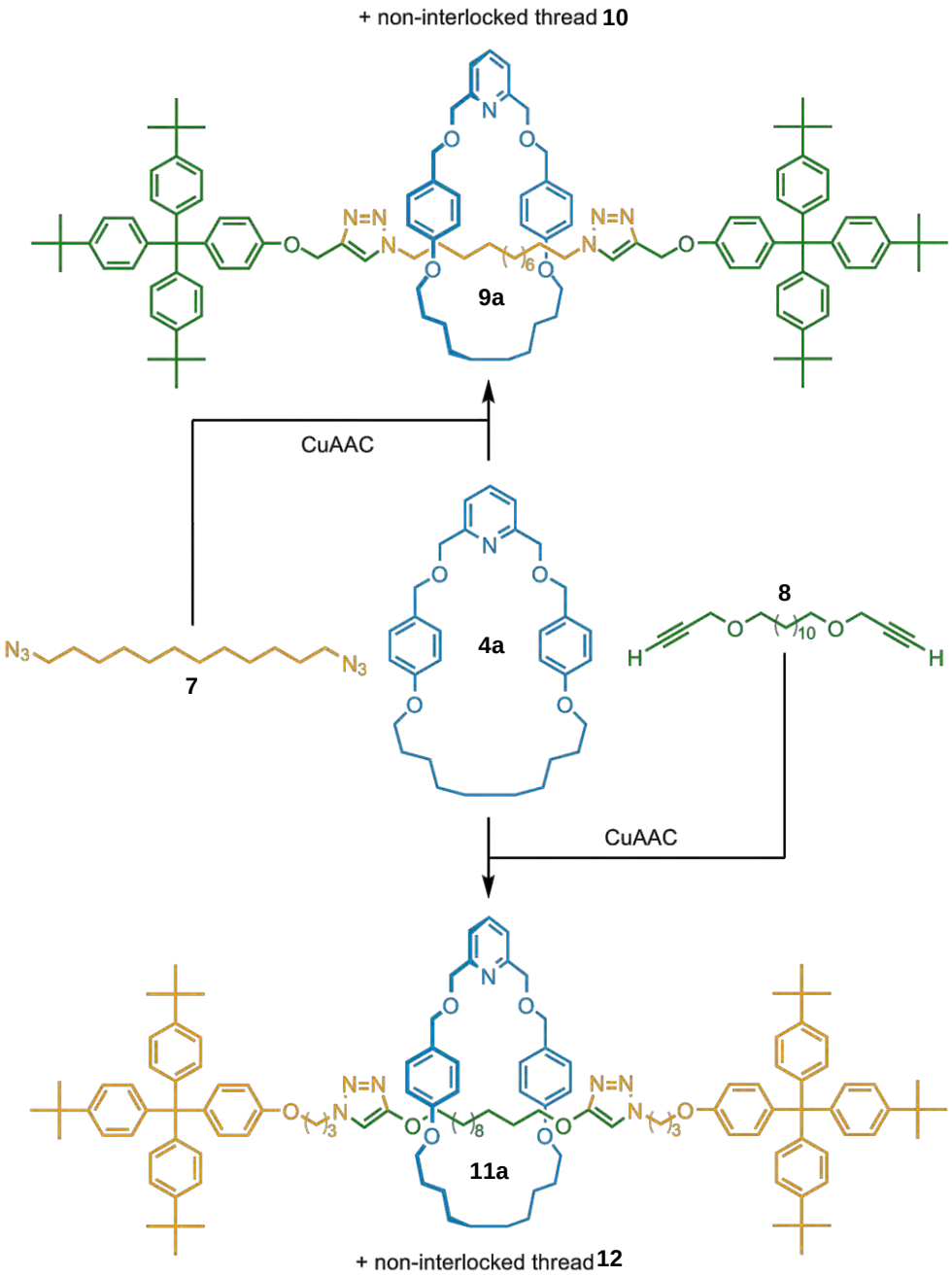

*Scheme 2.7 Synthesis of bistriazole molecular shuttles **9** and **11** via CuAAC.*

2.3.7 Transition Metal-mediated Control of the Shuttling Rate in Degenerate *Bis*Triazole-Station Molecular Shuttles

It proved possible to introduce diamagnetic TM such as Cu(I) or Pd(II) in order to control the shuttling of the ring in the degenerate two-station *bis*-triazole rotaxane **9a.** This was investigated using ^{1}H NMR spectroscopy in d_3-MeCN/$CDCl_3$ 9:1. In contrast with most previously reported molecular shuttles where the interactions used to direct the synthesis of the rotaxanes persist in the interlocked structure, there are no strong

non-covalent interactions between the components of metal-free **9a**. Comparison of the ^{1}H NMR spectrum of the free thread **10** (Figure 2.5, a) with that of the rotaxane **9a** (Figure 2.5, b) shows uniform shielding of the thread signals (H_{d-h}), indicating that the macrocycle randomly explores the full length of the thread. Reintroducing copper(I) into the *bis*-triazole rotaxane[23] to form Cu**9a**PF_6 (Scheme 2.8, top) gave a complex that exhibited fast shuttling of the macrocycle between the two triazole stations in the room temperature ^{1}H NMR spectra (Figure 2.5,*c*). Although fast shuttling between well-defined macrocycle binding sites is very unusual for metal-coordinated molecular shuttles,[24] Cu(I) complexes can exhibit extremely fast exchange rates.[25] Molecular models (Spartan™) have shown that a folded complex, wherein the two triazole rings are together bound to the Cu(I) centre, is viable but very improbable. Indeed, the resulting steric hindrance induced by the presence of both the metal centre and the aliphatic chain (H_{h-m}) inside the macrocycle's cavity makes the formation of this complex very unlikely. Additionally, the NMR spectrum of Cu**9a**PF_6 (Figure 2.5c) exhibits a simple pattern, suggesting a symmetrical structure. A folded form, where the loop created by the aliphatic chain is to one side or the other of the macrocycle, would produce an unsymmetrical complex and its corresponding NMR spectrum would exhibit a more complicated pattern (i.e. splitting of signals such as H_d, H_e, H_f, H_{h-m}). In contrast to the dynamic behaviour of Cu**9a**PF_6, the ^{1}H NMR spectrum (Figure 2.5, d) of rotaxane **9a** following by coordination of $PdCl_2$ (Scheme 2.8, bottom) displays two sets of peaks for protons close to the thread triazole rings (e.g. $H_{f/f'}$, $H_{g/g'}$). The chemical shifts of one set of the duplicated signals (e.g. H_f) correspond closely to those of the free thread **10** (Figure 2.5, a). This observation is indicative of the macrocycle in the Pd**9a**Cl_2 complex being unable to shuttle between the triazole stations on the NMR timescale. This shuttling restriction also manifests itself in the geminal splitting of the H_C and H_D signals of the macrocycle, which occurs as a consequence of the two faces of the ring being in different chemical environments. The chemical shifts of one set of the duplicated signals (e.g. H_f) correspond closely to those of the free thread **10**. The other set of duplicate signals (e.g. $H_{f'}$) correspond closely to a model single-triazole rotaxane-$PdCl_2$ complex, Pd**4a**Cl_2. Heating the sample of Pd**10**Cl_2 to 343 K did not lead to any broadening of the signals, indicating that the macrocycle shuttling is blocked by coordination to a Pd(II) centre. The formation of folded complexes, in this case, is also very unfavourable. Molecular models (Spartan™) demonstrated that the cavity of the macrocycle is too small to accommodate the corresponding aggregate (i.e. the metal

centre, the chloride ligand, the aliphatic chain and both triazole rings in *cis* and *trans* configurations).

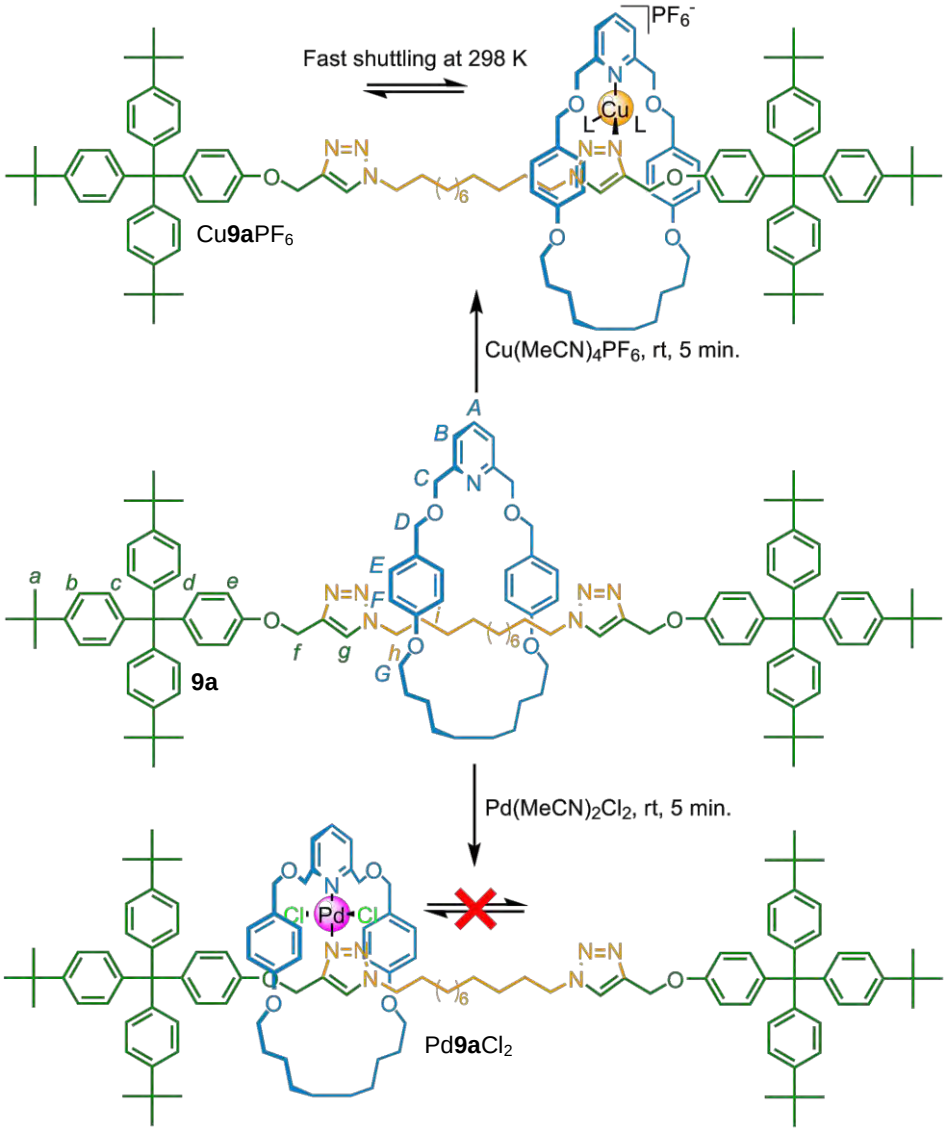

Scheme 2.8 Controlling the dynamics of bis-triazole molecule shuttle ***9a*** *by coordination to Cu(I) or Pd(II).*

The notable features of these degenerate two-station *bis*-triazole rotaxanes are:

(i) To our knowledge these are the first examples of molecular shuttles containing two degenerate transition-metal-binding stations.

(ii) The dynamics of the macrocycle exchange between the two well-defined discrete binding sites can be controlled with remarkable ease, simply through the judicious choice of different transition-metal ions.

(iii) An AMT strategy is much more amendable to the synthesis of such shuttles than traditional (passive) metal template strategies, because the number of recognition sites in the products is not necessarily related to the number of template sites used for the shuttle synthesis.

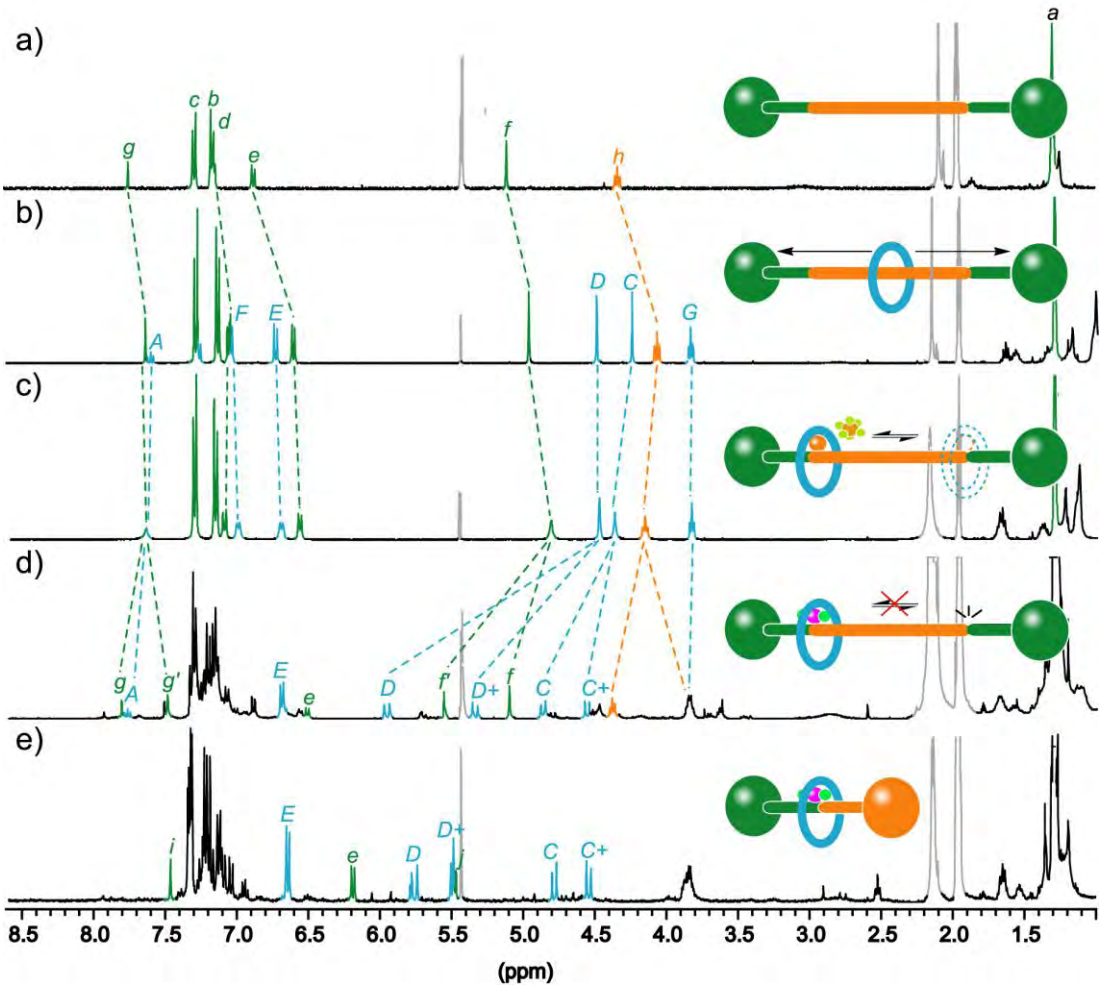

Figure 2.5 ^{1}H NMR spectra (400 MHz, d_3-MeCN/CD_2Cl_2 9:1, 298 K) of a) bis-triazole thread ***10****, b)* bis-*triazole rotaxane* ***9a*** *c) copper-* bis-*triazole rotaxane complex Cu****9a****PF_6, d) palladium-* bis-*triazole rotaxane-dichloride complex Pd****9a****Cl_2, e) palladium-triazole rotaxane-dichloride complex Pd****4a****Cl_2. The assignments correspond to the lettering shown in Scheme 2.8.*

2.4 Conclusion

The Cu(I)-catalysed 1,3-cycloaddition of azides with terminal alkynes is a highly effective reaction for the AMT synthesis of rotaxanes, as illustrated with both stoichiometric (up to 94% yields) and catalytic (up to 82% yields) versions of the strategy. The rotaxane-forming reaction tolerates a wide variety of both monodentate and bidentate macrocyclic ligands, although they inherently make the reaction slower than the ligand-free Cu(I)-catalysed reaction. They are still competitive by

sequestration of the majority of the Cu(I) present in solution. The addition of pyridine enables the Cu(I) active-metal template to turn over without significantly compromising the rotaxane production. Among several potentially attractive features of this type of synthetic strategy is that it offers an unusual experimental probe of the reaction mechanism. The increase in rates of rotaxane formation by an excess of ligand-free Cu(I) supports the suggestion that in CH_2Cl_2 the copper *σ*-acetylide is activated by coordination to a second ligandless copper atom. In addition, the sluggish reaction rates and remarkable formation of [3]rotaxanes with monodentate macrocycles at high macrocycle:Cu(I) ratios suggest that, under these conditions, the CuAAC reaction proceeds *via* a doubly bridged two copper atom intermediate (type IIb, Scheme 2.2) when using a monodentate macrocyclic ligand and *via* a simpler *π*-coordinated two copper atom intermediate (type Ib, Scheme 2.2) when using a bidentate macrocyclic ligand. The experimental results concerning the active-metal template CuAAC synthesis of *bis*-triazole rotaxanes suggest that the macrocycle-Cu(I) complex acts processively to catalyse the formation of more than one triazole ring per thread molecule. The resulting two-triazole-station molecular shuttles have interesting and unusual dynamic properties: coordination of the rotaxane macrocycle to Cu(I) gives a metal-complexed shuttle in which the ring still shuttles rapidly between the two triazole stations, even at low temperatures in non-coordinating solvents. In contrast, complexation of the same two-triazole shuttle to $PdCl_2$ gives a rotaxane in which shuttling does not occur even at 343 K in the presence of d_3-acetonitrile.

2.5 *Experimental Section*

2.5.1 General Procedure for the Formation of AMT-CuAAC Rotaxanes

CAUTION: copper acetylides, which are potential by-products of this reaction, are shock-sensitive when dry. Care should be taken if performing these reactions on a large scale that these are not isolated in other than trace amounts by washing with basic ammonium citrate or dilute HCl.

A solution of macrocycle, (1 equiv.), azide, (1 equiv.), alkyne, (1 equiv.) and $Cu(MeCN)_4PF_6$ (1.1 equiv.) in dry CH_2Cl_2 (5 mL) and under N_2 was stirred at room temperature for 24 h. The resulting mixture was diluted with CH_2Cl_2 (5 mL) and methanol (15 mL). A solution of KCN (10 equiv.) in methanol (2 mL) was added and the resulting suspension stirred vigorously for 1 h. Solvents were evaporated (80 ºC) and the residue was partitioned between water (15 mL) and CH_2Cl_2 (20 mL). The layers

were separated and the aqueous layer was extracted with CH_2Cl_2 (3 × 10 mL). The combined organic fractions were washed with water (10 mL) and brine (10 mL), then dried ($MgSO_4$) and concentrated under reduced pressure. The resulting solid was purified by flash column chromatography and/or preparative TLC to give pure rotaxane.

2.5.2 Preparation of Half-threads

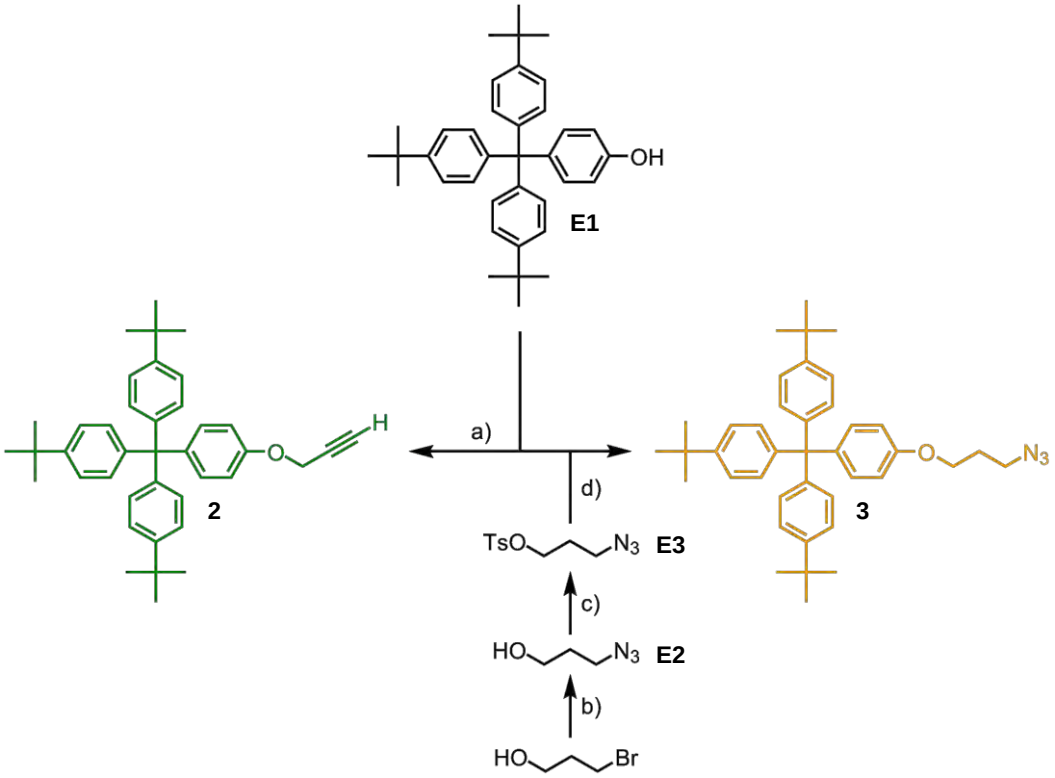

Scheme 2.9 a) Propargyl bromide, K_2CO_3, DMF, 80 °C, 18 h, 95%; b) NaN_3, H_2O, 80 °C, 18 h, 78%; c) p-TsCl, CH_2Cl_2, 0 °C → RT, 18 h, 75%; d) K_2CO_3, butanone, 80 °C, 18 h, 75%.

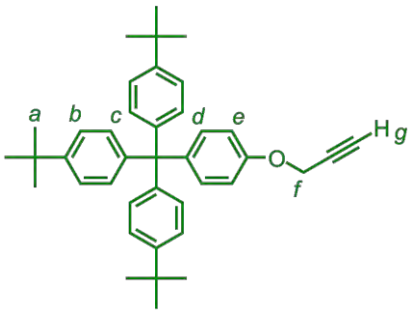

1-(prop-3-ynoxy)-4-(*tris*-(4-*tert*-butyl-phenyl)-methyl)-benzene (2)

To a solution of 4-[*tris*-(4-*tert*-butyl-phenyl)-methyl]-phenol (**E1**)[26] (1.60 g, 3 mmol, 1 equiv.) and propargyl bromide (80 % solution in toluene, 0.49 mL, 4.5 mmol, 1.5 equiv.) in DMF (30 mL) was added potassium carbonate (2.08 g, 15 mmol, 5 equiv.). The

suspension was heated at 80 °C for 18 h under an atmosphere of nitrogen. After cooling, the solution was concentrated under reduced pressure then diluted with water (30 mL) and extracted with EtOAc (3 x 20 mL). The resulting yellow solid was recrystallized from 5% $CHCl_3$ in MeCN to give the expected alkyne as a colorless solid. (1.53 g, 95%). m.p. 267-269°C (dec.); ^{1}H NMR (400 MHz, $CDCl_3$, 298 K): δ = 1.30 (s, 27H, H_a), 2.62 (t, 1H, *J* = 2.4 Hz, H_g), 4.66 (d, 2H, *J* = 2.4 Hz, H_f), 6.84 (d, 2H, *J* = 8.9 Hz, H_e), 7.07 (d, 6H, *J* = 8.6 Hz, H_b), 7.11 (d, 2H, *J* = 8.9 Hz, H_d), 7.23 (d, 6H, *J* = 8.6 Hz, H_c); ^{13}C NMR (100 MHz, $CDCl_3$, 298 K): δ = 31.4, 34.1, 55.8, 63.1, 75.4, 78.8, 113.3, 124.1, 130.7, 132.3, 140.5, 144.0, 148.4, 155.5; LRFAB-MS (3-NOBA matrix): *m/z* = 542 $[M]^+$; HRFAB-MS (3-NOBA matrix): *m/z* = 542.35433 $[M]^+$ (calcd. for $C_{40}H_{46}O$, 542.35487).

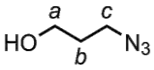

3-azido-propan-1-ol (E2)

To a solution of 3-bromo-propan-1-ol (1.92 g, 13.8 mmol, 1 equiv.) in water (40 mL) was added sodium azide (1.80 g, 28.0 mmol, 2 equiv.) and the solution was heated at 80 °C for 18 h. The aqueous solution was extracted with EtOAc (5 x 40 mL). The organic layers were washed with brine (30 mL), dried over $MgSO_4$, filtered and concentrated under reduced pressure* to give pure 3-azido-propanol as a colorless oil (1.09 g, 78%). ^{1}H NMR (400 MHz, $CDCl_3$, 298 K): δ = 3.76 (t, 2H, *J* = 6.0 Hz, H_a), 3.45 (t, 2H, *J* = 6.6 Hz, H_c), 1.79-1.87 (m, 2H, H_b); LRESI-MS: m/z = 102 $[M+1]^+$.

** as low molecular weight organic azides have been reported as potential explosives, care must be taken during the concentration operation. The authors used a standard PVC blast shield.*

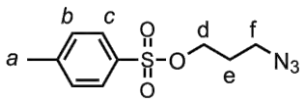

3-azidopropyl tosylate (E3)

A solution of 3-azido-propan-1-ol (1.09 g, 10.8 mmol, 1 equiv.) and Et_3N (3.04 mL, 21.6 mmol, 2 equiv.) in CH_2Cl_2 (100 mL) was cooled to 0 °C. *p*-Toluenesulfonyl chloride (2.17 g, 11.4 mmol, 1.05 equiv.) was added and the solution was stirred at RT for 18 h. The reaction was quenched with water (50 mL). The organic layer was separated, dried over $MgSO_4$, filtered, concentrated under reduced pressure and the resulting crude oil was purified by column chromatography (Petrol/CH_2Cl_2 9:1 to 5:5) to yield 3-azidopropyl tosylate as a colorless oil (2.06 g, 75%). ^{1}H NMR (400 MHz, $CDCl_3$, 298 K): δ = 7.78 (d, 2H, *J* = 8.1 Hz, H_c), 7.35 (d, 2H, *J* = 8.1 Hz, H_b), 4.09 (t, 2H, *J* = 6.5 Hz, H_d), 3.75

(t, 2H, J = 6.3 Hz, H_f), 2.47 (s, 3H, H_a), 1.85-1.95 (m, 2H, H_e); ^{13}C NMR (100 MHz, $CDCl_3$, 298 K): 145.1, 132.7, 130.0, 127.9, 67.0, 47.3, 28.4, 21.7; LRESI-MS: m/z = 256 $[M+1]^+$.

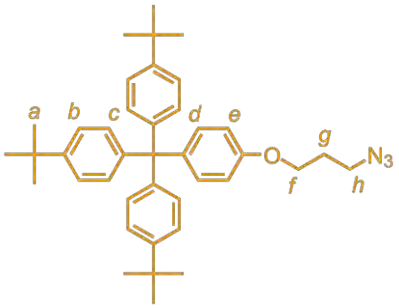

1-(3-azido-propoxy)-4-(*tris*-(4-*tert*-butyl-phenyl)-methyl)-benzene (3)

To a solution of 4-[*tris*-(4-*tert*-butyl-phenyl)-methyl]-phenol (**E1**)[26] (1.30 g, 2.58 mmol, 1 equiv.) and 3-azidopropyl tosylate (**E3**) (658 mg, 2.58 mmol, 1 equiv.) in butanone (25 mL), was added potassium carbonate (1.78 g, 12.9 mmol, 5 equiv.). The suspension was heated at 80 °C for 18 h under an atmosphere of nitrogen. After cooling, the solution was filtrated through a sintered glass funnel then concentrated under reduced pressure. The resulting yellow solid was purified by column chromatography (Petrol/CH_2Cl_2 7:3) to yield azide **3** as a colorless solid (1.14 g, 75%). m.p. 212-214 °C; ^{1}H NMR (400 MHz, $CDCl_3$, 298 K): δ = 7.30 (d, 6H, J = 8.6 Hz, H_c), 7.09 (d, 2H, J = 8.9 Hz, H_d), 7.08 (d, 6H, J = 8.6 Hz, H_b), 6.76 (d, 2H, J = 8.9 Hz, H_e), 4.02 (d, 2H, J = 6.0 Hz, H_h), 3.51 (d, 2H, J = 6.7 Hz, H_f), 2.00-2.07 (m, 2H, H_g), 1.30 (s, 27H, H_a); ^{13}C NMR (100 MHz, $CDCl_3$, 298 K): δ = 28.8, 31.4, 34.3, 48.3, 63.0, 64.3, 112.9, 124.1, 130.7, 132.3, 139.9, 144.1, 148,3, 156.4 ; LRFABMS (3-NOBA matrix): m/z = 588 $[M+H]^+$; HRFAB-MS (3-NOBA matrix): m/z = 587.38756 $[M]^+$ (calcd. for $C_{40}H_{49}N_3O$, 587.38747).

2.5.3 Preparation of Macrocycles

The syntheses presented in this section are the ones specifically made (or remade) by the author. For the synthesis of all the macrocycles, please see reference 19.

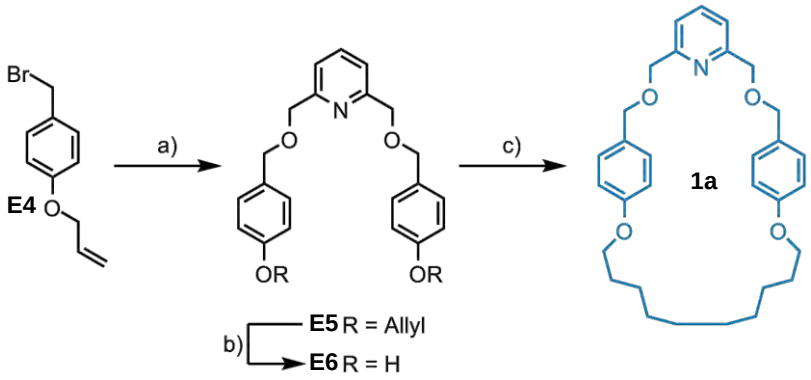

Scheme 2.10 a) 2,6-bis(hydroxymethyl)pyridine, NaH,, DMF, 0 °C → RT, 16 h, 72%; b) $Pd(PPh_3)_4$, aniline, 30 °C, 2 h, 78%; c) 1,10-dibromodecane, K_2CO_3, DMF, 65 °C, 16 h, 35%.

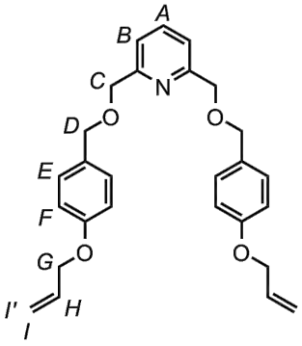

E5

To a suspension of 2,6 pyridine dimethanol (12.0 g, 90 mmol, 1 equiv.) in DMF (1.4 L) at 0 °C was added NaH (60% dispersion in mineral oil, 10.4 g, 260 mmol, 2.9 equiv.) and the mixture stirred until effervescence ceased. 1-Allyloxy-4-bromomethylbenzene (**E4**)[27] (58.0 g, 260 mmol, 2.9 equiv.) was added, the cooling bath removed and the mixture was stirred at RT for 16 h. The reaction mixture was partitioned between H_2O (500 mL) and $CHCl_3$/*i*PrOH (3:1, 500 mL) and the layers separated. The aqueous phase was extracted with $CHCl_3$/*i*PrOH (3:1, 2 × 500 mL), the organic layers combined, dried ($MgSO_4$) and the solvent removed under reduced pressure. Chromatography (Gradient, CH_2Cl_2 to MeOH/CH_2Cl_2, 2:98) gave **E5** as a pale yellow oil (25 g, 72%). ^{1}H NMR (400 MHz, $CDCl_3$, 298 K): δ = 7.77 (t, 1H, *J* = 7.8 Hz, H_A), 7.45 (d, 2H, *J* = 7.8 Hz, H_B), 7.37 (d, 4H, *J* = 8.6 Hz, H_F), 6.97 (d, 4H, *J* = 8.7 Hz, H_E), 6.13 (tdd, 2H, *J* = 17.2, 10.5, 5.31 Hz, H_H), 5.48 (dq, 1H, *J* = 17.24, 1.53 Hz, H_I), 5.36 (dq, 2H, *J* = 10.5, 1.30 Hz, one of $H_{I'}$), 4.71 (s, 4H, H_C), 4.64 (s, 4H, H_D), 4.61 (dt, 4H, *J* = 5.3, 1.5 Hz, H_G): ^{13}C NMR (100 MHz, $CDCl_3$, 298 K): δ = 157.7 (x 2), 137.2, 133.2, 129.5, 120.0, 117.7, 114.7, 72.8, 72.6, 68.8; LRESI-MS (MeOH/TFA): *m/z* = 432 $[M+H]^+$.

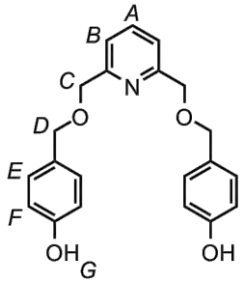

E6

To a solution of diallyl ether **E5** (25 g, 60 mmol, 1 equiv.) in THF (80 mL) was added aniline (6.2 mL, 68 mmol, 1.1 equiv.) then $Pd(PPh_3)_4$ (2.8 g, 2.4 mmol, 0.04 equiv.) and the mixture stirred at 30 °C for 2 h. The mixture was partitioned between H_2O (500 mL) and $CHCl_3$/*i*PrOH (3:1, 500 mL) and the layers separated. The organic phase was washed with H_2O (500 mL) then brine (500 mL), dried ($MgSO_4$) and the solvent concentrated under reduced pressure. Chromatography (Gradient, CH_2Cl_2 then CH_2Cl_2/acetone 95:5) gave **E6** as a pale yellow solid (16.4 g, 78%). M.p. 53-57 °C; ^{1}H NMR (400 MHz, d_4-MeOD, 298 K): δ = 7.79 (t, 1H, *J* = 7.8 Hz, H_A), 7.40 (d, 2H, *J* = 7.8 Hz, H_B), 7.19 (d, 4H, *J* = 8.5 Hz, H_F), 6.76 (d, 4H, *J* = 8.5 Hz, H_E), 4.56 (s, 4H, H_C), 4.50 (s, 4H, H_D); 13C NMR (100 MHz, d_4-MeOD, 298 K): δ = 159.0, 158.2, 139.1, 130.8, 129.8, 121.7, 116.0, 73.7, 72.9; LRESI-MS (MeOH/TFA): *m/z* = 352 $[M+H]^+$.

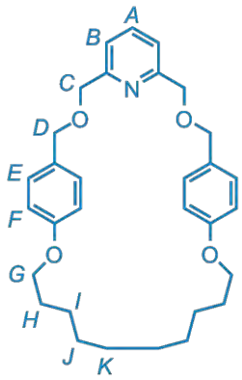

1a

K_2CO_3 (12 g, 87 mmol, 8.3 equiv.) was added to a stirred solution of diphenol **E6** (3.70 g, 10.5 mmol, 1 equiv.) and 1,10-dibromodecane (3.16 g, 10.5 mmol, 1 equiv.) in DMF (1.8 L) and the mixture heated at 65 °C for 16 h. The solvent was removed under reduced pressure and the residue partitioned between brine (500 mL) and EtOAc (500 mL) and the layers separated. The aqueous phase was extracted with CH_2Cl_2 (2 × 500 ml), the organic layers combined, dried ($MgSO_4$) and the solvent removed under reduced pressure. Chromatography (Gradient, CH_2Cl_2 then 99:1 CH_2Cl_2/acetone) gave macrocycle **1a** as a white solid (1.8 g, 35%). M.p. 61-62 °C; ^{1}H NMR (400 MHz, $CDCl_3$, 298 K): δ = 7.69 (t, 1H, *J* = 7.8 Hz, H_A), 7.36 (d, 2H, *J* = 7.8 Hz, H_B), 7.23 (d, 4H, *J* = 8.6 Hz, H_E), 6.80 (d, 4H, *J* = 8.6 Hz, H_F), 4.60 (s, 4H, H_C), 4.43 (s, 4H, H_D), 3.97 (t, 4H, *J* = 6.3 Hz, H_G), 1.73 (m, 4H, H_H), 1.22-1.48 (m, 12H, H_I, H_J and H_K); ^{13}C NMR (100 MHz, $CDCl_3$, 298 K): δ = 158.7, 157.7, 137.1, 130.0, 129.2, 119.9, 114.5, 72.2, 71.2, 67.3, 29.3, 28.6, 28.5, 25.6. LRESI-MS (MeOH/TFA): *m/z* = 490 $[M+H]^+$.

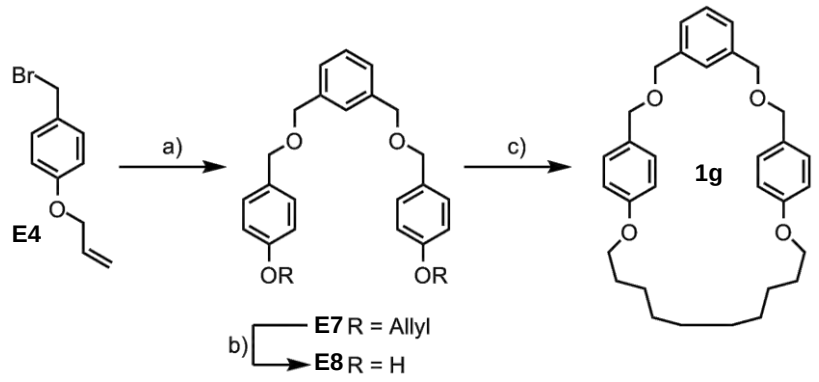

Scheme 2.11 a) 1,3-bis(bromomethyl)benzene, NaH, THF, Reflux, 40 h; b) Pd/C, KOH, MeOH, Reflux, 24h, 60% (over 2 steps); c) 1,10-dibromodecane, K_2CO_3, butanone, reflux, 24 h, 20%.

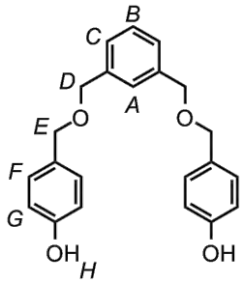

E8

To a solution of 1-Allyloxy-4-hydroxymethyl-benzene (**E4**)[27] (6.56 g, 0.04 mol, 2.5 equiv.) and 1,3-*bis*(bromomethyl)benzene (4.10 g, 0.016 mmol, 1.0 equiv.) in THF (150 mL) under a nitrogen atmosphere was added NaH (5.00 g, 60% dispersion in mineral oil, 0.128 mol, 8.0 equiv.). The reaction was refluxed for 40 h. The solvents were removed under reduced pressure and the resulting oil was dissolved in CH_2Cl_2 (20 mL) and washed with a saturated aqueous NH_4Cl solution (2 × 100 mL), saturated aqueous NaCl solution (2 x 100 mL). The organic layer was dried with $MgSO_4$, filtered, concentrated under reduced pressure then passed through a plug of silica to yield the corresponding diallyl ether U-shape **E7** as a yellow oil (4.10 g). Without further purification, this oil was dissolved into CH_2Cl_2 (75 mL) and 10 % KOH/MeOH (75 mL). 10% Pd/C (0.80 g, 0.2 equiv.) was added and the resulting mixture was refluxed for 24 h. The reaction mixture was cooled to room temperature and filtered through celite. The solvents were removed under reduced pressure and the resulting yellow oil was purified by flash column chromatography (CH_2Cl_2/Et_2O 9:1) to give the diphenol U-shape **E8** as a clear oil (2.05 g, 60%). ^{1}H NMR (400 MHz, $CDCl_3$, 298 K):): δ = 7.36 (s, 1H, H_A), 7.23-7.33 (m, 3H, H_B and H_C), 7.15 (d, *J* = 8.48 Hz, 4H, H_F), 6.65 (d, *J* = 8.52 Hz, 4H, H_G), 6.19 (s, 2H, H_H), 4.52 (s, 4H, H_D), 4.43 (s, 4H, H_E). ^{13}C NMR (100 MHz, $CDCl_3$, 298

K): δ = 155.5, 138.2, 129.9 (x 2), 129.6, 128.6, 127.4, 115.4, 71.8, 71.7; LRESI-MS (MeOH, NH_3): *m/z* = 349 $[M-H]^-$; HRFAB-MS (3-NOBA matrix): *m/z* = 350.15140 $[M]^+$ (calc. for $C_{22}H_{22}O_4$ 350.15181).

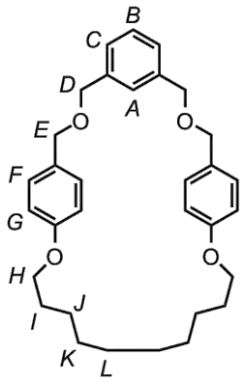

1g

To a solution of **E8** (285 mg, 0.82 mmol, 1 equiv.) and 1,10-dibromodecane (243 mg, 0.82 mmol, 1 equiv.) in butanone (900 mL) was added potassium carbonate (570 mg, 4.1 mmol, 5 equiv.). The suspension was heated at 80 °C for 18 hours under a nitrogen atmosphere. After cooling, the suspention was concentrated under reduced pressure and the residue was dissolved in CH_2Cl_2 (50 mL). The organic layer was washed with water (3 x 50 mL), dried ($MgSO_4$), filtered and concentrated under reduced pressure. The resulting yellow oil was purified by flash column chromatography (petrol-CH_2Cl_2 95:5 to 0:100 then petrol/AcOEt 96:4 to 92:8) to yield the macrocycle **1g** as a colourless solid (75 mg, 20%). M.p. 46-48 °C, ^{1}H NMR (400 MHz, $CDCl_3$, 298 K): δ = 7.30-7.34 (m, 3H, H_B, H_C), 7.28 (s, 1H, H_A), 7.25 (d, *J* = 8.5 Hz, 4H, H_F), 6.86 (d, *J* = 8.6 Hz, 4H, H_G), 4.49 (s, 4H, H_E), 4.48 (s, 4H, H_D), 3.98 (t, *J* = 6.3 Hz, 4H, H_H), 1.73-1.82 (m, 4H, H_I), 1.41-1.52 (m, 4H, H_J), 1.28-1.38 (m, 8H, H_K and H_L). ^{13}C NMR (100 MHz, $CDCl_3$, 298 K): δ = 158.1, 138.0, 129.4, 129.0, 127.7, 126.4, 126.3, 113.9, 71.2, 70.7, 67.0, 28.0, 27.9, 27.6, 24.9; LRFAB-MS (3-NOBA matrix): *m/z* = 488 $[M]^+$; HRFAB-MS (THIOG matrix): m/z = 488.29291 $[M]^+$ (calc. for $C_{32}H_{40}O_4$ 488.29266).

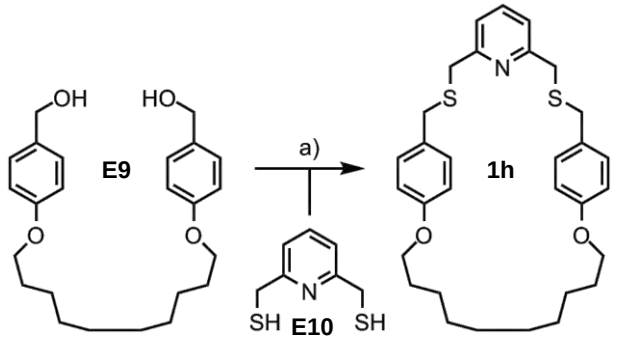

Scheme 2.12 a) TFA, CH_2Cl_2, RT, 20 h, 12%.

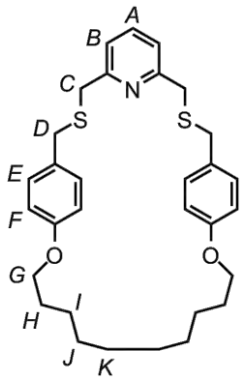

1h

To a solution of pyridine 2,6-di-methanethiol (**E10**)[28] (128 mg, 0.75 mmol, 1 equiv.) and 1,10-(4-hydroxymethyl-phenoxy)-decane (**E9**)[17b] (289 mg, 0.74 mmol, 1.0 equiv.) in CH_2Cl_2 (500 mL) under N_2 atmosphere was added TFA (10 mL). The reaction was stirred at room temperature for 20 h. Solvents were removed under reduced pressure, the resulting oil was dissolved in CH_2Cl_2 (20 mL) and washed with a saturated aqueous $KHCO_3$ solution (2 × 5mL). The organic layer was dried ($MgSO_4$), filtered, concentrated under reduced pressure then purified by flash column chromatography (petrol/CH_2Cl_2 35:65 then 25:75) to give the macrocycle **1h** as a yellow solid (48 mg, 12%). M.p. 69-73°C; ^{1}H NMR (400 MHz, $CDCl_3$, 298 K): δ = 7.64 (t, 1H, *J* = 7.7 Hz, H_A), 7.31 (d, 2H, *J* = 7.7 Hz, H_B), 7.22 (d, 4H, *J* = 8.6 Hz, H_E), 6.79 (d, 4H, *J* = 8.6 Hz, H_F), 3.93 (t, 4H, *J* = 6.3 Hz, H_G), 3.70 (s, 4H, H_D), 3.6 (s, 4H, H_C), 1.75 (dt., 4H, *J* = 6.8, 6.8 Hz, H_H), 1.51-1.41 (m, 4H, H_I), 1.39-1.29 (m, 8H, H_J, H_K); 13C NMR (100 MHz, $CDCl_3$, 298 K): δ = 158.0 (× 2), 137.5, 130.1, 129.8, 121.1, 114.4, 67.5, 36.5, 34.8, 28.5, 28.0, 27.7, 25.2; LRFAB-MS (3-NOBA matrix): *m/z* = 522 $[M+H]^+$; HRFAB-MS (3-NOBA matrix): *m/z* = 522.25074 $[M+H]^+$ (calc. for $C_{31}H_{40}NO_2S_2$ 522.25005).

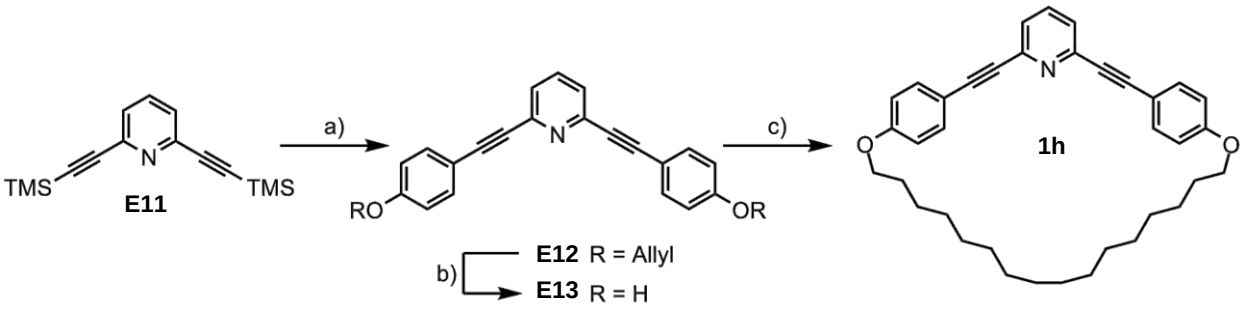

Scheme 2.13 a) 4-allyloxyiodobenzene, $Pd(PPh_3)_2Cl_2$, CuI, benzene, H_2O, DABCO, RT, 20 h,[29] b) Pd/C, KOH, MeOH, reflux, 24 h, 60%; c) 1,16-bis-(O-tosyl)hexadecane,[30] K_2CO_3, butanone, reflux, 24 h, 10%.

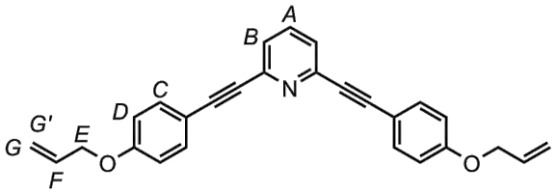

E12

2,6-*bis*{(trimethylsilyl)ethynyl}pyridine,[31] (2.00 g, 7.38 mmol, 1 equiv.) and 4-allyloxyiodophenol (4.70 g, 18.50 mmol, 2.5 equiv.) were dissolved in benzene (25 mL). $Pd(PPh_3)_2Cl_2$ (0.50 g, 0.71 mmol. 0.1 equiv.) and CuI (0.30 g, 1.57 mmol. 0.2 equiv.) were added as solids, and the reaction flask was sealed with a septum and purged with nitrogen. DBU (6.73 g, 44.2 mmol, 6 equiv.) and H_2O (0.053 g, 2.95 mmol, 0.4 equiv.) were added to the reaction mixture and the resulting brown solution was stirred at room temperature for 20 h, during which time a white prepitate formed and the color of the solution became black. The reaction mixture was quenched with water (10 mL) and extracted with EtOAc (3 × 50ml). The organic layer was then washed with an aqueous saturated NH_4Cl solution (2 × 50 ml), and brine (2 × 50 ml). The combined organic fractions were dried ($MgSO_4$), filtered, concentrated under reduced pressure then subjected to flash column chromatography (Et_2O) to give a tan coloured solid. This tan coloured material was washed with boiling hexanes to provide the diallylprotected-U-shape **E12** as a white solid (1.70 g, 70 %). M.p 138-140 °C; ^{1}H NMR (400 MHz, $CDCl_3$, 298 K): δ = 7.52 (t, 1H, *J* = 7.8 Hz, H_A), 7.41 (d, 4H, *J* = 8.9 Hz, H_D), 7.29 (d, 2H, *J* = 7.8 Hz, H_B), 6.77 (d, 4H, *J* = 8.9 Hz, H_C), 5.93 (m, 2H, H_F), 5.30 (dd, 2H, *J* = 1.6, 17.3 Hz, H_G), 5.19 (dd, 2H, *J* = 1.3 Hz, 10.5 Hz, $H_{G'}$), 4.44 (td, 4H, *J* = 1.5 Hz, Hz H_E); ^{13}C NMR (100 MHz, $CDCl_3$, 298 K): δ = 159.2, 144.0, 136.3, 133.6, 132.7, 125.7, 118.0, 114.8, 114.3, 89.8, 87.4, 68.8; LRESI-MS (MeOH/TFA): *m/z* = 392 $[M+H]^+$.

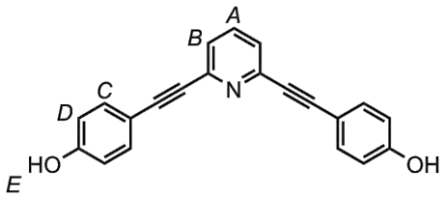

E13·HCl

Diallylprotected U-shape **E12** (0.50 g, 1.27 mmol, 1 equiv.) was dissolved in a mixture of CH_2Cl_2 (20 mL) and 10 % KOH/MeOH (20 mL). 10% Pd/C (0.10 g, 0.2 equiv.) was added and the resulting suspension was refluxed for 24 h, after which time the reaction mixture was cooled to room temperature and filtered through celite. The solvents were removed under reduced pressure and then resulting yellow oil was purified by flash column chromatography (Et_2O) to give the diphenol U-shape **E13** as a yellow oil. This was dissolved into a mixture of EtOAc/Et_2O 1:1 and excess HCl in Et_2O was added to preciptate a yellow/ orange solid. This solid was recrystallised from MeOH/Et_2O to provide **E13**·HCl as a yellow solid (0.20 g, 60%). M.p. 192-194 °C (dec.); ^{1}H NMR (400 MHz, d_4-MeOD, 298 K): δ = 8.50 (t, 1H, *J* = 8.1 Hz, H_A), 8.04 (d, 2H, *J* = 8.1 Hz, H_B), 7.86 (d, 4H, *J* = 8.8 Hz, H_C), 7.06 (d, 4H, *J* = 8.8 Hz, H_D), 4.74 (s, 3H, H_E and HCl) 13C NMR (100 MHz, d_4-MeOD): δ = 164.2, 148.1, 140.7, 137.8, 131.0, 119.2, 113.1, 105.5, 83.3; LRESI-MS (MeOH): *m/z* = 312 $[M+H-Cl]^+$; HRFAB-MS (THIOG matrix): *m/z* = 312.10249 $[M+H]^+$ (calc. for $C_{21}H_{14}NO_2$ 312.10245).

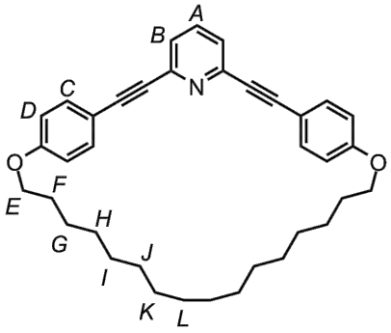

1k

To a solution of **E13**·HCl (150 mg, 0.43 mmol, 1 equiv.) and 1,16-*Bis*-(O-tosyl) hexadecane[30] (243 mg, 0.43 mmol, 1 equiv.) in butanone (600 mL) was added potassium carbonate (297 mg, 2.15 mmol, 5 equiv.). The suspension was heated at 80 °C for 18 hours under nitrogen atmosphere. After cooling, the suspension was concentrated under reduced pressure and the residue was extracted with CH_2Cl_2 (100 mL). The organic layer was washed with water (3 x 50 mL), dried ($MgSO_4$) filtered and

concentrated under reduced pressure. The resulting yellow solid was purified by column chromatography (AcOEt/petrol 1:9 to 2:8) to yield the macrocycle **1k** as a white solid (5 mg, 2 %). M.p. 130-132 °C. ^{1}H NMR (400 MHz, $CDCl_3$, 298 K): δ = 7.66 (t, *J* = 7.8 Hz, 1H, H_A), 7.51 (d, *J* = 8.8 Hz, 4H, H_C), 7.36 (d, *J* = 7.8 Hz, 2H, H_B), 6.87 (d, *J* = 8.8 Hz, 4H, H_D), 4.17 (t, *J* = 6.6 Hz, 4H, H_E), 1.62-1.73 (m, 4H, H_F), 1.13-1.39 (m, 24H, H_{G-L}). ^{13}C NMR (100 MHz, $CDCl_3$, 298 K): δ = 210.5, 136.6, 133.5, 124.2, 115.4, 103.4, 90.0, 87.8, 85.6, 67.8, 30.6, 30.4 (x 2), 29.6, 29.1, 27.9, 25.2. LRESI-MS (MeOH/TFA): *m/z* = 534 $[M+H]^+$; LRFAB-MS (3-NOBA matrix): *m/z* = 534.33775 $[M+H]^+$ (calc. for $C_{37}H_{44}NO_2$: 534.33720).

2.5.4 Preparation of CuAAC-AMT Rotaxanes

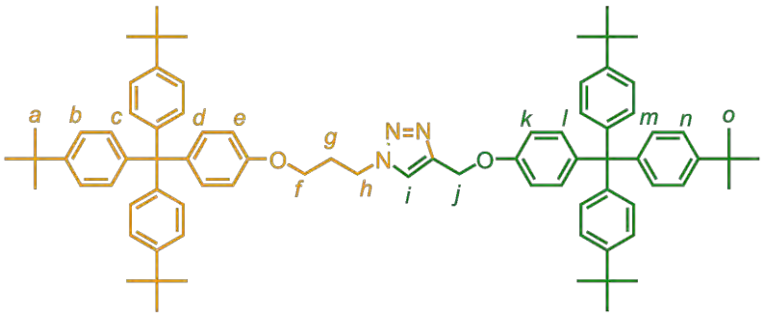

5

Spectroscopic data of the non-interlocked thread **5** generated during AMT-CuAAC rotaxane-formation reactions: ^{1}H NMR (400 MHz, $CDCl_3$, 298 K): δ = 7.61 (s, 1H, H_i), 7.21 (d, 12H, *J* = 8.5 Hz, H_b, H_n), 7.03-7.11 (m, 16H, H_c, H_d, H_m, H_l), 6.82 (d, 2H, *J* = 8.9 Hz, H_k), 6.72 (d, 2H, *J* = 8.9 Hz, H_e), 5.17 (s, 2H, H_j), 4.59 (t, 2H, *J* = 6.9 Hz, H_h), 3.94 (t, 2H, *J* = 5.5 Hz, H_f), 1.23-1.43 (m, 2H, *J* = 6.26 Hz, H_g), 1.29 (s, 54H, H_a and H_o). ^{13}C NMR (100 MHz, $CDCl_3$, 298 K): δ = 156.1, 156.0, 148.3 (×2), 144.3, 144.0 (×2), 140.1 (×2), 132.3 (×2), 130.6 (×2), 124.0 (×2), 123.1, 113.2, 112.9, 63.7, 63.0 (×2), 61.9, 47.2, 34.2 (×2), 31.3 (×2), 29.9; HRFAB-MS (3-NOBA matrix): *m/z* = 1130.75171 $[M+H]^+$ (calcd. for $C_{80}H_{96}N_3O_2$, 1130.75025).

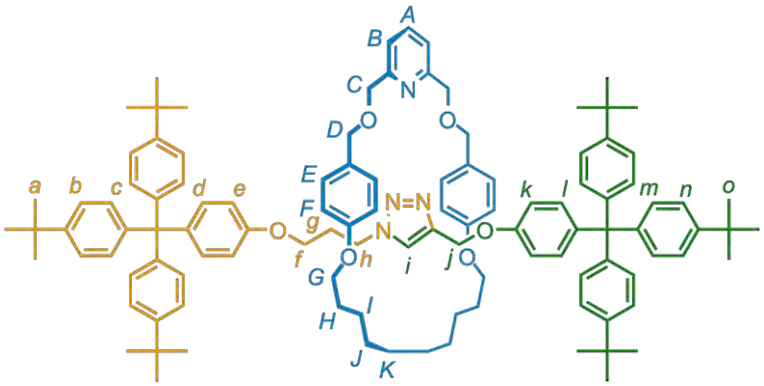

4a

Following the general procedure with macrocycle **1a** (100 mg, 0.2 mmol, 1 equiv.) alkyne **2** (542 mg, 1.0 mmol, 5.0 equiv.), azide **3** (587 mg, 1 mmol, 5.0 equiv.), $Cu(CH_3CN_4)PF_6$ (75 mg, 0.2mmol, 1 eq) and KCN (130 mg, 2.0 mmol, 10.0 equiv.). Purification by column chromatography (CH_2Cl_2 then a gradient from 5 to 20 % MeCN in CH_2Cl_2) gave pure rotaxane **4a** as a colorless solid (180 mg, 54%). ^{1}H NMR (400 MHz, $CDCl_3$, 298 K): δ = 7.50 (t, 1H, *J* = 7.7 Hz, H_A), 7.31 (s, 1H, H_i), 7.22-7.30 (m, 14H, H_B, H_b and H_n), 7.09-7.17 (m, 12H, H_m and H_c), 7.08 (d, 2H, *J* = 8.6 Hz, H_l), 7.04 (d, 2H, *J* = 8.6 Hz, H_d), 6.97 (d, 4H, *J* = 8.3 Hz, H_E), 6.77 (d, 2H, *J* = 8.6 Hz, H_k), 6.56 (d, 4H, *J* = 8.3 Hz, H_F), 6.48 (d, 2H, *J* = 8.6 Hz, H_e), 4.91 (br s, 2H, H_j), 4.49 (br s, 4H, H_D), 4.31 (bs, 4H, H_C), 3.76-3.87 (m, 4H, H_G), 3.71 (t, 2H, *J* = 7.1 Hz, H_h), 3.34 (t, 2H, *J* = 5.4 Hz, H_f), 1.61-1.73 (m, 4H, H_H), 1.54-1.62 (m, 2H, H_g), 1.34 (s, 27H, H_a or H_o), 1.33 (s, 27H, H_a or H_o), 1.17-1.41 (m, 12H, H_I, H_J and H_K); ^{13}C NMR (100 MHz, $CDCl_3$, 298 K): δ = 158.8, 157.7, 156.4 (× 2), 146.4 (×2), 144.4, 144.3, 143.5, 139.9, 139.7, 137.3, 132.3, 132.1, 130.1, 130.0, 129.1 (× 2), 124.2, 124.1, 123.6, 120.2, 114.4, 113.3, 113.1, 72.6, 71.4, 67.2, 64.0 (× 2), 63.2, 61.6, 46.7, 34.4, 34.3, 31.5 (× 2), 29.7, 29.5, 28.7 (× 2), 25.8; LRESI-MS: *m/z* = 1619 $[M+H]^+$; HRFAB-MS (3-NOBA matrix): m/z = 1621.04087 $[M+1+H]^+$ (calcd. for $^{13}C^{12}C_{110}H_{135}N_4O_6$, 1621.04152).

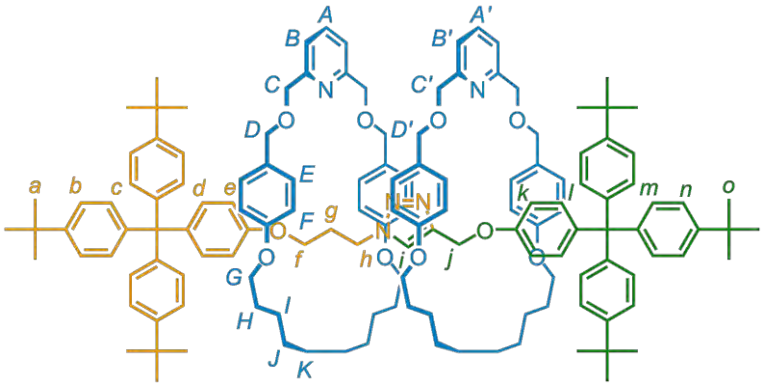

6a

A solution of macrocycle **1a** (400 mg, 0.817 mmol, 10 equiv.), alkyne **2** (48.0 mg, 8.17 µmol, 1.0 equiv.), azide **3** (44.3 mg, 8.17 µmol, 1.0 equiv.), $Cu(MeCN)_4PF_6$ (30.0 mg, 38.5 µmol, 1.0 equiv.) in dry CH_2Cl_2 (10 mL) and under N_2 was stirred at RT for 72 h. The solution was refluxed for further 48 h then cooled to RT. The resulting mixture was diluted with CH_2Cl_2 (15 mL) and methanol (25 mL). A solution of KCN (106 mg, 1.63 mmol, 20 equiv.) in methanol (2 mL) was added and the resulting suspension stirred vigorously for 2 h. Solvents were evaporated (80 °C) and the residue was partitioned between water (15 mL) and CH_2Cl_2 (20 mL). The layers were separated and the aqueous layer was extracted with CH_2Cl_2 (3 × 15 mL). The combined organic fractions were washed with water (10 mL) and brine (10 mL), then dried ($MgSO_4$) and concentrated under reduced pressure to give the crude product as a mixture of [2]-rotaxane **4a**, [3]-rotaxane **6a**, thread **5** (90:5:5, by ^1H NMR spectroscopy) and macrocycle **1a**. Purification by column chromatography (MeCN-CH_2Cl_2-Petrol; 5:35:60) followed by preparative TLC on silica gel (5 elutions in MeCN-CH_2Cl_2-Petrol; 7:33:60) gave pure rotaxane **6a** as a white solid (3.5 mg, 2%); m.p. 210-212 °C; ^1H NMR (400 MHz, $CDCl_3$, 298 K): δ = 7.48 (m, 2H, H_A, $H_{A'}$), 7.27-7.20 (m, 16H, H_B, $H_{B'}$, H_b, H_n), 7.19 (s, 1H, H_i), 7.10 (d, 6H, *J* = 8.5 Hz, H_c or H_m), 7.07 (d, 6H, *J* = 8.5 Hz, H_c or H_m), 6.98 (d, 4H, *J* = 8.4 Hz, H_E or $H_{E'}$), 6.94 (d, 4H, *J* = 8.4 Hz, H_E or $H_{E'}$), 6.76 (t, 4H, *J* = 8.8 Hz, H_d, H_l), 6.52 (d, 4H, *J* = 8.5 Hz, H_F or $H_{F'}$), 6.49 (d, 4H, *J* = 8.5 Hz, H_F or $H_{F'}$), 6.15 (d, 2H, *J* = 8.8 Hz, H_k), 5.99 (d, 2H, *J* = 8.8 Hz, H_e), 4.54-4.45 (m, 8H, H_C, $H_{C'}$), 4.39 (s, 2H, H_j), 4.25(s, 8H, H_D, $H_{D'}$), 3,84-3.66 (m, 8H, H_G, $H_{G'}$), 3.66-3.56 (m, 2H, H_h), 3.00 (t, 2H, *J* = 5.8 Hz, H_f), 1.70-1.52 (m, 10H, H_H, $H_{H'}$, H_g), 1.47-0.93 (m, 24H, H_I, $H_{I'}$, H_J, $H_{J'}$, H_K, $H_{K'}$), 1.31 (2s, 54H, H_a, H_o); δ = ^{13}C NMR (100 MHz, $CDCl_3$, 298 K): δ = 158.6 (×2), 157.6 (×2), 155.9 (×2), 148.0 (×2), 144.3(×2), 143.1, 139.1, 139.0, 136.9 (×2), 131.6, 131.5, 130.7 (×2), 129.8 (×2), 129.0, 128.8, 124.0 (×2), 123.2, 119.4 (×2), 114.3 (×2), 112.8, 112.7, 72.4, 72.3, 70.9, 70.8, 67.0

(×2), 63.8, 62.9 (×2), 61.0, 46.7, 34.2 (×2), 31.4 (×2), 29.6 (×2), 29.6, 28.7, 28.6, 28.5 (×2), 25.6, 25.5; LRFAB-MS (3-NOBA matrix): *m/z* = 2110 $[M+H]^+$; HRFAB-MS (3-NOBA matrix): *m/z* = 2110.33050 $[M+1+H]^+$ (calc. for $^{13}C^{12}C_{141}H_{174}N_5O_{10}$, 2110.32943).

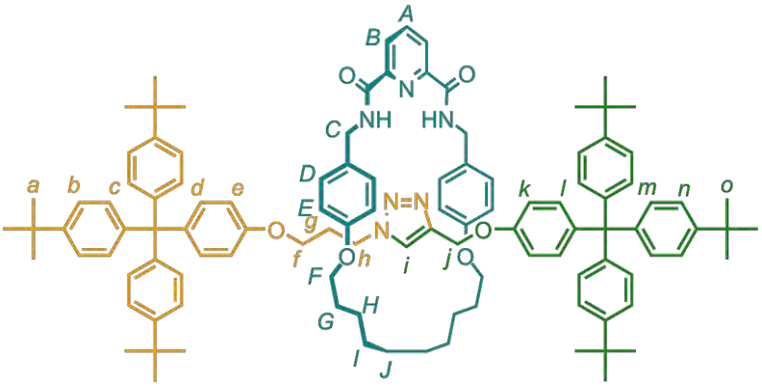

4b

Following the general procedure with macrocycle **1b** (260 mg, 0.50 mmol, 1.0 equiv.), alkyne **2** (300 mg, 0.55 mmol, 1.1 equiv.), azide **3** (296mg, 0.50 mmol, 1.0 equiv.), $Cu(CH_3CN_4)PF_6$ (206 mg, 0.55 mmol, 1.1 eq) and KCN (327 mg, 5.03 mmol, 10 equiv.). Purification by flash column chromatography (Acetone/CH_2Cl_2; 2:96 to 5:95) followed by preparative TLC on silica gel (2 elutions in Acetone/CH_2Cl_2; 4:96) gave the rotaxane **4b** as a white solid (20 mg, 3%). M.p. 165-168 °C; ^{1}H NMR (400 MHz, $CDCl_3$, 298 K): δ = 9.02 (t, 2H, *J* = 6.3 Hz, H_C), 8.37 (d, 2H, *J* = 7.8 Hz, H_B), 7.90 (t, 1H, *J* = 7.9 Hz, H_A), 7.24-7.22 (m, 12H, H_b and H_n), 7.13-7.03 (m, 16H, H_c, H_d, H_m, H_l), 6.90 (s, 1H, H_i), 6.72 (d, 4H, *J* = 8.5 Hz, H_E), 6.66 (d, 2H, *J* = 8.9 Hz, H_k), 6.61 (d, 2H, *J* = 8.9 Hz, H_e), 6.41 (d, 4H, *J* = 8.6 Hz, H_F), 4.58 (s, 2H, H_j), 4.48 (dd, 2H, *J* = 6.6 Hz, *J* = 14.6 Hz, H_D), 4.29 (dd, 2H, *J* = 6.5 Hz, *J* = 14.6 Hz, $H_{D'}$), 3.77 (t, 4H, *J* = 6.0 Hz, H_G), 3.66 (t, 2H, *J* = 7.5 Hz, H_h), 3.55 (t, 2H, *J* = 5.8 Hz, H_f), 1.71-1.54(m, 6H, H_g, H_H), 1.47-1.10 (m, 12H, H_I, H_J, H_K), 1.30 (s, 27H, H_a or H_o), 1.29 (s, 27H, H_a or H_o); ^{13}C NMR (100 MHz, $CDCl_3$, 298 K): δ = 163.6, 157.7, 155.8, 155.6, 149.1, 148.3, 148.3, 143.9 (×2), 143.8, 140.4, 140.2, 138.6, 132.2 (×2), 130.6 (×2), 130.2, 129.0, 125.2, 124.1 (×2), 122.4, 113.8, 112.8, 112.6, 66.7, 63.8, 63.0 (×2), 60.8, 46.7, 42.5, 34.2 (×2), 31.3 (×2), 29.4, 28.6, 28.4, 28.3 and 25.5; LRFAB-MS (3-NOBA matrix): *m/z* = 1647 $[M+H]^+$; HRFAB-MS (3-NOBA matrix): *m/z* = 1646.03336 (calcd. for $^{13}C^{12}C_{110}H_{133}N_6O_6$, 1646.02866).

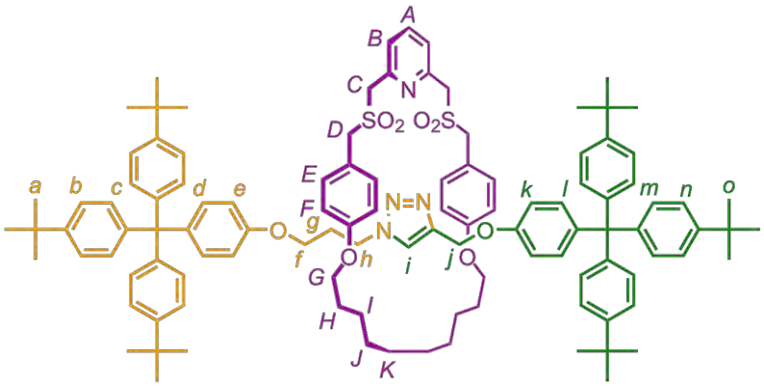

4i

Following the general procedure with macrocycle **1i** (20.0 mg, 34.1 µmol, 1.0 equiv.), alkyne **2** (20.3 mg, 37.5 µmol, 1.1 equiv.), azide **3** (20.0 mg, 34.1 µmol, 1.0 equiv.), $Cu(MeCN)_4PF_6$ (14.0 mg, 37.5 µmol, 1.1 eq) and KCN (22.2 mg, 0.34 mmol, 10 equiv.). Purification by preparative TLC on silica gel (1 elution in $MeCN/CH_2Cl_2$/Petrol; 11:29:60) gave the rotaxane **4i** as a white solid (5 mg, 8%). M.p. 92-95°C; ^{1}H NMR (400 MHz, $CDCl_3$, 298 K): δ = 7.67 (t, 1H, *J* = 7.6 Hz, H_A), 7.48 (s, 1H, H_i) 7.46 (d, 2H, *J* = 8 Hz, H_B), 7.26-7.15 (m, 12H, H_b, H_n), 7.15-7.00 (m, 16H, H_c, H_d, H_m, H_l), 6.93 (d, 4H, *J* = 8.6 Hz, H_E), 6.75 (d, 2H, *J* = 8.9 Hz, H_k), 6.59 (d, 2H, *J* = 8.9 Hz, H_e), 6.49 (d, 4H, *J* = 8.6 Hz, H_F), 4.88 (s, 2H, H_j), 4.11 (s, 4H, H_C), 4.09 (s, 4H, H_D), 3.87 (t, 2H, *J* = 7.3 Hz, H_h), 3.78-3.69 (m, 4H, H_G), 3.52 (t, 2H, J = 6.0 Hz, H_f), 1.73 (quint., 2H, *J* = 6.5 Hz, H_g), 1.67 (dt, 4H, *J* = 6.6, 6.6 Hz, H_H), 1.47-1.09 (m, 12H, H_I, H_J, H_K); 1.30 and 1.29 (2s, 54H, H_a, H_o); ^{13}C NMR (100 MHz, CDCl3): δ = 159.6, 156.2 (×2), 148.2, 147.7 (×2), 144.1, 144.0, 143.3, 139.7, 139.6, 137.5, 132.1, 132.0, 131.6, 130.6 (×2), 126.3, 124.0 (×2), 123.8, 118.4, 114.9, 113.0 (×2), 67.4, 64.2, 63.0 (×2), 60.1, 58.3 (×2), 46.6, 34.2 (×2), 31.3 (×2), 29.6, 29.0, 28.5, 28.3, 25.4; LRFAB-MS (3-NOBA matrix): *m/z* = 1716 $[M+H]^+$; HRFABMS (3-NOBA matrix): *m/z* = 1716.97173 $[M+1+H]^+$ (calcd. for $^{13}C^{12}C_{110}H_{135}N_4O_8S_2$, 1716.97549).

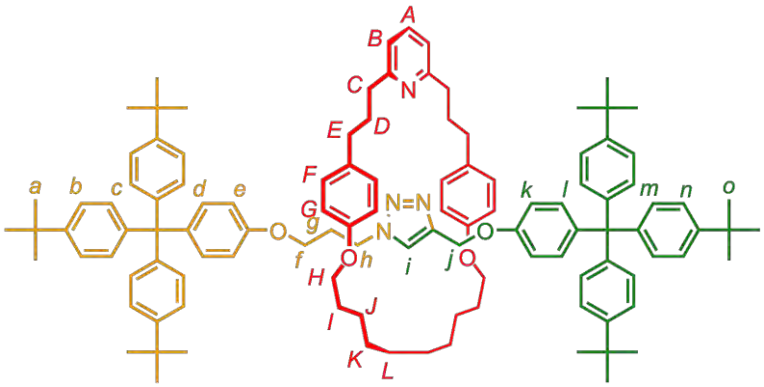

4j

Following the general procedure with macrocycle **1j** (12.1 mg, 25.0 µmol, 1.0 equiv.), alkyne **2** (14.9 mg, 27.5 µmol, 1.1 equiv.), azide **3** (14.7 mg, 25.0 µmol, 1.0 equiv.), $Cu(MeCN)_4PF_6$ (10.0 mg, 27.5 µmol, 1.1 eq) and KCN (16.0 mg, 0.25 mmol, 10 equiv.). Purification by preparative TLC on silica gel (2 elutions in $MeCN/CH_2Cl_2$/Petrol; 3.5:40:56.5) gave the rotaxane **4j** as a white solid (17 mg, 42%). M.p. 128-132 °C; 1H NMR (400 MHz, $CDCl_3$, 298 K): δ = 7.33 (t, 1H, *J* = 7.6 Hz, H_A), 7.24 (d, 6H, *J* = 8.5 Hz, H_n), 7.21-7.01 (m, 23H, H_b, H_c, H_d, H_i, H_l, H_m), 6.83 (d, 2H, *J* = 7.7 Hz, H_B), 7.74 (bd, 6H, *J* = 8.4 Hz, H_F, H_k), 6.48 (d, 6H, *J* = 8.6 Hz, H_G, H_e), 4.91 (s, 2H, H_j), 3.81-3.70 (m, 6H, H_H, H_h), 3.34 (t, 2H, *J* = 5.8 Hz, H_f), 2.60 (2d, 4H, *J* = 6.8 Hz, H_C), 2.51 (t, 4H, *J* = 7.3 Hz, H_E), 1.84-1.72 (m, 4H, H_D), 1.70-1.60 (m, 6H, H_l, H_g), 1.57-1.11 (m, 12H, H_J, H_K H_L), 1.31 and 1.30 (2s, 54H, H_a, H_o); ^{13}C NMR (100 MHz, $CDCl_3$, 298 K): δ = 161.4, 156.9, 156.1 (×2), 148.2 (×2), 144.1, 144.0, 143.5, 139.7, 139.5 (×2), 133.5, 132.1, 132.0, 130.6 (×2), 129.1, 124.0 (×2), 123.1, 119.6, 114.2, 113.0, 112.9, 67.0, 63.8, 63.0 (×2), 61.5, 46.7, 37.9, 35.0, 34.2 (×2), 32.4, 31.3 (×2), 29.4, 29.3, 28.6, 28.5, 25.6; LRFAB-MS (3-NOBA matrix): *m/z* = 1617 $[M+H]^+$; HRFAB-MS (3-NOBA matrix): *m/z* = 1617.08218 $[M+1+H]^+$ (calcd. for $^{13}C^{12}C_{112}H_{139}N_4O_4$, 1617.08299).

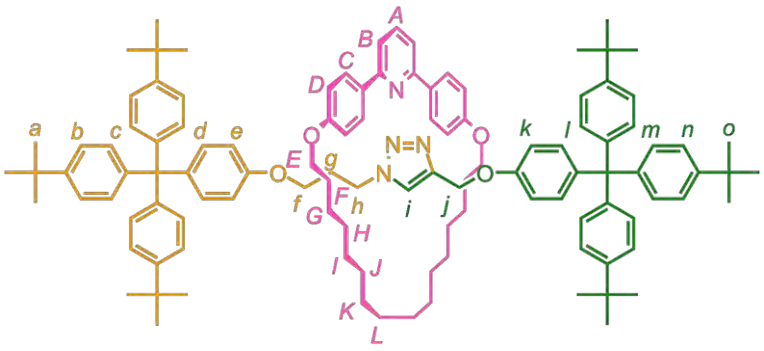

4l

Following the general procedure with macrocycle **1l** (29.0 mg, 60.4 µmol, 1.0 equiv.), alkyne **2** (36.0 mg, 66.4 µmol, 1.1 equiv.), azide **3** (35.5 mg, 60.4 µmol, 1.0 equiv.), $Cu(MeCN)_4PF_6$ (24.8 mg, 66.4 µmol, 1.1 eq) and KCN (40 mg, 0.66 mmol, 10 equiv.). Purification by flash column chromatography ($MeCN/CH_2Cl_2$/Petrol; 2.5:20:77.5) gave the rotaxane **4l** as a white solid (15 mg, 14%). M.p. 130-132°C; ^1H NMR (400 MHz, $CDCl_3$, 298 K): δ = 7.73 (d, 4H, *J* = 8.8 Hz, H_C), 7.61 (t, 1H, *J* = 7.8 Hz, H_A), 7.39 (d, 2H, *J* = 7.8 Hz, H_B), 7.22-7.18 (m, 12H, H_b, H_n), 7.10-7.03 (m, 16H, H_c, H_d, H_m, H_l), 6.89 (s, 1H, H_i), 6.82 (d, 4H, *J* = 8.8 Hz, H_D), 6.78 (d, 2H, *J* = 8.9 Hz, H_k), 6.66 (d, 2H, *J* = 8.9 Hz, H_e), 4.96 (s, 2H, H_j), 4.04 (t, 4H, *J* = 7.2 Hz, H_E), 4.00 (t, 2H, *J* = 7.1 Hz, H_h), 3.70 (t, 2H, *J* = 5.6 Hz, H_f), 1.97 (quint., 2H, *J* = 6.4 Hz, H_g), 1.60 (dt, 4H, *J* = 7.0, 7.0 Hz, H_F), 1.33-0.98 (m, 24H, H_G,

H_H, H_I, H_J, H_K, H_L), 1.30 and 1.29 (2s, 54H, H_a, H_o); ^{13}C NMR (100 MHz, $CDCl_3$, 298 K): δ = 158.9, 156.9, 156.2 (×2), 148.2 (×2), 144.0 (×2), 143.5, 139.8 (×2), 137.3, 132.5 (×2), 132.1, 130.7, 130.6, 128.8, 124.0 (×2), 123.2, 117.2, 115.3, 113.1, 112.8, 68.0, 63.9, 63.0 (×2), 61.7, 46.7, 34.2 (×2), 31.3 (×2), 30.1, 30.0, 29.6 (×2), 29.5 (×2), 28.2, 25.7; LRFAB-MS (3-NOBA matrix): *m/z* = 1617 $[M+H]^+$; HRFAB-MS (3-NOBA matrix): *m/z* = 1617.08485 $[M+1+H]^+$ (calcd. for $^{13}C^{12}C_{112}H_{139}N_4O_4$, 1617.08299).

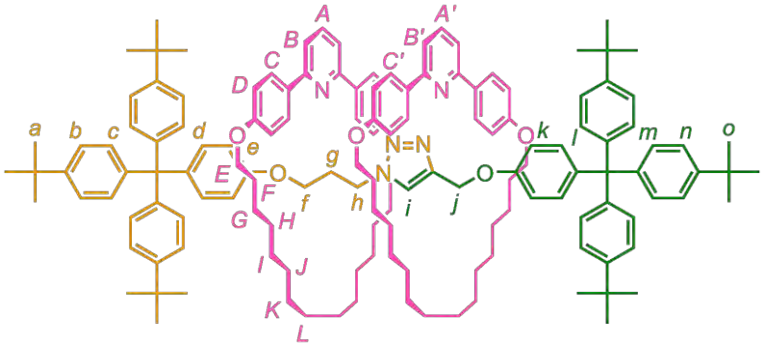

6l

A solution of macrocycle **1l** (170 mg, 0.35 mmol, 10 equiv.), alkyne **2** (19.0 mg, 35.0 µmol, 1.1 equiv.), azide **3** (20.6 mg, 35.0 µmol, 1.0 equiv.), $Cu(MeCN)_4PF_6$ (14.3 mg, 38.5 µmol, 1.1 eq) in CH_2Cl_2 (10 mL) under N_2 was stirred at RT for 8 days. The solution was then refluxed for further 48 h then cooled to RT. The resulting mixture was diluted with CH_2Cl_2 (5 mL) and methanol (15 mL). A solution of KCN (25 mg, 0.38 mmol, 10 equiv.) in methanol (2 mL) was added and the resulting suspension stirred vigorously for 1 h. Solvents were evaporated (80 °C) and the residue was partitioned between water (15 mL) and CH_2Cl_2 (20 mL). The layers were separated and the aqueous layer was extracted with CH_2Cl_2 (3 × 10 mL). The combined organic fractions were washed with water (10 mL) and brine (10 mL), then dried ($MgSO_4$) and concentrated under reduced pressure to give the crude product as a mixture of [2]rotaxane **4l**, [3]rotaxane **6l**, thread **5** (33:37:30, by ^1H NMR spectroscopy), macrocycle **1l**, remaining alkyne **2** and azide **3**, (75% overall conversion). Purification by preparative TLC on silica gel (3 elutions in $MeCN/CH_2Cl_2$/Petrol; 3.5:40:56.5) gave the [3]rotaxane **6l** as a white solid (15 mg, 20%). M.p. 302-304 °C; ^1H NMR (400 MHz, $CDCl_3$, 298 K): δ = 7.68 (m, 10H, H_C, $H_{C'}$, H_A, $H_{A'}$), 7.37 (d, 4H, *J* = 7.8 Hz, H_B, $H_{B'}$), 7.20 -7.10 (m, 12H, H_b, H_n), 7.09 (s, 1H, H_i), 7.05-6.91 (m, 16H, H_c, H_m, H_d, H_l), 6.82 (d, 2H, J = 8.9 Hz, H_k), 6.74-6,65 (m, 8H, H_D, $H_{D'}$), 6.46 (d, 2H, *J* = 8.9 Hz, H_e), 5.04 (s, 2H, H_j), 4.03-3.89 (m, 8H, *J* = 7.2 Hz, H_E, $H_{E'}$), 3.70 (t, 2H, *J* = 7.5 Hz, H_h), 3.50 (t, 2H, J = 5.7 Hz, H_f), 1.69 (br. quint., 2H, *J* = 6.7 Hz, H_g), 1.54 (br. quint, 8H, *J* = 7.35 Hz, H_F), 1.40-0.81 (m, 48H, H_G, $H_{G'}$, H_H, $H_{H'}$, H_I, $H_{I'}$, H_J, $H_{J'}$, H_K, $H_{K'}$, H_L,

$H_{L'}$), 1.27 and 1.26 (2s, 54H, H_a, H_o); ^{13}C NMR (100 MHz, $CDCl_3$, 298 K): δ = 158.9, 158.8, 156.8, 156.7, 156.2, 156.1, 148.1, 148.0, 144.0 (×2), 143.1, 139.7, 139.5, 137.1, 136.9, 132.5, 132.1, 132.0, 131.8, 130.6 (×2), 128.6 (×2), 123.9 (×2), 123.1, 116.9, 116.7, 115.2, 115.0, 113.3, 113.0, 68.2, 68.1, 64.1, 62.9 (×2), 61.7, 46.7, 34.2 (×2), 31.3 (×2), 30.1, 29.9 (×2), 29.7 (×2), 29.6 (×2) , 29.5 (×2), 29.4 (×2), 28.3, 28.2 and 25.7 (×2), LRFAB-MS (3-NOBA matrix): *m/z* = 2101 $[M]^+$; HRFAB-MS (3-NOBA matrix): *m/z* = 2102.41114 $[M+1+H]^+$ (calc. for $^{13}C^{12}C_{145}H_{182}N_5O_6$, 2102.41237).

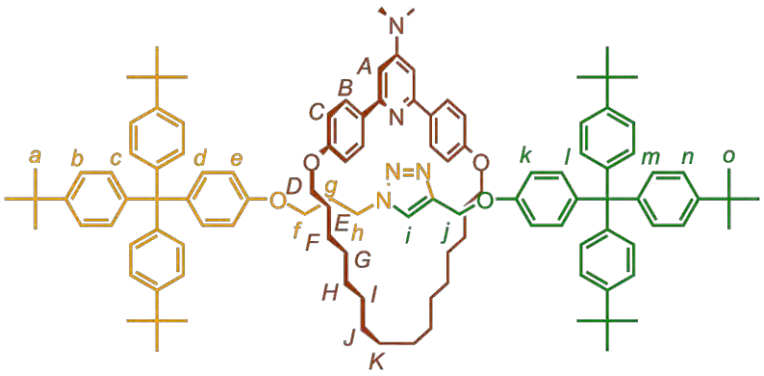

Following the general procedure with macrocycle **1m** (12.1 mg, 25.0 µmol, 1.0 equiv.), alkyne **2** (14.9 mg, 27.5 µmol, 1.1 equiv.), azide **3** (14.7 mg, 25.0 µmol, 1.0 equiv.), $Cu(MeCN)_4PF_6$ (10.0 mg, 27.5 µmol, 1.1 eq) and KCN (16.0 mg, 0.25 mmol, 10 equiv.). Purification by flash column chromatography ($MeCN/CH_2Cl_2$/Petrol; 3.5:20:76.5) followed by preparative TLC on alumina (3 elutions in $MeCN/CH_2Cl_2$/Petrol; 2.5:15:82.5) gave the rotaxane **4m** as a white solid (10 mg, 16 %). M.p. 99-101 °C; ^1H NMR (400 MHz, $CDCl_3$, 298 K): δ = 7.71 (d, 4H, *J* = 8.6 Hz, H_C), 7.21 (d, 6H, *J* = 8.5 Hz, H_b), 7.20 (d, 6H, *J* = 8.5 Hz, H_n) 7.12-7.03 (m, 16H, H_c, H_d, H_m, H_l), 6.99 (s, 1H, H_i). 6.80 (d, 6H, *J* = 8.6 Hz, H_D, H_k), 6.71 (s, 2H, H_B), 6.69 (d, 2H, *J* = 8.8 Hz, H_e), 4.91 (s, 2H, H_j), 4.04 (t, 4H, *J* = 7.1 Hz, H_E), 3.97 (t, 2H, *J* = 7.1 Hz, H_h), 3.72 (t, 2H, *J* = 5.8 Hz, H_f), 3.00 (s, 6H, H_A), 1.94 (br quint., 2H, *J* = 6.5 Hz, H_g), 1.58 (br quint, 4H, *J* = 7.1 Hz, H_F), 1.46-0.97 (m, 24H, H_G, H_H, H_I, H_J, H_K, H_L), 1.29 (s, 54H, H_a, H_o); ^{13}C NMR (100 MHz, $CDCl_3$, 298 K): δ = 158.5, 157.5, 156.3 (×2), 155.8, 148.2 (×2), 144.0 (×2), 143.3, 139.7 (×2), 133.8, 132.1 (×2), 130.7 (×2), 128.8, 124.0 (×2), 123.5, 115.1, 113.1, 112.9, 100.8, 68.0, 64.1, 63.0 (×2), 61.6, 46.7, 39.4, 34.2 (×2), 31.3 (×2), 30.1, 30.0, 29.7, 29.6, 29.5 (×2), 28.2, 25.7; LRFAB-MS (3-NOBA matrix): *m/z* = 1660 $[M+H]^+$; HRFAB-MS (3-NOBA): *m/z* = 1659.13501 $[M+1]^+$ (calc. for $^{13}C^{12}C_{114}H_{143}N_5O_4$, 1659.11736 $[M+H]^+$).

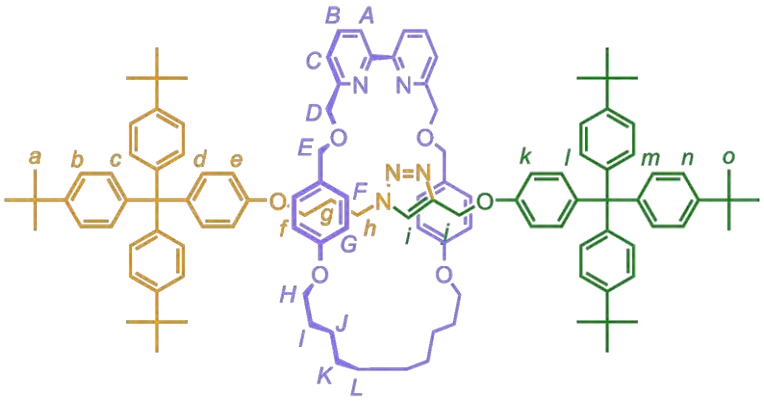

4n

Following the general procedure with macrocycle **1n** (9.9 mg, 17.4 µmol, 1.0 equiv.), alkyne **2** (10.4 mg, 19.2 µmol, 1.1 equiv.), azide **3** (10.2 mg, 17.4 µmol, 1.0 equiv.), $Cu(MeCN)_4PF_6$ (7.1 mg, 19.2 µmol, 1.1 eq) and KCN (11.4 mg, 0.17 mmol, 10 equiv.). Purification by flash column chromatography (Acetone/CH_2Cl_2; 4:96) followed by preparative TLC on alumina (3 elutions in Et_2O/Petrol; 1:1) gave the rotaxane **4n** as a white solid (10 mg, 35%). M.p. 90-94°C; ^{1}H NMR (400 MHz, $CDCl_3$, 298 K): δ = 7.89 (d, 2H, *J* = 7.7 Hz, H_A), 7.43 (t, 2H, *J* = 7.7 Hz, H_B), 7.30-7.17 (m, 14H, H_b, H_n, H_C), 7.17-7.00 (m, 16H, H_c, H_d, H_m, H_l), 7.00-6,92 (m, 5H, H_F, H_i), 6.66 (d, 2H, *J* = 8.8 Hz, H_k), 6.54 (d, 4H, *J* = 8.5 Hz, H_G), 6.33 (d, 2H, *J* = 8.8 Hz, H_e), 4.81 (s, 2H, H_j), 4.54 (s, 4H, H_D), 4.51 (s, 4H, H_E), 3.75- 3.66 (m, 6H, H_H, H_h), 3.24 (t, 2H, *J* = 5.6 Hz, H_f), 1.65-1.50 (m., 6H, H_l, H_g), 1.40-1.03 (m, 12H, H_J, H_K, H_L), 1.30 and 1.29 (2s, 54H, H_a, H_o); ^{13}C NMR (100 MHz, $CDCl_3$, 298 K): δ = 158.5 (×2), 158.1, 156.1 (×2), 148.2 (×2), 144.1, 144.0, 143.4, 139.8, 139.5, 137.1, 132.1, 131.9, 130.6 (×2), 129.6, 129.5, 124.0 (×2), 123.1, 121.5, 119.9, 114.2, 113.0, 112.7, 72.4, 72.2, 67.5, 63.6, 63.0 (×2), 61.5, 46.7, 34.2 (×2), 31.3 (×2), 29.6, 29.2, 28.7 (×2), 25.7; LRFAB-MS (3-NOBA matrix): *m/z* = 1698 $[M+H]^+$; HRFAB-MS (3-NOBA matrix): *m/z* = 1698.06527 $[M+1+H]^+$ (calc. for $^{13}C^{12}C_{115}H_{138}N_5O_6$ 1698.06807).

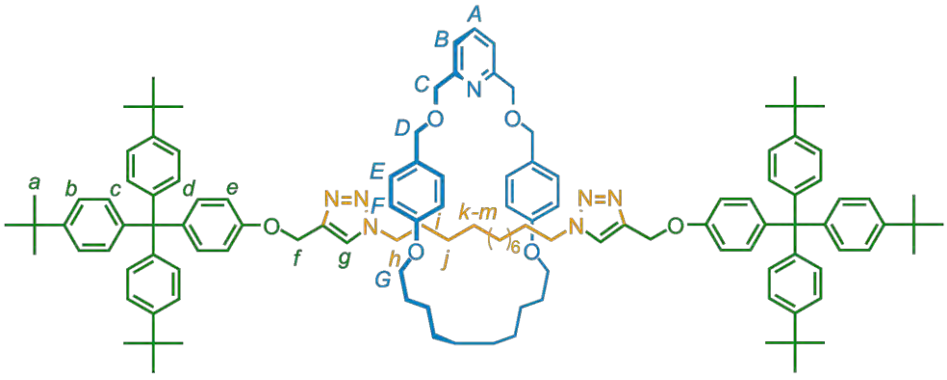

9a

Following the general procedure, macrocycle **1a** (50 mg, 0.1 mmol, 1 equiv.) was reacted with alkyne **2** (542 mg, 1 mmol, 10 equiv.) and diazide **8** (126 mg, 0.5 mmol, 5 equiv.) to give a crude yellow solid. Purification by column chromatography (CH_2Cl_2 then a gradient from 5% to 20 % MeCN in CH_2Cl_2) gave the rotaxane **9a** as a colorless solid (240 mg, 81%). M.p. 98-100°C; ^{1}H NMR (400 MHz, $CDCl_3$, 298 K): δ = 7.55 (t, 1H, *J* = 7.9 Hz, H_A), 7.44 (s, 2H, H_g), 7.27 (d, 2H, *J* = 8.0 Hz, H_B), 7.22 (d, 12H, *J* = 8.5 Hz, H_b), 7.04-7.09 (m, 4H, H_d), 7.07 (d, 12H, *J* = 8.5 Hz, H_c), 7.03 (d, 4H, *J* = 8.3 Hz, H_E), 6.79 (d, 4H, *J* = 8.8 Hz, H_e), 6.61 (d, 4H, *J* = 8.5 Hz, H_F), 5.04 (s, 4H, H_f), 4.50 (s, 4H, H_D), 4.30 (s, 4H, H_C), 3.93 (t, 4H, *J* = 7.5 Hz, H_h), 3.83 (t, 4H, *J* = 6.4 Hz, H_G), 1.64-1.71 (m, 4H, J = 6.8 Hz, H_H), 1.46-1.55 (m, 4H, H_i), 1.33-1.42 (m, 4H, H_I), 1.31 (s, 54H, H_a), 0.95-1.28 (m, 24H, H_{j-m} and H_{J-K}). ^{13}C NMR (100 MHz, $CDCl_3$, 298 K): δ = 158.7, 157.6, 157.4, 157.3, 156.2, 148.3, 144.1, 143.9, 140.0, 132.3, 130.7, 129.9, 129.0, 124.0, 122.7, 119.8, 114.2, 113.2, 72.5, 71.1, 67.1, 63.1, 61.9, 50.1, 34.3, 31.4, 30.0, 29.6, 29.5, 29.3, 29.0, 28.6, 26.4, 25.7. LRESI-MS: *m/z* = 1826 $[M+H]^+$; HRFAB-MS (3-NOBA matrix): *m/z* = 1828.21534 [M+1+H] (calcd. for $^{13}C^{12}C_{122}H_{156}N_7O_6$, 1828.21507).

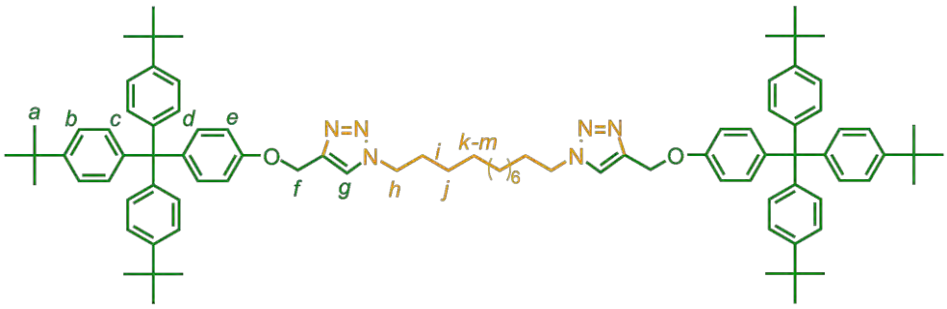

10

Spectroscopic data of the non-interlocked thread **10** generated during AMT-CuAAC rotaxane-formation reactions: ^{1}H NMR (400 MHz, $CDCl_3$, 298 K): δ = 7.58 (s, 2H, H_g), 7.23 (d, *J* = 8.6 Hz, 12H, H_b), 7.08 (d, *J* = 8.6 Hz, 16H, H_c and H_d), 6.85 (d, *J* = 8.9 Hz, 4H, H_e), 5.18 (s, 4H, H_f), 4.34 (t, *J* = 7.2 Hz, 4H, H_h), 1.85-1.97 (m, 4H, H_i), 1.30 (s, 54H, H_a), 1.23-1.34 (m, 16H, H_{j-m}). ^{13}C NMR (100 MHz, $CDCl_3$, 298 K): δ = 156.1, 148.3, 144.3, 144.0, 140.1, 132.3, 130.7, 124.0, 122.3, 113.2, 63.0, 62.1, 50.4, 34.3, 31.4, 30.3, 29.4, 29.3, 28.9, 26.4; LRFABMS (3-NOBA matrix): *m/z* = 1338.5 $[M+H]^+$; HRFAB-MS (3-NOBA matrix): *m/z* = 1337.92367 $[M+H]^+$ (calcd. for $C_{92}H_{117}N_6O_2$, 1337.92380).

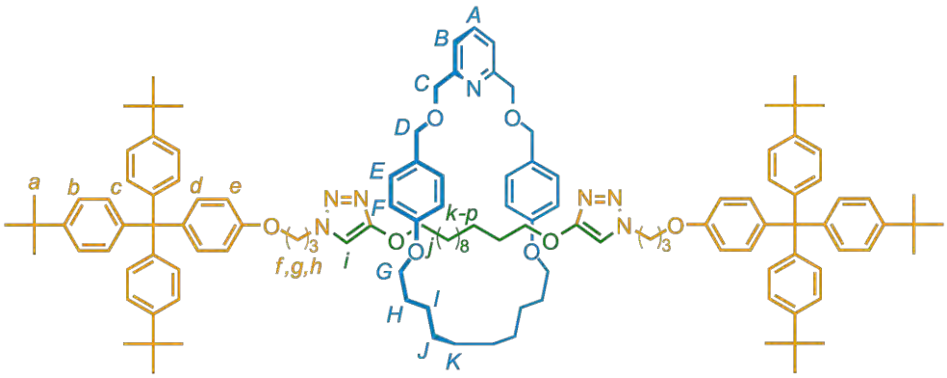

11a

Following the general procedure, macrocycle **1a** (50 mg, 0.1 mmol) was reacted with azide **3** (587 mg, 1 mmol, 10 equiv.) and dialkyne **9** (139 mg, 0.5 mmol, 5 equiv.) to give a crude white solid. Purification by column chromatography (CH_2Cl_2/Acetone 100:0 to 88:12) afforded **11a** (17 mg, 86%) as a colorless amorphous solid. ^{1}H NMR (400 MHz, $CDCl_3$, 298 K): δ = 7.55 (t, 1H, *J* = 7.7 Hz, H_A), 7.39 (s, 2H, H_i), 7.28 (s, 2H, H_B), 7.24 (d, 12H, *J* = 8.5 Hz, H_b), 7.09 (d, 12H, *J* = 8.5 Hz, H_c), 7.03 (m, 8H, H_d and H_E), 6.60 (d, 4H, *J* = 8.5 Hz, H_F), 6.56 (d, 4H, *J* = 8.9 Hz, H_e), 4.51 (s, 4H, H_D), 4.53 (s, 4H, H_j), 4.18 (t, 4H, *J* = 7.1 Hz, H_h), 4.29 (s, 4H, H_C), 3.82 (t, 4H, *J* = 6.3 Hz, H_G), 3.62 (t, 4H, *J* = 5.7 Hz, H_f), 3.43 (t, 4H, *J* = 6.7 Hz, H_k), 1.95-2.05 (m, 4H, *J* = 6.4 Hz, H_g), 1.58-1.70 (m, 4H, *J* = 6.7 Hz, H_H), 1.47-1.56 (m, 4H, *J* = 7.1 Hz, H_l), 1.30 (s, 54H, H_a), 1.11-1.27 (m, 28H, H_{m-p} and H_{I-K}). ^{13}C NMR (100 MHz, $CDCl_3$, 298 K): δ = 157.7, 156.6, 155.2, 147.3, 144.1, 143.1, 138.8, 136.1, 131.1, 129.7, 128.9, 128.0, 123.0, 121.8, 118.8, 113.3, 111.9, 71.4, 70.0, 69.9, 69.5, 66.1, 63.2, 62.8, 62.0, 45.9, 33.3, 30.4 (x 2), 28.7 (x 2), 28.6, 28.5, 27.7, 27.6, 25.1, 24.7. LRFAB-MS (3-NOBA matrix): *m/z* = 1944 $[M+H]^+$; HRFAB-MS (THIOG matrix): *m/z* = 1944.30187 $[M+1+H]^+$ (calc. for $^{13}C^{12}C_{128}H_{168}N_7O_8$ 1944.29880).

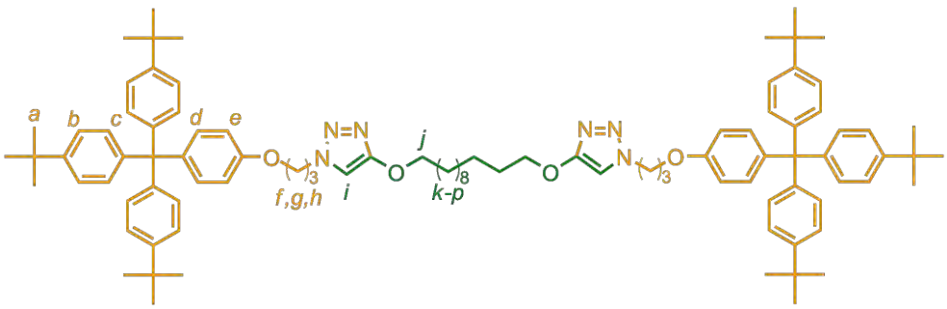

12

Spectroscopic data of the non-interlocked thread **12** generated during AMT-CuAAC rotaxane-formation reactions: ^{1}H NMR (400 MHz, $CDCl_3$, 298 K): δ = 7.59 (s, 2H, H_i),

7.28 (d, 12H, *J* = 8.5 Hz, H_b), 7.13 (d, 16H, *J* = 8.5 Hz, H_c and H_d), 6.78 (d, 4H, *J* = 8.9 Hz, H_e), 4.65 (s, 4H, H_j), 4.61 (t, 4H, *J* = 6.9 Hz, H_h), 3.99 (t, 4H, *J* = 5.6 Hz, H_f), 3.55 (t, 4H, *J* = 6.6 Hz, H_k), 2.36- 2.47 (m, 4H, H_g), 1.57-1.68 (m, 4H, H_l), 1.35 (s, 54H, H_a), 1.27-1.33 (m, 16H, H_{m-p}). ^{13}C NMR (100 MHz, $CDCl_3$, 298 K): δ = 156.1, 148.2, 145.3, 143.9, 140.0, 132.2, 130.6, 123.9, 122.7, 112.8, 70.8, 64.2, 63.7, 62.9, 62.8, 47.0, 34.2, 31.3, 29.9, 29.5, 29.5, 29.4, 26.0. LRFAB-MS (3-NOBA matrix): *m/z* = 1456 $[M+H]^+$; HRFAB-MS (THIOG matrix): *m/z* = 1455.01298 $[M]^+$ (calc. for $C_{98}H_{128}N_6O_4$ 1455.01381).

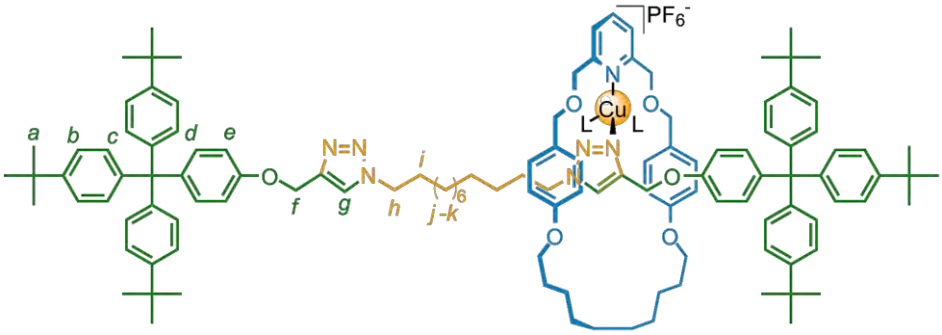

Cu**9a**PF_6

To a solution of *bis*-triazole rotaxane **9a** (5.0 mg, 0.0028 mmol, 1 equiv.) in CH_2Cl_2 was added $Cu(MeCN)_4PF_6$ (0.7 mg, 0.0028 mmol, 1 equiv.) and the solution stirred for 5 minutes. The solvent was removed *in vacuo* to yield a pale orange solid (5.1 mg, 91%). M.p. 142-144 °C. 1H NMR (400 MHz, d_3-MeCN/CD_2Cl_2 9:1, 298 K): δ = 7.61 (m, 3H, H_A and H_g), 7.27 (d, *J* = 8.5 Hz, 14H, H_B and H_c), 7.13 (d, *J* = 8.5 Hz, 12H, H_b), 7.06 (d, *J* = 7.6 Hz, 4H, H_d), 6.96 (d, *J* = 7.9 Hz, 4H, H_F), 6.66 (d, *J* = 8.1 Hz, 4H, H_E), 6.54 (d, *J* = 8.1 Hz, 4H, H_e), 4.78 (s, 4H, H_f), 4.44 (s, 4H, H_D), 4.33 (s, 4H, H_C), 4.12 (t, *J* = 7.1 Hz, 4H, H_h), 3.79 (t, *J* = 6.2, 4H, H_G), 1.56-1.70 (m, 8H, H_H and H_i), 1.28-1.39 (m, 4H, H_l), 1.25 (s, 54H, H_a), 1.02-1.22 (m, 24H, H_{J-K} and H_{j-m}). ^{13}C NMR: (100 MHz, d_3-MeCN/CD_2Cl_2 9:1, 298 K): δ = 211.0, 193.2, 159.4, 157.4, 156.7, 149.1, 145.2, 140.8, 138.8, 132.4, 130.9, 125.2, 121.7, 114.5, 114.0, 73.3, 71.5, 67.7, 63.8, 54.9, 54.7, 54.4, 54.1, 51.3, 34.7, 31.4, 30.4, 30.1, 29.7, 29.7, 29.3, 29.2, 26.8, 26.3. LRFAB-MS (3-NOBA matrix): *m/z* = 1890.4 $[M+H]^+$; HRFAB-MS (3-NOBA matrix): *m/z* = 1890.13790 $[M+1+H]^+$ (calc. for $^{13}C^{12}C_{122}H_{155}CuN_7O_6$ 1890.14684).

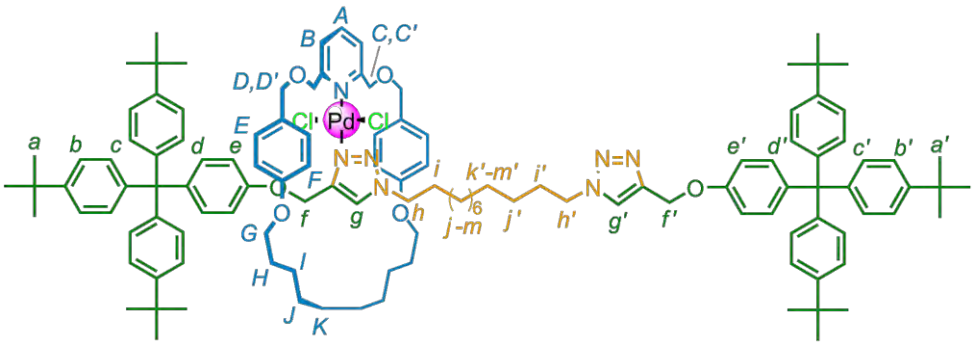

Pd**9a**Cl_2

To a solution of *bis*-triazole rotaxane **9a** (5.0 mg, 0.0028 mmol, 1 equiv.) in CH_2Cl_2 was added $Pd(MeCN)_2Cl_2$ (0.7 mg, 0.0028 mmol, 1 equiv.) and the solution stirred for 5 minutes. The solvent was removed in vacuo to yield a pale orange solid (5.1 mg, 91%). M.p. 208-210°C (dec.). ^{1}H NMR (400 MHz, d_3-MeCN/CD_2Cl_2 9:1): δ = 7.81 (s, 1H, H_g), 7.77 (t, $_J$ = 7.8 Hz, 1H, H_A), 7.49 (m, 3H, $H_{g'}$ and H_B), 7.36-6.86 (m, 34H, $H_{b\text{-}d}$, $H_{e'}$ $H_{b'\text{-}d'}$ and H_F), 6.71 (d, $_J$ = 8.6 Hz, 4H, H_E), 6.52 (d, $_J$ = 8.5 Hz, 2H, H_e), 5.96 (d, $_J$ = 14.8 Hz, 2H, H_D), 5.56 (s, 2H, $H_{F'}$), 5.34 (d, $_J$ = 14.9 Hz, 2H, $H_{D'}$), 5.10 (s, 2H, H_f), 4.87 (d, $_J$ = 12.4 Hz, 2H, H_C), 4.56 (d, $_J$ = 12.3 Hz, 2H, $H_{C'}$), 4.38 (t, $_J$ = 7.02 Hz, 2H, $H_{h'}$), 3.79-3.90 (m, 6H, H_G and H_h), 1.61-1.75 (m, 4H, H_H), 0.81-1.48 (m, 86H, H_a,and $_{a'}$, $H_{I\text{-}K}$ and $H_{i\text{-}i'}$). ^{13}C NMR The complex was insufficiently soluble to obtain satisfactory data. LRFAB-MS (3-NOBA matrix): *m/z* = 1932 $[M\text{-}2Cl]^+$; HRFAB-MS (THIOG matrix): *m/z* = 1933.10664 $[M+1\text{-}2Cl]^+$ (calc. for $^{13}C^{12}C_{122}H_{155}N_7O_6Pd$ 1933.11044).

2.6 References

(1) R. Huisgen, G. Szeimies, L. Möbius, *Chem. Ber*, **1967**, *100*, 2494-2507.

(2) C. W. Tornøe, M. Meldal, Peptidotriazoles: *Copper(I)-catalysed 1,3-dipolar cycloadditions on solid phase. Proc. A. Pept. Symp.* American Peptide Society and Kluwer Academic Publishers: San Diego, **2001**, 263-264.

(3) C. W. Tornøe, C. Christensen, M. Meldal, *J. Org. Chem*. **2002**, *67*, 3057-3064.

(4) V. V. Rostovtsev, L. G. Green, V. V. Fokin, B. K. Sharpless, *Angew. Chem. Int. Ed*. **2002**, *41*, 2596-2599.

(5) a) M. Meldal, C. W. Tornøe, *Chem. Rev*. **2008**, *108*, 2952-3015. b) A. Dondoni, *Chem Asian J*. **2007**, *2*, 700-708. c) J. E. Moses, A. D. Moorhouse, *Chem. Soc. Rev*. **2007**, *36*, 1249-1262. d) H. C. Kolb, M. G. Finn, K. B. Sharpless, *Angew. Chem., Int. Ed*. **2001**, *40*, 2004-2021. e) H. C. Kolb, K. B. Sharpless, *Drug DiscoVery Today*, **2003**, *8*, 1128-1137. f) P. Ball, *Chem. World*, **2007**, *4*, 46-51.

(6) V. D. Bock, H. Hiemstra, J. H. van Maarseveen, *Eur. J. Org. Chem.* **2005**, 51-68.

(7) L. D. Pachon, J. H. van Maarseveen, G. Rothenberg, *Adv. Synth. Catal.* **2005**, *347*, 811-815.

(8) a) T. R. Chan, R. Hilgraf, K. B. Sharpless, V. V. Fokin, *Org. Lett.* **2004**, *6*, 2853-2855. b) W. G. Lewis, F. G. Magallon, V. V. Fokin, M. G. Finn, *J. Am. Chem. Soc.* **2004**, *126*, 9152-9153.

(9) F. Perez-Balderas, M. Ortega-Munoz, J. Morales-Sanfrutos, F. Hernandez-Mateo, F. G. Calvo-Flores, J. A. Calvo-Asin, J. Isac-Garcia, F. Santoyo-Gonzalez, *Org. Lett.* **2003**, *5*, 1951-1954.

(10) L. Zhang, X. Chen, P. Xue, H. H. Y. Sun, I. D. Williams, K. B. Sharpless, V V. Fokin, G. Jia, *J. Am. Chem. Soc*. **2005**, *127*, 15998-15999.

(11) a) F. Himo, T. Lovell, R. Hilgraf, V. V. Rostovtsev, L. Noodleman, K. B. Sharpless, V. V. Fokin, *J. Am. Chem. Soc.* **2005**, *127*, 210-216. b) M. Ahlquist, V. V. Fokin, *Organometallics*, **2007**, *26*, 4389–4391.

(12) B. M. Mykhalichko, O. N. Temkin, M. G. Mys'kiv, *Russ. Chem. Rev*. **2000**, *69*, 957-984.

(13) V. O. Rodionov, V. V. Fokin, M. G. Finn, M. G. *Angew. Chem., Int. Ed.* **2005**, *44*, 2210-2215.

(14) C. Nolte, P. Mayer, B. F. Straub, *Angew. Chem., Int. Ed.* **2007**, *46*, 2101-2103.

(15) P. Wu, V. V. Fokin, *Aldrichimica Acta* **2007**, *40*, 7-17.

(16) a) F. Bohlmann, H. Schönowsky, E. Inhoffen, G. Grau, *Chem. Ber*. **1964**, *97*, 794-800. b) P. Siemsen, R. C. Livingston, F. Diederich, *Angew. Chem., Int. Ed.* **2000**, *39*, 2632-2657.

(17) a) A.-M. Fuller, D. A. Leigh, P. J. Lusby, I. D. H. Oswald, S. Parsons, D. B. Walker, *Angew. Chem. Int. Ed.* **2004**, *43*, 3914-3918. b) A.-M. Fuller, D. A. Leigh, P. J. Lusby, A. M. Z. Slawin, D. B. Walker, *J. Am. Chem. Soc.* **2005**, *127*, 12612-12619. c) D. A. Leigh, P. J. Lusby, A. M. Z. Slawin, D. B. Walker, *Chem. Commun.* **2005**, 4919-4921. d) D. A. Leigh, P. J. Lusby, A. M. Z. Slawin, D. B. Walker, *Angew. Chem Int. Ed.* **2005**, *44*, 4557-4564. e) A.-M. Fuller, D. A. Leigh, P. J. Lusby, *Angew. Chem. Int. Ed*. **2007**, *46*, 5015-5019.

(18) V. Aucagne, K. D. Hänni, D. A. Leigh, P. J. Lusby, D. B. Walker, *J. Am. Chem. Soc*. **2006**, *128*, 2186-2187.

(19) V. Aucagne, J. Berná, J. D. Crowley, S. M. Goldup, K. D. Hänni, D. A. Leigh, P. J. Lusby, V. E. Ronaldson, A. M. Z. Slawin, A. Viterisi, D. B. Walker, *J. Am. Chem. Soc.* **2007**, *129*, 11950-11963.

(20) A. J. Goshe, J. D. Crowley, B. Bosnich, *Helv. Chim. Acta* **2001**, *84*, 2971-2985.

(21) a)S. Saito, E. Takahashi, K. Nakazono, *Org. Lett.* **2006**, *8*, 5133-5136. b) Y. Sato, R. Yamasaki, S. Saito, *Angew. Chem. Int. Ed*. **2009**, *48*, 504 –507.

(22) E. R. Kay, D. A Leigh, *Top. Curr. Chem*. **2005**, *262*, 133-177.

(23) For examples of 1,2,3-triazoles as ligands see: a) D. Liu, W. Gao, Q. Dai, X. Zhang, *Org. Lett*. **2005**, *7*, 4907-4910. b) Q. Dai, W. Gao, D. Liu, L. M. Kapes, X. Zhang, *J. Org. Chem*. **2006**, *71*, 3928-3934. c) T. L. Mindt, H. Struthers, L. Brans, T. Anguelov, C. Schweinsberg, V. Maes, D. Tourwe, R. Schibli, *J. Am. Chem. Soc*. **2006**, *128*, 15096-15097. d) B. M. J. M. Suijkerbuijk, B. M. H. Aerts, H. P. Dijkstra, M. Lutz, A. L. Spek, G. van Koten, R. J. M. Klein Gebbink, *Dalton Trans*. **2007**, 1273-1276. e) J. C. Huffman, A. H. Flood, Y. Li, *Chem. Commun*. **2007**, 2692-2694.

(24) F. Durola, J.-P. Sauvage, *Angew. Chem. Int. Ed*. **2007**, *46*, 3537-3540.

(25) E. Riesgo, Y.-Z. Hu, F. Bouvier, R. P. Thummel, *Inorg. Chem.* **2001**, *40*, 2541-2546.

(26) H. W. Gibson, S. H. Lee, P. T. Engen, P. Lecavalier, J. Sze, Y. X. Shen, M. Bheda, *J. Org. Chem.* **1993**, *58*, 3748-3756.

(27) T. Nakayama, M. Nomura, K. Haga, M. Ueda, *Bull. Chem. Soc. Jpn*. **1998**, *71*, 2979-2984.

(28) E. C. Constable, A. C. King, P. R. Raithby, *Polyhedron*, **1998**, *17*, 4275-4289.

(29) M. J. Mio, L. C. Kopel, J. B. Braun, T. L. Gadzikwa, K. L. Hull, R. G. Brisbois, C. J. Markworth, P. A. Grieco, *Org. Lett*. **2002**, *4*, 3199-3202.

(30) I. Merino, J. D. Thompson, C. B. Millard, J. J. Schmidt, Y.-P. Pang, Bioorg. *Med. Chem. Lett*. **2006**, *14*, 3583-3591.

(31) B. H. Dana, B. H. Robinson, J. J. Simpson, *Organomet. Chem*. **2002**, *648*, 251-269.

Chapter III

A Catalytic Palladium Active-metal Template Pathway to [2]Rotaxanes

Published as *A Catalytic Palladium Active-Metal Template Pathway to [2]Rotaxanes*, J. Berná, J. D. Crowley, S. M. Goldup, K. D. Hänni, A.-L. Lee, D. A. Leigh, *Angewandte Chem. Int. Ed.* **2007**, 46, 5709-5713. Highlight: *Palladium-Catalyzed Synthesis of Rotaxanes*, T. M. Swager, R. M. Moslin, Synfacts, **2007**, 11, 1158.

Acknowledgments

The following people are gratefully acknowledged for their contribution to this Chapter: Dr. José Berná synthesised rotaxane **4a** for the first time and determined reaction conditions; Dr. Ai-Lan Lee isolated and characterised rotaxanes **4b** and **4c**, created the stacked plots presented in Paragraphs 3.3.2; Dr. James Crowley obtained Pd-complexes **2a-c** and obtained an X-ray quality crystal of **2c** (Figure 3.1); Prof. Alexandra Slawin solved the solid structure of **2c** and Dr. Stephen Goldup investigated alternative synthetic strategies that are not described here.

3.1 Synopsis

This chapter describes a method to assemble [2]rotaxanes using stoichometric and catalytic amounts of palladium. A trans-dichloridepalladium(II) complex undergoes transmetallation with alkynyl cuprate half-threads. The reductive elimination of the resulting complex produces interlocked structures. The metal can turnover during the reaction by the use of iodine to reoxidise the metal, resulting in a catalytic AMT assembly process.

A variety of mono-, bi- and tridentate Pd-macrocycle complexes were investigated under palladium rotaxane-formation conditions. The minimum of two available binding sites is necessary for the reaction to proceed, as the metal centre has to accommodate two stoppered ligands in order to produce a rotaxane.

3.2 Introduction

The rapid growth in the number and variety of palladium-catalysed transformations over the latter part of the 20th century has seen palladium become the workhorse of modern synthetic chemistry.[1] Palladium-catalysed processes include the formation of C-O, C-N, C-S, and, most notably, C-C bonds. Since Glaser publication in 1869,[2] considerable efforts were directed towards the development of facile and efficient methodologies for the preparation of symmetrical and dissymmetrical 1,4-diynes. Traditional protocols of alkyne coupling reactions include: Cadiot-Chodkiewicz,[3] Eglington,[4] Glaser,[2,5] Hay,[6] and Sonogashira[7] coupling. It has been shown that catalytic systems using Pd(0) or Pd(II) species are the most efficient, mild and selective[1c] for the oxidative coupling of alkynes over the traditional copper-mediated methodologies (Cu^{I}: Cadiot, Glaser, Hay; Cu^{II}: Eglington). Palladium-catalysed homocoupling reactions are generally carried out in the presence of phosphines (PPh_3) or amine ligands (*i*Pr_2NH, iPr_2NEt, DABCO, NEt_3), although recent literature reports the use of ligand-free conditions.[8] A typical Pd-mediated alkyne homocoupling is shown in Scheme 3.1: the formation of a copper-acetylide occurs first by base-assisted deprotonation of the alkyne in the presence of CuI. Further transmetallation with Pd(II) gives a dialkynylpalladium(II) species **I** (Scheme 3.1). Reductive elimination of **I** releases the diyne product and Pd(0). Reoxidation of Pd(0) to Pd(II) with various oxidants (i.e. I_2, $Cu(OAc)_2$ or benzoquinone) completes the catalytic cycle.

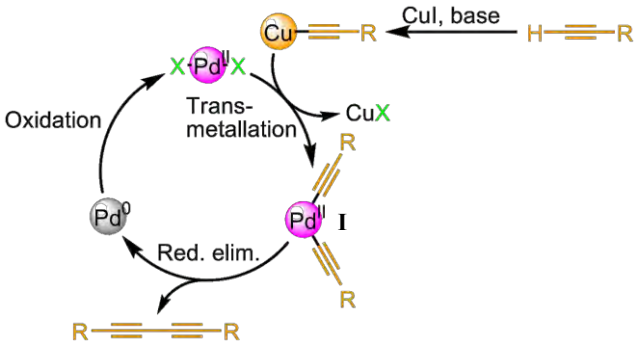

Scheme 3.1 General mechanism of the Pd-mediated alkyne homocoupling reaction.

3.3 Results and Discussion

Although Pd(II) has a square-planar coordination geometry, it has proved possible to use its two dimensional motif to assemble rotaxanes[9] and catenanes[10] in classical passive template strategies by utilising steric control over the required crossover point in the third dimension (see also Chapter I, Paragraph 1.5.4, 1.5.10 and 1.5.12).

Macrocycle **1a** (Scheme 3.2) was chosen as a suitable candidate ligand for developing a novel palladium active-template rotaxane synthesis. X-ray crystallography of a related palladium(II) [2]catenate shows that the *trans*-coordinated chloride ligands protrude from opposite sides of the macrocycle cavity (Scheme 3.2, right). We reasoned that if the chloride ligands of *trans*-**2a** could be replaced by suitably functionalized stoppered groups it would generate a threaded complex of type **I** (Scheme 3.2). If the palladium centre is able to retain the stoppered ligands until it has mediated a covalent bond forming reaction between them (**II**, Scheme 3.2), a [2]rotaxane would be formed. This idea was investigated using the palladium(II)-mediated homocoupling of terminal alkynes.[11]

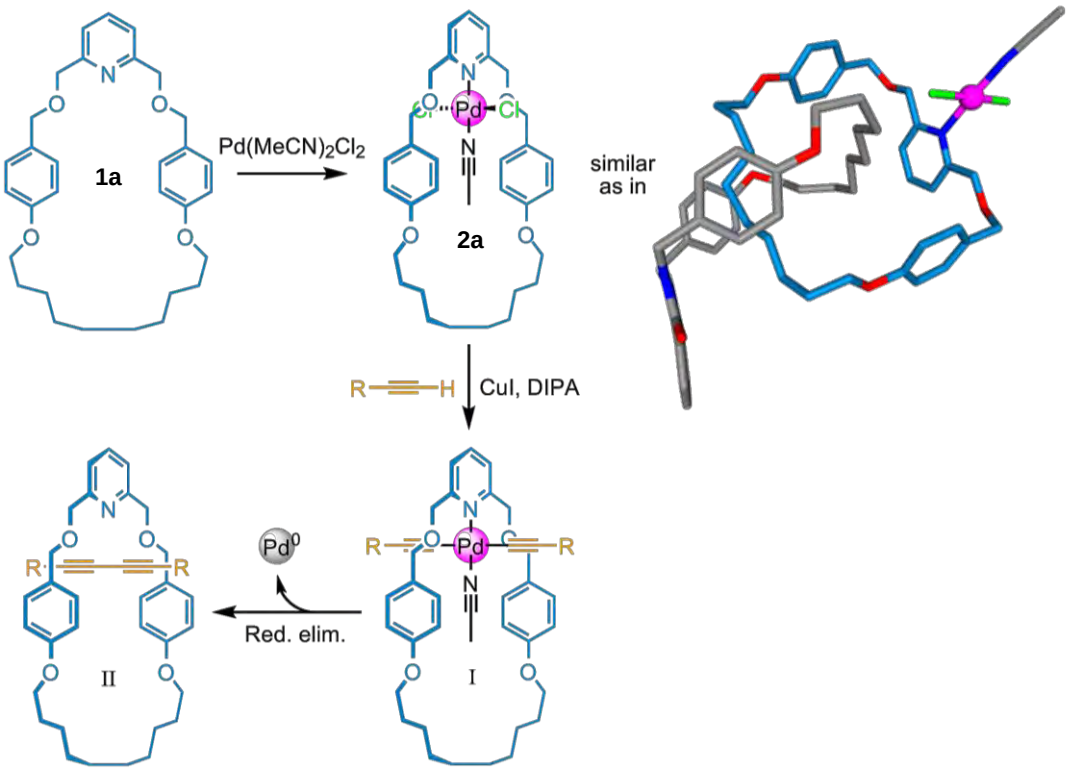

Scheme 3.2 Initial idea of using Pd-catalysed alkyne homocoupling. Chloride ligands in trans configuration in the X-Ray crystal structure.

Initial attempts in subjecting a propargylic half-thread, previously used in Chapter II, to standard Pd-mediated alkyne homo-coupling conditions together with **2a** led to the complete consumption of the alkyne. Unfortunately, instead of observing the desired homocoupled diyne as major products, the corresponding deprotected phenol was obtained in nearly quantitative yield. This observation is consistent with the publication of Pal *et al.* in 2003,[12] wherein they report a facile protocol to cleave propargyl protecting groups on phenols using Pd(0) (Scheme 3.3). To prevent phenol-

derived by-products, the half-thread spacer between the bulky stoppered unit and the alkyne functionality was extended from one to three carbon atoms as in half-thread **3**. This avoids the allenyl-palladium intermediate necessary for the deprotection.

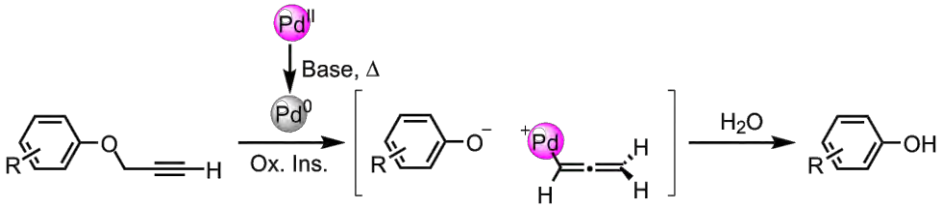

Scheme 3.3 Deprotection of the propargyl protected phenol with help of Pd(0) by Pal et al.

Complex *trans*-**2a** was treated with 2.5 equivalents of an appropriately derivatised alkyne (**3**) and CuI (5 mol% with respect to **3**) in diisopropylamine (DIPA; Table 3.1, entry 1). After 12 h at room temperature the desired [2]rotaxane **4a** was formed in 43% yield (based on **2a**), while the homocoupling reaction proceeded to completion (>98% conversion into the diyne products, rotaxane **4a**, and non-interlocked thread **5**, Scheme 3.4).

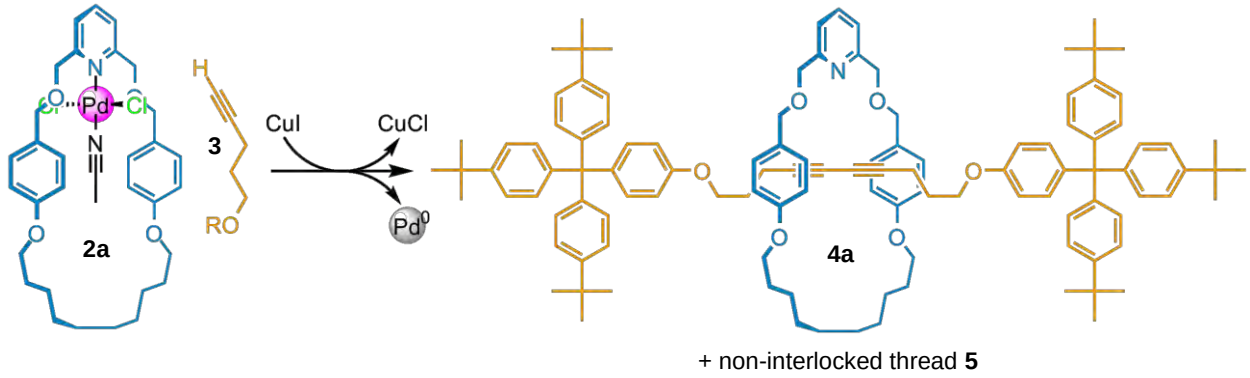

*Scheme 3.4 Pd-mediated alkyne homocoupling active template synthesis of rotaxane **4a**.*

Carrying out the reaction using a five-fold excess of **3** increased the yield of [2]rotaxane **4a** to 61% (Table 3.1, entry 2). The proposed mechanism for rotaxane formation is shown in Scheme 3.5. Standard Pd ligand-substitution chemistry[1,13] dictates that under transmetallation conditions the acetylide units should directly replace the chloride ligands of *trans*-**2a**, initially retaining their relative stereochemistry and thus leading to the threaded *trans* palladium *bis*(alkyne) adduct **I**. Isomerisation of **I** to the *cis* geometry necessary for the reductive elimination must occur without breaking either Pd–acetylide bond, as models (Spartan™) show that the unthreaded *cis* isomer (which would generate non-interlocked macrocycle **1a** and thread **5** rather than [2]rotaxane **4a**) would be preferred on steric grounds. Reductive elimination then generates the

Pd(0)–rotaxane complex **II** and decomplexation of the weakly binding Pd(0) liberates the free rotaxane **4a**.

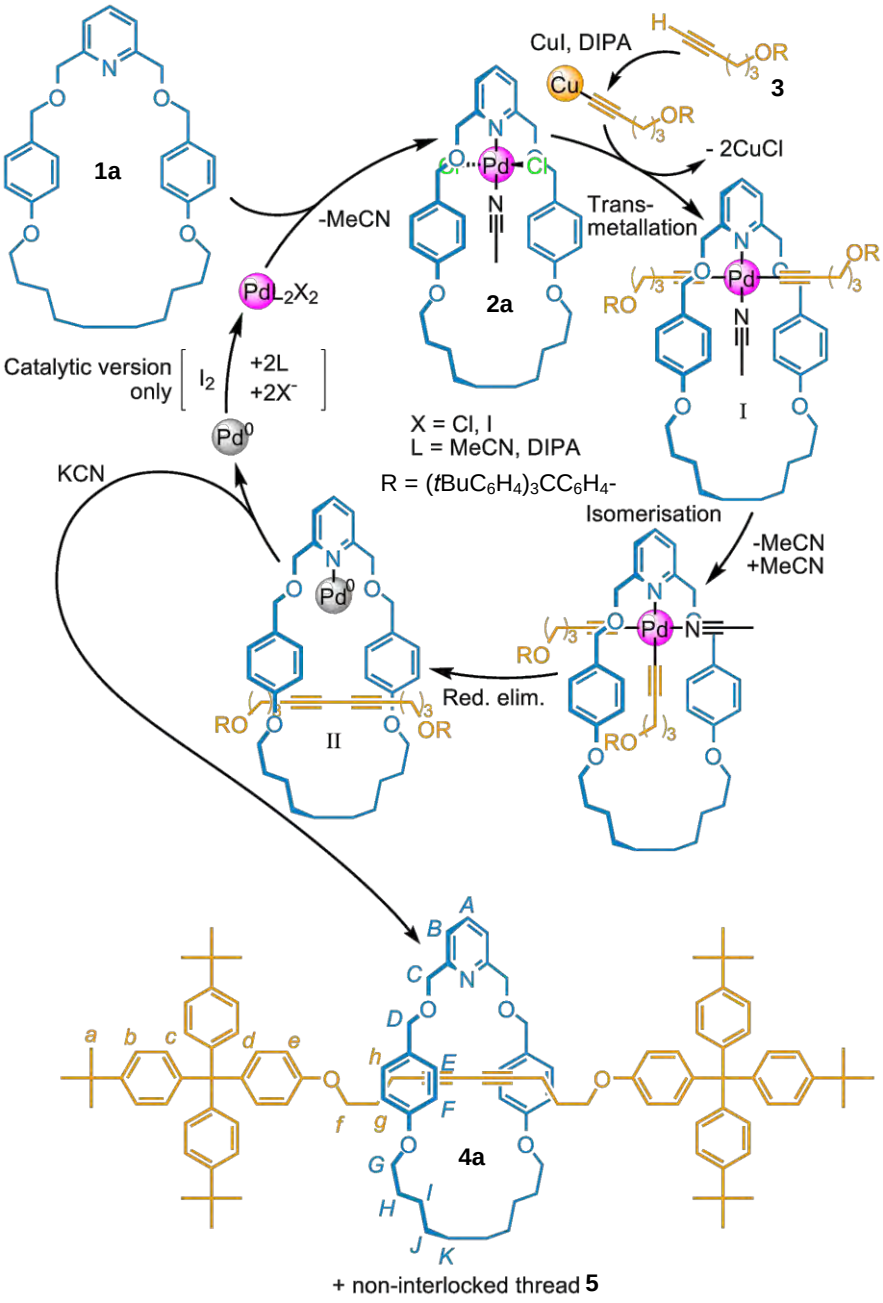

*Scheme 3.5 Pd(II)-mediated AMT synthesis of [2]rotaxane **4a**. For yields and conditions see Table 1.*

Having achieved an efficient stoichiometric version of the active-metal template reaction, we turned our attention towards developing a synthesis that was catalytic with respect to palladium (Table 3.1, entries 3–7). This required that the metal turn over as both a template and a covalent bond forming catalyst. The palladium-mediated alkyne homocoupling reaction is particularly well-suited in this respect because diyne

formation is accompanied by reduction of the Pd(II) to intrinsically weaker coordinating Pd(0). A combination of iodine and oxygen is typically used as the oxidant to render such reactions catalytic.[1] We initially tried conditions similar to those employed in the stoichiometric rotaxane-forming reaction, but using 10 mol% of *trans*-**2a** in the presence of I_2 (Table 3.1, entry 3). No rotaxane was produced under these conditions, however, and the overall conversion of alkyne to diyne products was only 37%. Switching from DIPA to benzene as the solvent led to a significant improvement in both the yield of diyne products and the formation of [2]rotaxane **4a** (57% and 27%, respectively, entry 4). Increasing the reaction time from 12 to 24 h gave further improvements (83% diyne products, 35% [2]rotaxane, entry 5). Finally, increasing the equivalents of **3**, reducing the loading of **2a** to 5 mol% (with respect to **1a**), and further extending the reaction time to 72 h improved the yield of rotaxane **4a** to up to 90% (entries 6 and 7 respectively). Increasing the temperature up to 50 °C led to no ameliorations: only 52% of total conversion was achieved with 47% of rotaxane **4a**.

*Table 3.1 Effect of reactant stoichiometry and experimental conditions on the Pd(II)-mediated AMT synthesis of [2]rotaxane **4a**.*[a]

Entry	Amt. of **1a** [equiv]	Amt. of **2a** [equiv]	Amt. of **3** [equiv]	Amt. of I_2 [equiv]	Time	Conv. to diynes **3**→**4a**+**5** [%]	Yield of rot. **1a**→**4a** [%][d]
1[b]	**-**	**1**	**2.5**	**-**	**12 h**	**>98**	**43**
2[b]	-	1	10	-	12 h	>98	61
3[b]	0.9	0.1	10	0.5	12 h	37	<1
4[c]	0.9	0.1	10	0.5	12 h	57	27
5[c]	0.9	0.1	10	0.5	24 h	83	35
6[c]	0.95	0.05	15	0.5	72 h	94	81
7[c]	**0.95**	**0.05**	**30**	**0.5**	**72 h**	**49**	**90**

*[a]All Reactions were carried out at 298 K using anhydrous solvents and protection from moisture. [b]10 mM trans-**2a**, CuI (5 mol% with respect to **3**), neat DIPA; [c]14 mM macrocycle (**1a**+trans-**2a**) CuI (5 mol% with respect to **3**), DIPA (5 equiv), benzene.*

Control experiments were carried out to confirm the necessity of the presence of both Pd and Cu in the palladium(II)-mediated homocoupling of terminal alkynes reaction. Conditions described in Table 3.1, entry 2 (stoichiometric) or Table 3.1, entry 6 (catalytic) were repeated, firstly in the absence of Pd, and then in the absence of CuI: no diyne products were detected by ^{1}H NMR in either cases. Even the Cu(I)-mediated Glaser alkyne homocoupling[14] occurs to a negligible extent under these reaction conditions (< 1%).

3.3.1 Effect of the Macrocycle Structure on [2]Rotaxane Formation

Mono- (**2b**), bi- (**2c**), and tridentate (**2d** and **2e**) Pd-macrocycle complexes shown in Figure 3.1 (their syntheses are detailed in the Experimental Section) were used to explore the influence of the nature of the macrocyclic ligand on the AMT reaction. Reaction of **2b** and **2c** under the standard stoichiometric conditions resulted in the formation of the corresponding [2]rotaxanes **4b** and **4c** in 38% and 10% yields respectively (Table 2, entries 1 and 4). The low yield obtained with the bidentate complex **2c** presumably reflects the fact that the two chloride ligands are necessarily *cis* for transmetallation. Even with the larger macrocycle cavity of **2c** relative to **2a**, the *cis* orientation significantly decreases the chance of the two alkyne substitutions occurring through opposite faces of the macrocycle. Carrying out the same reactions in the presence of 10 equivalents of **3** increased the yield of [2]rotaxane **4c** to 20% (Table 2, entry 5) but, to our surprise, resulted in a decrease in the yield of rotaxane **4b** from 38% to 30%(Table 2, entry 2). As expected, reaction of **3** with the tridentate palladium complexes **2d** and **2e** failed to generate any reaction products (Table 2, entries 7 and 8), as two labile coordination sites on the metal are necessary for the alkyne homocoupling mechanism (Scheme 3.5).

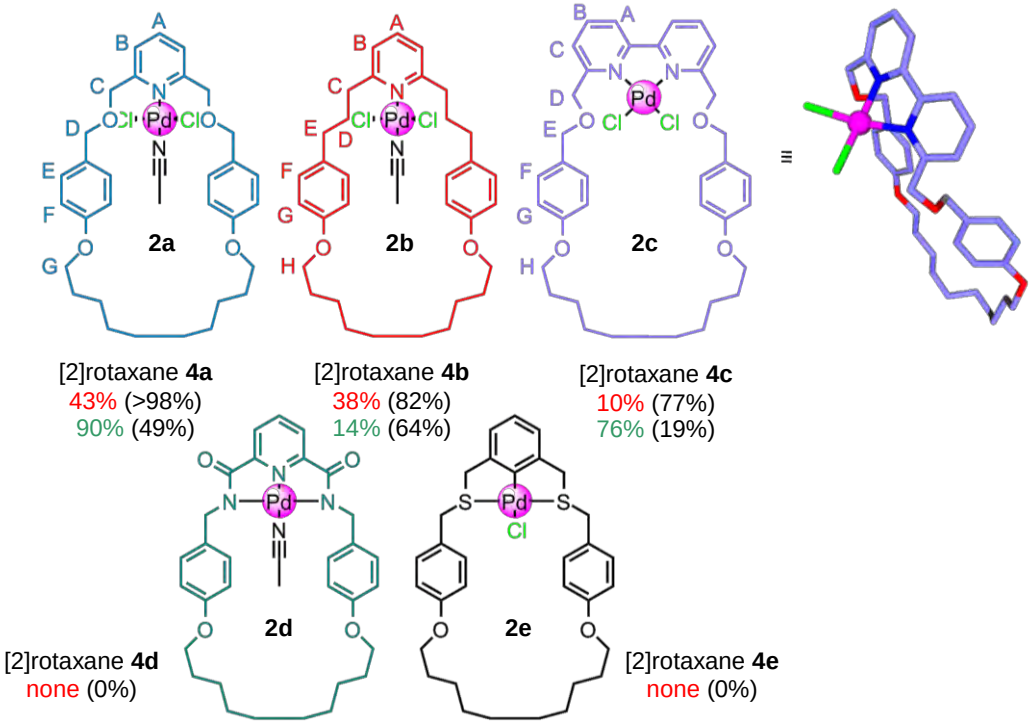

*Figure 3.1 Screening of different Pd-macrocycle complexes for the Pd(II)-mediated active-metal template synthesis of [2]rotaxanes. Conversion of complex into rotaxane (**2** → **4**) is given in red (stoichiometric conditions: Table 3.1, entry 1). Conversion of macrocycle into rotaxane (**1** → **4**) is given in green (catalytic conditions: Table 3.1, entry 7). **1a-e** are the metal-free macrocycles.*

As found earlier for **4a** (Table 1, entries 2 and 7), the yield of rotaxane **4c** was greatly improved (from 20% to 76%; Table 2, entries 5 and 6) by changing from stoichiometric to catalytic palladium conditions. In contrast, the yield of rotaxane **4b** decreased to 14% under similar catalytic conditions, although the overall conversion into diyne products (**4b**+**5**) was a respectable 63% (Table 2, entry 3). It is possible that this disparity occurs because the benzylic oxygen atoms in **2a** can play a role in dynamic ligation to the palladium centre. In their absence the macrocycle is a poorer ligand. Thus, when the amount of alkyne **3** present with respect to **2b** is increased (Table 2, entries 2 or 3), the excess alkyne is able to compete with the pyridine macrocycle for the palladium, thereby reducing the yield of rotaxane **4b**. In addition, the pyridine coordination site on the macrocycle is crucial for rotaxane formation: when conditions used in Table 1, entry 1 were repeated with the non-pyridine version of macrocycle **1a** (pyridine replaced by benzene), no rotaxane was detected and non-interlocked thread **5** was only formed in 19% yield after 3 days. It is interesting to note that the catalytic conditions with **2a** and **2c** provide much cleaner conversions and higher yields of [2]rotaxanes than the stoichiometric conditions. The use of stoichiometric amounts of Pd(II), especially with the solvent concentrations of DIPA required for high conversions in the stoichiometric reactions, probably gives rise to side-reactions and other macrocycle–Pd species that do not afford [2]rotaxane.

Table 3.2 Effect of macrocycle structure on the Pd(II)-mediated active-metal template synthesis of [2]rotaxanes.[a]

Entry	Pd-mac complex	Amt. of **3** [equiv]	Time	Conv. to diynes **3**→**4a**+**5** [%]	Yield of rot. **1a**→**4a** [%][e]
1[b]	**2b**	2.5	18 h	82	38
2[b]	**2b**	10	18 h	75	30
3[c]	**2b**	30	72 h	63	14
4[b]	**2c**	2.5	18 h	75	10
5[b]	**2c**	10	18 h	87	20
6[c]	**2c**	30	72 h	19	76
7[b]	**2d**	2.5	72 h	0[d]	0[d]
8[b]	**2e**	2.5	72 h	0[d]	0[d]

[a]All reactions were carried out at 298 K using anhydrous solvents and protection from moisture. [b]stoichiometric conditions (10 mm). [c]Catalytic conditions (14 mm). [d]No diyne products were detected. [e]With respect to the Pd-complexes.

3.3.2 ^{1}H NMR of the Interlocked Compound

The ^{1}H NMR spectrum of **4a** in $CDCl_3$ (Figure 3.2 b) shows the upfield shift of several signals with respect to the non-interlocked components (a, c and d). The shielding, typical of interlocked architectures in which the aromatic rings of one component are positioned face-on to another component, occurs for all the non-stopper resonances of the axle ($H_{f\text{-}h}$) indicating that in the metal-free rotaxane the macrocycle is able to access the full length of the thread.

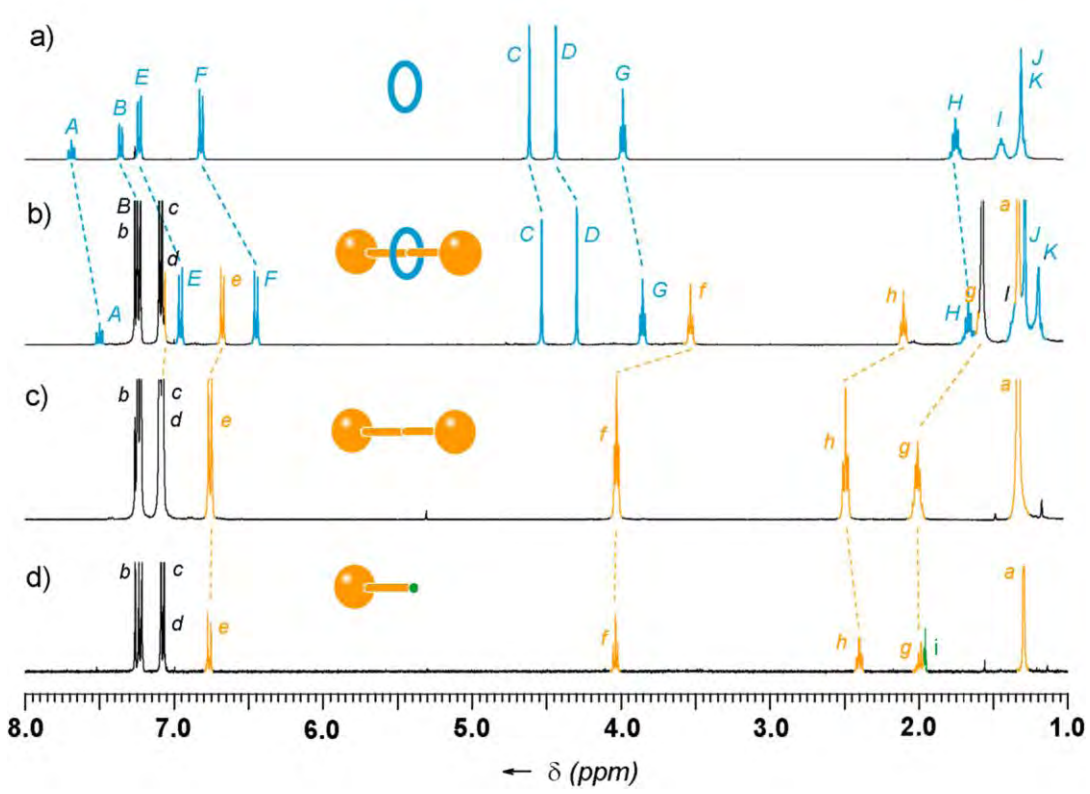

*Figure 3.2 ^{1}H NMR spectra (400 MHz, $CDCl_3$, 298 K) of a) macrocycle **1a**, b) [2]rotaxane **4a**, c) non-interlocked thread **5**, d) half-thread **3**. The assignments correspond to the lettering in Scheme 3.5.*

3.4 Conclusion

The template-directed assembly of otherwise difficult-to-access molecules and the catalysis of covalent-bond formation are two of the most useful tasks that transition metals can perform in organic chemistry. The present work demonstrates that the currently rare combination of these apparently disparate functions can produce high-yielding, mild and effective synthetic routes to complex molecular architectures that require only sub-stoichiometric amounts of metal.

3.5 Experimental Section

3.5.1 Preparation of Half-thread 3

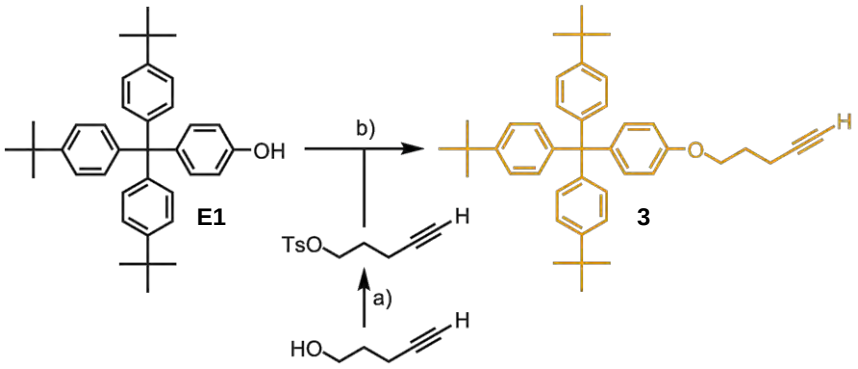

Scheme 3.6 a) p-TsCl, CH_2Cl_2, 0 °C → RT, 18 h, 71%; d) K_2CO_3, butanone, 80 °C, 18 h, 82%.

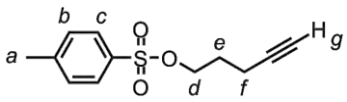

E2

A solution of 4-pentyn-1-ol (5.96 g, 70.9 mmol, 1 equiv.) and Et_3N (20 mL, 138 mmol, 2 equiv.) in anhydrous CH_2Cl_2 (200 mL) was cooled to 0 °C. *p*-Toluenesulfonyl chloride (14.33 g, 75.2 mmol, 1.05 equiv.) was added and the solution was stirred at RT for 18 h. The reaction was quenched with water (100 mL). The organic layer was separated, dried ($MgSO_4$), filtered, concentrated under reduced pressure and the resulting crude oil was purified by column chromatography (Gradient, hexane/CH_2Cl_2 9:1 then 5:5) to yield tosylate **E2** as a colorless oil (11.99 g, 71%). ^{1}H NMR (400 MHz, $CDCl_3$, 298 K): δ = 7.77 (d, *J* = 8.3 Hz, 2H, H_c), 7.33 (d, *J* = 8.3 Hz, 2H, H_b), 4.12 (t, *J* = 6.1 Hz, 2H, H_d), 2.43 (s, 3H, H_a), 2.23 (td, *J* = 6.9 Hz, 2.6 Hz, 2H, H_f), 1.87 (t, *J* = 2.6 Hz 1H, H_g), 1.84 (m, 2H, H_e); ^{13}C NMR (100 MHz, CDCl3): δ = 144.8, 132.8, 129.8, 127.8, 82.0, 69.4, 68.7, 27.6, 21.6, 14.6; LRESI-MS: *m/z* = 238 $[M]^+$; HRESI-MS: *m/z* = 238.06547 $[M]^+$ (calcd. for $C_{12}H_{14}O_3S$, 238.06582).

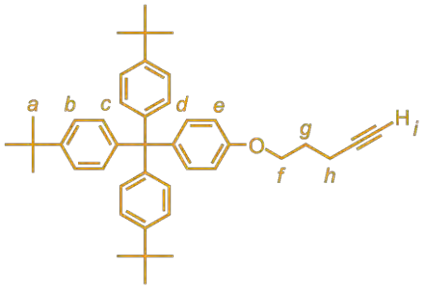

1-(pent-5-ynoxy)-4-(*tris*-(4-*tert*-butyl-phenyl)-methyl)-benzene (3)

A solution of 4-[*tris*-(4-*tert*-butylphenyl)methyl]phenol (**E1**) [15] (5.00 g, 9.95 mmol, 1 equiv.) and tosylate **E2** (3.81 g, 15.91 mmol, 1.6 equiv.) in butanone (75 mL) containing K_2CO_3 (6.9 g, 50 mmol, 5 equiv.) and 18-crown-6 (50 mg) was heated under reflux for 42 h. After cooling to room temperature, the reaction mixture was filtered through a sintered glass funnel and the solid washed with CH_2Cl_2 (50 mL). The combined organic phases were concentrated under reduced pressure and the resulting residue was dissolved in CH_2Cl_2 (150 mL), washed with water (2 × 100 mL), and dried ($MgSO_4$). After removal of the solvent the residue was purified by column chromatography (CH_2Cl_2/MeOH 97:3) to give alkyne **3** as a colorless solid which was recrystallized from hot hexane (4.66 g, 82%). M.p. 228-230 °C; ^{1}H NMR (400 MHz, $CDCl_3$, 298 K): δ = 7.22 (d, *J* = 8.7 Hz, 6H, H_b), 7.07 (d, *J* = 8.7 Hz, 6H, H_c), 6.76 (d, *J* = 9.0 Hz, 2H, H_d), 6.76 (d, *J* = 9.0 Hz, 2H, H_e), 4.04 (t, *J* = 6.1 Hz, 2H, H_f), 2.40 (td, *J* = 7.0Hz, 2.7 Hz, 2H, H_h), 1.99 (m, 2H, H_g), 1.96 (t, *J* = 2.7 Hz, 1H, H_i), 1.30 (s, 27H, H_a); ^{13}C NMR (100 MHz, $CDCl_3$, 298 K): δ = 156.6, 148.3, 144.1, 139.6, 132.2, 130.7, 124.0, 12.9, 83.6, 68.8, 65.9, 63.0, 34.3, 31.4, 28.2, 15.2; LRFAB-MS (3-NOBA matrix): *m/z* = 570 $[M]^+$; HRFAB-MS (3- NOBA matrix): *m/z* = 570.38676 $[M]^+$ (calcd. for $C_{42}H_{50}O$, 570.38617).

3.5.2 Preparation of Pd-complexes

Complexes **2a**[10a] and **2d**[10b] were prepared according to literature procedures.

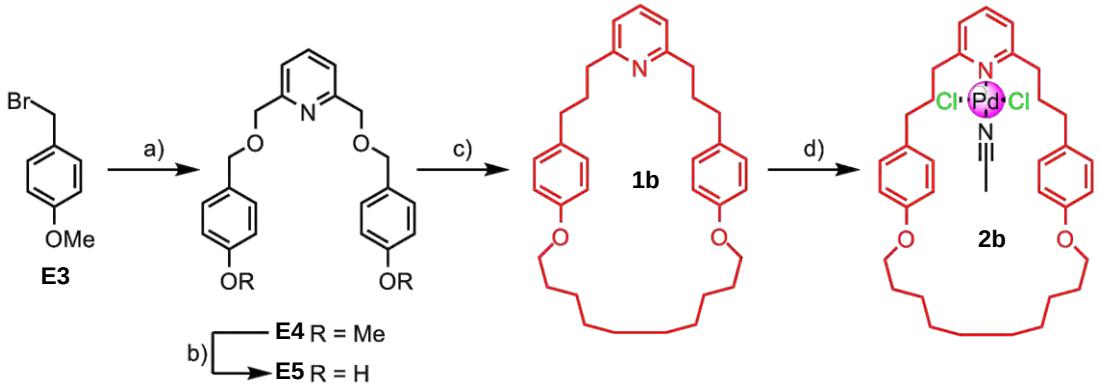

Scheme 3.7 a) 1. Zn, I_2, DMF, 80 °C, 4 h, 2. 2,6-dibromopyridine, $Pd(PPh_3)_4$, DMF, RT, 20 h; b) BBr_3, CH_2Cl_2, -78 °C → RT, 1 h, 50% (over three steps); c) 1,10-dibromodecane, K_2CO_3, DMF, 100 °C, 24 h, 36%; d) $Pd(MeCN)_2Cl_2$, CH_2Cl_2, RT, 1 h, 90%.

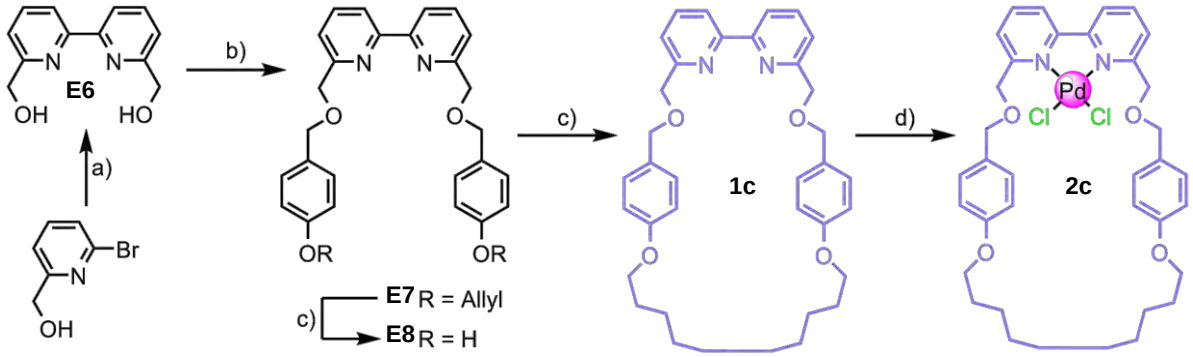

Scheme 3.8 a) $NiCl_2 \cdot 6H_2O$, PPh_3, Zn, DMF, 50 °C, 3 h, 82%; b) 1-Allyloxy-4-bromomethylbenzene,[16] NaH, DMF, 0 °C → RT, 16 h, 84%; c) $Pd(PPh_3)_4$, aniline, 30 °C, 2 ., 88%; d) 1,10-dibromodecane, K_2CO_3, DMF, 80 °C, 16 h, 31%; d) $Pd(MeCN)_2Cl_2$, CH_2Cl_2, RT, 2.5 h, 88%.

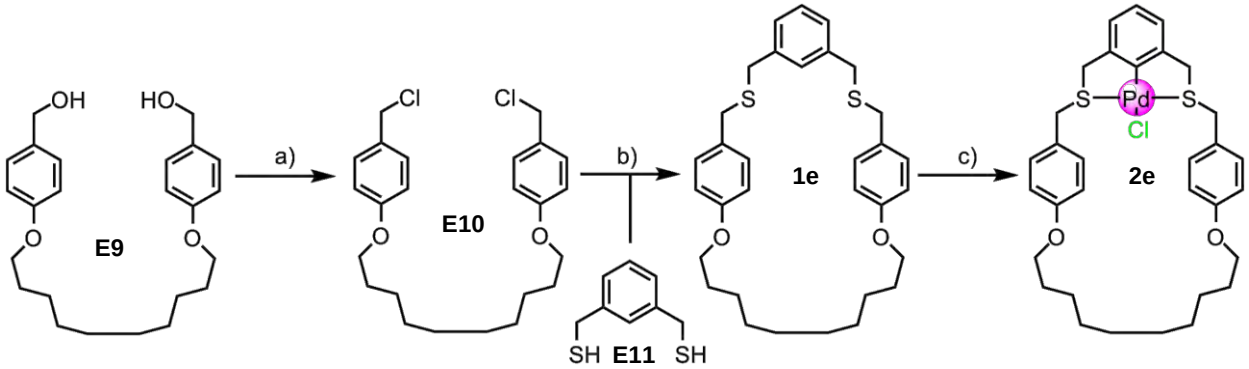

Scheme 3.9 a) $SOCl_2$, pyridine, CH_2Cl_2, 0 °C → RT, 16 h, 99%; b) K_2CO_3, butanone, 80 °C, 72 h, 19%; c) $Pd(MeCN)_4(BF_4)_2$, MeCN, reflux, 2 h, then brine, RT, 2 h, 41%.

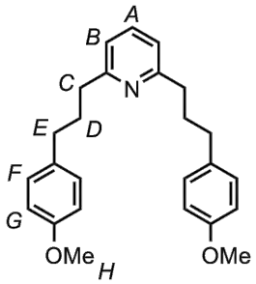

E4

To a stirred suspension of Zn (0.98 g, 15 mmol, 1.50 equiv.) in DMF (10 mL) at RT was added I_2 (130 mg, 0.50 mmol, 0.05 equiv.) and the mixture stirred until the colour of the iodine had disappeared (approximately 2 min). 4-(4-Methoxyphenyl)propyl bromide (**E3**)[17] (2.3 g, 10 mmol, 1.00 equiv.) was added and the reaction mixture was heated to 80 °C for 4 h after which time the reaction mixture was cooled to RT and 2,6-dibromopyridine (0.95 g, 4.0 mmol, 0.40 equiv.) was added followed by $Pd(PPh_3)_4$ (0.12 g, 0.10 mmol, 0.01 equiv.) and the reaction mixture stirred for a further 16 h at RT. The suspension was then partitioned between aqueous NH_3 (10 M, 200 mL) and EtOAc (200

ml) and the layers separated. The organic phase was washed with H_2O (200 mL) and brine (200 mL), dried ($MgSO_4$) and the solvent removed under reduced pressure. Purification by column chromatography (CH_2Cl_2 then 2% MeOH in CH_2Cl_2) gave 2,6-*bis*-[3-(4-methoxyphenyl)propyl]pyridine (**E4**) as a pale yellow oil (1.2 g, 80%). ^{1}H NMR (400 MHz, d_4-MeOD, 298 K): δ = 7.48 (t, *J* = 7.5, 1H, H_A), 7.11 (d, *J* = 8.5, 4H, H_F), 6.94 (d, *J* = 7.5, 2H, H_B), 6.82 (d, *J* = 8.5, 4H, H_G), 3.78 (s, 6H, O_H), 2.79 (t, *J* = 8.0, 4H, H_C), 2.62 (t, *J* = 8.0, 4H, H_E), 2.05-1.97 (m, 4H, H_D); ^{13}C NMR (100 MHz, d_4-MeOD, 298 K) δ = 161.3, 157.5, 136.3, 134.3, 129.2, 119.7, 113.6, 55.1, 37.9, 34.5, 31.9; LRESI-MS (MeOH/TFA): *m/z* = 376 $[M+H]^+$.

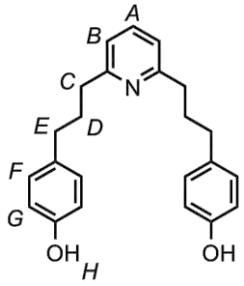

E5

To a solution of dimethylether **E4** (1.2 g, 3.2 mmol, 1 equiv.) in CH_2Cl_2 (20 mL) at -78 °C was added BBr_3 (1.5 mL, 16 mmol, 5 equiv.) and the reaction warmed to RT over 2 h. At this time the reaction was diluted with CH_2Cl_2 (200 mL) and sat. $NaHCO_3$ (200 mL) followed by MeOH until all the solids dissolved. The layers were separated and the aqueous phase extracted with CH_2Cl_2/MeOH 98:2 (200 mL). The combined organic extracts were dried ($MgSO_4$) and concentrated under reduced pressure. Purification by column chromatography (CH_2Cl_2 then 5% MeOH in CH_2Cl_2) gave the diphenol U-shape **E5** as a pale yellow solid (700 mg, 63%). M.p. 42-44 °C; ^{1}H NMR (400 MHz, $CDCl_3$, 298 K): δ = 9.14 (s, 2H, H_H), 7.57 (t, *J* = 7.5 Hz, 1H, H_A), 7.02 (d, *J* = 7.5 Hz, 2H, H_B), 6.97 (d, *J* = 8.5, 4H, H_F), 6.66 (d, *J* = 8.5, 4H, H_G), 2.67 (t, *J* = 7.5, 4H, H_C), 2.48 (t, *J* = 7.5, 4H, H_E), 1.92-1.85 (m, 4H, H_D); ^{13}C NMR (100 MHz, $CDCl_3$, 298 K): δ = 160.7, 156.2, 136.6, 132.0, 129.1, 119.8, 115.0, 36.9, 33.9, 31.4; LRFAB-MS (3-NOBA matrix): *m/z* = 348 $[M+H]^+$; HRFAB-MS (3-NOBA matrix): *m/z* = 348.19629 $[M+H]^+$ (calcd. for $C_{23}H_{26}NO_2$, 348.19635).

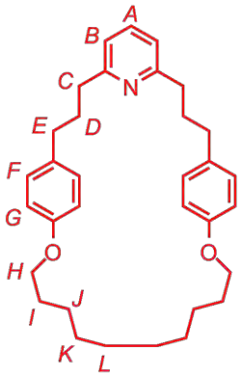

1b

To a solution of diphenol U-shape **E5** (348 mg, 1 mmol, 1 equiv.) in DMF (500 mL) was added K_2CO_3 (2.76 g, 20 mmol, 20 equiv.) and 1,10-dibromodecane (300 mg, 1 mmol, 1 equiv.) and the resulting suspension stirred for 24 h at 100 °C. The solvent was removed under reduced pressure and the residue dissolved in EtOAc (200 mL). This solution was washed with $NaHCO_3$ (200 mL), H_2O (200 mL) and brine (200 mL), then dried ($MgSO_4$). The solvent was removed under reduced pressure and the residue purified by column chromatography (hexane/EtOAc 9:91) to provide macrocycle **1b** as a colourless oil which crystallised as a colourless solid on standing (174 mg, 36%); M.p. 50-54 °C; ^{1}H NMR (400 MHz, $CDCl_3$, 298 K): δ = 7.49 (t, *J* = 7.6 Hz, 1H, H_A), 7.06 (d, *J* = 8.6 Hz, 4H, H_F), 6.97 (d, *J* = 7.7 Hz, 2H, H_B), 6.78 (d, *J* = 8.6 Hz, 4H, H_G), 3.94 (t, *J* = 6.4 Hz, 4H, H_H), 2.80 (t, *J* = 7.8 Hz, 4H, H_C), 2.64-2.52 (m, 4H, H_E), 2.05-1.93 (m, 4H, H_D), 1.76 (dt, *J* = 6.7, 6.7 Hz, 4H, H_I), 1.51-1.31(m, 4H, H_J), 1.31-1.25 (m, 8H, HK, H_L); ^{13}C NMR (100 MHz, CDCl3): δ = 161.3, 157.1, 136.4, 134.2, 129.2, 119.9, 114.3, 67.4, 37.9, 34.7, 32.4, 28.8, 28.6, 28.2, 25.5; LRFAB-MS (3-NOBA matrix): *m/z* = 486 $[M+H]^+$; HRFAB-MS (3-NOBA matrix): *m/z* = 486.33723 $[M+H]^+$ (calcd. for $C_{33}H_{44}NO_2$, 486.33721).

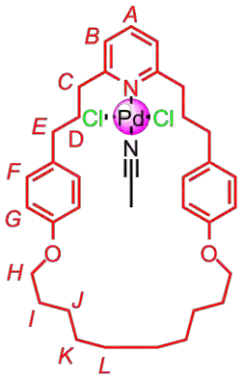

2b

A solution of pyridine macrocycle **1b**[18] (116 mg, 0.24 mmol, 1 equiv.) and *trans-bis*(acetonitrile)dichloropalladium(II) (62 mg, 0.24 mmol, 1 equiv.) in CH_2Cl_2 (5 mL) was allowed to stir at room temperature under N_2 for 1 h. The solvent was removed under reduced pressure and the resulting orange solid was purified by recrystallisation (CH_2Cl_2/MeCN 1:1) to give palladium complex **2b** as a yellow-orange solid (152 mg, 90%). M.p. 214-218 °C; ^{1}H NMR (400 MHz, $CDCl_3$/d_3-MeCN 9:1, 298 K): δ = 7.35 (t, *J* = 7.7 Hz, 1H, H_A), 7.15 (d, *J* = 8.5 Hz, 4H, H_F), 6.87 (d, *J* = 7.7 Hz, 2H, H_B), 6.70 (d, *J* = 8.5 Hz, 4H, H_G), 4.01 (t, *J* = 8.0 Hz, 4H, H_H), 3.87 (t, *J* = 6.6 Hz, 4H, H_C), 2.77 (t, *J* = 6.8 Hz, 4H, H_E), 2.25 (tt, *J* = 6.8 Hz, 6.6 Hz, 4H, H_D), 1.64 (tt, *J* = 6.8 Hz, 8.0 Hz, 4H, H_I), 1.38-1.13 (m, 12H, H_J, H_K, H_L); ^{13}C NMR (100 MHz, $CDCl_3$/d_3-MeCN 9:1, 298 K): δ = 163.7, 156.8, 138.1, 133.4, 129.8, 122.4, 116.4, 114.4, 67.5, 39.8, 34.4, 30.5, 28.8, 28.5, 28.4, 25.5, 0.95 (m); LRFAB-MS (3-NOBA matrix): *m/z* = 626 $[M–Cl–MeCN]^+$; HRFAB-MS (3-NOBA matrix): *m/z* = 626.20161 $[M\text{-}Cl–MeCN]^+$ (calcd. for $C_{33}H_{43}ClNO_2{}^{106}Pd$, 626.20143).

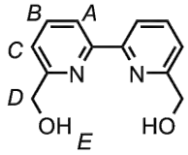

E6·HCl

To a solution of PPh_3 (89.3 g, 340 mmol, 4.00 equiv.) and $NiCl_2.6H_2O$ (20.3 g, 85.4 mmol, 1.00 equiv.) in DMF (350 mL) was added Zn (5.6 g, 85.4 mmol, 1.00 equiv.) and the resultant suspension stirred for 1 h (6-Bromo-pyridin-2-yl)-methanol (16.0 g, 85.1 mmol, 0.99 equiv.) was added to the deep red suspension and the reaction mixture stirred for 2 h then allowed to cool to RT. The mixture was poured into a mixture of conc. NH_3 (250 mL), H_2O (250 mL) and sat. EDTA/K_2CO_3 (100 mL) and extracted with $CHCl_3$/*i*PrOH 3:1 (4 × 500 mL). The combined organic phases were dried ($MgSO_4$) and the solvent removed under reduced pressure. The residue was dissolved in CH_2Cl_2 (500 mL) and HCl gas bubbled through the solution to give a white suspension. Suction filtration gave salt **E6**·HCl as a colourless solid (8.8 g, 82%); M.p. 208-212 °C; ^{1}H NMR (400 MHz, d_6-DMSO, 298 K): δ = 8.38 (d, *J* = 7.9 Hz, 2H, H_A), 8.17 (t, *J* = 7.8 Hz, 2H, H_B), 7.72 (d, *J* = 7.8 Hz, 2H, H_C), 4.77 (s, 4H, H_D); ^{13}C NMR (100 MHz, d_6-DMSO, 298 K): δ = 170.7 (× 2), 149.6, 131.6, 129.8, 72.7; LRESI-MS (MeOH): *m/z* = 217 $[M+H]^+$; HRESI-MS (MeOH): *m/z* = 216.0887 $[M]^+$ (calcd. for $C_{12}H_{12}N_2O_2$, 216.08933).

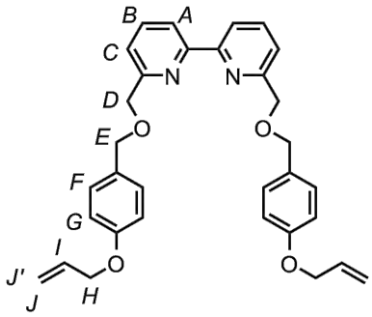

E7

To a suspension of salt **E6**·HCl (1.56 g, 6.17 mmol, 1 equiv.) in DMF (30 mL) at 0 °C was added NaH (60% dispersion in mineral oil, 0.99 g, 24.7 mmol, 4 equiv.) and the mixture stirred until effervescence ceased. 1-Allyloxy-4-bromomethylbenzene[16] (4.20 g, 18.5 mmol, 3 equiv.) was added, the cooling bath removed and the mixture was stirred at RT for 16 h. The reaction mixture was partitioned between H_2O (150 mL) and $CHCl_3$/*i*PrOH 3:1 (150 mL) and the layers separated. The aqueous phase was extracted with $CHCl_3$/*i*PrOH 3:1 (2 × 150 mL), the combined organic layers were dried ($MgSO_4$) and the solvent removed under reduced pressure. Chromatography (Gradient CH_2Cl_2 then acetone/CH_2Cl_2, 2:98) gave diallyl ether **E7** as a pale yellow solid (2.64 g, 84%); M.p. 86-90 °C; ^{1}H NMR (400 MHz, $CDCl_3$, 298 K): δ = 8.27 (d, J = 7.8 Hz, 2H, H_A), 7.80 (t, J = 7.8 Hz, 2H, H_B), 7.49 (d, J = 7.7 Hz, 2H, H_C), 7.32 (d, J = 8.6 Hz, 4H, H_G), 6.91 (d, J = 8.6 Hz, 4H, H_F), 6.05 (ddt, J = 17.3, 10.5, 5.3 Hz, 2H, H_I), 5.41 (ddt, J = 17.3, 1.6, 1.6 Hz, 2H, H_J), 5.28 (ddt, J = 10.5, 1.4, 1.3 Hz, 2H, $H_{J'}$), 4.74 (s, 4H, H_D), 4.61 (s, 4H, H_E) 4.54 (dt, J = 5.3, 1.5 Hz, 4H, H_H); ^{13}C NMR (100 MHz, $CDCl_3$, 298 K): δ = 158.3, 158.2, 155.4, 137.4, 133.2, 130.3, 129.4, 121.2, 119.7, 117.7, 114.6, 73.0, 72.5, 68.8; LRFAB-MS (3-NOBA matrix): *m/z* = 509 $[M+H]^+$; HRFAB-MS (3-NOBA matrix): *m/z* = 509.24403 $[M+H]^+$ (calcd. for $C_{32}H_{33}N_2O_4$, 509.24403).

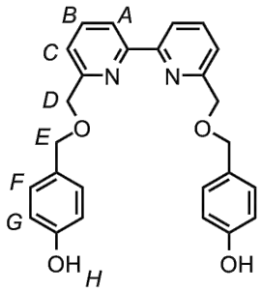

E8

To a solution of diallyl ether **E7** (2.64 g, 5.20 mmol, 1.00 equiv.) in THF (6 mL) was added aniline (1.85 mL, 20.40 mmol, 4.00 equiv.) then $Pd(PPh_3)_4$ (0.86 g, 0.74 mmol,

0.15 equiv.) and the mixture stirred at 30 °C for 2 h. The mixture was poured into H_2O (100 mL) and extracted with $CHCl_3$/*i*PrOH 3:1 (3 × 100 mL). The combined organic phases were dried ($MgSO_4$) and the solvent removed under reduced pressure. Purification by column chromatography (CH_2Cl_2 to MeOH/CH_2Cl_2, 3:97) gave the diphenol U-shape **E8** as a pale yellow oil which crystallised on standing (2.0 g, 88%); M.p. 128-130 °C; ^{1}H NMR (400 MHz, d_4-MeOD, 298 K): δ = 8.20 (d, J = 7.7 Hz, 2H, H_A), 7.84 (t, J = 7.8 Hz, 2H, H_B), 7.55 (d, J = 7.6 Hz, 2H, H_C), 7.22 (d, J = 8.6 Hz, 4H, H_G), 6.78 (d, J = 8.6 Hz, 4H, H_F), 4.90 (s, 2H, H_H), 4.66 (s, 4H, H_D), 4.54 (s, 4H, H_E); ^{13}C NMR (100 MHz, d_4-MeOD, 298 K): δ = 159.6, 158.4, 156.7, 138.9, 130.9, 130.1, 122.8, 121.2, 116.2, 73.8, 73.6; LRFAB-MS (3-NOBA matrix): *m/z* = 429 $[M+H]^+$.

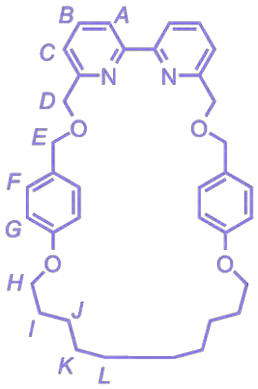

1c

K_2CO_3 (7.5 g, 48 mmol, 10 equiv.) was added to a stirred solution of diphenol U-shape **E8** (2.06 g, 4.80 mmol, 1 equiv.) and 1,10-dibromodecane (1.44 g, 4.80 mmol, 1 equiv.) in DMF (2 L) and the mixture heated at 80 °C for 16 h. The solvent was removed under reduced pressure and the residue partitioned between H_2O (500 mL) and EtOAc (500 mL) and the layers separated. The aqueous phase was extracted with CH_2Cl_2 (3 × 500 ml). The combined organic layers were dried ($MgSO_4$) and the solvent removed under reduced pressure. Purification by column chromatography (Petrol/EtOAc 93:7 to 75:25) gave macrocycle **1c** as a colourless solid (0.85 g, 31%); M.p. 90-94 °C; ^{1}H NMR (400 MHz, $CDCl_3$, 298 K): δ = 8.04 (d, J = 7.7 Hz, 2H, H_A), 7.72 (t, J = 7.8 Hz, 2H, H_B), 7.40 (d, J = 7.6 Hz, 2H, H_C), 7.19 (d, J = 8.5 Hz, 4H, H_F), 6.76 (d, J = 8.6 Hz, 4H, H_G), 4.66 (s, 4H, H_D), 4.64 (s, 4H, H_E), 3.91 (t, J = 6.5 Hz, 4H, H_H), 1.70 (dt, J = 6.6, 6.6 Hz, 4H, H_I), 1.50-1.35 (m, 4H, H_J), 1.34-1.18 (m, 8H, H_K, H_L); ^{13}C NMR (100 MHz, $CDCl_3$, 298 K): δ = 158.6, 158.5, 155.6, 137.1, 129.8, 129.6, 121.2, 119.9, 114.4, 72.5, 72.1, 67.6, 29.2, 28.8, 28.6, 25.7; LRFAB-MS (3-NOBA matrix): *m/z* = 567 $[M+H]^+$; HRFAB-MS (THIOG matrix): *m/z* = 567.32262 $[M+H]^+$ (calcd. for $C_{36}H_{43}N_2O_4$, 567.32228).

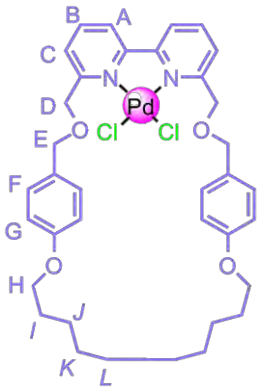

2c

A solution of bipyridine macrocycle **1c**[18] (75 mg, 0.14 mmol, 1 equiv.) and *trans-bis*(acetonitrile)dichloropalladium(II) (35 mg, 0.14 mmol, 1 equiv.) in CH_2Cl_2 (5 mL) was allowed to stir at room temperature under N_2 for 2.5 h. The solvent was removed under reduced pressure and the resulting orange solid was purified by recrystallisation (CH_2Cl_2/Et_2O 1:1) to yield the palladium-macrocycle complex **2c** as an orange solid (87 mg, 88%). Mp 186-190 °C; ^{1}H NMR (400 MHz, $CDCl_3$, 298 K): δ = 7.96 (t, *J* = 7.9 Hz, 2H, H_B), 7.86 (d, *J* = 7.9 Hz, 2H, H_A), 6.87 (d, *J* = 7.9 Hz, 2H, H_C), 7.28 (d, *J* = 8.6 Hz, 4H, H_F), 6.79 (t, *J* = 8.6 Hz, 4H, H_G), 5.20 (s, 4H, H_D), 4.64 (s, 4H, H_E), 3.87 (t, *J* = 6.3 Hz, 4H, H_H), 1.65 (tt, *J* = 6.3 Hz, 6.6 Hz, 4H, H_I), 1.41-1.21 (m, 16H, H_{J-L}); ^{13}C NMR (100 MHz, $CDCl_3$, 298 K): δ = 166.1, 158.8, 156.1, 140.0, 130.0, 129.1, 126.1, 120.6, 114.6, 73.6, 72.6, 67.6, 28.4, 28.12, 28.05, 25.0; LRFAB-MS (3-NOBA matrix): *m/z* = 707 $[M–Cl]^+$; HRFAB-MS (3-NOBA matrix): *m/z* = 707.18589 $[M–Cl]^+$ (calcd. for $C_{36}H_{42}ClN_2O_4{}^{106}Pd$, 707.18651 $[M–Cl]^+$). X-ray quality crystals were grown by slow cooling in a saturated MeCN solution of **2c**.

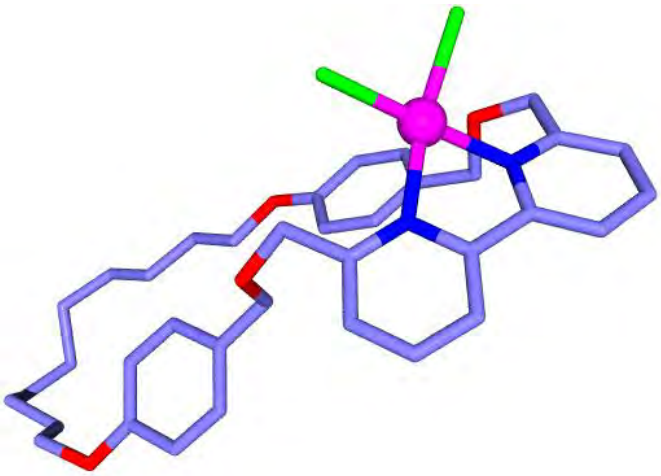

Table 3.3 Crystal data and structure refinement for 2c.

Empirical formula	$C_{36}H_{42}Cl_2N_2O_4Pd$	
Formula weight	744.02	
Temperature	93(2) K	
Wavelength	0.71073 Å	
Crystal system	Monoclinic	
Space group	P2(1)/c	
Unit cell dimensions	a = 15.7455(9) Å	α= 90°
	b = 21.3155(12) Å	β = 102.575(3)°
	c = 10.3932(6) Å	γ = 90°
Volume 3404.5(3) $Å^3$		
Z	4	
Density (calculated)	1.452 Mg/m^3	
Absorption coefficient	0.743 mm^{-1}	
F(000)	1536	
Crystal size	0.050 × 0.050 × 0.030 mm3	
Theta range for data collection	3.11 to 25.35°.	
Index ranges	-18<=h<=18, -25<=k<=24, -12<=l<=12	
Reflections collected	28560	
Independent reflections	6096 [R(int) = 0.0517]	
Completeness to theta = 25.00°	98.6 %	
Absorption correction	Multiscan	
Max. and min. transmission	1.0000 and 0.4740	
Refinement method	Full-matrix least-squares on F2	
Data / restraints / parameters	6096 / 0 / 407	
Goodness-of-fit on F2	1.135	
Final R indices [I>2sigma(I)]	R1 = 0.0347, wR2 = 0.0769	
R indices (all data)	R1 = 0.0387, wR2 = 0.0786	
Largest diff. peak and hole	0.533 and -0.501 $e.Å^{-3}$	

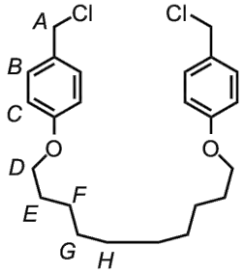

E10

At 0 °C, $SOCl_2$ (2.2 mL, 0.029 mol, 3 equiv.) was added to a solution of 1,10-(4-hydroxymethylphenoxy)decane (**E9**)[10a] (3.86 g, 0.010 mol, 1 equiv.) and pyridine (3.20 mL, 0.039 mol, 1.3 equiv.) in chloroform (500 mL). The reaction mixture was stirred under nitrogen atmosphere for 16 h. The solvent was removed under reduced pressure and the residue was dissolved in CH_2Cl_2 (100 mL). The organic layer was washed with sat. NH_4Cl solution (2 × 100 mL) then with brine (1 × 100 mL), dried ($MgSO_4$), filtered and concentrated under reduced pressure. The residue was purified by flash column chromatography (Petrol/CH_2Cl_2 1:1) to yield dichloride **E4** as a colourless solid (4.23g, 99%); M.p. 72-74 °C; ^{1}H NMR (400 MHz, $CDCl_3$, 298 K): δ = 7.24 (d, 4H, *J* = 8.6 Hz, H_B), 6.82 (d, 4H, *J* = 8.7 Hz, H_C), 4.52 (s, 4H, H_A), 3.90 (t, 4H, *J* = 6.5 Hz, H_D), 1.68- 1.78 (m, 4H, H_E), 1.36-1.46 (m, 4H, H_F), 1.25-1.36 (m, 8H, H_G and H_H); ^{13}C NMR (100 MHz, $CDCl_3$, 298 K): δ = 159.3, 130.0, 129.5, 114.7, 68.0, 46.4, 29.5, 29.3, 29.2, 26.0. LRFAB-MS (3- NOBA matrix): *m/z* = 422.5 $[M]^+$, 387.4 $[M\text{-}Cl]^+$. HRFAB-MS (3-NOBA matrix): *m/z* = 422.17753 $[M]^+$ (calcd. for $C_{24}H_{32}Cl_2O_2$, 422.17793).

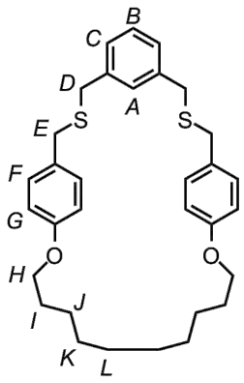

1e

To a solution of dichloride **E4** (1.50 g, 3.54 mmol, 1 equiv.) and 1,3 *bis*(mercaptomethyl)benzene (**E11**)[19] (0.60 g, 3.54 mmol, 1 equiv.) in butanone (700 mL) was added potassium carbonate (5.00 g, 35.4 mmol, 10 equiv.). The suspension was heated at 80 °C for 72 h under nitrogen atmosphere. After cooling, the suspension

was concentrated under reduced pressure and the residue was dissolved in CH_2Cl_2 (50 mL). The organic layer was washed with water (2 × 150 mL), dried ($MgSO_4$), filtered and concentrated under reduced pressure. The residue was purified by flash column chromatography (Petrol/CH_2Cl_2 6:4) to yield macrocycle **1e** as a colourless solid (346 mg, 19%); M.p. 66-68 °C; ^{1}H NMR (400 MHz, $CDCl_3$, 298 K): δ = 7.25 (s, 2H, H_C), 7.21 (s, 1H, H_B), 7.12 (d, 4H, *J* = 8.6 Hz, H_F), 6.91 (b, 1H, H_A), 6.77 (d, 4H, *J* = 8.6 Hz, H_G), 3.91 (t, 4H, *J* = 6.3 Hz, H_H), 3.52 (s, 4H, H_E), 3.50 (s, 4H, H_D), 1.67-1.77 (m, 4H, H_I), 1.38-1.48 (m, 4H, H_J), 1.25-1.34 (m, 8H, H_K and H_L); ^{13}C NMR (100 MHz, $CDCl_3$, 298 K): δ = 158.1, 137.9, 129.9, 129.8, 128.9, 127.5, 114.4, 68.0, 67.6, 35.1, 35.0, 28.5, 28.2, 27.9, 25.3; LRFAB-MS (3-NOBA matrix): *m/z* = 521.2 $[M+H]^+$; HRFAB-MS (3-NOBA matrix): *m/z* = 521.25295 $[M+H]^+$ (calcd. for $C_{32}H_{41}O_2S_2$, 521.25480).

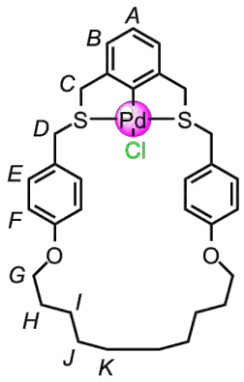

2e

A solution of macrocycle **1e** (100 mg, 0.19 mmol, 1 equiv.) and $Pd(MeCN)_4(BF_4)_2$ (85.3 mg, 0.19 mmol, 1 equiv.) in acetonitrile (20 mL) was stirred under reflux until the colour changed to pale yellow. After cooling to RT and evaporation of the solvent, the resulting yellow solid was dissolved in a mixture of CH_2Cl_2/MeCN 3:1 (20 mL) and the reaction mixture was stirred vigorously for 2 h with brine (20 mL). The layers were separated and the organic layer was washed with water (50 mL), dried ($MgSO_4$), filtered and concentrated under reduced pressure to afford palladium complex **2e** as a yellow solid (52 mg, 41%); M.p. 88-90 °C; ^{1}H NMR (400 MHz, $CDCl_3$/d_6-acetone 9:1, 323 K): δ = 7.52 (d, 4H, *J* = 8.6 Hz, H_F), 6.74 (d, 4H, *J* = 8.7 Hz, H_E), 6.63-6.71 (m, 3H, H_A and H_B), 3.91 (t, 4H, *J* = 6.2 Hz, H_G), 3.72-4.40 (bm, 8H, H_C and H_D), 1.66-1.77 (m, 4H, H_H), 1.38-1.49 (m, 4H, H_I), 1.28-1.35 (m, 8H, H_J and H_K); ^{13}C NMR (100 MHz, d_6-acetone, 298 K): δ = 158.4, 147.9, 131.2, 125.2, 123.6, 120.9, 114.0, 67.0, 42.5, 39.9, 29.1, 27.7, 27.1, 27.0, 24.5; LRFAB-MS (3-NOBA matrix): *m/z* = 627.1 $[M-Cl]^+$; HRFAB-MS (3-NOBA

matrix): *m/z* = 625.14262 $[M\text{-}Cl]^+$ (calcd. for $C_{32}H_{39}O_2S_2{}^{106}Pd$, 625.14262), *m/z* = 627.13991 $[M\text{-}Cl]^+$ (calc. for $C_{32}H_{39}O_2S_2{}^{108}Pd$, 627.14304).

3.5.3 Preparation of AMT Alkynes Homocoupling Rotaxanes

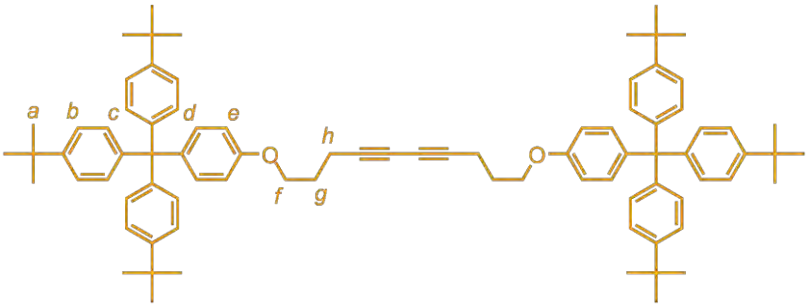

5

Spectroscopic data of the non-interlocked thread **5** generated during AMT Alkynes Homocoupling rotaxane-formation reactions: Mp 140 °C (dec.); ^1H NMR (400 MHz, $CDCl_3$, 298 K): δ = 7.23 (d, *J* = 8.6 Hz, 12H, H_b), 7.08 (d, *J* = 8.6 Hz, 12H, H_c), 6.75 (d, *J* = 8.9 Hz, 4H, H_d), 6.76 (d, *J* = 9.0 Hz, 4H, H_e), 4.01 (t, *J* = 6.0 Hz, 4H, H_f), 2.47 (t, *J* = 6.9 Hz, 4H, H_h), 1.98 (m, 4H, H_g), 1.30 (s, 54H, H_a); ^{13}C NMR (100 MHz, $CDCl_3$, 298 K): δ = 156.5, 148.2, 144.1, 139.6, 132.2, 130.7, 124.0, 112.9, 76.6, 65.9, 65.7, 63.0, 34.3, 31.4, 28.2, 16.1; LRFAB-MS (glycerol matrix): *m/z* = 1139.7 $[M]^+$; HRFAB-MS (glycerol matrix): *m/z* = 1138.75907 $[M]^+$ (calcd. for $C_{84}H_{98}O_2$, 1138.75668).

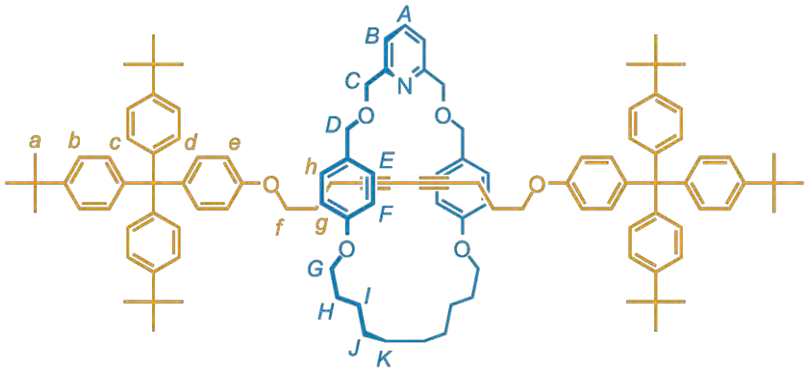

4a

A 5 mL round-bottomed flask, equipped with a drying $CaCl_2$ tube, was charged with a solution of alkyne **3** (484 mg, 0.84 mmol, 30 equiv.) in anhydrous benzene (2 mL). Diisopropylamine (28 mg, 0.28 mmol, 10 equiv.), copper iodide (8 mg, 42.0 µmol 1.5 equiv.), macrocycle **1a** (13 mg, 26.6 µmol, 0.95 equiv.) and iodine (4 mg, 14 µmol, 0.5 equiv.) were added sequentially. A solution of the corresponding palladium macrocycle complex **2a** (1 mg, 1.4 µmol, 0.05 equiv) in anhydrous benzene (1 mL) was slowly

added over a period of 12 h using a syringe pump. When addition was complete the reaction mixture was allowed to stir for a further 72 h at room temperature after which time the crude was taken into a partition of CH_2Cl_2 and sat. Na_4EDTA solution (15 mL) and stirred for 1 h. The layers were separated and the aqueous layer extracted with CH_2Cl_2 (2 × 5 mL). The combined organic phase was then washed with brine (15 mL), dried ($MgSO_4$), filtered and concentrated under reduced pressure. The resulting residue was purified by column chromatography (hexane/CH_2Cl_2/MeCN 70:25:5) to afford **4a** (41 mg, 90%). ^{1}H NMR (400 MHz, $CDCl_3$, 298 K): δ = 7.50 (t, *J* = 7.7 Hz, 1H, H_A), 7.23 (d, *J* = 8.6 Hz, 12H, H_b), 7.23 (d, *J* = 7.7 Hz, 2H, H_B), 7.07 (d, *J* = 8.6 Hz, 12H, H_c), 7.07 (d, *J* = 8.6 Hz, 4H, H_d), 6.95 (d, *J* = 8.9 Hz, 4H, H_E), 6.67 (d, *J* = 8.6 Hz, 4H, H_e), 6.44 (d, *J* = 8.9 Hz, 4H, H_F), 4.52 (s, 4H, H_C), 4.28 (s, 4H, H_D), 3.84 (t, *J* = 6.5 Hz, 4H, H_G), 3.51 (t, *J* = 6.0 Hz, 4H, H_f), 2.08 (t, *J* = 7.0 Hz, 4H, H_h), 1.64 (m, 4H, H_H), 1.55 (m, 4H, H_g), 1.30 (s, 54H, H_a), 1.35-1.16 (m, 12H, H_I, H_J, H_K); ^{13}C NMR (100 MHz, $CDCl_3$, 298 K): δ = 158.7, 157.7, 156.4, 148.2, 144.2, 139.3, 136.9, 132.0, 130.7, 129.8, 129.1, 124.0, 119.4, 114.5, 112.8, 72.2, 70.8, 67.2, 65.8, 65.6, 63.0, 34.3, 31.4, 29.7, 29.6, 28.74, 28.69, 28.0, 25.7, 15.8; HRFAB-MS (3-NOBA matrix): *m/z* = 1630.05527 $[M+1+H]^+$ (calcd. for $^{13}C^{12}C_{114}$ $H_{138}NO_6$, 1630.05577).

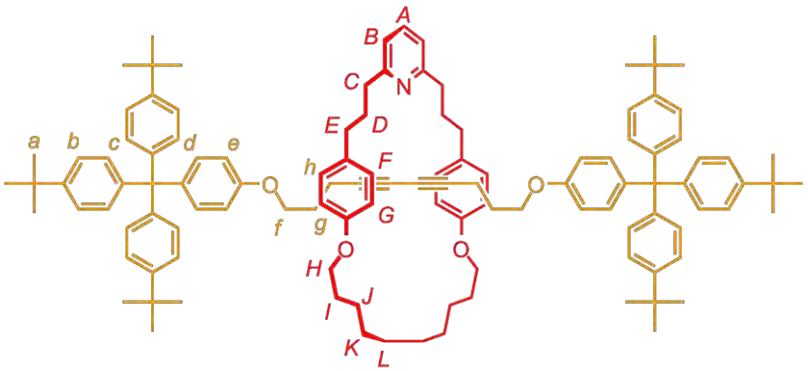

4b

A suspension of alkyne **3** (30 mg, 0.053 mmol, 2.5 equiv.), Pd-macrocycle **2b** (15 mg, 0.021 mmol, 1 equiv.) and diisopropylamine (2 mL) was sonicated at RT for 10 min. Copper(I) iodide (1 mg, 5.3 μmol, 0.25 equiv.) was added and the resulting suspension allowed to stir at RT for 23 h CH_2Cl_2, silica and a basic solution of EDTA (aq.) were added and air was bubbled through the resulting suspension for 1 h. The aqueous layer was extracted with CH_2Cl_2 (× 3) and the combined organic layers dried ($MgSO_4$). The crude mixture was purified by preparative TLC (hexane/CH_2Cl_2/MeCN 7:2.5:0.5) to yield **4b** as a pale yellow film (10 mg, 30%). ^{1}H NMR (400 MHz, $CDCl_3$, 298 K): δ = 7.31

(t, *J* = 7.6 Hz, 1H, H_A), 7.23 (d, *J* = 8.6 Hz, 12H, H_b), 7.09 (d, *J* = 8.6 Hz, 12H, H_c), 6.97 (d, *J* = 8.9 Hz, 4H, H_F), 6.88 (d, *J* = 8.5 Hz, 4H, H_d), 6.82 (d, *J* = 7.6 Hz, 2H, H_B), 6.64 (d, *J* = 8.5 Hz, 4H, H_e), 6.49 (d, *J* = 8.9 Hz, 4H, H_G), 3.85 (t, *J* = 6.5 Hz, 4H, H_H), 3.51 (t, *J* = 6.1 Hz, 4H, H_f), 2.67 (t, J = 8.3 Hz, 4H, H_C), 2.54 (t, *J* = 8.0 Hz, 4H, H_E), 2.02 (t, *J* = 7.1 Hz, 4H, H_h), 1.78 (m, 4H, H_D), 1.64 (m, 4H, H_I), 1.53 (m, 4H, H_g), 1.35-1.19 (m, 12H, H_J, H_K, H_L), 1.30 (s, 54H, H_a); ^{13}C NMR (100 MHz, CDCl3): δ = 161.5, 157.0, 156.4, 148.2, 144.2, 139.3, 136.5, 133.9, 132.0, 130.7, 129.2, 124.0, 119.7, 114.6, 112.9, 67.3, 65.9, 65.7, 63.0, 38.5, 35.3, 34.3, 33.0, 31.4, 29.6, 29.7, 28.74, 28.70, 28.0, 25.7, 15.8. LRFAB-MS (3-NOBA matrix): *m/z* = 1626 $[M+H]^+$; HRFAB-MS (3-NOBA matrix): *m/z* = 1626.09732 $[M+H+1]^+$ (calcd. for $^{13}C^{12}C_{161}H_{142}NO_4$, 1626.09724).

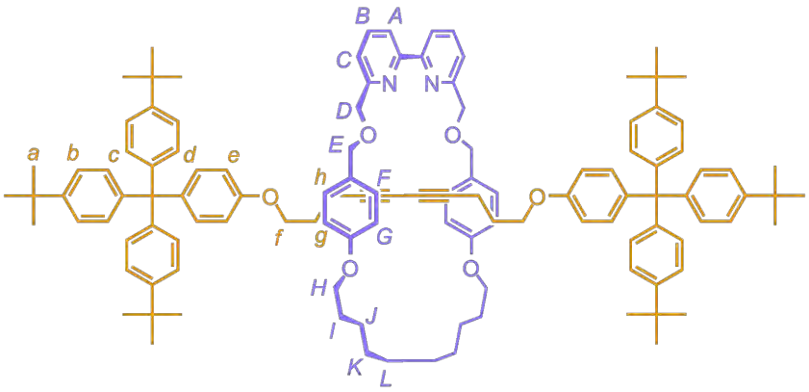

4c

A 5 mL round-bottomed flask, equipped with a drying $CaCl_2$ tube, was charged with a solution of alkyne **3** (470 mg, 0.82 mmol, 30 equiv.) in anhydrous benzene (1 mL). Diisopropylamine (28 mg, 0.28 mmol, 10 equiv.), copper iodide (10 mg, 53.0 µmol, 1.5 equiv.), macrocycle **1c** (15 mg, 26.9 µmol, 0.95 equiv.) and iodine (4 mg, 14.0 µmol, 0.5 equiv.) were added sequentially. A solution of the corresponding palladium macrocycle complex **2c** (1 mg, 1.37 µmol, 0.05 equiv.) in anhydrous benzene (1 mL) was slowly added over a period of 12 h using a syringe pump. When addition was complete the reaction mixture was allowed to stir for a further 72 h at room temperature after which time the crude was taken into a partition of CH_2Cl_2 and sat. Na_4EDTA solution (15 mL) and stirred for 1 h. The layers were separated and the aqueous layer extracted with CH_2Cl_2 (2 × 5 mL). The combined organic phase was then washed with brine (15 mL), dried ($MgSO_4$), filtered and concentrated under reduced pressure. A solution of KCN (19 mg, 0.28 mmol, 10 equiv.) in MeOH (3 mL) was added to the solution of the crude products in CH_2Cl_2 (3 mL). After stirring at RT for 1 h, the solvents were removed under reduced pressure. The resulting residue was dissolved in CH_2Cl_2, washed with water,

brine and dried ($MgSO_4$). The resulting residue was purified by column chromatography (hexane/CH_2Cl_2/MeCN 70:25:4) to afford the **4c** (37 mg, 76%). ^1H NMR (400 MHz, $CDCl_3$, 298 K): δ = 8.02 (d, *J* = 7.6 Hz, 2H, H_A), 7.51 (dd, *J* = 7.8, 7.6 Hz, 2H, H_B), 7.28 (d, *J* = 7.8 Hz, 2H, H_C), 7.16 (d, *J* = 8.6 Hz, 12H, H_b), 7.00 (d, *J* = 8.6 Hz, 12H, H_c), 6.96 (d, *J* = 8.6 Hz, 4H, H_d), 6.86 (d, *J* = 8.9 Hz, 4H, H_F), 6.54 (d, *J* = 8.6 Hz, 4H, H_e), 6.32 (d, *J* = 8.9 Hz, 4H, H_G), 4.51 (s, 4H, H_D or H_E), 4.49 (s, 4H, H_D or H_E), 3.69 (t, *J* = 6.6 Hz, 4H, H_H), 3.44 (t, *J* = 6.0 Hz, 4H, H_f), 2.02 (t, *J* = 7.0 Hz, 4H, H_h), 1.56-1.41 (m, 8H, H_g, H_I), 1.23 (s, 54H, H_a), 1.21-1.06 (m, 12H, H_L, H_K, H_J); ^{13}C NMR (100 MHz, $CDCl_3$, 298 K): δ = 158.6, 158.2, 156.4, 155.3, 148.2, 144.2, 139.3, 137.0, 134.7, 132.0, 130.7, 129.7, 124.0, 121.3, 119.6, 114.4, 112.8, 72.4, 72.2, 67.6, 65.8, 65.6, 64.2, 63.0, 34.3, 31.4, 29.4, 28.9, 28.8, 28.0, 25.8, 15.8; LRFAB-MS (3-NOBA matrix): *m/z* = 1707 $[M+1+H]^+$; HRFAB-MS (3-NOBA matrix): *m/z* = 1707.08219 [M+1+H]+ (calcd. for $^{13}C^{12}C_{119}H_{141}N_2O_6$, 1707.08232).

3.6 References

(1) a) J. Tsuji, *Palladium Reagents and Catalysts: Innovations in Organic Synthesis*, Wiley-VCH, Weinheim, **1995**. b) Handbook *of Organopalladium Chemistry for Organic Synthesis, Vol. 1* (Ed.: E.-i. Negishi), Wiley-VCH,Weinheim, **2002**. c) *Handbook of Organopalladium Chemistry for Organic Synthesis, Vol. 2* (Ed.: E.-i. Negishi), Wiley-VCH, Weinheim, **2002**. d) J. Tsuji, *Palladium Reagents and Catalysts: New Perspectives for the 21st Century,* 2nd ed. Wiley, Chichester, **2004**. e) *Metal-Catalyzed Cross-Coupling* Reactions, *Vol. 1*, Completely Revised and Enlarged, 2nd ed. (Eds.: A. de Meijere, F. Diederich), Wiley- VCH, Weinhiem, **2004**, p. 317-394; f) S. S. Stahl, *Angew. Chem. Int. Ed.* **2004**, *43*, 3400-3420.

(2) C. Glaser, *Ber. Dtsch. Chem. Ges*. **1869**, *2*, 422.

(3) a) W. Chodkiewicz, *Ann. Chim*. Paris **1957**, *2*, 819-869; b) P. Cadiot, W. Chodkiewicz, in *Chemistry of Acetylene*, H. G. Viehe Ed. Marcel Dekker, New York **1969**, p 597.-647.

(4) G. Eglington, R. Galbraith, *J. Chem. Soc*. **1959**, 889.

(5) R. J. K. Taylor, In *Organocopper Reagents: A Practical Approach*; Oxford University Press: New York, **1994**.

(6) A. S. Hay, *J. Org. Chem*. **1962**, *27*, 3320-3321.

(7) a) K. Sonogashira, Y. Tohda, N. Hagihara, *Tet. Lett*. **1975**, *50*, 4467-4470; b) K. Sonogashira, in *Metal-Catalyzed Cross-Coupling Reactions*, F. Diederich, P. J. Stang, Eds. Wiley-WCH: Weinhein, Germany, **1998**, p 203-230; c) K. Sonogashira, in *Comprehensive Organic Synthesis*; Pergamon Press, **1990**, Vol. 3, p 521.

(8) J.-H. Li, Y. Liang, X.-D. Zhang, *Tetrahedron*, **2005**, *61*, 1903-1907.

(9) a) A.-M. Fuller, D. A. Leigh, P. J. Lusby, I. D. H. Oswald, S. Parsons, D. B. Walker, *Angew. Chem. Int. Ed*. **2004**, *43*, 3914-3918. b) Y. Furusho, T. Matsuyama, T. Takata, T. Moriuchi, T. Hirao, *Tetrahedron Lett*. **2004**, *45*, 9593-9597.

c) D. A. Leigh, P. J. Lusby, A. M. Z. Slawin, D. B. Walker, *Angew. Chem. Int. Ed*. **2005**, *44*, 4557-4564.

(10) a) A.-M. Fuller, D. A. Leigh, P. J. Lusby, A. M. Z. Slawin, D. B. Walker, *J. Am. Chem. Soc*. **2005**, *127*, 12612-12619. b) D. A. Leigh, P. J. Lusby, A. M. Z. Slawin, D. B.Walker, *Chem. Commun*. **2005**, 4919-4921.

(11) a) Q. Liu, D. J. Burton, *Tetrahedron Lett*. **1997**, *38*, 4371–4374; b) A. Lei, M. Srivastava, X. Zhang, *J. Org. Chem.* **2002**, *67*, 1969–1971; c) V. Gevorgyan in *Handbook of Organopalladium Chemistry for Organic Synthesis*, Vol. 1, (Ed.: E.-i. Negishi), Wiley-VCH, Weinheim, **2002**, p 1463–1469; d) J. A. Marsden, J. J. Miller, M. M. Haley, *Angew. Chem.* **2004**, *116*, 1726–1729; *Angew. Chem. Int. Ed*. **2004**, *43*, 1694–1697; e) C. H. Oh, V. R. Reddy, *Tetrahedron Lett*. **2004**, *45*, 5221–5224; f) M. Bandini, R. Luque, V. Budarin, D. J. Macquarrie, *Tetrahedron* **2005**, *61*, 9860–9868; g) A. S. Batsanov, J. C. Collings, I. J. S. Fairlamb, J. P. Holland, J. A. K. Howard, Z. Lin, T. B. Marder, A. C. Parsons, R. M. Ward, J. Zhu, *J. Org. Chem.* **2005**, *70*, 703–706; h) J. Gil-Moltó, C. Nájera, *Eur. J. Org. Chem.* **2005**, 4073–4081; i) J.-H. Li, Y. Liang, Y.-X. Xie, *J. Org. Chem.* **2005**, *70*, 4393–4396; j) J.-H. Li, Y. Liang, X.-D. Zhang, *Tetrahedron* **2005**, *61*, 1903–1907; k) M. Shi, H. Qian, *Appl. Organometal. Chem.* **2006**, *20*, 771–774; l) C. Chen, Z. Ai, J. Lin, X. Hong, C. Xi, *Synlett* **2006**, 2454–2458; m) F. Yang, X. Cui, Y. Li, J. Zhang, G. Ren, Y. Wu, *Tetrahedron* **2007**, *63*, 1963–1969.

(12) M. Pal, K. Parasuraman, K. R. Yeleswarapu, *Org. Lett*. **2003**, *5*, 349-352.

(13) For a similar example involving platinium, see: C. J. Adams, S. L. James, P. R. Raithby, *Chem. Commun*. **1997**, 2155-2156.

(14) P. Siemsen, R. C. Livingston, F. Diederich, *Angew. Chem. Int. Ed.* **2000**, *39*, 2632–2657.

(15) H. W. Gibson, S. H. Lee, P. T. Engen, P. Lecavalier, J. Sze, Y. X. Shen, M. Bheda, *J. Org. Chem.* **1993**, *58*, 3748-3756.

(16) T. Nakayama, M. Nomura, K. Haga, M. Ueda, *Bull. Chem. Soc. Jpn.* **1998**, *71*, 2979-2984.

(17) S. E. N. Mohamed, D. A. Whiting, *J. Chem. Soc., Perkin Trans. 1* **1983**, 2577-2582.

(18) V. Aucagne, J. Berná, J. D. Crowley, S. M. Goldup, K. D. Hänni, D. A. Leigh, P. J. Lusby, V. E. Ronaldson, A. M. Z. Slawin, A. Viterisi, D. B. Walker, *J. Am. Chem. Soc.* **2007**, *129*, 11950-11963.

(19) R. Filler, G. L. Cantrell, D. Wolanin, D. Naqvi, S. M. *J. Fluor. Chem*. **1986**, 30, 399-414.

Chapter IV

[2]Rotaxanes through Palladium Active-Template Oxidative Heck Cross-Couplings

Published as *[2]Rotaxanes through Palladium Active-Template Oxidative Heck Cross-Couplings*, J. D. Crowley, K. D. Hänni, A.-L. Lee, D. A. Leigh, *J. Am. Chem. Soc.* **2007**, *129*, 12092-12093.

Acknowledgments

The work presented in this chapter was equally divided between Dr. Ai-Lan Lee and the author. Dr. James Crowley is acknowledged for his useful discussions and Dr. Roy McBurney for providing us with half-thread **9**.

4.1 Synopsis

This Chapter presents an extension of the Pd(II)-catalysed alkyne homocoupling strategy towards the accomplishment of a cross-coupling AMT protocol for the preparation of [2]rotaxanes. Because Pd(0) species do not ligate to our macrocycles and produce only non-interlocked products, they have to be replaced by Pd(II)-based catalyst. The Pd(II) oxidative Heck cross-coupling reaction was used to achieve this goal. Coordination of Pd(II) to an endotopic bipy-containing macrocycle allows the boronic acids and alkenes to bind to the transition metal in such a way that the metal-mediated bond-forming reaction takes place through the cavity of the macrocycle, forming a rotaxane.

A variety of boronic acids and alkenes are demonstrated to form [2]rotaxanes in excellent yields using catalyst's loadings as low as 1 mol%, which makes it one of the most efficient and powerful methods for the preparation of MIAs.

4.2 Introduction

Palladium-catalysed cross-coupling reactions are extremely powerful tools for organic synthesis, routinely providing efficient protocols for the construction of C-C bonds.[1] Following the success of the palladium(II) catalysed alkyne homocoupling for the active-template synthesis of [2]rotaxanes (see Chapter III), we attempted to extend this methodology to palladium cross-coupling reactions. Typical Pd catalysed cross-coupling reactions are mediated by Pd(0) (Heck, Suzuki, Negishi, Kumada, Stille, Hiyama, Sonogashira). As seen in Chapter III, as a consequence of the reductive elimination of the two alkyne ligands into the corresponding diyne product, the Pd(0) produced is not anymore – or is weakly – bound to the pyridine nitrogen atom of the macrocyclic ligand. This observation, together with the lack of success utilising classical Heck reaction conditions to assemble [2]rotaxanes (Paragraph 4.3.1), suggests that Pd(0) is not ligated successfully by our pyridine-based macrocycles. This allows the catalyst to direct the reaction not through the cavity of the macrocycle to afford [2]rotaxane, but freely in solution wherein only non-interlocked products are produced. There are two possible ways to overcome this issue: the design and fastidious synthesis of novel macrocyclic ligands able to maintain the Pd(0) catalyst (i.e. phosphines, carbene) as seen in Scheme 4.1a, or to turn our attention towards *Pd(II)*-mediated cross-couplings as to avoid Pd(0) ones (Scheme 4.1, b).

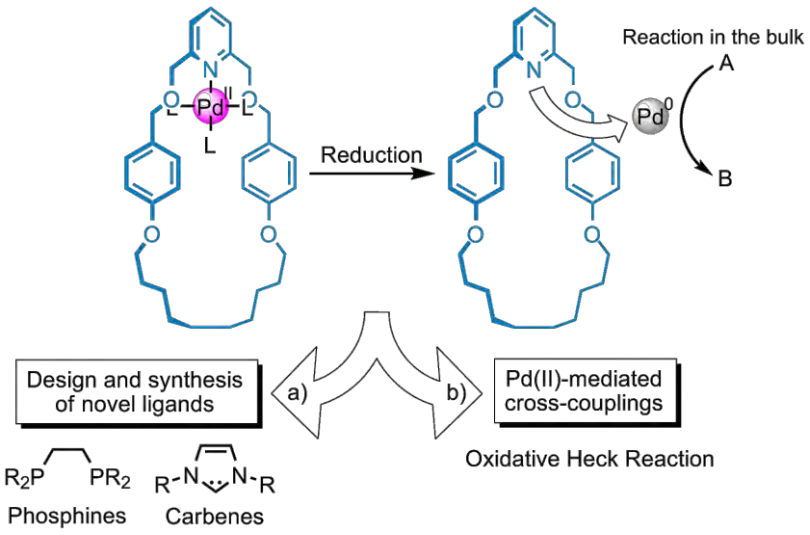

Scheme 4.1 Strategies to avoid Pd(0)-mediated cross-couplings: a) Design and synthesis of new macrocyclic ligands (phosphines or NHC); b) Using reactions mediated by Pd(II).

Recently, Pd(II)-catalysed cross-couplings have been developed as a novel alternative to the traditional Pd(0) systems, offering a change in both mechanism and reaction

parameters.[2] Studies have shown that bidentate ligands such as bipyridine and phenanthroline are the most efficient for promoting oxidative Heck reactions at room temperature.[2a,c]

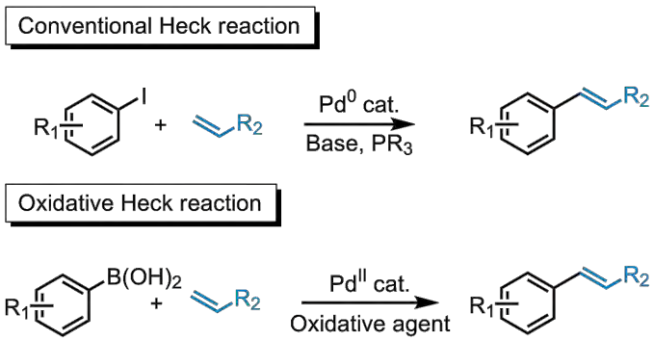

Scheme 4.2 Conventional vs. oxidative conditions for the Heck reaction.

4.3 Results and Discussion

4.3.1 Initial Attempts using Pd⁰-mediated Heck Cross-coupling

Initial attempts to construct rotaxanes using Pd(0)-catalysed reactions with various mono-, bi-, and tridentate macrocycles, shown in Scheme 4.3, were unsuccessful in producing rotaxanes: non-interlocked thread **5** was generated in good yields in all cases (80-90%) but the desired [2]rotaxanes were detected neither by ^{1}H NMR nor by ESI-MS.

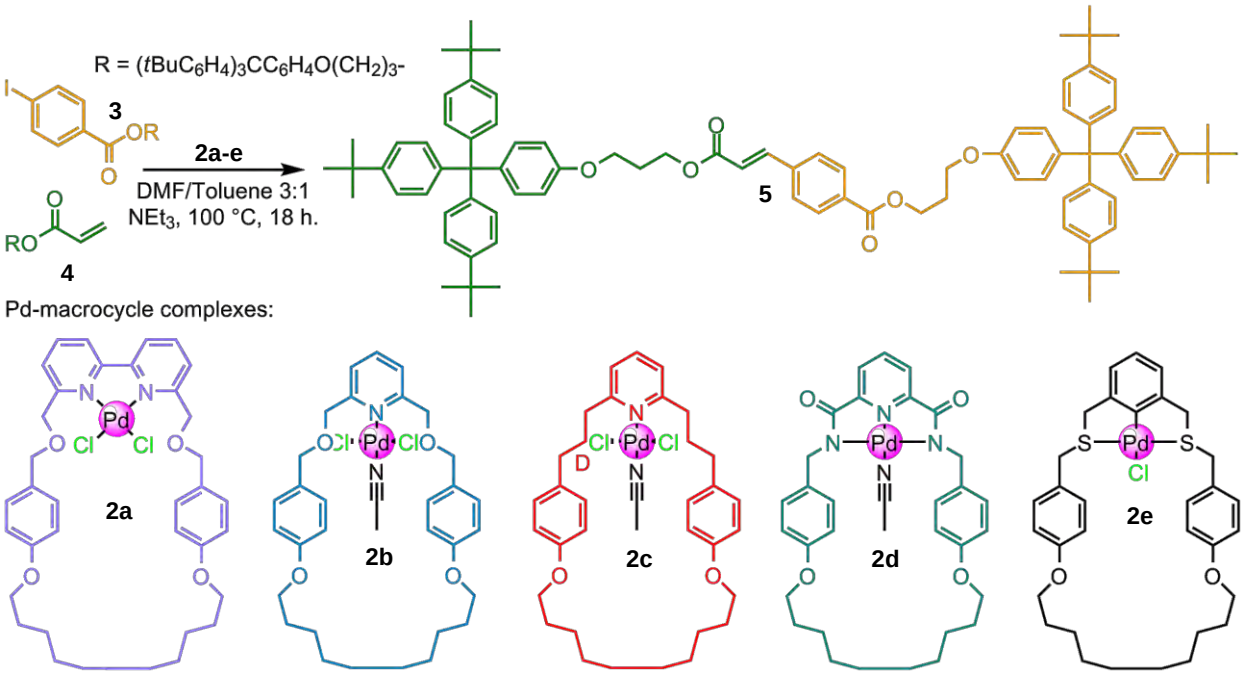

*Scheme 4.3 Attempted active-template Pd(0)-catalyzed heck cross-couplings. **1a-e** are the corresponding metal-free macrocycles.*

Because the Pd(0) does not remain coordinated to the macrocycle during key stages of the catalytic cycle, we reasoned that Pd(II) should be ligated strongly by the bipyridine macrocycle **1a**, thereby remaining attached inside the cavity of the macrocycle during the crucial C-C bond-forming step.

4.3.2 Pd(II) Oxidative Heck: Initial Screening Conditions

A number of different oxidants and solvent systems were screened for the reaction shown in Scheme 4.4: The Pd-macrocycle complex is formed *in situ* by mixing macrocycle **1a** (1 equiv) with a catalytic quantity (10 mol %) of $Pd(OAc)_2$. Addition of boronic acid **6** (2 equiv), alkene **4** (1 equiv), and an oxidising agent (1 equiv), followed by simple stirring under an atmosphere of oxygen at room temperature for 72 h, led to the desired [2]rotaxane **7** and its corresponding non-interlocked thread **8**. According to Jung and co-workers,[2b] the oxidative Heck cross-coupling shows the greatest efficiency in polar aprotic solvents. However, owing to the low solubility of both half-threads in solvents such as DMF and DMA, we decided to turn our attention to a mixture of DMF/chloroform 1:1 as solvent system.

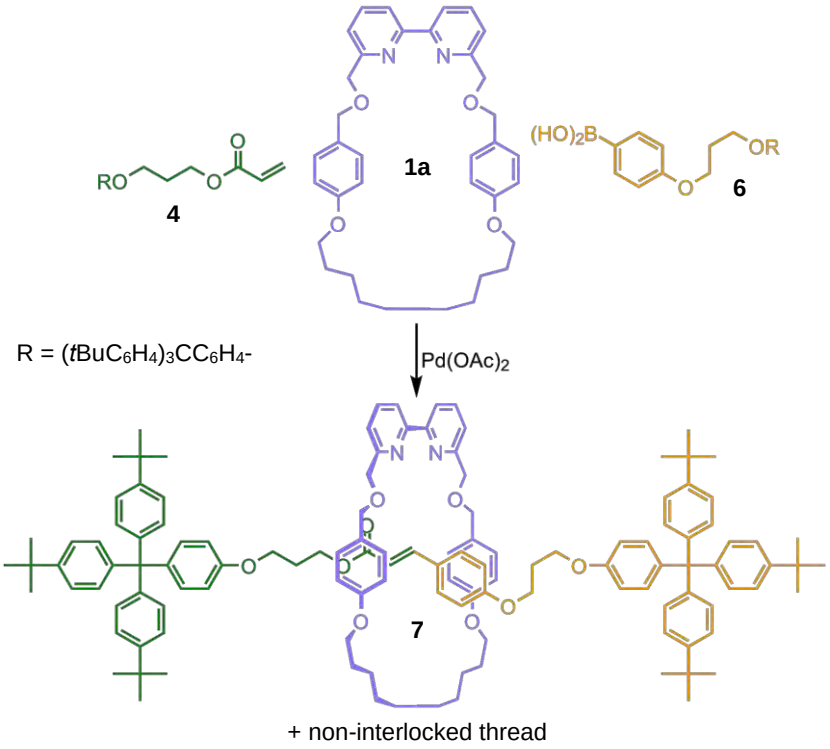

*Scheme 4.4 Oxidative Heck cross-coupling for AMT the synthesis of rotaxane **5** from boronic acid **3** and activated vinyl ester **4**.*

The reaction in DMF/$CHCl_3$ under an oxygen atmosphere gave an excellent conversion (>98%) but only 40% yield of the corresponding [2]rotaxane **7** (Table 4.1, entry 1).

Substituting oxygen for iodine (Table 4.1, entry 2) seems to completely shut down the reaction, possibly due to the fact that boronic acids can be converted into the corresponding aryl iodide with the presence of iodide ions in oxidative conditions,[3,4] and therefore are unable to react under the oxidative Heck cross-coupling conditions. The use of $Cu(OAc)_2$ led to very little reaction conversion (22%, no rotaxane, entry 3). Using benzoquinone (BQ) as an oxidising agent provides much cleaner conversion (entry 4) even if the yield of the [2]rotaxane was sightly lower (22%). Based on these observations, we decided to use a combination of BQ and oxygen as oxidising agents. As expected, the rotaxane-formation reaction in neat DMF (BQ + O_2 as oxidants, entry 5) did not lead to a significant improvement (55% conversion, 16% of **7**). However, carrying out the same reaction in neat chloroform (entry 6) and in CH_2Cl_2 (entry 7) gave similar results as the conditions used in Table 4.1, entry 1 (70% conversion, 48% of **7**, >98% conversion, 45% of **7**, respectively). Surprisingly, the use a 1:1 mixture of $CHCl_3/CH_2Cl_2$ was found to be the optimal solvent system for the studies presented here (73% of **6**, entry 8). The presence of BQ is necessary for an efficient rotaxane-formation reaction as seen in Table 4.1, entry 8: optimal conditions with O_2 as the only oxidant reduced the yield of rotaxane **7** to 24% (entry 9).

*Table 4.1 Effect of oxidant and solvent the Pd(II) oxidative Heck cross-coupling to [2]rotaxane **7***

Entry	Solvent system	Oxidant	Conversion **4**+**6** → **7**+**8**	Yield of rotaxane **1a**→**7**
1[a]	DMF/$CHCl_3$ 1:1[b]	O_2	>98%	40%
2[a]	DMF/$CHCl_3$ 1:1	I_2	<1%	0%
3[a]	DMF/$CHCl_3$ 1:1	$Cu(OAc)_2$	22%	0%
4[a]	DMF/$CHCl_3$ 1:1	BQ	78%	22%
5[a]	DMF	O_2 + BQ	55%	16%
6[a]	$CHCl_3$	O_2 + BQ	70%	48%
7[a]	CH_2Cl_2	O_2 + BQ	>98%	45%
8[a]	**$CHCl_3/CH_2Cl_2$ 1:1**	**O_2 + BQ**	**>98%**	**73%**
9[a]	$CHCl_3/CH_2Cl_2$ 1:1	O_2	>98%	24%

*[a]All reactions were carried out at 16 mM concentration with respect to **1a**. Reaction conditions: **6** (2 equiv.), **4** (1 equiv.) and $Pd(OAc)_2$ (10 mol% with respect to **1a**).[b]Using 30 mol% of $Pd(OAc)_2$ led to 68% of conversion and 19% of [2]rotaxane **7**.*

We next investigated the effect of lowering the amount of the palladium catalyst in the rotaxane-forming reaction. When reaction conditions presented in Table 4.1, entry 8 ($CHCl_3/CH_2Cl_2$ 1:1, 1 equiv. of **1a**, **4** and BQ, 2 equiv. of **6**, under an O_2 atm.) were used

with a loading of 5 mol% of $Pd(OAc)_2$, 52% of rotaxane **7** was obtained (Table 4.2, entry 2). Letting the reaction continue for a further 9 days (12 days in total) led to a complete conversion with an impressive 70% yield of rotaxane **7** (Table 4.2, entry 3). Lowering the amount of Pd down to 1 mol% afforded 21% of rotaxane after 3 days (entry 4) and still produced a 66% yield of rotaxane (i.e., the metal template turns over 65 times during the reaction!), albeit over a 16 day reaction time (entry 5).

*Table 4.2 Effect of Lowering $Pd(OAc)_2$ Loading for the Formation of rotaxane **5**.*

Entry	Amt of $Pd(OAc)_2$ [equiv.]	Time	Conversion **4**+**6** → **7**+**8**	Yield of rotaxane **1a**→**7**
1	0.1	72 h	>98%	73%
2	0.05	72 h	66%	52%
3	0.05	12 d.	>98%	70%
4	0.01	72 h	33%	21%
5	0.01	16 d	>98%	66%

*[a]All reactions were carried out at 16 mM concentration with respect to **1a**. Reaction conditions: **5** (2 equiv.), **3** (1 equiv.) in $CHCl_3/CH_2Cl_2$ 1:1.*

The proposed mechanism for rotaxane formation is shown in Scheme 4.5: transmetalation of the aryl boronic acid **6** with the Pd(II) complex **2a**, followed by π-coordination of alkene **4**, affords intermediate **I**. In order to achieve successful rotaxane formation, the two building blocks that ultimately form the thread need to be held on opposite faces of the macrocycle and the palladium needs to retain the stoppered ligands until it has mediated a covalent bond-forming reaction between them. Migratory insertion followed by β-Hydride elimination thus forms a mechanical as well as a covalent bond. Decomplexation of the weakly binding Pd(0) liberates free rotaxane **7**. Reoxidation of Pd(0) to Pd(II) regenerates the catalytically active complex **2a** and enables the reaction to be conducted using substoichiometric amounts of palladium.

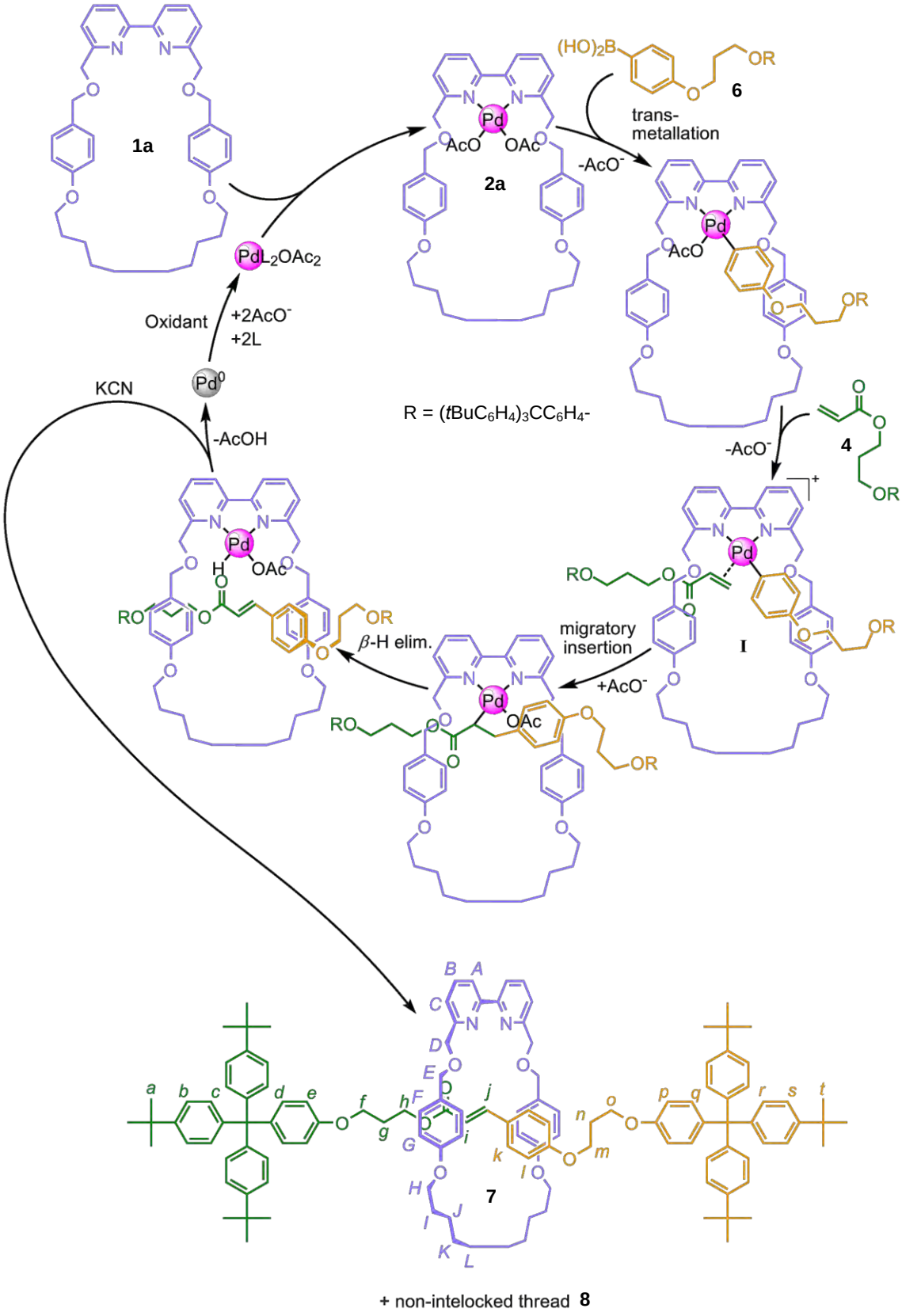

*Scheme 4.5 Proposed catalytic cycle for the oxidative Heck active-template synthesis of [2]rotaxane **7** from **1a**, **4**, and **6**.*

4.3.3 ^{1}H NMR of the Interlocked Structure

The ^{1}H NMR spectrum of rotaxane **7** in $CDCl_3$ (Figure 4.1, b) shows an upfield shift of several signals with respect to the non-interlocked components (Figure 4.1, a and c). The shielding, typical of interlocked architectures in which the aromatic rings of one component are positioned face-on to another component, occurs for all nonstopper resonances of the axle ($H_{f\text{-}o}$), indicating that the macrocycle accesses the full length of the thread in the rotaxane. However, the resonances of the protons on the half of the axle bearing the aryl ring ($H_{m\text{-}o}$) are shielded to a greater extend than those on the other half ($H_{f\text{-}h}$). This preference of the macrocycle for the aromatic region of the thread is probably a result of both π-stacking interactions and solvation effects.

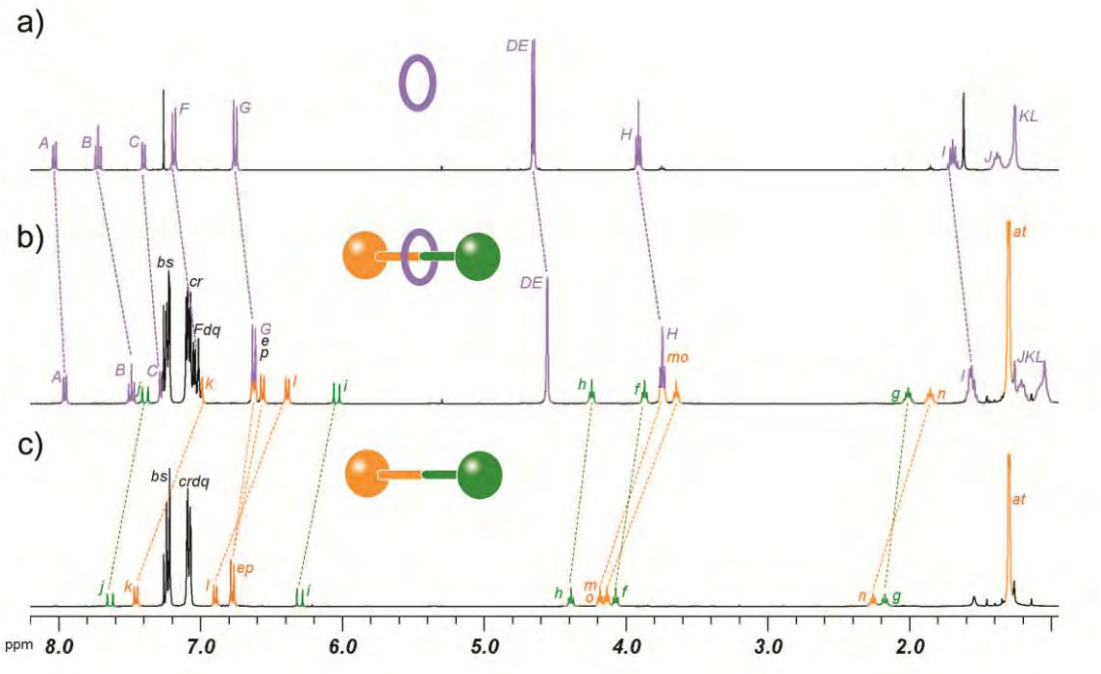

*Figure 4.1 ^{1}H NMR spectra (400 MHz, $CDCl_3$, 298 K) of a) macrocycle **1a**, b) [2]rotaxane **7**, c)non-interlocked thread **8**. The assignments correspond to the lettering shown in Scheme 4.5.*

4.3.4 Substrate Scope

To examine if this new cross-coupling approach to [2]rotaxanes is tolerant of a range of different cross-coupling partners, we screened a number of alkene and boronic acid functionalised half-threads, generating a variety of [2]rotaxanes (Table 4.3). Vinyl ketone **9** and styrene derivative **11** can replace vinyl ester **4** as the alkene cross-coupling partner to produce the corresponding rotaxanes **10** and **12** in 70% and 50% yields, respectively (Table 4.3, entries 2 and 3). The electron-poor aryl boronic acid **13** can also be used in place of the electron-rich aryl boronic acid **6** without affecting the

yield (**14**, 76%, entry 4). The rotaxane-forming reaction, however, is sensitive to steric hindrances although trisubstituted alkenes can be formed in high yields using the oxidative Heck method; the attempted coupling of disubstituted alkene **15** with boronic acid **3** resulted in only traces of the corresponding rotaxane **16**. Alkene boronic acid **17** also proved suitable as a substrate, giving butadiene [2]rotaxane **18** in 30% yield (Table 4.3, entry 6).

Table 4.3 Substrate Scope in the Oxidative Heck Active-Template Synthesis of [2]Rotaxanes.[a]

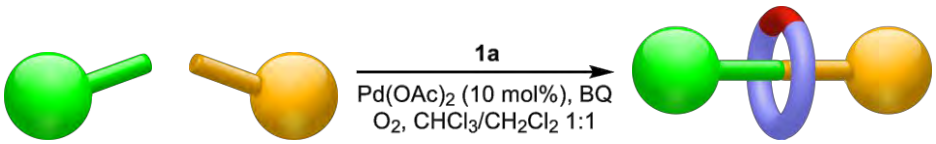

Entry	Alkene used	Boronic acid used	Rotaxane, yield [%]
1	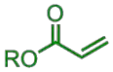 **4**	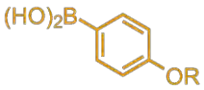 **6**	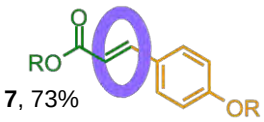 **7**, 73%
2	 **9**	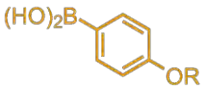 **6**	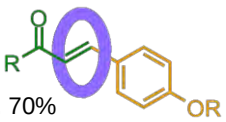 **10**, 70%
3	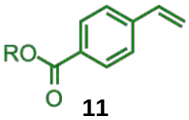 **11**	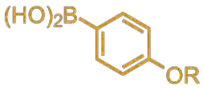 **6**	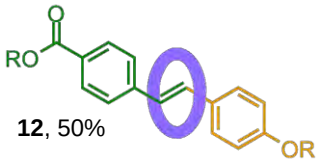 **12**, 50%
4	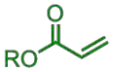 **4**	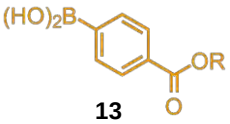 **13**	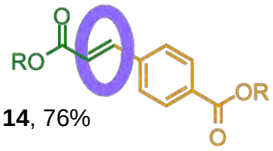 **14**, 76%
5	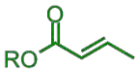 **15**	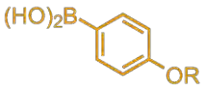 **6**	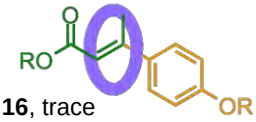 **16**, trace
6[b]	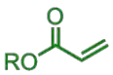 **4**	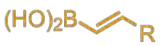 **17**	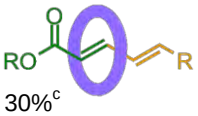 **18**, 30%[c]

[a]*R = $(tBuC_6H_4)_3CC_6H_4O(CH_2)_3$-. Reaction conditions: macrocycle 1 (1 equiv), $Pd(OAc)_2$ (10 mol %), alkene (1 equiv), boronic acid (2 equiv) and benzoquinone (BQ, 1 equiv) in $CHCl_3/CH_2Cl_2$ 1:1 were allowed to stir under O_2 at RT for 72 h.* [b]*Conditions as for other entries except alkene **4** (1.2 equiv.), boronic acid **17** (3 equiv), no benzoquinone, $CHCl_3$/DMF 1:1 as solvent. All reactions were carried out at a concentration of 16 mM.* [c]*Unoptimised yield. Rotaxane **18** proved difficult to isolate free from the accompanying by-product thread.*

4.4 Conclusion

The introduction of active-template palladium cross-coupling routes to [2]rotaxanes opens up the possibility of using one of the most powerful bond-forming methodologies in organic chemistry for the assembly of MIAs. The reaction is mild, substrate-tolerant, and essentially traceless with respect to the thread, and as little as 1% of the catalytic Pd(II) template is required.

4.5 Experimental Section

4.5.1 Preparation of Half-threads

Half-thread **9** was prepared according to the literature procedure.[5]

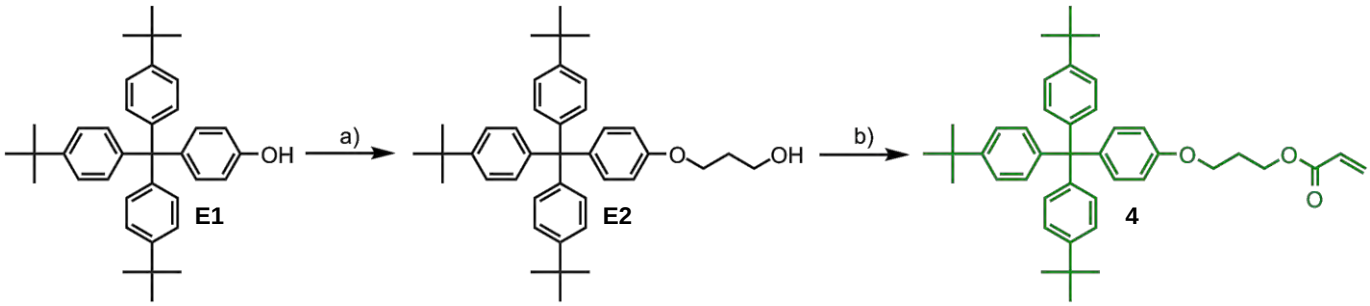

Scheme 4.6 a)1-bromopropanol, K_2CO_3, butanone, 80 °C, 48h, 92%; b) acryloyl chloride, EDCI, NEt_3 DMAP, CH_2Cl_2, 0 °C → RT, 2h, 63%.

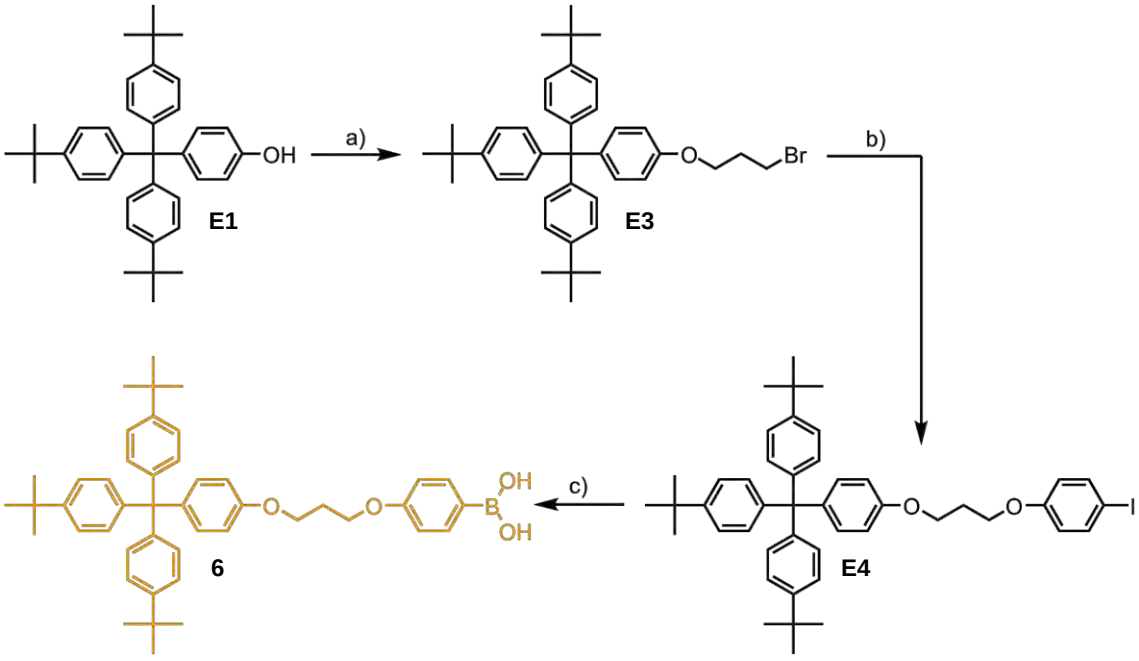

Scheme 4.7 a) 1-bromopropanol, PPh_3, DIAD, THF, 0°C → RT, 48h, 72%; b) p-iodophenol, K_2CO_3, butanone, 80 °C, 48 h, 91%; c) n-BuLi, THF, -78 °C, 30 min. then $B(OMe)_3$, -78 °C → RT, 18 h, then HCl, 71%.

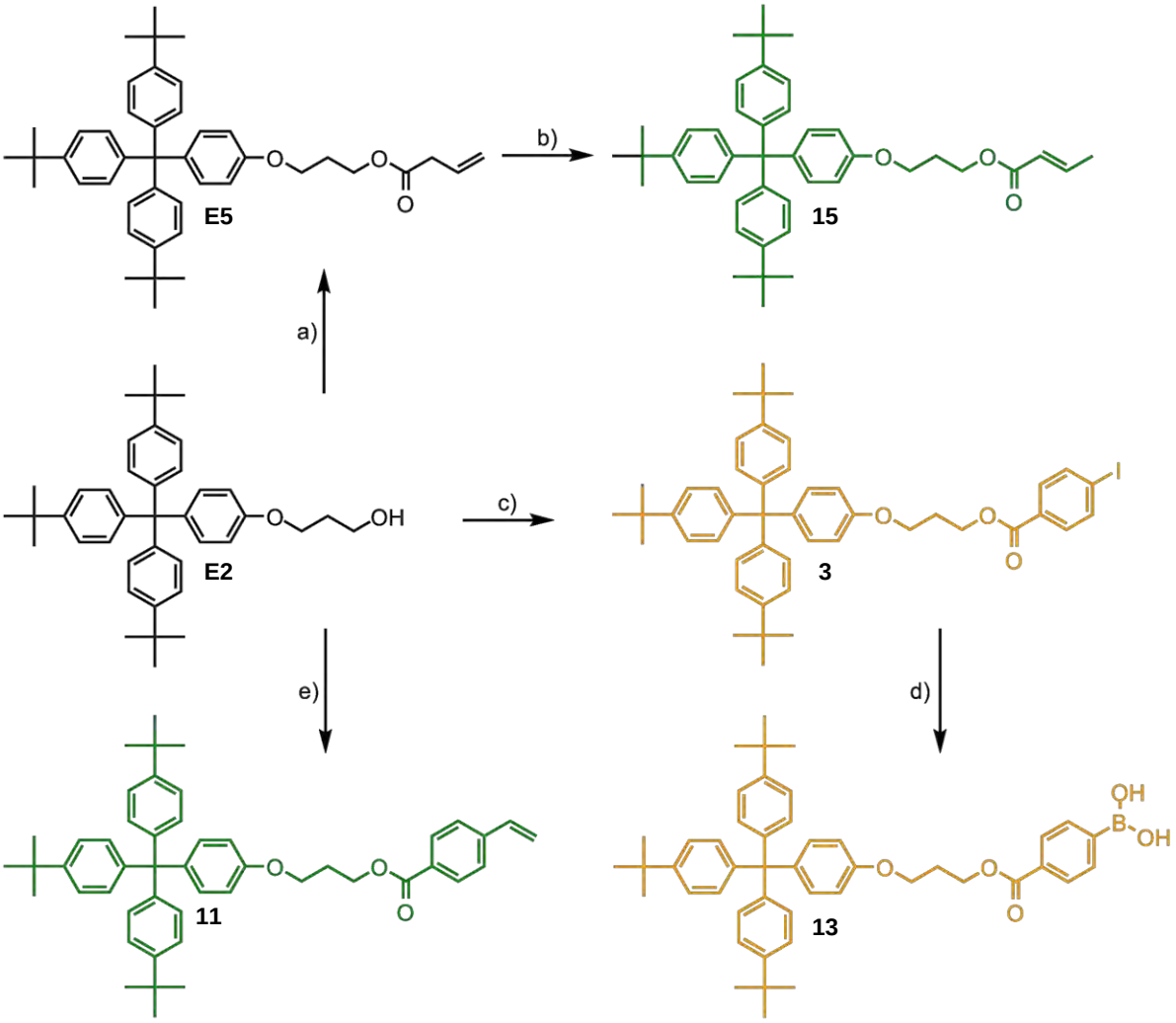

Scheme 4.8 a) Crotonoyl chloride, EDCI, NEt_3 DMAP, CH_2Cl_2, 0 °C → RT, 18h, 53%; b) DBU, THF, 0°C → RT, 18 h, 87%; c) p-iodo-benzoic acid, EDCI, NEt_3, DMAP, 0 °C → RT, 19h, 71%; d) bis-(2-dimethylaminoethyl)-ether, iPrMgCl, THF, 15 °C, $B(OMe)_3$, 0 °C, 20 min. 77%. e) 4-vinylbenzoic acid, EDCI, NEt_3 DMAP, CH_2Cl_2, 0 °C → RT, 18h, 72%;

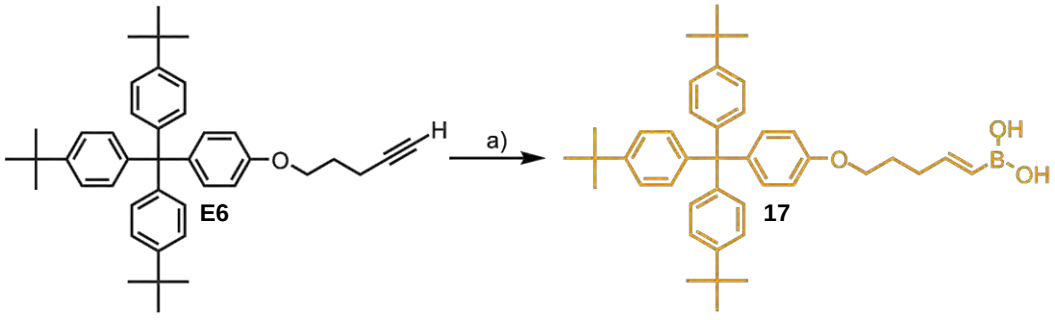

Scheme 4.9 a) Catechol borane, THF, 0 °C, then 18 h, reflux, 42%.

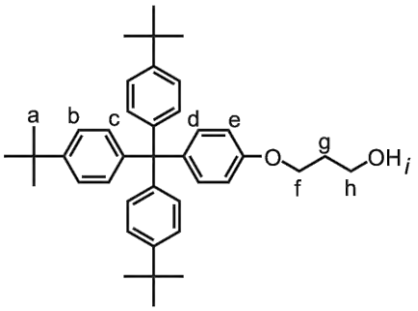

E2

To a solution of 4-[*tris*-(4-*tert*-butylphenyl)methyl]phenol (**E1**)[6] (2.00 g, 4.00 mmol, 1.0 equiv.) and 1-bromopropanol (0.52 mL, 6.00 mmol, 1.5 equiv.) in butanone (160 mL) was added potassium carbonate (5.94 g, 39.6 mmol, 10 equiv.). The suspension was heated at 80 °C for 48 h under nitrogen atmosphere. After cooling, the suspension was concentrated under reduced pressure and the residue was dissolved in CH_2Cl_2 (50 mL). The organic layer was washed with water (3 × 50 mL), dried ($MgSO_4$), filtered and concentrated under reduced pressure. The residue was redissolved in CH_2Cl_2 (10 mL) and precipitated with MeOH. The precipitate was filtered, washed with MeOH and dried under reduced pressure to yield the alcohol **E2** as a colorless solid (2.05 g, 92%). M.p. 290-292 °C. ^{1}H NMR (400 MHz, $CDCl_3$, 298 K): δ = 7.23 (d, *J* = 8.6 Hz, 6H, H_b), 7.08 (d, *J* = 8.6 Hz, 8H, H_c and H_d), 6.77 (d, *J* = 8.9 Hz, 2H, H_e), 4.10 (t, *J* = 5.9 Hz, 2H, H_f), 3.86 (q, *J* = 4.8 Hz, 2H, H_h), 2.04 (m, 2H, H_g), 1.78 (t, *J* = 4.8 Hz, 1H, H_i), 1.30 (s, 27H, H_a). 13C NMR (100 MHz, $CDCl_3$, 298 K): δ = 156.4, 148.2, 144.0, 139.8, 132.2, 130.6, 124.0, 112.9, 65.7, 63.0, 60.7, 34.2, 31.9, 31.3. LRFAB-MS (3-NOBA matrix): *m/z* = 562.4 $[M]^+$; HRFAB-MS (3-NOBA matrix): *m/z* = 562.38193 $[M]^+$ (calcd. for $C_{40}H_{50}O_2$, 562.38108).

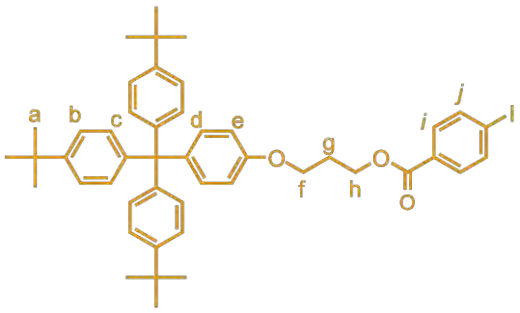

3

4-Iodobenzoic acid (264 mg, 1.07 mmol, 2 equiv.), DMAP (6.50 mg, 53.0 µmol, 0.1 equiv.) and EDCI (118 mg, 0.61 mmol, 1.2 equiv.) were added successively to a solution of the alcohol **E2** (300 mg, 0.53 mmol, 1 equiv.) in CH_2Cl_2 (10 mL). The resulting

solution was allowed to stir at RT for 19 h. The reaction mixture was quenched by addition of water, the aqueous layer extracted with CH_2Cl_2 (×3) and the combined organic layers dried ($MgSO_4$). Purification by flash column chromatography (hexane/EtOAc 91:9) yielded the title compound **3** as a colourless solid (300 mg, 71%); M.p. 232-234 °C. ^{1}H NMR (400 MHz, $CDCl_3$, 298 K): δ = 7.79 (d, *J* = 8.6 Hz, 2H, H_i), 7.73 (d, *J* = 8.6 Hz, 2H, H_j), 7.23 (d, *J* = 8.6 Hz, 6H, H_b), 7.08 (d, *J* = 9.0 Hz, 2H, H_d), 7.07 (d, *J* = 8.6 Hz, 6H, H_c), 6.76 (d, *J* = 9.0 Hz, 2H, H_e), 4.51 (t, *J* = 6.3 Hz, 2H, H_h), 4.10 (t, *J* = 6.1 Hz, 2H, H_f), 2.27-2.20 (m, 2H, H_g), 1.30 (s, 27H, H_a). ^{13}C NMR (100 MHz, $CDCl_3$, 298 K): δ = 166.0, 156.5, 148.3, 144.1, 139.8, 137.7, 132.3, 131.0, 130.7, 129.7, 124.0, 112.9, 100.7, 64.1, 63.0, 62.2, 34.3, 31.4, 28.7. LRFAB-MS (3-NOBA matrix): *m/z* = 792 $[M]^+$; HRFAB-MS (3-NOBA matrix): *m/z* = 792.3024 $[M]^+$ (calcd. for $C_{47}H_{53}O_3I$, 792.3040).

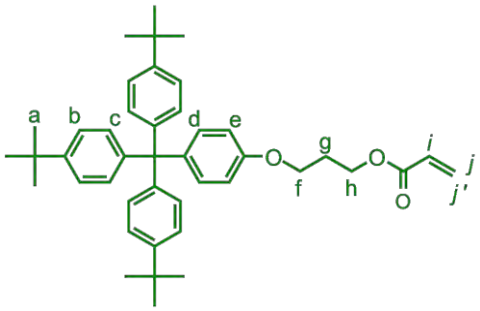

4

Triethylamine (1.86 mL, 13.3 mmol, 5.00 equiv.) was added to a solution of alcohol **E2** (1.50 g, 2.67 mmol, 1.00 equiv.) in CH_2Cl_2 (40 mL) and the resulting mixture was cooled to 0 °C. Acryloyl chloride (0.54 mL, 6.66 mmol, 2.50 equiv.) and DMAP (49 mg, 0.40 mmol, 0.15 equiv.) was added. The resulting mixture was allowed to stir at 0 °C for 2 h before the reaction was quenched by addition of water. The aqueous layer was extracted with CH_2Cl_2 (×3), washed with brine and dried ($MgSO_4$). Purification by column chromatography (hexane/EtOAc 75:25) provided the alkene **4** as a colourless solid (1.04 g, 63%); M.p. 210-212 °C. ^{1}H NMR (400 MHz, $CDCl_3$, 298 K): δ = 7.23 (d, *J* = 8.6 Hz, 6H, H_b), 7.08 (d, *J* = 8.6 Hz, 8H, H_c and H_d), 7.76 (d, *J* = 8.9 Hz, 2H, H_e), 6.40 (d, *J* = 17.3 Hz, 1H, H_j), 6.12 (dd, *J* = 17.3 and 11.9 Hz, 1H, H_i), 5.82 (d, *J* = 11.9 Hz, 1H, $H_{j'}$), 4.36 (t, *J* = 6.3 Hz, 2H, H_h), 4.04 (t, *J* = 6.1 Hz, 2H, H_f), 2.19-2.10 (m, 2H, H_g), 1.30 (s, 27H, H_a). ^{13}C NMR (100 MHz, $CDCl_3$, 298 K): δ = 166.2, 156.6, 148.3, 144.1, 139.8, 139.5, 132.3, 130.7, 128.4, 124.0, 113.0, 64.1, 63.1, 61.5, 34.3, 31.4, 28.7. LRFAB-MS (3-NOBA matrix): *m/z* = 616 $[M]^+$; HRFAB-MS (3-NOBA matrix): *m/z* = 616.3928 $[M]^+$ (calcd. for $C_{43}H_{52}O_3$, 616.3917).

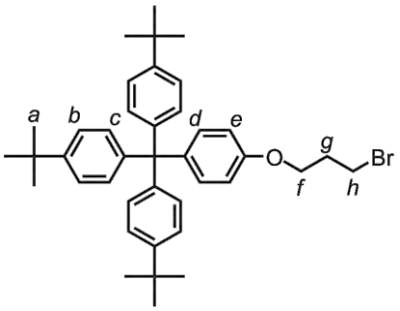

E3

4-[*Tris*-(4-*tert*-butylphenyl)methyl]phenol (**E1**)[6] (3.00 g, 5.94 mmol, 1 equiv.), 3-bromo-1-propanol (1.00 mL, 11.9 mmol, 2 equiv.) and triphenylphosphine (3.20 g, 11.9 mmol, 2 equiv.) were dissolved in THF at 0 °C. DIAD (2.30 mL, 11.9 mmol, 2 equiv.) was added dropwise. When addition was complete the reaction mixture was allowed to stir for a further 48 h at RT. The solution was concentrated under reduced pressure, the residue was dissolved in CH_2Cl_2 (10 mL) and precipitated with MeOH. The precipitate was filtered, washed with MeOH (3 × 10 mL) and redissolved in CH_2Cl_2. The solution was passed through a plug of silica (CH_2Cl_2) to afford **E3** as a colourless powder (2.68 g, 72%); M.p. 244-246 °C. ^{1}H NMR (400 MHz, $CDCl_3$, 298 K): δ = 7.23 (d, *J* = 8.6 Hz, 6H, H_b), 7.08 (d, *J* = 8.6 Hz, 8H, H_c and H_d), 6.77 (d, *J* = 8.9 Hz, 2H, H_e), 4.08 (t, *J* = 5.8 Hz, 2H, H_f), 3.60 (t, *J* = 6.4 Hz, 2H, H_h), 2.27-2.35 (m, 2H, H_g), 1.54 (s, 27H, H_a). 13C NMR (100 MHz, $CDCl_3$, 298 K): δ = 156.4, 148.3, 144.1, 139.8, 132.2, 130.7, 124.0, 112.9, 65.1, 63.0, 34.3, 32.4, 31.4, 30.2. LRFAB-MS (3-NOBA matrix): *m/z* = 625.1 $[M+H]^+$; HRFAB-MS (3-NOBA matrix): *m/z* = 624.29625 $[M]^+$ (calcd. for $C_{40}H_{49}BrO$, 624.29668).

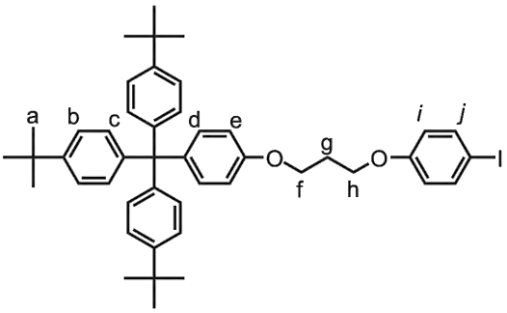

E4

To a solution of **E3** (1.00 g, 1.59 mmol, 1 equiv.) and 4-iodophenol (700 mg, 3.18 mmol, 2 equiv.) in butanone (160 mL) was added potassium carbonate (2.20 g, 16.0 mmol, 10 equiv.) The suspension was heated at 80 °C for 48 h under nitrogen atmosphere. After cooling, the suspension was concentrated under reduced pressure and the residue was

dissolved in CH_2Cl_2 (50 mL). The organic layer was washed with a solution of NaOH 1 M (3 x 50 mL) then with water (1 × 50 mL), dried ($MgSO_4$), filtered and concentrated under reduced pressure. The residue was redissolved in CH_2Cl_2 (10 mL) and precipitated with MeOH. The precipitate was filtered, washed with MeOH and dried under reduced pressure to yield the aryl iodide **E4** as a colourless solid (1.10 g, 91%); M. p. 201-203 °C. ^{1}H NMR (400 MHz, $CDCl_3$, 298 K): δ = 7.53 (d, *J* = 8.9 Hz, 2H, H_j), 7.22 (d, *J* = 8.6 Hz, 6H, H_b), 7.07 (d, *J* = 8.6 Hz, 8H, H_c and H_d), 6.76 (d, *J* = 8.9 Hz, 2H, H_i), 6.68 (d, *J* = 8.9 Hz, 2H, H_e), 4.11 (t, *J* = 6.0 Hz, 4H, H_f and H_h), 2.19-2.27 (m, 2H, H_g), 1.30 (s, 27H, H_a). 13C NMR (100 MHz, $CDCl_3$, 298 K): δ = 158.7, 156.5, 148.3, 144.1, 139.7, 138.1, 132.2, 130.7, 124.0, 116.9, 112.9, 82.7, 64.6, 64.0, 63.0, 34.3, 31.3, 29.2. LRFAB-MS (3-NOBA matrix): *m/z* = 764 $[M+H]^+$; HRFAB-MS (3-NOBA matrix): *m/z* = 764.30903 $[M]^+$ (calcd. for $C_{46}H_{53}IO_2$, 764.30903).

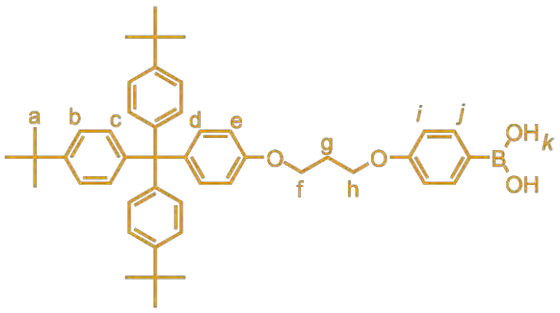

6

n-BuLi, (1.04 mL, 2.5 M solution in hexanes, 2.60 mmol) was added dropwise to a solution of **E4** (1.00 g, 1.30 mmol, 1 equiv.) in THF (20 mL) at -78 °C. After 30 min. of stirring at -78 °C, trimethyl borate (0.73 mL, 6.50 mmol, 5 equiv.) was added. The solution was stirred at -78 °C for another 2 h before it was allowed to stir for a further 18 h at RT. The reaction mixture was quenched with MeOH (2 mL) and the solvents removed under reduced pressure. The residue was dissolved in CH_2Cl_2 (10 mL) and stirred vigorously for 1 h with 5% HCl (aq.) (10 mL) until the colour of the organic layer became orange. The layers were separated and the organic layer washed with water (50 mL), dried ($MgSO_4$), filtered and concentrated under reduced pressure. The residue was purified by column chromatography (gradient 1% to 5% of MeOH in CH_2Cl_2) to afford the boronic acid **6** as a pale yellow powder (631 mg, 71%), M.p. 184-186 °C . ^{1}H NMR (400 MHz, $CDCl_3$/d_6-DMSO 95:5, 298 K): δ = 7.73 (d, *J* = 8.6 Hz, 2H, H_j), 7.18 (d, *J* = 8.6 Hz, 6H, H_b), 7.03 (d, *J* = 8.6 Hz, 8H, H_c and H_d), 6.85 (d, *J* = 8.6 Hz, 2H, H_i), 6.72 (d, *J* = 9.0 Hz, H_e), 6.14 (s, 2H, H_k), 4.13 (t, *J* = 6.1 Hz, 2H, H_f), 4.08 (t, *J* = 6.2 Hz, 2H,

H_h), 2.20 (tt, *J* = 6.2, 6.1 Hz, 2H, H_g), 1.25 (s, 27H, H_a). ^{13}C NMR (100 MHz, $CDCl_3$, 298 K): δ = 156.6, 148.2, 144.1, 139.6, 137.4, 135.8, 132.2, 130.6, 124.0, 113.9, 113.7, 112.9, 64.2, 63.0, 40.1, 34.2, 31.3, 29.3; LRESI-MS (MeOH/CH_2Cl_2): *m/z* = 696 $[M+MeOH-H_2O]^+$.

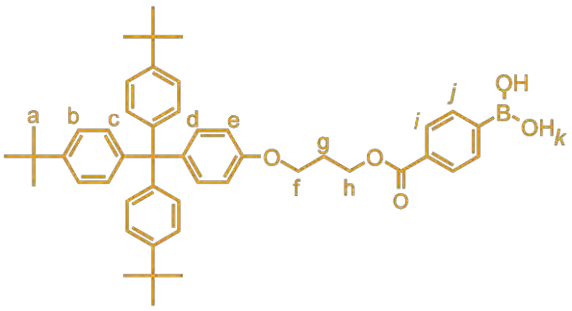

13

To a solution of **E2** (100 mg, 0.12 mmol, 1 equiv.) and *bis*-(2-dimethylaminoethyl)-ether (0.028 mL, 0.15 mmol, 1.25 equiv.) in THF (1 mL) was added isopropylmagnesium chloride (0.075 mL, 0.15 mmol, 1.25 equiv.) at 15 °C. The mixture was stirred at RT for 20 min. and trimethylborate (0.067 mL, 0.6 mmol, 5 equiv.) was added at 0 °C. The mixture was then quenched with HCl 1 M (2 mL), extracted with CH_2Cl_2 (3 mL) and the organic phase was dried ($MgSO_4$), filtered and concentrated under reduced pressure. The residue was purified by column chromatography (CH_2Cl_2/MeOH 100:0 to 95:5) to afford the boronic acid **13** as a colourless powder (66 mg, 77%). M.p. 192-194 °C. ^1H NMR (400 MHz, $CDCl_3$/d_6-DMSO 97:3, 298 K): δ = 7.91 (d, J = 8.0 Hz, 2H, Hi), 7.83 (d, J = 8.1 Hz, 2H, Hj), 7.13 (d, J = 8.5 Hz, 6H, Hb), 6.98 (d, J = 8.4 Hz, 8H, Hc and Hd), 6.68 (d, J = 8.8 Hz, 2H, He), 6.36 (s, 2H, Hk), 4.41 (t, J = 6.1 Hz, 2H, Hh), 4.02 (t, J = 6.0 Hz, 2H, Hf), 2.10-2.20 (m, 2H, Hg), 1.20 (s, 27H, Ha). 13C NMR (100 MHz, CDCl3/ d6-DMSO 9:1, 298 K): 156.2, 154.2, 148.0, 143.8, 139.4, 133.9, 131.9, 130.4, 128.2, 123.8, 112.7, 111.0, 106.9, 95.3, 63.9, 61.6, 34.0, 31.1, 28.5; LRESI-MS (MeOH/CH_2Cl_2): *m/z* = 724 $[M+MeOH-H_2O]^+$;

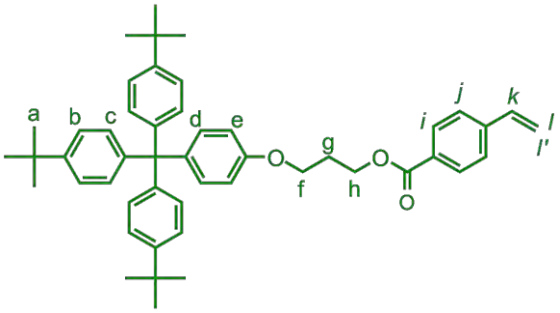

11

A solution of alcohol **E2** (1.00 g, 1.72 mmol, 1.0 equiv.) and 4-vinylbenzoic acid (310 mg, 2.06 mmol, 1.2 equiv.) in CH_2Cl_2 (50 mL) was cooled to 0 °C. EDCI (430 mg, 2.25 mmol, 1.5 equiv.) and DMAP (210 mg, 1.72 mmol, 1.0 equiv.) were added. The resulting mixture was allowed to stir overnight at RT. The reaction was quenched by addition of water and the resulting aqueous layer extracted with CH_2Cl_2 (×3). The combined organic layers were dried over anhydrous $MgSO_4$. Purification by column chromatography (hexane/EtOAc 9:1) provided the alkene **11** as a colourless solid (850 mg, 72%); M.p. 180-183 °C. ^{1}H NMR (400 MHz, $CDCl_3$, 298 K): δ = 7.91 (d, *J* = 8.3 Hz, 2H, H_i), 7.36 (d, *J* = 8.3 Hz, 2H, H_j), 7.14 (d, *J* = 8.5 Hz, 6H, H_b), 7.00 (d, *J* = 8.5 Hz, 6H, H_c), 7.00 (d, *J* = 8.8 Hz, 2H, H_d), 6.69 (d, *J* = 8.8 Hz, 2H, H_e), 6.66 (dd, *J* = 17.6, 10.9 Hz, 1H, H_k), 5.77 (d, *J* = 17.6 Hz, 1H, H_l), 5.29 (d, *J* = 10.9 Hz, 1H, $H_{l'}$), 4.43 (t, *J* = 6.2 Hz, 2H, H_h), 4.02 (t, *J* = 6.1 Hz, 2H, H_f), 2.16 (tt, *J* = 6.2, 6.1 Hz, 2H, H_g), 1.21 (s, 27H, H_a). ^{13}C NMR (100 MHz, 298 K, $CDCl_3$): δ = 166.3, 156.6, 148.3, 144.1, 142.0, 139.8, 136.0, 132.3, 130.7, 129.9, 129.4, 126.1, 124.3, 116.5, 113.0, 64.3, 63.1, 61.9, 34.3, 31.4, 28.9. LRFAB-MS (3-NOBA matrix): *m/z* = 692.8 $[M]^+$; HRFAB-MS (3-NOBA matrix): *m/z* = 692.4226 $[M]^+$ (calcd. for $C_{49}H_{56}O_3$, 692.4230).

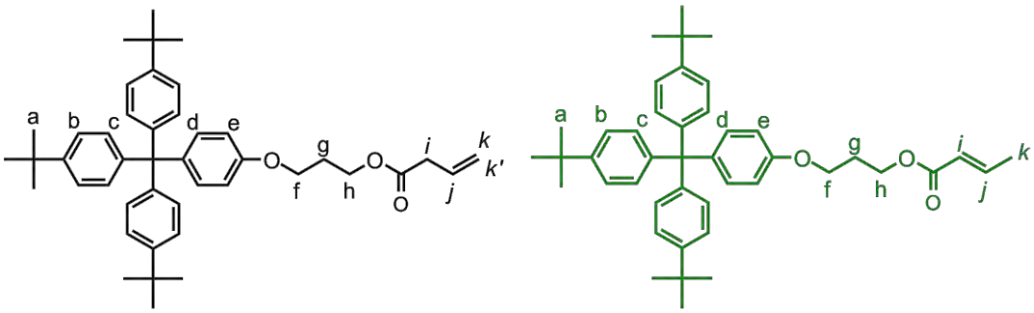

E5 + 15

A solution of alcohol **E2** (1.00 g, 1.78 mmol, 1.00 equiv.) and triethylamine (1.24 mL, 8.88 mmol, 5.00 equiv.) in CH_2Cl_2 (30 mL) was cooled to 0 °C. Crotonyl chloride (0.43 mL, 4.44 mmol, 2.50 equiv.) and DMAP (33 mg, 0.27 mmol, 0.15 equiv.) were added before allowing the reaction mixture to stir overnight at RT. The reaction was quenched by addition of water and the resulting aqueous layer extracted with CH_2Cl_2 (×3). The combined organic layers were washed with brine and dried ($MgSO_4$). Purification by column chromatography (hexane:EtOAc 91:9) provided the alkene **E5** as a pale yellow solid (593 mg, 53%). ^{1}H NMR (400 MHz, $CDCl_3$, 298 K): δ = 7.23 (d, *J* = 8.7 Hz, 6H, H_b), 7.08 (d, *J* = 8.7 Hz, 6H, H_c), 7.08 (d, *J* = 8.9 Hz, 2H, H_d), 6.75 (d, *J* = 8.9 Hz, 2H, H_e), 5.92 (m, 1H, H_j), 5.16 (m, 2H, H_k), 4.29 (t, *J* = 6.3 Hz, 2H, H_h), 4.02 (t, *J* = 6.1 Hz,

2H, H_f), 3.10 (dt, *J* = 7.0, 1.4 Hz, 2H, H_i), 2.11 (tt, *J* = 6.3, 6.1 Hz, 2H, H_g), 1.30 (s, 27H, H_a). DBU (0.18 mL, 1.19 mmol, 1.25 equiv.) was added dropwise to a solution of **E5** (593 mg, 0.94 mmol, 1 equiv.) in THF (12 mL) at 0 °C. The resulting mixture was allowed to warm slowly to RT and stirred overnight. THF was removed under reduced pressure and the resulting oil redissolved in CH_2Cl_2. The organic layer was washed with 1M HCl (aq.) (×3), the aqueous layer extracted with CH_2Cl_2 (×3) and the combined organic layers washed with dilute NaOH (aq.), 1M HCl (aq.), water and dried ($MgSO_4$) to yield the alkene **15** as a pale yellow solid (515 mg, 87%); M.p. 185-188 °C. ^{1}H NMR (400 MHz, $CDCl_3$, 298 K): δ = 7.13 (d, *J* = 8.5 Hz, 6H, H_b), 6.99 (d, *J* = 8.5 Hz, 6H, H_c), 6.99 (d, *J* = 8.9 Hz, 2H, H_d), 6.88 (dq, *J* = 15.5, 6.9 Hz, 1H, H_j), 6.66 (d, *J* = 8.9 Hz, 2H, H_e), 5.75 (dq, *J* = 15.5, 1.6 Hz, 1H, H_i), 4.22 (t, *J* = 6.2 Hz, 2H, H_h), 3.93 (t, *J* = 6.1 Hz, 2H, H_f), 2.03 (tt, *J* = 6.2, 6.1 Hz, 2H, H_g), 1.77 (dd, *J* = 6.9, 1.6 Hz, 2H, H_k), 1.21 (s, 27H, H_a). ^{13}C NMR (100 MHz, CDCl3, 298 K): δ = 166.5, 156.6, 148.3, 144.8, 144.2, 139.7, 132.3, 130.4, 123.7, 122.6, 113.0, 64.2, 63.1, 61.1, 34.3, 31.4, 28.8, 18.0. LRFAB-MS (3-NOBA matrix): *m/z* = 630.8 $[M]^+$; HRFAB-MS (3-NOBA matrix): *m/z* = 630.4072 $[M]^+$ (calcd. for $C_{44}H_{54}O_3$, 630.4073).

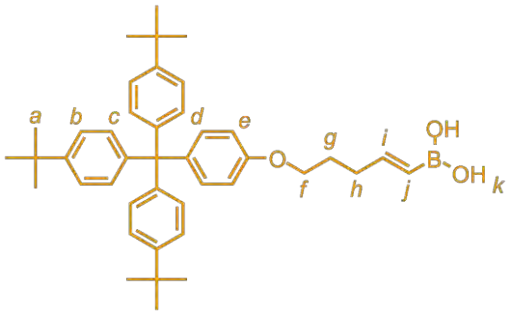

17

At 0 °C, Catechol borane (0.12 mL, 1.09 mmol, 1.25 equiv.) was added dropwise to a solution of alkyne **E6**[7] (500 mg, 0.87 mmol, 1 equiv.) in THF (2mL) under an atmosphere of nitrogen. The resulting mixture was refluxed for 18 h. After cooling, water was added dropwise and the reaction mixture was allowed to stir at RT for 1 h CH_2Cl_2 and water were added (10 mL). The aqueous layer was washed with CH_2Cl_2 (3 × 10 mL) and the combined organic layers were washed with water and dried ($MgSO_4$). Purification by column chromatography (hexane/EtOAc 5:5) yielded the boronic acid **17** as a pale yellow solid (225 mg, 42%). ^{1}H NMR (400 MHz, $CDCl_3$/d_6-DMSO 95:5, 298 K): δ = 7.22 (d, *J* = 8.6 Hz, 6H, H_b), 7.03-7.10 (m, 8H, H_c and H_d), 6.79 (d, *J* = 8.9 Hz, 2H, H_e), 6.57 (dt, *J* = 6.3, 17.9, 1H, H_j), 5.46 (dt, *J* = 1.3, 17.9, 1H, H_i), 5.23 (bs, 2H, H_k), 3.93 (t,

J = 6.4 Hz, 2H, H_f), 2.33 (dt, *J* = 1.3, 6.8 Hz, 2H, H_h), 1.89 (dt, *J* = 6.8, 6.8 Hz, 2H, H_g), 1.29 (s, 27H, H_a).^{13}C NMR (100 MHz, $CDCl_3$, 298 K) δ = 156.7, 151.0, 148.2, 144.1 (×2), 139.4, 132.2, 130.7, 124.0, 112.9, 66.9, 63.0, 34.3, 31.9, 31.3, 28.0. LRESI-MS: *m/z* = 630.4 $[M+MeOH-H_2O]^+$.

4.5.2 General Experimental Procedure for the Oxidative Heck Active-Metal Template Reaction

A solution of the alkene half-thread (1 equiv.), boronic acid half-thread (2 equiv.), bipy macrocycle **1a** (1 equiv.), $Pd(OAc)_2$ (0.1 equiv.) and benzoquinone (1 equiv.) in a 1:1 mixture of $CHCl_3/CH_2Cl_2$ was allowed to stir under a balloon of O_2. After 72 h, a solution of KCN (10 equiv.) in MeOH was added and the resulting suspension allowed to stir at RT for 1 h. The solvents were removed under reduced pressure and the resulting crude mixture dissolved in CH_2Cl_2 and water. The aqueous layer was extracted with CH_2Cl_2 (×3), washed with brine and dried ($MgSO_4$). Purification by column chromatography (hexane/CH_2Cl_2/MeCN 5:4.5:0.5) provided the rotaxane as a colourless film.

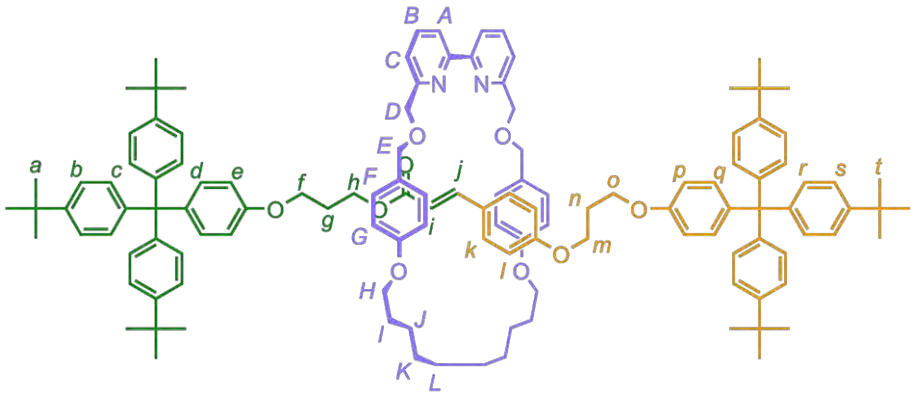

6

Following the general procedure with macrocycle **1a** (9 mg, 0.016 mmol, 1 equiv.), alkene **4** (11 mg, 0.016 mmol, 1 equiv.), boronic acid **6** (22 mg, 0.032 mmol, 2 equiv.), $Pd(OAc)_2$ (0.4 mg, 1.0 μmol, 0.1 equiv.) benzoquinone (1.7 mg, 0.016 mmol, 1 equiv.) and KCN (11 mg, 0.160 mmol, 10 equiv.) gave a crude yellow solid. Purification by column chromatography (hexane/CH_2Cl_2/MeCN 5:4.5:0.5) afforded **6** (18 mg, 62%) as a colourless film. ^{1}H NMR (400 MHz, $CDCl_3$, 298 K): δ = 7.96 (d, *J* = 7.6 Hz, 2H, H_A), 7.49 (dd, *J* = 7.8, 7.6 Hz, 2H, H_B), 7.39 (d, *J* = 15.9 Hz, 1H, H_j), 7.28 (d, *J* = 7.8 Hz, 2H, Hc), 7.23 (d, *J* = 8.7 Hz, 12H, H_b, H_s), 7.10-6.99 (m, 22H, H_c, H_r, H_F, H_d, H_q, H_k), 6.62 (d, *J* = 8.6 Hz, 6H, H_G, H_e), 6.56 (d, *J* = 8.9 Hz, 2H, H_p), 6.39 (d, *J* = 8.7 Hz, 2H, H_l), 6.04 (d, *J* = 15.9 Hz, 1H, H_i), 4.56 (s, 4H, $H_{D/E}$), 4.55 (s, 4H, $H_{D/E}$), 4.24 (t, *J* = 6.2 Hz, 2H, H_h), 3.85 (t, *J* = 6.2 Hz, 2H,

H_f), 3.74 (t, *J* = 6.2 Hz, 6H, H_H, $H_{m/o}$), 3.64 (t, *J* = 6.2 Hz, 2H, $H_{m/o}$), 2.00 (tt, *J* = 6.2, 6.2 Hz, 2H, H_g), 1.85 (tt, *J* = 6.2, 6.2 Hz, 2H, H_n), 1.59-1.53 (m, 4H, H_l), 1.30 (s, 54H, H_a, H_t), 1.26-1.05 (m, 12H, H_J, H_K, H_L). ^{13}C NMR (100 MHz, 298 K, $CDCl_3$): δ = 167.1, 160.3, 158.5, 158.2, 156.5, 156.4, 155.1, 148.2, 148.2, 144.5, 144.1 (×2), 139.5, 139.4 (×2), 136.8, 132.1, 132.0, 130.6, 129.7, 129.3, 126.6, 124.0, 124.0, 121.0, 119.5, 114.9, 114.3, 114.2, 112.8 (×2), 112.8, 72.4, 72.0, 67.5, 64.2, 63.9, 63.8, 63.0 (×2), 61.0, 34.2 (×2), 31.3 (×2), 29.7, 29.3, 28.9, 28.7 (×2), 25.7; LRFAB-MS (3-NOBA matrix): *m/z* = 1821 $[M+H]^+$; HRFAB-MS (3-NOBA matrix): *m/z* = 1820.1117 $[M+H]^+$ (calcd. for $C_{125}H_{147}N_2O_9$, 1820.1107).

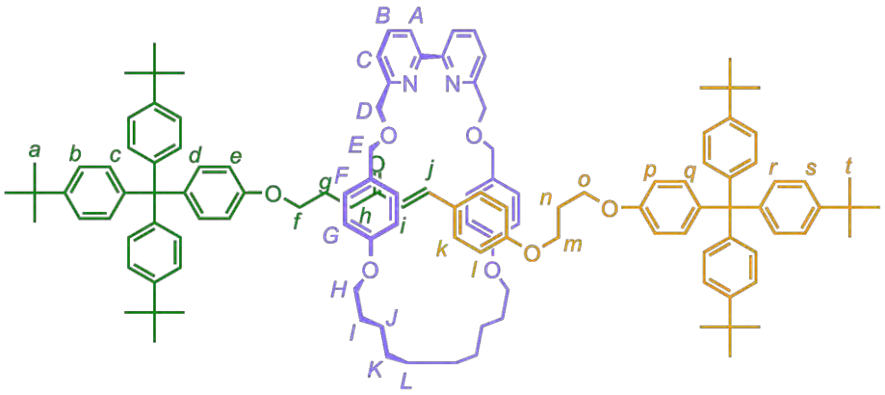

10

Following the general procedure with macrocycle **1a** (9 mg, 0.016 mmol, 1 equiv.), alkene **9** (9.5 mg, 0.016 mmol, 1 equiv.), boronic acid **6** (22 mg, 0.032 mmol, 2 equiv.), $Pd(OAc)_2$ (0.4 mg, 1.0 µmol, 0.1 equiv.) benzoquinone (1.7 mg, 0.016 mmol, 1 equiv.) and KCN (11 mg, 0.160 mmol, 10 equiv.) gave a crude yellow solid. Purification by column chromatography (hexane/CH_2Cl_2/MeCN 5:4.5:0.5) afforded **10** (18 mg, 62%) as a colourless film. ^{1}H NMR (400 MHz, $CDCl_3$, 298 K): δ = 7.94 (d, *J* = 7.7 Hz, 2H, H_A), 7.48 (dd, *J* = 7.7, 7.7 Hz, 2H, H_B), 7.27 (d, *J* = 7.7 Hz, 2H, Hc), 7.23 (d, *J* = 8.5 Hz, 12H, H_b, H_s), 7.18 (d, *J* = 16.3 Hz, 1H, H_j), 7.10-6.98 (m, 20H, H_c, H_r, H_F, H_d, H_q), 6.99 (d, *J* = 8.7 Hz, 2H, H_k), 6.65-6.57 (m, 8H, H_G, H_e, H_p), 6.41 (d, *J* = 8.7 Hz, 2H, H_l), 6.27 (d, *J* = 16.3 Hz, 1H, H_i), 4.55 (s, 8H, H_D, H_E), 3.80 (t, *J* = 6.2 Hz, 2H, H_f), 3.78 (t, *J* = 6.2 Hz, 2H, $H_{m/o}$), 3.74 (t, *J* = 6.4 Hz, 4H, H_H), 3.69 (t, *J* = 6.2 Hz, 2H, $H_{m/o}$), 2.58 (t, *J* = 7.1, 2H, H_h), 1.95 (tt, *J* = 7.1, 6.2 Hz, 2H, H_g), 1.90 (tt, *J* = 6.2, 6.2 Hz, 2H, H_n), 1.59-1.53 (m, 4H, H_l), 1.30 (s, 54H, H_a, H_t), 1.25-0.80 (m, 12H, H_J, H_K, H_L). ^{13}C NMR (100 MHz, 298 K, $CDCl_3$): δ = 199.4, 160.5, 158.6, 158.2, 156.7, 156.5, 155.2, 148.3, 148.2, 144.2 (×2), 142.3, 139.5 (×2), 139.4, 138.4, 136.9, 132.1 (×2), 130.7 (×2), 129.7, 129.7, 124.0 (×2), 123.6, 121.1, 119.6, 114.4, 114.3, 112.9, 112.9, 72.4, 72.1, 67.5, 66.7, 64.3, 63.8 (×2), 63.0, 36.7, 34.3 (×2), 31.4 (×2), 29.7,

29.4, 28.9, 28.8, 28.8, 23.6. LRESI-MS: *m/z* = 1804 $[M+H]^+$; HRFAB-MS (3-NOBA matrix): *m/z* = 1805.1256 $[M+1+H]^+$ (calcd. for $^{13}C^{12}C_{124}H_{147}N_2O_8$, 1805.1191).

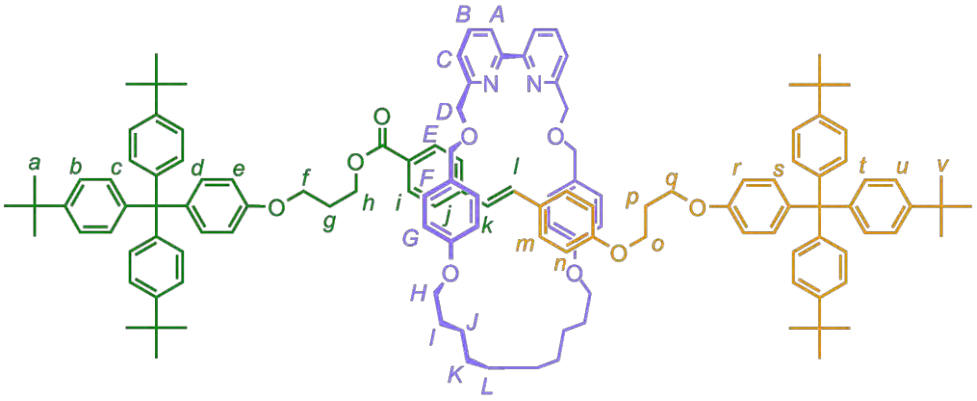

12

Following the general procedure with macrocycle **1a** (9 mg, 0.016 mmol, 1 equiv.), alkene **11** (11 mg, 0.016 mmol, 1 equiv.), boronic acid **6** (22 mg, 0.032 mmol, 2 equiv.), $Pd(OAc)_2$ (0.4 mg, 1.0 µmol, 0.1 equiv.) benzoquinone (1.7 mg, 0.016 mmol, 1 equiv.) and KCN (11 mg, 0.160 mmol, 10 equiv.) gave a crude yellow solid. Purification by column chromatography (hexane/CH_2Cl_2/MeCN 5:4.5:0.5) afforded **12** (14 mg, 48%) as a colourless film. ^{1}H NMR (400 MHz, $CDCl_3$, 298 K): δ = 7.93 (d, *J* = 7.7 Hz, 2H, H_A), 7.78 (d, *J* = 8.4 Hz, 2H, H_i), 7.46 (t, *J* = 7.7 Hz, 2H, H_B), 7.20-7.29 (m, H_b, H_u and H_C), 7.16 (d, *J* = 8.4 Hz, 2H, H_j), 7.02-7.11 (m, H_c, H_d, H_s, H_t and H_F), 6.74 (d, *J* = 15.9 Hz, 1H, H_k), 6.51-6.68 (m, 9H, H_e, H_l, H_r and H_G), 4.55 (2s, 8H, H_D and H_E), 4.38 (t, *J* = 6.4 Hz, 2H, H_h), 3.94 (t, *J* = 6.1 Hz, 2H, H_f), 3.87 (t, *J* = 5.8 Hz, 2H, H_o or H_q), 3.84 (t, *J* = 6.1 Hz, 2H, H_o or H_q), 3.74 (t, *J* = 6.4 Hz, 4H, H_H), 2.06-2.15 (m, 2H, H_g), 1.95-2.06 (m, 2H, H_p), 1.51-1.60 (m, 4H, H_I), 1.29 (2s, 54H, H_a and H_v), 1.15-1.24 (m, 4H, H_J), 1.00-1.10 (m, 4H, H_K), 0.79-0.91 (m, 4H, H_L). ^{13}C NMR (100 MHz, $CDCl_3$, 298 K): δ = 166.2, 158.5, 158..3, 158.1, 156.5, 156.4, 155.2, 148.2, 144.2, 144.2, 139.5, 136.9, 136.8, 132.3, 132.1, 132.1, 131.7, 130.7, 130.7, 130.0, 129.8, 129.7, 129.6, 129.5, 128.6, 127.9, 127.3, 124.0, 124.0, 121.1, 119.6, 114.4, 114.3, 114.0, 112.8, 72.4, 72.4, 72.1, 72.1, 67.5, 64.1, 63.9, 63.0, 51.7, 34.3, 34.3, 31.4, 31.4, 29.7, 29.4, 28.9, 28.8, 28.7. 25.8. LRESI-MS: *m/z* = 1897.25 $[M+H]^+$; HRFAB-MS (3-NOBA matrix): *m/z* = 1896.14476 $[M]^+$ (calcd. for $C_{131}H_{151}N_2O_9$, 1896.14796).

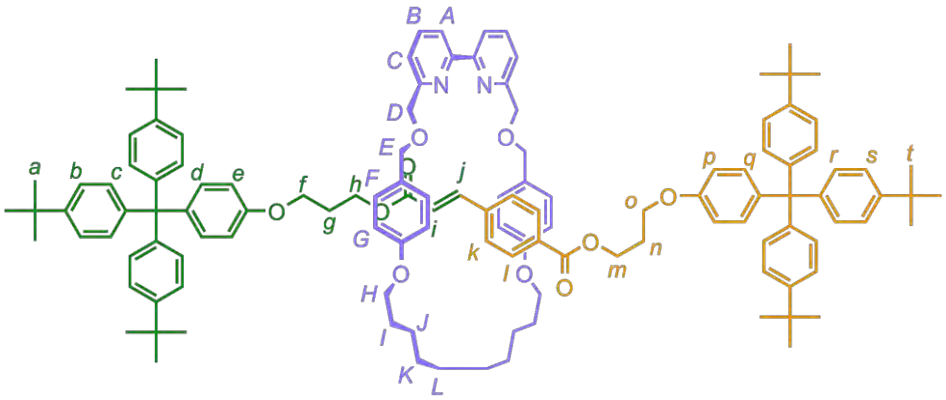

14

Following the general procedure with macrocycle **1a** (9 mg, 0.016 mmol, 1 equiv.), alkene **4** (10 mg, 0.016 mmol, 1 equiv.), boronic acid **13** (22.7 mg, 0.032 mmol, 2 equiv.), $Pd(OAc)_2$ (0.4 mg, 1.0 µmol, 0.1 equiv.), benzoquinone (1.7 mg, 0.016 mmol, 1 equiv.) and KCN (11 mg, 0.160 mmol, 10 equiv.) gave a crude yellow solid. Purification by column chromatography (hexane/CH_2Cl_2/MeCN 5:4.5:0.5) afforded **14**(8 mg, 27%) as a colourless film; M.p. 94-96 °C. ^{1}H NMR (400 MHz, $CDCl_3$, 298 K): δ = 7.90 (d, J = 7.7 Hz, 2H, H_A), 7.62 (d, J = 8.3 Hz, 2H, H_I), 7.47 (t, J = 7.7 Hz, 2H, H_B), 7.30 (d, J = 16.0 Hz, 1H, H_j), 7.25-7.28 (m, 2H, H_C), 7.22 (d, J = 8.5 Hz, 12H, H_b and H_s), 7.07 (d, J = 8.5 Hz, 16H, H_c, H_d, H_q and H_r), 7.00-7.05 (m, 6H, H_k and H_F), 6.59-6.65 (m, 8H, H_e, H_p and H_G), 6.12 (d, J = 16.0 Hz, 1H, H_i), 4.53 (2s, 8H, H_D and H_E), 4.31 (t, J = 6.3 Hz, 2H, H_m), 4.22 (t, J = 6.3 Hz, 2H, H_h), 3.81-3.88 (m, 4H, H_o and H_f), 3.74 (t, J = 6.4 Hz, 4H, H_H), 1.93-2.07 (m, 4H, H_g and H_n), 1.51-1.61 (m, 4H, H_l), 1.29 (s, 54H, H_a and H_t), 1.15-1.24 (m, 4H, H_J), 0.78-1.15 (m, 8H, H_K and H_L). ^{13}C NMR (100 MHz, $CDCl_3$, 298 K): δ = 166.3, 165.6, 158.5, 158.2, 156.4 (×2), 155.1, 148.2 (×2), 144.1 (×3), 143.1, 139.6 (×2), 136.8, 132.2 (×2), 130.7 (×2), 129.8, 129.7, 127.6, 124.0 (×2), 121.1, 120.0, 119.5, 114.3 (×2), 112.8 (×3), 72.4, 72.0, 67.5, 63.8 (×2), 63.0 (×2), 61.9, 61.4, 34.3 (×2), 31.4 (×2), 29.7, 29.4, 28.9, 28.8, 28.6, 25.8. LRFAB-MS (3-NOBA matrix): *m/z* = 1847.9 $[M+H]^+$; HRFAB-MS (3-NOBA matrix): *m/z* = 1849.11402 $[M+1+H]^+$ (calcd. for $^{13}C^{12}C_{125}H_{147}N_2O_{10}$, 1849.10893).

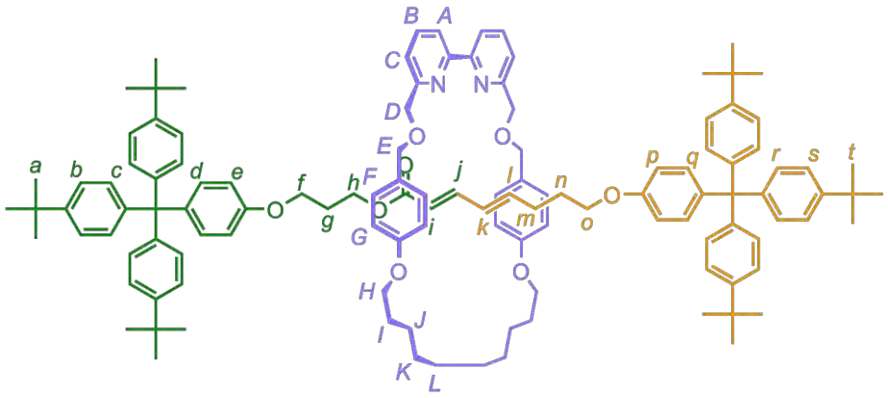

18

A solution of the alkene **4** (35 mg, 0.057 mmol, 3 equiv.), boronic acid **17** (14 mg, 0.023 mmol, 1.2 equiv.), bipy macrocycle **1a** (11 mg, 0.019 mmol, 1 equiv.), $Pd(OAc)_2$ (0.5 mg, 1.9 μmol, 0.1 equiv.) in a 1:1 mixture of DMF/$CHCl_3$ (1 mL) was allowed to stir under a balloon of O_2. After 72 h, a solution of KCN (13 mg, 0.190 mmol, 10 equiv.) in MeOH was added and the resulting suspension allowed to stir at RT for 1 h. The solvents were removed under reduced pressure and the resulting crude mixture dissolved in CH_2Cl_2 and water. The aqueous layer was extracted with CH_2Cl_2 (×3), washed with brine and dried ($MgSO_4$). Attempts of purification by column chromatography (hexane/ CH_2Cl_2/MeCN 5:4.5:0.5) afforded 7 mg of an impure sample of rotaxane **18** (20% yield) which proved to be highly difficult to isolate free from the accompanying homo-coupled by-product thread.

4.5.3 Spectroscopic Data of Corresponding Non-interlocked Threads

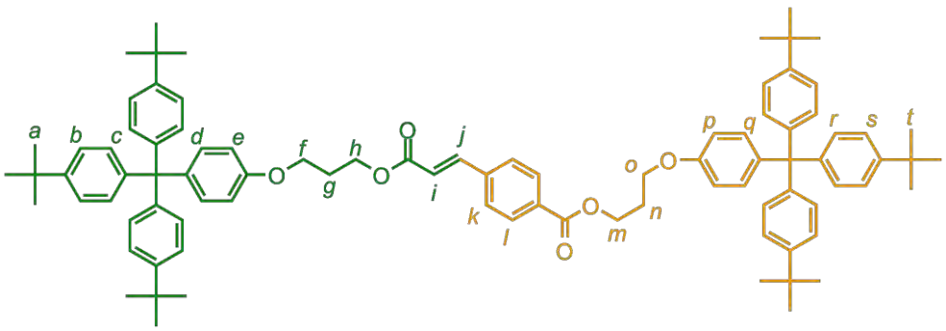

5

M.p. 152-156 °C. ^{1}H NMR (400 MHz, $CDCl_3$, 298 K): δ = 8.03 (d, *J* = 8.4 Hz, 2H, H_i), 7.69 (d, *J* = 16.0 Hz, 1H, H_j), 7.56 (d, *J* = 8.4 Hz, 2H, H_k), 8.53 (d, *J* = 8.5 Hz, 12H, H_b and H_s), 8.56 (d, *J* = 8.5 Hz, 16H, H_c, H_r, H_d, H_q), 6.77 (d, *J* = 8.9 Hz, 4H, H_e and H_p), 6.50 (d, *J* = 16.0 Hz, 1H, H_i), 4.53 (t, *J* = 6.3 Hz, 2H, $H_{h/m}$), 4.42 (t, *J* = 6.2 Hz, 2H, $H_{h/m}$), 4.13-4.06 (m, 4H,

H_o and H_f), 2.28-2.14 (m, 4H, H_g and H_n), 1.30 (s, 54H, H_t). 13C NMR (100 MHz, CDCl3): δ 166.5, 165.9, 156.5 (×2), 148.3 (×2), 144.1 (×2), 143.5, 139.8 (×2), 138.6, 132.3 (×2), 131.5, 130.7 (×2), 130.1, 127.9, 124.0 (×2), 120.4, 112.9 (×2), 64.13, 64.07, 63.0, 62.2, 61.7 (*plus one overlaping peak in this region*), 34.3(×2), 31.4 (×2), 28.8 (×2). LRFAB-MS (3-NOBA matrix): *m/z* = 1281 $[M+H]^+$; HRFAB-MS (THIOG matrix): *m/z* = 1280.7890 $[M]^+$ (calcd. for $C_{90}H_{104}O_6$, 1280.7833).

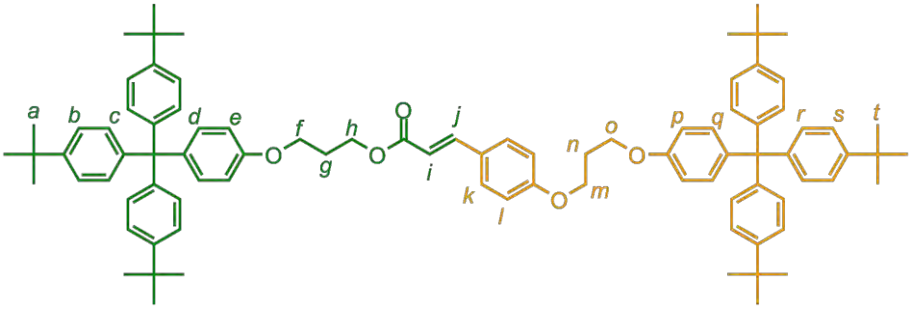

8

^1H NMR (400 MHz, $CDCl_3$, 298 K): δ = 7.63 (d, *J* = 15.9 Hz, 1H, H_j), 7.45 (d, *J* = 8.7 Hz, 2H, H_k), 7.22 (d, *J* = 8.4 Hz, 12H, H_b and H_s), 7.07 (d, *J* = 8.6 Hz, 16H, H_c, H_d, H_q and H_r), 6.89 (d, *J* = 8.7 Hz, 2H, H_l), 6.77 (d, *J* = 8.9 Hz, 4H, H_e and H_p), 6.29 (d, *J* = 15.9 Hz, 1H, H_i), 4.38 (t, *J* = 6.2 Hz, 2H, H_h), 4.18 (t, *J* = 6.1 Hz, 2H, $H_{m/o}$), 4.13 (t, *J* = 6.0 Hz, 2H, $H_{m/o}$), 4.07 (t, *J* = 6.1 Hz, 2H, H_f), 2.26 (tt, *J* = 6.1, 6.1 Hz, 2H, H_n), 2.18 (tt, *J* = 6.2, 6.0 Hz, 2H, H_g), 1.29 (s, 54H, H_a and H_t); ^{13}C NMR (100 MHz, $CDCl_3$, 298 K): δ = 167.2, 160.6, 156.5, 156.5, 148.2, 148.2, 144.5, 144.1, 144.1, 139.7, 139.6, 132.2, 132.2, 130.6 (×2), 129.7, 127.1, 124.0 (×2), 115.4, 114.8, 112.9, 112.8, 64.6, 64.2, 63.9, 63.0 (×2), 61.2, 34.2 (×2), 31.3 (×2), 29.2, 28.8; LRFAB-MS (3-NOBA): m/z = 1253 $[M]^+$. HRFAB-MS (3-NOBA): m/z = 1252.78975 $[M]^+$ (calcd. for $C_{89}H_{104}O_5$, 1252.78837).

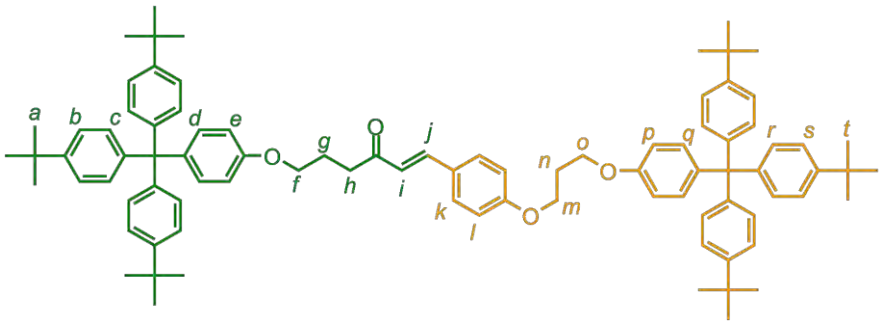

E6

^1H NMR (400 MHz, $CDCl_3$, 298 K): δ = 7.53 (d, *J* = 16.1 Hz, 1H, H_j), 7.47 (d, *J* = 8.8 Hz, 2H, H_k), 7.22 (d, *J* = 8.5 Hz, 12H, H_b and H_s), 7.07 (d, *J* = 8.5 Hz, 16H, H_c, H_d, H_q and H_r), 6.90

(d, J = 8.8 Hz, 2H, H_l), 6.77 (d, J = 8.8 Hz, 4H, H_e and H_p), 6.63 (d, J = 16.1 Hz, 1H, H_i), 4.18 (t, J = 6.0 Hz, 2H, $H_{m/o}$), 4.13 (t, J = 6.0 Hz, 2H, $H_{m/o}$), 4.01 (t, J = 6.0 Hz, 2H, H_f), 2.87 (t, J = 7.1 Hz, 2H, H_h), 2.26 (tt, J = 6.0, 6.0 Hz, 2H, H_n), 2.15 (tt, J = 7.1, 6.0 Hz, H_g), 1.30 (s, 54H, H_a, H_t). ^{13}C NMR (100 MHz, $CDCl_3$, 298 K): δ = 199.9, 161.1, 156.9, 156.8, 148.51, 148.47, 144.4, 144.3, 142.7, 140.0 (×2), 139.8, 132.5 (×2), 130.9 (×2), 130.2, 127.3, 124.3, 124.2, 114.8, 113.1 (×2), 68.0, 64.9, 64.2, 63.2 (×2), 37.1, 34.5 (×2), 31.6 (×2), 29.4, 24.2.

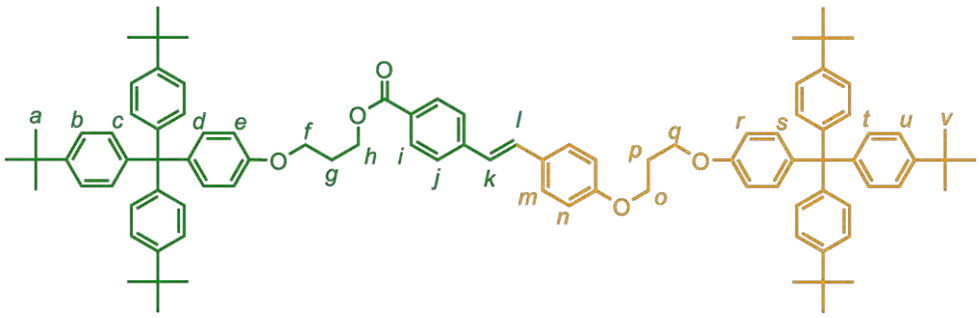

E7

Mixture of isomers: ^{1}H NMR (400 MHz, $CDCl_3$, 298 K): δ = 8.00 (d, J = 8.4 Hz, 2H, H_i), 7.46 (d, J = 8.3 Hz, minor isomer), 7.52 (d, J = 8.5 Hz, 2H, H_j), 7.46 (d, J = 8.7 Hz, 2H, H_m), 7.32 (d, J = 8.3 Hz, minor isomer), 7.17-7.25 (m, 13H, H_b, H_u and H_k), 7.05-7.11 (m, 16H, H_c, H_d, H_s and H_t), 6.98 (d, J = 16.3 Hz, 1H, H_l), 6.91 (d, J = 8.7 Hz, 2H, H_n), 6.72-6.81 (m, 4H, H_e and H_r), 6.55 (dd, J = 12.3, 49.5 Hz, minor isomer), 4.46-4.54 (m, 2H, H_h), 4.06-4.25 (m, 6H, H_f, H_o and H_p), 2.18-2.23 (m, 4H, H_g and H_p), 1.29 (2s, 54H, H_a and H_v). ^{13}C NMR (400 MHz, $CDCl_3$, 298 K): δ = 159.3, 152.0, 149.5 (×2), 141.2 (×2), 137.0, 135.5, 135.2, 132.6 (×2), 125.2, 123.7, 123.6, 123.1, 122.9, 122.5, 121.7, 121.0, 118.9, 118.3, 117.0, 107.7, 107.2, 105.9, 61.1, 57.5, 57.3, 57.2, 57.1, 57.0, 56.0, 54.8, 27.2, 24.3, 22.6, 22.2, 21.8 (×2). LRESI-MS: m/z = 1330.6 $[M+H]^+$.

4.6 References

(1) a) J. Tsuji, *Palladium Reagents and Catalysts: New Perspectives for the 21st Century*, 2nd ed. Wiley, Chichester, **2004**. b) *Metal-Catalyzed Cross-Coupling* Reactions, *Vol. 1*, Completely Revised and Enlarged, 2nd ed. (Eds.: A. de Meijere, F. Diederich), Wiley- VCH, Weinhiem, **2004**,

(2) a) Du, X.; Suguro, M.; Hirabayashi, K.; Mori, A. *Org. Lett.* **2001**, *3*, 3313-3316. b) Parrish, J. P.; Jung, Y. C.; Shin, S. I.; Jung, K. W. *J. Org. Chem.* **2002**, *67*, 7127-7130. c) Jung, Y. C.; Mishra, R. K.; Yoon, C. H.; Jung, K. W. *Org. Lett.* **2003**, *5*, 2231-2234. d) Inoue, A.; Shinokubo, H.; Oshima, K. *J. Am. Chem. Soc.* **2003**, *125*, 1484-1485. e) Andappan, M. M. S.; Nilsson, P.; von Schenck, H.; Larhed, M. *J. Org. Chem.* **2004**, *69*, 5212-5218. f) Andappan, M. M. S.; Nilsson, P.; Larhed, M. *Chem. Commun.* **2004**, 218-219.

g) Enquist, P.-A.; Lindh, J.; Nilsson, P.; Larhed, M. *Green Chem.* **2006**, *8*, 338-343. h) Yoo, K. S.; Yoon, C. H.; Jung, K. W. *J. Am. Chem. Soc.* **2006**, *128*, 16384-16393.

(3) M. D. Hylarides, D. S. Wilbur, S. W. Hadley, A. R. Fritzberg, *Journal of Organometallic Chemistry,* **1989**, *367*, 259-265

(4) a) G. W. Kabalka, R. S. Varma, Y. Z. Gai, R. M. Baldwin, *Tetrahedron Letters*, **1986**, 27(33), 3843-3844. b) A. L. Thompson, G. W. Kabalka, M. R. Akula, J. W. Huffman, *Synthesis*, **2005**, *4*, 547-550.

(5) S. M. Goldup, D. A. Leigh, P. J. Lusby, R. T. McBurney, A. M. Z. Slawin, *Angew. Chem. Int. Ed.* **2008**, *43*, 3381-3384.

(6) H. W. Gibson, S. H. Lee, P. T. Engen, P. Lecavalier, J. Sze, J. Shen, ;.Bheda, M. *J. Org. Chem.* **1993**, *58*, 3748-3756.

(7) J. Berná, J. D. Crowley, S. M. Goldup, K. D. Hänni, A.-L. Lee, D. A. Leigh, *Angew. Chem. Int. Ed.* **2007**, *46*, 5709-5713.

Chapter V

[2]Rotaxanes through Diels-Alder Active-Metal Template Strategy Mediated by Lewis Acids

Manuscript in preparation *[2]Rotaxanes through Diels-Alder Active-metal Template Strategy Mediated by Lewis-acids*, J. D. Crowley, K. D. Hänni, D. A. Leigh, A.M. Z. Slawin.

Acknowledgments

The following people are gratefully acknowledged for their contribution to this Chapter: Dr. James Crowley synthesised compound **E4** and provided useful advice and guidance. Prof. Alexandra Slawin solved the solid structures of complexes Zn**1a**-**c**Cl_2 and Cu**1a**Cl_2 shown in Figure 5.1.

5.1 Synopsis

The concept of the AMT has been extended to the well-known Diels-Alder (DA) cycloaddition. A synthetic approach to [2]rotaxanes is described in which Lewis acids (LAs) triflates such as Zn(II) and Cu(II) are able to catalyse a Diels-Alder (DA) cycloaddition while simultaneously acting as the template for the assembly of MIAs. Coordination of the LA to an endotopic pyridine-containing macrocycle allows the orientated chelation of the dienophile. The obtained LA-activated double bond can react with an incoming stoppered diene through the cavity of the macrocycle to afford [2]rotaxanes. A more complex two-station molecular shuttle was also prepared utilising this DA-AMT methodology. The translocation dynamics of the macrocycle could be controlled by coordination to different metal ions such as Zn(II) and Pd(II). This strategy is an affordable, high-yielding and effective synthetic route toward interlocked architectures.

5.2 Introduction

Since its discovery by Otto Diels and Kurt Alder in the early twentieth century,[1] there has been an explosive growth in the number of applications of the Diels-Alder (DA) reaction. Its ability to produce C-C, C-N, and C-O bonds makes it an essential tool for the design and the synthesis of new complex organic molecules (heterocycles, norbornene).[2] It has even proved possible to use it to control the motion in molecular machines[3] by utilising steric control to induce the shuttling of the macrocycle between two stations.[4] Lewis acids are involved in catalytic systems of many organic reactions and in particular in Diels-Alder cycloadditions.[5] As early as 1942, Wasserman had introduced Brönsted acids as catalysts for DA reactions,[6] but it was not until 1960 – twenty years later – with the work of Yate and Eaton[7] that the use of Lewis acids began, contributing to the development of diene catalytic reactions and their asymmetric versions.

For example, the reaction between isoprene and methyl vinyl ketone (Scheme 5.1a) [8] in a sealed tube at 120 °C (toluene), gives moderate yields (54%) with a poor *1,4*:*1,3* regioselectivity (*1,4*:*1,3* = 71:29). In the presence of Tin(IV) chloride as catalyst, however, the reaction goes smoothly at 0 °C, giving improved yields (71 %) with a high regioselectivity of *1,4*:*1,3* = 93:7. Similarly, the uncatalysed reaction between cyclopentadiene and methyl acrylate (Scheme 5.1b) at 0 °C (CH_2Cl_2) produces low yields (51%) with a moderate endo:exo enantioselectivity (endo:exo = 82:18). The presence of Tin chloride, however, affords improved yields (67-79%) with a high enantioselectivity of endo:exo = 95:5.

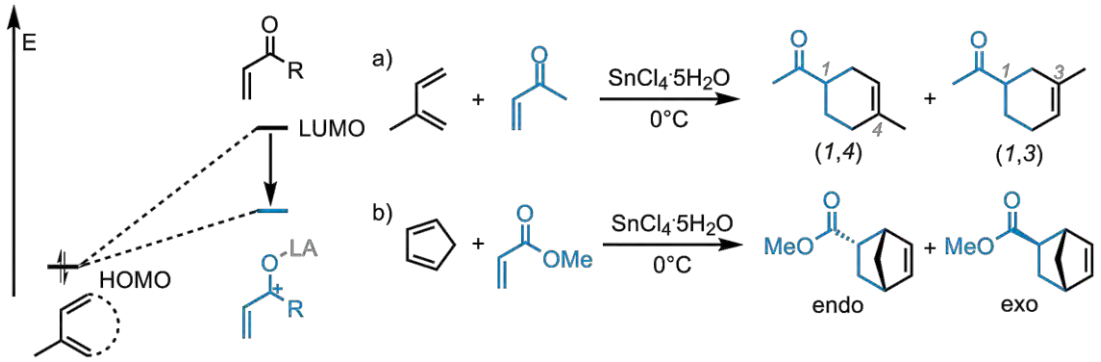

Scheme 5.1 Lowering of the dienophile LUMOs by the complexation with a Lewis acid.

The complexation of a dienophile to a Lewis acid results in an acceleration of the reaction rate by six orders of magnitude, increases the efficiency and improves the regio- (1,3/1,4) and the enantio- (endo/exo) selectivity. Pyridine ligands such as

pyridine-2,6-*bis*oxazoline (pybox),[9d-e] bipyridyl[10]or *bis*oxazolines (box)[9] have shown their efficiency to catalyse enantioselective Lewis acid promoted cycloaddition reactions. Diels-Alder cycloadducts can also be obtained in excellent yields using a wide range of Lewis acids – most often transition metal salts.[11] α,β-Unsaturated-2-acyl-oxazolidinones, imidazolidones or pyrazolidinones[12] are very convenient substrates on which to carry out these reactions: they provide an organised chelation around the metal centre allowing the LA-activated double bond to react with a selected diene.

5.3 Results and Discussion

Inspired by previous studies,[13] we postulated that the introduction of zinc chloride into well-defined macrocycles would lead to a trigonal bipyramidal configuration allowing the two chloride ligands to be located on opposite sides of the macrocycle (Scheme 5.2, top right). We reasoned that if an acroyl-imidazolidone half-thread could chelate to the metal centre inside the cavity of the macrocycle, it would generate an orientated complex of type **II** (Scheme 5.2) exposing the activated double bond to an incoming stoppered diene. Cycloaddition through the cavity would provide a [2]rotaxane.

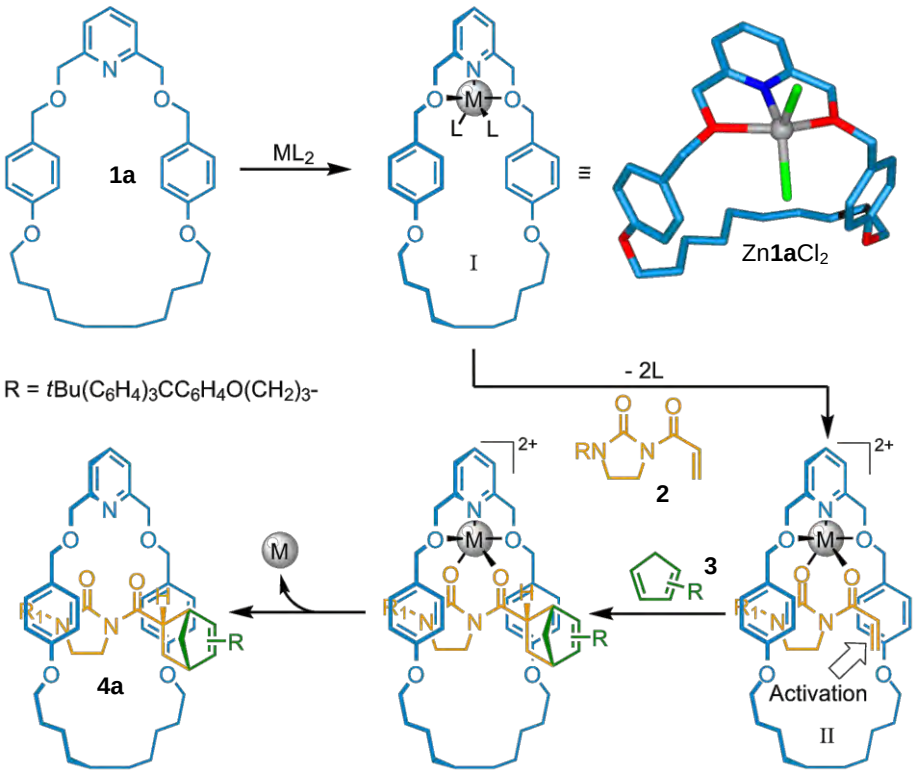

Scheme 5.2 Initial idea of using $ZnCl_2$-catalysed DA cycloaddition. Chloride ligands are in trans configuration in the X-Ray crystal structure.

Our initial attempts to produce rotaxane with $ZnCl_2$-complexes (Figure 5.1, a-c) were unsuccessful (Table 5.1, entry 1), probably owing to the fact that the two chloride ligands are too strongly coordinated to the metal. Non-coordinating ligands such as triflate were then preferred for our further investigations. Complex **I** is formed in situ by mixing macrocycle **1a** (1 equiv) with zinc triflate (1 equiv.) in CH_2Cl_2. Addition of acroyl-imidazolidone half-thread **2** (1 equiv.) at room temperature and cyclopentadiene half-thread **3** (1 equiv) at -78 °C, followed by stirring at that temperature for 20 h and at room temperature for 4 h, afforded the rotaxane **4a** in 8% yield (Table 5.1, entry 2). Changing the Lewis acid from zinc to copper triflate increased the yield of [2]rotaxane **4a** to 47 % (Table 5.1, entry 3). Increasing the equivalents of **2** and **3** and extending the reaction time to 96 h (48 h at -78 °C then 48 h at room temperature) improved the yield of rotaxane **4a** up to 83% (Table 5.1, entry 5).

*Table 5.1 Effect of reactant stoichiometry and experimental conditions on the DA Active-Metal template synthesis of the rotaxane **4a**.*[a]

Entry	LA	Amt. of **2** [equiv.]	Amt. of **3** [equiv.]	Time	Yield of rot. **1a→4a** [%][d]
1[b]	$ZnCl_2$	1	1	24 h	0%
2[b]	$Zn(OTf)_2$	1	1	24 h	8%
3[b]	$Cu(OTf)_2$	1	1	24 h	47%
4[c]	$Zn(OTf)_2$	1.2	2	72 d	43%
5[c]	$Cu(OTf)_2$	1.2	2	72 d	83%

*[a]All Reactions were carried out using anhydrous solvents under a nitrogen atmosphere, 9 mM. [b]Reaction mixture was stirred at -78 °C for 20 h and then allowed to stir at room temperature for 4 h. [c]Reaction mixture was stirred at -78 °C for 48 h, then allowed to stir at room temperature for 48 h. [d]With respect of **1a**.*

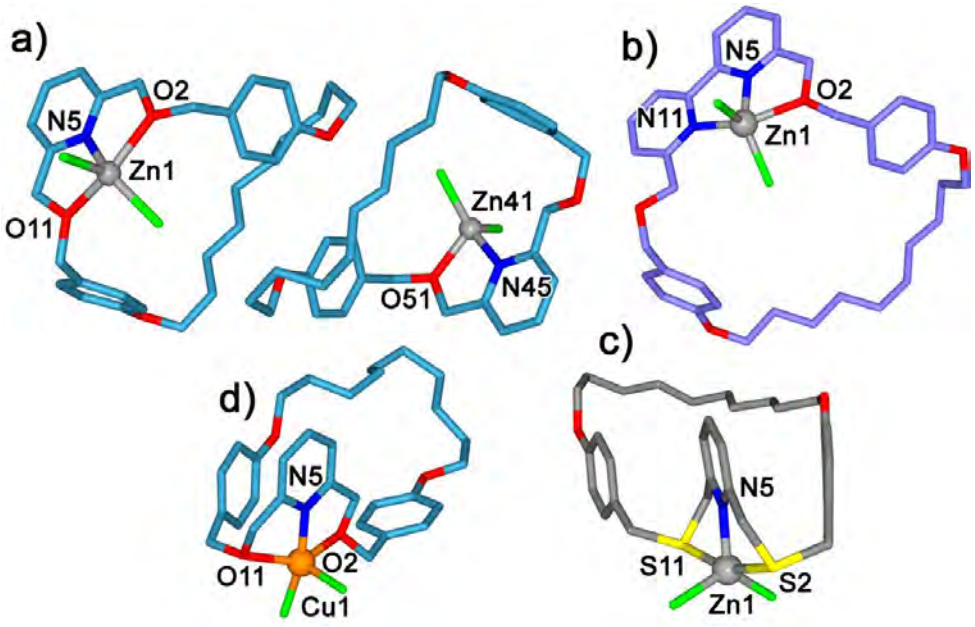

*Figure 5.1 X-ray crystal structure of complexes a) Zn**1a**Cl_2, please note the two Zn environments (trigonal bipyramidal and tetrahedral), b) Zn**1b**Cl_2, c) Zn**1c**Cl_2 and d) Cu**1a**Cl_2.*

The proposed mechanism of rotaxane formation is shown in Scheme 1. Replacement of the two labile ligands by the two oxygen atoms of the acroyl-imidazolidone half-thread **2** affords the activated, orientated complex of type **II** in which the double bond could react with the corresponding cyclopentadiene half-thread **3** (the 2-substitued isomer only). Demetallation by treatment with ammonia (or EDTA) liberates the metal-free rotaxane **4a**. Using a substoichiometric amount of copper triflate (30 mol%) yielded the [2]rotaxane **4a** in 37%, suggesting that the rotaxane is sequestering the metal after its formation.

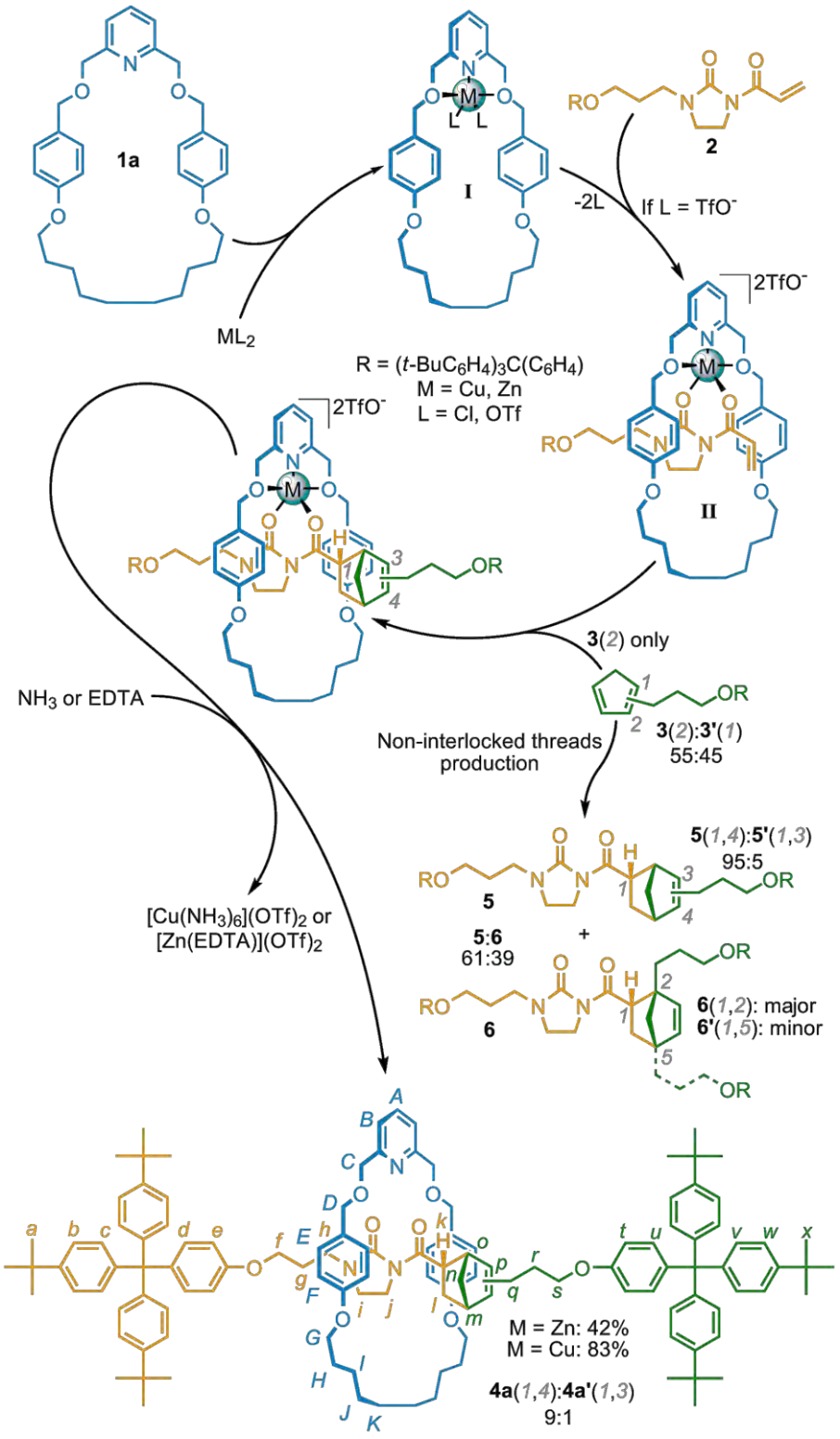

*Scheme 5.3 Proposed mechanism for the DA Active-Metal Template Synthesis of [2]Rotaxane **4a** from **1a**, **2** and **3**.*

The energy barrier of the [1,5]-sigmatropic shift of a monosubstitued cyclopentadiene such as 1-methyl cyclopentadiene (1-MCP) into 2-methyl cyclopentadiene (2-MCP) is known to be 28 kcal·mol^{-1} and the equilibrium ratio between 1-MCP and 2-MCP was determined to be 39:61 at 298 K and 1 atm.[14] Under the stated conditions, half-thread **3** was obtained as a mixture of 1- (**3′**) and 2-substituted (**3**) cyclopentadiene stoppered unit in a 55:45 ratio determined by ^{1}H NMR spectroscopy. Interestingly, when subjected to the DA-AMT rotaxane-formation conditions, only the 2-substitued isomer **3** was able to react with the activated double bond through the cavity of the macrocycle to afford rotaxanes **4a** and **4a′** as a mixture of two endo-adducts.* 1,4-Disubstitued rotaxane **4a** is favoured over its 1,3-disubstitued isomer **4a′** in a ratio of 9:1, most likely because **4a** is the product in which the two bulky 'stoppered' groups are farthest apart.

In contrast, when the reaction does not occur inside the cavity of the macrocycle, cyclopentadiene half-threads can create four distinct endo-adducts.* Non-interlocked threads **5** and **6**, respectively from **3** and **3′**, were produced in a 61:39 ratio, where the ratio of 1,3- (**5′**) over 1,4-disubstitued (**5**) thread was determined to be 95:5. As **6** and **6′** are indistinguishable by ^{1}H NMR and seemed to be impossible to separate by column chromatography, we were unable to determine the **6**:**6′** ratio. Knowing that only **3** reacts to form rotaxane (not **3′**), the modest yield of entry 3 Table 5.1, can be explained by the presence of only 0.55 equivalent of **3** during the process. The recalculated yield was determined to be 85% which is in accordance with the result of entry 5. In the absence of macrocycle, we observed a lack of selectivity for the production of non-interlocked threads (mixture of regio- and chemo-isomers **5** and **6**), suggesting that only the 2-substitued cyclopentadiene isomer (**3**) is able to form DA-adducts through the macrocycle cavity.

5.3.1 ^{1}H NMR of the Interlocked Product

The ^{1}H NMR spectrum of **4a** in $CDCl_3$ at 328 K (Figure 5.2, a) shows an upfield shift of several signals with respect to the non-interlocked components (Figure 5.2, a and c). The shielding, typical of interlocked architectures in which the aromatic rings of one component are positioned face-on to another component, occurs for all aliphatic non-stopper resonances of the axle ($H_{f\text{-}h}$, $H_{q\text{-}s}$ and $H_{i\text{-}j}$) indicating that the macrocycle is more likely to explore the non-hindered parts of the thread, avoiding the bulky norborene unit. This is probably owing to both high steric hindrance of the norbornene unit and

* The two exo adducts are probably also synthesised as minor side products.

electron repulsion between the lone pairs of both the *α*-carbonyl-imidazolidone unit and the macrocycle.

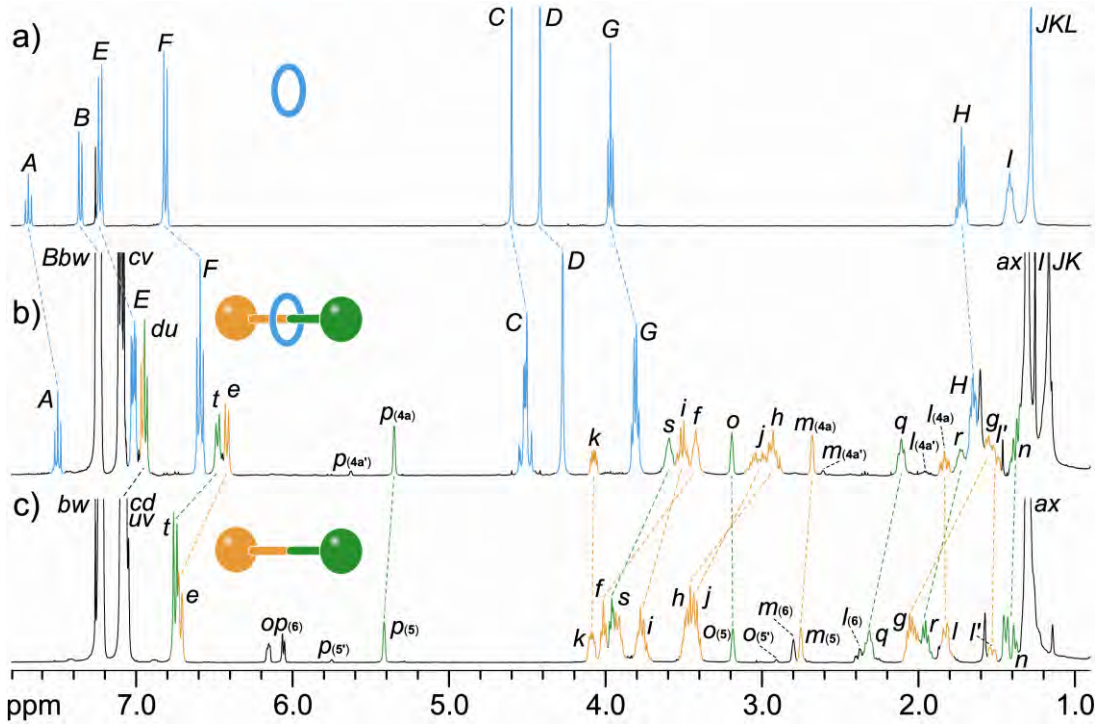

*Figure 5.2 ^{1}H NMR spectra (400 MHz, $CDCl_3$, 328 K) of a) macrocycle **1a**, b) [2]rotaxanes **4a**:**4a'** 9:1, c) thread **5** and **6** 61:39. The assignments correspond to the lettering shown in Scheme 5.3.*

5.3.2 Influence of the Macrocyclic Ligand on the DA-AMT Rotaxane Formation Reaction

To explore the influence of the nature of the macrocyclic ligand on the AMT cycloaddition reaction, we employed four different macrocycles shown in Figure 5.3. Pleasingly, reaction of **1b** under the same conditions resulted in the formation of the corresponding [2]rotaxane **4b** in 91% yield with a higher 1,4-/1,3-disubstitued ratio of 99:1. Substitution of the benzylic ether oxygen atoms of **1a** by strong coordinating atoms such as sulfur (**1c**) switches off the rotaxane formation, this is probably owing to the ability of sulfur atoms to lower the Lewis acidity of the metal centre and subsequently deactivate the formation of rotaxane. Similar results (i.e. no rotaxane formation) are observed when benzylic oxygen atoms are replaced by methylene groups (**1d**) or when the pyridine nitrogen atom is removed as in benzene analogue macrocycle **1e**, confirming the need of both nitrogen and ligating donor atoms such as oxygen for the coordination of the metal centre inside the macrocycle cavity.

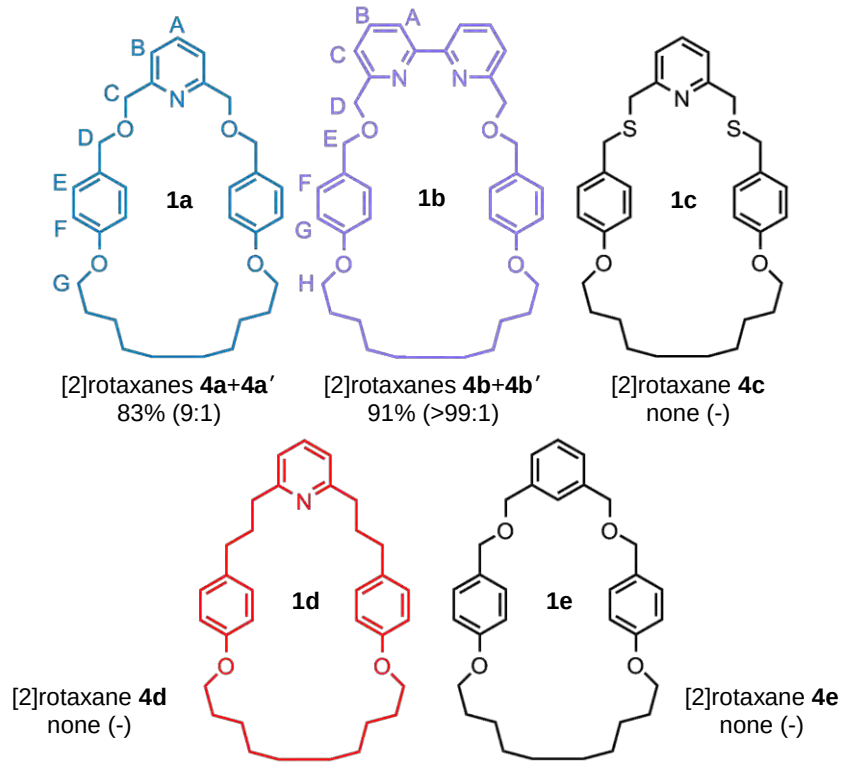

*Figure 5.3 Influence of the macrocyclic ligand on the DA AMT rotaxane-forming reaction. The ratio between **4** (1,4-) and **4′** (1,3-) is shown in parentheses.*

5.3.3 Transition Metal-mediated Control of the Shuttling in Two-Station Molecular Shuttle

To demonstrate the utility of this new active-metal template reaction, the metal-switchable molecular shuttle **8a** was prepared in 42% yield (ratio 1,4-/1,3-disubstitued 95:5) from a pyridine-containing dienophile building block (see Experimental section) and **3**. The pyridine and the α-carbonyl-imidazolidone functionalities could be then used as recognition sites for the shuttling of a metallated macrocycle as shown in Scheme 5.4.

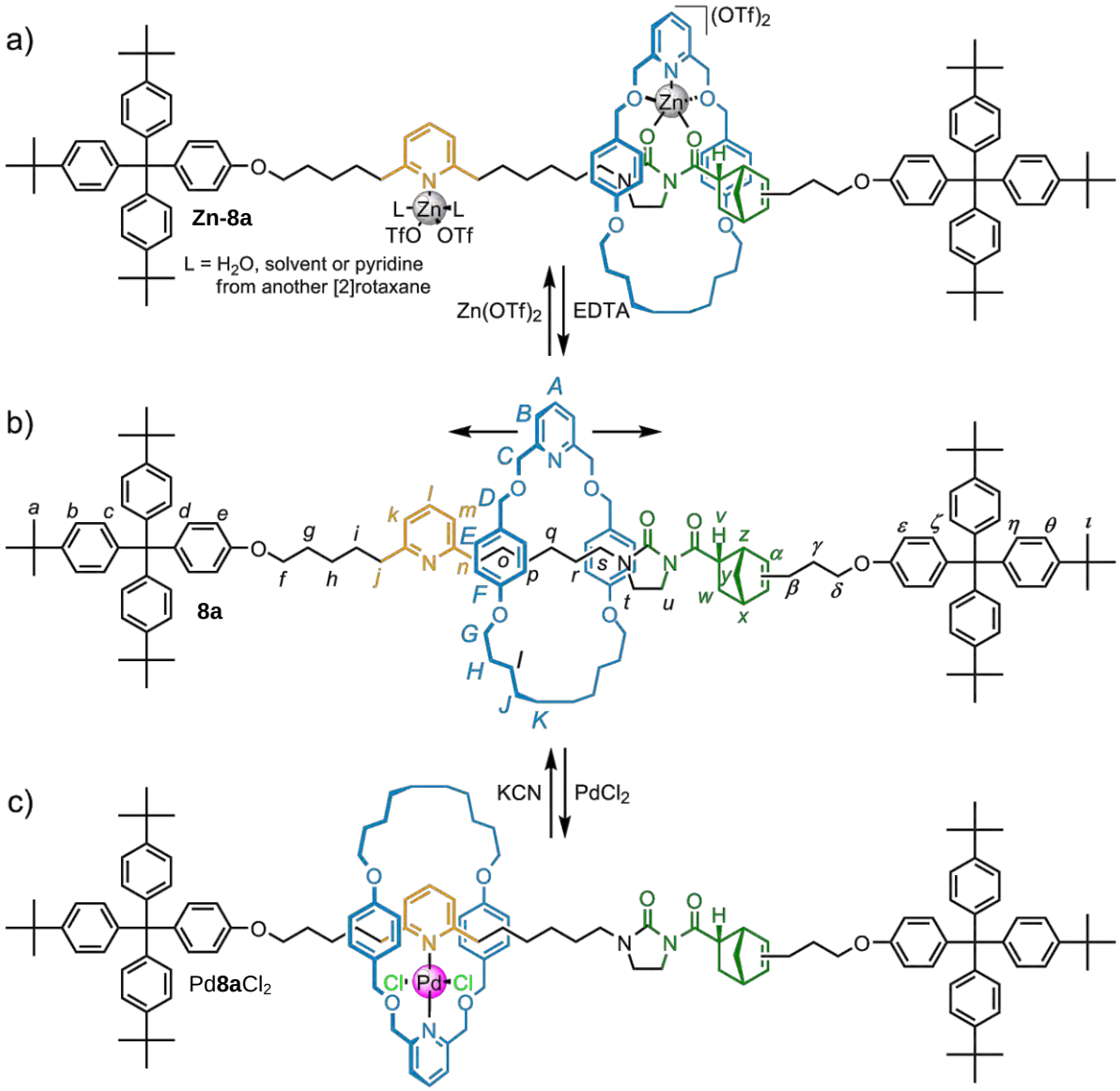

*Scheme 5.4 Controlling the dynamics of DA-Shuttle: a) coordination to Zn(II): [**8a**Zn](OTf)₂, b) metal-free rotaxane **8a** and c) coordination to Pd(II): [**8a**Pd]Cl₂.*

As with **4a**, the ^{1}H NMR spectrum of **8a** (CD_2Cl_2/CD_3CN 9:1 – Figure 5.4, b) shows an upfield shift of the aliphatic and pyridine signals with respect to the non-interlocked thread ($H_{f\text{-}h}$, $H_{\beta\text{-}\delta}$ and $H_{k\text{-}m}$ respectively – Figure 5.4, a), indicating that the macrocycle is more likely to explore the less-hindered parts of the thread, avoiding the bulky norbonene unit. The ^{1}H NMR spectrum of **8a** with only one equivalent of $Zn(OTf)_2$ (CD_2Cl_2/CD_3CN 9:1, 298 K) shows a very complicated pattern, suggesting that dynamics of both the metal (coordinated vs. in solution) and of the Zn-macrocycle unit (shuttling between the two stations) could be considered. Saturating all the binding sites by adding four more equivalents of $Zn(OTf)_2$ (5 equiv. in total) greatly simplifies the spectrum, however, and shows both significant upfield shifts of the *α*-carbonyl-

imidazolidone moiety (H_α, H_v, H_u, and H_z) and downfield shifts of the pyridine station ($H_{j\text{-}n}$). These observations suggest that more than one zinc ion is necessary to lock the macrocycle on the *α*-carbonyl-imidazolidone station: by coordination, one Zn centre is blocking the pyridine station while another metal is keeping the macrocycle sitting preferentially on the other station (Figure 5.4, c). Demetallation with EDTA (RT, 1 hour) returns the system to the metal-free rotaxane **8a**. In contrast, the ^{1}H NMR spectrum of complex Pd**8a**Cl_2 (Figure 5.4, d) displays two sets of peaks, for the pyridine protons (H_k and H_m) and those adjacent to the station (H_j and H_n), which are consistent with the chemical shifts of the switchable palladium-complexed molecular shuttle previously reported,[15] while signals of the *α*-carbonyl-imidazolidone moiety show similar shifts to the non-interlocked thread. Demetallation with KCN (MeOH/CH_2Cl_2 1:1, RT, 1 hour) returns **8a**.

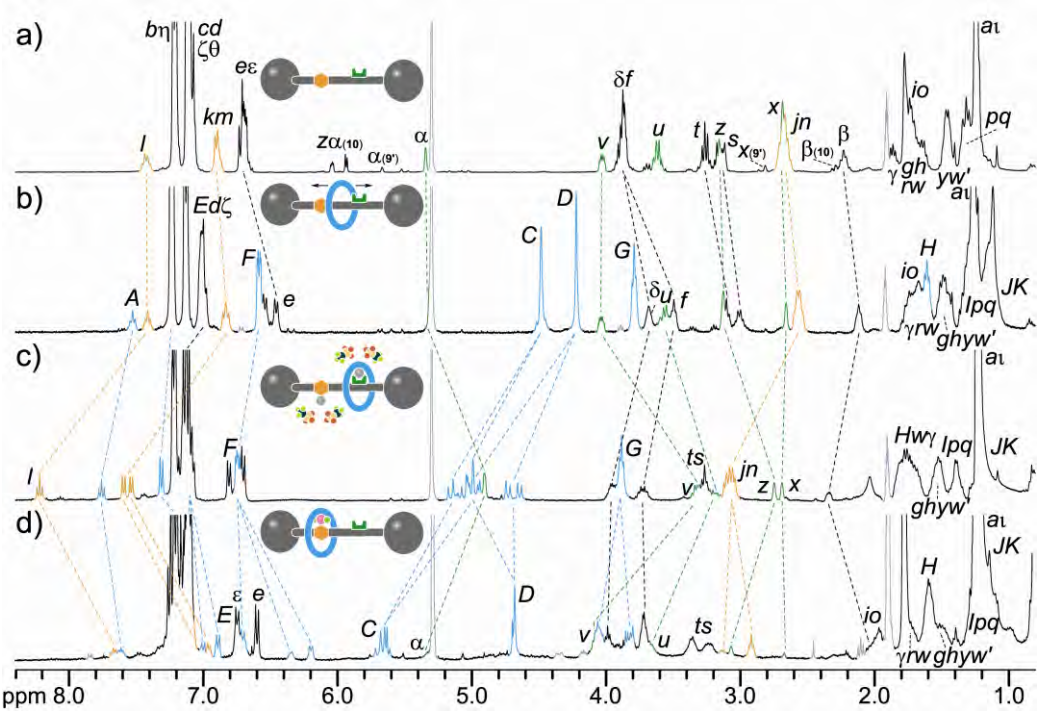

*Figure 5.4 ^{1}H NMR spectra (400 MHz, 298 K, CD_2Cl_2/CD_3CN 9:1) of a) threads **9** and **10** 68:32, b) [2]rotaxane **8a**:**8a'** 95:5, c) complex [**8a**Zn](OTf)$_2$ and d) complex [**8a**Pd]Cl_2. The assignments correspond to the lettering shown in Scheme 5.4.*

5.4 Conclusion

The development of the Diels-Alder Active-Metal template strategy has allowed us to use one of the most powerful recognised synthetic sequences in organic synthesis. It can produce affordable, high-yielding and effective synthetic routes towards [2]rotaxanes and molecular shuttles.

5.5 *Experimental Section*

5.5.1 General Procedure for the Preparation of Metal-complexes

Syntheses of macrocycle **1a**, **1b**, **1c**, **1d** and **1e** are described in previous chapters (Chapter II for **1a**, **1c** and **1e** – chapter III for **1b** and **1c**).

A solution of metal chloride (0.02 mmol, 1 equiv.) in MeOH (0.5 mL) was added dropwise to a solution of macrocycle (0.02 mmol, 1 equiv.) in acetone (0.5 mL) with stirring. The solution was slowly diluted with toluene (1 mL) and was allowed to evaporate slowly to afford metal-macrocycle complexes.

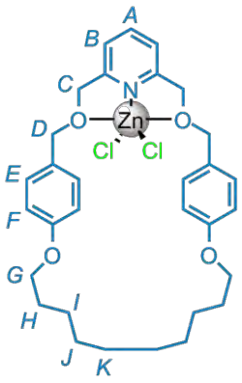

Zn**1a**Cl_2

Following the general procedure with $ZnCl_2$ (2.8 mg, 0.02 mmol, 1 equiv.), macrocycle **1a** (10.0 mg, 0.02 mmol, 1 equiv.) afforded complex Zn**1a**Cl_2 as colourless X-ray-quality crystals. ^{1}H-NMR (400 MHz, $CDCl_3$, 298 K): δ = 7.99 (t, *J* = 7.9 Hz, 1H, H_A), 7.41 (d, *J* = 8.6 Hz, 4H, H_E), 7.31 (d, *J* = 7.9 H, 2H, H_B), 6.86 (d, *J* = 8.7 Hz, 4H, H_F), 5.07 (s, 4H, H_C), 4.88 (s, 4H, H_D), 3.96 (t, *J* = 6.6 Hz, 4H, H_G), 2.90 (s, 2H, H_2O), 1.79 (dt, *J* = 6.8 Hz, 6.8 Hz, 4H, H_H), 1.43-1.54 (m, 4H, H_I), 1.33-1.43 (m, 8H, H_J and H_K). ^{13}C NMR (100 MHz, $CDCl_3$, 298 K) δ = 159.4, 154.4, 153.2, 140.3, 131.9, 126.2, 120.7, 114.5, 73.3, 67.7, 65.9, 28.8, 28.2, 25.4. LRESI-MS: m/z = 553.2 $[M-2Cl]^+$

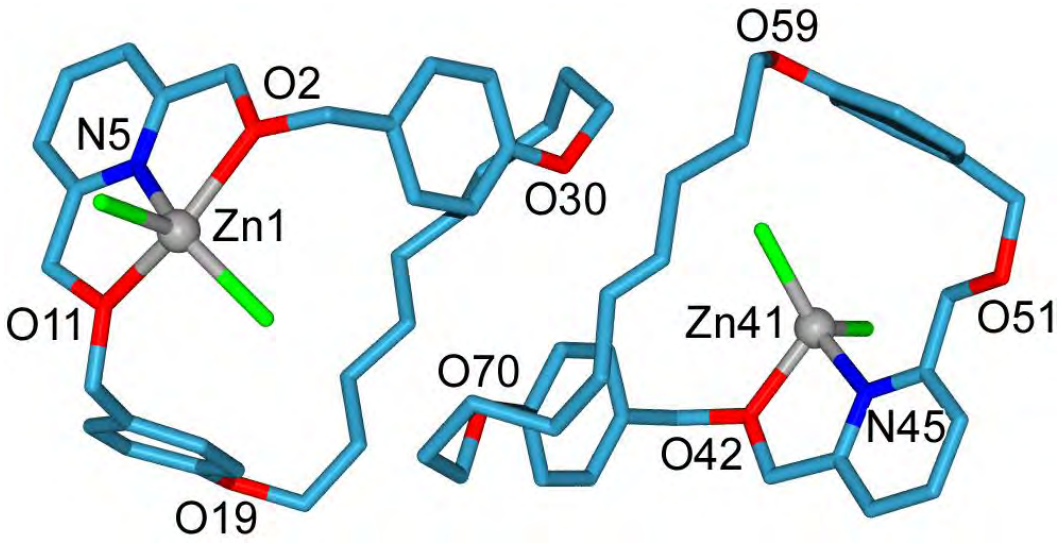

Table 5.2 Crystal data and structure refinement for $Zn1aCl_2$

Empirical formula	$C_{31}H_{39}Cl_2NO_4Zn$	
Formula weight	625.90	
Temperature	93(2) K	
Wavelength	0.71073 Å	
Crystal system	Triclinic	
Space group	P-1	
Unit cell dimensions	a = 13.0715(9) Å	α = 70.911(4)°
	b = 15.7296(10) Å	β = 75.535(4)°
	c = 15.7800(9) Å	γ = 81.991(5)°
Volume	2963.0(3) $Å^3$	
Z	4	
Density (calculated)	1.403 Mg/m^3	
Absorption coefficient	1.046 mm^{-1}	
F(000)	1312	
Crystal size	0.1000 x 0.0300 x 0.0300 mm^3	
Theta range for data collection	1.40 to 25.34°.	
Index ranges	-12<=h<=15, -18<=k<=13, -18<=l<=18	
Reflections collected	19564	
Independent reflections	10213 [R(int) = 0.0312]	
Completeness to theta = 25.00°	95.0 %	
Absorption correction	Multiscan	
Max. and min. transmission	1.0000 and 0.8661	
Refinement method	Full-matrix least-squares on F^2	

Data / restraints / parameters	10213 / 0 / 704
Goodness-of-fit on F^2	1.019
Final R indices [I>2sigma(I)]	R1 = 0.0439, wR2 = 0.0938
R indices (all data)	R1 = 0.0576, wR2 = 0.1025
Largest diff. peak and hole	1.435 and -1.410 e.Å^{-3}

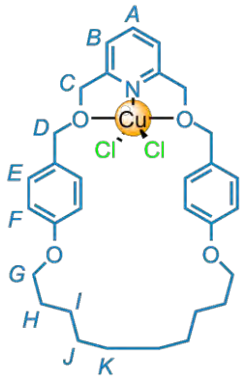

Cu**1a**Cl_2

Following the general procedure with $CuCl_2$ (2.8 mg, 0.02 mmol, 1 equiv.), macrocycle **1a** (10.0 mg, 0.02 mmol, 1 equiv.) afforded complex [**1a**Cu]Cl_2 as deep red X-ray-quality crystals.

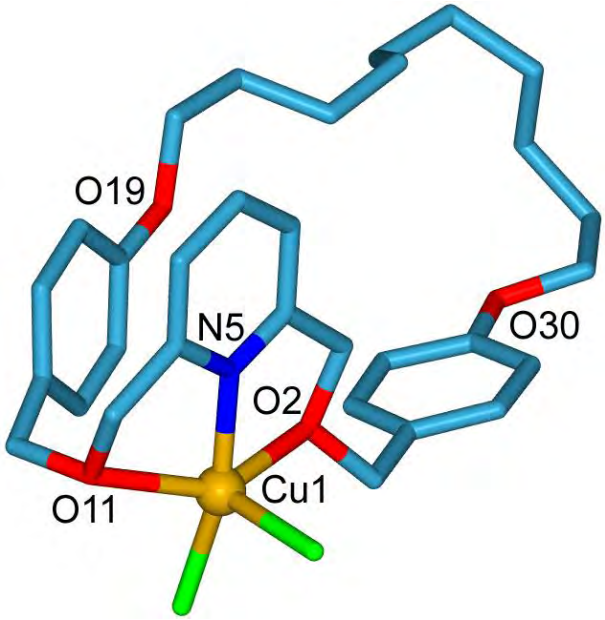

Table 5.3 Crystal data and structure refinement for Cu1aCl_2

Empirical formula	$C_{31}H_{39}Cl_2CuNO_4$
Formula weight	624.07
Temperature	93(2) K

Wavelength	0.71073 Å	
Crystal system	Monoclinic	
Space group	P2(1)/c	
Unit cell dimensions	a = 17.5116(11) Å	α = 90°.
	b = 8.6269(5) Å	β = 104.229(3)°.
	c = 21.0769(14) Å	γ = 90°.
Volume	3086.4(3) $Å^3$	
Z	4	
Density (calculated)	1.343 Mg/m^3	
Absorption coefficient	0.916 mm^{-1}	
F(000)	1308	
Crystal size	0.100 x 0.080 x 0.050 mm^3	
Theta range for data collection	2.40 to 25.35°.	
Index ranges	-21<=h<=21, -10<=k<=10, -24<=l<=25	
Reflections collected	28924	
Independent reflections	5627 [R(int) = 0.0466]	
Completeness to theta = 25.00°	99.3 %	
Absorption correction	Multiscan	
Max. and min. transmission	1.0000 and 0.9521	
Refinement method	Full-matrix least-squares on F^2	
Data / restraints / parameters	5627 / 0 / 353	
Goodness-of-fit on F^2	1.229	
Final R indices [I>2sigma(I)]	R1 = 0.0470, wR2 = 0.1098	
R indices (all data)	R1 = 0.0490, wR2 = 0.1108	
Largest diff. peak and hole	0.518 and -0.270 e. $Å^{-3}$	

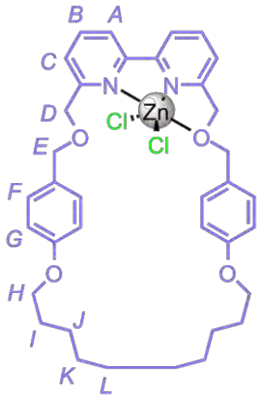

Zn**1b**Cl_2

Following the general procedure with $ZnCl_2$ (2.8 mg, 0.02 mmol, 1 equiv.), macrocycle **1b** (11.3 mg, 0.02 mmol, 1 equiv.) afforded complex Zn**2c**Cl_2 as colourless X-ray-quality crystals. ^{1}H NMR (400 MHz, $CDCl_3$, 298 K): δ = 7.96-8.04 (m, 4H, H_A and H_B), 7.68 (dd, *J* = 3.0 Hz, 5.7 Hz, 2H, H_B), 7.41 (d, *J* = 8.6 Hz, 4H, H_F), 6.85 (d, *J* = 8.6 Hz, 4H, H_G), 4.97 (s, 4H, H_D), 4.79 (s, 4H, H_E), 3.97 (t, J = 7.0 Hz, 4H, H_H), 1.72 (dt, *J* = 7.0 Hz, 7.0 Hz, 4H, H_I), 1.32-1.41 (m, 4H, H_J), 1.20-1.32 (m, 8H, H_K and H_L). ^{13}C NMR (100 MHz, $CDCl_3$, 298 K): δ = 159.9, 158.9, 148.3, 140.8, 130.5, 128.1, 123.8, 119.7, 114.8, 72.9, 68.1, 67.9, 29.2, 28.7, 28.4, 25.5.

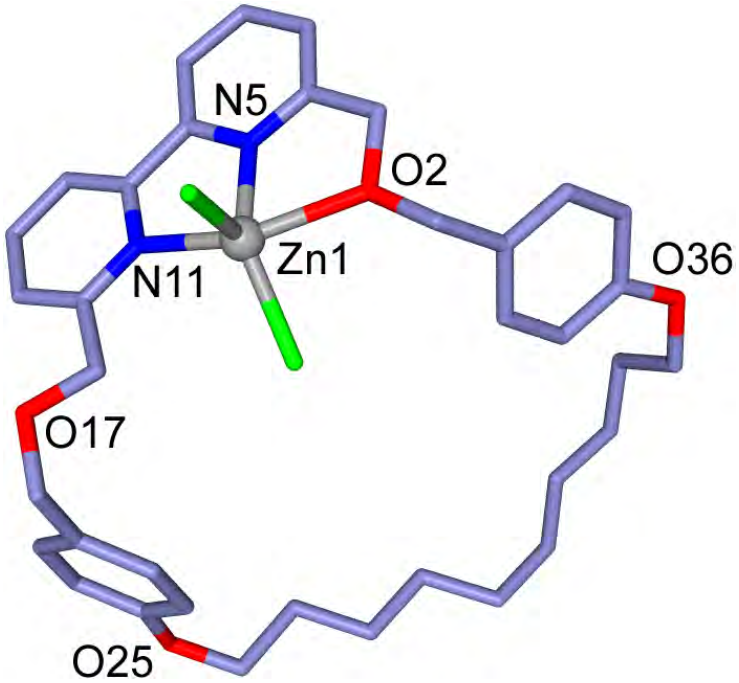

Table 5.4 Crystal data and structure refinement for Zn1cCl$_2$

Empirical formula	$C_{37.50}H_{46}Cl_2N_2O_5Zn$	
Formula weight	741.03	
Temperature	93(2) K	
Wavelength	0.71073 Å	
Crystal system	Monoclinic	
Space group	P2(1)/c	
Unit cell dimensions	a = 18.1258(18) Å	α = 90°.
	b = 15.0266(14) Å	β = 105.704(6)°.
	c = 14.6076(15) Å	γ = 90°.
Volume	3830.1(7) Å^3	
Z	4	

Density (calculated)	1.285 Mg/m^3
Absorption coefficient	0.823 mm^{-1}
F(000)	1556
Crystal size	0.150 x 0.100 x 0.030 mm^3
Theta range for data collection	1.79 to 25.35°.
Index ranges	-21<=h<=21, -18<=k<=18, -16<=l<=17
Reflections collected	32849
Independent reflections	6858 [R(int) = 0.1154]
Completeness to theta = 25.00°	98.2 %
Absorption correction	Multiscan
Max. and min. transmission	1.0000 and 0.8488
Refinement method	Full-matrix least-squares on F^2
Data / restraints / parameters	6858 / 29 / 452
Goodness-of-fit on F^2	1.167
Final R indices [I>2sigma(I)]	R1 = 0.0880, wR2 = 0.1971
R indices (all data)	R1 = 0.0978, wR2 = 0.2039
Largest diff. peak and hole	1.830 and -0.708 $e.Å^{-3}$

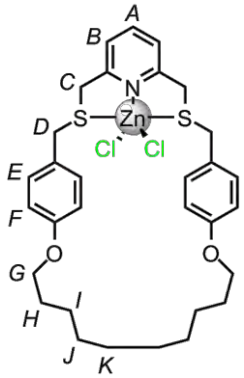

Zn**1b**Cl_2

Following the general procedure with $ZnCl_2$ (2.8 mg, 0.02 mmol, 1 equiv.), macrocycle **1c** (10.0 mg, 0.02 mmol, 1 equiv.) afforded complex Zn**1b**Cl_2 as colourless X-ray-quality crystals. ^{1}H NMR (400 MHz, $CDCl_3$, 298 K): δ = 7.32 (t, *J* = 7.7 Hz, 1H, H_A), 6.99 (d, *J* = 8.5 Hz, 2H, H_E), 6.62 (d, *J* = 7.7 Hz, 2H, H_B), 6.51 (d, *J* = 8.6 Hz, 4H, H_F), 3.38 (t, *J* = 6.1 Hz, 4H, H_G), 3.68 (s, 4H, H_C), 3.77 (s, 4H, H_D), 1.69 (dt, *J* = 6.5 HZ, 6.5 Hz, 4H, H_H), 1.36-1.45 (m, 4H, H_I), 1.21-1.34 (m, 8H, H_J and H_K). ^{13}C NMR (100 MHz, $CDCl_3$, 298 K): δ = 163.0, 158.2, 139.1, 130.9, 123.2, 114.3, 67.2, 35.7, 35.6, 29.7, 29.3, 28.7, 28.5, 25.5.

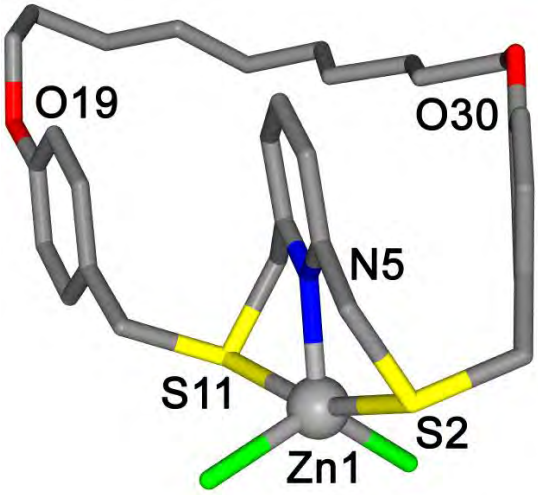

Table 5.5 Crystal data and structure refinement for Zn1cCl₂

Empirical formula	$C_{31}H_{39}Cl_2NO_2S_2Zn$
Formula weight	658.02
Temperature	93(2) K
Wavelength	0.71073 Å
Crystal system	Orthorhombic
Space group	Pbca
Unit cell dimensions	a = 26.267(9) Å α = 90°.
	b = 9.004(3) Å β = 90°.
	c = 26.253(9) Å γ = 90°.
Volume	6209(4) $Å^3$
Z	8
Density (calculated)	1.408 Mg/m^3
Absorption coefficient	1.127 mm^{-1}
F(000)	2752
Crystal size	0.1000 x 0.0300 x 0.0300 mm^3
Theta range for data collection	1.73 to 25.34°.
Index ranges	-29<=h<=31, -10<=k<=10, -31<=l<=27
Reflections collected	37530
Independent reflections	5649 [R(int) = 0.1853]
Completeness to theta = 25.00°	99.5 %
Absorption correction	Multiscan
Max. and min. transmission	1.0000 and 0.8493
Refinement method	Full-matrix least-squares on F^2

Data / restraints / parameters	5649 / 0 / 353
Goodness-of-fit on F^2	1.107
Final R indices [I>2sigma(I)]	R1 = 0.1293, wR2 = 0.3075
R indices (all data)	R1 = 0.1616, wR2 = 0.3398
Largest diff. peak and hole	4.254 and -0.896 e.Å^{-3}

5.5.2 Preparation of Half-threads

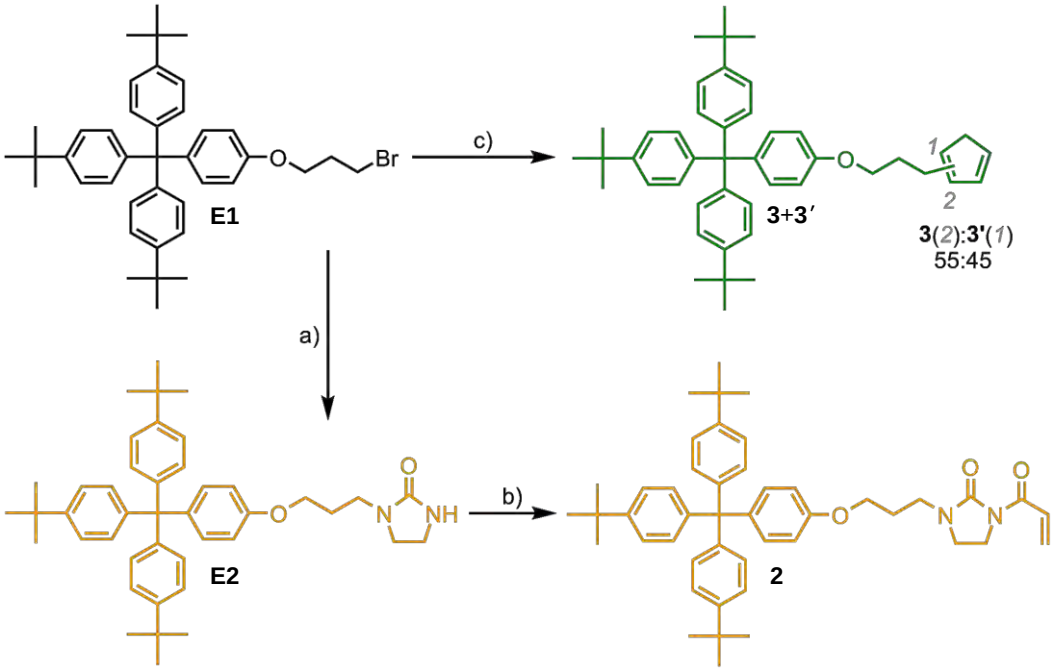

Scheme 5.5 a) Imidazolidone, NaH, DMF/THF 1:2, 10 h, RT, 33%; b) DIPEA, acryloyl chloride, CuCl, CH_2Cl_2, 8 h, 40 °C, 60%; c) NaCp 2M in THF, THF, 10 h, RT, 46%.

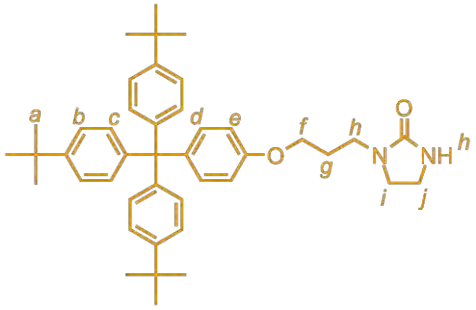

E2

Under nitrogen atmosphere, a solution of 2-imidazolidone (304.0 mg, 3.2 mmol, 2 equiv.) in dry DMF (75 mL) was stirred with molecular sieve for one hour. Sodium hydride (128.0 mg, 60% in oil, 3.2 mmol, 2 equiv.) was added in small portions and the reaction mixture was stirred for another hour before a solution of 1-(3-bromopropoxy)4-(*tris*(4-*tert*-butylphenyl)methyl)benzene (**E1**)[16] (1.0 g, 1.6 mmol, 1

equiv.) in dry THF (150 mL) was added dropwise through a cannula. The solution was stirred at room temperature for 10 hours and then quenched with MeOH (20 mL). The solvents were removed under reduced pressure and the resulting crude mixture dissolved in CH_2Cl_2 (20 mL). The organic layer was washed with brine (3 × 20 mL), dried ($MgSO_4$), filtered and concentrated under reduced pressure. Purification by column chromatography (CH_2Cl_2/Me_2CO 9:1 to 7:3) provided **E2** (334 mg, 33%) as a white powder; M.p. 225-227 °C. ^{1}H NMR (400 MHz, $CDCl_3$, 298 K): δ = 7.23 (d, *J* = 8.6 Hz, 6H, H_b), 7.08 (d, *J* = 8.5 Hz, 8H, H_c and H_d), 6.75 (d, *J* = 8.9 Hz, 2H, H_e), 4.55 (bs, 1H, H_k), 3.99 (t, *J* = 6.3 Hz, 2H, H_f), 3.38-3.50 (m, 4H, H_i and H_j), 3.37 (t, *J* = 7.0 Hz, 2H, H_h), 2.01 (dt, *J* = 6.7 Hz, 6.7 Hz, 2H, H_g), 1.30 (s, 27H, H_a). ^{13}C NMR (100 MHz, $CDCl_3$, 298 K): δ = 162.8, 156.6, 148.2, 144.1, 139.6, 132.2, 130.7, 124.0, 112.9, 65.3, 63.0, 45.5, 40.9, 38.2, 34.3, 31.4, 27.7. LRESI-MS: *m/z* = 631.5 $[M+H]^+$, HRFAB-MS (3-NOBA matrix): *m/z* = 631.42434 $[M+H]^+$ (calcd. for $C_{43}H_{55}O_2N_2$, 631.42581).

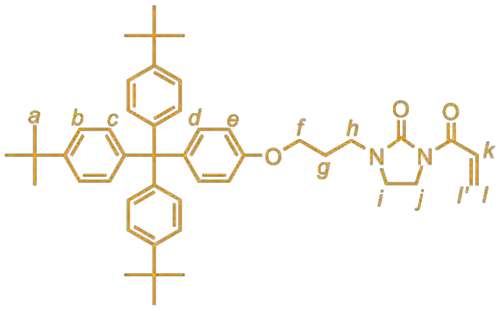

2

A solution of **E2** (334 mg, 0.53 mmol, 1 equiv.), diisopropyl ethyl amine (0.10 mL, 0.58 mmol, 1.1 equiv.), acryloyl chloride (0.45 mL, 0.58 mmol, 1.1 equiv.) and a catalytic amount of CuCl in dry CH_2Cl_2 (5 mL) was refluxed under nitrogen atmosphere. After 8 hours, ammonia (10 mL, 38% in water) was added and the organic phase was washed with water (2 × 10 mL), dried (Na_2SO_4), filtered and concentrated under reduced pressure. The residue was purified by column chromatography (CH_2Cl_2/Me_2CO, 99:1 to 98:2) to afford **3** (220 mg, 60%) as a white solid; M.p. 206-207 °C. ^{1}H NMR (400 MHz, $CDCl_3$, 298 K): δ = 7.59 (dd, *J* = 10.4 Hz, 17.1 Hz, 1H, H_k), 7.23 (d, *J* = 8.6 Hz, 6H, H_b), 7.04-7.10 (m, 8H, H_c and H_d), 6.74 (d, J = 8.9 Hz, 2H, H_e), 6.46 (dd, *J* = 2.0 Hz, 17.1 Hz, 1H, H_l), 5.76 (dd, *J* = 2.0 Hz, 10.5 Hz, 1H, $H_{l'}$), 4.00 (t, *J* = 6.0 Hz, 2H, H_f), 3.91 (t, *J* = 8.0 Hz, 2H, H_h), 3.46-3.52 (m, 4H, Hi and H_j), 2.05 (dt, *J* = 6.3 Hz, 6.3 Hz, 2H, H_g), 1.30 (s, 27H, H_a). ^{13}C NMR (100 MHz, $CDCl_3$, 298 K): δ = 165.5, 156.3, 154.6, 148.3, 144.0, 139.8, 132.3, 130.7, 129.4, 128.4, 124.0, 112.8, 65.1, 63.0, 41.4, 41.3, 39.7, 34.3, 31.3, 27.1. LSIMS-MS:

m/z = 685.5 $[M+H]^+$. HRFAB-MS (3-NOBA matrix): *m/z* = 684.42887 $[M]^+$ (calcd. for $C_{46}H_{56}N_2O_3$, 684.42909).

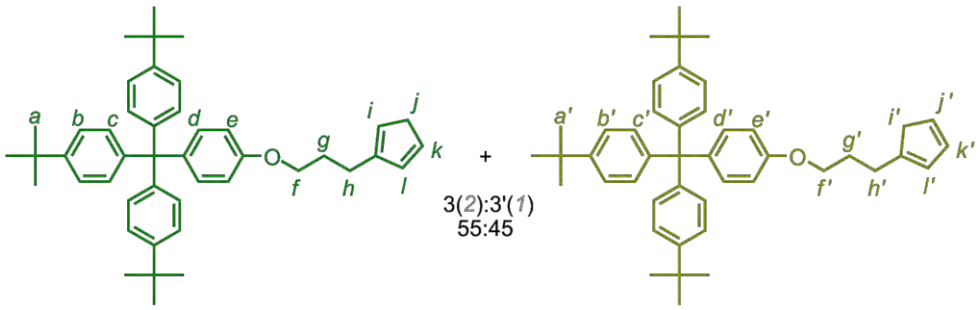

3 + **3′**

Sodium cyclopentadienide (3.2 mL, 2M in THF, 6.4 mmol, 4 equiv.) was added to a solution of 1-(3-bromopropoxy)4-(*tris*(4-*tert*-butylphenyl)methyl)benzene (**E1**)[16] (1.0g, 1.6 mmol, 1 equiv.) in dry THF (30 mL). The solution was stirred for 10 hours at room temperature and then quenched with MeOH (5 mL). The solvent was removed under reduced pressure and the resulting crude mixture dissolved in CH_2Cl_2 (20 mL). The organic layer was washed with brine (3 × 20 mL), dried ($MgSO_4$), filtered and concentrated under reduced pressure. Purification by column chromatography (CH_2Cl_2/Hexane 1:9) provided **3** as a mixture of isomers (ratio 2-substitued/1-substitued 55:45, 453 mg, 46%) as a white powder. The product was stored at -20 °C to avoid its dimerisation. M.p. 194-195 °C. ^{1}H NMR (400 MHz, $CDCl_3$, 298 K): δ = 7.23 (d, *J* = 8.6 Hz, 6H, $H_{bb'}$), 7.05-7.11 (m, 8H, $H_{cc'}$ and $H_{dd'}$), 6.76 (d, *J* = 8.9 Hz, 2H, $H_{ee'}$), 6.46 (dq, *J* = 1.4 Hz, 5.2 Hz, 0.55H, H_k), 6.41-6.44 (m, 1H, H_l and $H_{k'}$), 6.26 (dq, *J* = 1.3 Hz, 5.4 Hz, 0.45H, $H_{j'}$), 6.19 (dt, *J* = 1.5 Hz, 1.5 Hz, 0.45H, $H_{l'}$), 6.04 (dt, J = 1.6 Hz, 0.55H, H_i), 3.96 (t, *J* = 6.4 Hz, 2H, $H_{ff'}$), 2.94-2.96 (m, 1.1H, H_j), 2.90-2.92 (m, 0.9H, $H_{i'}$), 2.58 (td, *J* = 1.1 Hz, 7.3 Hz, 0.9H, $H_{h'}$), 2.54 (td, *J* = 1.1 Hz, 7.6 Hz, 1.1H, H_h), 1.97-2.08 (m, 2H, $H_{gg'}$), 1.30 (s, 27H, $H_{aa'}$). ^{13}C NMR (100 MHz, $CDCl_3$, 298 K): δ = 148.2, 144.1, 134.6, 133.9, 132.2, 130.7, 126.7, 126.3, 124.0, 112.9, 67.2, 43.3, 41.3, 34.3, 31.4, 29.2, 28.4, 27.1, 26.2. LRESI-MS: *m/z* = 610.5 $[M]^+$, HRESI-MS (3-NOBA matrix): *m/z* = 628.45086 $[M+NH_4]^+$ (calcd. for $C_{45}H_{58}NO$, 628.45184).

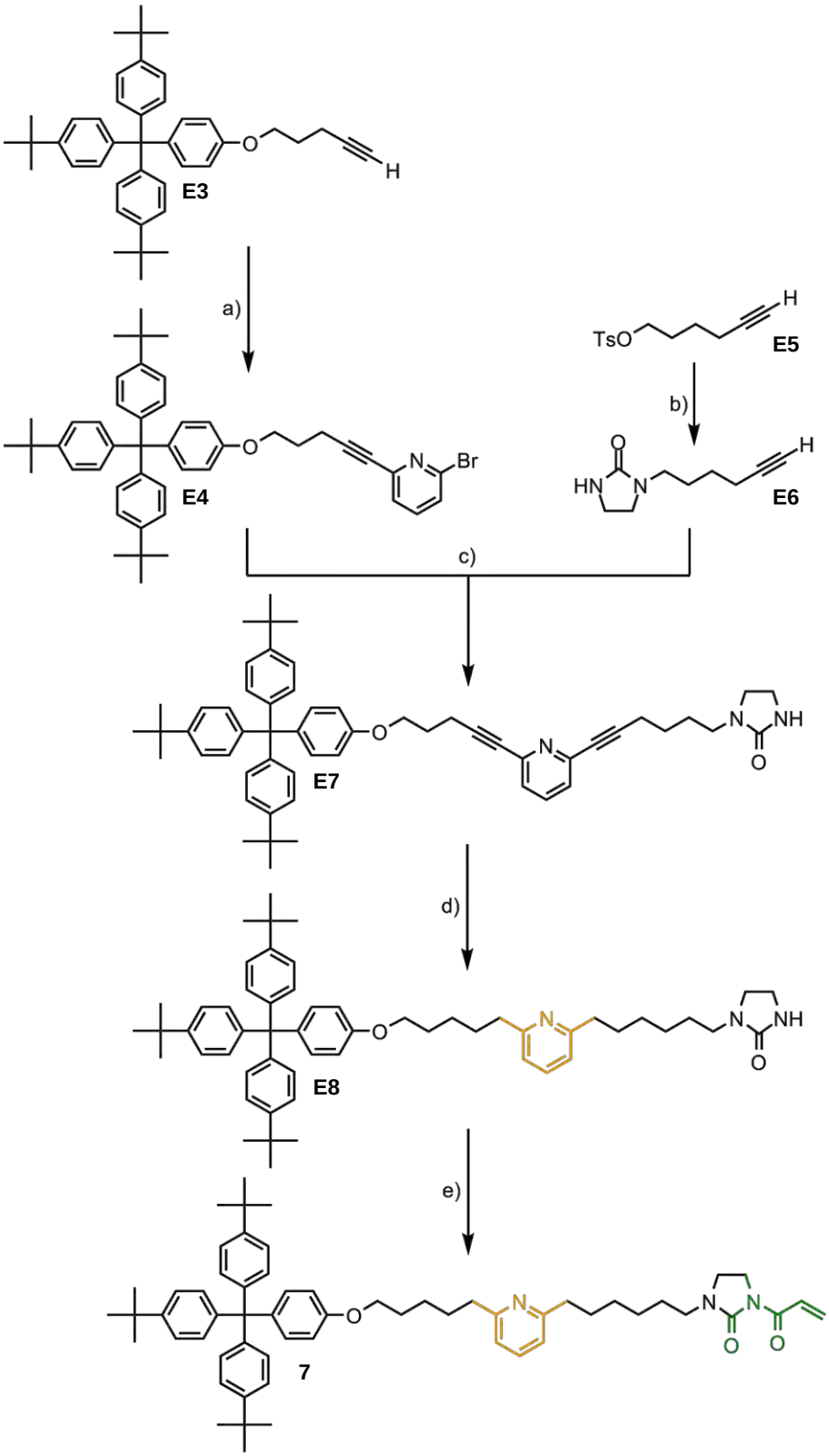

Scheme 5.6 a) 2-Bromo-6-iodopyridine, $Pd(PPh_3)_4$, CuI, THF/NEt_3 1:1, RT, 16 h, 74%; b) NaH, DMF, RT, 16 h, 23%; c) $Pd(PPh_3)_4$, CuI, THF/NEt_3 2:1, RT, 48 h, 73%; d) $Pd(OH)_2$/C, H_2, THF, RT, 2.5 h, 73%; e) DIPEA, acryloyl chloride, CuCl, CH_2Cl_2, 40 °C, 8 h, 46%.

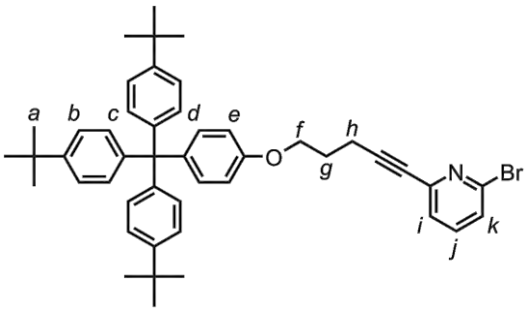

E4

A solution of 2-bromo-6-iodopyridine (546.0 mg, 1.92 mmol, 1.1 equiv.), **E3**[17] (1.0 g, 1.77 mmol, 1 equiv.), $Pd(PPh_3)_4$ (204.5 mg, 0.17 mmol, 0.1 equiv.) and CuI (67.4 mg, 0.35 mmol, 0.2 equiv.) in THF/NEt_3 1:1 (30 mL) was stirred at room temperature for 16 h. The solvents were removed under reduced pressure and the residue was extracted with CH_2Cl_2 (50 mL). The organic layer was washed with NH_4Cl sat. (2 × 50 mL) and with NH_3 (35% in water, 10 mL), dried ($MgSO_4$), filtered and concentrated under reduced pressure. Purification by column chromatography (Et_2O/Hexane 0:100 to 100:0) provided **E4** (1.03 g, 74%) as a yellow solid. M.p. 175-176 °C. ^{1}H NMR (400 MHz, $CDCl_3$, 298 K): δ = 7.45 (t, *J* = 7.7 Hz, 1H, H_j), 7.38 (dd, *J* = 0.9, 7.9 Hz, 1H, H_k), 7.30 (dd, *J* = 0.9, 7.4 Hz, 1H, H_i), 7.23 (d, *J* = 8.6 Hz, 6H, H_b), 7.08 (d, *J* = 8.4 Hz, 8H, H_c and H_d), 6.77 (d, *J* = 8.9 Hz, 2H, H_e), 4.06 (t, *J* = 5.9 Hz, 2H, H_f), 2.65 (t, *J* = 7.0 Hz, 2H, H_h), 2.08 (dt, *J* = 6.5, 6.5 Hz, 2H, H_g), 1.30 (s, 27H, H_a). ^{13}C NMR (100 MHz, $CDCl_3$, 298 K): δ = 156.5, 148.2, 144.1, 141.5, 139.6, 138.2, 132.2, 130.7, 127.0, 125.7, 124.0, 113.9, 112.9, 91.8, 79.7, 66.0, 63.0, 34.3, 31.4, 28.0, 16.2. LRESI-MS: *m/z* = 726.6 $[M]^+$, HRESI-MS: *m/z* = 726.3303 $[M+H]^+$ (calcd. for $C_{47}H_{53}BrNO$ 726.3305).

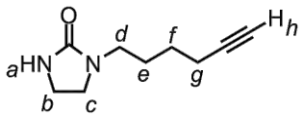

E6

Under nitrogen atmosphere, a solution of 2-imidazolidone (3.4 g, 35.7 mmol, 3 equiv.) in dry DMF (75 mL) was stirred with molecular sieve for one hour. Sodium hydride (714.0 mg, 60% in oil, 17.8 mmol, 1.5 equiv.) was added in small portions and the reaction mixture was stirred for another hour before hex-5-ynyl-4-methylbenzenesulfonate (**E5**)[18] (3.0 g, 11.9 mmol, 1 equiv.) was added dropwise. The solution was stirred at room temperature for 10 hours and then quenched with MeOH (20 mL). The solvent was removed under reduced pressure and the resulting crude

mixture dissolved in CH_2Cl_2 (100 mL). The organic layer was washed with brine (3 × 100 mL), dried ($MgSO_4$), filtered and concentrated under reduced pressure. Purification by column chromatography (CH_2Cl_2/Me_2CO/NEt_3 98:0:2 to 49:49:2) provided **E6** (456 mg, 23%) as a yellow oil. ^1H NMR (400 MHz, $CDCl_3$, 298 K): δ = 4.86 (bs, 1H, H_a), 3.38-3.41 (m, 4H, H_b and H_c), 3.18 (t, *J* = 7.0 Hz, 2H, H_d), 2.21 (td, *J* = 2.7, 6.8 Hz 2H, H_g), 1.93 (t, *J* = 2.7 Hz, 1H, H_h), 1.48-1.78 (m, 4H, H_e and H_f). ^{13}C NMR (100 MHz, $CDCl_3$, 298 K): δ = 162.9, 84.1, 68.6, 44.9, 42.9, 38.2, 26.5, 25.4, 18.1. LRESI-MS: *m/z* = 198.3 $[M+Na]^+$, HRESI-MS: *m/z* = 167.1180 $[M+H]^+$ (calcd. for $C_9H_{15}N_2O$, 167.1184).

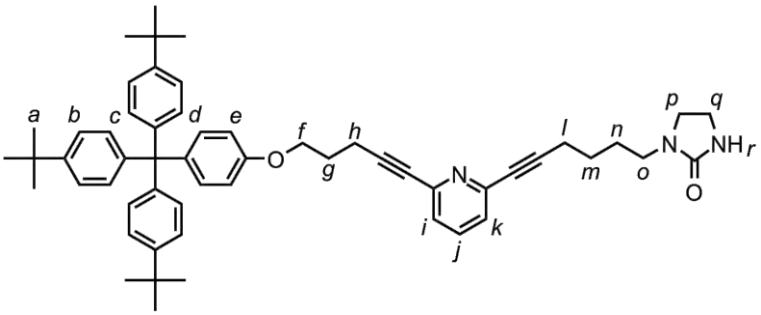

E7

A solution of **E5** (230.0 mg, 1.38 mmol, 1.2 equiv.), **E6** (191.0 mg, 1.15 mmol, 1 equiv.), $Pd(PPh_3)_4$ (127.1 mg, 0.11 mmol, 0.1 equiv.) and CuI (43.7 mg, 0.23 mmol, 0.2 equiv.) in THF/NEt_3 2:1 (15 mL) was stirred at room temperature for 48 hours. The solvents were removed under reduced pressure and the residue was extracted with CH_2Cl_2 (20 mL). The organic layer was washed with NH_4Cl sat. (2 × 10 mL) and with NH_3 (35% in water, 10 mL), dried ($MgSO_4$), filtered and concentrated under reduced pressure. Purification by column chromatography (CH_2Cl_2/Me_2CO/NEt_3 98:0:2 to 49:49:2) provided **S7** (888 mg, 73%) as a yellow foam. M.p. 178-180 °C (dec.) ^1H NMR (400 MHz, $CDCl_3$, 298 K): δ = 7.53 (t, *J* = 7.8 Hz, 1H, H_j), 7.20-7.28 (m, 8H, H_b, H_i and H_j), 7.07 (d, *J* = 8.5 Hz, 8H, H_c and H_d), 6.76 (d, *J* = 8.9 Hz, 2H, H_e), 4.21 (bs, 1H, H_r), 4.06 (t, *J* = 6.0 Hz, 2H, H_f), 3.38-3.48 (m, 4H, H_p and H_q), 3.22 (t, *J* = 6.7 Hz, 2H, H_o), 2.63 (t, *J* = 7.0 Hz, 2H, H_h), 2.47 (t, *J* = 6.6 Hz, 2H, H_l), 2.07 (dt, *J* = 6.5, 6.5 Hz, 2H, H_g), 1.60-1.73 (m, 4H, H_m and H_n), 1.29 (s, 27H, H_a). ^{13}C NMR (100 MHz, $CDCl_3$, 298 K): δ = 156.6, 148.2, 144.1, 139.6, 136.2 (×2), 132.2, 130.7, 125.5 (×2), 124.0, 112.9, 90.1, 80.4 (×2), 66.0 (×2), 44.9, 42.9, 38.1, 34.2, 31.3, 28.1 (×2), 26.8, 25.3, 22.0 (×2), 19.0, 16.1. LRESI-MS: *m/z* = 812.7 $[M]^+$, HRESI-MS: *m/z* = 812.5153 $[M+H]^+$ (calcd. for $C_{56}H_{66}N_3O_2$, 812.5155).

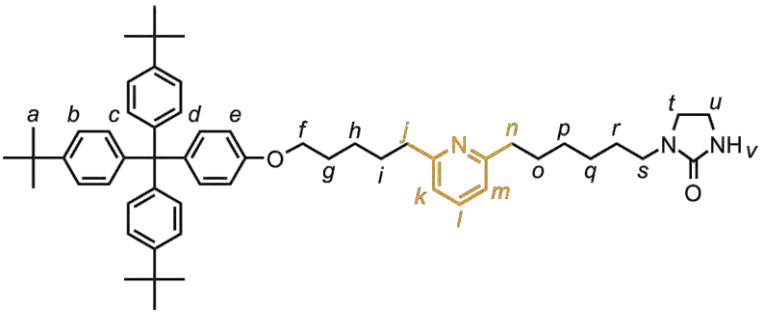

S8

$Pd(OH)_2$ on charcoal (142 mg, 20 wt%) was added to a solution of **E7** (710 mg, 0.87 mmol) in THF (22 mL). The resulting suspension was stirred at room temperature under a hydrogen atmosphere. After 2.5 hours, the reaction mixture was passed through neutralized celite and the solvent was removed under reduced pressure to afford **E8** (144 mg, quant.) as a white foam. M.p. 138-140 °C. ^{1}H NMR (400 MHz, $CDCl_3$, 298 K): δ = 7.48 (t, *J* = 7.6 Hz, 1H, H_l), 7.22 (d, *J* = 8.5 Hz, 6H, H_b), 7.04-7.10 (m, 10H, H_c, H_d and H_k), 6.94 (d, *J* = 7.7 Hz, 1H, H_m), 6.74 (d, *J* = 8.9 Hz, 2H, H_e), 4.18 (bs, 1H, H_v), 3.92 (t, *J* = 6.5 Hz, 2H, H_f), 3.36-3.41 (m, 4H, H_t and H_u), 3.16 (t, *J* = 7.3 Hz, 2H, H_s), 2.77 (t, *J* = 7.8 Hz, 2H, H_j), 2.74 (t, *J* = 7.8 Hz, 2H, H_n), 1.73-1.85 (m, 4H, H_g and H_i), 1.65-1.73 (m, 2H, H_o), 1.44-1.57 (m, 4H, H_h and H_r), 1.32-1.42 (m, 4H, H_p and H_q), 1.29 (s, 27H, H_a). ^{13}C NMR (100 MHz, $CDCl_3$, 298 K): δ = 161.7, 161.5, 156.8, 156.6, 148.2, 144.1, 139.3, 136.4, 132.1, 130.7, 124.0, 119.7 (×2), 112.8, 67.6, 63.0, 53.9, 44.9, 43.5, 38.4, 38.2, 34.2, 31.3, 30.1 (×2), 29.2 (×2), 27.5, 26.6, 25.9. LRESI-MS: *m/z* = 821.0 $[M+H]^+$, HRESI-MS: *m/z* = 820.5762 $[M+H]^+$ (calcd. for $C_{56}H_{74}N_3O_2$, 820.5781).

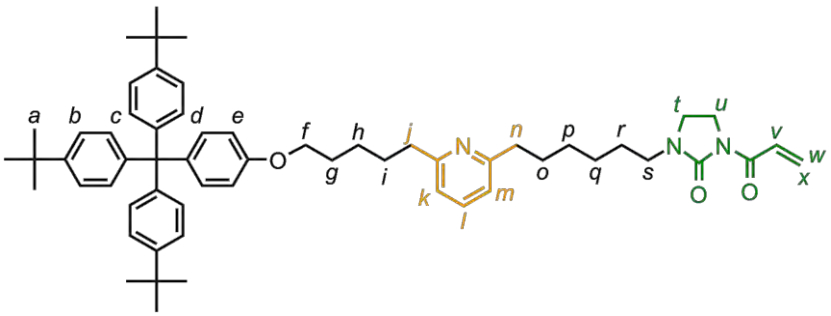

7

A solution of **E8** (144.0 mg, 0.17 mmol, 1 equiv.), diisopropyl ethyl amine (24.5 µL, 0.19 mmol, 1.1 equiv.), acryloyl chloride (15.6 µL, 0.19 mmol, 1.1 equiv.) and a catalytic amount of CuCl in dry CH_2Cl_2 (2 mL) was refluxed under nitrogen atmosphere. After 8 hours, ammonia (5 mL, 38% in water) was added and the organic phase was washed

with water (2 × 5 mL), dried (Na_2SO_4), filtered and concentrated under reduced pressure. The residue was purified by column chromatography (CH_2Cl_2, Me_2CO, 95:5 to 9:1) to afford **7** (68 mg, 46%) as a white film. M.p. 132-134 °C. ^{1}H NMR (400 MHz, $CDCl_3$, 298 K): δ = 7.63 (dd, *J* = 10.4, 17.1 Hz, 1H, H_v), 7.48 (t, *J* = 7.6 Hz, 1H, H_l), 7.22 (d, *J* = 8.6 Hz, 6H, H_b), 7.05-7.11 (m, 8H, H_c and H_d), 6.95 (d, *J* = 3.6 Hz, 1H, H_k), 3.94 (d, *J* = 3.6 Hz, 1H, H_m), 6.74 (d, *J* = 8.9 Hz, 2H, H_e), 6.47 (dd, *J* = 2.0, 17.1 Hz, 1H, H_w), 5.77 (dd, *J* = 2.0, 10.4 Hz, 1H, H_x), 3.85-3.95 (m, 4H, H_f and H_t), 3.41 (t, *J* = 8.0 Hz, 2H, H_u), 3.26 (t, *J* = 7.3 Hz, 2H, H_s), 2.71-2.80 (m, 4H, H_j and H_n), 1.74-1.85 (m, 4H, H_g and H_i), 1.66-1.74 (m, 2H, H_o), 1.49-1.57 (m, 4H, H_h and H_r), 1.32-1.43 (m, 4H, H_p and H_q), 1.30 (s, 27H, H_a). ^{13}C NMR (100 MHz, $CDCl_3$, 298 K): δ = 165.5, 161.6 (d), 156.8, 148.2, 144.1, 139.3, 136.4, 132.2, 130.7 (×2), 129.3, 128.4, 124.0, 119.7 (d), 112.8, 67.6, 63.0, 43.7, 40.8, 39.6, 38.4 (×2), 34.2, 31.3, 30.0 (×2), 29.2, 29.0, 27.0, 26.6, 25.9. LRESI-MS: *m/z* = 874.6 $[M+H]^+$, HRESI-MS: *m/z* = 874.5872 $[M+H]^+$ (calcd. for $C_{59}H_{76}N_3O_3$ 874.5881).

5.5.3 General Procedure for the DA-rotaxane Formation Reaction

A dry schlenk tube was charged with $M(OTf)_2$ (1.0 equiv, 0.014 mmol) and with macrocycle (1.0 equiv, 0.014 mmol) under a nitrogen atmosphere. Dry CH_2Cl_2 (0.5 mL) was added and the mixture was stirred at room temperature for 30 min. A solution of acroyl-imidazolidone stopper **2** (1.2 equiv, 0.017 mmol) in dry CH_2Cl_2 (0.5 mL) was added and the mixture was stirred for another 30 min. The mixture was then cooled to -78 °C and stirred for 5 minutes before a solution of cyclopentadiene stopper **3** (2 equiv, 0.028 mmol) in dry CH_2Cl_2 (0.5 mL) was added. The reaction mixture was stirred at -78 °C for 2 days then allowed to stir at room temperature for another two days. The reaction was quenched with ammonia (35% in water) and the aqueous layer was extracted with CH_2Cl_2 (2×). The organic layers were combined, washed with brine (3×), dried (Na_2SO_4), filtered and concentrated under reduced pressure. Purification by column chromatography (MeCN/Hexane/CH_2Cl_2 5:45:55) provided the rotaxane as a colourless film.

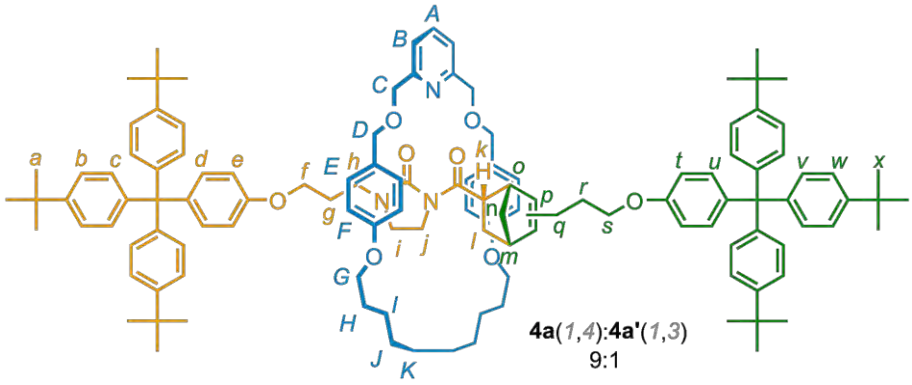

4a + 4a′

Following the general procedure, $Cu(OTf)_2$ (20.0 mg, 56.0 µmol, 1 equiv.), macrocycle **1a** (28.0 mg, 56.0 µmol, 1 equiv.) in dry CH_2Cl_2 (1.0 mL). Addition of **2** (46.0 mg, 68 µmol, 1.2 equiv.) in dry CH_2Cl_2 (1.0 mL). Addition of **3** (68.8 mg, 112 µmmol, 2 equiv.) in dry CH_2Cl_2 (1.0 mL). Ammonia (6 mL, 35% in water). Purification by column chromatography provided the rotaxane **4a** as a mixture of isomers (ratio 1,4-disubstitued/1,3-disubstitued 9:1, 77 mg, 75%) as a colourless film. M.p. 112-116 °C. ^{1}H NMR (400 MHz, $CDCl_3$, 328 K): δ = 7.50 (t, *J* = 7.7 Hz, 1H, H_A), 7.21-7.26 (m, 14H, H_B, H_b and H_v), 7.06-7.12 (m, 12H, H_c and H_w), 7.03 (d, *J* = 3.6 Hz, 2H, H_E), 7.01 (d, *J* = 3.6 Hz, 2H, $H_{E'}$), 6.96 (d, *J* = 6.9 Hz, 2H, H_d), 6.94 (d, *J* = 6.9 Hz, 2H, H_u), 6.56-6.62 (m, 4H, H_F), 6.48 (d, *J* = 8.3 Hz, 2H, H_t), 6.42 (d, *J* = 8.8 Hz, 2H, H_e), 5.63 (bs, 0.1H, $H_{p(\mathbf{4a'})}$), 5.35 (bs, 0.9H, $H_{p(\mathbf{4a})}$), 4.46-4.56 (m, 4H, H_D), 4.27 (s, 4H, H_C), 4.04-4.11 (m, 1H, H_k), 3.82 (t, *J* = 6.3 Hz, 2H, H_G), 3.80 (t, *J* = 6.3 Hz, 2H, $H_{G'}$), 3.56-3.64 (m, 2H, H_s), 3.46-3.56 (m, 2H, H_i), 3.42 (bt, *J* = 5.2 Hz, 2H, H_f), 3.19 (bs, 1H, H_o), 2.97-3.11 (m, 2H, H_j), 3.93 (t, *J* = 7.8 Hz, 2H, H_h), 2.68 (bs, 0.9H, $H_{m(\mathbf{4a})}$), 2.61 (bs, 0.1H, $H_{m(\mathbf{4a'})}$), 2.11 (bt, J = 7.3 Hz, 2H, H_q), 1.91-1.98 (m, 0.1H, $H_{l(\mathbf{4a'})}$), 1.83 (ddd, *J* = 3.5 Hz, 9.0 Hz , 12.5 Hz, 1H, $H_{l(\mathbf{4a})}$), 1.70-1.77 (m, 2H, H_r), 1.66 (dt, *J* = 6.6 Hz, 6.6 Hz, 2H, H_H), 1.65 (dt, *J* = 6.6 Hz, 6.6 Hz, 2H, $H_{H'}$), 1.35-1.44 (m, 3H, H_g and $H_{l'}$), 1.38 (d, J = 8.8 Hz, 2H, H_n), 1.31 (2s, 54H, H_a, H_x), 1.27-1.33 (m, 4H, H_l), 1.24-1.26 (m, 4H, H_J), 1.15-1.21 (m, 4H, H_K). ^{13}C NMR (100 MHz, $CDCl_3$, 328 K): δ = 174.8, 158.6 (×2), 157.6, 156.8, 156.3, 154.4, 151.5, 148.2, 144.2, 139.4, 138.9, 136.9, 131.9, 130.7, 129.8, 129.1, 124.0, 124.0, 123.6, 119.4 (×2), 114.3, 112.9 (×2), 77.3, 77.0, 76.7, 72.3, 71.0 (×2), 67.3, 67.1 (×2), 49.8, 47.2, 46.3, 44.7, 40.9, 40.8, 39.8, 34.3, 31.4, 29.7 (×2), 29.6, 29.1, 28.7, 28.6, 27.2, 27.0, 26.2, 25.6. LRESI-MS: *m/z* = 1785 $[M+H]^+$. HRFAB-MS (3-NOBA matrix): *m/z* = 1785.11478 $[M+H]^+$ (calcd. for $C_{122}H_{150}O_2N_3$, 1785.14229).

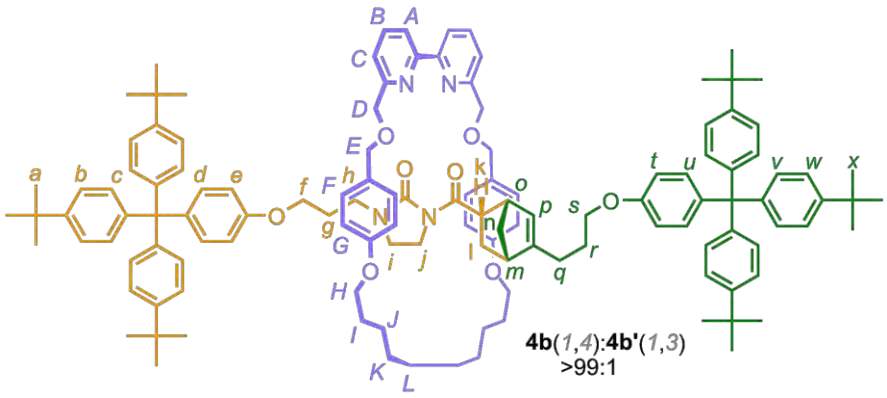

4b

Following the general procedure, $Cu(OTf)_2$ (15.0 mg, 42.0 µmol, 1 equiv.), macrocycle **1b** (24.0 mg, 42.0 µmol, 1 equiv.) in dry CH_2Cl_2 (1.5 mL). Addition of **2** (34.5 mg, 50.4 µmol, 1.2 equiv.) in dry CH_2Cl_2 (1.5 mL). Addition of **3** (51.6 mg, 84.0 µmmol, 2 equiv.) in dry CH_2Cl_2 (1.5 mL). Ammonia (6 mL, 35% in water). Purification by column chromatography provided the rotaxane **4b** (ratio 1,4-disubstitued/1,3-disubstitued 99:1, 69 mg, 87%) as a colourless film. M.p. 115-116 °C. ^{1}H NMR (400 MHz, $CDCl_3$, 298 K): δ = 7.99 (d, *J* = 7.8 Hz, 2H, H_A), 7.51 (t, *J* = 7.7 Hz, 2H, H_B), 7.29 (d, *J* = 7.6 Hz, 2H, H_C), 7.20-7.25 (m, 12H, H_b and H_w), 7.05-7.12 (m, 12H, H_c and H_v), 7.02 (d, *J* = 8.5 Hz, 2H, H_F), 7.01 (d, *J* = 8.6 Hz, 2H, $H_{F'}$), 6.97 (d, *J* = 5.8 Hz, 2H, H_d), 6.95 (d, *J* = 5.9 Hz, 2H, H_u), 6.55-6.60 (m, 4H, H_G), 6.48 (d, *J* = 9.0 Hz, 2H, H_t), 6.37 (d, *J* = 8.9 Hz, 2H, H_e), 5.32 (bs, 1H, H_p), 4.55 (2s, 8H, H_D and H_E), 4.00-4.05 (m, 1H, H_k), 3.75 (t, *J* = 6.4 Hz, 2H, H_H), 3.74 (t, *J* = 6.4 Hz, 2H, $H_{H'}$), 3.59-3.56 (m, 2H, H_s), 3.40-3.49 (m, 2H, H_i), 3.37 (t, *J* = 6.0 Hz, 2H, H_f), 3.14 (bs, 1H, H_o), 2.87-3.05 (m, 2H, H_j), 2.82 (t, J = 7.9 Hz, 2H, H_h), 2.64 (bs, 1H, H_m), 2.11 (t, *J* = 7.7 Hz, 2H, H_q), 1.76-1.83 (m, 1H, H_l), 1.67-1.76 (m, 2H, H_r), 1.52-1.67 (m, 4H, H_I), 1.40-1.52 (m, 3H, H_g and $H_{l'}$), 1.34 (d, J = 9.6 Hz, 2H, Hn), 1.30 (2s, 54H, H_a and H_x), 1.28-1.31 (m, 4H, H_J and H_K), 1.24-1.26 (m, 4H, H_L). ^{13}C NMR (100 MHz, $CDCl_3$, 298 K): δ = 158.5, 158.1, 155.3, 148.2, 148.1, 144.2, 144.2, 137.2 (×2), 137.0, 131.9 (×2), 130.7 (×2), 129.6 (×2), 124.0, 124.0, 123.6, 121.3 (×2), 119.7, 114.2, 112.8 (×2), 72.3, 72.1 (×2), 67.5, 67.3, 64.5, 49.8, 49.4, 47.2, 46.2, 44.7, 44.1, 41.9, 41.4, 41.3, 40.9, 40.8, 39.7, 34.2 (×2), 31.4, 29.7, 29.4, 28.9, 28.8, 27.2, 26.9, 25.8. LRFAB-MS: *m/z* = 1862.8 $[M]^+$. HRESI-MS: *m/z* = 1863.1669 $[M]^+$ (calcd. for $C_{127}H_{154}N_4O_8$ 1863.1767).

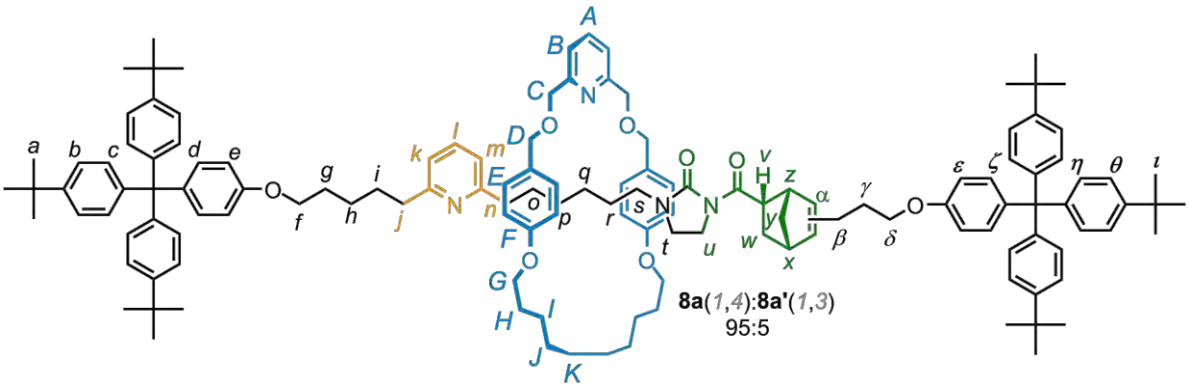

8a + **8a′**

Following the general procedure, $Cu(OTf)_2$ (36.0 mg, 0.10 mmol, 1 equiv.), macrocycle **1a** (50.0 mg, 0.10 mmol, 1 equiv.) in dry CH_2Cl_2 (5.0 mL). Addition of **7** (107.5 mg, 0.12 µmol, 1.2 equiv.) in dry CH_2Cl_2 (5.0 mL). Addition of **3** (122.0 mg, 0.20 mmmol, 2 equiv.) in dry CH_2Cl_2 (5.0 mL). Ammonia (15 mL, 35% in water). Purification by column chromatography provided the rotaxane **8a** (ratio 1,4-disubstitued/1,3-disubstitued 95:5, 83 mg, 42%) as a colourless film. M.p. 100-102 °C. ^{1}H NMR (400 MHz, $CDCl_3$, 298 K): δ = 7.52 (t, *J* = 7.7 Hz, 1H, H_A), 7.45 (t, *J* = 7.6 Hz, 1H, H_l), 7.23 (d, *J* = 8.4 Hz, 14H, H_B, H_b and H_η), 7.10 (d, *J* = 3.1 Hz, 6H, H_c), 7.07 (d, *J* = 3.2 Hz, 6H, H_θ), 7.04 (dd, *J* = 2.2, 8.5 Hz, 4H, H_E), 6.97 (d, *J* = 4.1 Hz, 2H, H_d), 6.95 (d, *J* = 4.1 Hz, 2H, H_ζ), 6.88 (d, *J* = 7.7 Hz, 1H, H_k), 6.86 (d, *J* = 7.8 Hz, 1H, H_m), 6.62 (dd, *J* = 3.4, 8.5 Hz, 4H, H_F), 6.56 (d, *J* = 8.2 Hz, 2H, H_ε), 6.49 (d, *J* = 8.8 Hz, 2H, H_e), 5.66 (bs, 0.14H, $H_{\alpha(\mathbf{8a'})}$), 5.38 (bs, 0.86H, $H_{\alpha(\mathbf{8a})}$), 4.47-4.57 (m, 4H, H_C), 4.28 (s, 4H, H_D), 4.07-4.14 (m, 1H, H_v), 3.82 (t, *J* = 6.0 Hz, 4H, H_G), 3.68-3.75 (m, 2H, H_δ), 3.57-3.68 (m, 2H, H_t), 3.50 (t, *J* = 6.3 Hz, 2H, H_f), 3.20 (bs, 1H, H_z), 2.97-3.17 (m, 4H, H_s and H_u), 2.69 (bs, 1H, H_x), 2.60-2.69 (m, 4H, H_j and H_n), 2.17 (bt, *J* = 7.1 Hz, 2H, H_β), 1.75-1.88 (m, 9H, H_i, H_o, H_r, H_w and H_γ), 1.60-1.70 (m, 4H, H_H), 1.44-1.60 (m, 7H, H_g, H_h, $H_{w'}$ and H_y), 1.32-1.44 (m, 6H, H_l, H_p and H_q), 1.30 (s, 54H, H_a and H_ι), 1.10-1.28 (m, H_J and H_K). ^{13}C NMR (100 MHz, $CDCl_3$, 298 K): δ = 174.9, 168.6, 161.5, 158.7, 157.6, 156.8, 156.7, 154.5, 151.4, 148.1, 144.2 (×2), 141.4, 141.1, 139.0, 136.8, 136.3, 132.0 (×2), 130.7, 129.8, 129.1, 124.0, 123.7, 119.6 (×2), 119.1, 114.3, 112.9 (×2), 72.2, 70.7, 67.4, 67.3, 67.0, 63.0, 49.8, 47.2, 46.3, 44.8, 43.6, 40.6, 39.8, 38.4 (×2), 34.2, 34.1, 31.4, 29.9, 29.8, 29.6 (×2), 29.2, 29.1 (×2), 28.7, 28.7, 27.2, 27.0 (×2), 26.6, 26.2, 25.8, 25.7, 22.3, 14.0. LRESI-MS: *m/z* = 1974.5 $[M+H]^+$, HRESI-MS: *m/z* = 1974.2853 $[M+H]^+$ (calcd. for $C_{135}H_{169}N_4O_8$ 1974.2940).

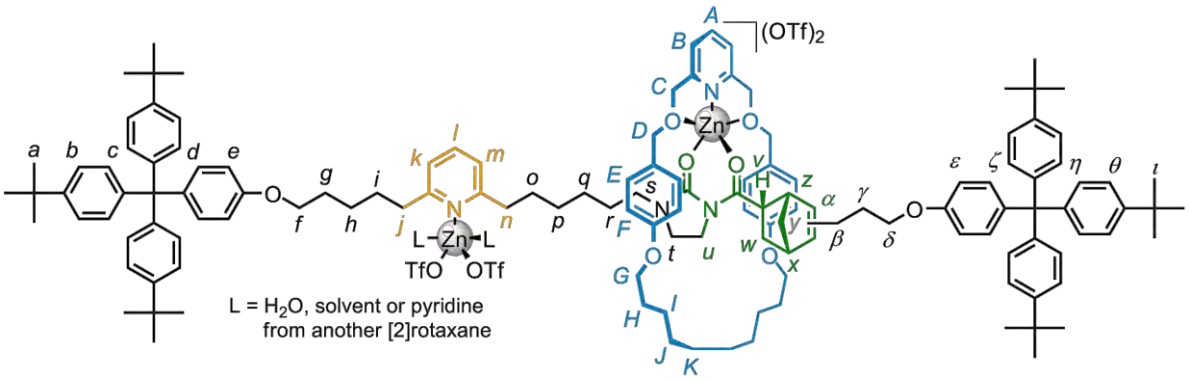

Zn-8a

A solution of $Zn(OTf)_2$ (9.5 mg, 8.5 μmol, 3 equiv) in MeOH (0.5 mL) was added dropwise to a solution of **8a** (10.0 mg, 5.0 μmol, 1 equiv.) in CH_2Cl_2 (0.5 mL) with stirring. The solution was stirred for 1 h at room temperature and the solvents were removed under reduced pressure to afford the complex **Zn-8a** as a white amorphous solid. ^{1}H NMR (400 MHz, CD_2Cl_2/CD_3CN 9:1, 298 K): δ = 8.22 (t, *J* = 7.9 Hz, 1H, H_l), 7.76 (t, *J* = 7.9 Hz, 1H, H_A), 7.58 (d, *J* = 7.9 Hz, 1H, H_k), 7.54 (d, *J* = 7.9 Hz, 1H, H_m), 7.31 (d, *J* = 7.9 Hz, 2H, H_B), 7.19-7.25 (m, 12H, H_b and H_η), 7.05-7.19 (m, 20H, H_c, H_d, H_ζ, H_θ and H_E), 6.81 (d, *J* = 8.5 Hz, 2H, H_ε), 6.67-6.78 (m, 6H, H_e and H_F), 4.61-4.76 and 4.91-5.20 (m, 8H, H_C and H_D), 4.90 (bs, 1H, H_α), 3.92-4.01 (m, 2H, H_δ), 3.89 (t, *J* = 5.9 Hz, 4H, H_G), 3.65-3.80 (m, 2H, H_f), 3.12-3.37 (m, 6H, H_s, H_t, H_u and H_v), 3.01-3.12 (m, 4H, H_j and H_n), 2.75 (bs, 1H, H_z), 2.69 (bs, 1H, H_x), 2.31-2.38 (m, 2H, H_β), 1.62-1.88 (m, 7H, H_w, H_γ and H_H), 1.45-1.62 (m, 7H, H_g, H_h, $H_{w'}$ and H_y), 1.31-1.45 (m, 8H, H_p, H_q and H_I), 1.25 (s, 54H, H_a and H_ι), 1.00-1.22 (m, 8H, H_J and H_K). ^{13}C NMR (100 MHz, CD_2Cl_2/CD_3CN 9:1, 298 K): δ = 158.1, 157.4, 156.8, 156.6, 156.3 (×2), 155.7, 155.5, 154.6, 151.9 (×2), 147.3, 147.2, 145.3, 143.4, 143.3, 140.1, 138.8, 138.4, 138.2, 138.1, 138.1, 136.9, 134.8, 130.8, 130.7, 129.7, 129.2 (×2), 123.2, 123.2, 122.4, 120.1, 112.6, 112.0 (×2), 73.6, 73.5, 69.6 (×2), 66.3, 66.2, 66.0, 48.1, 45.3, 44.7, 43.3, 40.0 (×2), 39.6, 33.0, 32.0, 31.9, 29.9, 28.6, 28.5, 28.3, 28.0, 27.6, 27.0, 25.9, 25.2 (×2), 24.8 (×2), 24.5, 24.3. LRESI-MS: *m/z* = 2336.3 $[M+H]^+$, 2189.7 $[M\text{-}OTf]^+$, 2037.1 $[M\text{-}2OTf]^+$, HRESI-MS: *m/z* = 2336.1 [M+H]+ (calcd. for $C_{137}H_{169}F_6N_4O_{14}S_2Zn$ 2336.12).

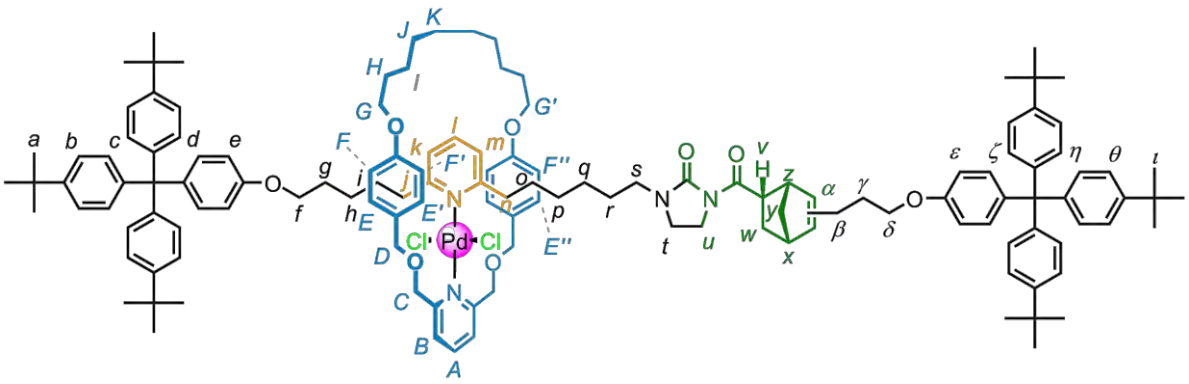

Pd**8a**Cl_2

$PdCl_2$ (0.9 mg, 5.1 µmol, 1.05 equiv.) was added to a solution of **8a** (10 mg, 5.0 µmol, 1.00 equiv.) in CH_2Cl_2 (0.5 mL). The suspension was stirred until the solid was dissolved and the solvent was removed under reduced pressure to afford Pd**8a**Cl_2 as a yellow amorphous solid (10.7 mg, quant.). ^{1}H NMR (400 MHz, CD_2Cl_2/CD_3CN 9:1, 298 K): δ = 7.68 (bt, *J* = 7.8 Hz, 1H, H_l), 7.62 (bt, *J* = 7.8 Hz, 1H, H_A), 7.02-7.30 (m, 31H, H_b, H_c, H_d, H_k, H_η, H_ζ, H_θ and H_E), 7.01 (d, *J* = 8.8 Hz, 1H, $H_{E'}$), 6.97 (d, *J* = 7.8 Hz, 1H, H_m), 6.90 (d, *J* = 8.7 Hz, 1H, $H_{E''}$), 6.76 (d, *J* = 8.7 Hz, 2H, H_ε), 6.72 (d, *J* = 8.6 Hz, 2H, H_F), 6.61 (d, *J* = 8.5 Hz, 2H, H_e), 6.36 (bd, *J* = 6.7 Hz, 1H, $H_{F'}$), 6.21 (bd, *J* = 7.9 Hz, 1H, $H_{F''}$), 5.6-5.75 (m, 4H, H_C), 5.34 (bs, 1H, H_α), 4.64-4.72 (m, 4H, H_D), 3.92-4.12 (m, 5H, H_v, H_δ and H_G), 3.60-3.92 (m, 5H, H_f, H_u and $H_{G'}$), 3.17-3.42 (m, 4H, H_s and H_t), 3.10-3.17 (m, 2H, H_j), 3.07 (bs, 1H, H_z), 2.92 (t, *J* = 6.3, 2H, H_n), 2.68 (bs, 1H, H_x), 1.93-2.08 (m, 4H, H_i and H_o), 1.68-1.74 (5H, H_r, H_w and H_γ), 1.54-1.66 (m, 4H, H_H), 1.34-1.54 (m, 7H, H_g, H_h, $H_{w'}$ and H_y), 1.25-1.34 (8H, H_p, H_q and H_I), 1.24 (s, 54H, H_a and H_ι), 0.95-1.22 (4H, H_J and H_K). ^{13}C NMR (100 MHz, CD_2Cl_2/CD_3CN 9:1, 298 K): δ = 162.7, 159.3 (×2, **8a′**), 157.8 (×2), 155.8, 147.1 (×3, **8a′**), 143.6, 143.4 (×3, **8a′**), 138.3, 137.8 (×3, **8a′**), 130.7, 130.6, 130.3, 129.3 (×2), 129.2 (×2), 129.1, 123.1 (×2), 121.3 (×2, **8a′**), 121.1, 120.9 (×2, **8a′**), 120.6, 120.5, 120.4, 113.2 (×2, **8a′**), 113.2 (×2, **8a′**), 112.9, 112.8, 112.1, 112.0 (×2), 72.0, 70.3, 70.2, 66.6, 66.3 (×2, **8a′**), 65.9, 65.7, 61.9, 42.3, 39.5 (×3, **8a′**), 39.3 (×3, **8a′**), 39.3, 38.8, 33.0, 29.9, 28.4 (×2, **8a′**), 27.9, 27.7, 27.4 (×2), 27.2, 27.1 (×2, **8a′**), 25.3 (×2), 25.2, 24.6, 24.2, 22.1. LRESI-MS: m/z = 2079.2 $[M-2Cl]^+$

5.5.4 Spectroscopic Data of Corresponding Non-interlocked Threads

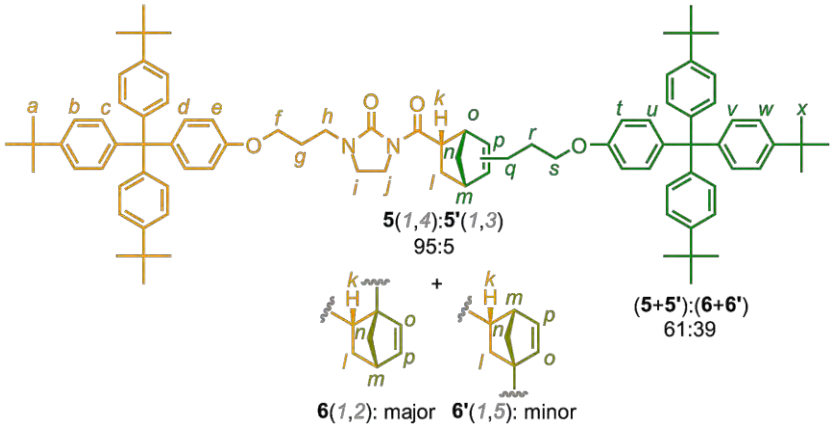

5 + 6

M.p. 142-144 °C. ^{1}H NMR (400 MHz, $CDCl_3$, 328 K): δ = 7.19-7.25 (m, 12H, H_b and H_v), 7.04-7.12 (m, 16H, H_c, H_d, H_u and H_w), 6.75 (d, *J* = 8.7 Hz, 2H, H_t), 6.72 (d, *J* = 8.2 Hz, 2H, H_e), 6.15 (dd, *J* = 3.1 Hz, 4.8 Hz, 0.38H, $H_{p(6)}$), 6.06 (d, *J* = 5.6 Hz, 0.38H, $H_{o(6)}$), 5.75 (bs, 0.03H, $H_{p(5')}$), 5.42 (bs, 0.56H, $H_{p(5)}$), 4.05-4.12 (m, 1H, H_k), 4.01 (t, *J* = 5.8 Hz, 2H, H_f), 3.90-3.94 (m, 2H, H_s), 3.72-3.94 (m, 2H, H_i), 3.38-3.52 (m, 4H, H_h and H_j), 3.19 (bs, 0.56H, H_o), 2.91 (bs, 0.03H, $H_{m(5')}$), 2.80 (bs, 0.38H, $H_{m(6)}$), 2.75 (bs, 0.56H, $H_{m(5)}$), 2.27-2.42 (m, 2.38H, $H_{l(6)}$ and H_q), 1.91-2.10 (m, 4H, H_g and H_r), 1.79-1.88 (m, 1H, H_l), 1.53 (bd, J = 11.9 Hz, $H_{l'}$), 1.44 (d, *J* = 10.2 Hz, 2H, H_n),1.30 (bs, 54H, H_a, and H_x). ^{13}C NMR (100 MHz, $CDCl_3$, 328 K): δ = 175.3, 175.0, 156.9 (d), 156.3 (d), 154.8, 154.6, 151.3, 148.2 (d), 144.1 (d), 139.7, 139.2 (d), 137.7, 136.0, 132.2 (×2), 130.6, 124.0 (×2), 112.9 (×2), 112.8 (d), 68.2, 67.5, 65.2 (×2), 62.9, 58.0, 52.4, 49.8, 47.2, 47.0, 46.3, 44.7, 42.3, 41.4 (×2), 41.2 (×2), 39.9 (×2), 35.8, 31.3, 29.0, 27.2 (×2), 26.6, 26.3. LRESI-MS: *m/z* = 1294.5 $[M]^+$.

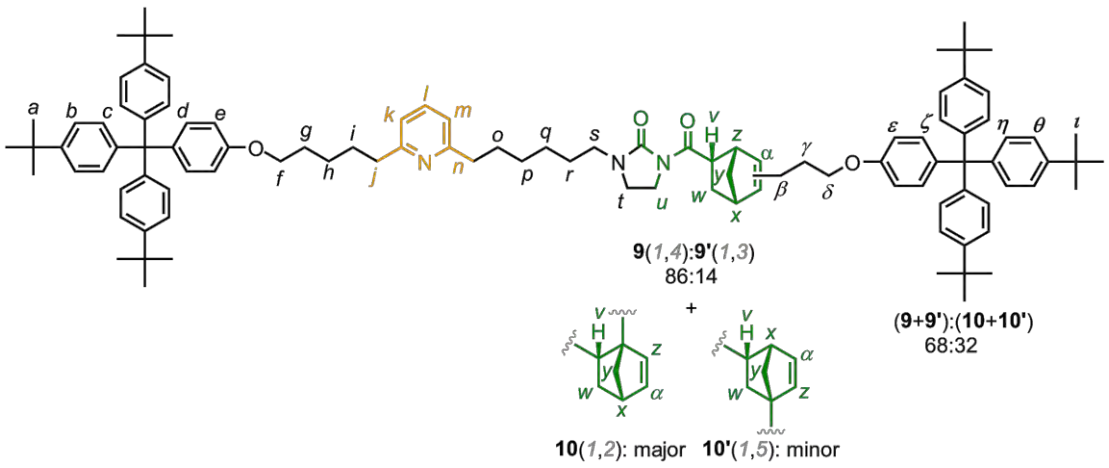

9 + 10

M.p. 135-136 °C. ^{1}H NMR (400 MHz, $CDCl_3$, 298 K): δ = 7.48 (bt, *J* = 6.9 Hz, 1H, H_l), 7.22 (d, *J* = 8.5 Hz, 12H, H_b and H_η), 7.03-7.10 (m, 16H, H_c, H_d, H_ζ and H_θ), 6.91-6.98 (bm, 2H, H_k and H_m), 6.70-6.78 (m, 4H, H_e and H_ε), 6.14 (dd, *J* = 3.1, 5.4 Hz, 0.24H, $H_{\alpha(\mathbf{10})}$), 6.06 (d, *J* = 5.5 Hz, 0.24H, $H_{z(\mathbf{10})}$), 5.75 (bs, 0.07H, $H_{\alpha(\mathbf{9'})}$), 5.42 (bs, 0.45H, $H_{\alpha(\mathbf{9})}$), 4.08-4.14 (m, 0.7H, $H_{v(\mathbf{9})}$), 4.04-4.08 (m, 0.3H, $H_{v(\mathbf{10})}$), 3.89-4.00 (m, 4H, H_f and H_δ), 3.68-3.78 (m, 2H, H_u), 3.28-3.39 (m, 2H, H_t), 3.19-3.28 (m, 3H, H_s and H_z), 2.92 (bs, 0.07H, $H_{x(\mathbf{9'})}$), 2.70-2.83 (m, 5H, H_j, H_n and H_x), 2.36-2.44 (m, 0.3H, $H_{\beta(\mathbf{10})}$), 2.30 (bt, *J* = 6.7 Hz, 0.7H, $H_{\beta(\mathbf{9})}$), 1.90-2.00 (m, 2H, H_γ), 1.64-1.75 (m, 7H, H_g, H_h, H_r and H_w) 1.75-1.90 (4H, H_i and H_o), 1.47-1.56 (m, 3H, $H_{w'}$ and H_y), 1.32-1.47 (m, 4H, H_p and H_q), 1.30 (s, 54H, H_a and H_ι). ^{13}C NMR (100 MHz, $CDCl_3$, 298 K): δ = 156.9, 156.8 (×2, **10**), 154.7, 154.5, 151.3, 148.2 (×2), 144.1, 139.3 (×2, **10**), 139.2, 137.9, 136.4 (×2), 135.9, 132.2, 130.7, 124.0, 123.9, 119.7, 112.9 (×2, **10**), 68.2, 67.6 (×2, **10**), 63.0, 58.0, 52.4, 49.9, 47.3 (×2, **10**), 46.4, 44.8, 43.7 (×2, **10**), 42.3, 40.8 (×2, **10**), 40.7, 39.9 (×2, **10**), 39.7, 38.4, 36.0, 34.2, 31.3, 30.0, 29.9, 29.2, 29.1, 29.0 (×2), 28.0, 27.2, 27.1, 27.0, 26.6 (×2, **10**), 26.3, 25.9. LRESI-MS: *m/z* = 1484.0 $[M]^+$, HRESI-MS: *m/z* = 1485.0028 $[M+H]^+$ (calcd. for $C_{104}H_{130}N_3O_4$ 1485.0061).

5.6 References

(1) O. Diels, K. Alder, *Liebigs Ann. Chem*. **1928**, *460*, 98.

(2) a) K. C. Nicolaou, S. A. Snyder, T. Montagnon, G. Vassilikogiannakis, *Angew. Chem. In. Ed*. **2002**, *41*, 1668-1698. b) E. J. Corey, *Angew. Chem. Int. Ed*. **2002**, *41*, 1650-1667.

(3) E. R. Kay, D. A. Leigh, F. Zerbetto, *Angew. Chem. Int. Ed*. **2007**, *46*, 72-191.

(4) D. A. Leigh, E. M. Perez, *Chem Commun*. **2004**, 2262-2263.

(5) a) *Cycloaddition Reactions in Organic Synthesis*, S. Kobayashi, K. A. Jøgensen, Ed, Wiley-VCH: Weinheim, **2002**. b) *Lewis Acids in Organic Synthesis*, H. Yamamoto, Ed, Wiley-VCH: Weinheim, **2000**; *Vols*. 1 and 2.

(6) a) A. Wassermann, *J. Chem. Soc.* **1942**, 618. b) A. Wassermann, *J. Chem. Soc.* **1942**, 623.

(7) P. Yate, P. Eaton, *J. Am. Chem. Soc*. **1960**, *82*, 4436.

(8) E. F. Lutz, G. M. Bailey, *J. Am. Chem. Soc*. **1964**, *86*, 3899.

(9) a) S. Crosignani, G. Desimoni, G. Faita, S. Filippone, A. Mortoni, P. P. Righetti, M. Zema, *Tet. Lett*., **1999**, *40*, 7007-7010; b) M. P. Sibi, J. Chen, *J. Am. Chem. Soc*. **2001**, *123*, 9472-9473; c) M. P. Sibi, K. Itoh, C. P. Jasperse, *J. Am. Chem. Soc*. **2004**, *126*, 5366-5367;d) M. P. Sibi, Z. Ma, K. Itoh, N. Prabagaran, C. P. Jasperse, *Org. Lett*. **2005**, *7*, 2349-2352; e) D. A. Evans, K. R. Fandrick, H.-J. Song, K. A. Scheidt, R. Xu, *J. Am. Chem. Soc*. **2007**, *129*, 10029-10041.

(10) T. Muraki, K. Fujita, M. Kujime, *J. Org. Chem*. **2007**, *72*, 7863-7870.

(11) a) S. Kanemasa, Y. Oderaotoshi, S. Sakagushi, H. Yamamoto, J. Tanaka, E. Wada, D. P. Curran, *J. Am. Chem. Soc*. **1998**, *120*, 3074-3088; b) K. Ishihara, M. Fushimi M.

Akakura, *Acc. Chem. Res.* **2007**, *40*, 1049-1055; c) For examples catalysed by lanthanide salts see: D. A. Evans, H.-J. Song, K. R. Fandrick, *Org. Lett*. **2006**, *8*, 3351; d) For examples catalysed by iminium activation see: A. B. Northrup, D. W. C. MacMillan, *J. Am. Chem. Soc*. **2002**, *124*, 2458-2460; d) For examples catalysed by cavitands see: R. J. Hooley, J. Rebek, Jr. *Org. Biomol. Chem*. **2007**, *5*, 3631-3636.

(12) M. P. Sibi, L. M. Stanley, X. Nie, L. Venkatraman, M. Liu, C. P. Jasperse, *J. Am. Chem. Soc*. **2007**, *129*, 395-405.

(13) a) M. Seitz, S. Stempfhuber, M. Zabel, M. Schütz, O. Reiser, *Angew. Chem. Int. Ed*. **2005**, *44*, 242-245; b) W. Lai, S. M. Berry, D. C. Bebout, *Inorg. Chem*. **2006**, *45*, 571-581; c) P.-K. Chen, Y.-X. Che, Y.-M. Li, J.-M. Zheng *J. Solid State Chem*. **2006**, 2656-2662.

(14) Q. Wang, Y. Zhang, W. J. Rogers, M. S. Mannan, *J. Hazard. Mater*. **2008**, *165*, 141-147.

(15) J. D. Crowley, D. A. Leigh, P. J. Lusby, R. T. McBurney, L.-E. Perret-Aebi, C. Petzold, A. M. Z. Slawin, M. D. Symes, M. D. *J. Am. Chem. Soc*. **2007**, *129*, 15085-15090.

(16) J. D. Crowley, K. D. Hänni, A.-L. Lee, D. A. Leigh, *J. Am. Chem. Soc*. **2007**, *129*, 12092-12093.

(17) J. Bernà, J. D. Crowley, S. M. Goldup, K. D. Hänni, A.-L. Lee, D. A. Leigh, *Angew. Chem. Int. Ed*. **2007**, *46*, 5709-5713.

(18) E. C. Davison, M. E. Fox, A. B. Holmes, S. D. Roughley, C. J. Smith, G. M. Williams, J. E. Davies, P. R. Raithby, J. P. Adams, I. T. Forbes, N. J. Press, M. J. Thompson, *J. Chem. Soc. Perkin Trans. 1*, **2002**, 1494-1514.

Outlook

The publication of the first example of an active-metal template strategy in 2006 marked a new area for the synthesis of mechanically interlocked architectures. The concept was rapidly adopted and expanded through a wide range of metal-catalysed reactions. This idea was exemplified with reactions such as the copper(I)-catalysed alkyne-azide cycladdition (CuAAC), the copper(I)-mediated Ulmann coupling, palladium- and copper-catalysed alkyne homocouplings and heterocouplings, palladium(II)-catalysed oxidative Heck cross-couplings and Michael additions, and Lewis acids-mediated Diels-Alder cycloadditions. In contrast with the passive metal template methods, wherein the metal is used only as a directional scaffold to arrange components into space, the active-metal template strategy takes advantage of both the spatial arrangements and catalytic proprieties of the metal ion to introduce a mechanical bond between three appropriately designed components. No permanent recognition motifs are required on any of the components (i.e. the assembly can be traceless) and the template can often be used in sub-stoichiometric quantities to produce rotaxanes and catenanes in exceptionally high yields. In addition to the construction of simple architectures such as rotaxanes and catenanes, the synthetic strategy can also be used to assemble switchable molecular shuttles with weak intercomponent interactions (a requirement for fast shuttling) and to provide insight into the mechanisms of transition metal-catalysed reactions.

The Leigh group is currently engaged in extending the active-metal template approach to more intricate structures including knots and Borromean rings and in exploring new concepts involving an active template-like clipping methodology or the development of an organocatalytic synthesis of interlocked systems.

Appendix

Published papers

"*The Application of CuAAC 'Click' Chemistry to Catenane and Rotaxane Synthesis*" K. D. Hänni, D. A. Leigh, *Chem. Soc. Rev.* **2010**, DOI: 10.1039/b901974j.

"[2]Rotaxanes through Palladium Active-Template Oxidative Heck Cross-Couplings", J. D. Crowley, K. D. Hänni, A.-L. Lee, D. A. Leigh, *J. Am. Chem. Soc*. **2007**, *129*, 12092-12093.

"Catalytic 'Active-Metal' Template Synthesis of [2]Rotaxanes, [3]Rotaxanes and Molecular Shuttles, and Some Observations on the Mechanism of the Cu(I)-Catalyzed Azide-Alkyne 1,3-Cycloaddition", V. Aucagne, J. Berná, J. D. Crowley, S. M. Goldup, K. D. Hänni, D. A. Leigh, P. J. Lusby, V. E. Ronaldson, A. M. Z. Slawin, A. Viterisi, D. B. Walker, *J. Am. Chem. Soc*. **2007**, *129*, 11950-11963.

"A Catalytic Palladium Active-Metal Template Pathway to [2]Rotaxanes", J. Berná, J. D. Crowley, S. M. Goldup, K. D. Hänni, A.-L. Lee, D. A. Leigh*, Angew. Chem. Int. Ed*. **2007**, *46*, 5709-5713. Highlight: T. M. Swager, R. M. Moslin, *Synfacts*, **2007**, *11*, 1158

"Catalytic 'Click' Rotaxanes: A Substoichiometric Metal-Template Pathway to Mechanically Interlocked Architectures", V. Aucagne, K. D. Hänni, D. A. Leigh, P. J. Lusby, D. B. Walker, *J. Am. Chem. Soc*. **2006**, *128*, 2186-2187.

"Pendant-bridging-chelating-cleavage: A Series of Bonding Modes in Ruthenium(II)-BINAPO Complexes", T. J. GeldBach, A. B. Chaplin, K. D. Hänni, R. Scopelliti, P. J. Dyson, *Organometallics*, **2005**, *24*, 4974-4980.

Rotaxanes

DOI: 10.1002/anie.200701678

A Catalytic Palladium Active-Metal Template Pathway to [2]Rotaxanes**

*José Berná, James D. Crowley, Stephen M. Goldup, Kevin D. Hänni, Ai-Lan Lee, and David A. Leigh**

The preparation of rotaxanes and other mechanically interlocked molecules by the oriented assembly of ligands around metal ions is a classic demonstration[1] of the utility and effectiveness of template-directed synthesis.[2] However, besides organizing the organic fragments through its preferred coordination geometry, the metal template is usually otherwise passive during such reactions. To exploit the richness of the metal's chemistry more fully in synthesis, we recently started to explore a strategy for rotaxane formation in which the metal plays a dual role, acting as both a template for threading and catalyzing covalent-bond formation.[3] Unlike "passive" template methodologies, in which the rotaxane product is normally a better ligand for the metal than the non-interlocked components, this type of "active" template can, in principle, be made to work substoichiometrically. The feasibility of such an approach was first demonstrated[3] using tetrahedral Cu^{I} centers, which is both the most well-established[1b,h,4] coordination geometry for metal template rotaxane-forming reactions and an extremely structurally tolerant catalyst[5] for the azide–alkyne 1,3-cycloaddition (a so-called "click" reaction[6]). Herein we report an application of the active-metal template concept to palladium chemistry, which is rather more demanding in terms of template geometry, but somewhat more significant in terms of catalysis.

The explosive growth in the number and variety of palladium-catalyzed transformations over the latter part of the 20th century has seen palladium become the workhorse of modern synthetic chemistry.[7] Palladium-catalyzed processes include the formation of C–O, C–N, C–S, and, most notably, C–C bonds.[7] Although Pd^{II} has a square-planar coordination geometry, it has proved possible to use its two-dimensional motif to assemble rotaxanes[8] and catenanes[9] in classical passive template strategies by utilizing steric control over the required crossover point in the third dimension.[10]

Macrocycle **1a** (Scheme 1)[9] was chosen as a suitable candidate ligand for developing a palladium active-template rotaxane synthesis. X-ray crystallography of a related palladium(II) [2]catenate shows that the *trans*-coordinated chloride ligands protrude out of opposite sides of the macrocycle

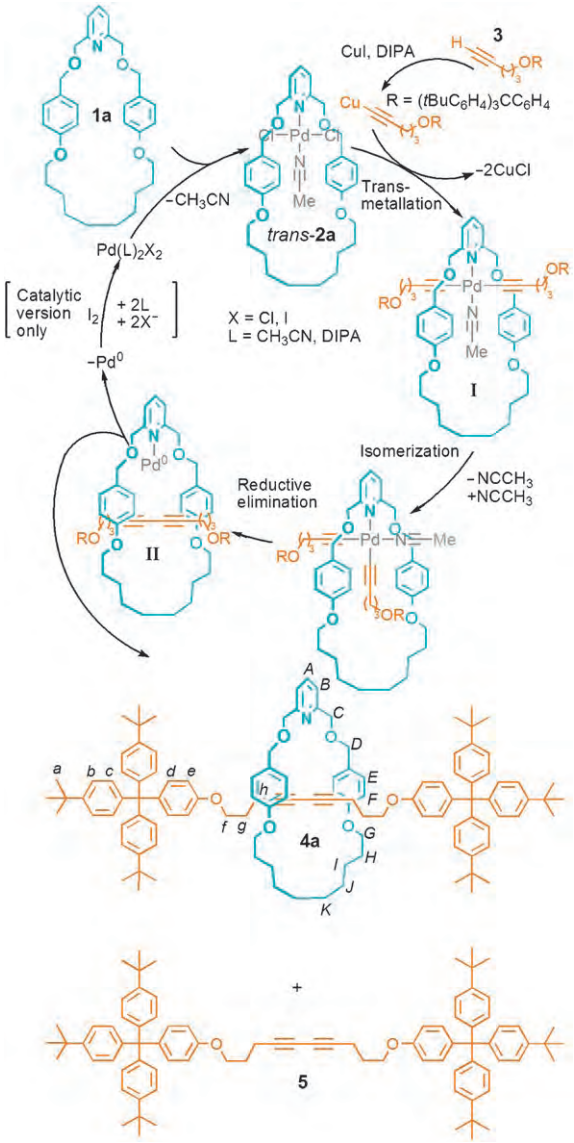

Scheme 1. Pd^{II}-mediated active-metal template synthesis of [2]rotaxane **4a**. For yields and conditions see Table 1.

[*] Dr. J. Berná, Dr. J. D. Crowley, Dr. S. M. Goldup, K. D. Hänni, Dr. A.-L. Lee, Prof. D. A. Leigh
School of Chemistry
The University of Edinburgh
The King's Buildings, West Mains Road, Edinburgh EH9 3JJ (UK)
Fax: (+44) 131-650-6453
E-mail: David.Leigh@ed.ac.uk
Homepage: http://www.catenane.net

[**] This work was supported by the European Union Future and Emerging Technology program Hy3M, the Ramsay Memorial Fellowships Trust, and the EPSRC. D.A.L. is an EPSRC Senior Research Fellow and holds a Royal Society Wolfson Research Merit Award. J.D.C. is a British Centenary Ramsay Fellow.

Supporting information for this article is available on the WWW under http://www.angewandte.org or from the author.

cavity.[9b] We reasoned that if the chloride ligands of *trans*-**2a**[9b] could be replaced by suitably functionalized stopper groups it would generate a threaded complex (e.g. **I**, Scheme 1). If the palladium center is able to retain the stoppered ligands until it has mediated a covalent bond forming reaction between them (**II**, Scheme 1), a [2]rotaxane would be formed.

This idea was investigated using the palladium(II)-mediated homocoupling of terminal alkynes (Scheme 1).[11–13] Complex *trans*-**2a** was treated with 2.5 equivalents of an appropriately derivatized alkyne (**3**) and CuI (5 mol% with respect to **3**) in diisopropylamine (DIPA; Table 1, entry 1).[14]

Table 1: Effect of reactant stoichiometry and experimental conditions on the Pd^{II}-mediated active-metal template synthesis of [2]rotaxane **4a**.[a]

Entry	**1a** [equiv]	*trans*-**2a** [equiv]	**3** [equiv]	I_2 [equiv]	*t* [h]	Conversion **3** → **4** + **5** [%]	Yield[d] of **4a** [%]
1[b]	–	1	2.5	–	12	>98	43
2[b]	–	1	10	–	12	>98	61
3[b]	0.9	0.1	10	0.5	12	37	<1
4[c]	0.9	0.1	10	0.5	12	57	27
5[c]	0.9	0.1	10	0.5	24	83	35
6[c]	0.95	0.05	15	0.5	72	94	81
7[c]	0.95	0.05	30	0.5	72	49	90

[a] Reactions were carried out at 298 K[18] using anhydrous solvents and protected from moisture (see the Experimental Section);[19] [b] 10 mM *trans*-**2a**, CuI (5 mol% with respect to **3**), DIPA; [c] 14 mM macrocycle (**1a** + *trans*-**2a**) CuI (5 mol% with respect to **3**), DIPA (5 equiv), benzene; [d] with respect to **1a** + *trans*-**2a**.

We were delighted to find that after 12 h at room temperature the desired [2]rotaxane **4a** was formed in 43% yield (based on **2a**). The homocoupling reaction essentially proceeded to completion (>98% conversion into the diyne products, rotaxane **4a**, and non-interlocked thread **5**).[15] Carrying out the reaction using a fivefold excess of **3** increased the yield of [2]rotaxane **4a** to 61% (Table 1, entry 2).

The ^{1}H NMR spectrum of **4a** in $CDCl_3$ (Figure 1b) shows an upfield shift of several signals with respect to the non-interlocked components (Figure 1a,c,d). The shielding, which is typical of interlocked architectures in which the aromatic rings of one component are positioned face-on to another component, occurs for all the nonstopper resonances of the axle (H_{f-h}), indicating that in the metal-free rotaxane the macrocycle is able to access the full length of the thread.[16]

The proposed mechanism for rotaxane formation is shown in Scheme 1. Standard Pd ligand-substitution chemistry[7,17] means that under transmetalation the acetylide units should directly replace the chloride ligands of *trans*-**2a**, initially retaining their relative stereochemistry and thus leading to the threaded *trans* palladium bis(alkyne) adduct **I**. Isomerization of **I** to the *cis* geometry necessary for the reductive elimination must occur without breaking either Pd–acetylide bond, as models show that the unthreaded isomer of the *cis* complex (which would generate noninterlocked macrocycle **1a** and thread **5** rather than [2]rotaxane **4a**) would be preferred on steric grounds. Reductive elimination then generates the Pd^0–rotaxane complex **II** and decomplexation of the weakly binding Pd^0 liberates the free rotaxane **4a**.

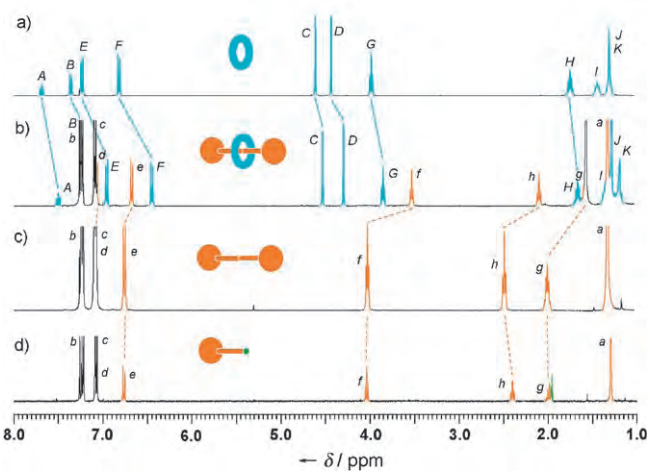

Figure 1. ^{1}H NMR spectra (400 MHz, $CDCl_3$, 300 K) of a) macrocycle **1a**, b) [2]rotaxane **4a**, c) thread **5**, d) half-thread **3**. The assignments correspond to the lettering shown in Scheme 1.

Having achieved an efficient stoichiometric version of the active-metal template reaction, we turned our attention towards developing a synthesis that was catalytic with respect to palladium (Table 1, entries 3–7). This requires the metal to turn over as both a template and a covalent bond forming catalyst. The palladium-mediated alkyne homocoupling reaction is particularly well-suited in this respect because diyne formation is accompanied by reduction of the Pd^{II} to intrinsically weaker coordinating Pd^0. A combination of iodine and oxygen is typically used as the oxidant to render such reactions catalytic.[7]

We initially tried conditions similar to those employed in the stoichiometric rotaxane-forming reaction, but using 10 mol% of *trans*-**2a** in the presence of I_2 (Table 1, entry 3). However, no rotaxane was produced under these conditions and the overall conversion of alkyne to diyne was only 37%. Switching from DIPA to benzene as the solvent led to a significant improvement in both the total yield of diyne products and the formation of [2]rotaxane **4a** (57% and 27%, respectively, entry 4). Increasing the reaction time from 12 to 24 h gave further improvements (83% diyne products; 35% [2]rotaxane, entry 5). Finally, increasing the equivalents of **3**, reducing the loading of **2a** to 5 mol% with respect to **1a**, and further extending the reaction time to 72 h improved the yield of rotaxane **4a** to up to 90% (entries 6 and 7).[18,19]

We used the mono- (**2b**), bi- (**2c**), and tridentate (**2d** and **2e**) macrocycles shown in Scheme 2 (their syntheses are detailed in the Supporting Information) to explore the influence of the nature of the macrocyclic ligand on the active-metal template reaction.[20] Reaction of **2b** or **2c** under the standard stoichiometric conditions resulted in the formation of the corresponding [2]rotaxanes **4b** and **4c**[21] in 38% and 10% yields, respectively (Table 2, entries 1 and 4). The low yield obtained with the bidentate complex **2c** presumably reflects the fact that the two chloride ligands are necessarily *cis* for transmetalation. Even with the larger

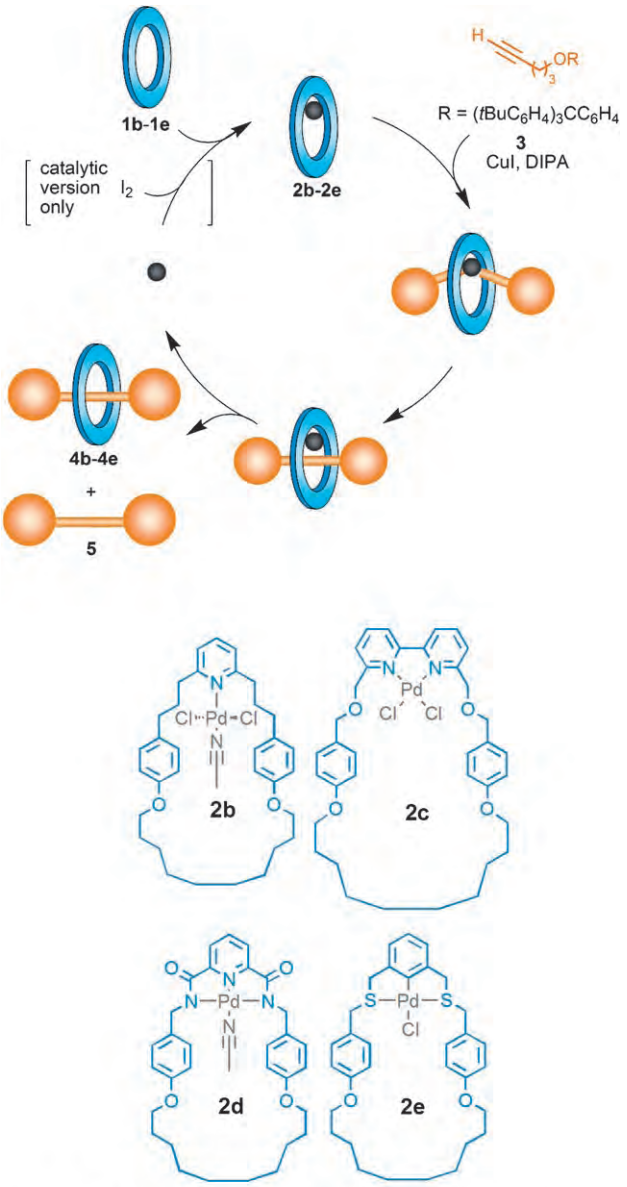

Scheme 2. Screening of different macrocyclic ligands for the palladium(II)-mediated active-metal template synthesis of [2]rotaxanes. For yields and conditions see Table 2.

macrocycle cavity of **2c** relative to **2a**, the *cis* orientation significantly decreases the chance of the two alkyne substitutions occurring through opposite faces of the macrocycle.[22] Carrying out the same reactions in the presence of 10 equivalents of **3** increased the yield of [2]rotaxane **4c** to 20% (Table 2, entry 5) but, to our surprise, resulted in a decrease in the yield of rotaxane **4b** from 38% to 30% (Table 2, entry 2). As expected, reaction of **3** with the tridentate palladium complexes **2d** and **2e** failed to generate any reaction products (Table 2, entries 7 and 8), as two labile coordination sites on the metal are necessary for the alkyne homocoupling mechanism (Scheme 1).

As found earlier for **4a** (Table 1, entries 2 and 7), the yield of rotaxane **4c** was greatly improved (from 20% to 76%; Table 2, entries 5 and 6) by changing from stoichiometric to catalytic palladium conditions. In contrast, the yield of rotaxane **4b** decreased to 14% under similar catalytic conditions, although the overall conversion into diyne products **4b**+**5** is a respectable 63% (Table 2, entry 3). It is possible that this disparity occurs because the benzylic oxygen atoms in **2a** can play a role in dynamic ligation to the palladium center. In their absence the macrocycle is a poorer ligand. Thus, when the amount of alkyne **3** present with respect to **2b** is increased (Table 2, entries 2 or 3), the excess alkyne is able to compete with the pyridine macrocycle for the palladium, thereby reducing the yield of rotaxane **4b**.

Table 2: Effect of macrocycle structure on the Pd^{II}-mediated active-metal template synthesis of [2]rotaxanes (Scheme 2).[a]

Entry	Macrocycle–Pd^{II} complex	**3** [equiv]	*t* [h]	Conversion **3**→ **4**+**5** [%]	Yield[e] of **4b–e** [%]
1[b]	**2b**	2.5	18	82	38
2[b]	**2b**	10	18	75	30
3[c]	**2b**	30	72	63	14
4[b]	**2c**	2.5	18	77	10
5[b]	**2c**	10	18	85	20
6[c]	**2c**	30	72	19	76
7[b]	**2d**	2.5	72	0[d]	0[d]
8[b]	**2e**	2.5	72	0[d]	0[d]

[a] Reactions were carried out at 298 K using anhydrous solvents and protected from moisture (see the Supporting Information); [b] stoichiometric conditions (10 mM **2b–e**): macrocycle–Pd complex **2b–e** (1 equiv), CuI (0.05 equiv), DIPA; [c] catalytic conditions (14 mM **1b**+**2b** or **1c**+**2c**): macrocycle **1b** or **1c** (0.95 equiv), macrocycle–Pd complex *trans*-**2b** or *cis*-**2c** (0.05 equiv), benzene, CuI (5 mol% with respect to **3**), I_2 (0.5 equiv), DIPA (5 equiv); [d] no diyne product was detected; [e] with respect to **2b–e** (entries 1, 2, 4, 5, 7 and 8), **1b**+**2b** (entry 3), or **1c**+**2c** (entry 6).

It is interesting to note that the catalytic conditions with **2a** and **2c** provide much cleaner conversions and higher yields of [2]rotaxanes than the stoichiometric conditions. The use of stoichiometric amounts of Pd^{II}, especially with the solvent concentrations of DIPA required for high conversions in the stoichiometric reactions, probably gives rise to side-reactions and other macrocycle–Pd species that do not afford [2]rotaxane.

The template-directed assembly of otherwise difficult-to-access molecules and the catalysis of covalent-bond formation are two of the most useful tasks that transition metals can perform in organic chemistry. The present work demonstrates that the currently rare combination of these apparently disparate functions can produce high-yielding, mild, and effective synthetic routes to complex molecular architectures that require only substoichiometric amounts of metal. Studies directed towards the design and development of other active template systems are in progress.

Experimental Section

General procedure for catalytic rotaxane synthesis: A 5-mL round-bottomed flask, equipped with a drying $CaCl_2$ tube, was charged with a solution of the terminal alkyne **3** (484 mg, 0.84 mmol) in anhydrous benzene (2 mL). Diisopropylamine (28 mg, 0.28 mmol), copper

iodide (8 mg, 42.0 μmol), macrocycle **1a–c** (26.6 μmol), and iodine (4 mg, 14.0 μmol) were added sequentially. A solution of the corresponding palladium–macrocycle complex **2a–c** (1.4 μmol) in anhydrous benzene (1 mL) was slowly added over a period of 12 h with a syringe pump. When addition was complete the reaction mixture was allowed to stir for a further 72 h after which time the crude product was taken into a partition of dichloromethane and a saturated solution of sodium ethylenediaminetetraacetate (Na_4EDTA, 15 mL) and stirred for 1 h. The layers were separated and the aqueous layer extracted with dichloromethane (2×5 mL). The combined organic extracts were then washed with brine (15 mL), dried over anhydrous magnesium sulfate, filtered, and concentrated under reduced pressure. The resulting residue was purified by column chromatography on silica gel to afford the corresponding [2]rotaxane (**4a** 90%; **4b** 14%; **4c** 76%).

Full details of the experimental procedures and compound characterization are given in the Supporting Information.

Received: April 17, 2007
Published online: June 26, 2007

Keywords: C–C coupling · homogeneous catalysis · palladium · rotaxanes · template synthesis

[1] For reviews that highlight various aspects of template strategies to rotaxanes, see: a) D. B. Amabilino, J. F. Stoddart, *Chem. Rev.* **1995**, *95*, 2725–2828; b) *Molecular Catenanes, Rotaxanes and Knots: A Journey Through the World of Molecular Topology* (Eds.: J.-P. Sauvage, C. Dietrich-Buchecker), Wiley-VCH, Weinheim, **1999**; c) G. A. Breault, C. A. Hunter, P. C. Mayers, *Tetrahedron* **1999**, *55*, 5265–5293; d) T. J. Hubin, D. H. Busch, *Coord. Chem. Rev.* **2000**, *200*, 5–52; e) L. Raehm, D. G. Hamilton, J. K. M. Sanders, *Synlett* **2002**, 1742–1761; f) K. Kim, *Chem. Soc. Rev.* **2002**, *31*, 96–107; g) F. Aricó, J. D. Badjić, S. J. Cantrill, A. H. Flood, K. C.-F. Leung, Y. Liu, J. F. Stoddart, *Top. Curr. Chem.* **2005**, *249*, 203–259; h) C. Dietrich-Buchecker, B. X. Colasson, J.-P. Sauvage, *Top. Curr. Chem.* **2005**, *249*, 261–283; i) E. R. Kay, D. A. Leigh, *Top. Curr. Chem.* **2005**, *262*, 133–177; j) S. J. Loeb, *Chem. Commun.* **2005**, 1511–1518; k) A. Bogdan, Y. Rudzevich, M. O. Vysotsky, V. Böhmer, *Chem. Commun.* **2006**, 2941–2952; l) M. S. Vickers, P. D. Beer, *Chem. Soc. Rev.* **2007**, *36*, 211–225; m) S. J. Loeb, *Chem. Soc. Rev.* **2007**, *36*, 226–235.

[2] *Templated Organic Synthesis* (Eds.: F. Diederich, P. J. Stang), Wiley-VCH, Weinheim, **2000**.

[3] V. Aucagne, K. D. Hänni, D. A. Leigh, P. J. Lusby, D. B. Walker, *J. Am. Chem. Soc.* **2006**, *128*, 2186–2187.

[4] For the earliest Cu^I template syntheses of rotaxanes, based on the seminal catenate template motif conceived in Strasbourg [a) J.-P. Sauvage, *Acc. Chem. Res.* **1990**, *23*, 319–327], see: b) C. Wu, P. R. Lecavalier, Y. X. Shen, H. W. Gibson, *Chem. Mater.* **1991**, *3*, 569–572; c) J.-C. Chambron, V. Heitz, J.-P. Sauvage, *J. Chem. Soc. Chem. Commun.* **1992**, 1131–1133.

[5] a) V. V. Rostovtsev, L. G. Green, V. V. Fokin, K. B. Sharpless, *Angew. Chem.* **2002**, *114*, 2708–2711; *Angew. Chem. Int. Ed.* **2002**, *41*, 2596–2599; b) C. W. Tornøe, C. Christensen, M. Meldal, *J. Org. Chem.* **2002**, *67*, 3057–3064; c) V. D. Bock, H. Hiemstra, J. H. van Maarseveen, *Eur. J. Org. Chem.* **2005**, 51–68; d) P. Wu, V. V. Fokin, *Aldrichimica Acta* **2007**, *40*, 7–17.

[6] H. C. Kolb, M. G. Finn, K. B. Sharpless, *Angew. Chem.* **2001**, *113*, 2056–2075; *Angew. Chem. Int. Ed.* **2001**, *40*, 2004–2021.

[7] a) J. Tsuji, *Palladium Reagents and Catalysts: Innovations in Organic Synthesis*, Wiley-VCH, Weinheim, **1995**; b) *Handbook of Organopalladium Chemistry for Organic Synthesis*, *Vol. 1* (Ed.: E.-i. Negishi), Wiley-VCH, Weinheim, **2002**; c) *Handbook of Organopalladium Chemistry for Organic Synthesis*, *Vol. 2* (Ed.: E.-i. Negishi), Wiley-VCH, Weinheim, **2002**; d) J. Tsuji, *Palladium Reagents and Catalysts: New Perspectives for the 21st Century*, 2nd ed., Wiley, Chichester, **2004**; e) *Metal-Catalyzed Cross-Coupling Reactions*, *Vol. 1*, Completely Revised and Enlarged, 2nd ed. (Eds.: A. de Meijere, F. Diederich), Wiley-VCH, Weinhiem, **2004**, p. 317–394; f) S. S. Stahl, *Angew. Chem.* **2004**, *116*, 3480–3501; *Angew. Chem. Int. Ed.* **2004**, *43*, 3400–3420.

[8] a) A.-M. Fuller, D. A. Leigh, P. J. Lusby, I. D. H. Oswald, S. Parsons, D. B. Walker, *Angew. Chem.* **2004**, *116*, 4004–4008; *Angew. Chem. Int. Ed.* **2004**, *43*, 3914–3918; b) Y. Furusho, T. Matsuyama, T. Takata, T, Moriuchi, T. Hirao, *Tetrahedron Lett.* **2004**, *45*, 9593–9597; c) D. A. Leigh, P. J. Lusby, A. M. Z. Slawin, D. B. Walker, *Angew. Chem.* **2005**, *117*, 4633–4640; *Angew. Chem. Int. Ed.* **2005**, *44*, 4557–4564.

[9] a) A.-M. L. Fuller, D. A. Leigh, P. J. Lusby, A. M. Z. Slawin, D. B. Walker, *J. Am. Chem. Soc.* **2005**, *127*, 12612–12619; b) D. A. Leigh, P. J. Lusby, A. M. Z. Slawin, D. B. Walker, *Chem. Commun.* **2005**, 4919–4921.

[10] Pseudorotaxanes, rotaxanes, and catenanes have also been made featuring Pd^{II} incorporated into the framework of at least one of the components, see: a) M. Fujita, F. Ibukuro, H. Hagihara, K. Ogura, *Nature* **1994**, *367*, 720–723; b) A. Hori, H. Kataoka, T. Okano, S. Sakamoto, K. Yamaguchi, M. Fujita, *Chem. Commun.* **2003**, 182–183; c) C. Dietrich-Buchecker, B. Colasson, M. Fujita, A. Hori, N. Geum, S. Sakamoto, K. Yamaguchi, J.-P. Sauvage, *J. Am. Chem. Soc.* **2003**, *125*, 5717–5725; d) A. Hori, K. Yamashita, T. Kusukawa, A. Akasaka, K. Biradha, M. Fujita, *Chem. Commun.* **2004**, 1798–1799; e) A. Hori, K. Yamashita, M. Fujita, *Angew. Chem.* **2004**, *116*, 5126–5129; *Angew. Chem. Int. Ed.* **2004**, *43*, 5016–5019; f) A. Hori, T. Sawada, K. Yamashita, M. Fujita, *Angew. Chem.* **2005**, *117*, 4974–4977; *Angew. Chem. Int. Ed.* **2005**, *44*, 4896–4899; g) M. Fujita, M. Tominaga, A. Hori, B. Therrien, *Acc. Chem. Res.* **2005**, *38*, 369–378; h) B. A. Blight, K. A. Van Noortwyk, J. A. Wisner, M. C. Jennings, *Angew. Chem.* **2005**, *117*, 1523–1528; *Angew. Chem. Int. Ed.* **2005**, *44*, 1499–1504; i) B. A. Blight, J. A. Wisner, M. C. Jennings, *Chem. Commun.* **2006**, 4593–4595; j) B. A. Blight, J. A. Wisner, M. C. Jennings, *Angew. Chem.* **2007**, *119*, 2893–2896; *Angew. Chem. Int. Ed.* **2007**, *46*, 2835–2838.

[11] For an excellent review of metal-mediated alkyne homocouplings, see P. Siemsen, R. C. Livingston, F. Diederich, *Angew. Chem.* **2000**, *112*, 2740–2767; *Angew. Chem. Int. Ed.* **2000**, *39*, 2632–2657.

[12] The palladium-catalyzed homocoupling of alkynes has attracted considerable attention, see a) Q. Liu, D. J. Burton, *Tetrahedron Lett.* **1997**, *38*, 4371–4374; b) A. Lei, M. Srivastava, X. Zhang, *J. Org. Chem.* **2002**, *67*, 1969–1971; c) V. Gevorgyan in *Handbook of Organopalladium Chemistry for Organic Synthesis*, *Vol. 1* (Ed.: E.-i. Negishi), Wiley-VCH, Weinheim, **2002**, p. 1463–1469; d) J. A. Marsden, J. J. Miller, M. M. Haley, *Angew. Chem.* **2004**, *116*, 1726–1729; *Angew. Chem. Int. Ed.* **2004**, *43*, 1694–1697; e) C. H. Oh, V. R. Reddy, *Tetrahedron Lett.* **2004**, *45*, 5221–5224; f) M. Bandini, R. Luque, V. Budarin, D. J. Macquarrie, *Tetrahedron* **2005**, *61*, 9860–9868; g) A. S. Batsanov, J. C. Collings, I. J. S. Fairlamb, J. P. Holland, J. A. K. Howard, Z. Lin, T. B. Marder, A. C. Parsons, R. M. Ward, J. Zhu, *J. Org. Chem.* **2005**, *70*, 703–706; h) J. Gil-Moltó, C. Nájera, *Eur. J. Org. Chem.* **2005**, 4073–4081; i) J.-H. Li, Y. Liang, Y.-X. Xie, *J. Org. Chem.* **2005**, *70*, 4393–4396; j) J.-H. Li, Y. Liang, X.-D. Zhang, *Tetrahedron* **2005**, *61*, 1903–1907; k) M. Shi, H. Qian, *Appl. Organomet. Chem.* **2006**, *20*, 771–774; l) C. Chen, Z. Ai, J. Lin, X. Hong, C. Xi, *Synlett* **2006**, 2454–2458; m) F. Yang, X. Cui, Y. Li, J. Zhang, G. Ren, Y. Wu, *Tetrahedron* **2007**, *63*, 1963–1969; n) M. Hoffmann, C. J. Wilson, B. Odell, H. L. Anderson, *Angew. Chem.* **2007**, *119*, 3183–3186; *Angew. Chem. Int. Ed.* **2007**, *46*, 3122–3125.

[13] For stoichiometric active-metal template Cu^{I}-mediated Ullman and Glaser coupling rotaxane syntheses, in which the metal does not turnover, see: S. Saito, E. Takahashi, K. Nakazono, *Org. Lett.* **2006**, *8*, 5133 – 5136.
[14] Attempts to generate [2]rotaxanes from various metal acetylides of **3** (Li, Cu, and Zn) with Pd complex *trans*-**2a** in nonbasic solvents were unsuccessful.
[15] This reaction is ligand-accelerated: Repeating the reaction with $Pd(MeCN)_2Cl_2$ in place of *trans*-**2a** resulted in only 20% conversion into the homocoupled product **5** during the same reaction time.
[16] All rotaxanes were fully characterized by ^{1}H and ^{13}C NMR spectroscopy, as well as LRESI-MS and HRMS. ^{1}H NMR stack plots of [2]rotaxanes **4b** and **4c** with their non-interlocked components are provided in the Supporting Information.
[17] For a similar example involving platinum, see: C. J. Adams, S. L. James, P. R. Raithby, *Chem. Commun.* **1997**, 2155 – 2156.
[18] Attempts at increasing the reaction rate by heating to 50 °C, with the other reaction conditions as for Table 1, entry 6, resulted in a lower yield of rotaxane **4a** (47%) and lower overall conversions into diyne products (52%).
[19] Several control reactions were carried out to confirm the necessity of both Pd and Cu. When the conditions used for Table 1, entry 2 (i.e. stoichiometric) or Table 1, entry 6 (i.e. catalytic) were repeated in the absence of Pd (i.e. with macrocycle **1a** replacing the Pd complex **2a**), no diyne products were detected by ^{1}H NMR spectroscopy. Thus, under these conditions the Cu^{I}-mediated Glaser alkyne homocoupling[11] does not operate to any significant extent (< 1%). Similarly, when the same reactions were run in the absence of CuI instead of in the absence of Pd, no diyne products were detected by ^{1}H NMR spectroscopy.
[20] The pyridine coordination site on the macrocycle is crucial for rotaxane formation. When the conditions used for Table 1, entry 1 were repeated with the non-pyridine version of macrocycle **1a** (pyridine replaced by benzene), no rotaxane was detected and non-interlocked thread **5** was formed in only 19% yield after 3 days. See the Supporting Information for further details.
[21] A further decomplexation reaction using KCN in MeOH/CH_2Cl_2 was necessary before [2]rotaxane **4c** could be isolated.
[22] For an X-ray crystal structure of **2c** and the corresponding crystallographic data, see the Supporting Information.

The application of CuAAC 'click' chemistry to catenane and rotaxane synthesis†

Kevin D. Hänni and David A. Leigh*

Received 1st September 2009
First published as an Advance Article on the web
DOI: 10.1039/b901974j

The copper(I)-catalysed azide–alkyne cycloaddition (the CuAAC 'click' reaction) is proving to be a powerful new tool for the construction of mechanically interlocked molecular-level architectures. The reaction is highly selective for the functional groups involved (terminal alkynes and azides) and the experimental conditions are mild and compatible with the weak and reversible intermolecular interactions generally used to template the assembly of interlocked structures. Since the CuAAC reaction was introduced as a means of making rotaxanes by an 'active template' mechanism in 2006, it has proven effective for the synthesis of numerous different types of rotaxanes, catenanes and molecular shuttles by passive as well as active template strategies. Mechanistic insights into the CuAAC reaction itself have been provided by unexpected results encountered during the preparation of rotaxanes. In this *tutorial review* we highlight the rapidly increasing utility and future potential of the CuAAC reaction in mechanically interlocked molecule synthesis.

1. Introduction

A quarter of a century after the first template synthesis of a mechanically interlocked molecule,[1] there now exists a plethora of strategies for the construction of mechanically bonded molecular-level structures. Rotaxanes, catenanes, knots and links have all been accessed *via* template methods using a diverse range of recognition motifs, such as electron-rich–electron-poor π-stacking systems, hydrogen bonding and metal ion coordination.[2] These molecules, in which some of the components are connected mechanically rather than by covalent bonds, could potentially find application in the modification of physical and chemical properties,[1] encapsulating and delivering substrates (such as dyes and drugs),[3,4] as smart materials with switchable surface properties[5,6] and in molecular electronics[7,8] and other types of molecular machinery.[9]

Three distinct approaches[10] have been devised for the template synthesis of rotaxanes and catenanes (Scheme 1):

(i) The *capping* (or threading-followed-by-stoppering) method[11] involves the covalent capture of a threaded supramolecular complex (a pseudorotaxane) by attachment of two bulky units at each end of the linear thread to give the corresponding rotaxane. The bulky 'stoppers' prevent disassociation

School of Chemistry, University of Edinburgh, The King's Buildings, West Mains Road, Edinburgh, UK EH9 3JJ.
E-mail: David.Leigh@ed.ac.uk; Fax: +44 (0)131 650 6453
† Part of a themed issue reviewing the applications of click chemistry.

Kevin Hänni

Kevin Hänni obtained his MSc degree in biological and molecular chemistry in April 2006 from the Swiss Federal Institute of Technology (EPFL). For his Masters thesis project he introduced (with Dr V. Aucagne) the 'active metal template' concept for the synthesis of mechanically interlocked architectures using the CuAAC reaction, conducted in Prof. Leigh's group at the University of Edinburgh. He was awarded the Ciba Spécialités Chimiques Prize for this work. Kevin subsequently pursued a PhD with Prof. Leigh, expanding on the concepts he introduced in his Masters thesis. His PhD work was awarded the RSC Laurie Vergnano Prize in 2008.

David Leigh

David Leigh is the Forbes Professor of Organic Chemistry and an EPSRC Senior Research Fellow at the University of Edinburgh. His research interests include the synthesis of catenanes and rotaxanes and the development of new paradigms and mechanisms for synthetic molecular-level motors and machines. In 2009 he was elected a Fellow of the Royal Society.

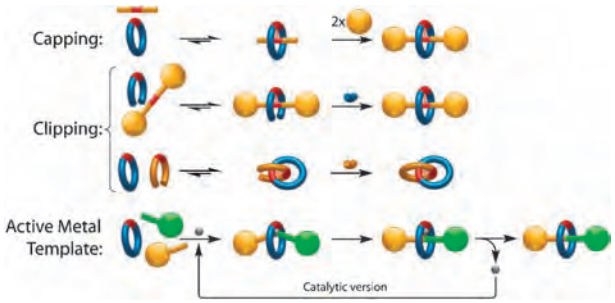

Scheme 1 Template strategies for the synthesis of rotaxanes and catenanes.

(dethreading) of the macrocycle and, since the breaking of a covalent bond is then required to disassemble the structure, the rotaxane is a molecule not a supramolecular complex.[10]

(ii) The *clipping* approach,[12] in which the interlocked structure is obtained by macrocyclisation of an acyclic ligand around the template site of an already stoppered thread (rotaxane) or another macrocycle (catenane).

(iii) The *active metal template* strategy,[13] where the substrate used as a template also plays an active role in promoting the crucial covalent bond formation used to capture the interlocked structure.

Although a number of different types of reactions have been used to covalently capture interlocked architectures, the most widely used in the early years of template-directed catenane and rotaxane synthesis were Williamson ether synthesis, amide and ester bond forming reactions, Glaser and Eglinton couplings, imine-bond formation, metal–ligand coordination and the Kröhnke alkylation of pyridines with alkyl halides.[2] The invention[14] of highly efficient ring-closing olefin metathesis (RCM) catalysts significantly increased the yields of many catenane and rotaxane template strategies.[15–18] There are three principal reasons for the effectiveness of RCM in these mechanical bond forming reactions:

(i) The intrinsic high functional group specificity of the reaction—it is highly selective and few other groups interfere with the reaction or are incompatible with the reaction conditions.

(ii) The reaction can be carried out in relatively non-polar solvents in which the non-covalent interactions generally used to template the interlocked architecture are maximised.

(iii) The reactive end-groups are sufficiently stable, even when attached to the transition metal catalyst, that they react overwhelmingly in the desired fashion even when accessing the required reaction geometry is a rare event (as it is for the cyclisation of large rings). The yield of interlocked *versus* non-interlocked products then depends on how effectively the template pre-organises the ring-closing reaction to take place while one component is threaded through the cavity of the other.

The Huisgen–Meldal–Fokin Cu(I)-catalysed 1,3-cycloaddition of azides with terminal alkynes (the CuAAC 'click' reaction[19–22]) also fulfills these criteria—indeed, it is even more functional group specific, substrate tolerant and higher yielding than typical RCM reactions—and so it is unsurprising that its discovery and development has rapidly led to it becoming a—perhaps even the—reaction of choice for catenane and rotaxane synthesis.[23]

To date the CuAAC reaction has been used in catenane and rotaxane synthesis in four different ways: to build hard-to-obtain structures by linking together small fragments into bigger and more complex structures or covalently capturing threaded supramolecular complexes, the modification of pre-existing structures (including decoration and post-synthetic functionalisation), the combination of both of these approaches where the CuAAC is used to link building blocks *and* as a functionalisation tool, and finally the use of pre-formed triazole rings as ligands for the assembly of, and to play a role in controlling the dynamics of, mechanically interlocked architectures.

2. Rotaxanes containing triazole rings

Early examples of triazole-containing rotaxanes were prepared by Mock in the 1980's[24] and Stoddart in the 1990's.[12] Mock established that cucurbit[6]uril (CB[6]) is able to bind ammonium-derivatised alkyl azides and alkynes and hold the reactive functional groups in close proximity to each other, promoting their cycloaddition.[24–26] When bulky *tert*-butyl groups were used as the second alkyl group on the secondary ammonium salts (*e.g.* **1** and **2**), the reaction inside CB[6] gave [2]rotaxane **3** in 76% yield (Scheme 2a).[24] This approach has subsequently been used to produce a series of cucurbituril-based[27] rotaxanes[28,29] and pseudorotaxanes.[30] Stoddart employed the thermal (*i.e.* uncatalysed) Huisgen 1,3-azide–alkyne cycloaddition[31] to convert **4** (which forms pseudorotaxane **5** with dibenzo-24-crown-8) into [2]rotaxane **6** in 31% yield (Scheme 2b). The modest yield of rotaxane **6**, despite the near quantitative formation of the threaded supramolecular complex **5**, is typical of the poorly effective methods for covalent capture employed in that era.

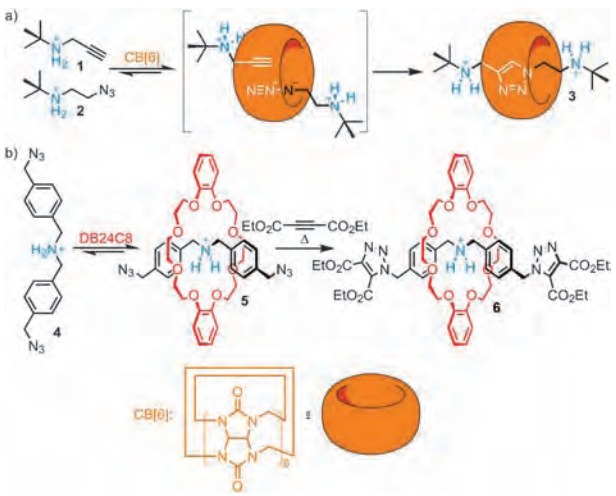

Scheme 2 (a) Mock's synthesis of [2]rotaxane **3**, utilising the ability of CB[6] to catalyse the cycloaddition between **1** and **2**.[24] (b) Stoddart's synthesis of [2]rotaxane **6**, exploiting the binding of secondary dialkylammonium salts by crown ethers through capping of the resulting pseudorotaxane intermediate **5** *via* a Huisgen 1,3-dipolar azide–alkyne cycloaddition.[12]

2.1 CuAAC active-metal template synthesis of rotaxanes

In 2006 the copper(I)-catalysed version of the azide–alkyne cycloaddition was first used to prepare mechanically interlocked architectures.[32] The CuAAC reaction formed part of a strategy in which both the preferred coordination geometry of a metal ion (in this case Cu(I)), and its catalytic properties, are used to both template the assembly and promote the formation of the covalent bond that captures the interlocked structure (the active metal template strategy, Scheme 1).[32,33]

It was envisaged that the tetrahedral arrangement of ligands about Cu(I) should direct the CuAAC reaction of appropriately 'stoppered' alkyne and azide units through the cavity of pyridine and bipyridine macrocycles **7a–c** to afford the corresponding [2]rotaxanes. Indeed, stirring an equimolar mixture of the pyridine-containing macrocycle **7a**, alkyne **8**, azide **9**, and $Cu(MeCN)_4PF_6$ in CH_2Cl_2 for 24 h afforded—after demetalation with KCN—a mixture of [2]rotaxane **10a** and non-interlocked thread **11** in 57% and 41% yield, respectively (Scheme 3).[32]

Reaction conditions were optimised using a five-fold excess of both **8** and **9** (yielding 94% of **10a**). Addition of pyridine as a competitive ligand—in order to remove the metal catalyst from the sequestrating rotaxane—enabled the catalyst to turn over, giving 82% (incorrectly reported as 38% in ref. 23) of rotaxane **10a** using only 20 mol% Cu(I). This marked the first time that only catalytic quantities of a template were necessary to synthesise a mechanically interlocked architecture.

In addition to the strongly coordinating pyridine nitrogen, macrocycle **7a** has two ether oxygen atoms that could potentially be involved in (albeit weak) coordination to the metal atom during the active metal template reaction (Scheme 3). To test whether other macrocycle geometries would be tolerated by the active-template reaction, macrocycle **7b**—in which the substituted benzylic units are replaced by aryl groups—was tested.[27] The aromatic rings flanking the pyridine in **7b** sterically encumbers the nitrogen donor atom, and a combination of sterics and electronic factors probably reduces the binding affinity of this ligand for Cu(I) ions. The weaker binding leads to more ligand Cu(I) (*i.e.* not bound to macrocycle) in solution, resulting in higher conversion of the building blocks into non-interlocked thread **11** and a relatively modest yield of [2]rotaxane **10b** (25%). The bipyridine macrocycle **7c** directs the CuAAC reaction through its cavity to form rotaxane almost as efficiently as **7a** (45% of rotaxane **10c**). However, the rate of the CuAAC reaction is severely inhibited by this ligand and the reaction took 3 days to go to completion. The sluggish reactivity is likely a result of the steric bulk around the Cu(I) centre in the complex changing the course of the productive mechanism of the CuAAC reaction (*vide infra*).[33]

2.1.1 The unexpected formation of [3]rotaxanes. In an attempt to minimise the amount of ligand-free Cu(I) (which causes formation of the non-interlocked thread) in the active-template CuAAC reaction, the effect of carrying out the reaction with 10 equivalents of macrocycle **7b** was investigated.[33] This resulted in the unexpected formation of [3]rotaxane **12b** in 37% yield (Scheme 4). The only way in which *two*

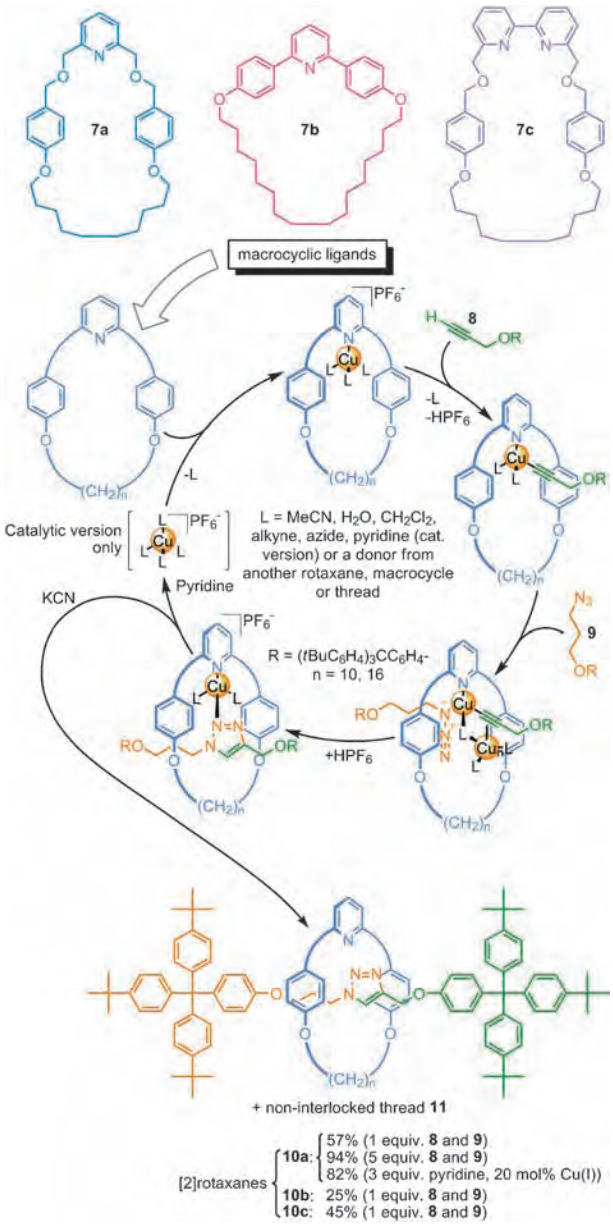

Scheme 3 Active metal template synthesis of [2]rotaxanes **10a–c** *via* the CuAAC reaction.[32,33]

Cu(I)-binding macrocycles can be threaded onto an axle when only *one* triazole is being formed is for two Cu(I) ions to be involved in the dominant mechanism of the CuAAC reaction. Such a bimetallic intermediate had been proposed by Rodionov *et al*. in 2005.[34]

The slowing down of the reaction rates when 10 equivalents of macrocycle are used was also strongly suggestive that the dominant mechanism of the CuAAC reaction under these conditions involved the activation of the copper-σ-acetylide by a second (probably not coordinated to the macrocycle for steric reasons) copper atom. No [3]rotaxane was observed with bidentate ligand **7c**, which when complexed to Cu(I) does not leave sufficient coordination sites to proceed *via* a bimetallic intermediate mechanism, and so it seems likely that the monodentate pyridine ligand promoted CuAAC reaction

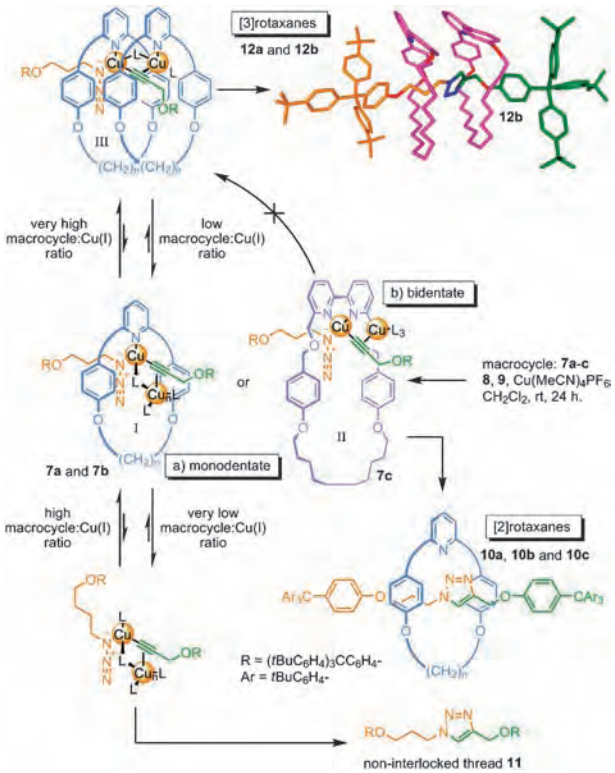

Scheme 4 Effect of the macrocycle: Cu(I) ratio on the active metal template CuAAC reaction.[33]

proceeds *via* a bridged intermediate such as **I** (and **III**), while the bidentate bipyridine ligand promoted CuAAC active-template reaction occurs *via* a simple π-coordinated complex such as **II** (Scheme 4).

2.2 Copper(I)-template [2]rotaxanes using CuAAC as a capping reaction

Sauvage and co-workers were the first to apply the CuAAC reaction to traditional 'passive template' rotaxane synthesis (Scheme 5).[35] Phenanthroline macrocycle **13** and bipyridine diazide rod **14** were complexed with a stoichiometric amount of $Cu(MeCN)_4PF_6$ in CH_2Cl_2–MeCN 1 : 1 to give Cu(I)–pseudorotaxane **15**. Subjecting **15** to a CuAAC capping reaction with stopper **8** ($Cu(MeCN)_4PF_6$, Na_2CO_3, CH_2Cl_2–MeCN 1 : 1, rt for 21 h) provided Cu(I)–rotaxane complex **Cu-16** in 62% yield. Use of a more sterically restricted phenanthroline-based axle increased the stability of the complex to the CuAAC reaction conditions, generating the corresponding Cu(I)–rotaxane complex in 67% yield.[36]

2.3 Octahedral metal template [3]rotaxanes using CuAAC as a capping reaction

The Strasbourg group have explored a passive template methodology which exploits the assembly of three distinct bidentate ligands around a single transition metal centre (Scheme 6). Triply entwined complexes, such as **19**, could be generated around various octahedral transition metal ions, such as Ru(II), Fe(II) and Co(III), using bis-isoquinoline **17a** (R = Me).[37] This motif was used to create a [3]rotaxane[38] **21**, which unusually features two axles threaded through a single

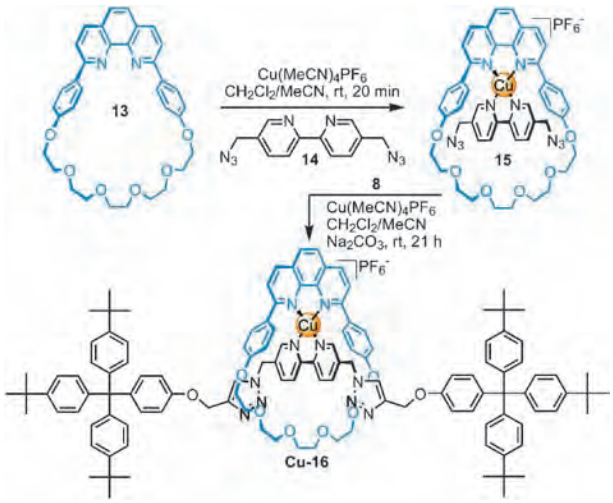

Scheme 5 Copper(I) template synthesis of [2]rotaxane **Cu-16**.[35,36]

macrocycle (Scheme 6).[39,40] Two bis-isoquinoline rods derivatised with azide groups at each end (**17b**) were threaded through the cavity of macrocycle **18** to generate metal complexes **M-20** (M = Fe(II) or Co(III)). Stoppering with bulky alkyne unit **8** *via* the CuAAC reaction afforded $\mathbf{Fe^{II}}$**-21** and $\mathbf{Co^{III}}$**-21** in good yields (82% and 89%, respectively). The iron(II)–rotaxane complex was stable to mild conditions (Na_3-HEDTA, MeOH–CH_2Cl_2 1 : 1, room temperature) for attempted demetallation, while harsher conditions (Cs_2CO_3, DMF, 70 °C) which removed the metal ion also resulted in the dethreading of the two stoppered threads from the cavity. The metal-free [3]rotaxane could be obtained, however, by replacing iron(II) as the template with cobalt(III).[23] Oxidation of Co(III) into labile Co(II) made the rotaxane decomplexation quick and efficient (Na_3HEDTA, DMSO) affording the metal-free [3]rotaxane **21** in quantitative yield. The dethreading process[36] of metal-free **21** was followed by ^{1}H NMR and its half-life was determined to be one week in CH_2Cl_2 at room temperature.

2.4 π-Stacking rotaxanes using CuAAC as a capping reaction

The Stoddart group have employed the CuAAC reaction in the preparation of a range of rotaxanes, catenanes, lariats and molecular shuttles.[41–46] The viologen units used in Stoddart-type interlocked molecules are notoriously sensitive to bases, reducing agents and nucleophiles and so the mild conditions of the CuAAC reaction are well-suited for assembling these sometimes difficult to handle building blocks.

Threading of a bis-azide functionalised π-electron-rich 1,5-dioxynaphthalene (DNP) rod (**22**) through a π-electron-poor cyclobis(paraquat-*p*-phenylene) ($CBPQT^{4+}$) macrocycle (**23**) afforded pseudorotaxane **24** (Scheme 7).[41] This was covalently captured using the CuAAC reaction and alkyne stopper **25** to give the corresponding [2]rotaxane (**26**). The yield is good (82% at −10 °C) compared to other capping methods for this assembly system, although for the $CBPQT^{4+}$ tetrafluoro derivative **22b** the yield of rotaxane (**26**) falls to just 11%. Similar methodology was used to prepare lariat compound **27** in 43% yield (Scheme 7b).[42]

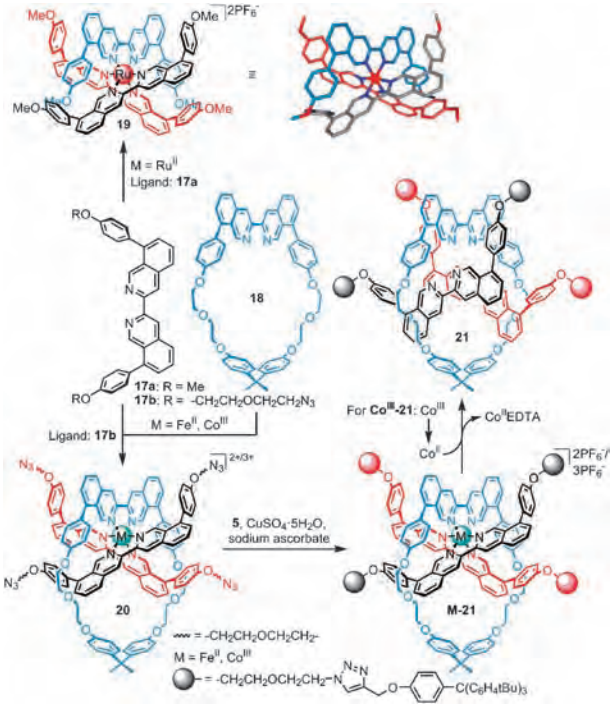

Scheme 6 Octahedral metal template synthesis of [3]rotaxane[38] **21**.[37,39,40]

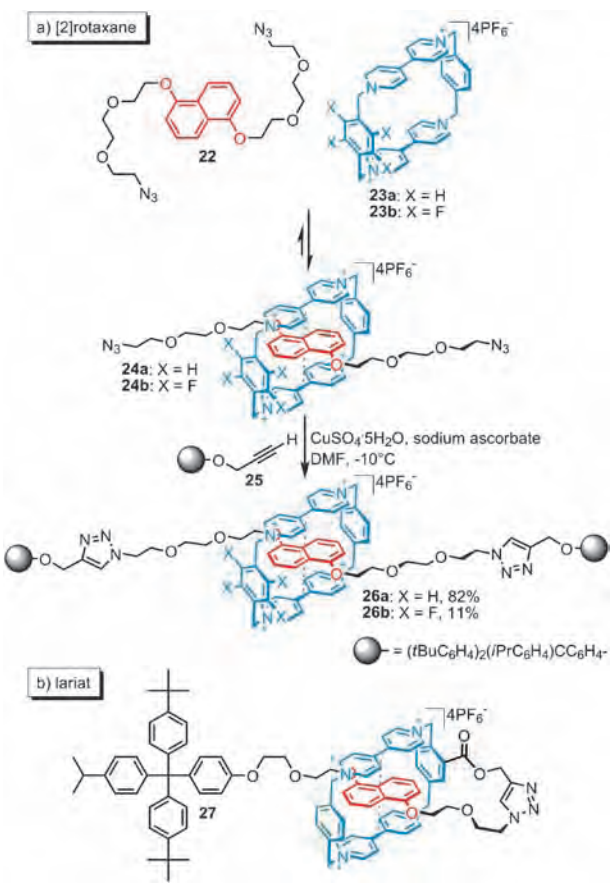

Scheme 7 Synthesis of (a) [2]rotaxanes **26a** and **26b** and (b) lariat **27** by CuAAC capping methodology.[41,42]

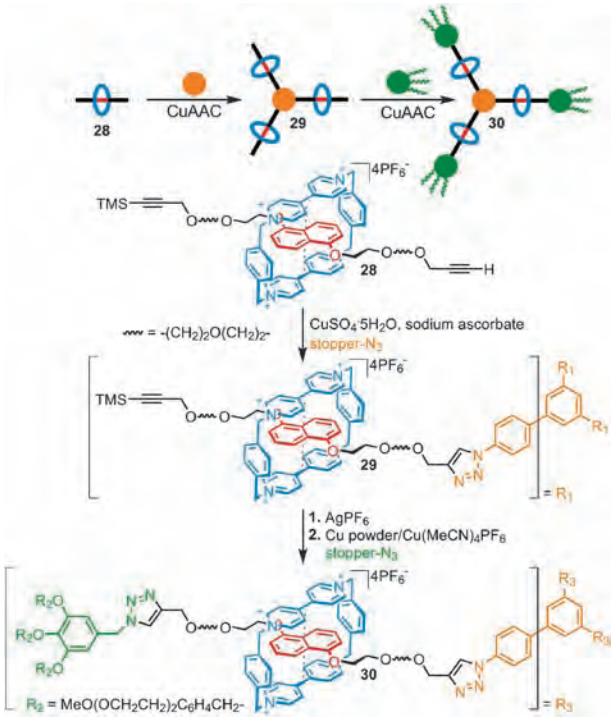

Scheme 8 CuAAC 'click–click' chemistry for the preparation of branched [4]rotaxane **30**.[49]

The syntheses of more complex structures, such as [3]rotaxanes, [4]rotaxanes, polyrotaxanes, polycatenanes and molecular shuttles, has also been accomplished using the CuAAC stoppering reaction.[43–47] Using a sequential 'click–click' CuAAC technique previously developed for oligopeptide ligation,[48] a one-pot synthesis of branched [4]rotaxanes was achieved (Scheme 8).[49] A DNP-containing thread bearing both terminal and TMS-(trimethylsilyl-) protected alkynes was treated with the $CBPQT^{4+}$ macrocycle **23a** to form the corresponding pseudorotaxane **28**. The first azide-derivatised bulky stopper (orange, Scheme 8) was attached using a standard CuAAC stoppering reaction (DMF, $CuSO_4 \cdot 5H_2O$–ascorbic acid, 25 °C) affording TMS-protected [4]pseudorotaxane **29**. *In situ* removal of the TMS-protecting group with $AgPF_6$, followed by reaction with a second azide-derivatised stopper (green, Scheme 8) under a second set of 'click–click' CuAAC conditions ($Cu/Cu(MeCN)_4PF_6$, DMF, rt), provided the branched [4]rotaxane **30** in excellent yield (>98%).

2.5 Cyclodextrin-based lariats, threaded complexes and supramolecular polyrotaxanes using CuAAC as a linking reaction

Cyclodextrins (CDs) form threaded inclusion complexes driven primarily by hydrophobic interactions. Chen's group have used triazole chemistry to covalently connect the host and guest in threaded β-cyclodextrin-based azobenzene complexes (Scheme 9).[50] A supramolecular polyrotaxane (**35**), CD-lariat (**33**) and self-threaded supramolecular dimer (**34**) could each be prepared in good yield (69–71%) from the same building blocks (azido-β-CD derivative **31** and azobenzene-alkyne **32**) by varying the reaction conditions (Scheme 9). Covalent

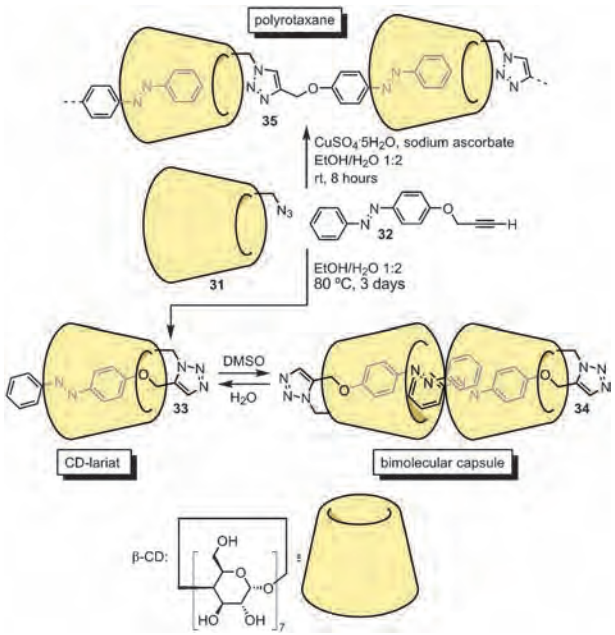

Scheme 9 Covalent linking of the threaded components of azobenzene-β-CD complexes *via* the thermal Huisgen cycloaddition (lariat **33** and self-threaded dimer **34**) and the CuAAC reaction (supramolecular polyrotaxane **35**).[50]

linking of the components of the pseudorotaxane intermediate by a thermal Huisgen 1,3-cycloaddition (EtOH–H_2O 1 : 2 at 85 °C for 3 days) yielded the 1,5-triazole-containing lariat **33** (Scheme 9). In water, **33** spontaneously forms dimer **34**, a capsular structure in which the threaded azobenzene rods are also complexed by the adjacent β-CD's cavity, a structure characterised in solution by ^{1}H NMR and maintained in the solid state, as determined by X-ray crystallography. In DMSO, however, ^{1}H NMR spectroscopy shows that the molecules largely exist as the monomeric lariat **33**. Covalent coupling of the components of the pseudorotaxane with the CuAAC reaction ($CuSO_4 \cdot 5H_2O$, Na ascorbate, EtOH–H_2O 1 : 2, rt, 8 h), however, led to the 1,4-triazole-containing isomer which formed the supramolecular polyrotaxane **35** (Scheme 9, top). The authors were able to observe the supramolecular polyrotaxane **35** by high resolution TEM imaging and the trimer could be detected by FTICR-MS.

2.6 Cyclodextrin-based [2]-, [3]- and higher rotaxanes using CuAAC as a capping and linking reaction

The spontaneous threading of CDs onto a linear aliphatic thread in aqueous solution can provide [*n*]pseudorotaxanes in a facile and efficient way, the corresponding [*n*]rotaxanes being obtained by aqueous-tolerant stoppering reactions. α-CD-based [2]-, [3]- and higher order rotaxanes could all be prepared from pseudorotaxane **38** (assembled from mono-stoppered axle **36** and lactose-derivatised α-CD **37**) under CuAAC reaction conditions ($CuSO_4 \cdot 5H_2O$, Na ascorbate, H_2O) with various mono- and di-alkyne linkers and stoppers in modest to good yields (Scheme 10).[51] [2]Rotaxane **40** was synthesised in 54% yield by reacting **38** with alkyne stopper **39** (Scheme 10a). Replacing **39** with dialkyne thread **41** under these reaction conditions gave [3]rotaxane **42** (24%) as the major product, together with smaller amounts of the corresponding [2]- and [4]-rotaxanes (Scheme 10b). [4]Rotaxane **44** (27%) and [6]rotaxane **45** (67%) were obtained by reacting **36** and extended dialkyne thread **43** with 3 and 15 equivalents of Lac-CD **37**, respectively (Scheme 10c). The average number of CDs threaded were determined by ^{1}H NMR and MS experiments. Lactose is a potent inhibitor of *Arachis hypogaea* peanut lectin,[52,53] and high lectin binding affinities were determined for the [4]rotaxane **44** (five lactose units) and [6]rotaxane **45** (seven lactose units) in enzyme-linked lectin assays.

2.7 Squaraine-based [2]rotaxanes using CuAAC as a capping reaction

Rotaxanes with squaraine-dye-based axles and amide macrocycles have been prepared by capping hydrogen bonded pseudorotaxanes using the CuAAC reaction (Scheme 11).[54] [2]Rotaxanes **47** and **48** were prepared in 40% and quantitative yields, respectively, from a bis-alkyne thread, amide macrocycles and azide-terminated stopper groups (Scheme 10).

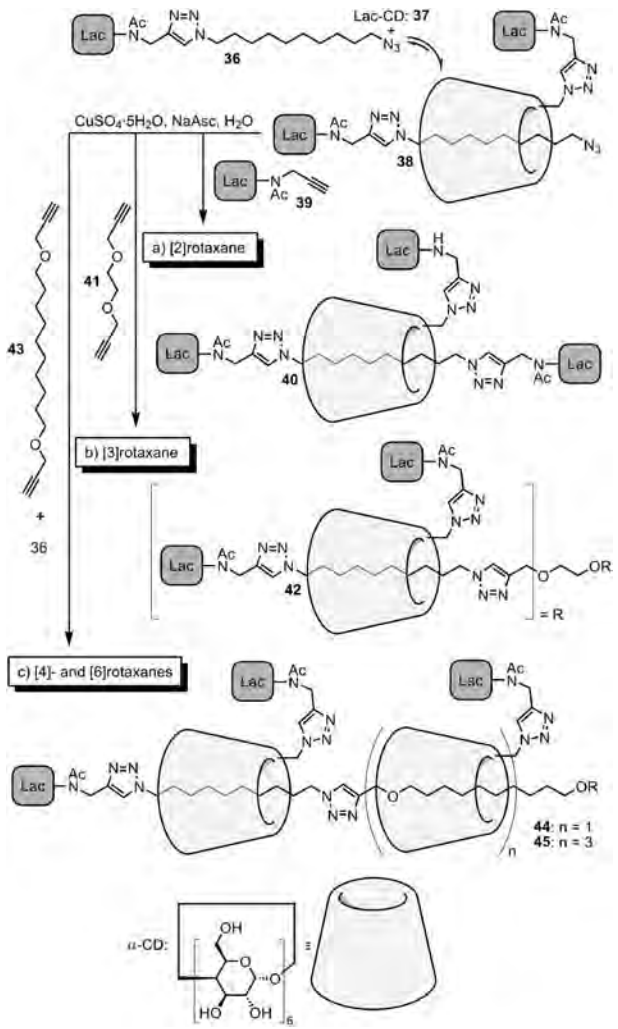

Scheme 10 Lactose-derivatised α-CD-based rotaxanes accessed *via* CuAAC capping and linking reactions. (a) [2]Rotaxane **40**, (b) [3]rotaxane **42** and (c) [4]rotaxane **44** and [6]rotaxane **45**.[51]

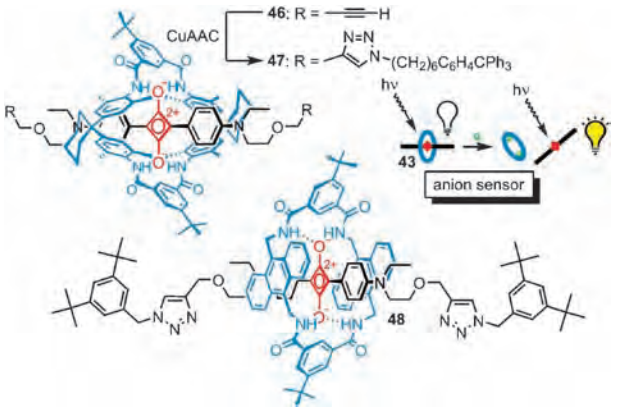

Scheme 11 Squaraine [2]rotaxane **47** and **48** obtained through CuAAC capping reactions. Pseudorotaxane **46** acts as an anion sensor through the dethreading of the macrocycle by competitive binding with various anions (Cl^-, AcO^-, BzO^-).[54]

The rotaxane architecture modifies the photophysical properties of the squaraine dye in significant ways. Rotaxane **47** has a 3-fold decrease in fluorescence quantum yield compared with the non-interlocked thread (Φ = 0.24 and Φ = 0.65, respectively). The fluorescence of pseudorotaxane **46** is similarly quenched by the macrocycle hydrogen bonding to the dye, but treatment of **46** with tetrabutylammonium chloride, acetate or benzoate salts results in decomplexation of the pseudorotaxane and the fluorescence intensity of the squaraine unit is restored. Both rotaxanes **47** and **48** exhibit an intense IR absorption/emission spectra and are being investigated as possible motifs for molecular probes for biological imaging.

2.8 Halide–triazolium template formation of [2]rotaxanes

Beer's group has imaginatively used the triazolium group itself (made by methylation of a triazole ring formed by a CuAAC reaction) to template the formation of rotaxanes *via* halide–triazolium ion pairing (Fig. 1).[55] Triazole-containing thread **11** (see Schemes 3 and 4) was methylated (Me_3OBF_4) in close-to-quantitative yield. Three-component complexation of the methylated thread, tetrabutylammonium chloride and an isophthalamide bis-olefin unit known to bind Cl^- ions through hydrogen bonding, followed by RCM, yielded the chloride-complexed triazolium-rotaxane **49-Cl** in 21% yield. The chloride ion could be removed by washing with a solution of NH_4PF_6. The yield is slightly improved (31%) using bromide ion instead of chloride.

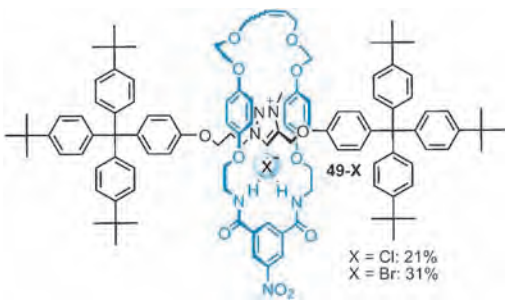

Fig. 1 Beer's anion-complexed rotaxanes **49-Cl/Br**, assembled *via* a halide–triazolium ion pair template.[55]

3. Molecular shuttles constructed *via* CuAAC

One of the most interesting features of rotaxanes and catenanes is that, as they are not covalently attached to one another, their mechanically interlocked components can often undergo large amplitude motions with respect to each other.[9] These 'molecular shuttles' are seen as prototypical building blocks for various types of molecular machinery.[9]

As a consequence of the template methods employed in their synthesis, rotaxanes often have thread binding sites for the macrocycle between which the ring moves under random thermal motion ('shuttling'). If the binding sites are identical this is often referred to as a 'degenerate' molecular shuttle. If the binding sites are different, however, a net change of position of the macrocycle on the thread can sometimes be brought about by use of an external signal, constituting a type of molecular switch. These stimuli-switchable shuttles have been shown to operate through a wide variety of different stimuli including pH changes, competitive binding, redox control and light.[9]

3.1 Degenerate molecular shuttles containing triazole rings

Using CuAAC active metal template methodology,[33] molecular shuttles can be efficiently prepared with two triazole rings on the thread of a [2]rotaxane. [2]Rotaxane **50** was assembled in good yield (81%) through the coupling of a bis-azide unit with alkyne stopper **8** (analogous to the types of reactions shown in Scheme 3).

Since triazole rings can act as ligands for transition metal ions, the two triazole groups in **50** can function as binding sites for a metal-coordinated macrocycle (Scheme 12). For Cu(I) complex (**Cu-50**), the ^{1}H NMR spectrum shows that the Cu-macrocycle unit shuttles rapidly between the two triazole ligands at room temperature (CD_2Cl_2–CD_3CN 1 : 9, 298 K). In contrast, the ^{1}H NMR spectrum of **Pd-50** shows that the Pd-macrocycle unit is kinetically locked to one triazole station on the NMR time scale, even at 343 K.[33]

3.2 Rh–porphyrin-based molecular shuttles

Mullen and Gunther have also used the coordinating abilities of the triazole group in molecular shuttles (Scheme 13).[56] A bis-alkyne-functionalised diimide axle forms a pseudorotaxane with a DNP macrocycle bearing a zinc–porphyrin unit. Stoppering through the CuAAC reaction (DIPEA, Cu(MeCN)$_4$BF$_4$, toluene, rt, 8 d) yielded the Zn–rotaxane **Zn-51** in 20% yield. ^{1}H NMR studies ($CDCl_3$, 298 K) showed that the triazole ring is not coordinated to the Zn atom and the porphyrin is located over the diimide unit of the thread. Exchanging Zn(II) for Rh(III) *via* the metal-free porphyrin rotaxane (**51**) afforded **Rh-51**. In contrast to **Zn-51**, the ^{1}H NMR spectrum of rotaxane **Rh-51** shows fast shuttling of the Rh–porphyrin unit between the two triazole stations. At −20 °C the Rh–porphyrin unit is localised to only one triazole ring on the NMR time scale. Attempts to remove the rhodium ion from **Rh-51** whilst maintaining the rotaxane structure were unsuccessful.

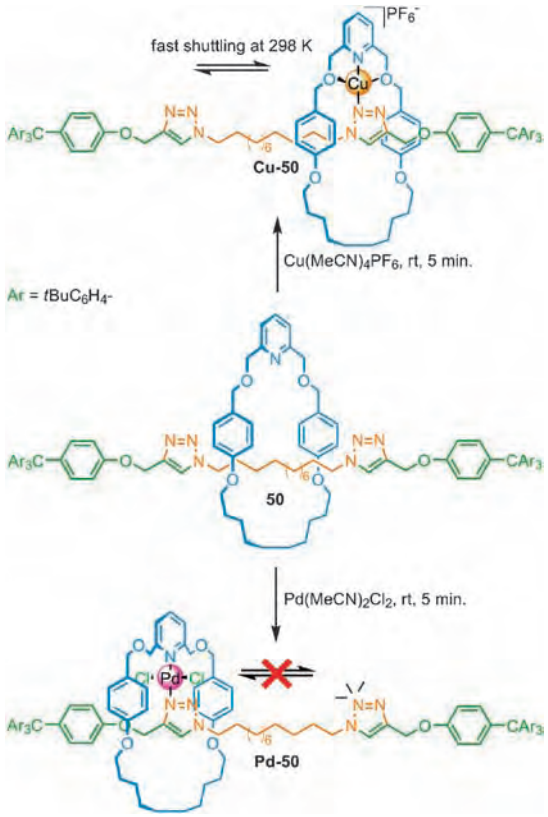

Scheme 12 Controlling macrocycle shuttling dynamics in bis-triazole molecular shuttle **50** by coordination of Cu(I) or Pd(II).[33]

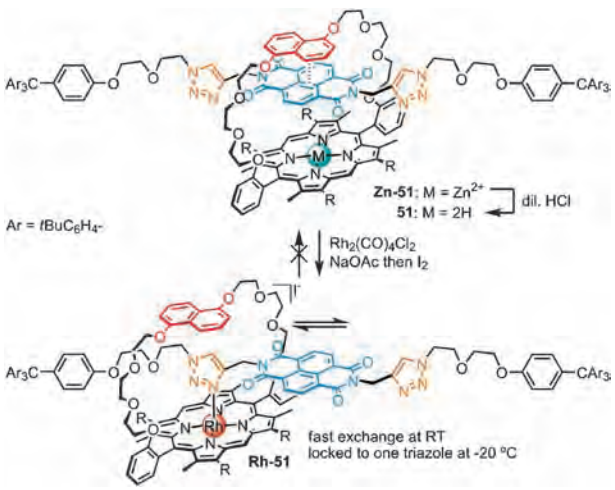

Scheme 13 [2]Rotaxanes **Zn-51** and **51** and the corresponding Rh-containing degenerate molecular shuttle **Rh-51**.[56]

3.3 Redox-switchable molecular shuttles

Molecular shuttles **52–54** (Scheme 14) were constructed using standard CuAAC capping methodologies. The degenerate shuttle **52** was obtained in 16% yield from the corresponding monoazide-derivatised DNP pseudorotaxane and *p*-diethynylbenzene.[42] The shuttling rate of the macrocycle between the two DNP stations was determined to be 15.5 kcal mol^{-1} in d_6-acetone by variable temperature ^{1}H NMR spectroscopy. This value, by comparison to many similar published structures,[57]

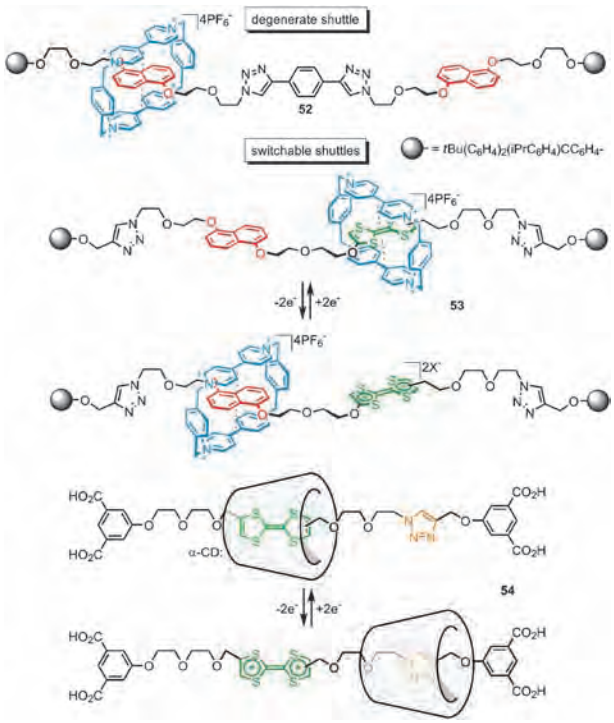

Scheme 14 CuAAC-assembled donor–acceptor molecular shuttles: degenerate shuttle **52**, redox two-station shuttle **53** and α-CD-containing shuttle **54**.[42,58,59]

suggests that the triazole rings do not significantly interfere with the shuttling process. [2]Rotaxane **53** which contains two different—tetrathiafulvalene (TTF) and DNP—potential binding sites was prepared in 60% yield from the corresponding pseudorotaxane complex. ^{1}H NMR spectroscopy (d_6-acetone, 298 K) indicated that the macrocycle was predominantly (>95%) located on the TTF unit. The electrochemistry of the shuttle (CV and differential pulse voltametry—DPV) again suggested that the triazole rings do not affect the thermodynamics or the kinetics of the switching process. This approach was recently extended to make a tripodal shuttle[58] and a redox-switchable α-CD-containing molecular shuttle **54**.[59]

3.4 Anion-switchable molecular shuttles

A novel type of chloride-switchable molecular shuttle that utilises the triazole unit introduced during the CuAAC reaction as a metal coordinating site was recently reported (Scheme 15).[60] Rotaxane **55-Cl** was assembled in 64% yield by CuAAC capping of the corresponding pseudorotaxane. Upfield shifts (^{1}H NMR, $CDCl_3$, 298 K) of the pyridinium and adjacent protons indicated that the anionic-PdCl macrocycle is located over the pyridinium station (Scheme 15, top). Treatment of **55-Cl** with $AgPF_6$ exchanged the chloride ligand by the non-coordinating PF_6^- anion thus inducing translocation of the Pd-complexed macrocycle to the triazole coordinating site (**55-PF$_6$**, Scheme 15, bottom). Simple addition of NBu_4Cl in chloroform reverses the process.

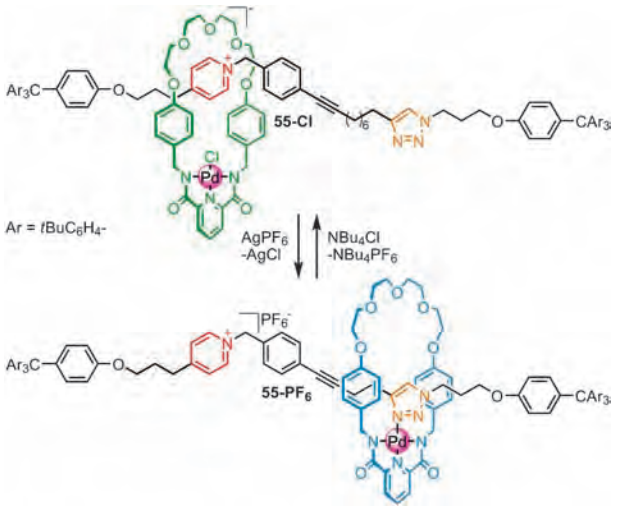

Scheme 15 Chloride-switchable molecular shuttle **55**.[60]

3.5 pH-switchable triazolium-based molecular shuttles

Carbohydrate-derivatised rotaxanes have been prepared by covalent capture of a dialkylammonium-dibenzo-24-crown-8 pseudorotaxane by a CuAAC reaction of the alkyne at one end of the axle with 1-azido-mannose to give the corresponding rotaxane (**56-H**$^+$) (Scheme 16a).[61–64] Methylation of the triazole group in the rotaxane axle forms a triazolium unit that can function as a second potential binding site for the dibenzocrown ether (**56**).[61,62] When the amine group of the axle is protonated (*i.e.* **56-H**$^+$), the macrocycle lies predominantly over the dialkylammonium site. However, treatment with base forms the neutral amine (**56**) and translocation of the electron-rich crown ether to the triazolium station occurs (Scheme 16).[61,62] Remarkably, the changing position of the macrocycle can also be used to flip the chair conformation of the mannoside stopper from $^1C_4$ to $^4C_1$.[64]

This system has also been used to prepare 'molecular daisy chains' and 'molecular muscles' (Scheme 16).[63] Supramolecular dimerisation of a lariat compound (a macrocycle attached to an ammonium-containing rod decorated with a terminal alkyne) afforded a doubly threaded pseudorotaxane where each axle is threaded through the other macrocycle's cavity. Capping with 1-azido-mannose (2,6-lutidine, $Cu(MeCN)_4PF_6$, CH_2Cl_2, 24 h) followed by triazole ring methylation and anion exchange (I^- to PF_6^-) led to **57-2H**$^+$**-S**. Contraction of **57-2H**$^+$**-S** to **57-C** could be achieved *via* treatment with base (NaOH, CH_2Cl_2–H_2O) which causes translocation of the crown ethers to the triazolium rings (evidenced by ^{1}H NMR). Reprotonation with hydrochloric acid, followed by anion exchange (Cl^- to PF_6^-), converted **57-C** back to **57-2H**$^+$**-S**.

3.6 'Nanovalves'

The macrocycle of rotaxanes or pseudorotaxanes can be used to block the holes of a porous surface and act as so-called 'nanovalves' for the stimuli-induced release of substrates (typically rhodamine B dye to show proof-of-concept) trapped below the surface (Fig. 2a).[65] Mesoporous silica nanoparticles (SCSNs, 400 nm diameter) that have 2 nm diameter-pores

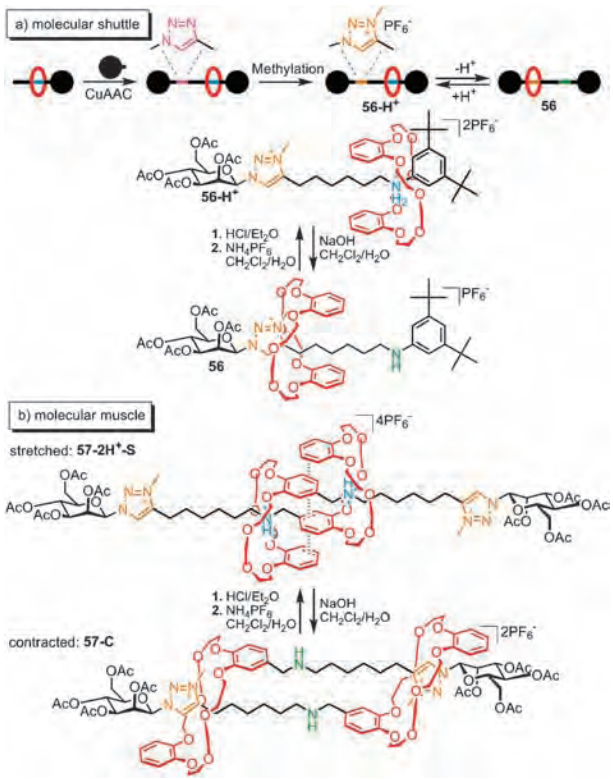

Scheme 16 pH-switchable glycorotaxanes. (a) Molecular shuttle **56**. (b) Stretching/contraction of 'molecular muscle' **57**.[61–64]

form suitable vessels for this purpose and can be derivatised to have azide–alkyne-modified surfaces that can be used as a handle to attach further functionalities, including rotaxanes and pseudorotaxanes, by CuAAC or the Huisgen 1,3-cycloaddition reaction.

A pH-switchable system based on cucurbituril pseudorotaxanes has been described (Fig. 2b).[65] Loading of the alkyne-decorated SCSNs with rhodamine B was followed by a [6]-cucurbitural-promoted 1,3-dipolar cycloaddition[25–30] to afford a pseudorotaxane-derivatised surface in which the cucurbituril (CB) units are held on the axles by hydrogen bonding to the two ammonium groups. Deprotonation of the ammonium groups at pH 10 liberates the CBs and releases the Rhodamine dye into the bulk. The release was followed by luminescence intensity (514 nm). The authors observed more efficient release when the CB units are held closer to the surface of the nanoparticle (n = 1).

Enzyme-responsive nanovalves were prepared through a similar strategy (Fig. 2c).[66] Azide-triethylene glycol rods were attached to the SCCNs surface before the loading. α-Cyclodextrins were threaded onto the rods (H_2O, 5 °C, 24 h) and trapped by a CuAAC stoppering reaction. Cleavage of the ester by porcine liver esterase causes dethreading of the CDs and liberates the cargo (Fig. 2c).

4. Catenanes *via* CuAAC strategies

The effectiveness of the CuAAC reaction for catenane synthesis lies in the high chemospecificity of the reaction. The azide and alkyne groups react overwhelmingly in the desired fashion

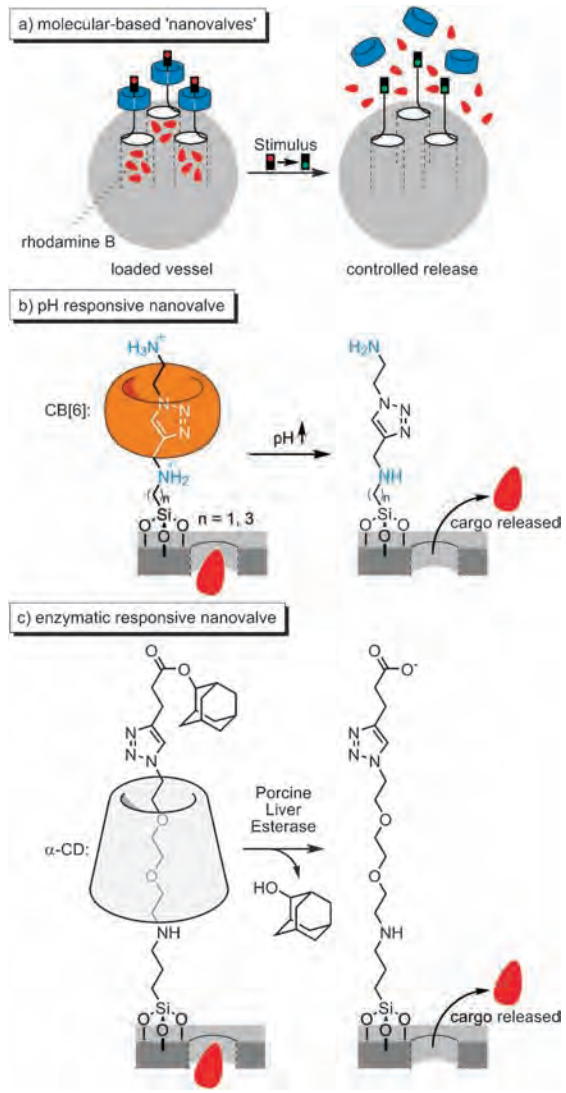

Fig. 2 Rotaxane and pseudorotaxane-based 'nanovalves'. (a) General mechanism. (b) pH-responsive operation.[65] (c) Enzyme-responsive operation.[66]

even when accessing the required reaction geometry is a rare event (as it is for the cyclization of large rings), and hence give predominantly macrocyclic products under high dilution. The yield of catenane *versus* non-interlocked macrocycle then depends on how effectively the template pre-organizes the ring-closing reaction to take place while one component is threaded through the cavity of the other.

4.1 π-Stacking catenanes using CuAAC as a ring-closing reaction

Stoddart and co-workers have applied the rotaxane-forming CuAAC strategy (see Scheme 7) to the more demanding task of catenane formation (Scheme 17).[67,68] Pseudorotaxanes **58a–c** were subjected to the CuAAC reaction conditions giving the corresponding [2]catenanes in modest (up to 41%) yields. The length of the DNP-rod had a critical effect on catenane yield, the best results obtained with pseudorotaxane **59b** (n = 1).

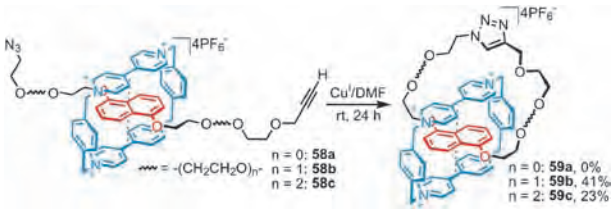

Scheme 17 Synthesis of [2]catenanes **59b–c** by CuAAC ring-closing reactions.[67,68]

4.2 DNA catenanes using CuAAC as a ring-closing reaction

DNA catenanes are formed naturally during several biological processes,[2] but Brown and co-workers have used the CuAAC reaction for oligonucleotide ligation to produce unnatural multiply entwined DNA rings (Scheme 18).[69] A [2]catenane with up to six crossover points was constructed from two carefully designed complementary DNA single strands. 3′-Azide and 5′-alkyne units were incorporated at the ends of 70-mer and 72-mer oligonuceotides **60** and **63**. Ring closure of **60** *via* CuAAC using the water-soluble Cu-ligand **61** afforded macrocycle **62**. Reaction of **62** with the complementary open strand **63** in the presence of the Cu(I) catalyst afforded [2]catenane **64** (Scheme 18). Gel electrophoresis confirmed the catenated structure of **64**, although it was not possible to determine whether all six of the potential crossover points are formed in the interlocked structure. Reacting **60** with **63** under CuAAC condition gave only small amounts of catenane **64**, suggesting that the preformed macrocycle **62** acts as a scaffold about which **63** can wind and become preorganised for formation of the catenane.

4.3 Copper(I)-template [2]- and [3]-catenanes using CuAAC as a ring-closing reaction

Megiatto and Schuster have conducted extremely efficient syntheses of both [2]-[70] and [3]-catenanes[71] utilising a CuAAC ring-closing strategy and Sauvage's well-established Cu(I)–phenanthroline template motif (Scheme 19). [2]Catenanes **67a** and **67b** (Scheme 19a) were prepared in excellent yields (92% and 80%, respectively) by reacting tetra-alkyne Cu(I)-complex **65** with bis-azide **66a–b** under semi-aqueous CuAAC conditions (CuI, Na ascorbate, H_2O–EtOH–PhMe, 70 °C, 24 h). [3]Catenanes **70a–b** were prepared in a similar fashion in 65–70% yields from the kinetically stable pseudorotaxane complexes **68** and **69a–b** (Scheme 19b). The authors suggest that further derivatisation of the R-groups could be used to attach the catenanes to surfaces or solid supports, or to make catenane-based polymers.

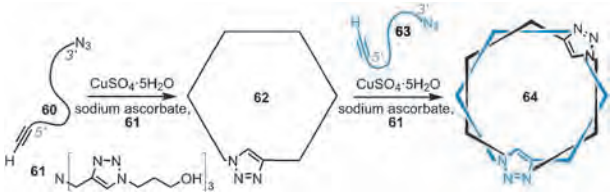

Scheme 18 Formation of multiply entwined bis-triazole DNA [2]catenane **64**.[69]

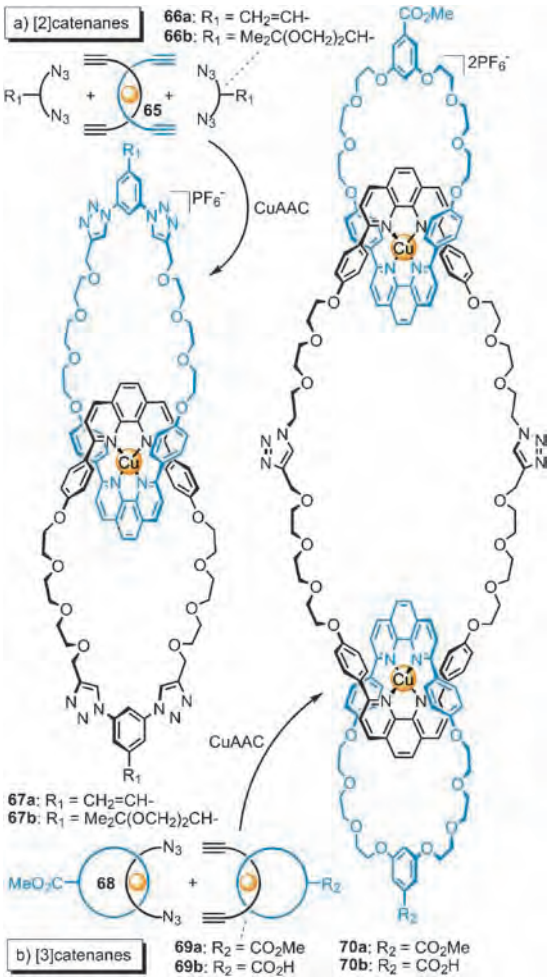

Scheme 19 (a) CuAAC assembled [2]catenanes **67a** and **67b** and (b) symmetrical and unsymmetrical [3]catenanes **70a** and **70b**.[70,71]

Very recently, the active template strategy for rotaxane synthesis has been successfully extended to catenanes through the use of the CuAAC reaction.[72]

5. Post-synthetic modifications of mechanically interlocked molecules

The substrate tolerance and mild conditions used for the CuAAC reaction makes it a reaction of choice for the functionalisation of complex structures while minimising the risk of denaturing them or unwanted side reactions occurring. However, the use of Cu(I) can create a problem in performing the CuAAC reaction in the presence of other redox-active metal ions or substrates containing multidentate binding sites capable of sequestering the copper catalyst. A transition metal tolerant CuAAC protocol has been developed for the preparation of homo- and mixed-metalated rotaxanes and other ligand systems (Scheme 20).[73] Metal-complexed alkyne **M-72** (M = Cu(II) or Cr(III)) could be attached *via* CuAAC to the azido-[2]rotaxane **Cu-71** to afford the corresponding rotaxane derivatives in good yields (**Cu_2-73**, 80% and **CrCu-73**, 82%). Owing to the difference in metal–ligand lability, Cu(II) could

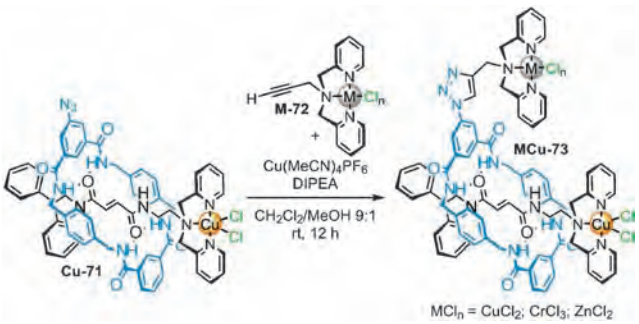

Scheme 20 Derivatisation of metal-containing rotaxane **Cu-71** to form homo- and mixed-metal complexes using the CuAAC reaction.[73]

be selectively removed from the mixed-metal-complex-rotaxanes with EDTA and subsequently replaced by Zn(II).

6. Conclusions

The CuAAC reaction has rapidly proved its efficacy for the construction of mechanically interlocked architectures and for their subsequent functionalisation and organisation. Its popularity with researchers is easily explained by the wide range of conditions in which the reaction can be carried out, the ease of introducing both alkyne and azide functionalities into building blocks, their stability and lack of reactivity towards other functional groups, the high yields obtained for the CuAAC reaction and its compatibility with the weak interactions involved in many template assembly processes. For all these reasons, the Cu(I)-catalysed alkyne–azide cycloaddition looks set to become one of the most powerful tools for the synthesis, functionalisation, derivatisation and application of mechanically interlocked molecular-level architectures in the 21st century.

Notes and references

1 C. O. Dietrich-Buchecker, J.-P. Sauvage and J.-P. Kintzinger, *Tetrahedron Lett.*, 1983, **24**, 5095–5098.
2 *Molecular Catenanes, Rotaxanes and Knots*, ed. J.-P. Sauvage and C. O. Dietrich-Buchecker, Wiley-VCH, Weinheim, 1999.
3 M. R. Craig, M. G. Hutchings, T. D. W. Claridge and H. L. Anderson, *Angew. Chem., Int. Ed.*, 2001, **40**, 1071–1074.
4 A. Fernandes, A. Viterisi, F. Coutrot, S. Potok, D. A. Leigh, V. Aucagne and S. Papot, *Angew. Chem., Int. Ed.*, 2009, **48**, 6443–6447.
5 J. Berná, D. A. Leigh, M. Lubomska, S. M. Mendoza, E. M. Pérez, P. Rudolf, G. Teobaldi and F. Zerbetto, *Nat. Mater.*, 2005, **4**, 704–710.
6 Y. Liu, A. H. Flood, P. A. Bonvallet, S. A. Vignon, B. H. Northrop, H.-R. Tseng, J. O. Jeppesen, T. J. Huang, B. Brough, M. Baller, S. Magonov, S. D. Solares, W. A. Goddard, C.-M. Ho and J. F. Stoddart, *J. Am. Chem. Soc.*, 2005, **127**, 9745–9759.
7 C. P. Collier, G. Mattersteig, E. W. Wong, Y. Luo, K. Beverly, J. Sampaio, F. M. Raymo, J. F. Stoddart and J. R. Heath, *Science*, 2000, **289**, 1172–1175.
8 E. Green, J. W. Choi, A. Boukai, Y. Bunimovich, E. Johnston-Halprin, E. DeIonno, Y. Luo, B. A. Sheriff, K. Xu, Y. S. Shin, H.-R. Tseng, J. F. Stoddart and J. R. Heath, *Nature*, 2007, **445**, 414–417.
9 E. R. Kay, D. A. Leigh and F. Zerbetto, *Angew. Chem., Int. Ed.*, 2006, **46**, 72–191.
10 Structures formed by 'slippage' are formally not rotaxanes, rather they are pseudorotaxanes that are kinetically stable under some

conditions. Rotaxanes are 'molecules in which a ring encloses another, rod-like molecule having end-groups too large to pass through the ring opening and thus holds the rod-like molecule in position without covalent bonding'. [A. D. McNaught and A. Wilkinson, *The IUPAC Compendium of Chemical Terminology*, Blackwell Science, 2nd edn, 1997]. A structure obviously cannot be said to have 'end-groups too large to pass through the ring opening' if they have passed through in order to form it.
11 P. R. Ashton, E. J. T. Chrystal, P. T. Glink, S. Menzer, C. Schiavo, N. Spencer, J. F. Stoddart, P. A. Tasker, A. J. P. White and D. J. Williams, *Chem.–Eur. J.*, 1996, **2**, 709–728.
12 P. R. Ashton, T. T. Goodnow, A. E. Kaifer, M. V. Reddington, A. M. Z. Slawin, N. Spencer, J. F. Stoddart, C. Vicent and D. J. Williams, *Angew. Chem., Int. Ed. Engl.*, 1989, **28**, 1396–1399.
13 J. D. Crowley, S. M. Goldup, A.-L. Lee, D. A. Leigh and R. T. McBurney, *Chem. Soc. Rev.*, 2009, **38**, 1530–1541.
14 R. H. Grubbs, *Angew. Chem., Int. Ed.*, 2006, **45**, 3760–3765.
15 B. Mohr, J.-P. Sauvage, R. H. Grubbs and M. Weck, *Angew. Chem., Int. Ed. Engl.*, 1997, **36**, 1308–1310.
16 T. J. Kidd, D. A. Leigh and A. J. Wilson, *J. Am. Chem. Soc.*, 1999, **121**, 1599–1600.
17 J. S. Hannam, T. J. Kidd, D. A. Leigh and A. J. Wilson, *Org. Lett.*, 2003, **5**, 1907–1910.
18 A. F. M. Kilbinger, S. J. Cantrill, A. W. Waltman, M. W. Day and R. H. Grubbs, *Angew. Chem., Int. Ed.*, 2003, **42**, 3281–3285.
19 C. W. Tornøe, C. Christensen and M. Meldal, *J. Org. Chem.*, 2002, **67**, 3057–3064.
20 V. V. Rostovtsev, L. G. Green, V. V. Fokin and B. K. Sharpless, *Angew. Chem., Int. Ed.*, 2002, **41**, 2596–2599.
21 J. E. Moses and A. D. Moorhouse, *Chem. Soc. Rev.*, 2007, **36**, 1249–1262.
22 M. Meldal and C. W. Tornøe, *Chem. Rev.*, 2008, **108**, 2952–3015.
23 O. Š. Miljanić, W. R. Dichtel, I. Aprahamian, R. D. Rohde, H. D. Agnew, J. R. Heath and J. F. Stoddart, *QSAR Comb. Sci.*, 2007, **26**, 1165–1174.
24 W. L. Mock, T. A. Irra, J. P. Wepsiec and M. Adhya, *J. Org. Chem.*, 1989, **54**, 5302–5308.
25 W. L. Mock and N.-Y. Shih, *J. Org. Chem.*, 1983, **48**, 3619.
26 P. Carlqvist and F. Maseras, *Chem. Commun.*, 2007, 748–750.
27 For a review on cucurbituril chemistry, see: J. Lagona, P. Mukhopadhyay, S. Chakrabarti and L. Isaacs, *Angew. Chem., Int. Ed.*, 2005, **44**, 4844–4870.
28 D. Tuncel and J. H. G. Steinke, *Chem. Commun.*, 2002, 496–497.
29 D. Tuncel and J. H. G. Steinke, *Macromolecules*, 2004, **37**, 288–302.
30 D. Tuncel and J. H. G. Steinke, *Chem. Commun.*, 1999, 1509–1510.
31 R. Huisgen, G. Szeimies and L. Möbius, *Chem. Ber.*, 1967, **100**, 2494–2507.
32 V. Aucagne, K. D. Hänni, D. A. Leigh, P. J. Lusby and D. B. Walker, *J. Am. Chem. Soc.*, 2006, **128**, 2186–2187.
33 V. Aucagne, J. Berná, J. D. Crowley, S. M. Goldup, K. D. Hänni, D. A. Leigh, P. J. Lusby, V. E. Ronaldson, A. M. Z. Slawin, A. Viterisi and D. B. Walker, *J. Am. Chem. Soc.*, 2007, **129**, 11950–11963.
34 V. O. Rodionov, V. V. Fokin and M. G. Finn, *Angew. Chem., Int. Ed.*, 2005, **44**, 2210–2215.
35 P. Mobian, J.-P. Collin and J.-P. Sauvage, *Tetrahedron Lett.*, 2006, **47**, 4907–4909.
36 S. Durot, P. Mobian, J.-P. Collin and J.-P. Sauvage, *Tetrahedron Lett.*, 2008, **64**, 8496–8503.
37 F. Durola, L. Russo, J.-P. Sauvage, K. Rissanen and O. S. Wenger, *Chem.–Eur. J.*, 2007, **13**, 8749–8753.
38 As metal-free 21 undergoes dethreading without breaking a covalent bond, it is technically a relatively kinetically stable pseudorotaxane, not a rotaxane. See ref. 10.
39 A. I. Prikhod'ko, F. Durola and J.-P. Sauvage, *J. Am. Chem. Soc.*, 2008, **130**, 448–449.
40 A. I. Prikhod'ko and J.-P. Sauvage, *J. Am. Chem. Soc.*, 2009, **131**, 6794–6807.
41 W. R. Dichtel, O. Š. Miljanić, J. M. Spruell, J. R. Heath and J. F. Stoddart, *J. Am. Chem. Soc.*, 2006, **128**, 10388–10390.
42 A. B. Braunschweig, W. R. Dichtel, O. Š. Miljanić, M. A. Olson, J. M. Spruell, S. I. Khan, J. R. Heath and J. F. Stoddart, *Chem. Asian J.*, 2007, **2**, 634–647.
43 W. Zhang, W. R. Dichtel, A. Z. Stieg, D. Benítez, J. K. Gimzewski, J. R. Heath and J. F. Stoddart, *Proc. Natl. Acad. Sci. U. S. A.*, 2008, **105**, 6514–6519.
44 W. R. Dichtel, O. Š. Miljanić, W. Zhang, J. M. Spruell, K. Patel, I. Aprahamian, J. R. Heath and J. F. Stoddart, *Acc. Chem. Res.*, 2008, **41**, 1750–1761.
45 I. Aprahamian, W. R. Dichtel, T. Ikeda, J. R. Heath and J. F. Stoddart, *Org. Lett.*, 2007, **9**, 1287–1290.
46 I. Aprahamian, T. Yasuda, T. Ikeda, S. Saha, W. R. Dichtel, K. Isoda, T. Kato and J. F. Stoddart, *Angew. Chem., Int. Ed.*, 2007, **46**, 4675–4679.
47 M. Bria, J. Bigot, G. Cooke, J. Lyskawa, G. Rabani, V. M. Rotello and P. Woisel, *Tetrahedron*, 2009, **65**, 400–407.
48 V. Aucagne and D. A. Leigh, *Org. Lett.*, 2006, **8**, 4505–4507.
49 J. M. Spruell, W. R. Dichtel, J. R. Heath and J. F. Stoddart, *Chem.–Eur. J.*, 2008, **14**, 4168–4177.
50 Y. Liu, Z.-X. Yang and Y. Chen, *J. Org. Chem.*, 2008, **73**, 5298–5304.
51 M. Chwalek, R. Auzély and S. Fort, *Org. Biomol. Chem.*, 2009, **7**, 1680–1688.
52 S. K. Natchiar, O. Srinivas, N. Mitra, S. Dev, N. Jayaraman, A. Surolia and M. Vijayan, *Curr. Sci.*, 2006, **90**, 1230–1237.
53 M. Ambrosi, N. R. Cameron, B. G. Davis and S. Stolnik, *Org. Biomol. Chem.*, 2005, **3**, 1476–1480.
54 J. J. Gassensmith, L. Barr, J. M. Baumes, A. Paek, A. Nguyen and B. D. Smith, *Org. Lett.*, 2008, **10**, 3343–3346.
55 K. M. Mullen, J. Mercurio, C. J. Serpell and P. D. Beer, *Angew. Chem., Int. Ed.*, 2009, **48**, 4781–4784.
56 K. M. Mullen and M. J. Gunter, *J. Org. Chem.*, 2008, **73**, 3336–3350.
57 S. Kang, S. A. Vignon, H.-R. Tseng and J. F. Stoddart, *Chem.–Eur. J.*, 2004, **10**, 2555–2564.
58 I. Aprahamian, J.-C. Olsen, A. Trabolsi and J. F. Stoddart, *Chem.–Eur. J.*, 2008, **14**, 3889–3895.
59 Y.-L. Zhao, W. R. Dichtel, A. Trabolsi, S. Saha, I. Aprahamian and J. F. Stoddart, *J. Am. Chem. Soc.*, 2008, **130**, 11294–11296.
60 M. J. Barrell, D. A. Leigh, P. J. Lusby and A. M. Z. Slawin, *Angew. Chem., Int. Ed.*, 2008, **47**, 8036–8039.
61 F. Coutrot, E. Busseron and J. L. Montero, *Org. Lett.*, 2008, **10**, 753–756.
62 F. Coutrot and E. Busseron, *Chem.–Eur. J.*, 2008, **14**, 4784–4787.
63 F. Coutrot, C. Romuald and E. Busseron, *Org. Lett.*, 2008, **10**, 3741–3744.
64 F. Coutrot and E. Busseron, *Chem.–Eur. J.*, 2009, **15**, 5186–5190.
65 S. Angelos, Y.-W. Yang, K. Patel, J. F. Stoddart and J. I. Zink, *Angew. Chem., Int. Ed.*, 2008, **47**, 2222–2226.
66 K. Patel, S. Angelos, W. R. Dichtel, A. Coskun, Y.-W. Yang, J. I. Zink and J. F. Stoddart, *J. Am. Chem. Soc.*, 2008, **130**, 2382–2383.
67 O. Š. Miljanić, W. R. Dichtel, S. Mortezaei and J. F. Stoddart, *Org. Lett.*, 2006, **8**, 4835–4838.
68 O. Š. Miljanić, W. R. Dichtel, S. I. Khan, S. Mortezaei, J. R. Heath and J. F. Stoddart, *J. Am. Chem. Soc.*, 2007, **129**, 8236–8246.
69 R. Kumar, A. El-Sagheer, J. Tumpane, P. Lincoln, L. M. Wilhelmsson and T. Brown, *J. Am. Chem. Soc.*, 2007, **129**, 6859–6864.
70 J. D. Megiatto Jr. and D. I. Schuster, *J. Am. Chem. Soc.*, 2008, **130**, 12872–12873.
71 J. D. Megiatto Jr. and D. I. Schuster, *Chem.–Eur. J.*, 2009, **15**, 5444–5448.
72 S. M. Goldup, D. A. Leigh, T. Long, P. R. McGonigal, M. D. Symes and J. Wu, *J. Am. Chem. Soc.*, 2009, DOI: 10.1021/ja9070317.
73 D. González-Cabrera, B. D. Koivisto and D. A. Leigh, *Chem. Commun.*, 2007, 4218–4220.

J|A|C|S
COMMUNICATIONS

Published on Web 01/31/2006

Catalytic "Click" Rotaxanes: A Substoichiometric Metal-Template Pathway to Mechanically Interlocked Architectures

Vincent Aucagne, Kevin D. Hänni, David A. Leigh,* Paul J. Lusby, and D. Barney Walker

School of Chemistry, University of Edinburgh, The King's Buildings, West Mains Road, Edinburgh EH9 3JJ, United Kingdom

Received October 9, 2005; E-mail: david.leigh@ed.ac.uk

The introduction of copper(I)-template strategies by Sauvage and colleagues in the mid-1980s marked the first practical synthetic routes to molecular catenanes, rotaxanes, and knots.[1] This seminal idea utilizes the tetrahedral coordination geometry of a Cu(I) atom to hold a pair of bidentate ligands in a mutually orthogonal orientation creating a crossover point that directs subsequent macrocyclization or "stoppering" reactions toward threaded architectures. Other template syntheses followed[2] (based on aromatic stacking, hydrogen bonding, hydrophobic interactions, etc.), leading to the rich variety of synthetic methods available today. However, all current approaches require a stoichiometric quantity of template and generally call for pre-established, strongly binding, recognition motifs on each of the components of the interlocked molecule. Here we describe a rotaxane-forming protocol in which the Cu(I) atom functions as a catalyst as well as a template and turns over during the reaction, permitting substoichiometric amounts of the metal to be used. A permanent coordination site is only needed on the macrocycle. The rest of the interlocked compound is assembled through functional groups that react together under catalysis of the metal, which also serves to hold the fragments in position such that their catalyzed reaction leads to the desired interlocked product.

The strategy utilizes the Cu(I)-catalyzed[3] 1,3-cycloaddition[4] of organic azides with terminal alkynes, recently popularized as a "click" reaction[5] by Sharpless and others.[3,6,7] In organic solvents, tertiary amines or, better, pyridines, considerably enhance the reaction kinetics,[3b,8] suggesting that a macrocycle bearing an endotopic ligating nitrogen atom could direct such a catalyzed reaction through its cavity.[9] The 2,6-disubstituted pyridine macrocycle **1**, previously used[10] as both a mono- and bidentate ligand in metal-coordinated rotaxanes and catenanes, appeared to be a suitable candidate to investigate this idea (Scheme 1). Commercially available $Cu(CH_3CN)_4PF_6$ was chosen as the copper source, avoiding ligands that might compete too strongly for the metal with the macrocycle and other reactants.

We were delighted to find that simple overnight stirring of an equimolar mixture of pyridine macrocycle **1**, alkyne **2**, azide **3**, and the Cu(I) salt in CH_2Cl_2 afforded—after demetalation with KCN—a mixture of [2]rotaxane **4** (57%) and the noninterlocked triazole thread **5** (41%), together with some of the unconsumed starting macrocycle (Table 1, entry 1). The ^{1}H NMR spectrum of **4** in $CDCl_3$ (Figure 1b) shows upfield shifts of several signals with respect to its noninterlocked components **1** and **5** (Figure 1a and c, respectively). The shielding, typical of interlocked architectures in which the aromatic rings of one component are positioned face-on to another component,[10] is observed for all the nonstopper resonances of the axle (H_{f-j}) in **4**, indicating that the macrocycle is able to access the full length of the thread. In contrast, the equivalent spectrum (Figure 1d) of the rotaxane re-metalated with $Cu(CH_3CN)_4PF_6$ (CH_3COCH_3, RT, 1 h, quantitative) shows pronounced shielding of H_j and H_k with respect to **5** (Figure 1c) but

Scheme 1. Proposed Catalytic Cycle for the Cu(I)-Template Synthesis of [2]Rotaxane **4** from **1**, **2**, and **3** (ref 9)

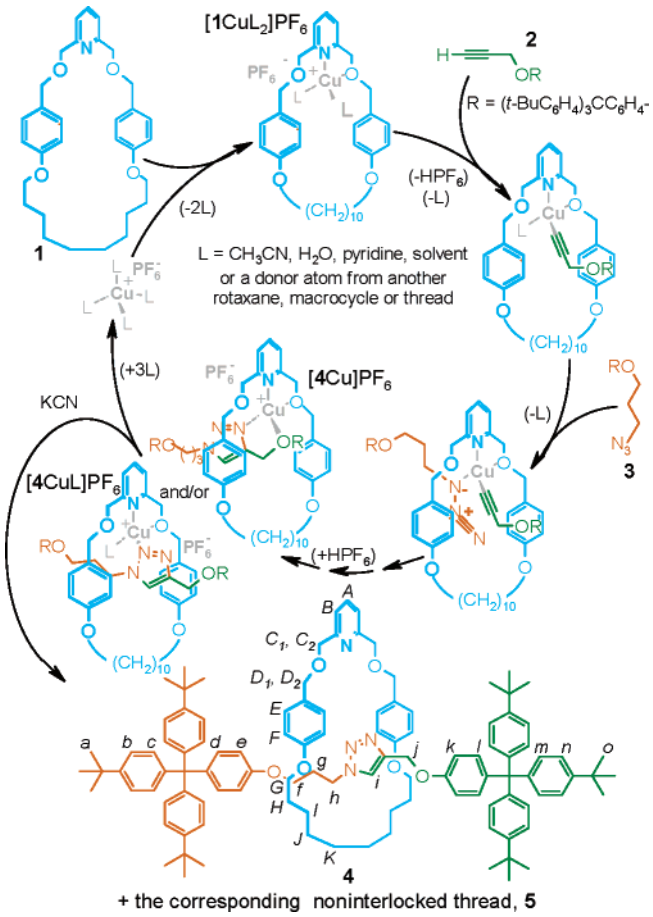

not H_h, H_g, or H_f. This suggests that the Cu binds to the macrocycle and thread in the rotaxane via two sets of bidentate N,O donor interactions (rapidly oscillating involvement between the two oxymethylene groups in the case of the macrocycle), fixing the interlocked components in a position consistent with the observed shielding effects. In other words, in $CDCl_3$, the structure of the rotaxane−metal complex corresponds to that of [**4**Cu]PF_6 shown in Scheme 1.

Although halogenated solvents give the highest yields of rotaxane, the reaction proved to be tolerant to a range of media, including semi-aqueous conditions (entry 2). The use of excess **2** and **3** generates high yields (up to 94%) of [2]rotaxane with respect to the amount of macrocycle used (entries 3 and 4); however, significant quantities of the noninterlocked thread (**5**) are produced in all the noncontrol entries in Table 1. Carrying out the reaction using the conditions of entry 4 but with no macrocycle present and starting with a stoichiometric equivalent of rotaxane (**4**) or thread

10.1021/ja056903f CCC: $33.50

Table 1. Variations in the Experimental Conditions and Reactant Stoichiometry for the Synthesis of [2]Rotaxane **4**[a]

entry	equiv of **2** and **3**	equiv of $CuPF_6$	solvent	*T* (°C)	duration	conversion to triazole **2**+**3**→**4**+**5**	yield of [2]rotaxane **1**→**4**
1	1	1	CH_2Cl_2	25	12 h	>95%	57%
2	1	1	H_2O/*t*BuOH	25	10 days	>95%	22%
3	3	1	CH_2Cl_2	25	24 h	>95%	83%
4[c]	**5**	**1**	**CH_2Cl_2**	**25**	**72 h**	**92%**	**94%**
5	1	0.2	CH_2Cl_2	25	10 days	30%	20%
6	1	0.2	CH_2Cl_2[b]	25	10 days	>95%	38%
7	5	0.2	CH_2Cl_2[b]	25	20 days	44%	59%
8	1	0	$ClCH_2CH_2Cl$[b]	25 then 70	12 h then 72 h	trace	0%
9	**5**	**0.2**	**$ClCH_2CH_2Cl$[b]**	**25 then 70**	**12 h then 24 h**	**94%**	**82%**

[a] All reactions were carried out at 0.1 mM concentration with respect to **2** and **3**, with 1 equiv of macrocycle **1**, and without the need for an inert atmosphere nor distilled or dried solvents. A general experimental procedure is provided in the Supporting Information. [b] With 3 equiv of pyridine. [c] To assess the efficacy of the rotaxane and thread as ligands for a catalytic copper species, the reaction conditions from entry 4 were repeated with no macrocycle present but starting with 1 equiv of **4** or **5** instead. The resulting conversions of **2** + **3** → **5** were 2 and 9%, respectively.

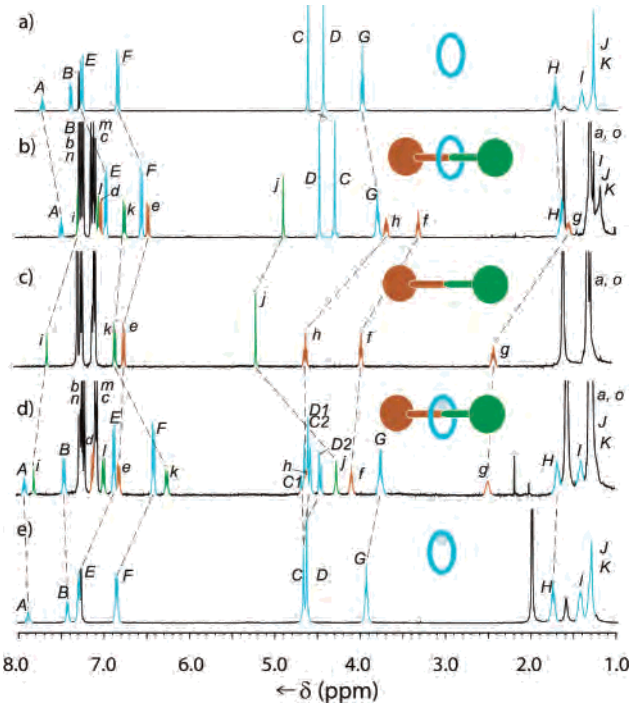

Figure 1. ^{1}H NMR spectra (400 MHz, $CDCl_3$, 298 K) of (a) macrocycle **1**, (b) [2]rotaxane **4**, (c) thread **5**, (d) [2]rotaxane−$CuPF_6$ complex [**4**Cu]PF_6, (e) macrocycle−$CuPF_6$ complex [**1**CuL_2]PF_6. The assignments correspond to the lettering shown in Scheme 1.

(**5**) instead gave low conversions to the triazole (2 and 9%, respectively; see Table 1 footnote b), showing that both rotaxane and thread are poor ligands for generating a catalytic copper species. Clearly, the noninterlocked thread produced in the rotaxane-forming reactions arises from the macrocycle-promoted Cu catalysis being able to take place around, rather than solely through, the cavity of **1**. We are currently exploring the noninterlocked:interlocked selectivity of other ligand designs.

We next investigated the use of substoichiometric amounts of copper to determine whether the metal would turn over as a template as well as a cycloaddition catalyst. When using 20 mol % (with respect to **1**) of $Cu(CH_3CN)_4PF_6$ at room temperature, the reaction appeared to stop after rotaxane equivalent to the amount of copper present had been formed (entry 5). This suggests that the multidentate rotaxane sequesters the transition metal during the reaction, inhibiting further catalytic activity. Addition of pyridine as a competing ligand enabled the catalyst to turn over producing a substoichiometric reaction (entries 6 and 7), but the reaction was extremely slow at 25 °C. Elevating the temperature (entry 9) gives an improved yield (82%) of rotaxane **4** in a reasonable period of time (36 h) using only 4 mol % Cu(I) with respect to both **2** and **3**.

The requirement for only a catalytic amount of a template represents a new development in the strategies available to mechanically interlocked architectures. Chelation to catalytic centers could lead to rotaxane- and catenane-forming protocols based on other metal-mediated reactions, including cross-couplings, condensations, and other cycloaddition reactions.

Supporting Information Available: General synthetic experimental procedure and characterization and spectroscopic data for **4**, **5**, and their precursors. This material is available free of charge via the Internet at http://pubs.acs.org.

References

(1) (a) Dietrich-Buchecker, C. O.; Sauvage, J.-P.; Kintzinger, J. P. *Tetrahedron Lett.* **1983**, *24*, 5095−5098. (b) Sauvage, J.-P. *Acc. Chem. Res.* **1990**, *23*, 319−327.

(2) (a) Amabilino, D. B.; Stoddart, J. F. *Chem. Rev.* **1995**, *95*, 2725−2828. (b) Sauvage, J.-P.; Dietrich-Buchecker, C. O. *Molecular Catenanes, Rotaxanes, and Knots*; Wiley-VCH: Weinheim, Germany, 1999.

(3) (a) Tornøe, C. W.; Christensen, C.; Meldal, M. *J. Org. Chem.* **2002**, *67*, 3057−3062. (b) Rostovstev, V. V.; Green, L. G.; Fokin, V. V.; Sharpless, K. B. *Angew. Chem., Int. Ed.* **2002**, *41*, 2596−2599.

(4) Huisgen, R. In *1,3-Dipolar Cycloaddition Chemistry*; Padwa, A., Ed.; Wiley: New York, 1984.

(5) (a) Kolb, H. C.; Finn, M. G.; Sharpless, K. B. *Angew. Chem., Int. Ed.* **2001**, *40*, 2004−2021. (b) Wang, Q.; Chittaboina, S.; Barnhill, H. N. *Lett. Org. Chem.* **2005**, *2*, 293−301.

(6) (a) Lee, L. V.; Mitchell, M. L.; Huang, S.-J.; Fokin, V. V.; Sharpless, K. B.; Wong, C.-H. *J. Am. Chem. Soc.* **2003**, *125*, 9588−9589. (b) Seo, T. S.; Li, Z.; Ruparel, H.; Ju, J. *J. Org. Chem.* **2003**, *68*, 609−612. (c) Löber, S.; Rodriguez, P.-L.; Gmeiner, P. *Org. Lett.* **2003**, *5*, 1753−1755. (d) Perez, F.-B.; Ortega, M.-M.; Morales, J.-S.; Hernández, F.-M.; Calvo, F. G.-F.; Calvo, J. A.-A.; Isac, J.-G.; Santoyo, F.-G. *Org. Lett.* **2003**, *5*, 1951−1954. (e) Himo, F.; Lovell, T.; Hilgraf, R.; Rostovtsev, V. V.; Noodleman, L.; Sharpless, K. B.; Fokin, V. V. *J. Am. Chem. Soc.* **2005**, *127*, 210−216. (f) Bock, V. D.; Hiemstra, H.; van Maarseveen, J. H. *Eur. J. Org. Chem.* **2006**, 51−68.

(7) The 1,3-cycloaddition of azides to terminal alkynes has previously been employed to prepare rotaxanes and polyrotaxanes by using cucurbituril to accelerate the reaction by organizing the reactants and increasing their effective molarity: (a) Mock, W. L.; Irra, T. A.; Wepsiec, J. P.; Adhya, M. *J. Org. Chem.* **1989**, *54*, 5302−5308. (b) Tuncel, D.; Steinke, J. H. G. *Chem. Commun.* **1999**, 1509−1510. (c) Tuncel, D.; Steinke, J. H. G. *Chem. Commun.* **2002**, 496−497. (d) Tuncel, D.; Steinke, J. H. G. *Macromolecules* **2004**, *37*, 288−302. The uncatalyzed 1,3-cycloaddition between azides and electron-poor internal alkynes has been used to form rotaxanes by a "threading-followed-by-stoppering" protocol: (e) Ashton, P. R.; Glink, P. T.; Stoddart, J. F.; Tasker, P. A.; White, A. J. P.; Williams, D. J. *Chem.−Eur. J.* **1996**, *2*, 729−736.

(8) Lewis, W. G.; Magallon, F. G.; Fokin, V. V.; Finn, M. G. *J. Am. Chem. Soc.* **2004**, *126*, 9152−9153.

(9) Kinetic studies[6e,f] indicate that the ligand-free aqueous alkyne−azide cycloaddition involves two, probably bridged, metal centers. In contrast, little is known about the details of the ligand-promoted reaction in organic solvents. It is not yet clear whether the formation of [**4**Cu]PF_6 proceeds via single copper atom intermediates, binuclear species, or structurally more complex aggregates. Further studies are ongoing.

(10) (a) Fuller, A.-M.; Leigh, D. A.; Lusby, P. J.; Oswald, I. D. H.; Parsons, S.; Walker, D. B. *Angew. Chem., Int. Ed.* **2004**, *43*, 3914−3918. (b) Leigh, D. A.; Lusby, P. J.; Slawin, A. M. Z.; Walker, D. B. *Angew. Chem., Int. Ed.* **2005**, *44*, 4557−4564. (c) Fuller, A.-M. L.; Leigh, D. A.; Lusby, P. J.; Slawin, A. M. Z.; Walker, D. B. *J. Am. Chem. Soc.* **2005**, *127*, 12612−12619. (d) Leigh, D. A.; Lusby, P. J.; Slawin, A. M. Z.; Walker, D. B. *Chem. Commun.* **2005**, 4919−4921.

JA056903F

J|A|C|S
ARTICLES
Published on Web 09/11/2007

Catalytic "Active-Metal" Template Synthesis of [2]Rotaxanes, [3]Rotaxanes, and Molecular Shuttles, and Some Observations on the Mechanism of the Cu(I)-Catalyzed Azide−Alkyne 1,3-Cycloaddition

Vincent Aucagne,[†] José Berná,[†] James D. Crowley,[†] Stephen M. Goldup,[†] Kevin D. Hänni,[†] David A. Leigh,*[,†] Paul J. Lusby,[†] Vicki E. Ronaldson,[†] Alexandra M. Z. Slawin,[‡] Aurélien Viterisi,[†] and D. Barney Walker[†]

Contribution from the Schools of Chemistry, University of Edinburgh, The King's Buildings, West Mains Road, Edinburgh EH9 3JJ, and University of St. Andrews, Purdie Building, St. Andrews, Fife KY16 9ST, United Kingdom

Received May 17, 2007; E-mail: David.Leigh@ed.ac.uk

Abstract: A synthetic approach to rotaxane architectures is described in which metal atoms catalyze covalent bond formation while simultaneously acting as the template for the assembly of the mechanically interlocked structure. This "active-metal" template strategy is exemplified using the Huisgen−Meldal−Fokin Cu(I)-catalyzed 1,3-cycloaddition of azides with terminal alkynes (the CuAAC "click" reaction). Coordination of Cu(I) to an endotopic pyridine-containing macrocycle allows the alkyne and azide to bind to metal atoms in such a way that the metal-mediated bond-forming reaction takes place through the cavity of the macrocycle—or macrocycles—forming a rotaxane. A variety of mono- and bidentate macrocyclic ligands are demonstrated to form [2]rotaxanes in this way, and by adding pyridine, the metal can turn over during the reaction, giving a catalytic active-metal template assembly process. Both the stoichiometric and catalytic versions of the reaction were also used to synthesize more complex two-station molecular shuttles. The dynamics of the translocation of the macrocycle by ligand exchange in these two-station shuttles could be controlled by coordination to different metal ions (rapid shuttling is observed with Cu(I), slow shuttling with Pd(II)). Under active-metal template reaction conditions that feature a high macrocycle:copper ratio, [3]-rotaxanes (two macrocycles on a thread containing a single triazole ring) are also produced during the reaction. The latter observation shows that under these conditions the mechanism of the Cu(I)-catalyzed terminal alkyne−azide cycloaddition involves a reactive intermediate that features at least two metal ions.

Introduction

Most noncovalent bond directed approaches[1] to rotaxanes developed to date require at least stoichiometric quantities of a template which often involves pre-established strongly binding recognition motifs that "live on"[2] in the mechanically interlocked molecule that is formed. Besides holding the reactive fragments in an orientation that directs interlocking, the template is generally otherwise passive during the reaction. Building on the principles of transition-metal catalysis, we recently[3] began to explore a strategy in which template ions could also play an active role in promoting the crucial final covalent bond forming reaction that captures the interlocked structure (i.e., the metal has a dual function, acting as a template for entwining the precursors *and* catalyzing covalent bond formation between the reactants). This "active-metal"[4] template process is shown schematically in Figure 1 in both stoichiometric (1 equiv of

[†] University of Edinburgh.
[‡] University of St. Andrews.

(1) For reviews which highlight various aspects of template strategies to rotaxanes, see: (a) Amabilino, D. B.; Stoddart, J. F. *Chem. Rev.* **1995**, *95*, 2725−2828. (b) *Molecular Catenanes, Rotaxanes and Knots: A Journey Through the World of Molecular Topology*; Sauvage, J.-P., Dietrich-Buchecker, C., Eds.; Wiley-VCH: Weinheim, Germany, 1999. (c) Breault, G. A.; Hunter, C. A.; Mayers, P. C. *Tetrahedron* **1999**, *55*, 5265−5293. (d) *Templated Organic Synthesis*; Diederich, F., Stang, P. J., Eds.; Wiley-VCH: Weinheim, Germany, 2000. (e) Hubin, T. J.; Busch, D. H. *Coord. Chem. Rev.* **2000**, *200*, 5−52. (f) Raehm, L.; Hamilton, D. G.; Sanders, J. K. M. *Synlett* **2002**, 1743−1761. (g) Kim, K. *Chem. Soc. Rev.* **2002**, *31*, 96−107. (h) Aricó, F.; Badjić, J. D.; Cantrill, S. J.; Flood, A. H.; Leung, K. C.-F.; Liu, Y.; Stoddart, J. F. *Top. Curr. Chem.* **2005**, *249*, 203−259. (i) Dietrich-Buchecker, C.; Colasson, B. X.; Sauvage, J.-P. *Top. Curr. Chem.* **2005**, *249*, 261−283. (j) Kay, E. R.; Leigh, D. A. *Top. Curr. Chem.* **2005**, *262*, 133−177. (k) Loeb, S. J. *Chem. Commun.* **2005**, 1511−1518. (l) Bogdan, A.; Rudzevich, Y.; Vysotsky, M. O.; Böhmer, V. *Chem. Commun.* **2006**, 2941−2952. (m) Nitschke, J. R. *Acc. Chem. Res.* **2007**, *40*, 103−112. (n) Vickers, M. S.; Beer, P. D. *Chem. Soc. Rev.* **2007**, *36*, 211−225. (o) Loeb, S. J. *Chem. Soc. Rev.* **2007**, *36*, 226−235. For reviews on polyrotaxanes, see: (p) Harada, A. *Acta Polym.* **1998**, *49*, 3−17. (q) Takata, T.; Kihara, N.; Furusho, Y. *Adv. Polym. Sci.* **2004**, *171*, 1−75. (r) Huang, F.; Gibson, H. W. *Prog. Polym. Sci.* **2005**, *30*, 982−1018. (s) Wenz, G.; Han, B.-H.; Müller, A. *Chem. Rev.* **2006**, *106*, 782−817.

(2) (a) Philp, D.; Stoddart, J. F. *Angew. Chem., Int. Ed. Engl.* **1996**, *35*, 1154−1196. For a discussion of how and why this feature can be usefully exploited in the field of molecular machinery, see: (b) Kay, E. R.; Leigh, D. A.; Zerbetto, F. *Angew. Chem., Int. Ed.* **2007**, *46*, 72−191.

(3) Aucagne, V.; Hänni, K. D.; Leigh, D. A.; Lusby, P. J.; Walker, D. B. *J. Am. Chem. Soc.* **2006**, *128*, 2186−2187.

(4) We use "active template" as a general term to describe a reaction in which a moiety both catalyzes covalent bond formation and acts as a template for the assembly of a particular structure. The term "active-metal template" describes a subset of active-template reactions in which the "active" moiety is a metal. A "catalytic active-metal template" reaction is one in which the metal catalyst turns over; a "stoichiometric active-metal template" reaction is one in which it does not.

10.1021/ja073513f CCC: $37.00

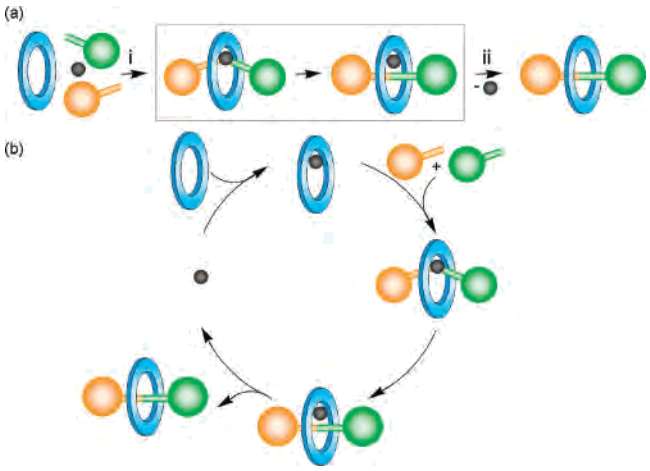

Figure 1. "Active-template" strategy to rotaxane architectures. The formation of a covalent bond between the green and orange "stoppered" units to generate the thread is promoted by the catalyst (shown in gray) and directed through the cavity of the macrocycle (shown in blue) by the catalyst's coordination requirements. (a) Stoichiometric active-metal template synthesis of a [2]rotaxane: (i) template assembly and covalent bond forming catalysis, (ii) subsequent demetalation. (b) Catalytic active-metal template synthesis of a [2]rotaxane.

the active template is required) and catalytic (the active template turns over during the reaction) forms. There are several potentially attractive features of such a synthetic approach to mechanically interlocked architectures, including (i) the inherent efficiency of a reaction in which the macrocycle−metal complex performs multiple functions, (ii) the lack of a requirement for permanent recognition elements in each component of the interlocked product, which increases the structural diversity possible in catenanes and rotaxanes and enables their formation to be "traceless", (iii) in some cases only substoichiometric quantities of the active template may be required (i.e., the catalytic active-metal template variant, Figure 1b), (iv) the strategy could prove applicable to many different types of well-known transition-metal-catalyzed (and even organocatalytic) reactions, (v) reactions that *only* proceed through a threaded intermediate would allow access to several currently inaccessible mechanically linked macromolecular architectures, and, finally, (vi) the coordination requirements during key stages of the catalytic cycle of active-template reactions could provide insight into the mechanisms of the catalyzed reactions.

Since the preliminary report[3] appeared on the realization of this strategy for rotaxane formation utilizing the Cu(I)-catalyzed[5−7] 1,3-cycloaddition[8] of organic azides and terminal alkynes (the CuAAC "click"[9,10] reaction), we have been delighted to see the concept be quickly adopted[11] to make rotaxanes[12] with other Cu(I)-catalyzed reactions, including alkyne-homocoupling and C−S bond forming reactions.[13,14] Here we expand on our investigation of the original system, showing that the active-metal template rotaxane-forming CuAAC reaction works well for both mono- and bidentate pyridine-containing macrocyclic ligands and can also be used to synthesize more complex two-station degenerate molecular shuttles whose interstation shuttling can be controlled by coordination to different metal ions. Furthermore, using a high macrocycle:copper ratio, [3]rotaxanes with two macrocycles on a single thread are somewhat unexpectedly produced during the active-metal template reaction. Together with some simple kinetic studies carried out under various rotaxane- and thread-forming reaction conditions, these experimental results provide some insight into the mechanism of the CuAAC reaction.

(5) (a) Tornøe, C. W.; Christensen, C.; Meldal, M. *J. Org. Chem.* **2002**, *67*, 3057−3064. (b) Rostovtsev, V. V.; Green, L. G.; Fokin, V. V.; Sharpless, K. B. *Angew. Chem., Int. Ed.* **2002**, *41*, 2596−2599.

(6) For some interesting examples of the CuAAC reaction, see: (a) Lee, L. V.; Mitchell, M. L.; Huang, S.-J.; Fokin, V. V.; Sharpless, K. B.; Wong, C.-H. *J. Am. Chem. Soc.* **2003**, *125*, 9588−9589. (b) Wang, Q.; Chan, T. R.; Hilgraf, R.; Fokin, V. V.; Sharpless, K. B.; Finn, M. G. *J. Am. Chem. Soc.* **2003**, *125*, 3192−3193. (c) Horne, W. S.; Yadav, M. K.; Stout, C. D.; Ghadiri, M. R. *J. Am. Chem. Soc.* **2004**, *126*, 15366−15367. (d) Diaz, D. D.; Punna, S.; Holzer, P.; McPherson, A. K.; Sharpless, K. B.; Fokin, V. V.; Finn, M. G. *J. Polym. Sci., Part A: Polym. Chem.* **2004**, *42*, 4392−4403. (e) Manetsch, R.; Krasiński, A.; Radić, Z.; Raushel, J.; Taylor, P.; Sharpless, K. B.; Kolb, H. C. *J. Am. Chem. Soc.* **2004**, *126*, 12809−12818. (f) Helms, B.; Mynar, J. L.; Hawker, C. J.; Frechet, J. M. J. *J. Am. Chem. Soc.* **2004**, *126*, 15020−15021. (g) Steffensen, M. B.; Simanek, E. E. *Angew. Chem., Int. Ed.* **2004**, *43*, 5178−5180. (h) Collman, J. P.; Devaraj, N. K.; Chidsey, C. E. D. *Langmuir* **2004**, *20*, 1051−1053. (i) Jang, H.; Fafarman, A.; Holub, J. M.; Kirshenbaum, K. *Org. Lett.* **2005**, *7*, 1951−1954; (j) Krasiński, A.; Radić, Z.; Manetsch, R.; Raushel, J.; Taylor, P.; Sharpless, K. B.; Kolb, H. C. *J. Am. Chem. Soc.* **2005**, *127*, 6686−6692. (k) Wu, P.; Malkoch, M.; Hunt, J. N.; Vestberg, R.; Kaltgrad, E.; Finn, M. G.; Fokin, V. V.; Sharpless, K. B.; Hawker, C. J. *Chem. Commun.* **2005**, 5775−5777. (l) Mocharla, V. P.; Colasson, B.; Lee, L. V.; Roeper, S.; Sharpless, K. B.; Wong, C.-H.; Kolb, H. C. *Angew. Chem., Int. Ed.* **2005**, *44*, 116−120. (m) Srinivasachari, S.; Liu, Y.; Zhang, G.; Prevette, L.; Reineke, T. M. *J. Am. Chem. Soc.* **2006**, *128*, 8176−8184. (n) Slater, M.; Snauko, M.; Svec, F.; Frechet, J. M. J. *Anal. Chem.* **2006**, *78*, 4969−4975. (o) Ladmiral, V.; Mantovani, G.; Clarkson, G. J.; Cauet, S.; Irwin, J. L.; Haddleton, D. M. *J. Am. Chem. Soc.* **2006**, *128*, 4823−4830. (p) White, M. A.; Johnson, J. A.; Koberstein, J. T.; Turro, N. J. *J. Am. Chem. Soc.* **2006**, *128*, 11356−11357. (q) Collman, J. P.; Devaraj, N. K.; Eberspacher, T. P. A.; Chidsey, C. E. D. *Langmuir* **2006**, *22*, 2457−2464. (r) Devaraj, N. K.; Dinolfo, P. H.; Chidsey, C. E. D.; Collman, J. P. *J. Am. Chem. Soc.* **2006**, *128*, 1794−1795. (s) Detz, R. J.; Arevalo Heras, S.; de Gelder, R.; van Leeuwen, P. W. N. M.; Hiemstra, H.; Reek, J. N. H.; van Maarseveen, J. H. *Org. Lett.* **2006**, *8*, 3227−3230. (t) Aucagne, V.; Leigh, D. A. *Org. Lett.* **2006**, *8*, 4505−4507. (u) Viguier, R. F. H.; Hulme, A. N. *J. Am. Chem. Soc.* **2006**, *128*, 11370−11371.

(7) For reviews of the CuAAC reaction, see: (a) Bock, V. D.; Hiemstra, H.; van Maarseveen, J. H. *Eur. J. Org. Chem.* **2005**, 51−68. (b) Wang, Q.; Chittaboina, S.; Barnhill, H. N. *Lett. Org. Chem.* **2005**, *2*, 293−301. (c) Wu, P.; Fokin, V. V. *Aldrichimica Acta* **2007**, *40*, 7−17.

(8) (a) *1,3-Dipolar Cycloadditions Chemistry*; Huisgen, R., Ed.; Wiley: New York, 1984; Vol. 1, pp 1−176. (b) Huisgen, R. *Pure Appl. Chem.* **1989**, *61*, 613−628.

(9) For reviews and discussion of the "click chemistry" concept, see: (a) Kolb, H. C.; Finn, M. G.; Sharpless, K. B. *Angew. Chem., Int. Ed.* **2001**, *40*, 2004−2021. (b) Kolb, H. C.; Sharpless, K. B. *Drug Discovery Today* **2003**, *8*, 1128−1137. (c) Ball, P. *Chem. World* **2007**, *4* (4), 46−51.

(10) A listing of examples of the use of "click" reactions is available at http://www.scripps.edu/chem/sharpless/click.html.

(11) Indeed, it was predicted[3] that, "Chelation to catalytic centers could lead to rotaxane- and catenane-forming protocols based on other metal-mediated reactions, including cross-couplings, condensations, and other cycloaddition reactions". For a recent example involving Pd(II)-catalyzed alkyne homocouplings, see: Berná, J.; Crowley, J. D.; Goldup, S. M.; Hänni, K. D.; Lee, A.-L.; Leigh, D. A. *Angew. Chem., Int. Ed.* **2007**, *46*, 5709−5713.

(12) For the synthesis of rotaxanes and catenanes using the CuAAC reaction in "passive" template stoppering or macrocyclization protocols, see: (a) Mobian, P.; Collin, J.-P.; Sauvage, J.-P. *Tetrahedron Lett.* **2006**, *47*, 4907−4909. (b) Dichtel, W. R.; Miljanić, O. Š.; Spruell, J. M.; Heath, J. R.; Stoddart, J. F. *J. Am. Chem. Soc.* **2006**, *128*, 10388−10390. (c) Miljanić, O. Š.; Dichtel, W. R.; Mortezaei, S.; Stoddart, J. F. *Org. Lett.* **2006**, *8*, 4835−4838. (d) Aprahamian, I.; Dichtel, W. R.; Ikeda, T.; Heath, J. R.; Stoddart, J. F. *Org. Lett.* **2007**, *9*, 1287−1290; (e) Braunschweig, A. B.; Dichtel, W. R.; Miljanić, O. Š.; Olson, M. A.; Spruell, J. M.; Khan, S. I.; Heath, J. R.; Stoddart, J. F. *Chem. Asian J.* **2007**, *2*, 634−647.

(13) Saito, S.; Takahashi, E.; Nakazono, K. *Org. Lett.* **2006**, *8*, 5133−5136.

(14) Saito et al. imply[13] that the concept of binding of a substrate in a cavity while simultaneously activating it to catalysis is an extension of Vögtle's anion template route to rotaxanes [(a) Seel, C.; Vögtle, F. *Chem.—Eur. J.* **2000**, *6*, 21−24]. Actually the two strategies are rather fundamentally different. In the Vögtle reaction the macrocycle does not increase the reactivity of any of the building blocks for the rotaxane. In fact, the hydrogen bonding of the macrocycle to the phenoxide anion, combined with the steric hinderance conferred by the presence of the macrocycle, greatly *decreases* its reactivity. The only reason that rotaxane is formed in the Vögtle system is that the more reactive unthreaded phenoxide anion is completely insoluble under the reaction conditions. The active-template strategy described in ref 3 and elaborated upon in this paper has much more in common with Sauvage's original (passive) metal template ideas combined with Mock's [(b) Mock, W. L.; Irra, T. A.; Wepsiec, J. P.; Adhya, M. *J. Org. Chem.* **1989**, *54*, 5302−5308] and later Steinke's [(c) Tuncel, D.; Steinke, J. H. G. *Chem. Commun.* **1999**, 1509−1510. (d) Tuncel, D.; Steinke, J. H. G. *Chem. Commun.* **2002**, 496−497. (e) Tuncel, D.; Steinke, J. H. G. *Macromolecules* **2004**, *37*, 288−302] use of curcubituril to accelerate a reaction within a macrocycle cavity to form rotaxanes.

Cu(I)-Catalyzed Terminal Alkyne−Azide Cycloaddition (CuAAC Reaction)

Recently, there has been a tremendous surge of interest in so-called click[9,10] methodologies for functional molecule synthesis, the most popular of which is the Huisgen−Meldal−Fokin[15] Cu(I)-catalyzed 1,3-cycloaddition of organic azides with terminal alkynes (the CuAAC reaction).[5−7] The most common catalyst systems for this reaction employ water or alcohol solvents and use a Cu(II) salt in the presence of a reducing agent (often sodium ascorbate) to generate the required Cu(I) catalyst in situ.[5b,7a] Metallic copper[5b,7a] or copper clusters[16] have also been employed as precatalysts, and in some cases Cu(I) salts can be used directly. However, in apolar solvents Cu(I) salts usually require the presence of nitrogen[5b,7a,17] or phosphorus[18] ligands, or acetonitrile as a cosolvent, to stabilize the Cu(I) oxidation state, and undesired alkyne−alkyne homocoupling products are often observed under such reaction conditions.[5b,7a]

The basic mechanism of the CuAAC reaction is believed to be that shown in Scheme 1. A [2+3] cycloaddition—the mechanism of the thermal (i.e., uncatalyzed) Huisgen reaction[8]—is ruled out[19] for the Cu(I)-catalyzed reaction on the basis of DFT calculations which show that reaction via a (formally Cu(III)) metallacycle is a more favorable pathway by up to 11.7 kcal mol^{-1} (Scheme 1).[5b,20,21] The same calculations suggest that the rate-determining step is the formation of the Cu metallacycle from a reactive intermediate involving copper-coordinated alkyne and, presumably, azide (organoazido−metal complexes are likely intermediates in many transition-metal-mediated reactions of azides, and Cu(I)−N_3R complexes have been characterized by X-ray crystallography[22]). However, the exact nature of this reactive intermediate is unclear (Scheme 1, types A−C).

In the absence of competing ligands,[23] copper(I) acetylides exist as complex multi metal atom aggregates,[24] and kinetic studies[17a,25] by Fokin and Finn on the generic ligand-free[23] Cu(I)-catalyzed alkyne−azide reaction show that in DMSO−water mixtures the reaction mechanism is second-order with respect to copper. The same studies found first-order kinetics with respect to the azide and alkyne (actually slightly higher than first-order with respect to the alkyne).[25] However, relatively little is known about the ligand-promoted Cu(I)-catalyzed cycloaddition in organic solvents. Recent experiments by Straub,[26] in which mononuclear copper(I) acetylides ligated to a sterically demanding *N*-heterocyclic carbene react efficiently with bulky organoazides at room temperature, support the notion that a single copper atom mechanism (A(i), Scheme 1) is viable for the reaction, at least when the copper is bound to bulky ligands. Recent DFT calculations[7c,21] suggest that π-activation of the copper acetylide unit by coordination of a second copper atom (e.g., A(ii) or, more likely under ligand-free conditions or with small monodentate ligands, bridged[27] intermediates such as B(i) or B(ii), Scheme 1) greatly enhances the reactivity of the copper σ-acetylide, accelerating formation of the metallacycle. Alternatively, a pathway[25] in which the reacting azide and alkyne are coordinated to different copper(I) atoms (intermediate C(i) or C(ii)) would also be consistent with the second-order kinetics observed in DMSO−water. It may well be that several of these types of intermediates[28] can provide viable pathways for the CuAAC reaction, with the different characteristics of the intermediates being relatively favored or inhibited by factors such as the solvent, bulk and coordination number of an added ligand, the strength of ligand−copper binding, and the amount of ligand-free Cu(I) present in solution. Given the tendency of copper(I) acetylides to aggregate, however, doubly bridged intermediates such as B or C should be abundant species under most conditions. Accordingly, if coordination of the azide to the same copper atom significantly increases the reactivity of the σ-acetylide, type B(ii) intermediates are probably involved in the dominant pathways in most reported CuAAC reactions.

Despite the uncertainty over the precise nature of the reactive intermediate, since tertiary amines and pyridines facilitate[5b,17] the reaction in organic solvents, we reasoned that a macrocycle, **1**, bearing an endotopic ligating nitrogen atom might be able to direct the CuAAC reaction of a "stoppered" alkyne, **2**, and a "stoppered" azide, **3**, through the macrocycle cavity to give a [2]rotaxane, **4**, in an active-metal template synthesis (Scheme 2).

Active-Metal Template CuAAC Rotaxane Synthesis

A 2,6-bis[(alkyloxy)methyl]pyridine macrocycle (**1a**), previously used[29] as both a mono- and bidentate ligand for various transition metals in classical "passive" template rotaxane and catenane syntheses, seemed a suitable candidate for initial investigations. Pleasingly, stirring of an equimolar mixture of

(15) The Cu(I)-catalyzed terminal alkyne−azide cycloaddition is often referred to as the "Sharpless copper click reaction" or the "Sharpless−Huisgen alkyne−azide cycloaddition". However, Sharpless gives Fokin the credit for the idea and recognition of the copper catalysis of this reaction at Scripps [Rouhi, A. M. *Chem. Eng. News* **2004**, *82* (7), 63−65]. The initial work at Scripps was carried out shortly after, and without knowledge of, the first paper (ref 5a) describing the Cu(I)-catalyzed alkyne−azide cycloaddition (on solid-supported resins) had been submitted by Meldal and co-workers.

(16) Pachon, L. D.; van Maarseveen, J. H.; Rothenberg, G. *Adv. Synth. Catal.* **2005**, *347*, 811−815.

(17) (a) Chan, T. R.; Hilgraf, R.; Sharpless, K. B.; Fokin, V. V. *Org. Lett.* **2004**, *6*, 2853−2855. (b) Lewis, W. G.; Magallon, F. G.; Fokin, V. V.; Finn, M. G. *J. Am. Chem. Soc.* **2004**, *126*, 9152−9153.

(18) Perez-Balderas, F.; Ortega-Munoz, M.; Morales-Sanfrutos, J.; Hernandez-Mateo, F.; Calvo-Flores, F. G.; Calvo-Asin, J. A.; Isac-Garcia, J.; Santoyo-Gonzalez, F. *Org. Lett.* **2003**, *5*, 1951−1954.

(19) If the [2+3] cycloaddition were the preferred mechanism of the Cu-catalyzed reaction, the structures A−C shown in Scheme 1 would still be relevant as reactive intermediates.

(20) Himo, F.; Lovell, T.; Hilgraf, R.; Rostovtsev, V. V.; Noodleman, L.; Sharpless, K. B.; Fokin, V. V. *J. Am. Chem. Soc.* **2005**, *127*, 210−216.

(21) Ahlquist, M.; Fokin, V. V. *Organometallics*, in press, cited in ref 7c.

(22) Dias, H. V. R.; Polach, S. A.; Goh, S.-K.; Archibong, E. F.; Marynick, D. S. *Inorg. Chem.* **2000**, *39*, 3894−3901.

(23) In this paper we use the phrases "ligandless" and "ligand-free" to describe copper that is not bound to the macrocyclic pyridine ligands added to the CuAAC reactions to generate the active-template synthesis. As discussed in the text and ref 28, any Cu(I) that is not coordinated to pyridine units will be complexed by molecules of acetonitrile, azide, alkyne, water, or other donor atoms present.

(24) Mykhalichko, B. M.; Temkin, O. N.; Mys'kiv, M. G. *Russ. Chem. Rev.* **2000**, *69*, 957−984.

(25) Rodionov, V. O.; Fokin, V. V.; Finn, M. G. *Angew. Chem., Int. Ed.* **2005**, *44*, 2210−2215.

(26) Nolte, C.; Mayer, P.; Straub, B. F. *Angew. Chem., Int. Ed.* **2007**, *46*, 2101−2103.

(27) (a) Bohlmann, F.; Schönowsky, H.; Inhoffen, E.; Grau, G. *Chem. Ber.* **1964**, *97*, 794−800. (b) Siemsen, P.; Livingston, R. C.; Diederich, F. *Angew. Chem., Int. Ed.* **2000**, *39*, 2632−2657.

(28) Note: Copper(I) acetylides are generally complex extended multiatom aggregates, at least in the solid state and in the absence of good nitrogen ligands (see ref 24). The types of reactive intermediates shown in Scheme 1 are not meant to be precise or definitive structures—indeed, some of them (e.g., A(ii) and B(ii)) are very closely related—but rather are meant to illustrate different (possible) features of the putative reactive intermediate: How many copper atoms are needed to play significant structural or electronic roles during the catalysis? Is the copper σ-acetylide π-activated by an additional Cu atom? If the intermediate has two or more copper atoms, is it doubly bridged—as envisaged for a Glaser coupling, which can be ruled out with bidentate ligands for Cu if azide is also coordinated—or singly bridged? Are the reacting azide and alkyne attached to the same or different Cu atoms?

Scheme 1. Proposed Mechanism of the Huisgen−Meldal−Fokin Cu(I)-Catalyzed Alkyne−Azide Cycloaddition (CuAAC) Reaction[48]

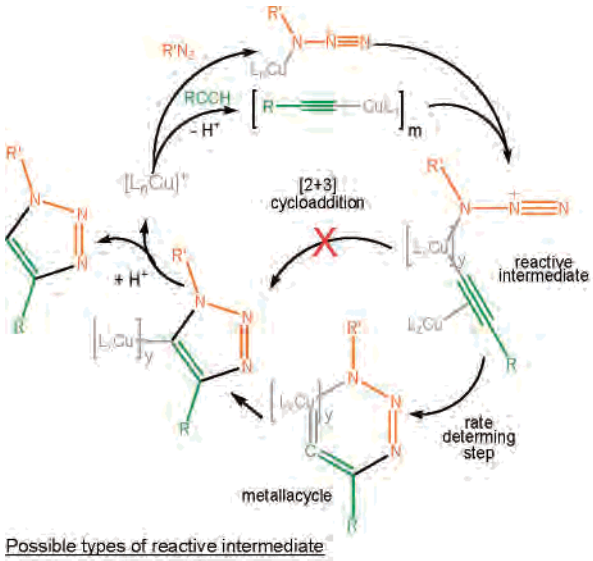

Possible types of reactive intermediate

Type A
(i) one copper atom or (ii) one copper atom + π-activation of Cu-acetylide by a second copper atom

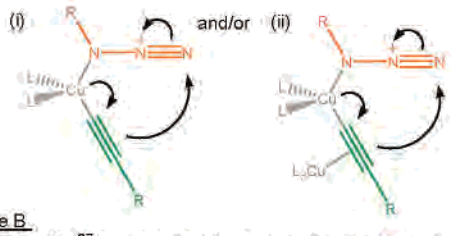

Type B
(i) Glaser-like[27] *bis*-alkyne bridged intermediate, or more generally since kinetic studies do not implicate two alkynes in the reaction, (ii) two μ-coordinated copper atoms featuring a π-activated Cu-acetylide. These structures differ from A(ii) only by the two copper atoms being doubly bridged. Doubly-bridged intermediates are not possible with bidentate ligands for copper (assuming RN_3 coordinates to Cu).

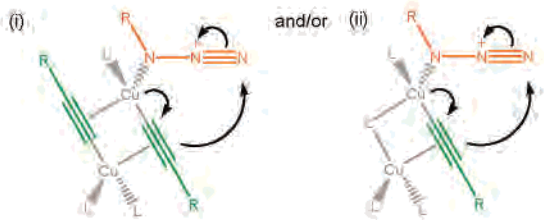

Type C
The azide and alkyne groups that react are on different copper atoms - (i) non-π-activated alkyne, (ii) π-activated alkyne. These differ from B only in the location of the alkyne which reacts with the azide. Doubly-bridged intermediates are not possible with bidentate ligands for copper (assuming RN_3 coordinates to Cu).

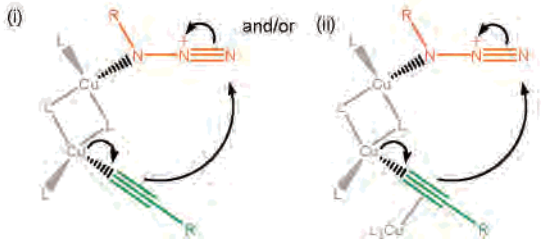

the pyridine macrocycle **1a**, alkyne **2**, azide **3**, and [Cu(CH_3-$CN)_4$](PF_6) in CH_2Cl_2 for 24 h afforded—after demetalation with KCN—a mixture of [2]rotaxane **4a** (57%) and the noninterlocked triazole thread **5** (41%), together with some of the unconsumed starting macrocycle (Scheme 2 and Table 1, entry 1).[3] By varying the reaction conditions and reactant stoichiometry (Table 1), yields of up to 94% of [2]rotaxane with respect to the amount of macrocycle used were achieved (5 equiv of **2** and **3**; Table 1, entry 2) for this stoichiometric active-metal template reaction (Figure 1a). The use of substoichiometric amounts of copper was investigated to determine whether the metal would turn over as both a template and a cycloaddition catalyst (i.e., a

Scheme 2. Active-Metal Template CuAAC Synthesis of [2]Rotaxanes **4a**−**o** from Alkyne **2**, Azide **3**, and Macrocycles **1a**−**o**[a]

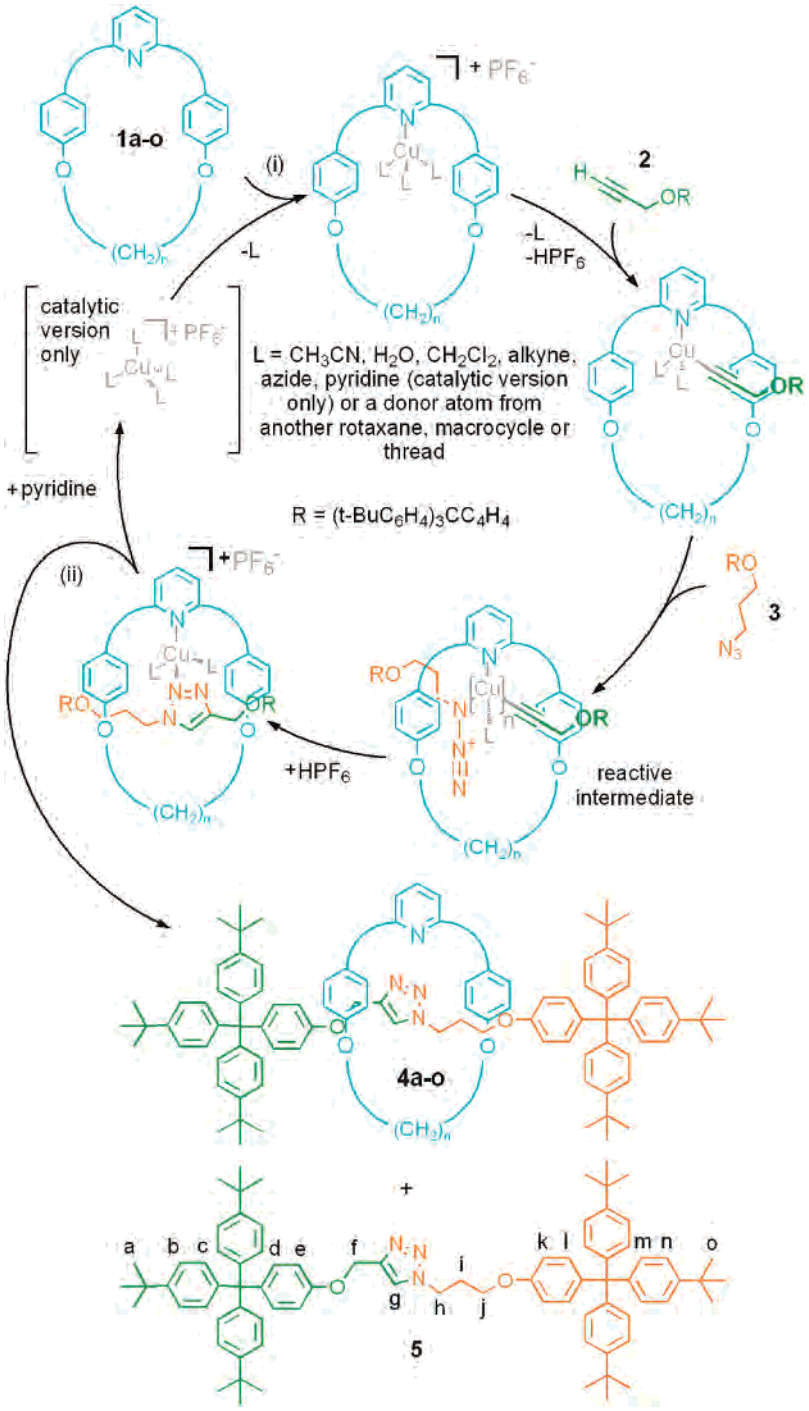

[a] Reagents and conditions: (i) **1a**−**o** (0.01 M), Cu(I) salt (generally $[Cu(CH_3CN)_4](PF_6)$; see the text), poorly coordinating solvent (generally CH_2Cl_2; see the text), and, in the catalytic version of the active-metal template reaction (Figure 1b), 3 equiv of pyridine; (ii) KCN, CH_2Cl_2/CH_3OH.[3] For the effect of the reaction conditions and reagent stoichiometry on the yields of **4a** and **5**, see Table 1. For the relative yields of **4a**−**o** using a standardized set of reaction conditions see Figure 4

.

catalytic active-metal template synthesis, Figure 1b). When using 20 mol % (with respect to **1a**) $[Cu(CH_3CN)_4](PF_6)$ at room temperature, the reaction appeared to stop after an amount of [2]rotaxane equivalent to the amount of copper present had been formed, suggesting that the multidentate rotaxane sequesters the transition metal during the reaction, inhibiting further catalytic activity. Addition of pyridine as a competing ligand enabled the catalyst to turn over, producing a substoichiometric reaction, but the reaction was extremely slow at 25 °C (Table 1, entry 3). Elevating the temperature (70 °C, $ClCH_2CH_2Cl$) gave an

(29) (a) Fuller, A.-M.; Leigh, D. A.; Lusby, P. J.; Oswald, I. D. H.; Parsons, S.; Walker, D. B. *Angew. Chem., Int. Ed.* **2004**, *43*, 3914−3918. (b) Fuller, A.-M. L.; Leigh, D. A.; Lusby, P. J.; Slawin, A. M. Z.; Walker, D. B. *J. Am. Chem. Soc.* **2005**, *127*, 12612−12619. (c) Leigh, D. A.; Lusby, P. J.; Slawin, A. M. Z.; Walker, D. B. *Chem. Commun.* **2005**, 4919−4921. (d) Leigh, D. A.; Lusby, P. J.; Slawin, A. M. Z.; Walker, D. B. *Angew. Chem., Int. Ed.* **2005**, *44*, 4557−4564. (e) Fuller, A.-M. L.; Leigh, D. A.; Lusby, P. J. *Angew. Chem., Int. Ed.* **2007**, *46*, 5015−5019.

Table 1. Effect of Reaction Conditions and Reagent Stoichiometry on the Active-Metal Template CuAAC Synthesis of [2]Rotaxane **4a** (Scheme 2)[3]

entry	amt of **2** and **3** (equiv)	amt of $[Cu(CH_3CN)_4](PF_6)$ (equiv)	solvent	*T* (°C)	conversion to triazole **2** + **3** → **4a** + **5** (%)	yield of rotaxane **1a** → **4a** (%)
1[a]	1	1	CH_2Cl_2	25[d]	>95	57
2[a]	5	1	CH_2Cl_2	25[d]	92	94
3[b]	5	0.2	CH_2Cl_2	25[d]	44	59
4[b]	5	0.2	$ClCH_2CH_2Cl$	25 → 70[e]	94	82
5[c]	1	0	$ClCH_2CH_2Cl$	25 → 70[f]	<5	0

[a] All reactions were carried out at 0.01 M concentration with respect to **1a** using the procedure shown in Scheme 2. [b] 3 equiv of pyridine. [c] Control experiment with no $[Cu(CH_3CN)_4](PF_6)$ present to demonstrate that the thermal reaction does not occur at these temperatures. [d] 24 h. [e] 12 h and then 24 h. [f] 12 h and then 72 h.

improved yield (82%) of rotaxane **4a** in a reasonable time period (36 h) using only 4 mol % Cu(I) with respect to both **2** and **3** (Table 1, entry 4).

Effect of the Nature of the Cu(I) Source

A number of different Cu(I) salts were screened for the reaction shown in Scheme 2 using the conditions shown in Table 1, entry 1, but replacing the $[Cu(CH_3CN)_4](PF_6)$ salt with other Cu(I) complexes. The use of CuOTf·benzene gave a 78% conversion of **2** and **3** into triazole products after 24 h but only a 46% yield of [2]rotaxane **4a**. By letting the reaction continue for a further 2 days (72 h in total), complete conversion of the starting azide and alkyne to triazole products was achieved (48% rotaxane). Substituting CuI for $[Cu(CH_3CN)_4](PF_6)$ led to very little reaction during the first 24 h (8% conversion to triazole), presumably due to the low solubility of CuI in CH_2Cl_2, but interestingly, what little alkyne and azide had reacted formed rotaxane with high selectivity (7:1 rotaxane:thread). The reaction proceeded slowly to completion (>98% conversion) over three weeks. However, at the end point of the reaction the product ratio (56:44 rotaxane:thread) was no different from that of the analogous $[Cu(CH_3CN)_4](PF_6)$-mediated experiment.

We also synthesized and isolated various discrete Cu(I)−**1a** complexes and tested their efficacy in the active-metal template reaction. The macrocycle **1a** and the different Cu(I) salts were mixed in CH_3CN solution and the resulting Cu(I)−**1a** complexes obtained through precipitation by vapor diffusion with diethyl ether. The preformed Cu(I)−**1a** complexes were submitted to the standard rotaxane-forming reaction conditions (Table 1, entry 1). The preformed $[Cu(CH_3CN)_4](PF_6)$−**1a** complex gave 76% conversion to triazole and a 53% yield of [2]rotaxane; the preformed CuOTf−**1a** complex gave 53% conversion to triazole but only a 5% yield of [2]rotaxane; the preformed CuI−**1a** complex gave results identical to those of the CuI−**1a** complex formed in situ (i.e., >98% triazole conversion over 3 weeks, 56% rotaxane).

Although there is some variation in the efficacy of the various Cu(I) salts on the rotaxane-forming reaction and some unexplained variation in the rotaxane:thread ratio during the course of the reaction with some sources of Cu(I), simple addition of $[Cu(CH_3CN)_4](PF_6)$ is the most convenient way of maximizing the CuAAC yield of rotaxane.[30]

(30) We also examined the effect of different alkyne substrates on the rotaxane formation. The alkynes (see the Supporting Information) were submitted to the standard click reaction conditions (Scheme 2). Using a longer, more flexible, alkylalkyne or an arylalkyne in the place of **2** led to similar yields of the corresponding [2]rotaxanes (and similar overall conversions of the substrates into triazole products), indicating the active-metal template rotaxane-forming reaction is rather insensitive to substrate modifications.

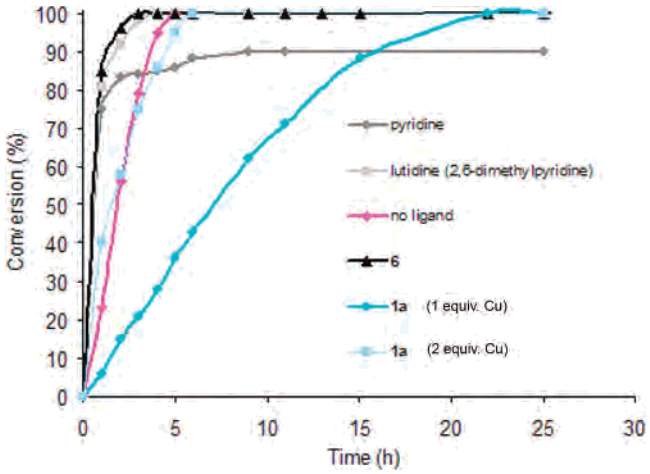

Figure 2. Conversion to triazole (i.e., thread + rotaxane if applicable) vs time for different pyridine-based ligands for the CuAAC reaction. Conditions: (i) ligand (1 equiv), alkyne **2** (1 equiv), azide **3** (1 equiv), $[Cu(CH_3CN)_4](PF_6)$ (1 equiv, 1 or 2 equiv with **1a**), CD_2Cl_2, rt, 0.01 M. The conversion of **2** and **3** into the triazole products (thread **5**, + rotaxane **4a** where relevant) was monitored by ^1H NMR.

Kinetic Studies

Some simple kinetic measurements were made to determine whether, under these reaction conditions, the Cu(I)-catalyzed alkyne−azide cycloaddition is actually accelerated by pyridine-based ligands. The rate of formation of triazole products (i.e., thread, plus rotaxane where relevant) was compared for the ligand-free[23] reaction and reactions containing pyridine, 2,6-dimethylpyridine (lutidine), 2,6-bis[(alkyloxy)methyl]pyridine macrocycle **1a**, and **6**, a close but acyclic analogue of **1a**.

The results (Figure 2) show that both lutidine and **6**, the acyclic analogue of **1a**, significantly accelerate the CuAAC reaction rate (essentially complete conversion to triazole after 3 h) compared to that of the Cu(I)-catalyzed reaction when no pyridine-based ligand is added (complete conversion after 6 h). The presence of pyridine also initially accelerates the reaction, but the conversion tails off after 2 h, suggesting that using unsubstituted pyridine as a ligand facilitates the oxidation of Cu(I) to noncatalytic Cu(II) under the reaction conditions. The role of the pyridine ligands in the rate acceleration is probably to break up extended copper(I) acetylide aggregates to form smaller reactive intermediates of the types shown in Scheme 1, although we cannot rule out an electronic effect of the ligand on the metal as well.

Interestingly, the Cu(I)-catalyzed formation of triazole products (both rotaxane and thread) in the presence of macrocycle **1a** (with 1 equiv of Cu)—which also presumably breaks up the

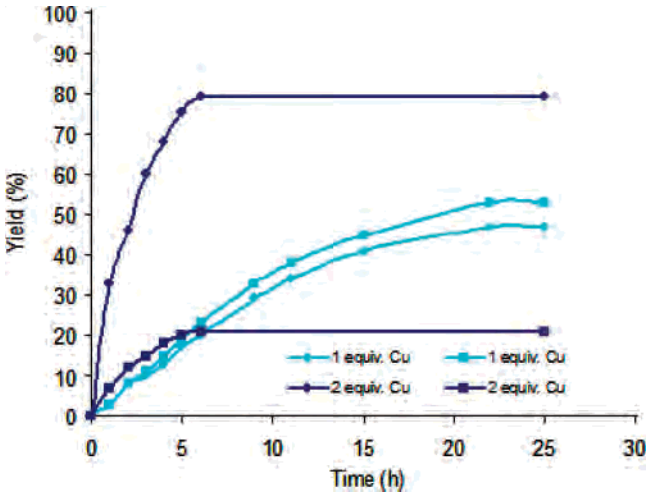

Figure 3. Formation of triazole products (rotaxane **4a,** ■; thread **5**, ●) vs time for the CuAAC reaction in the presence of macrocycle **1a**. Conditions: (i) **1a** (1 equiv), **2** (1 equiv), **3** (1 equiv), $[Cu(CH_3CN)_4](PF_6)$ (1 or 2 equiv), CD_2Cl_2, rt, 0.01 M. The conversion of **2** and **3** into thread **5** and rotaxane **4a** was monitored by ^1H NMR.

copper acetylide aggregates—is actually *slower* (24 h compared to 6 h) than the ligand-free Cu(I)-catalyzed reaction. While it might seem surprising that the active-metal template reaction is slower than the ligand-free reaction given that excellent yields of rotaxane are obtained under both stoichiometric and catalytic active-metal template conditions (Table 1), the rationale for this is quite straightforward. First, the alkyne−azide cycloaddition with the macrocyclic ligand must take place *through* the macrocycle cavity, a sterically restricted environment compared to the ligandless Cu(I)-catalyzed reaction, effecting the solvation of the reactive species as well as hindering any motion required to achieve bond formation or changes of geometry at the copper center. Second, the macrocyclic ligand might disfavor certain types of reactive intermediates (e.g., B) on steric grounds, so the reaction may proceed through another type of slower reacting, but still viable, intermediate (e.g., A or C rather than B). The reason that the ligandless formation of the triazole thread does not dominate given the slow rate of rotaxane formation is that the macrocycle is an excellent ligand for the Cu(I) and sequesters it, preventing the inherently faster ligand-free reaction (probably via B(ii)) from occurring. Accordingly, addition of a second equivalent of Cu(I) to the reaction containing **1a** should accelerate the rate of triazole formation to close to the ligand-free rate. Indeed, this was found to be the case (Figures 2 and 3). However, while one might expect this increase to be totally due to thread formation, analysis shows that the rate of *rotaxane* formation is also increased by adding an extra equivalent of Cu(I) to this reaction (Figure 3). In fact, the final yield of [2]-rotaxane only falls from 57% to 22% even though the triazole-forming reaction is complete in 6 h instead of 24 h. The acceleration of the rotaxane-forming reaction by excess Cu(I) strongly suggests that π-activation of the copper acetylide unit (see Scheme 1) is the dominant process in the CuAAC reaction mechanism of **1a**.

Effect of the Macrocycle Structure on [2]Rotaxane Formation

To further investigate both the scope and the mechanism of the active-template rotaxane-forming reaction shown in Scheme 2, we varied the structure of the pyridine-based macrocycle. The macrocycles used in the study are shown in Figure 4, and their syntheses are detailed in the Supporting Information. To compare the relative yields of rotaxane and thread within the ligand series, the macrocyclic ligands were screened using a standard, rather than optimized,[31] set of stoichiometric active-metal template reaction conditions in which the original macrocycle **1a** generates appreciable quantities of both rotaxane and thread. The conditions used were 1 equiv of macrocycles **1a**−**o**, 1 equiv of alkyne **2**, 1 equiv of azide **3**, and 1 equiv of $[Cu(CH_3CN)_4](PF_6)$ at a concentration of 0.01 M in CH_2Cl_2 at room temperature for 24 h. In most cases the starting alkyne **2** and azide **3** were completely consumed during the course of the reaction. After 24 h (72 h for **1n** and **1o**) each reaction was treated with KCN to remove the Cu(I), analyzed by ^1H NMR to determine the yield (shown in Figure 4) under the standard set of conditions, and then purified to give authentic samples of each [2]rotaxane. The yield (the percentage shown in red in Figure 4) of each rotaxane is the conversion of the macrocycles **1a**−**o** to the corresponding [2]rotaxanes **4a**−**o**. The conversion to triazole (the percentage shown in parentheses in Figure 4) is the overall conversion of the alkyne **2** and azide **3** into both thread **5** and rotaxanes **4a**−**o**.

Mono- and Tridentate Macrocycles. In addition to the strongly coordinating pyridine nitrogen, macrocycle **1a** has two ether oxygen atoms that could potentially be involved in (albeit weak) coordination to the metal atom during the active-template reaction, making **1a** a monodentate or possibly weakly bidentate or very weakly tridentate ligand.[32] Not only is macrocycle **1b** missing the ether oxygen atoms, but the pyridine nitrogen atom lone pair is tied up in strong intramolecular bifurcated hydrogen bonds to the adjacent amide groups,[33] so it was rather surprising to find that [2]rotaxane **4b** was successfully produced in the active-metal template reaction, albeit in only 6% yield. Coordination of **1b** to the copper occurs at the expense of the intramolecular hydrogen bonds[34,35] so that **1b** is able to act as an effective monodentate ligand. In contrast, the use of **1c**—a tridentate macrocyclic ligand with three hard donor atoms—gave a similar overall conversion to triazole but with no rotaxane

(31) The standard reaction conditions use 1 equiv of each reagent and low temperatures to minimize the background uncatalyzed thermal cycloaddition. These conditions were chosen to allow the relative efficacy of the different macrocycles in promoting rotaxane formation to be assessed. No attempt was made to optimize the reaction conditions to improve the rotaxane yields reported in Figure 4. For macrocycles **1a**, **1i**, **1j**, **1f**, **1l**, **1m**, and **1n**—all of which produce significant rotaxane and are not degraded under the reaction conditions—virtually all the macrocyclic ligand can be converted to rotaxane by using extended reaction times and an excess of the azide and alkyne building blocks.

(32) For an X-ray structure of **1a** as a monodentate ligand in a rotaxane (Pd(II) as the metal atom) see ref 29b; for X-ray structures of a related pyridine diether ligand acting as a bidentate ligand in a rotaxane (Cu(II) or Ni(II) as the metal atom) see ref 29d.

(33) (a) Hunter, C. A.; Purvis, D. H. *Angew. Chem., Int. Ed. Engl.* **1992**, *31*, 792−795. (b) Johnston, A. G.; Leigh, D. A.; Nezhat, L.; Smart, J. P.; Deegan, M. D. *Angew. Chem., Int. Ed. Engl.* **1995**, *34*, 1212−1216. (c) Leigh, D. A.; Moody, K.; Smart, J. P.; Watson, K. J.; Slawin, A. M. Z. *Angew. Chem., Int. Ed. Engl.* **1996**, *35*, 306−310. (d) Leigh, D. A.; Murphy, A.; Smart, J. P.; Slawin, A. M. Z. *Angew. Chem., Int. Ed. Engl.* **1997**, *36*, 728−732. (e) Leigh, D. A.; Murphy, A.; Smart, J. P.; Deleuze, M. S.; Zerbetto, F. *J. Am. Chem. Soc.* **1998**, *120*, 6458−6467. (f) Deleuze, M. S.; Leigh, D. A.; Zerbetto, F. *J. Am. Chem. Soc.* **1999**, *121*, 2364−2379. (g) Clegg, W.; Gimenez-Saiz, C.; Leigh, D. A.; Murphy, A.; Slawin, A. M. Z.; Teat, S. J. *J. Am. Chem. Soc.* **1999**, *121*, 4124−4129. (h) Biscarini, F.; Cavallini, M.; Leigh, D. A.; León, S.; Teat, S. J.; Wong, J. K. Y.; Zerbetto, F. *J. Am. Chem. Soc.* **2002**, *124*, 225−233. (i) Bottari, G.; Dehez, F.; Leigh, D. A.; Nash, P. J.; Pérez, E. M.; Wong, J. K. Y.; Zerbetto, F. *Angew. Chem., Int. Ed.* **2003**, *42*, 5886−5889. (j) Leigh, D. A.; Venturini, A.; Wilson, A. J.; Wong, J. K. Y.; Zerbetto, F. *Chem.—Eur. J.* **2004**, *10*, 4960−4969.

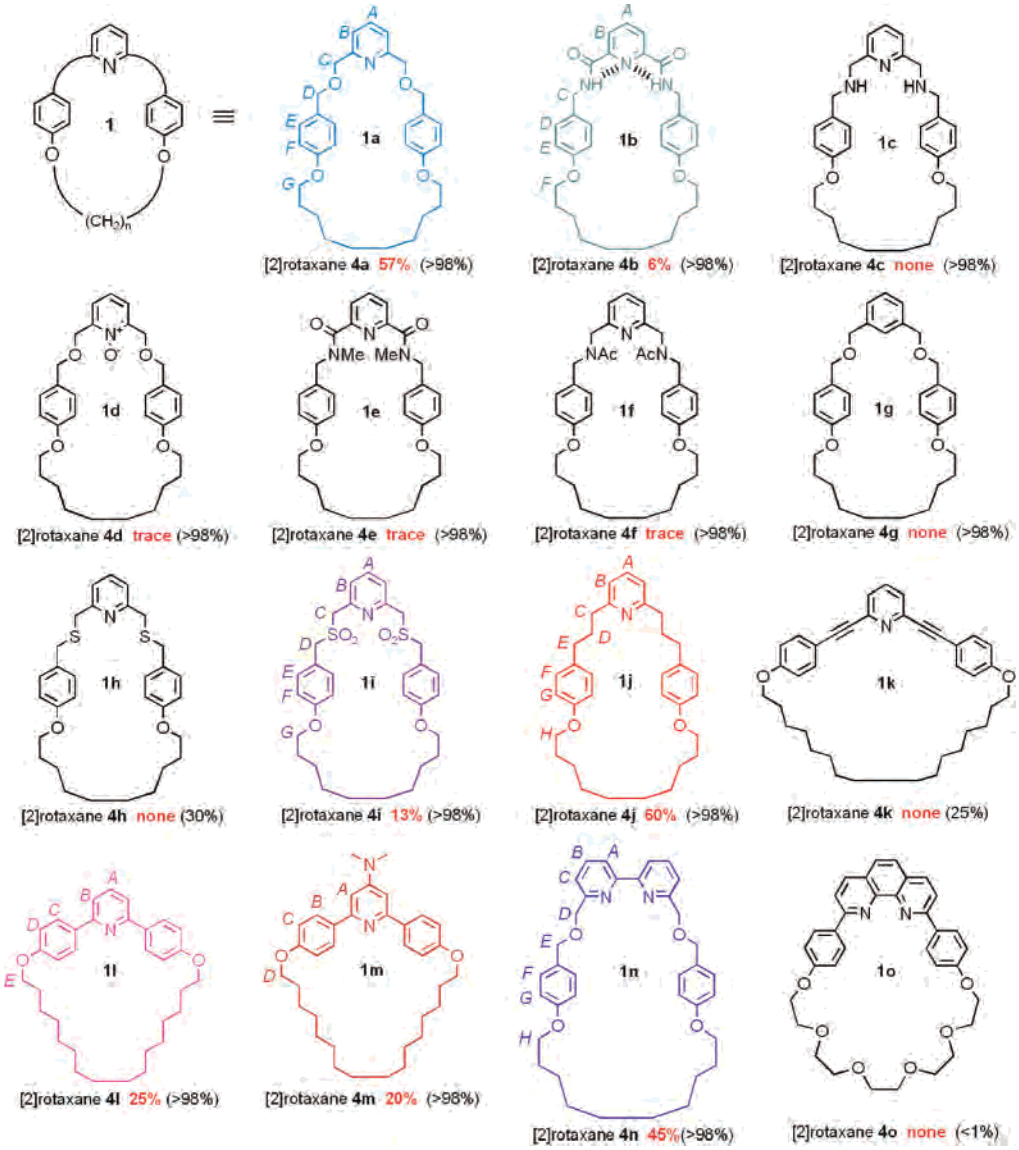

Figure 4. Influence of the macrocycle structure on the active-metal template CuAAC rotaxane-forming reaction in Scheme 2 under a standardized set of reaction conditions. Conditions for Scheme 2: (i) **1a**−**o**, **2**, **3**, $[Cu(CH_3CN)_4](PF_6)$, CH_2Cl_2, rt, 24 h (72 h for **4n** and **4o**), 0.01 M concentration with respect to each of **1a**−**o**, alkyne **2**, azide **3**, and $[Cu(CH_3CN)_4](PF_6)$; the reactions were not run under an inert atmosphere, nor using distilled or dried solvents; (ii) KCN, CH_2Cl_2/CH_3OH. The conversion of each macrocycle to [2]rotaxane is given as a percentage yield in red, and the overall conversion of **2** and **3** into triazole products (rotaxanes **4a**−**o** and thread **5**) is shown for each macrocycle in parentheses. The designation "trace" means that the rotaxane was observed by ESI-MS but could not be detected by ^{1}H NMR. The colors and lettering correspond to the signals and assignments of the ^{1}H NMR spectra shown in Figure 5.

formed. Upon addition of **1c** to the copper catalyst and other reagents the solution changed color immediately from colorless to blue-green. This suggests that most of the Cu(I) is rapidly oxidized to Cu(II) upon coordination to **1c**.[36] The resulting Cu(II)−**1c** complex is not catalytically active for the alkyne−azide cycloaddition, and any tridentate Cu(I)−**1c** complex lacks the free coordination sites necessary to bind azide and alkyne in the same aggregate.[37] However, enough of the copper in the reaction is not tied up as the **1c** complex for the ligandless thread-forming triazole reaction to proceed to completion within 24 h.

Macrocycle **1d** has a structure similar to that of **1a** except that the pyridine nitrogen is oxidized. The result, >98% conversion to triazole but only a trace of rotaxane when using **1d** as the macrocycle in the active-template reaction, shows that the *N*-oxygen atom greatly affects the ligand's ability to coordinate to Cu(I). Macrocycle **1e** also has a constitution

(34) Hydrogen bond energies are usually in the range of 1−10 kcal/mol, whereas coordinate bonds have energies of 20−80 kcal/mol;[35] thus, the stabilization of the copper(I) ion upon coordination should compensate for the loss of the two hydrogen bond interactions. In fact, all of the pyridine-containing macrocycles studied exhibit complexation-induced shifts in the ^{1}H NMR spectra ($CDCl_3$) upon addition of $[Cu(CH_3CN)_4](PF_6)$, indicating that copper(I) ions interact with the macrocycles in every case.

(35) Goshe, A. J.; Crowley, J. D.; Bosnich, B. *Helv. Chim. Acta* **2001**, *84*, 2971−2985.

(36) This oxidation of Cu(I) to Cu(II) in the presence of **1c** occurs even when great care is taken to exclude both moisture and oxygen from the reaction mixture. It appears that the macrocycle itself is the oxidant. However, there is some remaining $[Cu(CH_3CN)_4](PF_6)$ which catalyzes the formation of the thread **5**.

(37) The multidentate ligand tris[(1-benzyl-1*H*-1,2,3-triazol-4-yl)methyl]amine (TBTA) is a highly effective copper ligand for the CuAAC reaction [see refs 6b and 17a,b and Gupta, S. S.; Kuzelka, J.; Singh, P.; Lewis, W. G.; Manchester, M.; Finn, M. G. *Bioconjugate Chem.* **2005**, *16*, 1572−1579]. However, the individual triazole-functionalized "arms" of TBTA are weakly coordinating ligands, so TBTA probably functions by the alkyne and azide displacing two of the triazole groups to form the reactive intermediate.

similar to that of **1b**, but the secondary amides are methylated, eliminating their ability to form hydrogen bonds. AM1 calculations[38,39] using Spartan (see the Supporting Information) show that the methyl groups distort and partially fill the macrocycle cavity. The result is that, like that of **1d**, little of the CuAAC reaction is directed through the macrocycle cavity to form rotaxane. The same effect is seen for macrocycle **1f**, the bis-*N*-acetylated analogue of **1c**.

Removing the pyridine nitrogen atom, macrocycle **1g**, completely switches off rotaxane formation, confirming the need for a ligating donor atom. Replacing the benzylic oxygens of **1a** by more strongly coordinating sulfur atoms produces another tridentate macrocycle, **1h**. As with **1c**, no rotaxane is formed—consistent with the premise that tridentate ligand complexes of Cu(I) lack the vacant coordination sites necessary to bind both azide and alkyne[37]—and the yield of triazole is also only 30%, indicating that **1h** is particularly effective in sequestering the copper. Oxidation of the sulfide groups to sulfones, macrocycle **1i**, restores the ability of the macrocycle to bind to the Cu(I) as a monodentate ligand, and despite the increased bulk around the coordinated metal ion, a significant amount (13%) of [2]-rotaxane **4i** is formed by the stoichiometric active-metal template reaction. In fact, substitution of the benzylic ether oxygen atoms by methylene groups confirms that only a monodentate macrocycle with a single strongly coordinating donor atom is required for an efficient active-template rotaxane-forming reaction; macrocycle **1j** generates just as much [2]rotaxane as the parent macrocycle **1a**. Modeling suggests that the cavity of macrocycle **1j** is rather more flexible than that of **1a**, yet this is not detrimental for rotaxane formation.

To test whether other macrocycle geometries would be tolerated by the active-template reaction, we prepared **1k** and **1l** in which the substituted benzylic units were replaced by arylalkynyl and aryl groups, respectively. The 2,6-bisalkynylpyridine unit proved to be unstable[40,41] under the reaction conditions, suppressing the overall yield of the CuAAC reaction, with no rotaxane being produced. However, the active-metal template CuAAC reaction proceeded smoothly with **1l**, albeit generating rather less rotaxane (25%) than the most effective examples of other macrocycle geometries (**1a** and **1j**). AM1 calculations[38] using Spartan (see the Supporting Information) indicate that **1l** has a well-defined persistent cavity suitable for the threading of a molecular chain. However, the phenyl groups flanking the pyridine sterically encumber the nitrogen donor atom of the macrocycle, and a combination of steric and electronic factors probably reduces the binding strength of this macrocycle for Cu(I) ions. The weaker binding leads to more ligandless[23] Cu(I) in solution, resulting in higher conversion of the substrates into the noninterlocked thread **5** and the relatively modest yield of [2]rotaxane **4l**. Increasing the steric bulk at the 4-position of the pyridine group while simultaneously increasing the electron-donating ability of the heterocyclic nitrogen atom, macrocycle **1m**, had little effect on the rotaxane yield.

Bidentate Macrocycles. Having established that monodentate ligands of several different macrocycle geometries and donor atom orientations (**1a**, **1j**, **1l**, **1m**) efficiently promote active-template rotaxane formation, whereas strongly tridentate macrocycles (**1c** and **1h**) do not, we investigated the efficacy of bidentate macrocycles **1n** and **1o**.[17,42] The bipyridyl macrocycle **1n** directs the CuAAC reaction through its cavity to form rotaxane almost as efficiently as the best monodentate macrocycles (45% for **1n** → **4n** compared to 57% for **1a** → **4a** and 60% for **1j** → **4j**). However, it severely inhibits the rate of the Cu(I)-catalyzed reaction, and it took 3 days for the active-metal template reaction **1n** → **4n** to go to completion, compared to 24 h for **1a** → **4a** and 6 h for the ligand-free Cu(I)-catalyzed control reaction (Figure 3). The inhibition of the Cu(I)-catalyzed cycloaddition is even more dramatic with the other bidentate ligand investigated, the 2,9-diphenylphenanthroline macrocycle **1o** used extensively to assemble rotaxanes and catenanes by the Sauvage group.[1b,i] Macrocycle **1o** completely inhibits the CuAAC reaction. Even after 3 days under the standard stoichiometric active-metal reaction conditions in the presence of **1o**, no triazole products were observed. This latter result is particularly interesting given that phenanthroline ligands have previously been reported[17] to promote the CuAAC reaction. The lack of reactivity is presumably a result of the steric bulk about the Cu(I) center in the complex preventing the complex from undergoing the various structural variations required for reaction to take place (e.g., tolerating the change in geometry from Cu(I) to the formal Cu(III) species, Scheme 1), together with the macrocycle being very effective in sequestering the Cu(I) in this unreactive form. A related Cu(I)−macrocycle complex has recently been reported to promote the formation of [2]rotaxanes via a Glaser alkyne homocoupling.[13] However, in that case, intermediates of type B (Scheme 1) are possible with a bidentate ligand for copper because no azide need be coordinated to the metal atom.

^{1}H NMR Spectra of the Metal-Free [2]Rotaxanes

The ^{1}H NMR spectra (400 MHz, 300 K, $CDCl_3$) for each of the rotaxanes formed in >5% yield are shown in Figure 5. The ^{1}H NMR spectra of the rotaxanes (Figure 5b−g) all show upfield shifts of several signals with respect to the signals of the noninterlocked components (thread **5**, Figure 5a, and the macrocycles **1a**, **1b**, **1i**, **1j**, **1m**, and **1n**; see the Supporting Information). Such shielding is typical of interlocked structures in which the aromatic rings of one component are positioned face on to with another component and is observed for all the nonstopper resonances of the axle (H_{f-j}), indicating that the macrocycle accesses the full length of the thread. This is as expected; there should be no strong intercomponent noncovalent interactions between the thread and the macrocycle in the metal-free rotaxanes. The one exception is the amide-containing rotaxane **4b** (Figure 5c), which exhibits a significant downfield shift of the amide resonance with respect to that of the free macrocycle (see Supporting Information). This can be attributed to hydrogen bonding between the amides of the macrocycle and

(38) Minimum energy conformations were calculated for each of the metal-free macrocycles using the Spartan molecular modeling program (Semi-Empirical, AM1). The results are provided in the Supporting Information.
(39) In the case of **1e** no hydrogen bonds are present, thus allowing the Cu(I) ion better access to the macrocycle's pyridine nitrogen atom. However, in each of macrocycles **1e** and **1f** the nitrogen atom of the pyridine is more hindered, which may reduce the binding ability of the ligand.
(40) Internal alkynes have been found to react under CuAAC conditions; see: Díez-González, S.; Correa, A.; Cavallo, L.; Nolan, S. P. *Chem.—Eur. J.* **2006**, *12*, 7558−7564.
(41) Macrocycle **1k** is also photosensitive and decomposes slowly in ambient light.
(42) Bidentate bipyridine and phenanthroline ligands have been shown to significantly enhance the kinetics of the CuAAC reaction; see ref 17b.

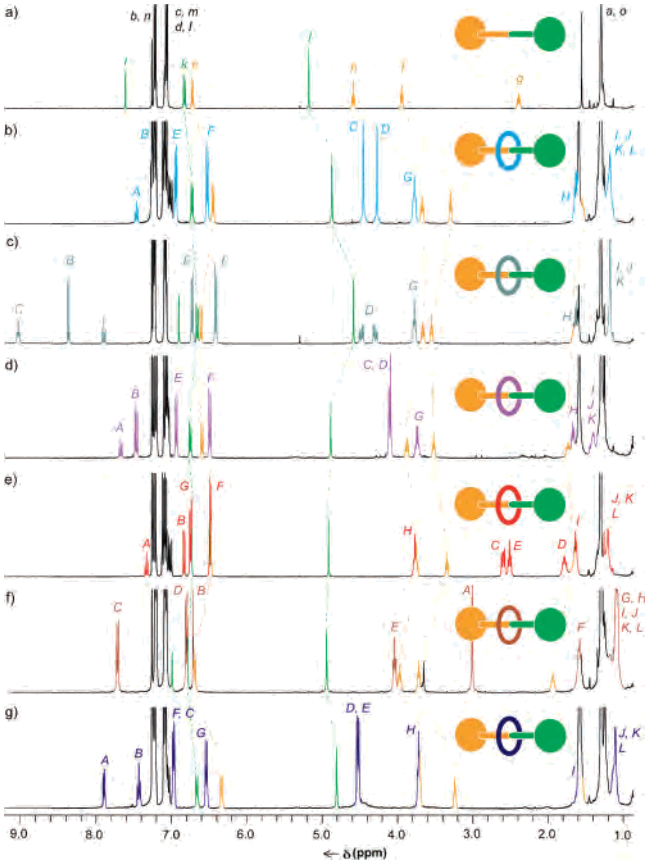

Figure 5. ^{1}H NMR spectra (400 MHz, $CDCl_3$, 300 K) of (a) triazole thread **5**, (b) [2]rotaxane **4a**, (c) [2]rotaxane **4b**, (d) [2]rotaxane **4i**, (e) [2]rotaxane **4j**, (f) [2]rotaxane **4m**, and (g) [2]rotaxane **4n**. The assignments correspond to the lettering shown in Scheme 2 and Figure 4.

the triazole unit of the thread in an interaction similar to that previously observed between interlocked amide and pyridine components in rotaxanes and catenanes.[1j,29]

Active-Metal Template CuAAC Reaction at High Macrocycle:Cu(I) Ratios: Unexpected Formation of [3]Rotaxanes

The picture of the active-metal template CuAAC reaction that we can build up that is consistent with the experimental observations so far is that the ligand-free $[Cu(CH_3CN)_4](PF_6)$ salt and macrocycles **1a**−**o** are in equilibrium with the corresponding copper(I)−macrocycle complex in which, in most cases, the metal atom directs the cycloaddition of the azide and alkyne through the macrocycle cavity. Although the ligand-free reaction is inherently faster than the active-metal template one, the coordinating ability of the macrocycle means that the rotaxane-forming reaction can become competitive with, or even dominate, the thread-forming reaction. In general, a stronger binding macrocyclic ligand (e.g., **1a** compared to **1b**) should move this equilibrium in favor of rotaxane formation. However, some changes in coordination geometry about the metal are required for the CuAAC mechanism to operate (Scheme 1), so the most strongly binding macrocycle (**1o**), which apparently does not tolerate such changes, actually inhibits the rotaxane-forming reaction. In view of this, we decided to investigate other conditions in which rotaxane formation might be increased at the expense of the thread.

In an attempt to minimize the amount of ligandless Cu(I) present in the reaction, we carried out the active-metal template CuAAC protocol under the standard set of conditions (1 equiv of **2**, 1 equiv of **3**, 1 equiv of $[Cu(CH_3CN)_4](PF_6)$, CH_2Cl_2, rt) used previously but in the presence of 10 equiv of macrocycle (Scheme 3). Our initial experiments[43] were carried out with monodentate macrocycle **1l**, and we were immediately intrigued to find that the reaction was much slower with 10 equiv of the macrocycle than it had been with 1 equiv, the higher macrocycle:Cu(I) reaction taking more than one week to go to completion. Upon reaching this end point, the mixture of triazole products was found to consist of 30% thread **5**, 37% [2]rotaxane **4l**, and, to our surprise, 33% [3]rotaxane **7l** (yields quoted with respect to the alkyne and azide reactants). A reaction using macrocycle **1a** under the same experimental conditions (1 equiv of **2**, 1 equiv of **3**, 1 equiv of $[Cu(CH_3CN)_4](PF_6)$, and 10 equiv of **1a**, CH_2Cl_2, rt) was again slower than the same reaction with 1 equiv of macrocycle (3 days to reach completion compared to 24 h), generating a product mixture of 5% thread **5**, 90% [2]rotaxane **4a**, and 5% [3]rotaxane **7a** (yields quoted with respect to the alkyne and azide reactants). A similar but less dramatic trend was seen with bidentate macrocycle **1n**; with 10 equiv of **1n** the reaction took 10 days to complete (cf. 3 days with 1 equiv), producing 3% thread **5** and 97% [2]rotaxane **4n** (in this case no [3]rotaxane **7n** could be detected by ^{1}H NMR spectroscopy).

The remarkable features of these high macrocycle:Cu(I) ratio active-metal template reactions are the following:

(i) Exceptional combined rotaxane yields: 95% ([2]rotaxane **4a** + [3]rotaxane **7a**) compared to 57% for **4a** with 1 equiv of **1a**; 70% ([2]rotaxane **4l** + [3]rotaxane **7l**) compared to 25% for **4l** with 1 equiv of **1l**; 97% ([2]rotaxane **4n**) compared to 45% for **4n** with 1 equiv of **1n**.

(ii) Significant slowing of the reaction rates compared to the low macrocycle:Cu(I) ratio reactions. The largest effect on the rate is seen with the weakly copper-binding macrocycle **1l**; the smallest effect on the rate occurs for the strongly copper-binding macrocycle **1n**. Again, this is strongly suggestive experimental evidence that the dominant mechanism of the CuAAC reaction under these conditions involves activation of the copper σ-acetylide unit by a second, preferably ligandless for steric reasons, copper atom (i.e., **I** or **II**, Scheme 3).

(iii) Formation of [3]rotaxane (in 33% yield using macrocycle **1l**)—i.e., *two* macrocycles being threaded during the formation of *one* triazole ring. Molecular models show that this can most reasonably occur through the sort of bridged two copper atom intermediate **III** shown in Scheme 3. Since such a doubly bridged intermediate cannot occur with bidentate ligands (and no [3]rotaxane is observed with **1n**), it seems likely that monodentate pyridine ligand-promoted CuAAC reactions proceed via doubly bridged intermediates such as **I** (Scheme 3), the equivalent of intermediate B(ii) in Scheme 1, whereas bidentate bipyridyl ligand-promoted CuAAC reactions proceed

(43) We chose macrocycle **1l** for this study because it is a rather poor ligand (indeed, we were unable to generate complexes with it using several other metals) due to the steric crowding around the pyridine nitrogen and the π-electron density presented to the low-oxidation-state copper from the adjacent aromatic rings. The rather weak Cu(I) binding affinity—meaning there is more ligandless[23] Cu(I) present in solution than many of the other macrocycles shown in Figure 4—is most likely the reason for the modest yield of rotaxane using 1 equiv of this macrocycle. We reasoned the yield should be improved by increasing the macrocycle:copper ratio.

Scheme 3. Effect of the Macrocycle:Cu(I) Ratio on the Active-Metal Template CuAAC Reaction[a,b]

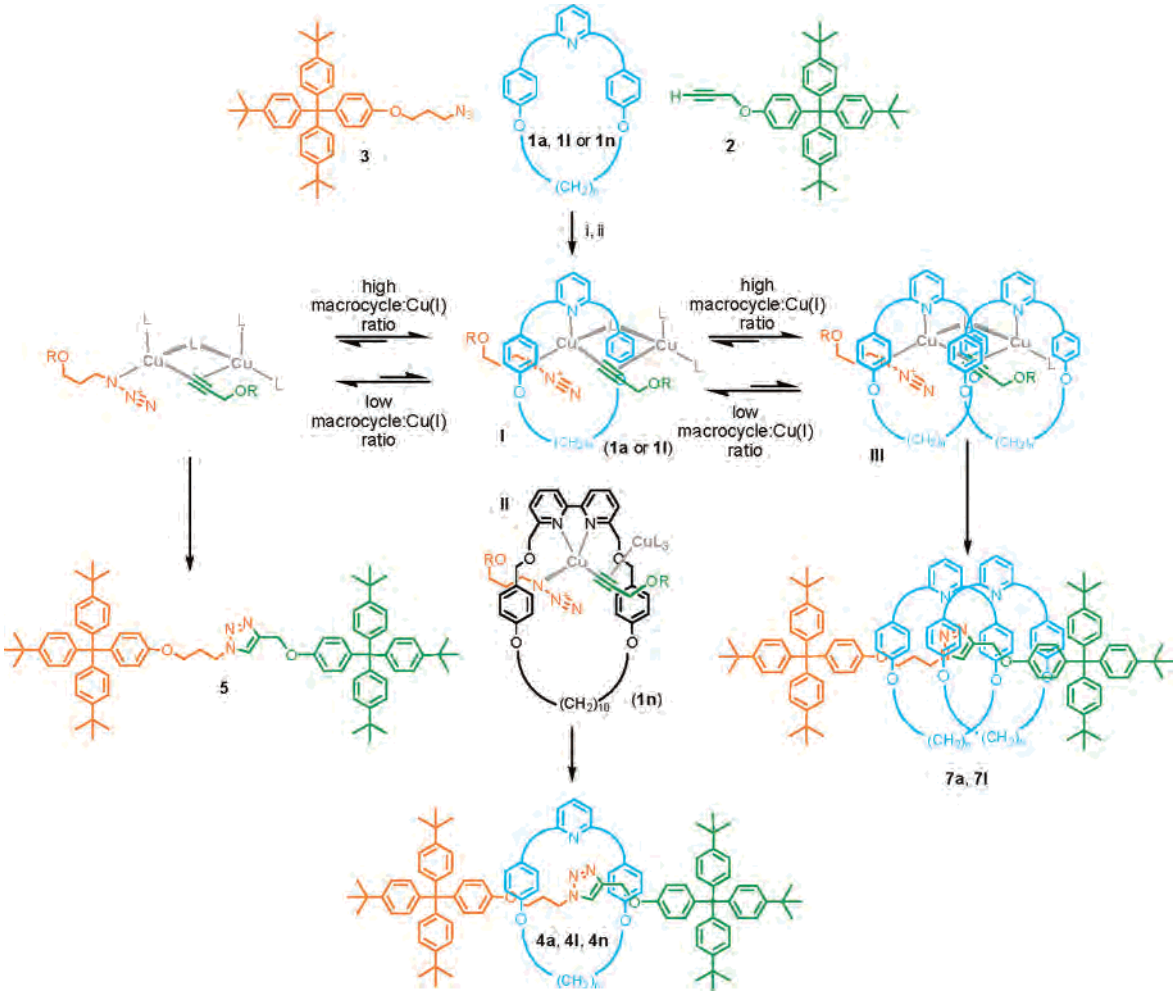

[a] Reagents and conditions: (i) **1a**, **1l**, or **1n** (10 equiv), **2** (1 equiv), **3** (1 equiv), $[Cu(CH_3CN)_4](PF_6)$ (1 equiv), CH_2Cl_2, rt, 24 h (**1a**), 7 days (**1l**), 10 days (**1n**); (ii) KCN, CH_2Cl_2/CH_3OH. Product yields starting from macrocycle **1a**: thread **5** (5%), [2]rotaxane **4a** (90%), [3]rotaxane **7a** (5%). Product yields starting from macrocycle **1a**: thread **5** (5%), [2]rotaxane **4i** (33%), [3]rotaxane **7l** (37%). Product yields starting from macrocycle **1n**: thread **5** (3%), [2]rotaxane **4n** (97%), [3]rotaxane **7n** (0%). [b]In the reactive intermediates shown, the copper azide (orange) reacts with any of the copper alkyne units shown in green. L can be any nonreacting ligand, including other alkyne and azide groups.

via simple π-coordinated complexes such as **II** (Scheme 3), the equivalent of intermediate A(ii) in Scheme 1.

The ^{1}H NMR spectra of [2]rotaxane **4l** and [3]rotaxane **7l** are shown in parts b and c, respectively, of Figure 6. The resonances for the axle (H_{f-j}) of the rotaxanes are shifted upfield compared to the signal for the free noninterlocked thread **5** (Figure 6a). The effect is more pronounced in the [3]rotaxane (Figure 6c) than in the [2]rotaxane (Figure 6b). Due to the asymmetry of the thread, the ^{1}H NMR spectrum of [3]rotaxane **7l** (Figure 6c) displays inequivalent but overlapping peaks for the two macrocycle components, which are double the intensity of the corresponding macrocycle signals in the [2]rotaxane. Single crystals of **7l** suitable for X-ray crystallography were grown by slow cooling of a hot saturated solution of **7l** in acetonitrile. The solid-state structure (Figure 7) confirmed the constitution of **7l** as a [3]rotaxane. Although it may superficially appear that face-to-face π-stacking interactions might aid the relative orientation of the two macrocycles on the thread, in the solid state the aromatic rings of adjacent macrocycles are not coplanar and their separation (>3.8 Å) is somewhat greater than that typically associated with aromatic stacking interactions.

Stoichiometric and Catalytic Active-Metal Template Synthesis of Bistriazole [2]Rotaxanes

To see whether the copper(I) would turn over catalytically during the formation of a single molecule, we investigated systems which require *two* cycloaddition reactions to be catalyzed in the formation of each molecule of [2]rotaxane (Scheme 4). [2]Rotaxanes **10** and **12** were each obtained in good yields (81% and 74%, respectively) using the conditions shown in Scheme 4 (0.5 equiv of Cu(I) for each triazole ring formed in a rotaxane) with either **1a**, **2**, and the diazide **8** or **1a**, **3**, and the dialkyne **9**. Since the rotaxane−Cu(I) complex in **4a** is strong enough to sequester the metal in the absence of pyridine, the lack of formation of more than trace amounts of [3]rotaxane in the reaction mixtures from Scheme 4 suggests that one macrocycle−Cu(I) complex may act processively to catalyze the formation of both triazole rings of an individual rotaxane thread. Such a hypothesis is consistent with the observation[25] by Rodionov et al. (albeit in a ligand-free Cu(I) system) of a strong kinetic enhancement in the second cycloaddition reaction when using diazide reactants. Reducing the amount of the copper salt to 20 mol % with respect to **1a** (10 mol % with respect to each

Scheme 4. Active-Metal Template CuAAC Synthesis of Bistriazole Molecular Shuttles **10** and **12**[a]

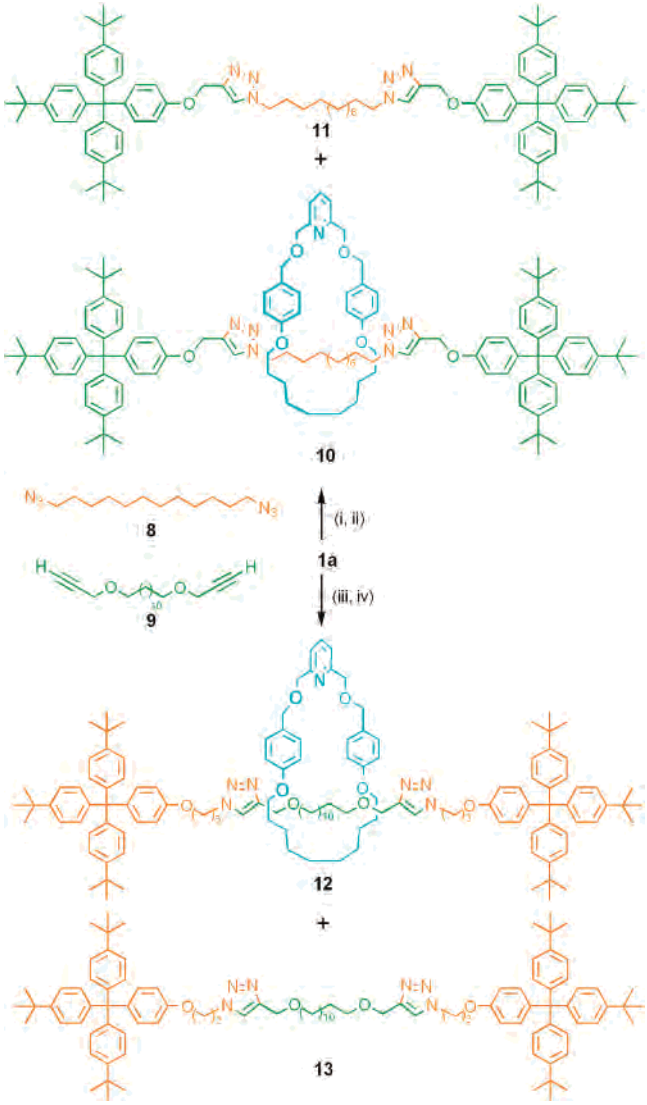

[a] Reagents and conditions: (i) **2**, $[Cu(CH_3CN)_4](PF_6)$, CH_2Cl_2, 25 °C, 72 h; (ii) KCN, CH_2Cl_2/CH_3OH, 81% ([2]rotaxane **10**) over two steps with 0.5 equiv of Cu(I), 63% ([2]rotaxane **10**) over two steps with 0.1 equiv of Cu(I) + 3 equiv of pyridine; (iii) **3**, $[Cu(CH_3CN)_4](PF_6)$, CH_2Cl_2, 25 °C, 72 h; (iv) KCN, CH_2Cl_2/CH_3OH, 74% ([2]rotaxane **12**) over two steps.

rotaxane triazole ring formed) and introducing 3 equiv of pyridine to the reaction of **1a**, **2**, and **8** to allow the processive catalyst to turn over intermolecularly still generated [2]rotaxane **10** in 63% yield (Scheme 4).

Transition-Metal-Mediated Control of the Shuttling Rate in Degenerate Two-Triazole-Station Molecular Shuttles

The shuttling of the ring in the degenerate two-station bistriazole rotaxane **10** in the presence of different diamagnetic transition-metal salts was investigated using ^{1}H NMR spectroscopy. Unlike most previously reported molecular shuttles—where the interactions used to direct the synthesis of the rotaxanes persist in the interlocked structure, resulting in a well-defined coconformation—there are no strong noncovalent interactions between the components of metal-free **10**. Comparison of the ^{1}H NMR spectrum of the free thread **11** (Figure 8a) with that of the rotaxane **10** (Figure 8b) shows uniform shielding of

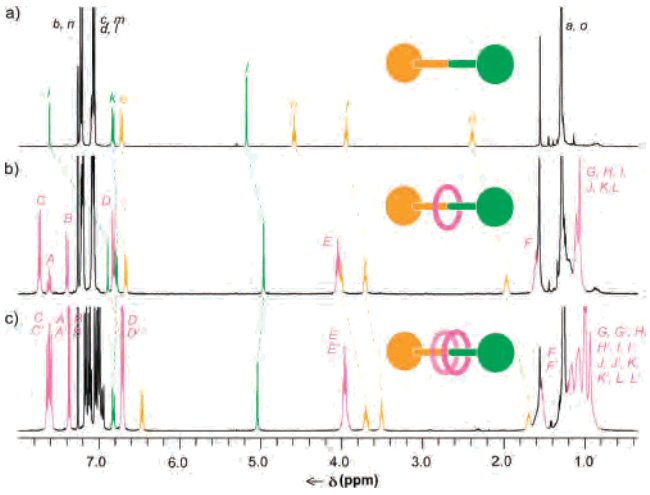

Figure 6. ^{1}H NMR spectra (400 MHz, $CDCl_3$, 300 K) of (a) triazole thread **5**, (b) [2]rotaxane **4l**, and (c) [3]rotaxane **7l**. The assignments correspond to the lettering shown in Scheme 2 and Figure 4.

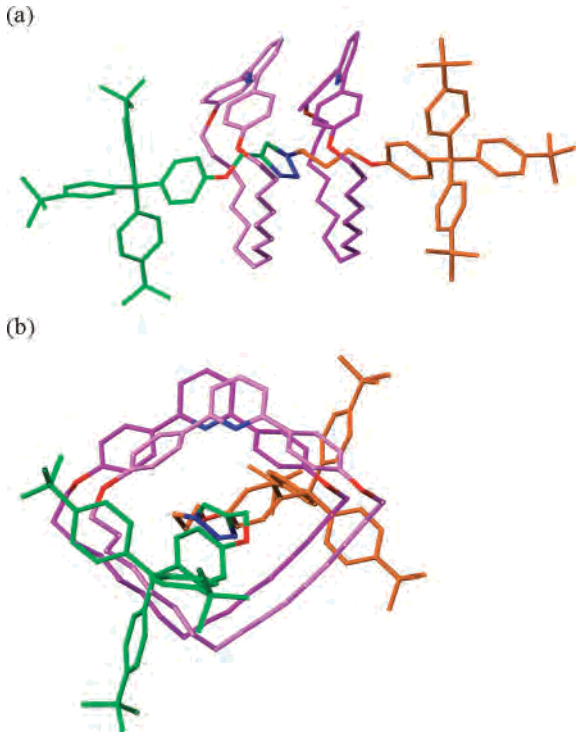

Figure 7. X-ray structure of [3]rotaxane **7l**, from a single crystal obtained from a saturated acetonitrile solution: (a) viewed side-on; (b) viewed along the axis of the thread. For clarity, different shades of purple are used for the carbon atoms of the two rings.

the thread signals (H_d, H_e, H_f, H_g, H_h), indicating that the macrocycle randomly explores the full length of the thread.

Reintroducing copper(I) into the bistriazole rotaxane[44] to form $[Cu\mathbf{10}](PF_6)$ (Scheme 5) gave a complex that exhibited fast shuttling of the macrocycle between the two triazole units in the room temperature ^{1}H NMR spectra in CD_3CN/CD_2Cl_2

(44) For examples of 1,2,3-triazoles as ligands see refs 3, 6s, and 17a,b and (a) Liu, D.; Gao, W.; Dai, Q.; Zhang, X. *Org. Lett.* **2005**, *7*, 4907−4910. (b) Dai, Q.; Gao, W.; Liu, D.; Kapes, L. M.; Zhang, X. *J. Org. Chem.* **2006**, *71*, 3928−3934. (c) Mindt, T. L.; Struthers, H.; Brans, L.; Anguelov, T.; Schweinsberg, C.; Maes, V.; Tourwe, D.; Schibli, R. *J. Am. Chem. Soc.* **2006**, *128*, 15096−15097. (d) Suijkerbuijk, B. M. J. M.; Aerts, B. N. H.; Dijkstra, H. P.; Lutz, M.; Spek, A. L.; van Koten, G.; Klein Gebbink, R. J. M. *Dalton Trans.* **2007**, 1273−1276. (e) Huffman, J. C.; Flood, A. H.; Li, Y. *Chem. Commun.* **2007**, 2692−2694.

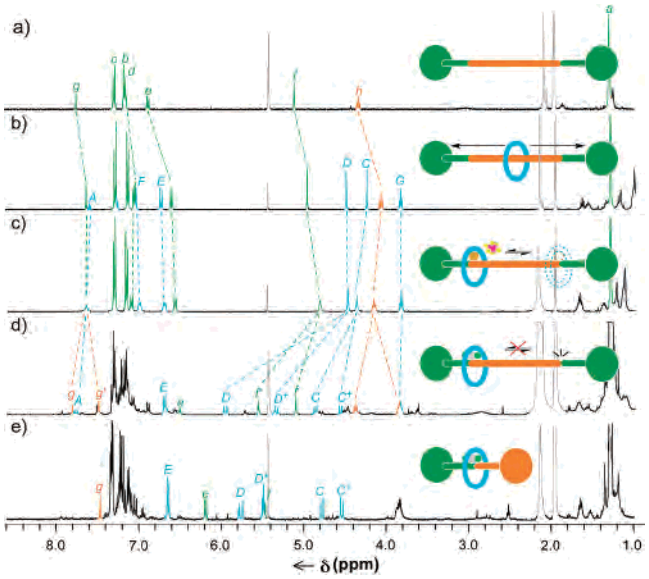

Figure 8. ^{1}H NMR spectra (400 MHz, CD_3CN/CD_2Cl_2 (9/1), 300 K) of (a) bistriazole thread **11**, (b) bistriazole [2]rotaxane **10**, (c) copper−bistriazole [2]rotaxane complex [Cu**10**](PF_6), (d) palladium dichloride−bistriazole [2]rotaxane complex Cl_2Pd**10**, and (e) palladium dichloride−triazole rotaxane complex Cl_2Pd**4a**. The assignments correspond to the lettering shown in Scheme 5.

(Figure 8c).[45] Although fast shuttling between well-defined macrocycle binding sites is very unusual for metal-coordinated molecular shuttles,[46] Cu(I) complexes can exhibit extremely fast exchange rates.[47] In contrast to this dynamic behavior, the ^{1}H NMR spectrum (Figure 8d) of rotaxane **10** following coordination of $PdCl_2$ (Scheme 5, ii) displays two sets of peaks for protons close to the thread triazole rings (e.g., $H_{f/f'}$, $H_{g/g'}$). This observation is indicative of the macrocycle in the Cl_2Pd**10** complex being unable to shuttle between the triazole stations on the NMR time scale. This restriction to shuttling also manifests itself in the geminal splitting of the signals corresponding to H_C and H_D of the macrocycle, which occurs as a consequence of the two "faces" of the ring being in different chemical environments. The chemical shifts of one set of the duplicated signals (e.g., H_f) correspond closely to those of the free thread **11** (Figure 8a). The other set of duplicate signals (e.g., $H_{f'}$) correspond closely to a model single-triazole rotaxane−$PdCl_2$ complex, Cl_2Pd**4a** (Figure 8e, Scheme 5). Heating the sample of Cl_2Pd**10** to 343 K (close to the solvent boiling point of CD_3CN) did not lead to any broadening of the signals in the ^{1}H NMR spectrum, indicating that the macrocycle shuttling is very effectively blocked by coordination to Pd.

The notable features of these degenerate two-station bistriazole rotaxanes are the following:

(i) To our knowledge these are the first examples of molecular shuttles containing two degenerate transition-metal-binding stations.

(ii) The dynamics of the macrocycle exchange between the two well-defined discrete binding sites can be controlled with remarkable ease, simply through the judicious choice of different transition-metal ions.

(iii) An active-metal template strategy is much more amendable to the synthesis of such shuttles than traditional (passive) metal template strategies, because the number of binding sites in the products is not necessarily related to the number of template sites used for the shuttle synthesis.

Scheme 5. Controlling the Dynamics of Bistriazole Molecule Shuttle **10** by Coordination to Cu(I) or Pd(II)[a]

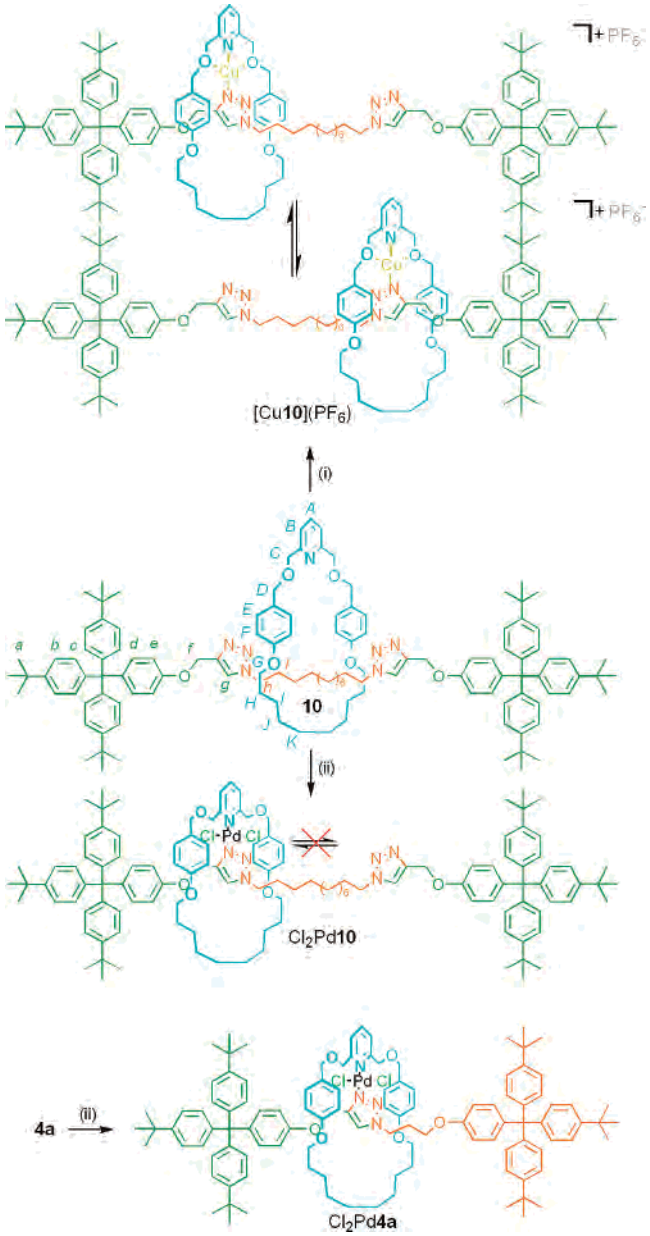

[a] Reagents and conditions: (i) $[Cu(CH_3CN)_4](PF_6)$ (1 equiv), CD_2Cl_2 (90%)/CD_3CN (10%), 25 °C, 5 min, >99%; (ii) $Pd(CH_3CN)_2Cl_2$ (1 equiv), CD_2Cl_2 (90%)/CD_3CN (10%), 25 °C, 5 min, >99%.

Conclusions

The Cu(I)-catalyzed 1,3-cycloaddition of azides with terminal alkynes is a highly effective reaction for the active-metal template synthesis of rotaxanes, as illustrated through both stoichiometric (up to 97% yields) and catalytic (up to 82% yields) versions of the strategy. The reaction tolerates a wide

(45) We were unable to slow the macrocycle shuttling dynamics in [Cu(**10**)](PF_6) sufficiently, nor isolate that motion from other conformational processes at low temperatures, to determine an accurate shuttling rate.
(46) Durola, F.; Sauvage, J.-P. *Angew. Chem., Int. Ed.* **2007**, *46*, 3537−3540.
(47) For an evaluation of ligand exchange rates at Cu(I) centers, see: Riesgo, E.; Hu, Y.-Z.; Bouvier, F.; Thummel, R. P. *Inorg. Chem.* **2001**, *40*, 2541−2546.

variety of both monodentate and bidentate macrocyclic ligands which, although inherently slower in promoting covalent bond formation than the ligand-free[23] Cu(I)-catalyzed reaction, all work by sequestering the majority of the Cu(I) present so that the rotaxane-forming CuAAC reaction becomes competitive with—and under many conditions dominates—the ligand-free CuAAC reaction. The addition of pyridine enables the Cu(I) active-metal template to turn over without significantly compromising the rotaxane yield. Among several potentially attractive features of this type of synthetic strategy is that it offers an unusual experimental probe of the reaction mechanism. The increase in rates of rotaxane formation by excess ligand-free Cu(I) supports the suggestion that in CH_2Cl_2 the copper σ-acetylide is activated by coordination to a second ligandless copper atom, and the sluggish reaction rates and remarkable formation of [3]rotaxanes with monodentate macrocycles at high macrocycle:Cu(I) ratios suggest that, under these conditions, the CuAAC reaction proceeds via a doubly bridged two copper atom intermediate (type B(ii), Scheme 1) when using a monodentate macrocyclic ligand and a simpler π-coordinated two copper atom intermediate (type A(ii), Scheme 1) when using a bidentate macrocyclic ligand.[48]

The experimental results concerning the active-metal template CuAAC synthesis of bistriazole rotaxanes suggest that the macrocycle−Cu(I) complex may act processively to catalyze the formation of more than one triazole ring per thread molecule. The resulting two-triazole-station molecular shuttles have interesting and unusual dynamic properties: coordination of the rotaxane macrocycle to Cu(I) gives a metal-complexed shuttle in which the ring still shuttles rapidly between the two triazole units of the thread, even at low temperatures in noncoordinating solvents. In contrast, complexation of the same two-triazole-station shuttle to $PdCl_2$ gives a rotaxane in which shuttling does not occur even at 343K in the presence of d_3-acetonitrile.

The template-directed assembly of otherwise difficult-to-access molecular architectures and the catalysis of covalent bond formation are two of the most useful tasks that transition metals can perform in organic chemistry. The active-template concept combines these two apparently disparate functions into one, which can produce—as the present work exemplifies—high-yielding, mild and effective synthetic routes to complex molecular structures requiring only catalytic quanitities of metal. The development of other active-template systems is in progress.

Acknowledgment. This work was supported by the European Union Future and Emerging Technology program Hy3M, the Ramsay Memorial Fellowships Trust, the Royal Society of Edinburgh, and the EPSRC. D.A.L. is an EPSRC Senior Research Fellow and holds a Royal Society-Wolfson Research Merit Award, P.J.L. is a Royal Society University Research Fellow, and J.D.C. is a British Ramsay Memorial Fellow. We thank Patrice Staub and Professor J.-P. Sauvage (Strasbourg) for generously providing us with a sample of macrocycle **1o**, termed "m-30" by the Strasbourg group in many papers. We thank Professor B. F. Straub (Munich) for a preprint of ref 26. We thank Professor V. V. Fokin (Scripps) for a preprint of ref 21 and for sharing with us his thoughts on the mechanism of the CuAAC reaction.

Supporting Information Available: Synthetic schemes, experimental procedures, and spectroscopic data for all new compounds. This material is available free of charge via the Internet at http://pubs.acs.org.

JA073513F

(48) Note added in proof: Very recent calculations (Straub, B. F. *Chem. Commun.* published online 12th July 2007 DOI: 10.1039/b706926j) suggest that the metallacycle formed in Scheme 1 consists of a strain-free Cu-C(Cu)=C unit rather than the depicted Cu=C=C unit. The second copper atom in the type B(ii) and A(ii) reactive intermediates shown in Scheme 1 means they are perfectly set up to form such a Cu-C(Cu)=C metallacycle.

J|A|C|S
COMMUNICATIONS

Published on Web 09/18/2007

[2]Rotaxanes through Palladium Active-Template Oxidative Heck Cross-Couplings

James D. Crowley, Kevin D. Hänni, Ai-Lan Lee, and David A. Leigh*

School of Chemistry, University of Edinburgh, The King's Buildings, West Mains Road, Edinburgh EH9 3JJ, United Kingdom

Received July 12, 2007; E-mail: david.leigh@ed.ac.uk

Palladium-catalyzed cross-coupling reactions are extremely powerful tools for organic synthesis, routinely proving the method of choice for the construction of C−C bonds.[1] Recently, Pd(II)-catalyzed cross-couplings have been developed as a novel alternative to the traditional Pd(0) systems, offering a change in both mechanism and reaction parameters.[2] Here we report on the utility of the Pd(II)-catalyzed oxidative Heck cross-coupling over Pd(0)-based methods in the active-metal template synthesis of [2]-rotaxanes.

Active-template syntheses differ from classical template reactions in that a single species acts as both a template AND a catalyst for covalent bond formation.[3] Combining these two roles within the action of the same metal center(s) has several potential advantages over conventional "passive" template syntheses, including inherent efficiency, scope, the possibility of traceless assembly, and—if it is able to turnover at the end of the catalytic cycle—only substoichiometric quantities of the template need to be employed.

The active-template concept has been demonstrated through the synthesis of rotaxanes using reactions such as the Cu(I)-catalyzed azide-alkyne cycloaddition—the CuAAC "click" reaction—and alkyne homocouplings.[3,4] However, to make active-template strategies truly attractive, it will be necessary to apply them to reactions that are synthetically versatile and applicable to a wide variety of different structural motifs. Palladium-catalyzed cross-couplings fit these criteria perfectly, of course. However, our initial attempts to make rotaxanes using Pd(0)-catalyzed reactions with various mono-, bi-, and tridentate macrocycles were unsuccessful, producing only the corresponding non-interlocked threads.[5] We attributed this to the Pd(0) not remaining attached to the macrocycle during key stages of the catalytic cycle. Accordingly, we switched our attention to the oxidative Heck cross-coupling[2] since Pd(II) should be ligated much more strongly than Pd(0) by nitrogen donor atoms[6] in macrocycles such as **1**.

Palladium(II) complex **2** was formed in situ by mixing macrocycle **1** (1 equiv) with a catalytic quantity (10 mol %) of $Pd(OAc)_2$ in 1:1 $CHCl_3/CH_2Cl_2$. Addition of boronic acid **3** (2 equiv), alkene **4** (1 equiv), and benzoquinone (1 equiv), followed by simple stirring under an atmosphere of oxygen at room temperature for 72 h, pleasingly led to the desired [2]rotaxane **5** in 73% yield.[7,8] These base-free conditions produced much higher yields of rotaxane **5** than standard oxidative Heck procedures,[2h] presumably because the formation of undesired homocoupled byproducts is reduced. Reducing the amount of Pd to 1 mol % still produced 66% [2]rotaxane (i.e., the metal template turns over 65 times during the reaction), albeit over a 16 day reaction time.

The proposed mechanism for rotaxane formation is shown in Scheme 1. Transmetalation of the aryl boronic acid **3** with the Pd(II) complex **2**, followed by π-coordination of alkene **4**, affords intermediate **I**. In order to achieve successful rotaxane formation, the two building blocks that ultimately form the thread need to be held on opposite faces of the macrocycle and the palladium needs to retain the stoppered ligands until it has mediated a covalent bond-forming reaction between them. Migratory insertion followed by β-H elimination thus forms a mechanical as well as a covalent bond. Decomplexation of the weakly binding Pd(0) liberates free rotaxane **5**. Reoxidation of Pd(0) to Pd(II) regenerates the catalytically active complex **2** and enables the reaction to be conducted using substoichiometric amounts of palladium.

Scheme 1. Proposed Catalytic Cycle for the Oxidative Heck Active-Template Synthesis of [2]Rotaxane **5** from **1**, **3**, and **4**

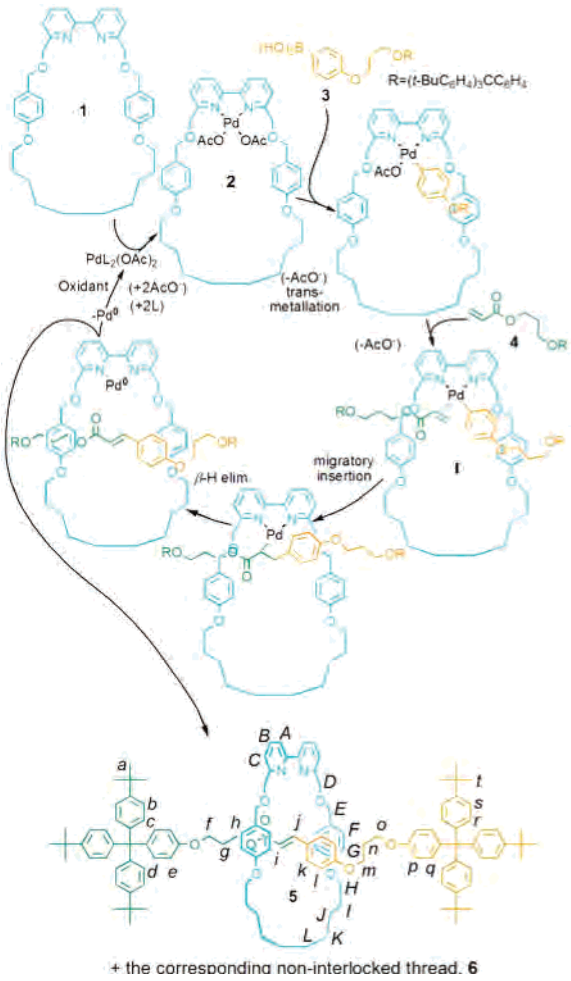

The ^{1}H NMR spectrum of rotaxane **5** in $CDCl_3$ (Figure 1b) shows an upfield shift of several signals with respect to the non-interlocked components (Figure 1a and c). The shielding, typical of interlocked architectures in which the aromatic rings of one component are positioned face-on to another component, occurs for all nonstopper resonances of the axle (H_{f-o}), indicating that the macrocycle accesses the full length of the thread in the rotaxane. However, the resonances of the protons on the half of the axle bearing the aryl ring (H_{m-o}) are shielded to a greater extend than those on the other

10.1021/ja075219t CCC: $37.00

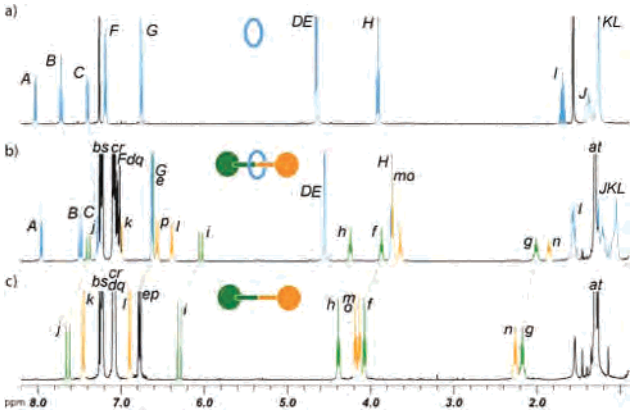

Figure 1. ^{1}H NMR spectra (400 MHz, $CDCl_3$, 298 K) of (a) macrocycle **1**, (b) [2]rotaxane **5**, (c) thread **6**. The assignments correspond to the lettering shown in Scheme 1.

Table 1. Substrate Scope in the Oxidative Heck Active-Template Synthesis of [2]Rotaxanes[a]

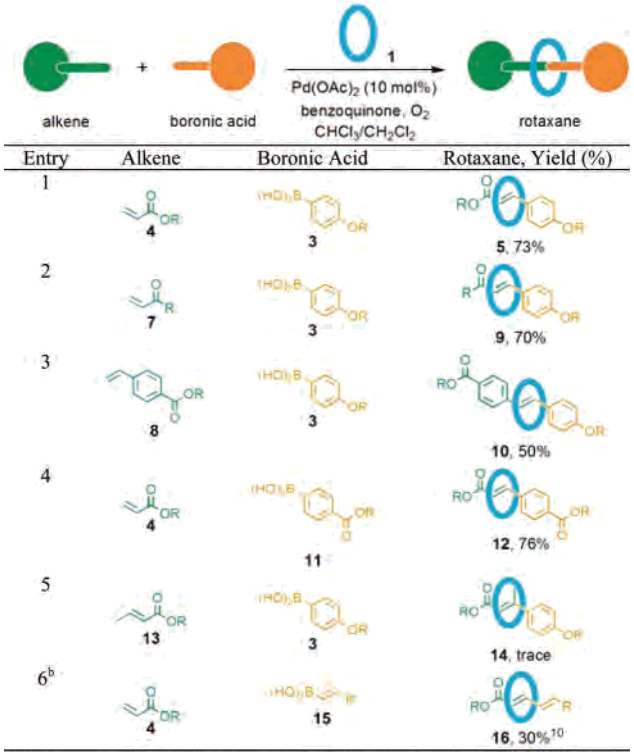

[a] R = $(t\text{-BuC}_6H_4)_3CC_6H_4O(CH_2)_3$–. Reaction conditions: macrocycle **1** (1 equiv), $Pd(OAc)_2$ (10 mol %), alkene (1 equiv), boronic acid (2 equiv), and benzoquinone (1 equiv) in 1:1 $CHCl_3/CH_2Cl_2$ were allowed to stir under O_2 at rt for 72 h. [b] Conditions as for other entries except alkene **4** (1.2 equiv), boronic acid **15** (3 equiv), no benzoquinone, 1:1 $CHCl_3$/DMF as solvent. All reactions were carried out at 16 mM concentration with respect to **1** without the need for dried or distilled solvents.

half (H_{f-h}). This preference of the macrocycle for the aromatic region of the thread is probably a result of both π-stacking interactions and solvation effects.

To examine if this new cross-coupling approach to [2]rotaxanes is tolerant of a range of different cross-coupling partners, we screened a number of alkene and boronic acid functionalized stoppers, generating a variety of [2]rotaxanes (Table 1).[9] Vinyl ketone **7** and styrene derivative **8** can replace vinyl ester **4** as the alkene cross-partner to produce the corresponding rotaxanes **9** and **10** in 70 and 50% yields, respectively. The electron-poor aryl boronic acid **11** can also be used in place of the electron-rich aryl boronic acid **3** without affecting the yield (**12**, 76%). The rotaxane-forming reaction, however, is sensitive to steric hindrance—although trisubstituted alkenes can be formed in high yields using the oxidative Heck method,[2h] the attempted coupling of disubstituted alkene **13** with boronic acid **3** resulted in only traces of the corresponding rotaxane **14**.[9] Alkene boronic acid **15** also proved suitable as a substrate, giving butadiene [2]rotaxane **16** in 30% yield.[10]

The introduction of active-template palladium cross-coupling routes to [2]rotaxanes opens up the possibility of using one of the most powerful bond-forming methodologies in organic chemistry for the assembly of mechanically interlocked architectures. The reaction is mild, substrate-tolerant, and essentially traceless with respect to the thread, and as little as 1% of the catalytic Pd(II) template is required.

Acknowledgment. This work was supported through the EU project Hy3M and the EPSRC. D.A.L. is an EPSRC Senior Research Fellow and holds a Royal Society Wolfson Research Merit Award. J.D.C. is a British Centenary Ramsay Fellow. We thank Roy T. McBurney for providing alkene **7**.

Supporting Information Available: Full experimental procedures and characterization of all products. This material is available free of charge via the Internet at http://pubs.acs.org.

References

(1) (a) Tsuji, J. *Palladium Reagents and Catalysis: New Perspectives for the 21st Century*, 2nd ed.; Wiley: Chichester, 2004. (b) *Metal-Catalyzed Cross-Coupling Reactions*, 2nd ed.; de Meijere, A., Diederich, F., Eds.; Wiley-VCH: Weinheim, Germany, 2004.

(2) (a) Du, X.; Suguro, M.; Hirabayashi, K.; Mori, A. *Org. Lett.* **2001**, *3*, 3313−3316. (b) Parrish, J. P.; Jung, Y. C.; Shin, S. I.; Jung, K. W. *J. Org. Chem.* **2002**, *67*, 7127−7130. (c) Jung, Y. C.; Mishra, R. K.; Yoon, C. H.; Jung, K. W. *Org. Lett.* **2003**, *5*, 2231−2234. (d) Inoue, A.; Shinokubo, H.; Oshima, K. *J. Am. Chem. Soc.* **2003**, *125*, 1484−1485. (e) Andappan, M. M. S.; Nilsson, P.; von Schenck, H.; Larhed, M. *J. Org. Chem.* **2004**, *69*, 5212−5218. (f) Andappan, M. M. S.; Nilsson, P.; Larhed, M. *Chem. Commun.* **2004**, 218−219. (g) Enquist, P.-A.; Lindh, J.; Nilsson, P.; Larhed, M. *Green Chem.* **2006**, *8*, 338−343. (h) Yoo, K. S.; Yoon, C. H.; Jung, K. W. *J. Am. Chem. Soc.* **2006**, *128*, 16384−16393.

(3) (a) Aucagne, V.; Hänni, K. D.; Leigh, D. A.; Lusby, P. L.; Walker, D. B. *J. Am. Chem. Soc.* **2006**, *128*, 2186−2187. (b) Berná, J.; Crowley, J. D.; Goldup, S. M.; Hänni, K. D.; Lee, A.-L.; Leigh, D. A. *Angew. Chem., Int. Ed.* **2007**, *46*, 5709−5713. (c) Aucagne, V.; Berná, J.; Crowley, J. D.; Goldup, S. M.; Hänni, K. D.; Leigh, D. A.; Lusby, P. J.; Ronaldson, V. E.; Slawin, A. M. Z.; Viterisi, A.; Walker, D. B. *J. Am. Chem. Soc.* **2007**, *129*, 11950-11963.

(4) For stoichiometric active-metal template Ullman and Glaser coupling rotaxane syntheses, in which the metal does not turnover, see: Saito, S.; Takahashi, E.; Nakazono, K. *Org. Lett.* **2006**, *8*, 5133−5136.

(5) An outline of these macrocycle−Pd(0) investigations is given in the Supporting Information. Pd(0)-catalyzed Suzuki reactions have been used as the stoppering reaction in the synthesis of cyclodextrin rotaxanes; see: (a) Terao, J.; Tang, A.; Michels, J. J.; Krivokapic, A.; Anderson, H. L. *Chem. Commun.* **2004**, 56−57. (b) Klotz, E. J. F.; Claridge, T. D. W.; Anderson, H. L. *J. Am. Chem. Soc.* **2006**, 128, 15374−15375. (c) Stone, M. T.; Anderson H. L. *Chem. Commun.* **2007**, 2387−2389.

(6) Studies[2f−h] suggest that bidentate N ligands such as bipyridine and phenanthroline are the most effective at promoting oxidative Heck reactions at room temperature. Carrying out the reaction in Table 1, entry 1, with a monodentate pyridine macrocycle resulted in no rotaxane formation and only 10% conversion to the thread.

(7) Use of $Cu(OAc)_2$ or I_2 as the oxidant produced no rotaxane; O_2 as the sole oxidant produced only 26% rotaxane (other reagents and conditions as per Table 1, entry 1). See Supporting Information for further details.

(8) According to Jung and co-workers,[2h] the base-free oxidative Heck cross-coupling shows the greatest efficiency in polar aprotic solvents. However, our rotaxane-forming reactions did not proceed efficiently in DMF (16% yield of **5**), probably due to the low solubility of the cross-coupling partners. A 1:1 mixture of $CHCl_3/CH_2Cl_2$ was found to be the optimal solvent system for the studies presented here. See Supporting Information for further details.

(9) Much lower yields of rotaxane (<5%) were obtained using pinacol boronic esters in place of boronic acids, even though the former generally gives higher yields in base-free oxidative Heck reactions.[2h] This difference is probably due to steric effects.

(10) Unoptimized yield. Rotaxane **16** proved difficult to isolate free from the accompanying byproduct thread.

JA075219T

Pendant−Bridging−Chelating−Cleavage: A Series of Bonding Modes in Ruthenium(II)-BINAPO Complexes

Tilmann J. Geldbach,* Adrian B. Chaplin, Kevin D. Hänni, Rosario Scopelliti, and Paul J. Dyson*

Institut des Sciences et Ingénierie Chimiques, Ecole Polytechnique Fédérale de Lausanne (EPFL), CH-1015 Lausanne, Switzerland

Received July 8, 2005

Reaction of 1,1′-bis(diphenylphosphino)binaphthol (BINAPO, **1**) with $[RuCl_2(\eta^6\text{-arene})]_2$ in methanol leads to dinuclear BINAPO-bridged Ru compounds $[\{RuCl_2(\eta^6\text{-}p\text{-cymene})\}_2(\mu\text{-BINAPO})]$, **2a**, in near quantitative yield. In dichloromethane or acetonitrile, **1** preferably affords mononuclear species in which one of the phosphine centers remains uncoordinated. These complexes can be further stabilized by reaction with BH_3 to afford, for example, $[RuCl_2(\eta^6\text{-}p\text{-cymene})(\eta^1\text{-BINAPO-}BH_3)]$, **4a**. Upon heating a mixture of **1** and $[RuCl_2(\eta^6\text{-}p\text{-cymene})]_2$ in DMF, P−O bond cleavage occurs to afford $[RuCl(\eta^2\text{-}PPh_2\text{-BINOL})(\eta^6\text{-}p\text{-cymene})]$, **5a**, bearing an anionic PO-chelating ligand. Ligand **1** acts as an intact chelate when reacted with $[Ru_2(\mu\text{-}Cl)_3(\eta^6\text{-}p\text{-cymene})_2][PF_6]$ to yield $[RuCl(\eta^6\text{-}p\text{-cymene})(\eta^2\text{-BINAPO})][PF_6]$, **7**. Reaction of **1** with $[RuCp(CH_3CN)_3][PF_6]$ in acetonitrile or chloroform affords $[\{RuCp(CH_3CN)_2\}_2(\mu\text{-BINAPO})][PF_6]_2$, **8**, and $[RuCp(CH_3CN)(\eta^2\text{-BINAPO})][PF_6]$, **9**, respectively. The solid-state structures of **1**, **2a**, **4a**, and **7** are reported, that of **2a** representing a rare structural example of a molecule with a bridging binaphthyl-type ligand.

1. Introduction

In recent years a plethora of complexes containing C_2-symmetric bisphosphine ligands have been synthesized and successfully used for a large range of asymmetric transformations. In particular, ruthenium(II) complexes with chiral BINAP ligands are excellent hydrogenation catalysts.[1−3] Given this background, it is interesting to note that only very few metal complexes containing the related phosphinite BINAPO ligand, **1**, have been reported, namely, of palladium,[4,5] rhodium,[6,7] and ruthenium.[8,9] This is even more surprising, as enantiopure BINAPO is accessible in a facile manner from the relatively inexpensive chiral precursor 1,1′-dinaphthol.[10]

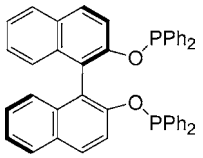

(*R*)-**1**

It has been demonstrated that with BINAPO ligands bearing substituents in the 3,3′-position of the binaphthyl backbone, good to excellent ee can be achieved in, for example, the rhodium-catalyzed hydrogenation of enamides[11] and the ruthenium-catalyzed hydrogenation of β-keto esters.[12] Yet, in both cases the catalysts were generated in situ and the nature of the active species was not determined. At present, well-defined ruthenium-BINAPO complexes are, to the best of our knowledge, restricted to the cationic $[RuXCp(BINAPO\text{-}F)]^+$ complexes prepared by Kündig and co-workers (bearing perfluorinated P-phenyl groups), which have been employed in asymmetric Diels−Alder reactions.[8] Herein, we report on the coordination chemistry of **1** with the widely used ruthenium complexes $[RuCp(CH_3CN)_3][PF_6]$, $[Ru_2(\mu\text{-}Cl)_3(\eta^6\text{-}p\text{-cymene})_2][PF_6]$, and $[RuCl_2(\eta^6\text{-arene})]_2$, of which the latter has been previously used for the in situ generation of a ruthenium-BINAPO hydrogenation catalyst.[12]

2. Results and Discussion

The reaction between the dimeric ruthenium-arene halide, $[RuCl_2(\eta^6\text{-}p\text{-cymene})]_2$, and **1** in methanol af-

* To whom correspondence should be addressed. E-mail: paul.dyson@epfl.ch.

(1) Shimizu, H.; Nagasaki, I.; Saito, T. *Tetrahedron* **2005**, *61*, 5405. (b) Crepy, K. V. L.; Imamoto, T. *Adv. Synth. Catal.* **2003**, *345*, 79. (c) Hu, A. G.; Ngo, H. L.; Lin, W. B. *Angew. Chem., Int. Ed.* **2004**, *43*, 2501.

(2) Kumobayashi, H. *Rec. Trav. Chim. Pays-Bas* **1996**, *115*, 201. (b) Zhang, X.; Mashima, K.; Koyano, K.; Sayo, N.; Kumobayashi, H.; Akutagawa, S.; Takaya, H. *J. Chem. Soc., Perkin Trans.* **1994**, 2309. (c) Miyake, T.; Seido, N.; Kumobayashi, H.; Takaya, H. *J. Org. Chem.* **1995**, *60*, 357.

(3) Mashima, K.; Kusano, K.; Ohta, T.; Noyori, R.; Takaya, H. *J. Chem. Soc., Chem. Commun.* **1989**, 1208. Ohta, T.; Takaya, H.; Noyori, R. *Inorg. Chem.* **1988**, *27*, 566. (b) Noyori, R.; Takaya, H. *Acc. Chem. Res.* **1990**, *23*, 345.

(4) Nishimata, T.; Yamaguchi, K.; Mori, M. *Tetrahedron Lett.* **1999**, *40*, 5713.

(5) Clyne, D. S.; Mermet-Bouvier, Y. C.; Nomura, N.; RajanBabu, T. V. *J. Org. Chem.* **1999**, *64*, 7601.

(6) Gergely, I.; Hegedüs, C.; Szöllösy, A.; Monsees, A.; Riermeier, T.; Bakos, J. *Tetrahedron Lett.* **2003**, *44*, 9025.

(7) Grubbs, R. H.; DeVries, R. A. *Tetrahedron Lett.* **1977**, *18*, 1879.

(8) Alerza, V.; Bernardinelli, G.; Corminboeuf, C.; Frey, U.; Kündig, P. E.; Merbach, A. E.; Saudan, C. M.; Viton, F.; Weber, J. *J. Am. Chem. Soc.* **2004**, *126*, 4843.

(9) Guo, R.; Chen, X.; Elpelt, C.; Song, D.; Morris, R. H. *Org. Lett.* **2005**, *7*, 1757. (b) Guo, R.; Elpelt, C.; Chen, X.; Song, D.; Morris, R. H. *Chem. Commun.* **2005**, 3050.

(10) Cox, P. J.; Wang, W.; Snieckus, V. *Tetrahedron Lett.* **1992**, *33*, 2253.

(11) Zhou, Y.-G.; Zhang, X. *Chem. Commun.* **2002**, 1124.

(12) Zhou, Y.-G.; Tang, W.; Wang, W.-B.; Li, L.; Zhang, X. *J. Am. Chem. Soc.* **2002**, *124*, 4952.

10.1021/om050568m CCC: $30.25
Publication on Web 09/08/2005

Scheme 1

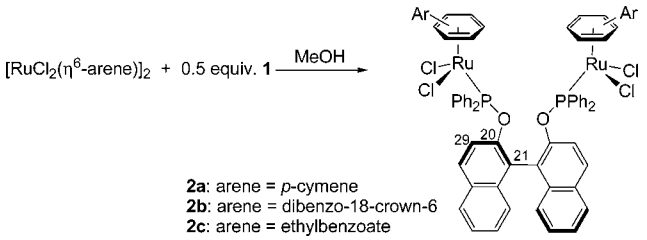

Table 1. Selected ^{13}C and ^{31}P NMR Chemical Shifts of Compounds 2a−5a and 7−9 (CD_2Cl_2 at 293 K)

	2a	3a	4a	5a	7	8	9
C1	106.9	108.9	109.3	109.7	132.8	77.7	84.7
C4	101.1	98.8	98.7	98.2	100.0		
C20	149.9	148.4	148.5	148.2	148.1	150.2	150.1
C21	121.3	121.2	120.6	119.2	124.1	122.6	124.3
C29	122.5	120.9	121.0	121.3	118.5	120.0	121.6
C20′		153.3	149.1	151.9	150.0		149.1
C21′		121.5	123.3	115.2	121.6		124.8
C29′		119.5	120.4	118.2	120.3		120.4
P1	117.8	115.1	114.3	114.1	129.5	146.7	155.9
P2	117.8	114.1	110.2		129.5	146.7	153.7

forded the phosphinite-bridged ruthenium dimer complex **2a** in near quantitative yield, as shown in Scheme 1. Irrespective of the stoichiometry, i.e., even in the presence of 2 equiv of BINAPO, **2a** was formed exclusively and no mononuclear product with a chelating ligand was observed. Neither electronic nor steric factors of the complexed arene appear to influence the course of the reaction, exemplified by the reactions with electron-rich, bulky $[RuCl_2(\eta^6\text{-dibenzo-18-6-crown})]_2$ and electron-poor $[RuCl_2(\eta^6\text{-ethylbenzoate})]_2$, respectively, which readily afford the corresponding dinuclear products **2b** and **2c**, respectively, in high yield. The solubility of these dinuclear products is very poor in methanol, allowing facile isolation and purification. Selected NMR data for **2a** (and other compounds described below) are listed in Table 1.

When the reaction between $[RuCl_2(\eta^6\text{-}p\text{-cymene})]_2$ and 2 equiv of **1** was performed in dichloromethane, four signals are observed in the ^{31}P NMR spectrum corresponding to the uncoordinated ligand ($\delta = 110.1$ ppm), complex **2a** ($\delta = 117.7$ ppm), and a new species, **3a**, with two singlets of equal intensity at $\delta = 114.1$ and 115.5 ppm, matching a ruthenium complex bearing a pendant bisphosphinite ligand. Similar spectra were also observed if the reaction was conducted in, for example, acetonitrile or DMSO. Compound **3a** is surprisingly stable with respect to coordination of the free phosphinite to a metal center, although to obtain the complex in an analytically pure form and to prevent oxidation of the pendant phosphinite moiety, **3a** was reacted with BH_3·THF to afford the borane adduct **4a** (Scheme 2). This is a common method for protecting valuable (usually chiral) phosphines from oxidation, during either storage or synthetic transformations.[13] Regeneration of the free phosphine is typically accomplished by, for example, addition of an amine base.

Attempts to introduce an additional donor ligand such as triphenylphosphine to either **2** or **4** resulted in

Scheme 2

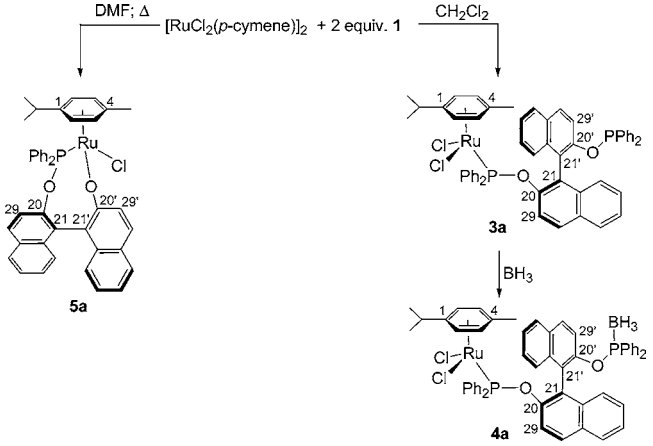

complex mixtures, presumably due to abstraction and subsequent decomposition (see below) of the BINAPO ligand.

A different product was obtained when a mixture of $[RuCl_2(\eta^6\text{-}p\text{-cymene})]_2$ and 2 equiv of **1** was heated at 100 °C in DMF, in accordance with the procedure described previously by Zhang et al. for the in situ generation of a hydrogenation catalyst.[12] Under such conditions P−O bond cleavage occurred, resulting in the mononuclear complex **5a** as the predominant species. Compound **5a** is highly soluble in organic solvents, even dissolving to some extent in diethyl ether. The structure was unambiguously assigned by NMR spectroscopy, notably from the absence of any phosphorus coupling to carbon atoms C20′, C21′, and C29′ (see Scheme 2 for numbering). This complex is likely to be the precursor to the catalytically active species in the asymmetric hydrogenation of β-keto esters. In that an eight-membered ring is formed, the chiral center is in closer proximity to the metal, providing a plausible explanation for the observed high ee when alkyl substituents on the binaphthyl moiety are present.[12]

The facile loss of a PPh_2 fragment from **1** indicates that this ligand has only limited thermal stability. Indeed, when a solution of BINAPO was heated in DMF, two new doublets were observed in the ^{31}P NMR spectrum at $\delta = 34.2$ and -24.4 ppm with a coupling constant of $J_{PP} = 222$ Hz. On the basis of these data, we tentatively suggest a product arising from P−O bond rupture and subsequent P−P bond formation, as exemplified in compound **6**. Related compounds have been synthesized previously, and their NMR data agree well with that of **6**.[14]

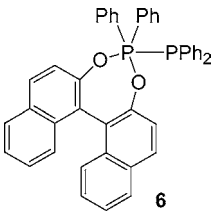

To prepare a ruthenium-arene complex where **1** acts as a chelating ligand, viz., $[RuCl(\eta^6\text{-}p\text{-cymene})(\eta^2\text{-BINAPO})]^+$, it was necessary to use an activated

(13) Recent reviews on the chemistry of amine- and phosphine-borane adducts: (a) Brunel, J. M.; Faure, B.; Maffei, M. *Coord. Chem. Rev.* **1998**, *178−180*, 665. (b) Carboni, B.; Monnier, L. *Tetrahedron* **1999**, *55*, 1197.

(14) Schmutzler, R.; Stelzer, O.; Weferling, N. *Chem. Ber.* **1988**, *121*, 391.

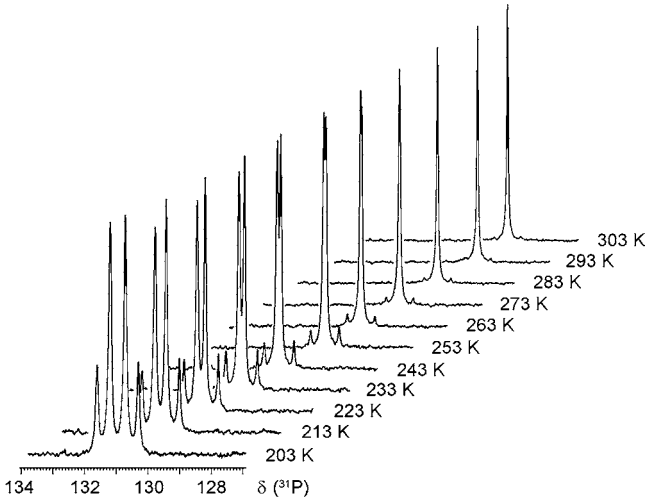

Figure 1. Variable-temperature ^{31}P NMR spectra of complex **7** between 203 and 303 K (CD_2Cl_2, 162 MHz).

Scheme 3

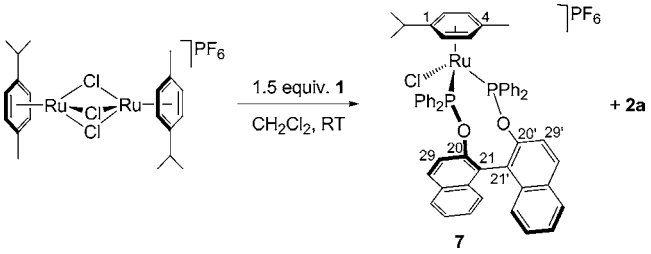

ruthenium arene precursor such as $[Ru_2(\mu\text{-}Cl)_3(\eta^6\text{-}p\text{-cymene})_2][PF_6]$. This species acts as the source for the coordinatively unsaturated, cationic synthon "$[RuCl(\eta^6\text{-}p\text{-cymene})]^+$" and readily reacts with **1** to afford complex **7**, as shown in Scheme 3. Attempts to synthesize **7** directly from **1** and $[RuCl_2(\eta^6\text{-}p\text{-cymene})]_2$ in the presence of $[NH_4][PF_6]$, $Ag[PF_6]$, or comparable chloride-abstracting agents were less successful, resulting in the formation of complex mixtures and low conversion toward the envisaged product, as evidenced by ^{31}P NMR.

With 1.5 equiv of ligand compound **2a** is formed as byproduct, facilitating the isolation of complex **7** from the reaction mixture by simple extraction with methanol. The ^{31}P NMR spectrum of **7** in CD_2Cl_2 at room temperature displays a broad singlet at $\delta = 129.5$ ppm, which upon cooling is resolved into an AB quartet with $^2J_{PP} = 67$ Hz at 203 K (see Figure 1), corroborating the proposed coordination mode. Such temperature-dependent characteristics are also known from ruthenium complexes with other chelating phosphines such as BINAP.[15] The ESI-MS of **7** exhibits a strong molecular ion peak at $[M]^+ = 925$, which upon selective fragmentation (MS/MS)[16] gives rise to a peak at $m/z = +791$ due to loss of the coordinated arene ligand.

Relative to complexes **2**−**5**, the C^1 carbon atom of the *p*-cymene ligand in **7** is shifted by more than 20 ppm to higher frequency, $\delta = 132.8$ ppm, as is readily established via C,H long-range correlation NMR, shown in Figure 2. These data suggest that in solution the interaction between C^1 and the metal is fairly weak. Accordingly, the bonding of the arene to the ruthenium is tending toward η^5-coordintaion rather than η^6, reflecting both a higher electron density at the metal due to the presence of two donor P atoms and increased steric bulk, pushing the isopropyl moiety away from the ruthenium. These effects are, though less pronounced, also present in the solid-state structure of **7** (vide infra).

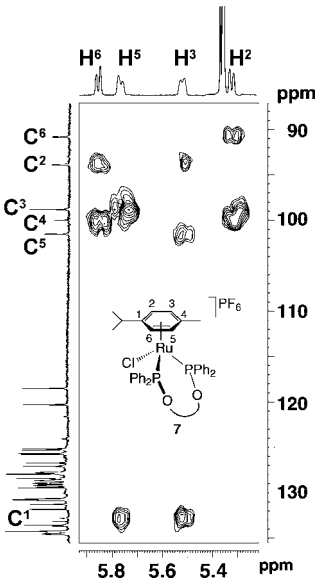

Figure 2. Section of the C,H long-range correlation spectrum of **7** showing the cross-peaks within the coordinated arene moiety arising predominantly from $^3J_{CH}$ couplings (CD_2Cl_2, 400 MHz).

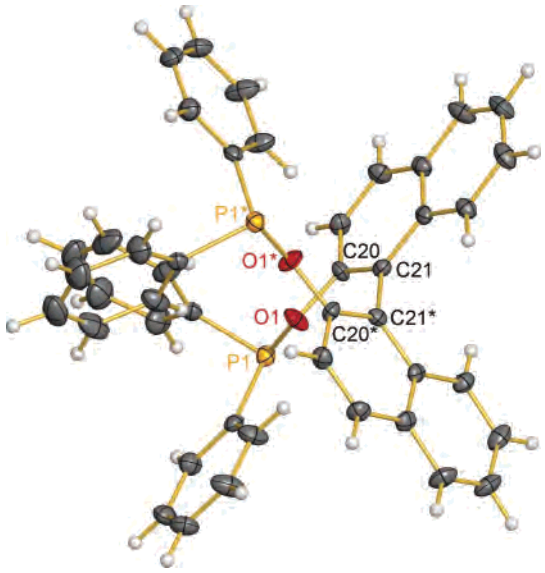

Figure 3. ORTEP plot of **1**; ellipsoids are drawn at the 40% probability level. The starred atoms are obtained by the symmetry operation $-x, y, -z$.

Crystals suitable for X-ray diffraction studies could be obtained of the free ligand **1** as well of those complexes where BINAPO acts as either bridging (**2a**), pendant (**4a**), or chelating (**7**) ligand, and representations of the structures are shown in Figures 3−6. In all crystals the binaphthyl ligand displays an *R*-configuration. Selected bond lengths and angles are given in Table 2, and relevant crystallographic data are listed in Table 3. Crystals of **2a** and **7** were of only poor quality, resulting in weak scattering and rather large thermal ellipsoids.

(15) Geldbach, T. J.; Rüegger, H.; Pregosin, P. S. *Magn. Reson. Chem.* **2003**, *41*, 703.
(16) Dyson, P. J.; McIndoe, J. S. *Inorg. Chima. Acta* **2003**, *354*, 68.

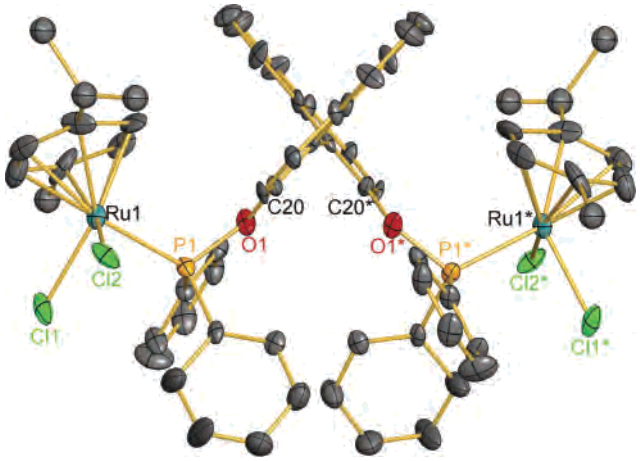

Figure 4. ORTEP plot of **2a**; ellipsoids are drawn at the 40% probability level; hydrogen atoms and solvent THF have been omitted for clarity. The starred atoms are obtained by the symmetry operation $-x$, $2-y$, z.

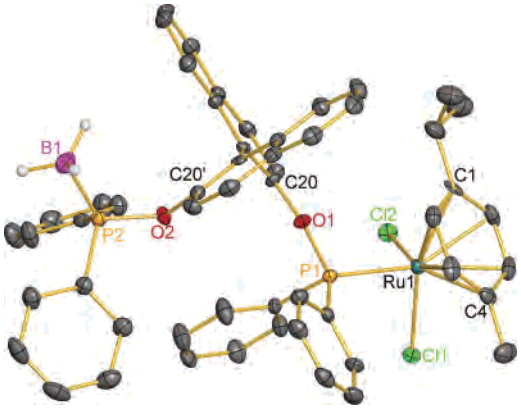

Figure 5. ORTEP plot of **4a**; ellipsoids are drawn at the 40% probability level; hydrogen atoms (except those of the BH_3) and solvent $CHCl_3$ have been omitted for clarity.

Table 2. Comparison of Selected Bond Lengths (Å) and Angles (deg) of 1, 2a, 4a, and 7

	1	2a	4a	7
Ru1−Cl1		2.365(4)	2.413(1)	2.390(2)
Ru1−Cl2		2.378(4)	2.414(1)	
Ru1−P1		2.299(4)	2.317(1)	2.323(2)
Ru1−P2				2.322(2)
P1−O1	1.659(2)	1.633(9)	1.637(3)	1.639(4)
P1−O2			1.616(3)	1.624(5)
O1−C20	1.377(2)	1.39(1)	1.403(4)	1.389(8)
O2−C20′			1.404(5)	1.383(8)
Cl1−Ru1−Cl2		87.3(1)	86.52(4)	
P1−Ru1−P2				95.65(8)
P1−Ru1−Cl1		87.6(1)	88.94(4)	85.77(7)
P2−Ru1−Cl1				82.46(7)
Cl2−Ru1−P1		90.1(1)	92.58(3)	
Ru1−P1−O1		114.1(4)	115.55(9)	121.5(2)
Ru1−P2−O2				115.0(2)

Coordination of the free ligand to the ruthenium leads to a moderate contraction of the P−O bond [1.659(2) Å in **1** versus 1.624(5)−1.640(9) Å], while interaction of the phosphinite with the Lewis acid BH_3 in **4a** has a more profound effect with an observed P(1)−O(1) bond of 1.616(3) Å. The P(2)−B(1) distance in **4a**, 1.894(6) Å,

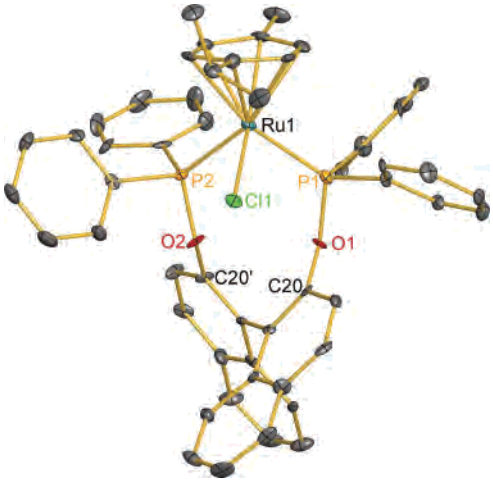

Figure 6. ORTEP plot of the cation of **7**; ellipsoids are drawn at the 40% probability level; hydrogen atoms and solvent CH_2Cl_2 have been omitted for clarity.

Scheme 4

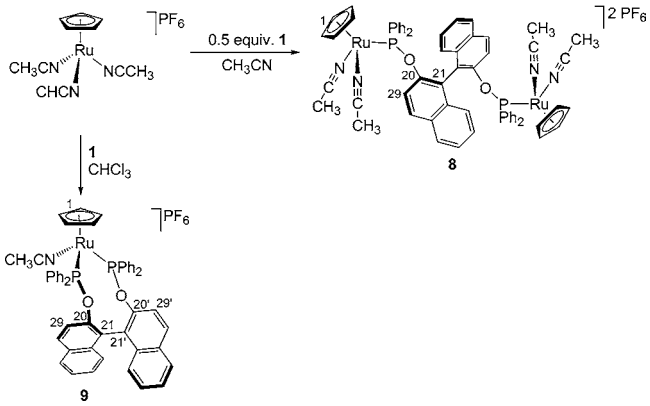

is comparable to other phosphine-BH_3 adducts.[17] The dihedral angle between the planes of the naphthyl rings in **1** is almost perpendicular, 87.75(4)°, and changes only moderately in complexes **2a** and **4a**, with values of 82.5(2)° and 89.91(5)°, respectively. However, in **7**, where **1** binds to the ruthenium in a chelating mode, a considerably smaller dihedral angle of 69.39(8)° is observed, differing from previously reported RuCp-(η^2-BINAPO-F) complexes, where the angle is close to 90°.[8]

Structural parameters around the metal center in **2a**, **4a**, and **7** are of routine nature, exhibiting the typical "piano-stool" geometry around the ruthenium. Ru−P distances are found in a range from 2.298(4) to 2.323(2) Å, Ru−Cl distances vary between 2.365(4) and 2.414(1) Å, and these data are in good agreement with those of related Ru(II) arene complexes.[18] Bond lengths

(17) McQuade, P.; Winter, R. E. K.; Rath, N. P.; Barton, L. *Inorg. Chim. Acta* **2005**, *358*, 1545. (b) McQuade, P.; Rath, N. P.; Barton, L. *Inorg. Chem.* **1999**, *38*, 5468.

(18) Representative examples: (a) Baldwin, R.; Bennet, M. A.; Hockless, D. C.; Pertici, P.; Verrazzani, A.; Barretta, G. V.; Marchetti, F.; Salvadori, P. *J. Chem. Soc., Dalton Trans.* **2002**, 4488. (b) Bhalla, R.; Boxwell, C. J.; Duckett, S. B.; Dyson, P. J.; Humphrey, D. G.; Steed, J. W.; Suman, P. *Organometallics* **2002**, *21*, 924. (c) Hansen, H. D.; Nelson, J. H. *Organometallics* **2000**, *19*, 4740. (d) Arena, C. G.; Drago, D.; Panzalorto, M.; Giuseppe, B.; Faraone, F. *Inorg. Chim. Acta* **1999**, *292*, 84. (e) Hafner, A.; Mühlebach, A.; van der Schaaf, P. A. *Angew. Chem., Int. Ed. Engl.* **1997**, *36*, 2121. (f) Elsegood, M. R.; Tocher, D. A. *Polyhedron* **1995**, *14*, 3147. (g) Bennet, M. A.; Robertson, G. B.; Smith, A. K. *J. Organomet. Chem.* **1972**, *43*, C41.

Table 3. Crystallographic Data for 1, 2a, 4a, and 7

formula	$C_{44}H_{32}O_2P_2$	$C_{64}H_{60}Cl_4O_2P_2Ru_2\cdot 2THF$	$C_{54}H_{49}BCl_2O_2P_2Ru\cdot CHCl_3$	$C_{54}H_{46}ClF_6O_2P_3Ru\cdot CH_2Cl_2$
M	654.64	1411.21	1094.02	1155.26
T [K]	140(2)	140(2)	140(2)	140(2)
cryst syst	monoclinic	orthorhombic	triclinic	orthorhombic
space group	$I2$	$P2_12_12$	$P1$	$P2_12_12_1$
a [Å]	12.3895(10)	13.776(2)	9.9885(9)	13.4669(15)
b [Å]	10.1181(6)	21.201(2)	10.8157(13)	14.7201(17)
c [Å]	13.7513(12)	10.796(2)	13.5361(10)	25.264(2)
α [deg]	90.0	90.0	99.160(10)	90.0
β [deg]	90.954(7)	90.0	99.000(7)	90.0
γ [deg]	90.0	90.0	117.294(9)	90.0
V [Å^3]	1723.6(2)	3153.0(8)	1238.3(2)	5008.2(9)
Z	2	2	1	4
density [Mg/m^3]	1.261	1.469	1.467	1.532
μ [mm^{-1}]	0.164	0.749	0.693	0.634
2θ range [deg]	$3.29 \le 2\theta \le 25.02$	$3.07 \le 2\theta \le 25.02$	$3.34 \le 2\theta \le 25.03$	$2.85 \le 2\theta \le 25.03$
no. of reflns collected	5151	19 418	7295	30 890
independent reflns	2715 [$R_{int} = 0.0239$]	5548 [$R_{int} = 0.1697$]	6434 [$R_{int} = 0.0301$]	8332 [$R_{int} = 0.1332$]
GooF on F^2	0.950	0.860	1.001	0.645
final R1, wR2 [$I > 2\sigma(I)$]	0.0314, 0.0669	0.0703, 0.1283	0.0277, 0.0639	0.0450, 0.0558
Flack x (esd)	−0.04(8)	0.20(10)	−0.02(2)	0.01(4)

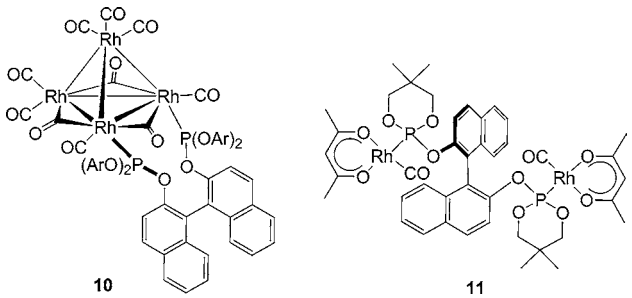

Figure 7.

between the metal and the carbon atoms of the coordinated arene are of comparable length in **2a** and **4a** [2.12(2)−2.255(4) Å] and somewhat longer in **7** [2.219(8)−2.345(8) Å], reflecting both higher electron density at the metal as well as increased steric bulk in the latter complex. In **7** the distance between the ruthenium and C(1), 2.345(8) Å, is relatively long, in agreement with the solution ^{13}C NMR data, but still sufficiently short to consider the coordination of the arene in the solid state as η^6. The bite angle of the bisphosphinite in complex **7** is 95.65(8)°, comparable to that of bisdiphenylphosphino ferrocene (dppf).[19]

A diverse coordination chemistry of ligand **1** also emerges when $[RuCp(CH_3CN)_3][PF_6]$ is employed as precursor instead of dimeric ruthenium-arene complexes; see Scheme 4. In acetonitrile, the ruthenium complex reacts with **1** to afford the dicationic complex **8** as the only product, as is evident from a singlet in the ^{31}P NMR spectrum, $\delta = 146.7$ ppm, as well as from ESI-MS, $[M]^{2+} = 575.3$. However, in noncoordinating solvents such as chloroform, **1** binds preferably in a chelating mode, affording the cationic complex **9**. This compound is readily identified from the appearance of two doublets in the ^{31}P NMR at $\delta = 155.9$ and 153.7 with a coupling constant $^2J_{PP} = 50$ Hz, as well as from the mass of the molecular ion, $[M]^+ = 861.7$.

While there are few examples for complexes bearing **1** as ligand, compounds with binaphthyl-based ligands bridging two metal centers are very rare. We are aware of only two examples where this is the case, both involving rhodium carbonyl complexes; see Figure 7. These examples differ in some respect from the compounds described herein in that they deal with phosphite ($P(OR)_3$) rather than phosphinite ($P(OR)R_2$) ligands. In **10**, a diphosphite-binaphthyl ligand coordinates to two rhodium centers in a tetranuclear Rh-carbonyl cluster,[20] whereas in the other example, assigned on the basis of its IR and ^{31}P NMR spectra, a similar ligand bridges between two rhodium centers, affording the dinuclear complex **11**.[21]

In conclusion a series of ruthenium(II) complexes bearing BINAPO ligands have been prepared, demonstrating that rather subtle changes in the reaction conditions can induce very different coordination modes of the ligand. Relative to other binaphthyl-based bisphosphines such as the widely used BINAP, ligand **1** is less likely to coordinate in a chelating manner and activated precursors are required to afford complexes of the type $[RuX(\eta^2\text{-BINAPO})(\eta^6\text{-arene})]^+$. Otherwise complexes where **1** acts as either bridging or pendant ligand predominate. These observations may have implications for the use of **1** as ligand in catalysis in that a change of solvent and/or reaction temperature may afford markedly different species, thereby potentially deciding over success or failure of a given transformation.

3. Experimental Section

General Techniques. All manipulations were performed under an atmosphere of nitrogen, using standard Schlenk techniques. Solvents were dried catalytically (Et_2O, CH_2Cl_2), distilled from calcium hydride (acetonitrile, DMF), or used as received following saturation with nitrogen (MeOH, chloroform). Chromatographic separations where carried out in air using 1.0 × 20 × 20 mm silica gel 60 F254 plates (Merck). $[RuCl_2(\eta^6\text{-}p\text{-cymene})]_2$,[22] $[RuCl_2(\eta^6\text{-dibenzo-18-crown-6})]_2$,[23] $[RuCl_2(\eta^6\text{-ethylbenzoate})]_2$,[24] $[Ru_2(\mu\text{-Cl})_3(\eta^6\text{-}p\text{-cymene})_2][PF_6]$,[25]

(19) Hamann, B. C.; Hartwig, J. F. *J. Am. Chem. Soc.* **1998**, *120*, 3694.

(20) Moasser, B.; Gladfelter W. L. *Inorg. Chim. Acta* **1996**, *242*, 125.

(21) Nifantev, E. E.; Rasadkina, E. N.; Batalova, T. A.; Bekker, A. R.; Stash, A. I.; Belskii V. K. *Zh. Obshch. Khim.* **1996**, *66*, 1109−1114.

(22) Bennett, M. A.; Huang, T. N.; Matheson, T. W.; Smith, A. K. *Inorg. Synth.* **1982**, *21*, 74.

(23) Geldbach, T. J.; Brown, M. R. H.; Scopelliti, R.; Dyson, P. J. *J. Organomet. Chem.* **2005**, in press.

(24) Therrien, B.; Ward, T. R.; Pilkington, M.; Hoffann, C.; Gilardoni, F.; Weber, J. *Organometallics* **1998**, *330*, 17.

$[RuCp(CH_3CN)_3][PF_6]$,[26] and (*R*)-**1**[27] were prepared according to methods described previously; all other compounds were commercially available and used as received. NMR spectra were recorded on a Bruker Avance 400 with chemical shifts δ given in ppm (internal lock as reference) and coupling constants *J* given in Hz as positive values regardless of their real individual signs. Electrospray ionization mass spectra (ESI-MS) were recorded on a ThermoFinnigan LCQ Deca XP Plus quadrupole ion trap instrument, and elementary analyses were carried out at the EPFL.

Synthesis of 2a. A suspension of $[RuCl_2(\eta^6\text{-}p\text{-cymene})]_2$ (100 mg, 0.16 mmol) and **1** (110 mg, 0.17 mmol) in methanol (10 mL) was heated to reflux for 5 min, and then stirring continued at room temperature for another 30 min, during which time a salmon-colored precipitate forms. The solvent was removed by filtration and the residue washed twice with methanol. Yield: 194 mg (94%). ^{1}H NMR (CD_2Cl_2, 400 MHz): 8.24 (d, $^3J_{HH}$ = 7.9, 2H, H^{26}), 8.23 (d, $^3J_{HH}$ = 9.1, 2H, H^{28}), 8.04 (d, $^3J_{HH}$ = 9.1, 2H, H^{29}), 7.76 (m, 6H), 7.61 (dd, 2H, H^{25}), 7.50 (dd, 2H, H^{24}), 7.21 (m, 2H), 7.00 (m, 4H), 6.92 (m, 4H), 6.22 (m, 4H), 5.52 (d, $^3J_{HH}$ = 6.7, 2H, H^3), 5.37 (br, 2H, H^2), 5.00 (br, 2H, H^6), 4.75 (d, $^3J_{HH}$ = 5.9, 2H, H^5), 1.83 (dq, 2H, H^7), 1.53 (s, 6H, H^{10}), 0.74 (d, $^3J_{HH}$ = 7.0, 6H, H$^{8/9}$), 0.47 (d, $^3J_{HH}$ = 6.7, 6H, H$^{8/9}$). ^{13}C NMR (CD_2Cl_2, 100 MHz): 149.9 (d, $^2J_{PC}$ = 3, C^{20}), 133.5 (C^{22}), 132.7 (d, $^2J_{PC}$ = 11), 130.5 (d, $^4J_{PC}$ = 3), 130.5 (C^{27}), 130.1 (d, $^4J_{PC}$ = 2), 130.0 (C^{28}), 129.5 (d, $^2J_{PC}$ = 9), 129.3 (C^{26}), 127.8 (d, $^3J_{PC}$ = 11), 127.6 (C^{24}), 127.0 (d, $^3J_{PC}$ = 11), 125.4 (C^{25}), 124.9 (C^{23}), 122.5 (d, $^3J_{PC}$ = 6, C^{29}), 121.3 (d, $^3J_{PC}$ = 6, C^{21}), 106.9 (C^1), 101.1 (C^4), 92.2 (d, $^2J_{PC}$ = 10, C^3), 91.6 (br, C^2), 85.5 (br, C^5), 85.1 (d, $^2J_{PC}$ = 3, C^6), 29.8 (C^7), 21.6 (C^9), 20.7 (C^8), 17.4 (C^{10}). ^{31}P NMR (CD_2Cl_2, 162 MHz): 117.8 (s). Anal. Calcd for $C_{64}H_{60}Cl_4O_2P_2Ru_2$: C, 60.67; H, 4.77. Found: C, 60.52; H, 5.03.

Synthesis of 2b. As described for **2a** but with $[RuCl_2(\eta^6\text{-dibenzo-18-crown-6})]_2$ as substrate. Yield: 92%. ^{1}H NMR (CD_2Cl_2, 400 MHz): 8.21 (d, $^3J_{HH}$ = 8.1, 2H, H^{26}), 8.20 (d, $^3J_{HH}$ = 9.2, 2H, H^{28}), 8.15 (d, $^3J_{HH}$ = 9.2, 2H, H^{29}), 7.78 (dd, br, 4H), 7.65 (d, $^3J_{HH}$ = 8.3, 2H, H^{23}), 7.61 (m, 2H, H^{25}), 7.49 (m, 2H, H^{24}), 7.21 (m, 2H), 7.03−6.97 (m, 10H), 6.90−6.81 (m, 8H), 6.36 (br, 4H), 5.29 (br, 2H, H^2), 4.76 (br, 2H, H^3), 4.55 (br, 2H, H^4), 4.32 (br, 2H, H^5), 4.24−3.72 (m, 24H), 3.61 (br, 2H), 3.24 (br, 4H), 2.67 (br, 2H). ^{13}C NMR (CD_2Cl_2, 100 MHz): 149.6 (d, $^2J_{PC}$ = 3, C^{20}), 148.6, 148.5, 133.6 (C^{22}), 132.6 (d, $^2J_{PC}$ = 11), 130.6 (d, $^4J_{PC}$ = 3), 130.5 (C^{27}), 130.2 (br), 129.9 (C^{28}), 129.4 (d, $^2J_{PC}$ = 10), 129.1 (C^{26}), 128.0 (d, $^3J_{PC}$ = 11), 127.7 (C^{24}), 127.2 (d, $^3J_{PC}$ = 10), 125.5 (C^{25}), 124.7 (C^{23}), 122.3 (br, C^6), 121.9 (d, $^3J_{PC}$ = 6, C^{29}), 121.2 (d, $^3J_{PC}$ = 6, C^{21}), 120.8, 120.7, 112.6, 112.5, 81.7 (br, C^3), 76.0 (br, C^2), 75.5 (br, C^4), 72.3 (br, C^5), 70.2, 70.0, 69.8, 69.1, 69.0, 68.9, 67.8, 67.7. ^{31}P NMR (CD_2Cl_2, 162 MHz): 124.1 (s). Anal. Calcd for $C_{84}H_{80}Cl_4O_{14}P_2Ru_2 \cdot 2H_2O$: C, 57.47; H, 4.82. Found: C, 57.38; H, 4.02.

Synthesis of 2c. As described for **2a** but with $[RuCl_2(\eta^6\text{-ethylbenzoate})]_2$ as substrate. Yield: 85%. ^{1}H NMR (CD_2Cl_2, 400 MHz): 8.23 (m, 2H, H^{26,28}), 8.11 (d, $^3J_{HH}$ = 9.1, 2H, H^{29}), 7.71 (dd, 4H), 7.66−7.62 (m, 4H, H^{25,23}), 7.49 (dd, 2H, H^{24}), 7.27 (dt, 2H), 7.12−6.97 (m, 10H), 6.50 (m, 4H), 6.45 (d, $^3J_{HH}$ = 6.2, 2H, H^2), 6.27 (d, $^3J_{HH}$ = 5.9, 2H, H^6), 5.32 (dd, 2H, H^4), 5.02 (dd, 2H, H^3), 4.60 (dd, 2H, H^5), 4.22 (m, 4H, H^8), 1.29 (t, $^3J_{HH}$ = 7.1, H^9). ^{13}C NMR (CD_2Cl_2, 100 MHz): 162.9 (C^7), 149.6 (d, $^2J_{PC}$ = 4, C^{20}), 133.5 (C^{22}), 132.6 (d, $^2J_{PC}$ = 11), 131.2 (d, $^4J_{PC}$ = 3), 130.8 (d, $^4J_{PC}$ = 2), 130.6 (C^{27}), 130.2 (C^{28}), 130.0 (d, $^2J_{PC}$ = 11), 129.2 (C^{26}), 127.9 (d, $^3J_{PC}$ = 11), 127.8 (C^{24}), 127.5 (d, $^3J_{PC}$ = 11), 125.7 (C^{25}), 124.9 (C^{23}), 121.7 (d, $^3J_{PC}$ = 6, C^{29}), 121.3 (d, $^3J_{PC}$ = 6, C^{21}), 98.6 (C^2), 97.3 (d, $^2J_{PC}$ = 3, C^6), 89.0 (d, $^3J_{PC}$ = 10, C^7), 88.6 (C^4), 83.6 (d, $^2J_{PC}$ = 3, C^3), 82.8 (C^5), 62.5 (C^8), 14.2 (C^9). ^{31}P NMR (CD_2Cl_2, 162 MHz): 117.2 (s). Anal. Calcd for $C_{62}H_{52}Cl_4O_6P_2Ru_2 \cdot 2H_2O$: C, 55.78; H, 4.23. Found: C, 56.07; H, 4.39.

Synthesis of 4a. A solution of $[RuCl_2(\eta^6\text{-}p\text{-cymene})]_2$ (468 mg, 0.076 mmol) and **1** (100 mg, 0.15 mmol) in CH_2Cl_2 (10 mL) was stirred at room temperature for 5 min, then cooled to 0 °C, and a solution of BH_3 in THF (∼1.2 M, 0.26 mL, 0.31 mmol) was added. Following stirring a further 30 min at room temperature, the solution was concentrated to ca. 2 mL in vacuo and subjected to preparative TLC (1:10 acetone−CH_2Cl_2). The product was isolated by extraction of the first orange band (R_f = 0.68) with THF. Yield: 66 mg (44%). ^{1}H NMR (CD_2Cl_2, 400 MHz): 8.16 (d, $^3J_{HH}$ = 9.1, 1H, H$^{28'}$), 8.10 (d, $^3J_{HH}$ = 8.2, 1H, H$^{26'}$), 8.00 (d, $^3J_{HH}$ = 7.9, 1H, H^{26}), 7.98 (d, $^3J_{HH}$ = 9.0, 1H, H^{29}), 7.91 (d, $^3J_{HH}$ = 9.0, 1H, H^{28}), 7.76 (d, $^3J_{HH}$ = 9.0, 1H, H$^{29'}$), 6.9−7.6 (m, 24H), 6.7−6.8 (m, 2H), 5.19 (d, $^3J_{HH}$ = 5.9, 1H, H^6), 5.15 (d, $^3J_{HH}$ = 5.8, 1H, H^3), 5.12 (d, $^3J_{HH}$ = 5.9, 1H, H^2), 5.03 (d, $^3J_{HH}$ = 6.0, 1H, H^5), 2.17 (septet, $^3J_{HH}$ = 6.9, 1H, H^7), 1.30 (s, 1H, H^{10}), 1.0 (br, 3H, BH_3), 0.75 (d, $^3J_{HH}$ = 6.7, 6H, H^{8,9}). ^{13}C NMR (CD_2Cl_2, 100 MHz): 149.1 (d, $^2J_{PC}$ = 5, C$^{20'}$), 148.5 (d, $^2J_{PC}$ = 5, C^{20}), 133.7 (C$^{22,22'}$), 132.2 (d, $^4J_{PC}$ = 2), 132.1 (d, $^4J_{PC}$ = 2), 131.5 (br), 131.3(br), 131.2 (d, J_{PC} = 12), 131.1 (d, J_{PC} = 11), 130.5 (C$^{27'}$), 130.5 (d, $^4J_{PC}$ = 2), 130.4 (d, $^4J_{PC}$ = 2), 130.0 (C^{27}), 129.6 (C$^{28,28'}$), 128.9 (d, J_{PC} = 11), 128.6 (C$^{26'}$), 128.4 (d, J_{PC} = 11), 128.2 (C^{26}), 127.6 (d, J_{PC} = 10), 127.4 (d, J_{PC} = 11), 127.3 (C^{24}), 127.1 (C$^{24'}$), 125.8, 125.6, 125.4, 125.1, 123.3 (d, $^3J_{PC}$ = 5, C$^{21'}$), 121.0 (d, $^3J_{PC}$ = 6, C^{29}), 120.6 (d, $^3J_{PC}$ = 6, C^{21}), 120.4 (d, $^3J_{PC}$ = 5, C$^{29'}$), 109.3 (C^1), 98.7 (C^4), 90.4 (br, C^3), 89.7 (br, C^5), 89.0 (d, $^2J_{PC}$ = 5, C^2), 87.6 (d, $^2J_{PC}$ = 4, C^6), 29.9 (C^7), 21.2 (C^{8,9}), 17.2 (C^{10}). ^{31}P NMR (CD_2Cl_2, 162 MHz): 114.3 (s, RuP), 110.2 (br, PBH_3). ^{11}B NMR (CD_2Cl_2, 128 MHz): −38.8 (br). Anal. Calcd for $C_{54}H_{49}BCl_2O_2P_2Ru \cdot 1^1/_3CH_2Cl_2$: C, 61.09; H, 4.79. Found: C, 61.17; H, 4.49.

Synthesis of 5a. A solution of $[RuCl_2(\eta^6\text{-}p\text{-cymene})]_2$ (35 mg, 0.06 mmol) and **1** (80 mg, 0.12 mmol) in DMF (6 mL) was heated to 100 °C for 10 min, then the solvent was removed in vacuo. The crude product was washed with Et_2O−pentane (1:1, 5 mL) and then extracted with Et_2O−methanol (10:1) to afford the product as an orange-red solid. Yield: 57 mg (68%). ^{1}H NMR (CD_2Cl_2, 400 MHz): 8.20 (d, $^3J_{HH}$ = 8.9, 1H, H$^{28'}$), 8.10 (d, $^3J_{HH}$ = 7.8, 1H, H^{26}), 8.07 (d, $^3J_{HH}$ = 9.1, 1H, H^{29}), 7.93 (d, $^3J_{HH}$ = 8.0, 1H, H^{26}), 7.87 (d, $^3J_{HH}$ = 9.1, 1H, H^{28}), 7.56 (d, $^3J_{HH}$ = 8.9, 1H, H$^{29'}$), 7.54−7.23 (m, 13H), 7.16−7.08 (m, 4H), 5.28 (d, $^3J_{HH}$ = 5.9, 1H, H^2), 5.20 (d, $^3J_{HH}$ = 5.9, 1H, H^6), 5.18 (d, $^3J_{HH}$ = 5.9, 1H, H^3), 5.15 (d, $^3J_{HH}$ = 5.9, 1H, H^5), 2.34 (dq, 1H, H^7), 1.53 (s, 3H, H^{10}), 0.85 (d, $^3J_{HH}$ = 6.9, 3H, H$^{8/9}$), 0.79 (d, $^3J_{HH}$ = 6.9, 3H, H$^{8/9}$). ^{13}C NMR (CD_2Cl_2, 100 MHz): 151.9 (C$^{20'}$), 148.2 (d, $^2J_{PC}$ = 8, C^{20}), 134.0 (C^{22}), 133.8 (C$^{22'}$), 131.9 (d, $^2J_{PC}$ = 11), 131.3 (d, $^2J_{PC}$ = 11), 130.6 (d, $^4J_{PC}$ = 2), 130.5 (d, $^4J_{PC}$ = 2), 130.3 (C^{27}), 130.2 (C$^{28,28'}$), 129.6 (C$^{27'}$), 128.5 (C^{26}), 128.4 (C$^{26'}$), 127.6 (d, $^3J_{PC}$ = 11), 127.5 (d, $^3J_{PC}$ = 11), 127.3 (C^{24}), 127.0 (C$^{24'}$), 125.1 (C^{23}), 124.9 (C^{25}), 124.5 (C$^{23'}$), 123.8 (C$^{25'}$), 121.3 (d, $^3J_{PC}$ = 6, C^{29}), 119.2 (d, $^3J_{PC}$ = 5, C^{21}), 118.2 (C$^{29'}$), 115.2 (C$^{21'}$), 109.7 (C^1), 98.2 (C^4), 91.3 (d, $^2J_{PC}$ = 5, C^5), 90.9 (d, $^2J_{PC}$ = 5, C^3), 88.0 (d, $^2J_{PC}$ = 6, C^2), 87.8 (d, $^2J_{PC}$ = 6, C^6), 30.0 (C^7), 21.2 (C^{8,9}), 17.3 (C^{10}). ^{31}P NMR (CD_2Cl_2, 162 MHz): 114.1 (s).

Synthesis of 7. To a solution of $[Ru_2(\mu\text{-Cl})_3(\eta^6\text{-}p\text{-cymene}_2)][PF_6]$ (78 mg, 0.107 mmol) in CH_2Cl_2 (20 mL) was added **1** (105 mg, 0.161 mmol) and the solution stirred at RT for 4 h before the solvent was removed in vacuo. The residue was washed with MeOH (2 × 5 mL), leaving an orange solid, and the washings were subjected to preparative TLC (CH_2Cl_2) following concentration. The first (broad) yellow band (R_f = 0.27) was extracted with CH_2Cl_2−MeOH to give the product as a yellow powder (yield: 14 mg). Further extraction of the orange solid with MeOH (100 mL) gave additional product (70 mg, >92% purity by ^{31}P NMR). Total yield: 68% per Ru_2. Analytically pure samples can be obtained (in low yield) by preparative TLC as described above. ^{1}H NMR

(25) Bennett, M. A.; Smith, A. K. J. *Chem. Soc., Dalton Trans.* **1974**, 233.

(26) Trost, B. M.; Older, C. M. *Organometallics* **2002**, *21*, 2544−2546.

(27) Grubbs, R. H.; DeVries, R. A. *Tetrahedron Lett.* **1977**, *22*, 1879. (b) Zhou, Y.-G.; Zhang, X. *Chem. Commun.* **2002**, 1124.

(CD_2Cl_2, 400 MHz): 7.98 (br, 2H), 7.90−7.80 (m, 4H), 7.69−7.53 (m, 9H), 7.47−7.29 (m, 9H), 7.26−7.18 (m, 2H, $H^{24,24'}$), 7.10 (br, 2H), 6.91 (d, $^3J_{HH}$ = 8.5, 1H, $H^{23'}$), 6.82 (d, $^3J_{HH}$ = 8.5, 1H, H^{23}), 6.40 (d, $^3J_{HH}$ = 9.4, 1H, $H^{29'}$), 6.11 (d, $^3J_{HH}$ = 9.4, 1H, H^{29}), 5.85 (m, 1H, H^2), 5.76 (m, 1H, H^3), 5.52 (m, 1H, H^5), 5.32 (m, 1H, H^6), 2.56 (dq, 1H, H^7), 1.29 (s, 3H, H^{10}), 1.24 (d, $^3J_{HH}$ = 7.0, 3H, $H^{8/9}$), 0.60 (d, $^3J_{HH}$ = 6.7, 3H, $H^{8/9}$). ^{13}C NMR (CD_2Cl_2, 100 MHz): 150.0 (br, $C^{20'}$), 148.1 (br, C^{20}), 134.5 (m), 134.3 (br), 133.7 (C^{22}), 133.6 (br), 133.1 ($C^{22'}$), 132.8 (C^1), 131.8 (br), 131.3 (br), 130.8 (br), 130.6 ($C^{27,27'}$), 129.4 (br), 129.2 (m), 129.0 (m), 128.7 (m), 128.1 (br), 128.0 (C^{26}), 127.9 ($C^{26'}$), 127.8 (m), 127.1 (C^{24}), 126.7 ($C^{24'}$), 125.8 (C^{23}), 125.7 ($C^{25'}$), 125.3 (C^{25}), 125.2 ($C^{23'}$), 124.1 (C^{21}), 121.6 ($C^{21'}$), 120.3 ($C^{29'}$), 118.5 (C^{29}), 101.5 (br, C^3), 100.0 (C^4), 98.8 (br, C^5), 93.8 (dd, $^2J_{PC}$ = 6, J_{PC} = 4, C^6), 90.8 (dd, $^2J_{PC}$ = 7, $^2J_{PC}$ = 4, C^2), 31.3 (C^7), 22.5 ($C^{8/9}$), 18.6 ($C^{8/9}$), 15.9 (C^{10}). ^{31}P NMR (CD_2Cl_2, 162 MHz): 129.5 (s). ESI-MS (CH_2Cl_2) positive ion: *m/z* +925 $[M]^+$. ESI-MS/MS(+925): *m/z* +791 $[M - C_{10}H_{14}]^+$. ESI-MS(CH_2Cl_2) negative ion: *m/z* −145 $[PF_6]^-$. Anal. Calcd for $C_{54}H_{46}ClF_6O_2P_3Ru$: C, 60.59; H, 4.33. Found: C, 60.22; H, 4.31.

Synthesis of 8. A solution of $[RuCp(NCCH_3)_3][PF_6]$ (50 mg, 0.12 mmol) and **1** (40 mg, 0.06 mmol) in acetonitrile (5 mL) was stirred at room temperature for 1 h, then concentrated, and diethyl ether was added, resulting in the precipitation of a yellow-brown solid, which was washed further with Et_2O to afford the product. Yield: 74 mg (89%). ^1H NMR (CD_2Cl_2, 400 MHz): 8.08 (d, $^3J_{HH}$ = 8.1, 2H, H^{26}), 8.04 (d, $^3J_{HH}$ = 9.1, 2H, H^{28}), 7.55 (m, 2H, H^{25}), 7.48−7.39 (m, 8H), 7.30 (d, $^3J_{HH}$ = 8.5, 2H, H^{23}), 7.30 (br, 2H), 7.25 (d, $^3J_{HH}$ = 9.1, 2H, H^{29}), 7.15−7.06 (m, 8H), 6.61 (m, 4H), 4.32 (s, 10H, H^1), 2.15 (s, 6H, CH_3), 1.95 (s, 6H, CH_3). ^{13}C NMR (CD_2Cl_2, 100 MHz): 150.2 (d, $^2J_{PC}$ = 4, C^{20}), 138.9 (d, $^1J_{PC}$ = 55), 136.7 (d, $^1J_{PC}$ = 38), 133.5 (C^{22}), 131.5 (d, $^3J_{PC}$ = 14), 131.5 (d, $^4J_{PC}$ = 2), 130.2 (C^{27}), 130.1 (d, $^4J_{PC}$ = 2), 129.3 (C^{28}), 129.0 (C^{26}), 128.8 (d, $^3J_{PC}$ = 10), 128.7 (d, $^2J_{PC}$ = 14), 128.1 (d, $^2J_{PC}$ = 10), 127.8 (*C*N), 127.7 (*C*N), 127.3 (C^{24}), 125.5 (C^{23}), 125.4 (C^{25}), 122.6 (d, $^3J_{PC}$ = 6, C^{21}), 120.0 (d, $^3J_{PC}$ = 8, C^{29}), 77.7 (d, $^2J_{PC}$ = 2, C^1), 3.9 (*C*H_3), 3.5 (*C*H_3). ^{31}P NMR (CD_2Cl_2, 162 MHz): 147.6 (s). ESI-MS (CH_2Cl_2): *m/z* +575.3 $[M]^{2+}$. Anal. Calcd for $C_{62}H_{54}F_{12}N_4O_2P_4Ru_2$: C, 51.67; H, 3.78; N, 3.89. Found: C, 52.04; H, 3.79; N, 3.94.

Synthesis of 9. A solution of $[RuCp(NCCH_3)_3][PF_6]$ (50 mg, 0.12 mmol) and **1** (80 mg, 0.12 mmol) in chloroform (25 mL) was heated to reflux for 1 h, then filtered through a glass fiber filter, and the solution was concentrated. Addition of diethyl ether led to the precipitation of the product as a pale yellow, almost white solid. Yield: 92 mg (79%). ^1H NMR (CD_2Cl_2, 400 MHz): 7.89 (d, $^3J_{HH}$ = 8.1, 1H, H^{26}), 7.79 (d, $^3J_{HH}$ = 9.1, 1H, H^{28}), 7.78 (d, $^3J_{HH}$ = 8.2, 1H, $H^{26'}$), 7.62 (d, $^3J_{HH}$ = 9.1, 1H, $H^{28'}$), 7.61 (m, 1H), 7.57−7.39 (m, 13H), 7.18 (d, $^3J_{HH}$ = 8.5, 1H, H^{23}), 7.14 (d, $^3J_{HH}$ = 9.1, 1H, H^{29}), 7.11 (m, 2H), 7.04 (d, $^3J_{HH}$ = 8.2, 1H, $H^{23'}$), 7.02 (m, 2H), 6.91 (m, 2H), 6.69 (m, 2H), 6.55 (d, $^3J_{HH}$ = 9.1, 1H, $H^{29'}$), 4.43 (s, 5H, H^1), 1.72 (s, 3H, CH_3). ^{13}C NMR (CD_2Cl_2, 100 MHz): 150.1 (d, $^2J_{PC}$ = 6, C^{20}), 149.1 (d, $^2J_{PC}$ = 6, $C^{20'}$), 143.3 (d, $^1J_{PC}$ = 48), 141.6 (d, $^1J_{PC}$ = 43), 139.6 (d, $^1J_{PC}$ = 60), 136.7 (d, $^1J_{PC}$ = 59), 133.8 (C^{22}), 133.6 ($C^{22'}$), 131.8 (d, $^4J_{PC}$ = 2), 131.5 (d, J_{PC} = 12), 131.4 (d, J_{PC} = 14), 131.3 (d, $^4J_{PC}$ = 2), 130.8 ($C^{27,27'}$), 130.5 ($C^{28'}$), 130.3 (d, $^4J_{PC}$ = 2), 130.0 (d, $^4J_{PC}$ = 2), 129.9 (d, J_{PC} = 12), 129.8 (d, J_{PC} = 13), 129.5 (C^{28}), 129.1 (*C*N), 128.7 (d, J_{PC} = 10), 128.6 (d, J_{PC} = 10), 128.2 ($C^{26'}$), 128.0 (C^{26}), 127.9 (d, J_{PC} = 11), 127.5 (d, J_{PC} = 14), 127.4 ($C^{24'}$), 127.3 (C^{24}), 125.8 (C^{25}), 125.6 ($C^{25'}$), 125.4 (C^{23}), 125.2 ($C^{23'}$), 124.8 (d, $^3J_{PC}$ = 5, $C^{21'}$), 124.3 (d, $^3J_{PC}$ = 4, $C^{21'}$), 121.6 (d, $^3J_{PC}$ = 3, C^{29}), 120.4 (d, $^3J_{PC}$ = 2, $C^{29'}$), 84.7 (d, $^2J_{PC}$ = 2, C^1), 4.3 (*C*H_3). ^{31}P NMR (CD_2Cl_2, 162 MHz): 155.9 (d, $^2J_{PP}$ = 50), 153.7 (d, $^2J_{PP}$ = 50). ESI-MS (CH_2Cl_2): *m/z* +861.7 $[M]^+$, +821.3 $[M - CH_3CN]^+$. Anal. Calcd for $C_{51}H_{40}F_6NO_2P_3Ru$: C, 60.84; H, 4.00; N, 1.39. Found: C, 61.06; H, 4.60; N, 1.81.

Crystallography. Data collection for the X-ray structure determinations were performed on a KUMA CCD diffractometer system using graphite-monochromated Mo Kα (0.71070 Å) radiation and a low-temperature device [*T* = 140(2) K]. Crystals suitable for X-ray diffraction studies of **1** were obtained by cooling a CH_2Cl_2−acetonitrile solution (1:1) to −25 °C for **1**, diffusion of diethyl ether into a THF solution for **2a**, diffusion of pentane into a $CHCl_3$ solution for **4a**, and diffusion of pentane into a CH_2Cl_2 solution for **7**. Data reductions were performed by CrysAlis RED.[28] The structures of **1**, **2a**, and **7** were solved with SHELX97,[29] and that of **4a** with SIR-97.[30] Refinement was performed on PCs using the SHELX97 software package. Graphical representations of the structures were made with DIAMOND 3.0. Structures were solved by direct methods and successive interpretation of the difference Fourier maps, followed by full matrix least-squares refinement (against F^2). An empirical absorption correction (DELABS)[31] was applied to **1** and **4a**. All non-hydrogen atoms were refined anisotropically except for those of the THF solvent molecule and carbon atoms C7−C10 in **2a**, which were kept isotropic. In **2a** and **7** the structure was restrained using the DELU command, and some atoms were further restrained using the ISOR command. The contribution of the hydrogen atoms, in their calculated positions, were included in the refinement using a riding model with the exception of the BH-hydrogen atoms, which were located on the Fourier difference map and then constrained to equal B−H bond lengths and H−B−H angles. Some of the fluorine atoms of the $[PF_6]^-$ anion in **7** were split over two positions. Relevant crystallographic data are compiled in Table 3.

Acknowledgment. We thank the New Zealand Foundation for Research, Science and Technology for a Top Achiever Doctoral Fellowship (A.B.C.), the EPFL, and the Swiss National Science Foundation for financial support.

Supporting Information Available: Additional NMR spectra and crystallographic information files (CIF) of **1**, **2a**, **4a**, and **7** are available free of charge via the Internet at http://pubs.acs.org.

OM050568M

(28) *CrysAlis RED*; Oxford Diffraction Ltd: Abingdon, M. P. OX14 4 RX, UK, 2003.
(29) Sheldrick, G. M. *SHELX-97*, Structure Solution and Refinement Package; Universität Göttingen, 1997.
(30) Altomare, A.; Burla, M. C.; Camalli, M.; Cascarano, G. L.; Giacovazzo, C.; Guagliardi, A.; Moliterni, A. G. G.; Polidori, G.; Spagna, R. *J. Appl. Crystallogr.* **1999**, *32*, 115−119.
(31) Walker, N.; Stuart, D. *Acta Crystallogr.* **1983**, *A39*, 158.